Forum for Interdisciplinary Mathematics

Hemen Dutta *Editor*

Mathematical Modelling in Health, Social and Applied Sciences

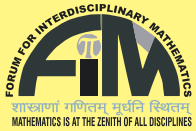

Forum for Interdisciplinary Mathematics

Forum for Interdisciplinary Mathematics is a Scopus-indexed book series. It publishes high-quality textbooks, monographs, contributed volumes and lecture notes in mathematics and interdisciplinary areas where mathematics plays a fundamental role, such as statistics, operations research, computer science, financial mathematics, industrial mathematics, and bio-mathematics. It reflects the increasing demand of researchers working at the interface between mathematics and other scientific disciplines.

More information about this series at http://www.springer.com/series/13386

Hemen Dutta
Editor

Mathematical Modelling in Health, Social and Applied Sciences

Springer

Editor
Hemen Dutta
Department of Mathematics
Gauhati University
Guwahati, Assam, India

ISSN 2364-6748 ISSN 2364-6756 (electronic)
Forum for Interdisciplinary Mathematics
ISBN 978-981-15-2285-7 ISBN 978-981-15-2286-4 (eBook)
https://doi.org/10.1007/978-981-15-2286-4

Mathematics Subject Classification (2010): 97Mxx, 68Uxx, 91G70, 90-XX, 41-XX

This Springer imprint is published by the registered company Springer Nature Singapore Pte Ltd.
The registered company address is: 152 Beach Road, #21-01/04 Gateway East, Singapore 189721, Singapore

Preface

This book is targeted to graduate students, teachers and researchers interested in various mathematical models associated with health, social and applied sciences. The readers should find several useful tools and techniques necessary to develop mathematical models and also various ways to solve them. The interpretation of the findings should help readers to understand better the several issues associated with health, social and applied sciences. The book consists of 10 chapters as follows:

The chapter on "Viral Immunology: Modeling and Analysis" aims to model and analyse the interactions between viruses and immune system by proposing two mathematical models that describe the role of adaptive immune response in infectious diseases caused by viruses such as the human immunodeficiency virus, hepatitis B virus and hepatitis C virus. The first model is based on delay differential equations and the second on partial differential equations. The models integrate the two main modes of virus propagation, namely virus-to-cell infection and direct cell-to-cell transmission. The dynamical behaviours of the models were further examined by five threshold parameters, and the biological aspects of the analytical results were also presented.

The chapter on "Modeling the Stochastic Dynamics of Influenza Epidemics with Vaccination Control, and the Maximum Likelihood Estimation of Model Parameters" discusses a family of stochastic models for the dynamics of influenza in a closed human population. It considers treatment for the disease in the form of vaccination and incorporates the periods of effectiveness of the vaccine and infectiousness for individuals in the population. The method of maximum likelihood and expectation–maximization algorithm has been applied in finding estimates for the parameters. Estimators for some special epidemiological control parameters, such as the basic reproduction number, are also computed. Further, a numerical simulation example has been incorporated to find the maximum likelihood estimators of the parameters of the model.

The chapter on "A Two-Dimensional Dynamical System for Local Transmission of Dengue with Time Invariant Mosquito Density" discusses a mathematical model describing the transmission of dengue. The critical parameters of the model equations are determined by the climate variation and techniques to model the

parameters are developed considering their uncertainty behaviour. The stability analysis of the model is carried out, and the model equations are numerically solved by using time-invariant parameters. Further, the simulated dengue infections are validated with the actual cases in Colombo, Sri Lanka.

The chapter on "A Mathematical Study of a Model for HPV with Two High-Risk Strains" aims to design a new two-sex deterministic model for two strains (HPV type-16/18 and type-31/45) of HPV infection and analyse for gaining insights into its transmission dynamics. The model is claimed to exhibit the phenomenon of backward bifurcation, where a stable disease-free equilibrium coexists with one or more stable endemic equilibria when the associated reproduction number is less than unity. It is further claimed that the backward bifurcation phenomenon is caused due to the imperfect vaccine as well as the re-infection of individuals who recover naturally from previous infection with the same strain of the disease. Numerical simulations of the model are also carried out, which reveal that increasing the fraction of vaccinated females against strain 1 (HPV type-16/18) infection can significantly bring down the burden of strain 2 (HPV type-31/45) infection.

The chapter on "The Impact of Fractional Differentiation in Terms of Fitting for a Prostate Cancer Model Under Intermittent Androgen Suppression Therapy" aims to introduce fractional calculus as a prospective mathematical tool for cancer dynamics and for prostate cancer modelling, in particular. It first attempts to handle the problem on the role of androgens for prostate cancer development. Based on the hypothesis of authors, a new mathematical model consisting of conventional logistic growth phenomena has been constructed. Another prospective model based on an ecological phenomenon, cell quota, has also been developed. It compared both the models demonstrating the mean squared error values for androgen- and prostate-specific antigen for the first 1.5 cycles of intermittent androgen suppression therapy administered to 62 selected patients from Vancouver Prostate Center (Vancouver, BC, Canada). It also generates the fractional version of the model to reduce the mean squared error values and verified that fractional differentiation provides nearly better data fitting for mathematical modelling.

The chapter on "Toward the Realization of the 'Europe 2020' Agenda for Economic Growth in the European Union: An Empirical Analysis Based on Goal Programming" proposes a weighted goal programming model that can be used to determine the optimal allocation of labour in each economic sector in order to minimize the deviation from the goals of four different criteria which model economic, environmental, energetic and social objectives. The model was applied to each country of the European Union and measured their performance with respect to the Europe 2020 agenda. The model claimed to provide insights and policy recommendations such as a better integration of the incoming workforce in a context of increasing immigration flows, development of renewable sources of energy and green sustained transformation of national economic environments.

The chapter on "On the Poincaré-Andronov-Melnikov Method for Modelling of Grazing Periodic Solutions in Discontinuous Systems" aims to derive Melnikov-like condition for the persistence of a periodic and grazing solution under autonomous perturbation for discontinuous systems. The grazing Poincaré map is derived

to fulfil the purpose. Then, its fixed point is investigated to determine desired solutions leading to Melnikov-like conditions. It was further emphasized to illustrate the theory by means of an example modelling the type of solutions discussed.

The chapter on "Modelling and Analysis of Predation System with Nonlocal and Nonsingular Operator" aims to model a novel system of predation involving two individuals or species which interact in a nonlinear fashion with the Atangana–Baleanu fractional derivative of order $0 < \gamma < 1$ in the sense of Caputo. This derivative has been used to model some important real-life phenomena such as heat flow, fractals, diffusion and groundwater flows, among many others. The local and global stability analysis of such model is given to accurately provide a good choice of parameters when numerically simulating the full process. Relevant numerical results for different instances of fractional power are also discussed in this chapter.

The chapter on "New Aspects of Fractional Epidemiological Model for Computer Viruses with Mittag–Leffler Law" aims to examine a fractional epidemiological model with strong memory effects. It uses a fractional derivative with Mittag-Leffler type kernel to moderate the epidemiological model in order to interpret the spreading and controlling of computer viruses. The solution to the mathematical model has been obtained by using q-HATM, a numerical algorithm used for solving epidemiological model of arbitrary order for computer viruses associated with the Mittag-Leffler type kernel. The existence and uniqueness of the solution are examined by employing the fixed point theory. Further, numerical simulations are carried out for demonstrating the results.

The chapter on "Numerical Simulation of Nonlinear Ecological Models with Nonlocal and Nonsingular Fractional Derivative" aims to focus on both non-spatial and spatially extended predator–prey systems whose dynamics are described by the Holling type-IV functional responses. It replaces the classical time derivative in such models by the Atangana–Baleanu fractional derivative with nonlocal and nonsingular properties. It claimed to formulate a two-step scheme based on the fractional Adams–Bashforth method for approximating this derivative. A brief linear stability analysis has been presented for the non-diffusive system and reported the Hopf and Turing bifurcation analysis for the spatial case. Further, numerical experiments are carried out to obtain range pattern results for different parameter values of α in (0, 1] as well as numerical simulation to justify the difference between integer and non-integer order results.

I am grateful to the contributors for their timely contribution and cooperation during the entire process of reviewing and editing the chapters. The reviewers deserve sincere gratitude for voluntarily offering their service for the success of the book. The editor and staff at Springer also deserve special thanks for their cooperation. I would like to acknowledge the encouragement of several friends and well-wishers for bringing out such a book.

Guwahati, India
November 2019

Hemen Dutta

Contents

About the Editor

Hemen Dutta is a regular faculty member at the Department of Mathematics, Gauhati University, Guwahati, India. He completed his PhD in mathematics from Gauhati University. He has to his credit 10 books and over 100 items as research papers and chapters in books published by leading publishers. He is member of noted scientific societies and has visited several foreign institutions with regards to research collaborations, conferences and delivering talks. His main research interests are summability theory, functional equations, fixed point theory and mathematical modelling.

Viral Immunology: Modeling and Analysis

Khalid Hattaf

1 Introduction

Immunity is a complex system that plays a vital role in the defense against infectious agents. It is comprised of two branches, the innate and adaptive immune responses. The innate immune response is the first line of defense against antigen which is rapid in response but non-specific. However, the adaptive immune response starts to work after the antigen has breached the innate or natural defense barrier. It is well known that the humoral and cellular immune responses are two fundamental types of adaptive immune response. The humoral immune response is mediated by antibodies that are produced by B-cells and are programmed to neutralize the pathogen, while the cellular immune response is carried out by cytotoxic T lymphocyte (CTL) cells to attack the infected cells.

Modeling the role of adaptive immune response in viral infections such as HIV, HBV and HCV has been studied in several researches. In 2003, Wodarz [1] introduced a mathematical model governed by five ordinary differential equations (ODEs) to investigate the role of CTL and antibody responses in HCV dynamics and pathology. The mathematical analysis of this model was studied in [2]. From this analysis, the authors have observed that the basic reproduction number of [1] is proportional to the total number of liver cells. This implies that an individual with a smaller liver may be more resistant to the HCV infection than an individual with a larger one. So, the model of [1] cannot be a reasonable model to describe the dynamics of HCV infection. This problem has been corrected in [3] by replacing the mass action process with a standard incidence function in order to model the role of adaptive immune response in HBV infection. In 2016, Hattaf and Yousfi [4] proposed a class

K. Hattaf (✉)
Centre Régional des Métiers de L'Education Et de la Formation (CRMEF), 20340, Derb Ghalef, Casablanca, Morocco

Laboratory of Analysis, Modeling and Simulation (LAMS), Faculty of Sciences Ben M'sik, Hassan II University, P.O Box 7955, Sidi Othman, Casablanca, Morocco

H. Dutta (ed.), *Mathematical Modelling in Health, Social and Applied Sciences*, Forum for Interdisciplinary Mathematics, https://doi.org/10.1007/978-981-15-2286-4_1

of delayed viral infection models with general incidence rate and adaptive immune response in order to extend the above models and the other ones presented in [5–9].

All the immunological models mentioned above considered only the classical mode of transmission that is virus-to-cell infection. However, viruses spread in the human body through two different ways, one by virus-to-cell infection and the other by cell-to-cell transmission via direct contact. It is shown that cell-to-cell transmission is the predominant mode of HIV spread and helps to explain why this virus replicates so efficiently in lymphoid organs [10]. Also, cell-to-cell viral transmission is a rapid and potent phenomenon [11, 12]. Motivated by these biological considerations, we propose the following model:

$$\begin{cases} \frac{dU}{dt} = \lambda - dU(t) - f\big(U(t), I(t), V(t)\big)V(t) - g\big(U(t), I(t)\big)I(t), \\ \frac{dI}{dt} = \int_0^\infty f_1(\tau)e^{-\alpha_1\tau}[f\big(U(t-\tau), I(t-\tau), V(t-\tau)\big)V(t-\tau) \\ \qquad +g\big(U(t-\tau), I(t-\tau)\big)I(t-\tau)]d\tau - aI(t) - pI(t)Z(t), \\ \frac{dV}{dt} = k\int_0^\infty f_2(\tau)e^{-\alpha_2\tau}I(t-\tau)d\tau - \mu V(t) - qV(t)W(t), \\ \frac{dW}{dt} = rV(t)W(t) - hW(t), \\ \frac{dZ}{dt} = cI(t)Z(t) - bZ(t), \end{cases} \tag{1}$$

where $U(t)$, $I(t)$, $V(t)$, $W(t)$ and $Z(t)$ are, respectively, the densities of uninfected cells, infected cells, free virus, antibodies and CTL cells at time t. The uninfected cells are generated at a constant rate λ, die at rate dU and become infected by contact with free virus at rate $f(U, I, V)V$ and by contact with infected cells at rate $g(U, I)I$. The positive constants a, h and b are the death rates of infected cells, antibodies and CTL cells. However, μ denotes the clearance rate of free virus. The virions are neutralized by antibodies at rate qVW, while the infected cells are killed by CTL cells at rate pIZ. The parameters k, r and c represent the birth rates of virus, antibodies and CTL cells, respectively. In addition, we assume that the free virus or infected cell contacts an uninfected cell at time $t-\tau$ and the cell becomes infected at time t, where τ is a random variable taken from a probability distribution $f_1(\tau)$ and $e^{-\alpha_1\tau}$ accounts for survival probability of infected but not yet virus-producing cells. Similarly, we assume that the time necessary for the newly produced virions to become mature and infectious is a random variable with a probability distribution $f_2(\tau)$. The survival probability of immature virions is given by $e^{-\alpha_2\tau}$, and the probability distribution functions are assumed to be nonnegative and $\int_0^\infty f_1(\tau)d\tau = \int_0^\infty f_2(\tau)d\tau = 1$.

The first purpose of this study is to analyze the global dynamics of model (1) which extends and generalizes many cases existing in the literature such as the models with only cellular immune response [13–19], with only humoral immune response [20–27] and with both cellular and humoral immune responses [1, 3–9, 28].

Modeling with PDEs allows to describe the evolution in time and space of viral infections. Hence, the second purpose of this work is to introduce the spatial dependence into model (1). This model becomes

$$\begin{cases} \dfrac{\partial U}{\partial t} = \lambda - dU(x,t) - f\big(U(x,t), I(x,t), V(x,t)\big)V(x,t) \\ \qquad\quad -g\big(U(x,t), I(x,t)\big)I(x,t), \\ \dfrac{\partial I}{\partial t} = \int_0^\infty f_1(\tau)e^{-\alpha_1\tau}[f\big(U(x,t-\tau), I(x,t-\tau), V(x,t-\tau)\big)V(x,t-\tau) \\ \qquad\quad +g\big(U(x,t-\tau), I(x,t-\tau)\big)I(x,t-\tau)]d\tau - aI(x,t) - pI(x,t)Z(x,t), \\ \dfrac{\partial V}{\partial t} = d_V \triangle V + k\int_0^\infty f_2(\tau)e^{-\alpha_2\tau}I(x,t-\tau)d\tau - \mu V(x,t) - qV(x,t)W(x,t), \\ \dfrac{\partial W}{\partial t} = rV(x,t)W(x,t) - hW(x,t), \\ \dfrac{\partial Z}{\partial t} = cI(x,t)Z(x,t) - bZ(x,t), \end{cases} \tag{2}$$

where $U(x,t)$, $I(x,t)$, $V(x,t)$, $W(x,t)$ and $Z(x,t)$ are the densities of uninfected cells, infected cells, free virus, antibodies and CTL cells at position x and time t, respectively. d_V is the diffusion coefficient and $\triangle$ is the Laplacian operator. The other parameters have the same biological meanings as those in model (1).

For both models (1) and (2), the incidence functions $f(U,I,V)$ and $g(U,I)$ are assumed to be continuously differentiable and satisfy the following hypotheses:

(H_0) g(0,I)=0, for all $I \geq 0$; $\dfrac{\partial g}{\partial U}(U,I) \geq 0$(or $g(U,I)$ is a strictly monotone increasing function with respect to U when $f \equiv 0$) and $\dfrac{\partial g}{\partial I}(U,I) \leq 0$, for all $U \geq 0$ and $I \geq 0$.

(H_1) $f(0,I,V) = 0$, for all $I \geq 0$ and $V \geq 0$,

(H_2) $f(U,I,V)$ is a strictly monotone increasing function with respect to U(or $\dfrac{\partial f}{\partial U}(U,I,V) \geq 0$ when $g(U,I)$ is a strictly monotone increasing function with respect to U), for any fixed $I \geq 0$ and $V \geq 0$,

(H_3) $f(U,I,V)$ is a monotone decreasing function with respect to I and V.

The organization of this chapter is as follows. The next section deals with the mathematical analysis of the generalized DDE model including well-posedness, threshold parameters and global stability of equilibria. Section 3 is devoted to the analysis of the generalized PDE model. An application of the analytical results to HIV infection is given in Sect. 4. The biological and mathematical conclusions are presented in the last section.

2 Analysis of the Generalized DDE Model

In this section, we first establish the well-posedness of the DDE model (1) and the threshold parameters for the existence of equilibria. After, we focus on the global stability on these equilibria.

2.1 Well-Posedness and Threshold Parameters

For the nonnegativity of solutions, we consider model (1) under the following initial conditions:

$$\begin{array}{lll} U(\theta) = \phi_1(\theta) \geq 0, & I(\theta) = \phi_2(\theta) \geq 0, & V(\theta) = \phi_3(\theta) \geq 0, \\ W(\theta) = \phi_4(\theta) \geq 0, & Z(\theta) = \phi_5(\theta) \geq 0, & \theta \in (-\infty, 0]. \end{array} \tag{3}$$

For the existence of solutions, we need the following Banach space:

$$C_\alpha = \Big\{ \varphi \in C((-\infty, 0], \mathbb{R}^5_+) : \ \varphi(\theta)e^{\alpha\theta} \text{ is uniformly continuous on } (-\infty, 0] \text{ and } \|\varphi\| = \sup_{\theta \leq 0} |\varphi(\theta)|e^{\alpha\theta} < \infty \Big\},$$

where α is a positive constant and $\mathbb{R}^5_+ = \{(x_1, ..., x_5) : x_i \geq 0, \ i = 1, ..., 5\}$.

Theorem 2.1 *For any initial condition $\phi = (\phi_1, \phi_2, \phi_3, \phi_4, \phi_5) \in C_\alpha$ satisfying (3), the DDE model (1) has a unique solution defined on $[0, +\infty)$. Also, this solution remains nonnegative and bounded for all $t \geq 0$.*

Proof. From the standard theory of functional differential equations [29–31], the DDE model (1) with initial condition $\phi \in C_\alpha$ has a unique local solution on its maximal interval of existence $[0, t_{\max})$.

First, we show that $U(t) > 0$ for all $t \in [0, t_{\max})$. On the contrary, let $t_1 > 0$ be the first time such that $U(t_1) = 0$ and $\frac{dU(t_1)}{dt} \leq 0$. According to the first equation of (1), we have $\frac{dU(t_1)}{dt} = \lambda > 0$ which is a contradiction. Then, $U(t) > 0$ for all $t \in [0, t_{\max})$. From (1), we obtain

$$\begin{aligned} I(t) &= \phi_2(0)e^{-\int_0^t (a+pZ(\theta))d\theta} \\ &\quad + \int_0^t e^{-\int_\xi^t (a+pZ(\theta))d\theta} \int_0^\infty f_1(\tau)e^{-\alpha_1\tau}[f\big(U(\xi-\tau), I(\xi-\tau), V(\xi-\tau)\big)V(\xi-\tau) \\ &\quad + g\big(U(\xi-\tau), I(\xi-\tau)\big)\big)I(\xi-\tau)]d\tau d\xi, \\ V(t) &= \phi_3(0)e^{-\int_0^t (\mu+qW(\theta))d\theta} + k\int_0^t e^{-\int_\xi^t (\mu+qW(\theta))d\theta} \int_0^\infty f_2(\tau)e^{-\alpha_2\tau} I(\xi-\tau)d\tau d\xi, \\ W(t) &= \phi_4(0)e^{\int_0^t (rV(\theta)-h)d\theta}, \\ Z(t) &= \phi_5(0)e^{\int_0^t (cI(\theta)-b)d\theta}. \end{aligned}$$

Hence, $I(t) \geq 0$, $V(t) \geq 0$, $W(t) \geq 0$ and $Z(t) \geq 0$, for all $t \in [0, t_{\max})$.

Now, we prove the boundedness of the solution. The first equation of (1) gives $\frac{dU}{dt} \leq \lambda - dU(t)$. Then,

$$\limsup_{t \to +\infty} U(t) \leq \frac{\lambda}{d}, \tag{4}$$

which implies that $U(t)$ is bounded. Denote

$$F_1(t) = I(t) + \frac{p}{c}Z(t) + \int_0^\infty f_1(\tau)e^{-\alpha_1\tau}U(t-\tau)d\tau.$$

Then,

$$\begin{aligned}\frac{dF_1(t)}{dt} &= \lambda\int_0^\infty f_1(\tau)e^{-\alpha_1\tau}d\tau - d\int_0^\infty f_1(\tau)e^{-\alpha_1\tau}U(t-\tau)d\tau - aI(t) - \frac{pb}{c}Z(t)\\ &\le \lambda\eta_1 - \rho_1 F_1(t),\end{aligned}$$

where $\rho_1 = \min\{a, b, d\}$ and

$$\eta_i = \int_0^\infty f_i(\tau)e^{-\alpha_i\tau}d\tau, \quad i = 1, 2. \tag{5}$$

Hence, $G_1(t) \le \max\{F_1(0), \frac{\lambda\eta_1}{\rho_1}\}$, implying that $I(t)$ and $Z(t)$ are bounded. Let

$$F_2(t) = V(t) + \frac{q}{r}W(t).$$

Then,

$$\begin{aligned}\frac{dF_2(t)}{dt} &= k\int_0^\infty f_2(\tau)e^{-\alpha_2\tau}I(t-\tau)d\tau - \mu V(t) - \frac{hq}{r}W(t)\\ &\le k\varrho\eta_2 - \rho_2 F_2(t),\end{aligned}$$

where $\varrho = \max\{F_1(0), \frac{\lambda\eta_1}{\rho_1}\}$ and $\rho_2 = \min\{\mu, h\}$. So, $F_2(t) \le \max\{F_2(0), \frac{k\varrho\eta_2}{\rho_2}\}$ which implies that $G_2(t)$ is bounded and so are $V(t)$ and $W(t)$. From the above, we have proved that all sate variables of (1) are bounded. Therefore, $t_{\max} = +\infty$, and the proof is completed. ■

In addition to (3), if we assume that $\phi_i(0) > 0$ for all $i = 1, ..., 5$, then we have the following result.

Remark 2.2 If $\phi \in \mathcal{C}_\alpha$ satisfying (3) with $\phi_i(0) > 0$, then the solution of model (1) with initial condition ϕ remains positive and bounded for all $t \ge 0$.

On the other hand, model (1) has always a unique infection-free equilibrium $E_0(U_0, 0, 0, 0, 0)$, where $U_0 = \frac{\lambda}{d}$. Then, we define the first threshold parameter which is called the basic reproduction number as follows

$$\mathcal{R}_0 = \frac{k\eta_1\eta_2 f(\frac{\lambda}{d}, 0, 0) + \mu\eta_1 g(\frac{\lambda}{d}, 0)}{a\mu}. \tag{6}$$

From the biological point of view, the threshold parameter $\mathcal{R}_0$ describes the average number of secondary infections produced by one infected cell at the beginning of infection.

The other arbitrary equilibria of model (1) satisfy the following system

$$\begin{cases} \lambda - dU - f(U,I,V)V - g(U,I)I = 0, \\ \eta_1\big(f(U,I,V)V + g(U,I)I\big) - aI - pIZ = 0, \\ k\eta_2 I - \mu V - qVW = 0, \\ rVW - hW = 0, \\ cIZ - bZ = 0. \end{cases} \tag{7}$$

The last two equations of (7) lead to $W = 0$ or $V = \frac{h}{r}$, and $Z = 0$ or $I = \frac{b}{c}$.

Let us first consider $W = 0$ and $Z = 0$, then $V = \frac{k\eta_1\eta_2(\lambda - dU)}{a\mu}$ and

$$k\eta_1\eta_2 f\big(U, \frac{\eta_1(\lambda - dU)}{a}, \frac{k\eta_1\eta_2(\lambda - dU)}{a\mu}\big) + \mu\eta_1 g\big(U, \frac{\eta_1(\lambda - dU)}{a}\big) = a\mu.$$

Since $I = \frac{\eta_1(\lambda - dU)}{a} \geq 0$, we have $U \leq \frac{\lambda}{d}$. Then, there is no equilibrium if $U > \frac{\lambda}{d}$. In this case, we define a function ψ_1 on $[0, \frac{\lambda}{d}]$ as follows

$$\psi_1(U) = k\eta_1\eta_2 f\big(U, \frac{\eta_1(\lambda - dU)}{a}, \frac{k\eta_1\eta_2(\lambda - dU)}{a\mu}\big) + \mu\eta_1 g\big(U, \frac{\eta_1(\lambda - dU)}{a}\big) - a\mu.$$

By (H_0)-(H_3), we have $\psi_1(0) = -a\mu < 0$, $\psi_1(\frac{\lambda}{d}) = a\mu(\mathcal{R}_0 - 1)$ and

$$\psi_1'(U) = k\eta_1\eta_2\left(\frac{\partial f}{\partial U} - \frac{d\eta_1}{a}\frac{\partial f}{\partial I} - \frac{kd\eta_1\eta_2}{a\mu}\frac{\partial f}{\partial V}\right) + \mu\eta_1\left(\frac{\partial g}{\partial U} - \frac{d\eta_1}{a}\frac{\partial g}{\partial I}\right) > 0.$$

When $\mathcal{R}_0 > 1$, there exists a unique $U_1 \in (0, \frac{\lambda}{d})$ such as $\psi_1(U_1) = 0$. So, model (1) has a unique infection equilibrium without immunity $E_1(U_1, I_1, V_1, 0, 0)$, where $I_1 = \frac{\eta_1(\lambda - dU_1)}{a}$ and $V_1 = \frac{k\eta_1\eta_2(\lambda - dU_1)}{a\mu}$.

When $W \neq 0$ and $Z = 0$, we have $V = \frac{h}{r}$ and

$$ahf\big(U, \frac{\eta_1(\lambda - dU)}{a}, \frac{h}{r}\big) + r\eta_1(\lambda - dU)g\big(U, \frac{\eta_1(\lambda - dU)}{a}\big) = ar(\lambda - dU).$$

It follows from $W = \dfrac{kr\eta_1\eta_2(\lambda - dU) - ah\mu}{ahq} \geq 0$ that $U \leq \dfrac{\lambda}{d} - \dfrac{ah\mu}{dkr\eta_1\eta_2}$. So, define a function ψ_2 on the closed interval $[0, \dfrac{\lambda}{d} - \dfrac{ah\mu}{dkr\eta_1\eta_2}]$ as follows

$$\psi_2(U) = ahf\big(U, \frac{\eta_1(\lambda - dU)}{a}, \frac{h}{r}\big) + r\eta_1(\lambda - dU)g\big(U, \frac{\eta_1(\lambda - dU)}{a}\big) - ar(\lambda - dU).$$

We have $\psi_2(0) = -ar\lambda < 0$ and

$$\begin{aligned}\psi_2'(U) = ah\left(\frac{\partial f}{\partial U} - \frac{d\eta_1}{a}\frac{\partial f}{\partial I}\right) + rd\left(a - \eta_1 g\big(U, \frac{\eta_1(\lambda - dU)}{a}\big)\right)\\ + r\eta_1(\lambda - dU)\left(\frac{\partial g}{\partial U} - \frac{d\eta_1}{a}\frac{\partial g}{\partial I}\right) > 0.\end{aligned}$$

When the humoral immunity has not been established, we have $rV_1 - h \leq 0$. Then, we define the reproduction number for humoral immunity as

$$\mathcal{R}_1^W = \frac{rV_1}{h}, \tag{8}$$

which implies that $rV_1 - h \leq 0$ is equivalent to $\mathcal{R}_1^W \leq 1$.
If $\mathcal{R}_1^W < 1$, then $V_1 < \dfrac{h}{r}$, $U_1 > \dfrac{\lambda}{d} - \dfrac{ah\mu}{dkr\eta_1\eta_2}$ and

$$\psi_2\big(\frac{\lambda}{d} - \frac{ah\mu}{dkr\eta_1\eta_2}\big) = \frac{ah}{k\eta_1\eta_2}\psi_1\big(\frac{\lambda}{d} - \frac{ah\mu}{dkr\eta_1\eta_2}\big) < \frac{ah}{k\eta_1\eta_2}\psi_1(U_1) = 0.$$

So, there is no positive equilibrium if $\mathcal{R}_1^W < 1$.
When $\mathcal{R}_1^W > 1$, we have $V_1 > \dfrac{h}{r}$, $U_1 < \dfrac{\lambda}{d} - \dfrac{ah\mu}{dkr\eta_1\eta_2}$ and $\psi_2(\dfrac{\lambda}{d} - \dfrac{ah\mu}{dkr\eta_1\eta_2}) > 0$. Hence, if $\mathcal{R}_1^W > 1$, model (1) has a unique infection equilibrium with only humoral immunity $E_2(U_2, I_2, V_2, W_2, 0)$, where $U_2 \in (0, \dfrac{\lambda}{d} - \dfrac{ah\mu}{dkr\eta_1\eta_2})$, $I_2 = \dfrac{\eta_1(\lambda - dU_2)}{a}$, $V_2 = \dfrac{h}{r}$ and $W_2 = \dfrac{kr\eta_1\eta_2(\lambda - dU_2) - ah\mu}{ahq}$.

When $W = 0$ and $Z \neq 0$, we have $I = \dfrac{b}{c}$, $V = \dfrac{kb\eta_2}{c\mu}$ and

$$k\eta_2 f\big(U, \frac{b}{c}, \frac{kb\eta_2}{c\mu}\big) + \mu g\big(U, \frac{b}{c}\big) = \frac{c\mu}{b}(\lambda - dU).$$

By $Z = \dfrac{c\eta_1(\lambda - dU) - ab}{pb} \geq 0$, we have $U \leq \dfrac{\lambda}{d} - \dfrac{ab}{dc\eta_1}$. So, there is no equilibrium if $U > \dfrac{\lambda}{d} - \dfrac{ab}{dc\eta_1}$ or $\dfrac{\lambda}{d} - \dfrac{ab}{dc\eta_1} \leq 0$. Consider a function ψ_3 defined on $[0, \frac{\lambda}{d} - \dfrac{ab}{dc\eta_1}]$ by

$$\psi_3(U) = k\eta_2 f\big(U, \frac{b}{c}, \frac{kb\eta_2}{c\mu}\big) + \mu g\big(U, \frac{b}{c}\big) - \frac{c\mu}{b}(\lambda - dU).$$

When the cellular immunity has not been established, we have $cI_1 - b \leq 0$. Then, we define the reproduction number for cellular immunity as

$$\mathcal{R}_1^Z = \frac{cI_1}{b}. \tag{9}$$

If $\mathcal{R}_1^Z < 1$, then $I_1 < \dfrac{b}{c}$, $U_1 > \dfrac{\lambda}{d} - \dfrac{ab}{dc\eta_1}$ and

$$\psi_3(\frac{\lambda}{d} - \frac{ab}{dc\eta_1}) = \frac{1}{\eta_1}\psi_1(\frac{\lambda}{d} - \frac{ab}{dc\eta_1}) < \frac{1}{\eta_1}\psi_1(U_1) = 0.$$

So, there is no biological equilibrium if $\mathcal{R}_1^Z < 1$.

When $\mathcal{R}_1^Z > 1$, we have $I_1 > \dfrac{b}{c}$, $U_1 < \dfrac{\lambda}{d} - \dfrac{ab}{dc\eta_1}$ and $\psi_3(\frac{\lambda}{d} - \dfrac{ab}{dc\eta_1}) > 0$. Thus, if $\mathcal{R}_1^Z > 1$, model (1) has a unique infection equilibrium with only cellular immunity $E_3(U_3, I_3, V_3, 0, Z_3)$, where $U_3 \in (0, \dfrac{\lambda}{d} - \dfrac{ab}{dc\eta_1})$, $I_3 = \dfrac{b}{c}$, $V_3 = \dfrac{kb\eta_2}{\mu c}$ and $Z_3 = \dfrac{c\eta_1(\lambda - dU_3) - ab}{pb}$.

Finally, when $W \neq 0$ and $Z \neq 0$, we have $I = \dfrac{b}{c}$ and $V = \dfrac{h}{r}$ and

$$chf\big(U, \frac{b}{c}, \frac{h}{r}\big) + rbg\big(U, \frac{b}{c}\big) = rc(\lambda - dU).$$

By $Z = \dfrac{c\eta_1(\lambda - dU) - ab}{pb} \geq 0$, we have $U \leq \dfrac{\lambda}{d} - \dfrac{ab}{dc\eta_1}$. Then, there is no equilibrium if $U > \dfrac{\lambda}{d} - \dfrac{ab}{dc\eta_1}$ or $\dfrac{\lambda}{d} - \dfrac{ab}{dc\eta_1} \leq 0$. Define the function ψ_4 on the interval $[0, \frac{\lambda}{d} - \dfrac{ab}{dc\eta_1}]$ by

$$\psi_4(U) = chf\big(U, \frac{b}{c}, \frac{h}{r}\big) + rbg\big(U, \frac{b}{c}\big) - rc(\lambda - dU).$$

We have $\psi_4(0) = -rc\lambda < 0$ and

$$\psi_4'(U) = ch\frac{\partial f}{\partial U} + rb\frac{\partial g}{\partial U} + rcd > 0.$$

In this last case, we define the reproduction number for cellular immunity in competition as

$$\mathcal{R}_2^Z = \frac{cI_2}{b}. \tag{10}$$

If $\mathcal{R}_2^Z < 1$, then $I_2 < \frac{b}{c}$, $U_2 > \frac{\lambda}{d} - \frac{ab}{dc\eta_1}$ and

$$\psi_4(\frac{\lambda}{d} - \frac{ab}{dc\eta_1}) = \frac{c}{a}\psi_2(\frac{\lambda}{d} - \frac{ab}{dc\eta_1}) < \frac{c}{a}\psi_2(U_2) = 0.$$

Thus, there is no biological equilibrium when $\mathcal{R}_2^Z < 1$.
If $\mathcal{R}_2^Z > 1$, then $I_2 > \frac{b}{c}$, $U_2 < \frac{\lambda}{d} - \frac{ab}{dc\eta_1}$ and $\psi_4(\frac{\lambda}{d} - \frac{ab}{dc\eta_1}) > 0$. So, there exists a unique $U_4 \in (0, \frac{\lambda}{d} - \frac{ab}{dc\eta_1})$ such that $\psi_4(U_4) = 0$. From the third equation of (7), we get

$$W_4 = \frac{\mu}{q}(\mathcal{R}_3^W - 1),$$

where $\mathcal{R}_3^W$ is the reproduction number for humoral immunity in competition defined as

$$\mathcal{R}_3^W = \frac{rV_3}{h}. \tag{11}$$

Therefore, if $\mathcal{R}_2^Z > 1$ and $\mathcal{R}_3^W > 1$, model (1) has a unique infection equilibrium with both humoral and cellular immune responses $E_4(U_4, I_4, V_4, W_4, Z_4)$, where $U_4 \in (0, \frac{\lambda}{d} - \frac{ab}{dc\eta_1})$, $I_4 = \frac{b}{c}$, $V_4 = \frac{h}{r}$, $W_4 = \frac{\mu}{q}(\mathcal{R}_3^W - 1)$ and $Z_4 = \frac{c\eta_1(\lambda - dU_4) - ab}{pb}$.

Consequently, we get the following theorem.

Theorem 2.3

(i) *If $\mathcal{R}_0 \leq 1$, then model (1) always has one infection-free equilibrium $E_0(U_0, 0, 0, 0, 0)$, where $U_0 = \frac{\lambda}{d}$.*

(ii) *If $\mathcal{R}_0 > 1$, then model (1) has an infection equilibrium without immunity $E_1(U_1, I_1, V_1, 0, 0)$, where $U_1 \in (0, \frac{\lambda}{d})$, $I_1 = \frac{\eta_1(\lambda - dU_1)}{a}$ and $V_1 = \frac{k\eta_1\eta_2(\lambda - dU_1)}{a\mu}$.*

(iii) *If* $\mathcal{R}_1^W > 1$, *then model (1) has an infection equilibrium with only humoral immunity* $E_2(U_2, I_2, V_2, W_2, 0)$, *where* $U_2 \in (0, \frac{\lambda}{d} - \frac{ah\mu}{dkr\eta_1\eta_2})$, $I_2 = \frac{\eta_1(\lambda - dU_2)}{a}$, $V_2 = \frac{h}{r}$ *and* $W_2 = \frac{kr\eta_1\eta_2(\lambda - dU_2) - ah\mu}{ahq}$.

(iv) *If* $\mathcal{R}_1^Z > 1$, *then model (1) has an infection equilibrium with only cellular immunity* $E_3(U_3, I_3, V_3, 0, Z_3)$, *where* $U_3 \in (0, \frac{\lambda}{d} - \frac{ab}{dc\eta_1})$, $I_3 = \frac{b}{c}$, $V_3 = \frac{kb\eta_2}{\mu c}$ *and* $Z_3 = \frac{c\eta_1(\lambda - dU_3) - ab}{pb}$.

(v) *If* $\mathcal{R}_2^Z > 1$ *and* $\mathcal{R}_3^W > 1$, *then model (1) has an infection equilibrium with both humoral and cellular immune responses* $E_4(U_4, I_4, V_4, W_4, Z_4)$, *where* $U_4 \in (0, \frac{\lambda}{d} - \frac{ab}{dc\eta_1})$, $I_4 = \frac{b}{c}$, $V_4 = \frac{h}{r}$, $W_4 = \frac{\mu}{q}(\mathcal{R}_3^W - 1)$ *and* $Z_4 = \frac{c\eta_1(\lambda - dU_4) - ab}{pb}$.

On the other hand, it is very important to note that

$$\mathcal{R}_3^W = \frac{\mathcal{R}_1^W}{\mathcal{R}_1^Z} = \frac{rkb\eta_2}{h\mu c}, \ W_2 = \frac{\mu}{q}(\mathcal{R}_2^Z\mathcal{R}_3^W - 1) \text{ and } \mathcal{R}_3^W > \frac{1}{\mathcal{R}_2^Z}. \tag{12}$$

2.2 Global Dynamics

This subsection focuses on the global stability of the five equilibria of model (1) by means of Lyapunov functionals. First, we have the following result.

Theorem 2.4 *The infection-free equilibrium* E_0 *of model (1) is globally asymptotically stable if* $\mathcal{R}_0 \leq 1$.

Proof. To investigate the global dynamics of (1) when $\mathcal{R}_0 \leq 1$, we construct a Lyapunov functional as follows

$$\begin{aligned} L_0(t) = {} & \frac{1}{\eta_1}I(t) + \frac{\beta_1 U_0}{\mu}V(t) + \frac{qf(U_0,0,0)}{r\mu}W(t) + \frac{p}{c\eta_1}Z(t) \\ & + \frac{1}{\eta_1}\int_0^\infty f_1(\tau)e^{-\alpha_1\tau}\int_{t-\tau}^t \big[f\big(U(\theta), I(\theta), V(\theta)\big)V(\theta) + g\big(U(\theta), I(\theta)\big)I(\theta)\big]d\theta d\tau \\ & + \frac{kf(U_0,0,0)}{\mu}\int_0^\infty f_2(\tau)e^{-\alpha_2\tau}\int_{t-\tau}^t I(\theta)d\theta d\tau, \end{aligned}$$

For simplicity, denote $\varphi = \varphi(t)$ and $\varphi_\tau = \varphi(t-\tau)$ for any $\varphi \in \{U, I, V, W, Z\}$. The time derivative of L_0 along the solution of model (1) is

$$\frac{dL_0}{dt} = \Big(f(U,I,V) - f(U_0,0,0)\Big)V + \frac{a}{\eta_1}I\left(\frac{k\eta_1\eta_2 f(U_0,0,0) + \mu\eta_1 g(U,I)}{a\mu} - 1\right) - \frac{qhf(U_0,0,0)}{r\mu}W - \frac{pb}{c\eta_1}Z.$$

By (4), we have $\limsup_{t\to+\infty} U(t) \le U_0$. Then, all omega limit points verify $U(t) \le U_0$. So, it is sufficient to consider solutions for which $U(t) \le U_0$. According to (6) and (H_0)–(H_3), we have

$$\begin{aligned}\frac{dL_0}{dt} &\le \Big(f(U,I,V) - f(U_0,0,0)\Big)V + \frac{a}{\eta_1}\big(\mathcal{R}_0 - 1\big)I - \frac{qhf(U_0,0,0)}{r\mu}W - \frac{pb}{c\eta_1}Z\\ &\le \frac{a}{\eta_1}\big(\mathcal{R}_0 - 1\big)I - \frac{qhf(U_0,0,0)}{r\mu}W - \frac{pb}{c\eta_1}Z.\end{aligned}$$

Since $\mathcal{R}_0 \le 1$, we have $\frac{dL_0}{dt} \le 0$. Clearly, the largest compact invariant set in $\{(U,I,V,W,Z) | \frac{dL_0}{dt} = 0\}$ is $\{E_0\}$. From LaSalle's invariance principle [32], we deduce that E_0 is globally asymptotically stable if $\mathcal{R}_0 \le 1$. ■

When $\mathcal{R}_0 > 1$, we assume that the incidence functions f and g satisfy for each infection equilibrium E_i $(1 \le i \le 4)$, the following hypothesis

$$\begin{aligned}&\left(1 - \frac{f(U,I,V)}{f(U,I_i,V_i)}\right)\left(\frac{f(U,I_i,V_i)}{f(U,I,V)} - \frac{V}{V_i}\right) \le 0,\\ &\left(1 - \frac{f(U_i,I_i,V_i)g(U,I)}{f(U,I_i,V_i)g(U_i,I_i)}\right)\left(\frac{f(U,I_i,V_i)g(U_i,I_i)}{f(U_i,I_i,V_i)g(U,I)} - \frac{I}{I_i}\right) \le 0.\end{aligned} \tag{H_4}$$

Theorem 2.5 *Suppose that $\mathcal{R}_0 > 1$ and (H_4) holds for each E_i.*

(i) *The infection equilibrium without immunity E_1 of model (1) is globally asymptotically stable when $\mathcal{R}_1^W \le 1$ and $\mathcal{R}_1^Z \le 1$.*

(ii) *The infection equilibrium with only humoral immunity E_2 of model (1) is globally asymptotically stable when $\mathcal{R}_1^W > 1$ and $\mathcal{R}_2^Z \le 1$.*

(iii) *The infection equilibrium with only cellular immunity E_3 of model (1) is globally asymptotically stable when $\mathcal{R}_1^Z > 1$ and $\mathcal{R}_3^W \le 1$.*

(iv) *The infection equilibrium with both humoral and cellular immune responses E_4 of model (1) is globally asymptotically stable when $\mathcal{R}_2^Z > 1$ and $\mathcal{R}_3^W > 1$.*

Proof. For **(i)**, we consider the following Lyapunov functional

$$
\begin{aligned}
L_1(t) = U - U_1 - \int_{U_1}^{U} \frac{f(U_1, I_1, V_1)}{f(X, I_1, V_1)} dX + \frac{1}{\eta_1} I_1 \Phi\left(\frac{I}{I_1}\right) \\
+ \frac{f(U_1, I_1, V_1) V_1}{k\eta_2 I_1} V_1 \Phi\left(\frac{V}{V_1}\right) + \frac{qf(U_1, I_1, V_1) V_1}{rk\eta_2 I_1} W + \frac{p}{c\eta_1} Z \\
+ \frac{1}{\eta_1} f(U_1, I_1, V_1) V_1 \int_0^{\infty} f_1(\tau) e^{-\alpha_1 \tau} \int_{t-\tau}^{t} \Phi\left(\frac{f\big(U(\theta), I(\theta), V(\theta)\big) V(\theta)}{f(U_1, I_1, V_1) V_1}\right) d\theta d\tau \\
+ \frac{1}{\eta_1} g(U_1, I_1) I_1 \int_0^{\infty} f_1(\tau) e^{-\alpha_1 \tau} \int_{t-\tau}^{t} \Phi\left(\frac{g\big(U(\theta), I(\theta)\big) I(\theta)}{g(U_1, I_1) I_1}\right) d\theta d\tau \\
+ \frac{1}{\eta_2} f(U_1, I_1, V_1) V_1 \int_0^{\infty} f_2(\tau) e^{-\alpha_2 \tau} \int_{t-\tau}^{t} \Phi\left(\frac{I(\theta)}{I_1}\right) d\theta d\tau ?
\end{aligned}
$$

where $\Phi(\xi) = \xi - 1 - \ln \xi$, $\xi > 0$. By taking the time derivative of L_1 along the solution of model (1) and using $\lambda = dU_1 + f(U_1, I_1, V_1)V_1 + g(U_1, I_1)I_1 = dU_1 + \frac{a}{\eta_1} I_1$ and $k\eta_2 I_1 = \mu V_1$, we get

$$
\begin{aligned}
\frac{dL_1}{dt} = dU_1 \left(1 - \frac{U}{U_1}\right)\left(1 - \frac{f(U_1, I_1, V_1)}{f(U, I_1, V_1)}\right) + \frac{qhf(U_1, I_1, V_1) V_1}{rk\eta_2 I_1} (\mathcal{R}_1^W - 1) W \\
+ \frac{pb}{c\eta_1} (\mathcal{R}_1^Z - 1) Z + f(U_1, I_1, V_1) V_1 \left(- 1 - \frac{V}{V_1} + \frac{f(U, I_1, V_1)}{f(U, I, V)} + \frac{f(U, I, V) V}{f(U, I_1, V_1) V_1}\right) \\
+ g(U_1, I_1) I_1 \left(- 1 - \frac{I}{I_1} + \frac{f(U, I_1, V_1) g(U_1, I_1)}{f(U_1, I_1, V_1) g(U, I)} + \frac{f(U_1, I_1, V_1) g(U, I) I}{f(U, I_1, V_1) g(U_1, I_1) I_1}\right) \\
- \frac{1}{\eta_1} f(U_1, I_1, V_1) V_1 \int_0^{\infty} f_1(\tau) e^{-\alpha_1 \tau} \left[\Phi\left(\frac{f(U_1, I_1, V_1)}{f(U, I_1, V_1)}\right) + \Phi\left(\frac{f(U_\tau, I_\tau, V_\tau) V_\tau I_1}{f(U_1, I_1, V_1) V_1 I}\right) \right. \\
\left. + \Phi\left(\frac{f(U, I_1, V_1)}{f(U, I, V)}\right)\right] d\tau - \frac{1}{\eta_1} g(U_1, I_1) I_1 \int_0^{\infty} f_1(\tau) e^{-\alpha_1 \tau} \left[\Phi\left(\frac{f(U_1, I_1, V_1)}{f(U, I_1, V_1)}\right)\right. \\
\left. + \Phi\left(\frac{g(U_\tau, I_\tau) I_\tau}{g(U_1, I_1) I}\right) + \Phi\left(\frac{f(U, I_1, V_1) g(U_1, I_1)}{f(U_1, I_1, V_1) g(U, I)}\right)\right] d\tau \\
- \frac{1}{\eta_2} f(U_1, I_1, V_1) V_1 \int_0^{\infty} f_2(\tau) e^{-\alpha_2 \tau} \Phi\left(\frac{V_1 I_\tau}{V I_1}\right) d\tau .
\end{aligned}
$$

According to (H_2), we have

$$
\left(1 - \frac{U}{U_i}\right)\left(1 - \frac{f(U_i, I_i, V_i)}{f(U, I_i, V_i)}\right) \leq 0, \quad \text{for i=1,2,3,4.} \tag{13}
$$

By (H_4), we also have

$$
-1 - \frac{V}{V_i} + \frac{f(U, I_i, V_i)}{f(U, I, V)} + \frac{f(U, I, V) V}{f(U, I_i, V_i) V_i} = \left(1 - \frac{f(U, I, V)}{f(U, I_i, V_i)}\right)\left(\frac{f(U, I_i, V_i)}{f(U, I, V)} - \frac{V}{V_i}\right) \leq 0, \tag{14}
$$

and

$$\begin{aligned}&-1-\frac{I}{I_1}+\frac{f(U,I_i,V_i)g(U_i,I_i)}{f(U_i,I_i,V_i)g(U,I)}+\frac{f(U_i,I_i,V_i)g(U,I)I}{f(U,I_i,V_i)g(U_i,I_i)I_i}\\&=\left(1-\frac{f(U_i,I_i,V_i)g(U,I)}{f(U,I_i,V_i)g(T_i,I_i)}\right)\left(\frac{f(U,I_i,V_i)g(U_i,I_i)}{f(U_i,I_i,V_i)g(U,I)}-\frac{I}{I_i}\right)\le 0.\end{aligned}\tag{15}$$

Thus, $\frac{dL_1}{dt}\le 0$ if $\mathcal{R}_1^W\le 1$ and $\mathcal{R}_1^Z\le 1$. Further, we have $\frac{dL_1}{dt}=0$ if and only if $U=U_1$, $I=I_1$, $V=V_1$, $W=0$ and $Z=0$. It follows from LaSalle's invariance principle that E_1 is globally asymptotically stable when $\mathcal{R}_1^W\le 1$ and $\mathcal{R}_1^Z\le 1$.

For **(ii)**, we consider the following Lyapunov functional

$$\begin{aligned}L_2=&U-U_2-\int_{U_2}^{U}\frac{f(U_2,I_2,V_2)}{f(X,I_2,V_2)}dX+\frac{1}{\eta_1}I_2\Phi\left(\frac{I}{I_2}\right)\\&+\frac{f(U_2,I_2,V_2)V_2}{k\eta_2I_2}V_2\Phi\left(\frac{V}{V_2}\right)+\frac{qf(U_2,I_2,V_2)V_2}{rk\eta_2I_2}W_2\Phi\left(\frac{W}{W_2}\right)+\frac{p}{c\eta_1}Z\\&+\frac{1}{\eta_1}f(U_2,I_2,V_2)V_2\int_0^\infty f_1(\tau)e^{-\alpha_1\tau}\int_{t-\tau}^{t}\Phi\left(\frac{f\big(U(\theta),I(\theta),V(\theta)\big)V(\theta)}{f(U_2,I_2,V_2)V_2}\right)d\theta d\tau\\&+\frac{1}{\eta_1}g(U_2,I_2)I_2\int_0^\infty f_1(\tau)e^{-\alpha_1\tau}\int_{t-}^{t}\Phi\left(\frac{g\big(U(\theta),I(\theta)\big)I(\theta)}{g(U_2,I_2)I_2}\right)d\theta d\tau\\&+\frac{1}{\eta_2}f(U_2,I_2,V_2)V_2\int_0^\infty f_2(\tau)e^{-\alpha_2\tau}\int_{t-\tau}^{t}\Phi\left(\frac{I(\theta)}{I_2}\right)d\theta d\tau.\end{aligned}$$

By $\lambda=dU_2+f(T_2,I_2,V_2)V_2+g(U_2,I_2)I_2=dU_2+\frac{a}{\eta_1}I_2$, $V_2=\frac{h}{r}$ and $k\eta_2I_2=\mu V_2+qV_2W_2$, we have

$$\begin{aligned}\frac{dL_2}{dt}=&dU_2\left(1-\frac{U}{U_2}\right)\left(1-\frac{f(U_2,I_2,V_2)}{f(U,I_2,V_2)}\right)+\frac{pb}{c\eta_1}(\mathcal{R}_2^Z-1)Z\\&+f(U_2,I_2,V_2)V_2\left(-1-\frac{V}{V_2}+\frac{f(U,I_2,V_2)}{f(U,I,V)}+\frac{f(U,I,V)V}{f(U,I_2,V_2)V_2}\right)\\&+g(U_2,I_2)I_2\left(-1-\frac{I}{I_2}+\frac{f(U,I_2,V_2)g(U_2,I_2)}{f(U_2,I_2,V_2)g(U,I)}+\frac{f(U_2,I_2,V_2)g(U,I)I}{f(U,I_2,V_2)g(U_2,I_2)I_2}\right)\\&-\frac{1}{\eta_1}f(U_2,I_2,V_2)V_2\int_0^\infty f_1(\tau)e^{-\alpha_1\tau}\left[\Phi\left(\frac{f(U_2,I_2,V_2)}{f(U,I_2,V_2)}\right)+\Phi\left(\frac{f(U_\tau,I_\tau,V_\tau)V_\tau I_2}{f(U_2,I_2,V_2)V_2I}\right)\right.\\&\left.+\Phi\left(\frac{f(U,I_2,V_2)}{f(U,I,V)}\right)\right]d\tau-\frac{1}{\eta_1}g(U_2,I_2)I_2\int_0^\infty f_1(\tau)e^{-\alpha_1\tau}\left[\Phi\left(\frac{f(U_2,I_2,V_2)}{f(U,I_2,V_2)}\right)\right.\\&\left.+\Phi\left(\frac{g(U_\tau,I_\tau)I_\tau}{g(U_1,I_1)I}\right)+\Phi\left(\frac{f(U,I_2,V_2)g(U_2,I_2)}{f(U_2,I_2,V_2)g(U,I)}\right)\right]d\tau\\&-\frac{1}{\eta_2}f(U_2,I_2,V_2)V_2\int_0^\infty f_2(\tau)e^{-\alpha_2\tau}\Phi\left(\frac{V_2I_\tau}{VI_2}\right)d\tau.\end{aligned}$$

Since $\mathcal{R}_2^Z \leq 1$ and by (13)–(15), we have $\frac{dL_2}{dt} \leq 0$ with equality if and only if $U = U_2, I = I_2$ and $V = V_2$. From (1), we have $\frac{dI}{dt} = 0$ and $\frac{dV}{dt} = 0$ which implies $Z = 0$ and $W = W_2$. Hence, the singleton $\{E_2\}$ is the largest invariant subset of $\{(U, I, V, W, Z) | \frac{dL_2}{dt} = 0\}$. From LaSalle's invariance principle, we deduce that E_2 is globally asymptotically stable and we get **(ii)**.

For **(iii)**, we consider the following Lyapunov functional

$$
\begin{aligned}
L_3 = U - U_3 - \int_{U_3}^{U} \frac{f(U_3, I_3, V_3)}{f(X, I_3, V_3)} dX + \frac{1}{\eta_1} I_3 \Phi\left(\frac{I}{I_3}\right) + \frac{f(U_3, I_3, V_3) V_3}{k\eta_2 I_3} V_3 \Phi\left(\frac{V}{V_3}\right) \\
+ \frac{qf(U_3, I_3, V_3) V_3}{rk\eta_2 I_3} W + \frac{p}{c\eta_1} Z_3 \Phi\left(\frac{Z}{Z_3}\right) \\
+ \frac{1}{\eta_1} f(U_3, I_3, V_3) V_3 \int_0^{\infty} f_1(\tau) e^{-\alpha_1 \tau} \int_{t-\tau}^{t} \Phi\left(\frac{f\big(U(\theta), I(\theta), V(\theta)\big) V(\theta)}{f(U_3, I_3, V_3) V_3}\right) d\theta d\tau \\
+ \frac{1}{\eta_1} g(U_3, I_3) I_3 \int_0^{\infty} f_1(\tau) e^{-\alpha_1 \tau} \int_{t-\tau}^{t} \Phi\left(\frac{g\big(U(\theta), I(\theta)\big) I(\theta)}{g(U_3, I_3) I_3}\right) d\theta d\tau \\
+ \frac{1}{\eta_2} f(U_3, I_3, V_3) V_3 \int_0^{\infty} f_2(\tau) e^{-\alpha_2 \tau} \int_{t-\tau}^{t} \Phi\left(\frac{I(\theta)}{I_3}\right) d\theta d\tau.
\end{aligned}
$$

By using $\lambda = dU_3 + f(U_3, I_3, V_3) V_3 + g(U_3, I_3) I_3 = dU_3 + \frac{a}{\eta_1} I_3 + \frac{p}{\eta_1} I_3 Z_3$, $I_3 = \frac{b}{c}$ and $k\eta_2 I_3 = \mu V_3$, we can get

$$
\begin{aligned}
\frac{dL_3}{dt} = dU_3 \left(1 - \frac{U}{U_3}\right)\left(1 - \frac{f(U_3, I_3, V_3)}{f(U, I_3, V_3)}\right) + \frac{qhf(U_3, I_3, V_3) V_3}{rk\eta_2 I_3} (\mathcal{R}_3^W - 1) W \\
+ f(U_3, I_3, V_3) V_3 \left(-1 - \frac{V}{V_3} + \frac{f(U, I_3, V_3)}{f(U, I, V)} + \frac{f(U, I, V) V}{f(U, I_3, V_3) V_3}\right) \\
+ g(U_3, I_3) I_3 \left(-1 - \frac{I}{I_3} + \frac{f(U, I_3, V_3) g(U_3, I_3)}{f(U_3, I_3, V_3) g(U, I)} + \frac{f(U_3, I_3, V_3) g(U, I) I}{f(U, I_3, V_3) g(U_3, I_3) I_3}\right) \\
- \frac{1}{\eta_1} f(U_3, I_3, V_3) V_3 \int_0^{\infty} f_1(\tau) e^{-\alpha_1 \tau} \left[\Phi\left(\frac{f(U_3, I_3, V_3)}{f(U, I_3, V_3)}\right) + \Phi\left(\frac{f(U_\tau, I_\tau, V_\tau) V_\tau I_3}{f(U_3, I_3, V_3) V_3 I}\right) \right. \\
\left. + \Phi\left(\frac{f(U, I_3, V_3)}{f(U, I, V)}\right)\right] d\tau - \frac{1}{\eta_1} g(U_3, I_3) I_3 \int_0^{\infty} f_1(\tau) e^{-\alpha_1 \tau} \left[\Phi\left(\frac{f(U_3, I_3, V_3)}{f(U, I_3, V_3)}\right) \right. \\
\left. + \Phi\left(\frac{g(U_\tau, I_\tau) I_\tau}{g(U_3, I_3) I}\right) + \Phi\left(\frac{f(U, I_3, V_3) g(T_3, I_3)}{f(U_3, I_3, V_3) g(U, I)}\right)\right] d\tau \\
- \frac{1}{\eta_2} f(U_3, I_3, V_3) V_3 \int_0^{\infty} f_2(\tau) e^{-\alpha_2 \tau} \Phi\left(\frac{V_3 I_\tau}{V I_3}\right) d\tau.
\end{aligned}
$$

Thus, $\frac{dL_3}{dt} \leq 0$ with equality if and only if $U = U_3, I = I_3$ and $V = V_3$. Then $\frac{dI}{dt} = 0$ and $\frac{dV}{dt} = 0$ which leads to $Z = Z_3$ and $W = 0$. Therefore, the global asymptotic stability of E_3 is ensured by LaSalle's invariance principle when $\mathcal{R}_1^Z > 1$ and $\mathcal{R}_3^W \leq 1$.

It finally remains to prove **(iv)**. For this, we consider the following Lyapunov functional

$$
\begin{aligned}
L_4 = {} & U - U_4 - \int_{U_4}^{U} \frac{f(U_4, I_4, V_4)}{f(X, I_4, V_4)} dX + \frac{1}{\eta_1} I_4 \Phi\left(\frac{I}{I_4}\right) + \frac{f(U_4, I_4, V_4) V_4}{k\eta_2 I_4} V_4 \Phi\left(\frac{V}{V_4}\right) \\
& + \frac{qf(U_4, I_4, V_4) V_4}{rk\eta_2 I_4} W_4 \Phi\left(\frac{W}{W_4}\right) + \frac{p}{c\eta_1} Z_4 \Phi\left(\frac{Z}{Z_4}\right) \\
& + \frac{1}{\eta_1} f(U_4, I_4, V_4) V_4 \int_0^{\infty} f_1(\tau) e^{-\alpha_1 \tau} \int_{t-\tau}^{t} \Phi\left(\frac{f\big(U(\theta), I(\theta), V(\theta)\big) V(\theta)}{f(U_4, I_4, V_4) V_4}\right) d\theta d\tau \\
& + \frac{1}{\eta_1} g(U_4, I_4) I_4 \int_0^{\infty} f_1(\tau) e^{-\alpha_1 \tau} \int_{t-\tau}^{t} \Phi\left(\frac{g\big(U(\theta), I(\theta)\big) I(\theta)}{g(U_4, I_4) I_4}\right) d\theta d\tau \\
& + \frac{1}{\eta_2} f(U_4, I_4, V_4) V_4 \int_0^{\infty} f_2(\tau) e^{-\alpha_2 \tau} \int_{t-\tau}^{t} \Phi\left(\frac{I(\theta)}{I_4}\right) d\theta d\tau.
\end{aligned}
$$

Since $\lambda = dU_4 + f(U_4, I_4, V_4) V_4 + g(U_4, I_4) I_4 = dU_4 + \frac{a}{\eta_1} I_4 + \frac{p}{\eta_1} I_4 Z_4$, $I_4 = \frac{b}{c}$, $V_4 = \frac{h}{r}$ and $k\eta_2 I_4 = \mu V_4 + q V_4 W_4$, we have

$$
\begin{aligned}
\frac{dL_4}{dt} = {} & dU_3 \left(1 - \frac{U}{U_4}\right)\left(1 - \frac{f(U_4, I_4, V_4)}{f(U, I_4, V_4)}\right) \\
& + f(U_4, I_4, V_4) V_4 \left(- 1 - \frac{V}{V_4} + \frac{f(U, I_4, V_4)}{f(U, I, V)} + \frac{f(U, I, V) V}{f(U, I_4, V_4) V_4}\right) \\
& + g(U_4, I_4) I_4 \left(- 1 - \frac{I}{I_4} + \frac{f(U, I_4, V_4) g(U_4, I_4)}{f(U_4, I_4, V_4) g(U, I)} + \frac{f(U_4, I_4, V_4) g(U, I) I}{f(U, I_4, V_4) g(U_4, I_4) I_4}\right) \\
& - \frac{1}{\eta_1} f(U_4, I_4, V_4) V_4 \int_0^{\infty} f_1(\tau) e^{-\alpha_1 \tau} \left[\Phi\left(\frac{f(U_4, I_4, V_4)}{f(U, I_4, V_4)}\right) + \Phi\left(\frac{f(U_\tau, I_\tau, V_\tau) V_\tau I_4}{f(U_4, I_4, V_4) V_4 I}\right) \right. \\
& \left. + \Phi\left(\frac{f(U, I_4, V_4)}{f(U, I, V)}\right)\right] d\tau - \frac{1}{\eta_1} g(U_4, I_4) I_4 \int_0^{\infty} f_1(\tau) e^{-\alpha_1 \tau} \left[\Phi\left(\frac{f(U_4, I_4, V_4)}{f(U, I_4, V_4)}\right) \right. \\
& \left. + \Phi\left(\frac{g(U_\tau, I_\tau) I_\tau}{g(U_4, I_4) I}\right) + \Phi\left(\frac{f(U, I_4, V_4) g(U_4, I_4)}{f(U_4, I_4, V_4) g(U, I)}\right)\right] d\tau \\
& - \frac{1}{\eta_2} f(U_4, I_4, V_4) V_4 \int_0^{\infty} f_2(\tau) e^{-\alpha_2 \tau} \Phi\left(\frac{V_4 I_\tau}{V I_4}\right) d\tau.
\end{aligned}
$$

Therefore, $\frac{dL_4}{dt} \leq 0$ with equality holds if and only if $U = U_4, I = I_4$ and $V = V_4$. Let

$$
\Gamma = \left\{ (U, I, V, W, Z) | \frac{dL_4}{dt} = 0 \right\}.
$$

The second and third equations of (1) lead to

$$\dot{I} = \eta_1[f(U_4, I_4, V_4)V_4 + g(U_4, I_4)I_4] - aI_4 - pI_4Z = 0,$$
$$\dot{V} = k\eta_2 I_4 - \mu V_4 - qV_4W = 0,$$

which implies that $Z = Z_4$ and $W = W_4$. So, the largest compact invariant set in Γ is the singleton $\{E_4\}$. Consequently, E_4 is globally asymptotically stable. This ends the proof of Theorem 2.5. ■

From (12) and Theorem 2.5, it is not hard to get the following important remark.

Remark 2.6 Suppose that $\mathcal{R}_0 > 1$ and (H_4) holds for each E_i.

1. If $\max(\mathcal{R}_1^W, \mathcal{R}_1^Z) \leq 1$, then model (1) converges to E_1 without immunity.
2. If $\max(\mathcal{R}_1^W, \mathcal{R}_1^Z) > 1$, two cases occur:

(i) When $\max(\mathcal{R}_1^W, \mathcal{R}_1^Z) = \mathcal{R}_1^Z$, the cellular immunity is dominant and model (1) converges to E_3 without humoral immunity.
(ii) When $\max(\mathcal{R}_1^W, \mathcal{R}_1^Z) = \mathcal{R}_1^W$, the humoral immunity is dominant and model (1) converges to E_2 if $\mathcal{R}_2^Z \leq 1$, or to E_4 if $\mathcal{R}_2^Z > 1$.

As in [28], we can define the over-domination of cellular immunity when $\mathcal{R}_2^Z > 1$ and $\mathcal{R}_3^W < 1$ and the over-domination of humoral immunity when $\mathcal{R}_2^Z > 1$ and $\mathcal{R}_3^W > 1$.

3 Analysis of the Generalized PDE Model

In this section, we analyze the dynamical behaviors of the generalized PDE model (2) under initial conditions

$$\begin{aligned} &U(x,\theta) = \phi_1(x,\theta) \geq 0, \quad I(x,\theta) = \phi_2(x,\theta) \geq 0, \quad V(x,\theta) = \phi_3(x,\theta) \geq 0, \\ &W(x,\theta) = \phi_4(x,\theta) \geq 0, \quad Z(x,\theta) = \phi_5(x,\theta) \geq 0, \quad (x,\theta) \in \bar{\Omega} \times (-\infty, 0], \end{aligned} \tag{16}$$

and Neumann boundary condition

$$\frac{\partial V}{\partial \nu} = 0 \text{ on } \partial\Omega \times (0, +\infty), \tag{17}$$

where Ω is a bounded domain in $\mathbb{R}^n$ with smooth boundary $\partial\Omega$, and $\dfrac{\partial}{\partial \nu}$ is the outward normal derivative on the boundary $\partial\Omega$.

Obviously, $E_0(U_0, 0, 0, 0, 0)$ is also an equilibrium point of model (2). So, we have the following result.

Theorem 3.1 *The infection-free equilibrium E_0 of model (2) is globally asymptotically stable if $\mathcal{R}_0 \leq 1$.*

Proof. By applying the method presented in [33], we construct the Lyapunov functional for model (2) at E_0 as follows

$$\begin{aligned}\mathcal{L}_0 = \int_\Omega \Big\{ &\frac{1}{\eta_1} I(x,t) + \frac{\beta_1 U_0}{\mu} V(x,t) + \frac{qf(U_0,0,0)}{r\mu} W(x,t) + \frac{p}{c\eta_1} Z(x,t) \\ &+ \frac{1}{\eta_1} \int_0^\infty f_1(\tau) e^{-\alpha_1 \tau} \int_{t-\tau}^t \big[f\big(U(x,\theta), I(x,\theta), V(x,\theta)\big) V(x,\theta) \\ &+ g\big(U(\theta), I(x,\theta)\big) I(x,\theta) \big] d\theta d\tau + \frac{kf(U_0,0,0)}{\mu} \int_0^\infty f_2(\tau) e^{-\alpha_2 \tau} \int_{t-\tau}^t I(x,\theta) d\theta d\tau \Big\} dx.\end{aligned}$$

Denote $\Lambda = \Lambda(x,t)$ and $\Lambda_\tau = \Lambda(x, t-\tau)$ for any $\Lambda \in \{U, I, V, W, Z\}$. Then,

$$\begin{aligned}\frac{d\mathcal{L}_0}{dt} = \int_\Omega \Big\{ &\Big(f(U,I,V) - f(U_0,0,0) \Big) V + \frac{a}{\eta_1} I \Big(\frac{k\eta_1\eta_2 f(U_0,0,0) + \mu\eta_1 g(U,I)}{a\mu} - 1 \Big) \\ &- \frac{qhf(U_0,0,0)}{r\mu} W - \frac{pb}{c\eta_1} Z \Big\} dx.\end{aligned}$$

Thus,

$$\frac{d\mathcal{L}_0}{dt} \le \int_\Omega \Big\{ \frac{a}{\eta_1} (\mathcal{R}_0 - 1) I - \frac{qhf(U_0,0,0)}{r\mu} W - \frac{pb}{c\eta_1} Z \Big\} dx.$$

Since $\mathcal{R}_0 \le 1$, we have $\dfrac{d\mathcal{L}_0}{dt} \le 0$. Further, the largest compact invariant set in $\{(U, I, V, W, Z) | \dfrac{d\mathcal{L}_0}{dt} = 0\}$ is the singleton $\{E_0\}$. This completes the proof. ■

When $\mathcal{R}_0 > 1$, the points E_1, E_2, E_3 and E_4 are also the steady states of model (2). Similarly to above and based on the Lyapunov functionals L_1, L_2, L_3 and L_4 for DDE model (1), we easily get the following result.

Theorem 3.2 *Suppose that $\mathcal{R}_0 > 1$ and (H_4) holds for each E_i.*

(i) *The infection equilibrium without immunity E_1 of model (2) is globally asymptotically stable when $\mathcal{R}_1^W \le 1$ and $\mathcal{R}_1^Z \le 1$.*
(ii) *The infection equilibrium with only humoral immunity E_2 of model (2) is globally asymptotically stable when $\mathcal{R}_1^W > 1$ and $\mathcal{R}_2^Z \le 1$.*
(iii) *The infection equilibrium with only cellular immunity E_3 of model (2) is globally asymptotically stable when $\mathcal{R}_1^Z > 1$ and $\mathcal{R}_3^W \le 1$.*
(iv) *The infection equilibrium with both humoral and cellular immune responses E_4 of model (2) is globally asymptotically stable when $\mathcal{R}_2^Z > 1$ and $\mathcal{R}_3^W > 1$.*

4 Application

In this section, we apply our main analytical results to the following HIV infection model:

$$\begin{cases} \dfrac{\partial U}{\partial t} = \lambda - dU(x,t) - \dfrac{\beta_1 U(x,t)V(x,t)}{1+\epsilon_1 V(x,t)} - \dfrac{\beta_2 U(x,t)I(x,t)}{1+\epsilon_2 I(x,t)}, \\ \dfrac{\partial I}{\partial t} = \int_0^\infty f_1(\tau)e^{-\alpha_1\tau}[\dfrac{\beta_1 U(x,t-\tau)V(x,t-\tau)}{1+\epsilon_1 V(x,t-\tau)} + \dfrac{\beta_2 U(x,t-\tau)I(x,t-\tau)}{1+\epsilon_2 I(x,t-\tau)}]d\tau \\ \quad -aI(x,t) - pI(x,t)Z(x,t), \\ \dfrac{\partial V}{\partial t} = d_V \triangle V + k\int_0^\infty f_2(\tau)e^{-\alpha_2\tau}I(x,t-\tau)d\tau - \mu V(x,t) - qV(x,t)W(x,t), \\ \dfrac{\partial W}{\partial t} = rV(x,t)W(x,t) - hW(x,t), \\ \dfrac{\partial Z}{\partial t} = cI(x,t)Z(x,t) - bZ(x,t), \end{cases} \tag{18}$$

where $\epsilon_1,\ \epsilon_2 \geq 0$ are constants that measure the saturation effect. The rates of virus-to-cell infection and cell-to-cell transmission are, respectively, denoted by β_1 and β_2. The other parameters and state variables have the same biological meanings as in models (1) and (2). This HIV infection model is a special case of (2), it suffices to take $f(U,I,V) = \dfrac{\beta_1 U}{1+\epsilon_1 V}$ and $g(U,I) = \dfrac{\beta_2 U}{1+\epsilon_2 I}$. Also, we consider model (18) with initial conditions

$$\begin{aligned} &U(x,\theta) = \phi_1(x,\theta) \geq 0, \quad I(x,\theta) = \phi_2(x,\theta) \geq 0, \quad V(x,\theta) = \phi_3(x,\theta) \geq 0, \\ &W(x,\theta) = \phi_4(x,\theta) \geq 0, \quad Z(x,\theta) = \phi_5(x,\theta) \geq 0, \quad (x,\theta) \in \bar{\Omega} \times (-\infty, 0], \end{aligned} \tag{19}$$

and homogeneous Neumann boundary condition

$$\frac{\partial V}{\partial \nu} = 0 \ \text{ on } \ \partial\Omega \times (0, +\infty). \tag{20}$$

It is obvious to verify that the hypotheses (H_0)-(H_3) are satisfied. On the other hand, we have

$$\left(1 - \frac{f(U,I,V)}{f(U,I_i,V_i)}\right)\left(\frac{f(U,I_i,V_i)}{f(U,I,V)} - \frac{V}{V_i}\right) = \frac{-\epsilon_1(V-V_i)^2}{V_i(1+\epsilon_1 V_i)(1+\epsilon_1 V)} \leq 0,$$

$$\left(1 - \frac{f(U_i,I_i,V_i)g(U,I)}{f(U,I_i,V_i)g(U_i,I_i)}\right)\left(\frac{f(U,I_i,V_i)g(U_i,I_i)}{f(U_i,I_i,V_i)g(U,I)} - \frac{I}{I_i}\right) = \frac{-\epsilon_2(I-I_i)^2}{I_i(1+\epsilon_2 I_i)(1+\epsilon_2 I)} \leq 0.$$

Therefore, the hypothesis (H_4) is satisfied. By applying Theorems 3.1 and 3.2, we get the following result.

Corollary 4.1

1. *If $\mathcal{R}_0 \leq 1$, then the infection-free equilibrium E_0 of model (18) is globally asymptotically stable.*
2. *If $\mathcal{R}_0 > 1$, then model (18) has four infection equilibria that are:*

(i) *the infection equilibrium without immunity E_1 that is globally asymptotically stable if $\mathcal{R}_1^W \leq 1$ and $\mathcal{R}_1^Z \leq 1$;*
(ii) *the infection equilibrium with only humoral immunity E_2 that is globally asymptotically stable if $\mathcal{R}_1^W > 1$ and $\mathcal{R}_2^Z \leq 1$;*
(iii) *the infection equilibrium with only cellular immunity E_3 that is globally asymptotically stable if $\mathcal{R}_1^Z > 1$ and $\mathcal{R}_3^W \leq 1$;*
(iv) *the infection equilibrium with both humoral and cellular immune responses E_4 that is globally asymptotically stable if $\mathcal{R}_2^Z > 1$ and $\mathcal{R}_3^W > 1$.*

5 Conclusions

In this chapter, we have developed two immunological models, one with DDEs and the other with PDEs in order to describe the interactions between host cells, virus and adaptive immune system presented by CTL cells and antibodies. In both models, the classical virus-to-cell infection and the direct cell-to-cell transmission are modeled by two general incidence functions. Under some hypotheses on these incidence functions, dynamical analysis of both models shows that the global stability of equilibria is completely characterized by five threshold parameters called the reproduction numbers for viral infection $\mathcal{R}_0$, for humoral immunity $\mathcal{R}_1^W$, for cellular immunity $\mathcal{R}_1^Z$, for cellular immunity in competition $\mathcal{R}_2^Z$ and for humoral immunity in competition $\mathcal{R}_3^W$. More accurately, we have proved that when $\mathcal{R}_0 \leq 1$ the infection-free equilibrium is globally asymptotically stable which biologically means that the virus is cleared up. When $\mathcal{R}_0 > 1$, the virus persists in the host and four steady states appear, the first without immunity which is globally asymptotically stable if $\mathcal{R}_1^W \leq 1$ and $\mathcal{R}_1^Z \leq 1$; the second with only humoral immunity which is globally asymptotically stable if $\mathcal{R}_1^W > 1$ and $\mathcal{R}_2^Z \leq 1$; the third with only cellular immunity which is globally asymptotically stable if $\mathcal{R}_1^Z > 1$ and $\mathcal{R}_3^W \leq 1$; and the fourth with both cellular and humoral immune responses which is globally asymptotically stable if $\mathcal{R}_2^Z > 1$ and $\mathcal{R}_3^W > 1$. Therefore, the activation of one or both branches of adaptive immunity is unable to eradicate the virus in vivo, but plays a crucial role in the reduction of viral load and infected cells. This last biological result can obviously be obtained by a simple comparison between the components of viral load and infected cells before and after the activation of the immunity. Based on Remark 2.6, we also deduce other biological findings that are the over-domination of cellular immunity leads to the absence of the humoral immunity, while the over-domination of the humoral immunity leads to the persistence of viral infection with a weak response of both types of adaptive immunity. On the other hand, the PDE models and corresponding results presented in the more recent works [34, 35] are improved and extended.

References

1. D. Wodarz, Hepatitis C virus dynamics and pathology: The role of CTL and antibody responses. J. Gen. Virol. **84**, 1743–1750 (2003)
2. N. Yousfi, K. Hattaf, M. Rachik, Analysis of a HCV model with CTL and antibody responses. Appl. Math. Sci. **3**(57), 2835–2845 (2009)
3. N. Yousfi, K. Hattaf, A. Tridane, Modeling the adaptative immune response in HBV infection. J. Math. Biol. **63**(5), 933–957 (2011)
4. K. Hattaf, N. Yousfi, A class of delayed viral infection models with general incidence rate and adaptive immune response. Int. J. Dyn. Control. **4**, 254–265 (2016)
5. Y. Yan, W. Wang, Global stability of a five-dimensional model with immune responses and delay. Discret. Contin. Dyn. Syst.-B **17**(1), 401–416 (2012)
6. Y. Su, D. Sun, L. Zhao, Global analysis of a humoral and cellular immunity virus dynamics model with the Beddington-DeAngelis incidence rate. Math. Methods Appl. Sci. **38**(14), 2984–2993 (2015)
7. X. Wang, S. Liu, A class of delayed viral models with saturation infection rate and immune response. Math. Methods Appl. Sci. **36**(2), 125–142 (2013)
8. Y. Zhao, Z. Xu, Global dynamics for a delayed hepatitis C virus infection model. Electron. J. Differ. Equ.S **2014**(132), 1–18 (2014)
9. K. Hattaf, M. Khabouze, N. Yousfi, Dynamics of a generalized viral infection model with adaptive immune response. Int. J. Dyn. Control. **3**, 253–261 (2015)
10. M. Sourisseau, N. Sol-Foulon, F. Porrot, F. Blanchet, O. Schwartz, Inefficient human immunodeficiency virus replication in mobile lymphocytes. J. Virol. **81**, 1000–1012 (2007)
11. H. Sato, J. Orenstein, D. Dimitrov, M. Martin, Cell-to-cell spread of HIV-1 occurs within minutes and may not involve the participation of virus particles. Virology **186**, 712–724 (1992)
12. J.M. Carr, H. Hocking, P. Li, C.J. Burrell, Rapid and efficient cell-to-cell transmission of human immunodeficiency virus infection from monocyte-derived macrophages to peripheral blood lymphocytes. Virology **265**, 319–329 (1999)
13. M.A. Nowak, C.R.M. Bangham, Population dynamics of immune responses to persistent viruses. Science **272**, 74–79 (1996)
14. X. Wang, Y. Tao, X. Song, Global stability of a virus dynamics model with Beddington-DeAngelis incidence rate and CTL immune response. Nonlinear Dyn. **66**(4), 825–830 (2011)
15. K. Hattaf, N. Yousfi, A. Tridane, Global stability analysis of a generalized virus dynamics model with the immune response. Can. Appl. Math. Q. **20**(4), 499–518 (2012)
16. Y. Li, R. Xu, Z. Li, S. Mao, Global dynamics of a delayed HIV-1 infection model with CTL immune response. Discret. Dyn. Nat. Soc. **2011**, 1–13 (2011)
17. X. Li, S. Fu, Global stability of a virus dynamics model with intracellular delay and CTL immune response. Math. Methods Appl. Sci. **38**(3), 420–430 (2015)
18. J. Wang, M. Guo, X. Liu, Z. Zhao, Threshold dynamics of HIV-1 virus model with cell-to-cell transmission, cell-mediated immune responses and distributed delay. Appl. Math. Comput. **291**, 149–161 (2016)
19. A.M. Elaiw, A.A. Raezah, K. Hattaf, Stability of HIV-1 infection with saturated virus-target and infected-target incidences and CTL immune response. Int. J. Biomath. **10**(5), 1–29 (2017)
20. A. Murase, T. Sasaki, T. Kajiwara, Stability analysis of pathogen-immune interaction dynamics. J. Math. Biol. **51**, 247–267 (2005)
21. S.F. Wang, D.Y. Zou, Global stability of in-host viral models with humoral immunity and intracellular delays. Appl. Math. Model. **36**, 1313–1322 (2012)
22. T. Wang, Z. Hu, F. Liao, Stability and Hopf bifurcation for a virus infection model with delayed humoral immunity response. J. Math. Anal. Appl. **411**, 63–74 (2014)
23. T. Wang, ZHuF Liao, W. Ma, Global stability analysis for delayed virus infection model with general incidence rate and humoral immunity. Math. Comput. Simul. **89**, 13–22 (2013)
24. H. Miao, Z. Teng, C. Kang, A. Muhammadhaji, Stability analysis of a virus infection model with humoral immunity response and two time delays. Math. Methods Appl. Sci. **39**(12), 3434–3449 (2016)

25. X. Wang, S. Liu, A class of delayed viral models with saturation infection rate and immune response. Math. Methods Appl. Sci. **36**, 125–142 (2013)
26. J. Lin, R. Xu, X. Tian, Threshold dynamics of an HIV-1 virus model with both virus-to-cell and cell-to-cell transmissions, intracellular delay, and humoral immunity. Appl. Math. Comput. **315**, 516–530 (2017)
27. A.M. Elaiw, A.A. Raezah, A.S. Alofi, Effect of humoral immunity on HIV-1 dynamics with virus-to-target and infected-to-target infections. AIP Adv. **6**, 085204 (2016)
28. K. Hattaf, N. Yousfi, Modeling the adaptive immunity and both modes of transmission in HIV infection. Computation **6**(2), 1–18 (2018)
29. J.K. Hale, J. Kato, Phase space for retarded equations with infinite delay. Funkc. Ekvacioj **21**, 11–41 (1978)
30. Y. Hino, S. Murakami, T. Naito, Functional Differential Equations with Infinite Delay, In: Lecture Notes in Math, vol. 1473, (Springer, Berlin, 1991)
31. Y. Kuang, *Delay Differential Equations with Applications in Population Dynamics* (Academic Press, San Diego, 1993)
32. J.K. Hale, S.M. Verduyn Lunel, in *Introduction to Functional Differential Equations* (Springer, New York, 1993)
33. K. Hattaf, N. Yousfi, Global stability for reaction-diffusion equations in biology. Comput. Math. Appl. **66**, 1488–1497 (2013)
34. K. Hattaf, N. Yousfi, *Spatiotemporal Dynamics of a Class of Models Describing Infectious Diseases, Mathematics Applied to Engineering, Modelling, and Social Issues* (Springer, Cham, 2019), pp. 529–549
35. K. Hattaf, Spatiotemporal dynamics of a generalized viral infection model with distributed delays and CTL immune response. Computation **7**(2), 1–16 (2019)

Modeling the Stochastic Dynamics of Influenza Epidemics with Vaccination Control, and the Maximum Likelihood Estimation of Model Parameters

Divine Wanduku, C. Newman, O. Jegede and B. Oluyede

1 Introduction

Influenza ranks among the top ten most important diseases in the United States of America (USA). In fact, the *Center for Disease Control* (CDC) estimates that from 2010–2011 to 2013–2014, influenza-associated deaths in the USA ranged from a low of 12,000 (during 2011–2012) to a high of 56,000 (during 2012–2013) annually [1]. Globally, the *World Health Organization* (WHO) estimates that seasonal influenza results in approximately 290–650 thousand deaths each year from just influenza-related respiratory diseases alone [2, 3]. These statistics necessitate more investigation and understanding about the disease, in order to control or ameliorate the burdens of the disease.

For hundreds of years, influenza, more commonly know as the flu, has plagued mankind. The flu is caused by a virus and spreads from person to person through direct contact and through particulates in the air. Symptoms include fever, cough, sore throat, runny or stuffy nose, muscle or body aches, headaches, fatigue, and even vomiting and diarrhea [4].

There are several strains of the influenza virus, all causing similar symptoms with varying severity. Influenza viruses are generally categorized into four subgroups: A, B, C, and D. Human influenza A and B viruses are the most common and cause seasonal epidemics of disease almost every winter in the USA. The emergence of a new and very different influenza A virus to infect people can cause an influenza pandemic, for instance, the recent "swine flu" (officially called H1N1) and "bird flu" (H5N1) (cf. [5]).

An individual infected with the flu can spread it to others up to about 6 ft away through droplets from their mouth from coughing, sneezing, or merely talking. Once an individual has been infected with the flu virus, it usually takes about 2 days

D. Wanduku (✉) · C. Newman · O. Jegede · B. Oluyede
Department of Mathematical Sciences, Georgia Southern University,
65 Georgia Ave., Room 3042, Statesboro, GA 30460, USA
e-mail: dwanduku@georgiasouthern.edu

H. Dutta (ed.), *Mathematical Modelling in Health, Social and Applied Sciences*, Forum for Interdisciplinary Mathematics, https://doi.org/10.1007/978-981-15-2286-4_2

incubation period before symptoms start to show. From the onset of symptoms, it can take 7–10 days for an individual to recover. In general, adults who are infected with the influenza virus are capable of spreading it to others a day before symptoms show up as well as throughout the duration of the illness (cf. [6]).

In an attempt to slow the spread of seasonal influenza, the CDC recommends annual influenza vaccination for people 6 months of age and older. The most common vaccination is the seasonal flu injection, standard-dose trivalent shot (IIV3), and there are several other options available. One setback is that the flu virus constantly mutates and vaccination against one strain may not protect against other strains. Once vaccinated, it may take up to two weeks before the vaccine is completely effective (cf. [7]).

Various types of mathematical compartmental models have been used to investigate the dynamics of infectious diseases of humans [8–13] . For instance, in some studies [13, 14], deterministic models for influenza are presented. Malaria epidemic models [9, 15] have also been studied. Stochastic models with white noise perturbations for influenza have also been studied [10–12]. Some papers [16, 17] have presented mathematical models with perfect lifelong immunity conferred via vaccination, where all individuals vaccinated can no longer be infected. Other papers [14] study imperfect vaccination in influenza epidemics, where vaccinated individuals obtain partial immunity resulting in lower disease transition rates than the unvaccinated population.

The compartmental mathematical epidemic dynamic models are largely classified as SVIS, SVIRS, SIS, SIR, SIRS, SEIRS, SEIR, etc. epidemic dynamic models depending on the compartments of the disease states directly involved in the general disease dynamics [8–13]. For instance, SIR model represents transitions from the susceptible state to the infectious and then to the removed state. An SEIR model adds the incubation period via an exposed class E to the previous SIR model. SVIR models incorporate the vaccination class V and represent the dynamics of diseases that grant permanent immunity after recovery from disease, for example, influenza where naturally acquired immunity against a strain of the virus is conferred after viral infection [8, 18–20].

Stochastic epidemic dynamic models more realistically represent epidemic dynamic processes because they include the randomness which inevitably occurs during a disease outbreak, owing to the presence of constant random environmental fluctuations in the disease dynamics. For stochastic epidemic models, the state of the system over time, which usually represents the number of people susceptible (S), vaccinated (V), infected but not infectious (E), infected and infectious (I), or removed with natural immunity (R), is a stochastic process. Furthermore, the stochastic process for the disease dynamics can be a continuous-time–continuous-state, continuous-state–discrete-time, or discrete-time and discrete-state stochastic process. The choice on which type of stochastic process to use to represent the dynamics of the disease depends on the finiteness or infiniteness of the epidemiological features of the disease that are represented mathematically. Some exam-

ples of continuous-time–continuous-state stochastic epidemiological studies include [10–12, 21] and discrete-time–discrete-state models include [8, 18, 22, 23].

In our study, we derive a SVIR discrete-time and discrete-state stochastic chain model, wherein temporary artificial immunity through vaccination is considered, in addition to the lifelong naturally acquired immunity for influenza in a closed community of human beings.

Chain binomial models are an important class of Markov chain models, and they have been used to represent and study infectious disease epidemics over time [8, 22, 24–27]. This family of stochastic models represent the disease dynamics as a random process, where transition between some states such as from susceptible to infectious or from vaccinated to susceptible is characterized by binomial transition probabilities.

Some pioneer chain binomial models for infectious diseases include Greenwood and Reed–Frost models [24, 25]. Many other studies such as [8, 22, 23] have extended and expanded on the ideas of Greenwood and Reed–Frost, creating more realistic epidemic dynamic models. Greenwood [24] in the 1931 study presented a SIS chain binomial chain model for the spread of diseases in human populations, where a breakdown of the population into successive generations indexed by $t = 0, 1, 2, \ldots$ is used. Furthermore, the susceptible individuals are infected in a given generation and are only capable of infecting others within that generation. And after which, they remain infected, but isolated from subsequent disease spread. Greenwood assumed that a susceptible person meets only one infectious person at any instance and interaction with the infectious person leads to transmission of disease with probability p.

Reed–Frost [25] built upon most of the ideas of the Greenwood model and presented a SIR epidemic model. Moreover, Reed–Frost made a more realistic (i.e., more conforming to real-life scenario) assumption that a susceptible person at any instance t has a chance to interact independently with any of the infectious individuals present at that instance. Thus, the probability of the susceptible person getting infection at any instance t, from at least one of the y infectious individuals the susceptible person contacts in that instance, is given by $p(y) = 1 - (1 - p)^y$.

The previous Greenwood and Reed–Frost models consider generations of infections, and the infectious individuals no longer participate in subsequent transmission of disease to susceptible persons. This assumption is suitable for generalizations of disease dynamics, where the disease suddenly outbreaks in a given time generation, dies out, and reoccur in another time generation.

Tuckwell and Williams [8] utilized some ideas from Reed–Frost [25] and proposed a more realistic SIR epidemic dynamic model. In their model, infection takes place over discrete-time intervals, and the infectious population at any instance t comprises of all infectious persons at different ages $k = 0, 1, 2, \ldots, R - 2$ of their infectiousness over the constant duration of the infectious period R. The age k represents how long an individual has been infectious since initial infection from the susceptible state. In their model, the total infectious individuals at any instance participates in the disease transmission process, and it is assumed that at the end of the infectious period R, all infectious persons are treated, fully recovered, and join the removed class R.

Tuckwell and Williams [8] also assume that the ith individual in the population at any instant t encounter a fixed number of people (family, office mates, employees) denoted n_i, and also a random number of people $M_i(t)$, where the random variables $M_i(t)$ are mutually independent and independent of the state of the population. This assumption leads to a more realistic random process description for the total number of people the ith individual encounters at any instance $N_i(t) = n_i + M_i(t), t \geq 0$. Moreover, the probability of getting infection at any instance becomes dependent on the number of infectious people the ith susceptible individual meets among the $N_i(t)$ people.

Using ideas from Tuckwell–Williams [8], we propose a susceptible, vaccinated, infected, and removed (SVIR) epidemic discrete-time and discrete-state family of chain binomial models for influenza. Treatment in the form of vaccination is available, where the vaccine confers temporary effective artificial immunity against the disease, but ultimately wanes over time. In line with [8], the infectious population involves in the disease transmission process overall generations of the population over time and overall ages of infectiousness. However, unlike [8], the vaccination class is incorporated, and the total infectious and vaccinated populations are characterized based on the ages of infection and vaccination since initial infection and vaccination, over the constant and finite infectious and effective vaccination periods, respectively. Moreover, as far as we know, no other discrete-time, discrete-state chain binomial study in the line of thinking of Tuckwell–Williams [8] with multiple time delays and with the vaccination class exists in the literature. This study provides a suitable and more realistic extension of the chain binomial models: Greenwood, Reed–Frost, and Tuckwell–William models above.

The rest of this paper is organized as follows: In Sect. 2, we present an adequate description of the SVIR human population over discrete time. In Sect. 3, we derive the transition probabilities of the SVIR Markov chain family of models, and present special cases of the general SVIR Markov chain model. In Sect. 5, we present the method of maximum likelihood estimation to find important parameters of the SVIR chain models. In Sect. 6, we estimate some important epidemiological parameters for the influenza epidemic model. Finally, in Sect. 7, we present numerical examples for the SVIR influenza model and make general concluding remarks.

2 Description of the SVIR Influenza Epidemic Process

In this section, we describe and represent the influenza epidemic in the human population. We present the procedure to discretize time and decompose the human population into the different states of the disease involved in the influenza epidemic

We consider (1) a human population of size n living in a closed natural environment over a period of time consistent with the duration of an epidemic outbreak, where it can be assumed that human movement into and out of the population is negligible or nonexistent. In addition, the population is relatively safe, and no natural deaths occur during the duration of the epidemic outbreak. Also, it is assumed no births occur

during the duration of the epidemic or very strong measures are taken medically to protect all newborns, such that they can be ignored from the effective diseased population.

Furthermore, it is assumed (2) that a particular strain of an infectious disease such as a flu or other similar respiratory infectious diseases breaks out in the closed population, and the disease causes major suffering in the human being, but with no mortal consequences due to disease-related causes. The scenario of influenza epidemic driven by multiple strains of the virus is not considered. The readers are referred to [28] for examples of influenza studies involving multiple strains of the virus.

It is also assumed (3) that the infectious disease has a vaccine which provides temporary effective artificial immunity against the strain of the infectious agent (strain of the influenza virus) that lasts over a constant immunity period T_1. At the end of the immunity period T_1, the vaccinated person becomes susceptible again to the particular strain of the disease. It is assumed that individuals are vaccinated only once throughout the season of the influenza epidemic. The disease also confers natural immunity after recovery from the infection. The naturally acquired immunity also provides effective natural protection against the strain of the disease agent, that lasts over a period of time longer than the duration of the epidemic in the population. Unlike the temporary artificial immunity period T_1, it is assumed that the naturally acquired immunity period is constant infinite.

It is also assumed (4) that the strain of the infectious agent has strong infectious abilities, moreover, the human population is homogenous in susceptibility to the strain of the virus, such that all susceptible individuals who contract the infectious agent exhibit symptoms of illness after a relatively small time interval (roughly between 2 and 4 days [6]), and become infectious to other susceptible persons. Thus, using one-time unit for the model to be more than the incubation period, for instance, 1 week, the incubation period of the disease is considered relatively small (i.e., by the time scale for the influenza epidemic model presented in this study, the incubation period is small enough such that it cannot form a distinct disease class), and consequently, the exposure class can be ignored. Note that the general susceptible population consisting of (i.) those who have never been vaccinated or infected and (ii.) those who were previously vaccinated and have lost their artificial immunity are vulnerable to infection of the strain of the virus.

It is further assumed (5) that the infectious period of all individuals who have contracted the disease is constant and finite, and it is denoted T_2. At the end of that period T_2, it is assumed that the immune system of the infected individual has established sufficient natural immunity against the particular strain of the disease, which lasts longer than the overall duration of the epidemic, and as a result individuals with naturally acquired immunity are removed from the epidemic process.

From the above description, (6) the human population of size n is subdivided into four major human subclasses, namely susceptible (S), vaccinated (V), infectious (I), and removed (R). The susceptible class (S) does not have the disease, but are vulnerable to infection from the infectious class (I). A portion of the susceptible individuals is vaccinated artificially against the disease, and after a small time lapse

until the vaccine takes effect, the individuals become the vaccinated class (V). The vaccinated class (V) can no longer contract the disease during the effective artificially acquired temporary immunity period T_1 of the vaccine (however, over the small time lapse until the vaccine is effective, the vaccinated person can still be infected by influenza). At the end of the period T_1, the vaccine wanes, and the vaccinated individuals become susceptible again to the disease. When the infectious class (I) recovers from the disease at the end of the constant infectious period of time T_2, the individuals acquire natural immunity against the disease that can be considered to be constant and infinite. The removed class denoted R consists of all individuals with naturally acquired immunity. It is further assumed that the naturally acquired immunity is very effective such that the removed class never becomes susceptible again to the disease over the overall duration of the disease.

(7) The general susceptible population $S(t)$ at any time $t = 0, 1, 2, 3, \ldots$ over the duration of the epidemic can be further broken down into two subclasses $\underbrace{S}(t)$ and $\overbrace{S}(t)$, where $\underbrace{S}(t)$ represents all susceptible individuals present at time t, who have never contracted the disease nor been vaccinated, and $\overbrace{S}(t)$ represents the number of susceptible individuals present at time t, who were previously vaccinated, and have lost the artificial immunity against the disease after the effective period T_1. That is,

$$S(t) = \underbrace{S}(t) + \overbrace{S}(t). \tag{2.1}$$

Note that over the duration of the epidemic, when it is assumed that all individuals are vaccinated only once against that strain of influenza virus, regardless whether the vaccine wanes over time, it follows that, only the class $\underbrace{S}(t)$ will be liable to be vaccinated. When vaccination occurs multiple times, then all susceptible individuals $S(t)$ will be liable to be vaccinated at any time t. Also, at any time t, the general susceptible class $S(t)$ is vulnerable to infection. A compartmental framework exhibiting the transitions between the different states in the population is shown in Fig. 1.

In the following, we characterize the different disease subclasses, namely susceptible, vaccinated, infectious, and removed individuals over discrete-time intervals of unit length, for example, days, weeks, months, etc. The description of the discretization of time is presented in the following.

Definition 2.1 Time discretization process:

The different disease subclasses, namely susceptible, vaccinated, infectious, and removal individuals, shall be counted over discrete-time intervals of unit length. That is, over the time subintervals $(t_0, t_0 + 0] \equiv t_0$, $(t_0, t_0 + 1]$, $(t_0 + 1, t_0 + 2]$, $(t_0 + 2, t_0 + 3], \ldots, (t_0 + (t - 2), t_0 + (t - 1)]$, $(t_0 + (t - 1), t_0 + t]$, where $t_0 \geq 0$ is any nonnegative real number. Furthermore, the number of individuals in any subclass of the population at any time t are taken to be the number of people in that state present in the subinterval of time $(t_0 + (t - 1), t_0 + t]$, counted up to and including the point $t_0 = t$, where t is a positive integer, that is, $t = 0, 1, 2, \ldots$. Moreover, all events that occur at the initial time $t = 0$ refer explicitly to every event that occurred at

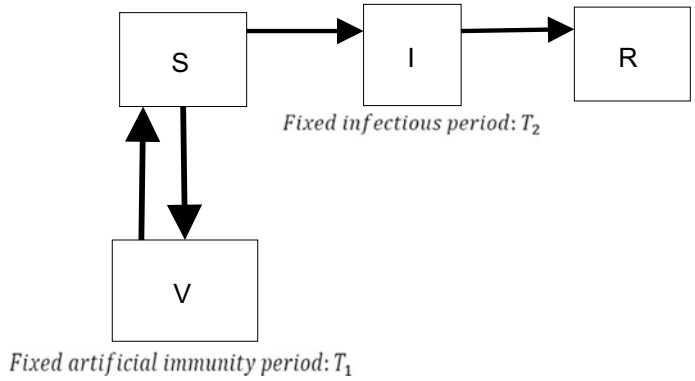

Fig. 1 Shows the framework of transitions between the different disease states (S,V,I,R) in the population during the outbreak of the disease

the initial point t_0, or equivalently, in the initial subinterval $(t_0, t_0 + 0]$, which forms an initial state for the epidemic. In addition, when $t_0 = 0$, then the initial interval $(t_0, t_0 + 0]$ reduces to the point $t = t_0 = 0$.

For example, the number of susceptible people present at time $t = 2$, denoted $S(2)$, refer to the number of people in the susceptible state S, who are present in the subinterval of time $(t_0 + 1, t_0 + 2]$. More generally, $S(t)$ is the number of susceptible people present in the subinterval $(t_0 + (t - 1), t_0 + t]$.

Another discrete measure of time denoted by $k = 0, 1, 2, \ldots, t$, represents how long individuals in the different disease states S, V, I, and R have been in the given states since their initial conversion into the states. We let $S_k(t)$, $V_k(t)$, $I_k(t)$, and $R_k(t)$, $\forall k = 0, 1, 2, 3, \ldots, t$ denote the number of susceptible, vaccinated, infectious, and removal individuals, respectively, present at time t, who have been in their different states for k discrete-time units, where $k = 0, 1, 2, 3, \ldots, t$. Note that according to the description of the time measure k, then $S_0(t)$, $V_0(t)$, $I_0(t)$ and $R_0(t)$ signify the number of people present at time t, who have just become susceptible, vaccinated, infectious, and removed at time t.

For example, for $t = 5, k = 2$, $S_2(5)$ denotes the number of susceptible people present at the end of week 5 (i.e., in $(t_0 + 4, t_0 + 5]$), who were previously vaccinated, and lost their artificial immunity 2 weeks ago. Furthermore, $S_5(5)$ denotes the number of susceptible people present at the end of week 5, who have never been vaccinated or infected. Also, $V_2(5)$ denotes the number of vaccinated people present at the end of week 5, who were vaccinated two weeks ago.

The decomposition of the susceptible population is presented in the following.

Definition 2.2 Decomposition and Aggregation of the Susceptible Population:

We decompose the susceptible population over the discrete times $t = 0, 1, 2, \ldots$ into subcategories based on (1) when a person first becomes susceptible to the disease, given that the person was previously vaccinated against the disease, and the artificial

vaccine has worn out after the effective vaccination period T_1, and (2) how long a person has remained susceptible to the disease, since the initial time $t = 0$.

For $t = 0, 1, 2, \ldots$, let $S_k(t), \forall k = 0, 1, 2, 3, \ldots, t$ denote the number of susceptible individuals present at time t, who have been susceptible for k discrete-time units, where $k = 0, 1, 2, 3, \ldots, t$. That is, the number of susceptible individuals $S(t)$ present at time $t = 0, 1, 2, \ldots$ can be written in the two equivalent ways

$$\begin{aligned} S(t) = S_0(t) + S_1(t) + S_2(t) + S_3(t) + S_4(t) + \cdots \\ + S_{t-3}(t) + S_{t-2}(t) + S_{t-1}(t) + S_t(t), \end{aligned} \tag{2.2}$$

where from (2.1),

$$\begin{aligned} \underbrace{S}(t) = S_0(t) + S_1(t) + S_2(t) + S_3(t) + S_4(t) + \cdots \\ + S_{t-3}(t) + S_{t-2}(t) + S_{t-1}(t), \end{aligned} \tag{2.3}$$

and

$$\overbrace{S}(t) = S_t(t). \tag{2.4}$$

From (2.3) to (2.4), since infection and vaccination occur over every time $t = 0, 1, 2, \ldots$, it follows that $S_k(t) \leq S_0(t-k), \forall k = 0, 1, 2, \ldots, t$, and $S_k(k) \geq S_{k+1}(k+1), \forall k = 0, 1, 2, \ldots, t-1$.

Furthermore, for any time t at least as large as the maximum of the artificial immunity and the infectious periods T_1 and T_2, respectively, that is, for $t \geq \max(T_1, T_2)$ it is easy to see that the relationship between susceptibility and vaccination is given as follows:

$$\begin{aligned} S_k(t) \leq S_0(t-k) &= V_{T_1}(t-k) = V_{T_1+k}(t) \\ &= V_0(t-(T_1+k)) \geq 0, k = 0, 1, \ldots, t - T_1. \end{aligned} \tag{2.5}$$

It follows from (2.2) to (2.5) that the total susceptible population $S(t) = \underbrace{S}(t) + \overbrace{S}(t)$ at any time $t \geq T_1$, or $t \geq \max(T_1, T_2)$, can be written as follows:

$$\overbrace{S}(t) = S_0(t) + S_1(t) + S_2(t) + \cdots + S_{t-T_1}(t) \quad \textit{and} \quad \underbrace{S}(t) = S_t(t). \tag{2.6}$$

Also, for any time $t < T_1$, or $t \leq \min(T_1, T_2)$ then

$$\overbrace{S(t)} = 0, \quad \textit{and} \quad \underbrace{S(t)} = S_t(t). \tag{2.7}$$

Also, under the assumption that the population is closed and there is no migration of susceptible, vaccinated, infectious, and removal individuals, then it follows from above that $S(0) > 0$, $S_0(0) \geq 0$, and $S_k(0) = 0, \forall k \geq 1$.

To illustrate the above with an example, suppose influenza breaks out in the population at time $t = 0$, and the artificial immunity period is $T_1 = 5$ weeks, then the susceptible population at time $t = 2$ (2nd week after the outbreak) is given by (2.7) as follows

$$\overbrace{S(2)} = 0, \underbrace{S(2)} = S_2(2), \quad \textit{and} \quad S(2) = \underbrace{S(2)} = S_2(2). \tag{2.8}$$

The susceptible population at time $t = 8$ (8th week after the outbreak) is given by (2.6) as follows

$$\overbrace{S}(8) = S_0(8) + S_1(8) + S_2(8) + S_3(8) \quad \textit{and} \quad \underbrace{S}(8) = S_8(8). \tag{2.9}$$

The decomposition of the vaccinated class $V(t)$ at time t is presented in the following.

Definition 2.3 Decomposition and Aggregation of the Vaccinated Population:

We also decompose the vaccinated population class into subcategories based on how long individuals have been vaccinated before returning to the susceptible class of the population, whenever the artificial immunity wanes. As with the previous definition, we decompose the vaccinated population over the discrete times $t = 0, 1, 2, \ldots$ into subcategories based on (1) when a person first becomes vaccinated against the disease, and (2) how long a person has been vaccinated against the disease, since the initial time $t = 0$, or simply how long a person has been vaccinated before the artificial immunity wears off completely after the period of effectiveness of the vaccines T_1. For $t = 0, 1, 2, \ldots$, let $V_k(t), \forall k = 0, 1, 2, 3, \ldots, t$ denote the number of vaccinated individuals present at time t, who have been vaccinated for k discrete-time units, where $k = 0, 1, 2, 3, \ldots, t$. Letting $V(t)$ be the number vaccinated people present at time t, then it can be seen that for any $t = 0, 1, 2, \ldots$, then V(t) can be written in two different equivalent ways as follows: For $t < T_1$ or $t < \min(T_1, T_2)$,

$$\begin{aligned} V(t) = {} & V_0(t) + V_1(t) + V_2(t) + V_3(t) + V_4(t) + \cdots + V_{t-3}(t) \\ & + V_{t-2}(t) + V_{t-1}(t) + V_t(t) \end{aligned} \tag{2.10}$$

and since $V_0(t - k) = V_k(t), k = 0, 1, \ldots, t$, then $V(t)$ is equivalently expressed as follows:

$$\begin{aligned} V(t) = {} & V_0(t) + V_0(t-1) + V_0(t-2) + V_0(t-3) \\ & + V_0(t-4) + \cdots + V_0(3) + V_0(2) + V_0(1) + V_0(0). \end{aligned} \tag{2.11}$$

Also for any time t at least as large as T_1, or at least as large as the maximum of the artificial immunity and the infectious periods T_1 and T_2, respectively, that is, for $t \geq T_1$, or $t \geq \max(T_1, T_2)$ it is easy to see that some of the subclasses $V_k(t)$'s in in

the expression (2.10) are no longer in the vaccinated state, but have been converted into susceptible individuals. That is,

$$\begin{aligned} V_0(t-T_1) &= V_{T_1}(t) = S_0(t), \\ V_0(t-(T_1+k)) &= V_{T_1+k}(t) = V_{T_1}(t-k) \\ &= S_0(t-k) \geq S_k(t), \forall k = 0, 1, \ldots, t-T_1 \end{aligned} \tag{2.12}$$

Therefore, for $t \geq T_1$, or $t \geq \max(T_1, T_2)$, the number of people in the vaccinated class at time t is given by

$$V(t) = V_0(t) + V_1(t) + V_2(t) + \cdots + V_{T_1-1}(t)$$

or equivalently

$$V(t) = V_0(t) + V_0(t-1) + V_0(t-2) + \cdots + V_0(t-(T_1-1)). \tag{2.13}$$

The decomposition of the infectious class $I(t)$ at time t is presented in the following.

Definition 2.4 Decomposition and Aggregation of the Infectious Population:

We also decompose the infectious population class into subcategories based on how long individuals have been infectious before transitioning into the removed class of the population. As with the previous definition, we decompose the infectious population over the discrete times $t = 0, 1, 2, \ldots$ into subcategories based on (1) when a person first becomes infectious and (2) how long a person has been infectious, since the initial time $t = 0$, and until the infectious period T_2 is lapsed, where it is assumed that all infectious individuals are identified, treated, and fully recovered over the constant finite time period T_2.

For $t = 0, 1, 2, \ldots$, let $I_k(t), \forall k = 0, 1, 2, 3, \ldots, t$ denote the number of infectious individuals present at time t, who have been infectious for k discrete-time units, where $k = 0, 1, 2, 3, \ldots, t$. It follows that for any $t = 0, 1, 2, \ldots$, the number of infectious persons present at time t, denoted $I(t)$, is written as follows: For $t < T_2$ or $t < \min(T_1, T_2)$,

$$I(t) = I_0(t) + I_1(t) + I_2(t) + I_3(t) + I_4(t) + \cdots + I_{t-3}(t) + I_{t-2}(t) + I_{t-1}(t) + I_t(t),$$

or (2.14)

$$\begin{aligned} I(t) = {} & I_0(t) + I_0(t-1) + I_0(t-2) + I_0(t-3) + I_0(t-4) + \cdots \\ & + I_0(3) + I_0(2) + I_0(1) + I_0(0), \end{aligned} \tag{2.15}$$

where $I_k(t) = I_0(t-k), \forall k = 0, 1, \ldots t$.

In addition, for any time t at least as large as the infectious period T_2, or at least as large as the maximum of the artificial immunity and the infectious periods T_1 and T_2 respectively, that is, for $t \geq T_2$, or $t \geq \max(T_1, T_2)$, it is easy to see that some of the subcategories in expression (2.14) are no longer in the infectious class, but have

been converted into the removed state. That is, for $t \geq T_2$, or $t \geq \max(T_1, T_2)$, it is easy to see that

$$I(t) = I_0(t) + I_1(t) + I_2(t) + \cdots + I_{T_2-1}(t),$$

or

$$I(t) = I_0(t) + I_0(t-1) + I_0(t-2) + \cdots + I_0(t-(T_2-1)),$$

and the following infectious classes are removed:

$$\begin{aligned} I_0(t-T_1) &= I_{T_2}(t) = R_0(t), \\ I_0(t-(T_2+k)) &= I_{T_2+k}(t) = I_{T_2}(t-k) = R_0(t-k) = R_k(t), \forall k = 0, 1, 2, \ldots, t-T_2 \end{aligned} \tag{2.16}$$

The decomposition of the removed class $R(t)$ at time t is presented in the following:

Definition 2.5 Decomposition and Aggregation of the Removed Population:

Finally, we decompose the removed population class into subcategories based on how long individuals have been removed from the infectious state. As with the previous definition, we decompose the removed population over the discrete times $t = 0, 1, 2, \cdots$ into subcategories based on (1) when a person first becomes removed, and (2) how long a person has been removed from the infectious state since the initial time $t = 0$ of disease outbreak, or simply how long the person has been removed from the time when the person transitioned from the infectious state to the removal state. For $t = 0, 1, 2, \ldots$, let $R_k(t), \forall k = 0, 1, 2, 3, \ldots, t$ denote the number of removed individuals present at time t, who have been removed for k discrete-time units, where $k = 0, 1, 2, 3, \ldots, t$. It follows that for any time $t = 0, 1, 2, \ldots$, the number of removed individuals at time t denoted $R(t)$, can be written in two different equivalent ways as follows: For $t < T_2$ or $t < \min(T_1, T_2)$,

$$R(t) = R_t(t) = R_0(0) = R(0) \geq 0. \tag{2.17}$$

That is, $R(t)$ in (2.17) is the removed population at the initial time.

Furthermore, for any time t at least as large as the infectious period T_2, or at least as large as the maximum of the artificial immunity and the infectious periods T_1 and T_2 respectively, that is, for $t \geq T_2$ or $t \geq \max(T_1, T_2)$,

$$\begin{aligned} R(t) = {} & R_0(t) + R_1(t) + R_2(t) + R_3(t) + R_4(t) + \cdots + R_{t-3}(t) + R_{t-2}(t) + \\ & R_{t-1}(t) + R_t(t) \end{aligned}$$

or equivalently,

$$\begin{aligned} R(t) = {} & R_0(t) + R_0(t-1) + R_0(t-2) + R_0(t-3) + R_0(t-4) + \cdots + \\ & R_0(3) + R_0(2) + R_0(1) + R_0(0), \end{aligned} \tag{2.18}$$

where $R_k(t) = R_0(t-k), \forall k = 0, 1, \ldots t$.

It is also easy to see that some of the subcategories in (2.18) are equivalent to some infectious subclasses as shown below:

$$\begin{aligned} &R_0(t) = I_{T_2}(t) = I_0(t - T_2), \\ &R_k(t) = R_0(t-k) = I_{T_2}(t-k) = I_{T_2+k}(t) = I_0(t-(T_2+k)), k = 0, 1, \ldots, t - T_2. \end{aligned} \tag{2.19}$$

Therefore, for $t \geq T_2$ or $t \geq \max(T_1, T_2)$, the number of removed individuals at time t, $R(t)$ is given by:

$$\begin{aligned} R(t) &= R_0(t) + R_1(t) + R_2(t) + \cdots + R_{t-T_2}(t) \\ &\text{or} \\ R(t) &= R_0(t) + R_0(t-1) + R_0(t-2) + \cdots + R_0(t-(t-T_2)). \\ &= R_0(t) + R_0(t-1) + R_0(t-2) + \cdots + R_0(T_2). \end{aligned} \tag{2.20}$$

Definition 2.6 Decomposition and Aggregation of the total human population:

It can be seen from Definitions 2.2–2.5 that the total human population of size n can be written as follows:
For all $t \in \mathbb{Z}_+ = 0, 1, 2, 3, \ldots$

$$n = S(t) + V(t) + I(t) + R(t), \tag{2.21}$$

or

$$n = \underbrace{S(t)} + \overbrace{S(t)} + V(t) + I(t) + R(t). \tag{2.22}$$

It is easy to see from (2.21) that since the total population is fixed at any time $t \geq 0$, then given the values of the states $S(t)$, $V(t)$ and $I(t)$, the value of the state $R(t)$ can be determined using the formula in (2.21). Furthermore, since all individuals are vaccinated only once in the population; therefore, at any time t, only the susceptible class $\underbrace{S(t)} = S_t(t)$ is liable to be vaccinated. In addition, note that at all movement from the vaccinated class V to the susceptible class $\overbrace{S(t)}$ are deterministic by translation over the artificial immunity period T_1. Therefore, the most relevant partition for the susceptible class $S(t)$ is $S(t) = \underbrace{S(t)} + \overbrace{S(t)}$. Also, due to connectivity between the susceptible state component $\underbrace{S(t)} = S_t(t)$ and the susceptible state component $\overbrace{S(t)}$, via the vaccinated class $V(t)$, it is relevant to represent all microscopic sub-vaccinated classes $V_k(t), k = 0, \ldots, T_1$. Similarly, to explain connectivity between $S(t)$ and $R(t)$, it is relevant to represent all the microscopic sub-infectious classes $I_k(t), k = 0, \ldots, T_2$. Thus, using the above information, the following decompositions and vectors will be sufficient to characterize the influenza epidemic at any time t.

So for $T_1 \leq t < T_2$, the vector

$$B(t) = (S(t) = \underbrace{S(t)} + \overbrace{S(t)}, V_0(t), V_1(t), \ldots, V_{T_1-1}(t), I_0(t), I_1(t), \ldots, I_t(t))$$

is sufficient to define all states of the process. Also,

$$n = \underbrace{S(t)} + \sum_{i=0}^{t-T_1} S_i(t) + \sum_{i=0}^{T_1-1} V_i(t) + \sum_{i=0}^{t} I_i(t) + R(t), \tag{2.23}$$

where $R_t(t) = R(0) \geq 0$.

For $T_2 \leq t < T_1$, the vector

$$B(t) = (S(t) = \underbrace{S(t)}, V_0(t), V_1(t), \ldots, V_t(t), I_0(t), I_1(t), \ldots, I_{T_2-1}(t))$$

is sufficient to define all states of the process. Also,

$$n = \underbrace{S(t)} + \sum_{i=0}^{t} V_i(t) + \sum_{i=0}^{T_2-1} I_i(t) + \sum_{i=0}^{t-T_2} R_i(t). \tag{2.24}$$

Also, for $t \leq \min(T_1, T_2)$, the vector

$$B(t) = (S(t), V_0(t), V_1(t), \ldots, V_t(t), I_0(t), I_1(t), \ldots, I_t(t))$$

is sufficient to define all states of the process. Also,

$$n = \sum_{i=0}^{t} S_i(t) + \sum_{i=0}^{t} V_i(t) + \sum_{i=0}^{t} I_i(t) + R_t(t), \tag{2.25}$$

where $R_t(t) = R(0) = 0$.

In addition, for $t \geq \max(T_1, T_2)$, the vector

$$B(t) = (S(t) = \underbrace{S(t)} + \overbrace{S(t)}, V_0(t), V_1(t), \ldots, V_{T_1-1}, I_0(t), I_1(t), \ldots, I_{T_2-1}(t))$$

is sufficient to define all states of the process. Also,

$$n = \underbrace{S(t)} + \sum_{i=0}^{t-T_1} S_i(t) + \sum_{i=0}^{T_1-1} V_i(t) + \sum_{i=0}^{T_2-1} I_i(t) + \sum_{i=0}^{t-T_2} R_i(t). \tag{2.26}$$

3 Derivation of the SVIR Influenza Markov Chain Model and Transition Probabilities

In this section, we derive the SVIR chain-binomial epidemic dynamic model for the influenza epidemic. The epidemic model presented is an extension of the studies by Tuckwell and Williams [8], Greenwood [24], and Ajelli et al. [29]. That is, we derive a random process that characterizes the dynamics of influenza in the human population structured over time as described above and derive the general formula for the transition probabilities of the Markov chain.

Let $(\Omega, \mathfrak{F}, \mathbb{P})$ be a complete probability space. Define the following nonnegative integer valued random vector measurable function:

$$B : \mathbb{Z}_+ \times \Omega \to \mathbb{Z}_+^{T_1+T_2+1}, \tag{3.1}$$

where for each $t \in \mathbb{Z}_+$, and $t \geq \max\{T_1, T_2\}$, the random vector B is given by

$$B(t) = (S(t), V_0(t), V_1(t), \ldots, V_{T_1-1}(t), I_0(t), I_1(t), \ldots, I_{T_2-1}(t)) \in \mathbb{Z}_+^{T_1+T_2+1}. \tag{3.2}$$

Also, for each $t \in \mathbb{Z}_+$, an observed vector value $b(t)$ for the random vector $B(t)$ is defined as follows:

$$b(t) = (x_t, y_{0_t}, y_{1_t}, y_{2_t}, \ldots, y_{(T_1-1)_t}, z_{0_t}, z_{1_t}, \ldots, z_{(T_2-1)_t}) \in \mathbb{Z}_+^{T_1+T_2+1}. \tag{3.3}$$

Note that for each $t \in \mathbb{Z}_+$, the observed values $x_t, y_{0_t}, y_{1_t}, y_{2_t}, \ldots, y_{(T_1-1)_t}, z_{0_t}, z_{1_t}, \ldots, z_{(T_2-1)_t}$ are nonnegative integers. Furthermore,

$$B(t) = b(t)$$

if and only if

$$\begin{aligned} &S(t) = x_t, \quad V_0(t) = y_{0_t}, \quad V_1(t) = y_{1_t}, \ldots, V_{T_1-1}(t) = y_{(T_1-1)_t}, \\ &I_0(t) = z_{0_t}, \ldots, I_{T_2-1}(t) = z_{(T_2-1)_t}. \end{aligned} \tag{3.4}$$

The random process $\{B(t), t = 1, 2, 3, \ldots\}$ describes the evolution of the influenza epidemic in the $SVIR$ population characterized above.

Furthermore, for $t < \min\{T_1, T_2\}$,

$$B(t) = (S(t), V_0(t), V_1(t), V_2(t) \ldots, V_t(t), I_0(t), I_1(t), \ldots, I_t(t)) \tag{3.5}$$

is sufficient to define all the states of the process.

For $T_1 \leq t < T_2$

$$B(t) = (S(t) = \underbrace{S(t)} + \overbrace{S(t)}, V_0(t), V_1(t), \ldots, V_{T_1-1}(t), I_0(t), I_1(t), \ldots, I_t(t)) \tag{3.6}$$

is sufficient to define all the states of the process.

For $T_2 \leq t < T_1$

$$B(t) = (S(t) = \underbrace{S(t)}, V_0(t), V_1(t), \ldots, V_t(t), I_0(t), I_1(t), \ldots, I_{T_2-1}(t)) \tag{3.7}$$

is sufficient to define all states of the process.

And for $t \geq \max\{T_1, T_2\}$

$$B(t) = (S(t) = \underbrace{S(t)} + \overbrace{S(t)}, V_0(t), V_1(t), \ldots, V_{T_1-1}(t), I_0(t), I_1(t), \ldots, I_{T_2-1}(t)) \tag{3.8}$$

is sufficient to define all states of the process.

The SVIR model given by random process $\{B(t), t = 1, 2, 3, \ldots\}$ suitably describes influenza epidemics for the following reasons. (1) Influenza epidemics are seasonal epidemics, exhibiting timescales that can be approximated with small discrete-time intervals. Moreover, the sizes of closed populations that experience influenza outbreaks are often relatively small. These properties make discrete-time and discrete-state (DTDS) random processes such as $\{B(t), t = 1, 2, 3, \ldots\}$ more suitable to model influenza epidemics. See [30] for more properties of DTDS stochastic epidemic models. (2) During influenza epidemics, vaccination is an integral part of disease control. Also, as earlier remarked in the introduction of this chapter, the incubation period of influenza is relatively short compared to the periods of infectiousness and artificial immunity T_2 and T_1, respectively. Therefore, considering units of time, for instance, weekly defined in Definition 2.1, the incubation period of approximately 2 days for influenza [6] can be ignored. Thus, the SVIR epidemic model $\{B(t), t = 1, 2, 3, \ldots\}$ sufficiently describes the evolution of influenza over time, in the susceptible, vaccinated, and infectious states of the population.

It should be noted from (3.5) to (3.8) that the random process $\{B(t) : t \geq 0\}$ takes different simplifications for different subintervals of the time interval, $t \in [0, \infty)$, relative to the magnitude of the delays T_1, T_2 in the system. In addition, the most interesting features of influenza dynamics, such as the outbreak turning into an epidemic, and persistence of the disease occur when $t \geq \max\{T_1, T_2\}$.

We make the following additional assumptions about the influenza epidemic. We assume that the influenza epidemic in this scenario is caused by a new viral strain that is sufficiently persistent, and the vaccine against the influenza viral strain, despite the fact that it is available and relatively effective, it confers relatively shorter-term protection compared to the duration of the influenza season. Moreover, the period of infectiousness is also relatively shorter compared to the duration of the epidemic in the population. These assumptions suggest that at time $t \geq \max\{T_1, T_2\}$, the disease is still persistent in the population. Thus, we present the general form of the transition

probability of the random process $\{B(t) : t \geq 0\}$ in the case where $t \geq \max\{T_1, T_2\}$. In the following theorem, we show that the random process $\{B(t), t = 1, 2, 3, \dots\}$ is a Markov chain.

Theorem 3.1 *For $t \geq \max\{T_1, T_2\}$, the random process $\{B(t), t = 1, 2, 3, \dots\}$, where the $(T_1 + T_2 + 1)$ nonnegative integer value random vector function*

$$B(t) = (S(t), V_0(t), V_1(t), \dots, V_{T_2-1}(t), I_0(t), I_1(t), \dots, I_{T_2-1}(t)), \forall t = 0, 1, \dots,$$

defines a Markov chain for all $t = 0, 1, 2, 3, \dots$. Furthermore, the transition probabilities are completely specified by the conditional distribution of the states V_0 and I_0. That is,

$$\begin{aligned} P(B(t+1) = b(t+1)|B(t) = b(t)) &= P(V_0(t+1) \\ &= y_{0_{t+1}}, I_0(t+1) = z_{0_{t+1}}|B(t) = b(t)), \end{aligned} \tag{3.9}$$

where the terms $S(t+1) = x_{t+1}$, $V_0(t+1) = y_{0_{t+1}}$, $I_0(t+1) = z_{0_{t+1}}$, and $S(t) = x_t$ are related as follows

$$y_{0_{t+1}} = x_t - x_{t+1} - z_{0_{t+1}}. \tag{3.10}$$

That is,

1. *If $S(t+1) = x_{t+1} = 0$, then*

$$\begin{aligned} P(B(t+1) &= b(t+1)|B(t) = b(t)) \\ &= P(V_0(t+1) = y_{0_{t+1}}, I_0(t+1) = x_t - y_{0_{t+1}}|B(t) = b(t)), \\ &= P(V_0(t+1) = x_t - z_{0_{t+1}}, I_0(t+1) = z_{0_{t+1}}|B(t) = b(t)), \end{aligned} \tag{3.11}$$

2. *If $S(t+1) = x_{t+1} = x_t$, then*

$$\begin{aligned} P(B(t+1) &= b(t+1)|B(t) = b(t)) \\ &= P(V_0(t+1) = 0, I_0(t+1) = 0|B(t) = b(t)), \end{aligned} \tag{3.12}$$

3. *If $S(t+1) = x_{t+1} \in (0, x_t)$, then*

$$\begin{aligned} P(B(t+1) &= b(t+1)|B(t) = b(t)) \\ &= P(V_0(t+1) = x_t - x_{t+1} - z_{0_{t+1}}, I_0(t+1) = z_{0_{t+1}}|B(t) = b(t)), \\ &= P(V_0(t+1) = y_{0_{t+1}}, I_0(t+1) = x_t - x_{t+1} - z_{0_{t+1}}|B(t) = b(t)). \end{aligned} \tag{3.13}$$

Proof As mentioned earlier, we show that $\{B(t) : t \geq 0\}$ is a Markov chain without loss of generality for $t \geq \max(T_1, T_2)$. Moreover, we assume further without loss of generality that $T_1 \geq T_2$. Indeed, for most influenza epidemics where vaccination is available, it is expected that the artificial immunity from the vaccine protects against the viral attack over the whole season of the influenza epidemic, which is typically longer on average than the length of time until infected people recover from the disease. Thus, $\max(T_1, T_2) = T_1$.

To show that $\{B(t), t \in \mathbb{Z}_+\}$ is a Markov chain, it suffices to show that the Markov property holds in $\{B(t), t \in \mathbb{Z}_+\}$. That is, we show that for all t $\geq \max(T_1, T_2) = T_1 \geq T_2$,

$$\begin{aligned} P(B(t+1) &= b(t+1)|B(t) = b(t), B(t-1) \\ &= b(t-1), \ldots, B(1) = b(1), B(0) = b(0)) \\ &= P(B(t+1) = b(t+1)|B(t) = b(t)), \end{aligned} \tag{3.14}$$

where $B(t)$ and $b(t)$ are defined in (3.2) and (3.3). Indeed, from (3.8),

$$\begin{aligned} P(B(t+1) &= b(t+1)|B(t) = b(t), B(t-1) \\ &= b(t-1), \ldots, B(1) = b(1), B(0) = b(0)) \\ &= P(S(t+1) = x_{(t+1)}, V_0(t+1) \\ &= y_{0_{t+1}}, \ldots, V_{(T_1-1)}(t+1) = y_{(T_1-1)_{t+1}}, \\ &\quad I_0(t+1) = z_{0_{t+1}}, \ldots, I_{(T_2-1)}(t+1) \\ &\quad = z_{(T_2-1)_{(t+1)}}|B(t) = b(t), \ldots, B(0) = b(0)) \\ &\equiv RHS. \end{aligned} \tag{3.15}$$

Observe that at time $t+1$, $S(t+1)$ is expressed as follows:

$$S(t+1) = S(t) - V_0(t+1) - I_0(t+1), \quad \forall t \geq \max(T_1, T_2). \tag{3.16}$$

The right-hand side (RHS) of (3.15) can be expressed explicitly as follows:

$$\begin{aligned} RHS \equiv\ & P(S_{t+1}(t+1) = x_{t+1}, V_0(t+1) = y_{0_{t+1}}, V_1(t+1) = y_{1_{t+1}}, V_2(t+1) = y_{2_{t+1}}, \ldots \\ & V_{T_1-1}(t+1) = y_{T_1-1_{t+1}}, I_0(t+1) = z_{0_{t+1}}, I_1(t+1) = z_{1_{t+1}}, I_2(t+1) = z_{2_{t+1}}, \ldots \\ & I_{t_2-1}(t+1) = z_{t_2-1_{t+1}} | \underbrace{S_t(t)} = x_t, V_0(t) = y_{0_t}, V_1(t) = y_{1_t}, V_2(t) = y_{2_t}, \ldots \\ & V_{T_1-1}(t) = y_{T_1-1_t}, I_0(t) = z_{0_t}, I_1(t) = z_{1_t}, I_2(t) = z_{2_t}, \ldots, I_{t_2-1}(t) = z_{t_2-1_t}, \\ & B(t-1) = b(t-1), B(t-2) = b(t-2), \ldots, B(1) = b(1), B(0) = b(0)). \end{aligned} \tag{3.17}$$

By applying (3.16)–(3.17), it is easy to see that (3.17) reduces to

$$
\begin{aligned}
&RHS\\
&\equiv P(V_0(t+1) = y_{0_{t+1}} = x_t - x_{t+1} - z_{0_{t+1}}, V_1(t+1) = y_{0_t}, V_2(t+1) = y_{1_t}, \dots\\
&V_{(T_1-1)}(t+1) = y_{(T_1-2)_t}, I_0(t+1) = z_{0_{t+1}}, I_1(t+1) = z_{0_t},\\
&I_2(t+1) = z_{1_t}, \dots, I_{(t_2-1)}(t+1) = z_{(t_2-2)_t} | S_t(t) = x_t,\\
&V_0(t) = y_{0_t}, V_1(t) = y_{1_t}, V_2(t) = y_{2_t}, \dots V_{(T_1-1)}(t) = y_{(T_1-1)_t},\\
&I_0(t) = z_{0_t}, I_1(t) = z_{1_t}, I_2(t) = z_{2_t}, \dots, I_{t_2-1}(t) = z_{(t_2-1)_t},\\
&B(t-1) = b(t-1), B(t-2) = b(t-2), \dots, B(1) = b(1), B(0) = b(0)).
\end{aligned}
\tag{3.18}
$$

Since most of the terms in the argument of the conditional probability in (3.18) are already given as the conditions of the probability, and $V_0(t+1)$ and $I_0(t+1)$ have no relationship with $B(t-1), B(t-2), \dots, B(1)$, and $B(0)$, the Markov property in (3.14) follows immediately. Moreover, (3.18) further reduces to:

$$
\begin{aligned}
RHS \equiv\ & P(V_0(t+1) = y_{0_{t+1}} = x_t - x_{t+1} - z_{0_{t+1}}, I_0(t+1) = z_{0_{t+1}} | S(t) = x_t, V_0(t) = y_{0_t},\\
& V_1(t) = y_{1_t}, \dots, V_{T_1-1}(t) = y_{(T_1-1)_t}, I_0(t) = z_{0_t},\\
& I_1(t) = z_{1_t}, \dots, I_{(T_2-1)}(t) = z_{(T_2-1)_t}),
\end{aligned}
\tag{3.19}
$$

or to

$$
\begin{aligned}
RHS \equiv\ & P(V_0(t+1) = y_{0_{t+1}}, I_0(t+1) = z_{0_{t+1}} = x_t - x_{t+1} - y_{0_{t+1}} | S(t) = x_t, V_0(t) = v_{0_t},\\
& V_1(t) = y_{1_t}, \dots, V_{T_1-1}(t) = y_{(T_1-1)_t}, I_0(t) = z_{0_t},\\
& I_1(t) = z_{1_t}, \dots, I_{(T_2-1)}(t) = z_{(T_2-1)_t}).
\end{aligned}
\tag{3.20}
$$

Thus, the second part (3.9) is proved.

Remark 3.1 Observe Theorem 3.1[1.] for $S(t+1) = x_{t+1} = 0$ signifies that at the $t+1$ time step, all susceptible individuals x_t at the previous time step t, are either vaccinated or infected by the virus. Theorem 3.1[2.] for $S(t+1) = x_{t+1} = x_t$ signifies that no infection or vaccination occurs at the $t+1$ time step, and Theorem 3.1[3.] for $S(t+1) = x_{t+1} \in (0, x_t)$ signifies that either $y_{0_{t+1}}$ number of people are vaccinated, $x_t - x_{t+1} - y_{0_{t+1}}$ are infected, and x_{t+1} remain susceptible at time $t+1$, or $z_{0_{t+1}}$ number of people are infected, $x_t - x_{t+1} - z_{0_{t+1}}$ are vaccinated, and x_{t+1} remain susceptible at time $t+1$. Thus, the transition probabilities (3.11)–(3.13) represent tri-variate distributions for $S(t+1)$, V_0 and I_0.

In reality, the relationship between the events of getting vaccinated and getting infected exhibit various mathematical forms determined by the properties of the particular disease scenario. That is, the joint conditional distributions of the random variables $V_0(t)$ and $I_0(t)$, for any time $t = 0, 1, \dots$, can be expressed in various forms depending on the disease scenario.

For instance, in more organized societies, the decision to be vaccinated, in some cases, is not influenced by the outbreak of influenza, since influenza seasons are predictable and periodic vaccination against influenza is encouraged. In other disease scenarios especially when the influenza outbreak is unpredictable, more people tend to get vaccinated whenever the influenza epidemic breaks out, and more influenza cases have been reported. Also, in other influenza scenarios, the vaccine may not be sufficiently strong to prevent infection, but mainly to reduce the severity of infection. These scenarios can also create independence between vaccination and infection. One of such special influenza disease scenarios is described in the next section.

4 Special SVIR Models

As remarked in Theorem 3.1, the transition probabilities of the chain $\{B(t), t = 0, 1, 2, \dots\}$ are completely defined by the joint conditional distribution of the discrete random variables $S(t+1)$, V_0 and I_0. In fact, the general discrete tri-variate distribution in (3.9) defines a family of trinomial distributions, since a susceptible individual at any instant has three possible outcomes in the next time step, namely getting infected, or getting vaccinated, or remaining susceptible. Furthermore, there are several different ways to characterize the explicit form of the discrete trinomial distribution in (3.9), which are used to specify the transition probabilities for the chain. Thus, the stochastic process $\{B(t), t = 0, 1, 2, \dots\}$ with general transition probabilities in Theorem 3.1 defines a family of chain-trinomial models.

Each particular chain-trinomial model in the family is defined in a unique manner based on the assumptions for the influenza scenario, and consequently on the structure, and interrelationship between the probabilities of getting vaccination, infection or remaining susceptible in the next time step, for each susceptible individual in the population. We consider an influenza scenario in this section, where the events of getting infection and vaccinated are interconnected or correlated. That is, the drive for vaccination is inspired by infectious encounters. Furthermore, the trinomial distribution will be used to characterize the transition probabilities for the chain $\{B(t), t = 0, 1, 2, \dots\}$. Other scenarios for the influenza epidemic such as when vaccination and infection are uncorrelated will be studied elsewhere in the second part of this work.

4.1 The SVIR Influenza Model with Vaccination Correlated with Infectious Encounters

The following assumptions are made for the influenza epidemic in this subsection:

(a) It is assumed that the influenza epidemic is very severe and highly contagious, and the population is also well sensitized about the disease, and there are available vaccines for those seeking vaccination.

There are several different ways to express the relationship between the events of vaccination and infection in an influenza epidemic. Note that influenza vaccines do not always completely protect against subsequent influenza infections. In fact, in some instances, infection may occur even after vaccination, as well as protection through vaccination may take effect after infection has occurred [7]. Informed by these facts in [4, 6, 7], we consider a hypothetical influenza-vaccination scenario, where people who receive influenza vaccines require a time lapse after inoculation until the vaccine takes effect. The inoculated person may still be infected during this time lapse before the vaccine takes effect, and as a result the person becomes infectious despite being vaccinated. On the other hand, a recently infected person incubates the disease over a time lapse, during which the individual may also be vaccinated. The vaccinated person may become asymptomatic to the disease or less severely ill after receiving the vaccine. That is, it is assumed that the vaccine may intercept and reverse early infection and vice versa.

Mathematically, these assumptions are adapted in the model $\{B(t), t = 0, 1, 2, \dots\}$, and expressed as follows. For $i = 1, 2, \dots, S(t-1) = \underbrace{x_{t-1}} + \overbrace{x_{t-1}}$, if the ith susceptible person in the time interval $(t-2, t-1]$ is infected at time $t-1$, the individual remains exposed for at most one-time unit and becomes infectious $I_0(t)$ at time t, provided that no vaccination occurs in the interval $(t-1, t]$, otherwise, the individual is counted in the vaccinated class $V_0(t)$. That is, if infection occurs first in any interval before vaccination, then vaccination reverses the infectious state. Note that the infected person must be incubating the disease, and not fully infectious.

On the other hand, if the ith susceptible person in the time interval $(t-2, t-1]$ is vaccinated at time $t-1$, the individual remains vulnerable for one-time unit and becomes vaccinated $V_0(t)$ at time t, provided that no infection occurs in the interval $(t-1, t]$, otherwise, the individual is counted in the infected class $I_0(t)$. That is, if vaccination occurs first in any interval before infection, then infection reverses the vaccination state. Note that reversal of vaccination status only occurs during the time lapse until the vaccine is effective.

Observe that assuming reversal of early infection by vaccination, and vice versa, requires in Theorem 3.1 that for each $t = 0, 1, 2, \dots$, the sample space $S(t) = \underbrace{x_t} + \overbrace{x_t}$ for the random variables $V_0(t+1)$ and $I_0(t+1)$ does not change within the time interval $(t, t+1)$, but at the endpoint $t+1$ of the interval. Furthermore, because of the high prevalence of the disease, every susceptible person in the population at the end of any time interval t, that is, $(t-1, t]$ is either infected, vaccinated, or remains susceptible. Moreover, the probability of the ith susceptible individual from the $(t-1)$th generation $S(t-1) = x_{t-1}$ escaping infection and avoiding vaccination at time t is denoted $P_S^i(t)$.

(b) Using ideas from [8, 25], we assume further that p is the probability of becoming infected after one interaction with an infected individual, and all interactions between a susceptible person and infectious individuals are independent. Thus,

at time t, the probability that the ith susceptible individual from the $(t-1)$th generation $S(t-1) = x_{t-1}$ becomes infectious after interaction with j infectious individuals is denoted $p_j^i(t) \equiv p_j^i$, and is given by

$$p_j^i = 1 - (1-p)^j, i = 1, 2, 3, \ldots, x_{t-1}, \text{ where } \quad S(t-1) = x_{t-1}. \tag{4.1}$$

(c) Let $N_i(t)$ represent the number of people the ith susceptible individual interacts with at time t. Note that $N_i(t)$ is a random variable for each $t = 0, 1, 2, \ldots$. In fact, $\{N_i(t), t = 0, 1, 2, \ldots\}$ is a random process. For the purpose of illustrating the method of expectation–maximization (EM) algorithm to find the maximum likelihood estimators (MLEs) for the parameters of the influenza epidemic model, we shall assume for simplicity that $N_i(t)$ is a constant $N > 0$, that is $N_i(t) \equiv N$ (note that such a simplifying assumption was utilized in [8]). Moreover, we assume that N is chosen in such a way that the binomial approximation for the number of infectious people a susceptible person meets can be used. In the next part of this study, we characterize the random process $\{N_i(t), t = 0, 1, 2, \ldots\}$ as a Poisson process.

(d) Furthermore, it is assumed that there is homogenous mixing in the population, and as a result, the probability that the ith susceptible person $S(t-1) = x_{t-1}$ at the beginning of the tth time interval $(t-1, t]$ meets an infectious person $I(t-1)$ also from the $(t-1)$th generation present at time t is given as $\frac{I(t-1)}{n-1}$. Thus, the probability that the ith individual meets exactly j infectious individuals is defined as follows:

$$P_j^i(N_i(t)) = \binom{N_i(t)}{j} \left(\frac{I(t-1)}{n-1}\right)^j \left(1 - \frac{I(t-1)}{n-1}\right)^{N_i(t)-j}, \quad 0 \le j \le N_i(t). \tag{4.2}$$

It follows from the assumptions (a)–(d) above that the probability of the ith susceptible individual of $S(t-1) = x_{t-1}$ meeting infectious individuals and becoming infected at time t is given by

$$P_I^i(t) = \sum_{j=1}^{N_i(t)} (1-(1-p)^j) \binom{N_i(t)}{j} \left(\frac{I(t-1)}{n-1}\right)^j \left(1 - \frac{I(t-1)}{n-1}\right)^{N_i(t)-j}, \tag{4.3}$$

which simplifies to

$$P_I^i(t) \equiv P_I^t = 1 - \left(1 - \frac{pI(t-1)}{n-1}\right)^{N_i(t)}. \tag{4.4}$$

(e) It is assumed further that susceptible individuals are motivated to seek vaccination due to their encounter with infectious individuals, and such encounters

within any one time unit which do not lead to infection, give rise to immediate desire in the susceptible person to get vaccinated within the very one-time unit.

Furthermore, it is assumed that the disease has an incubation period at most one-time unit (e.g., one week, etc.), and the vaccine is relatively strong to reverse any infection that occurs within the span of one-time unit, such that all susceptible people who get infected and are also vaccinated within the one-time unit, obtain artificial immunity, and join the vaccinated class instead. That is, suppose a susceptible person is infected at the beginning of the time interval $(t-1, t]$, without the interception by vaccination, the exposed person develops full-blown disease by the end of the interval t. On the contrary, if the person exposed at time $t-1$ or at any instant within the time interval $(t-1, t]$ is also vaccinated within the very time interval $(t-1, t]$, then the infection is reversed by the vaccination, and the individual joins the vaccination class instead. The reversibility of vaccination by infection is not considered in this influenza scenario.

Also, suppose a susceptible person eludes infection within a one-time unit $(t-1, t]$, we let $\phi \in (0, 1)$ be the probability that the susceptible individual experiences an attitude change toward vaccination due to the encounters with infectious persons and gets vaccinated within the very time interval. Thus, with probability $1-\phi$, the individual who has eluded infection after infectious contacts remains the same in attitude about not getting vaccination, and also remaining susceptible by the end of the time interval $(t-1, t]$. Moreover, it is assumed that ϕ is independent of the size of the infectious encounters at any time interval $(t-1, t]$, $\forall t$. Vaccination without the impact of infection is not considered in this scenario.

From above, it is easy to see that the probability that the ith susceptible person $S(t-1) = x_{t-1}$ present at the beginning of the tth time interval $(t-1, t]$ meets j $(\forall j = 1, 2, \ldots, N)$ infectious persons of the class $I(t-1)$ (also from the $(t-1)$th generation) also present in the tth time interval $(t-1, t]$, and eludes infection from the j infectious persons, and subsequently becomes vaccinated before or by the end of the interval t, is given as follows:

$$(\phi(1-p)^j)\binom{N_i(t)}{j}\left(\frac{I(t-1)}{n-1}\right)^j\left(1-\frac{I(t-1)}{n-1}\right)^{N_i(t)-j}, \forall j = 1, 2, \ldots, N. \quad (4.5)$$

Also, from assumption (a), since three outcomes are possible for any susceptible person of a previous time step $t-1$, present at time t, therefore, the probability that the ith susceptible person $S(t-1) = x_{t-1}$ at the beginning of the tth time interval $(t-1, t]$ meets at least one infectious person $I(t-1)$ (also from the $(t-1)$th generation) present at time t, and eludes infection from the infectious persons, and subsequently becomes vaccinated at time t, is denoted $P^i_V(t)$. Moreover, $P^i_V(t)$ satisfies $P^i_V(t) + P^i_I(t) = 1 - P^i_S(t)$, and is derived as follows:

$$P^i_V(t) = \sum_{j=1}^{N_i(t)}(\phi(1-p)^j)\binom{N_i(t)}{j}\left(\frac{I(t-1)}{n-1}\right)^j\left(1-\frac{I(t-1)}{n-1}\right)^{N_i(t)-j}, \quad (4.6)$$

which simplifies to

$$P_V^i(t) \equiv P_V^t = \phi\left(1 - \frac{pI(t-1)}{n-1}\right)^{N_i(t)}. \tag{4.7}$$

We now present the transition probabilities for the SVIR stochastic process $\{B(t), t = 1, 2, 3, \dots\}$, whenever $t \geq \max\{T_1, T_2\}$.

Theorem 4.1 *Let the conditions of Theorem 3.1 be satisfied, and let the probability that the ith, $\forall i = 1, 2, \dots, x_t$ susceptible gets vaccinated at time t, denoted $P_V^i(t)$ be as defined in (4.7), the probability that the ith, $\forall i = 1, 2, \dots, x_t$ susceptible gets infected at time t, denoted $P_I^i(t)$ be as defined in (4.4), where $P_V^i(t) + P_I^i(t) + P_S^i(t) = 1$. It follows that for $t \geq \max\{T_1, T_2\}$, the transition probabilities for the stochastic process $\{B(t), t = 1, 2, 3, \dots\}$, are given as follows. For $S(t+1) = x_{t+1} \in (0, x_t)$, and with every susceptible individual vaccinated only once, it follows that*

$$\begin{aligned} P(B(t+1) = b_{t+1}|B(t)) = &\underbrace{\binom{x_t}{y_{0_{t+1}}}}\binom{x_t - y_{0_{t+1}}}{z_{0_{t+1}}} \left(P_V^i(t)\right)^{y_{0_{t+1}}} \left(P_I^i(t)\right)^{z_{0_{t+1}}} \\ &\times \left(P_S^i(t)\right)^{x_t - z_{0_{t+1}} - y_{0_{t+1}}}, \end{aligned} \tag{4.8}$$

where $x_{t+1} + y_{0_{t+1}} + z_{0_{t+1}} = x_t$.

For $S(t+1) = x_{t+1} \in (0, x_t)$, and with multiple vaccination in the population, it follows that

$$\begin{aligned} P(B(t+1) = b_{t+1}|B(t)) = &\binom{x_t}{y_{0_{t+1}}}\binom{x_t - y_{0_{t+1}}}{z_{0_{t+1}}} \left(P_V^i(t)\right)^{y_{0_{t+1}}} \left(P_I^i(t)\right)^{z_{0_{t+1}}} \\ &\times \left(P_S^i(t)\right)^{x_t - z_{0_{t+1}} - y_{0_{t+1}}}, \end{aligned} \tag{4.9}$$

where $x_{t+1} + y_{0_{t+1}} + z_{0_{t+1}} = x_t$. In addition, the conditional marginal distributions of V_0 and I_0 are given as follows:

$$P(V_0(t+1) = y_{0_{t+1}}|B(t)) = \binom{x_t}{y_{0_{t+1}}} \left(P_V^i(t)\right)^{y_{0_{t+1}}} \left(1 - P_V^i(t)\right)^{x_t - y_{0_{t+1}}}, \tag{4.10}$$

and

$$P(I_0(t+1) = z_{0_{t+1}}|B(t)) = \binom{x_t}{z_{0_{t+1}}} \left(P_I^i(t)\right)^{z_{0_{t+1}}} \left(1 - P_I^i(t)\right)^{x_t - z_{0_{t+1}}}. \tag{4.11}$$

Proof Let $not(V_0(t) \vee I_0(t))$ be the random variable representing the number of people who remain susceptible at time t. It follows from basic probability rules that

$$
\begin{aligned}
P(B(t+1) = b_{t+1}|B(t)) &= P(V_0(t=1) = y_{0_{t+1}}|B(t) = b(t)) \\
&\quad \times P(I_0(t+1) = z_{0_{t+1}}|V_0(t+1) = y_{0_{t+1}}, B(t) = b(t)) \times \\
&\quad \times P(not(V_0(t+1) \vee I_0(t+1)) = x_t - y_{0_{t+1}} - z_{0_{t+1}}|I_0(t=1) \\
&\quad = z_{0_{t+1}}, V_0(t=1) \\
&= y_{0_{t+1}}, B(t) = b(t)).
\end{aligned} \tag{4.12}
$$

From the assumptions (a)–(d) above, it is easy to see that since $not(V_0(t+1) \vee I_0(t+1)) + V_0(t+1) + I_0(t+1) = x_t$, then

$$
\begin{aligned}
P(B(t+1) = b_{t+1}|B(t)) = &\binom{\underbrace{x_t}}{y_{0_{t+1}}} \binom{x_t - y_{0_{t+1}}}{z_{0_{t+1}}} \binom{x_t - y_{0_{t+1}} - z_{0_{t+1}}}{x_t - y_{0_{t+1}} - z_{0_{t+1}}} \left(P_V^i(t)\right)^{y_{0_{t+1}}} \\
&\times \left(P_I^i(t)\right)^{z_{0_{t+1}}} \left(1 - P_V^i(t) - P_I^i(t)\right)^{x_t - z_{0_{t+1}} - y_{0_{t+1}}}
\end{aligned} \tag{4.13}
$$

Note that (4.13) reduces to (4.8). Also, the results for (4.10)–(4.11) follows immediately from the assumptions (a)–(d) above.

5 Parameter Estimation

In this section, we find estimators for the true parameters of the SVIR Markov chain model using observed data for the state of the process over time. In Sect. 4.1, observe that both $P_V^i(t)$ and $P_I^i(t)$ depend on the probability of getting infection from one interaction with an infectious person, p. Also, $P_V^i(t)$ depends on ϕ-the probability that a susceptible person who has eluded infection develops desire and becomes vaccinated at time t. Therefore, utilizing ideas from [23], we find a maximum likelihood estimators (MLEs) for the probability of getting infection from one interaction with an infectious person, p, and also for ϕ, for the chain $\{B(t), t = 0, 1, 2, \dots\}$ in the case defined in Sect. 4.1. That is, when the transition probabilities are defined in (4.8).

Furthermore, we consider the random process $\{B(t), t = 0, 1, 2, \dots\}$, whenever $t \geq \max\{T_1, T_2\}$ without loss of generality. Also, note that the parameter $\Theta = (p, \phi)$ represent fixed measures in the population at each time t, that is, p and ϕ represent fixed measurements for events occurring in the population during the tth time interval $(t-1, t]$, where the population at any time $t = 0, 1, 2, \dots$ is defined by the random vector

$$
B(t) = (S(t), V_0(t), V_1(t), \dots, V_{T_1-1}(t), I_0(t), I_1(t), \dots, I_{T_2-1}(t)), \tag{5.1}
$$

whenever $t \geq \max\{T_1, T_2\}$.

Let $\hat{b}(t)$ be the observed value of the random vector $B(t)$ at time $t \geq \max\{T_1, T_2\}$, $t = 0, 1, 2, \ldots$, defined in (3.3). That is,

$$\hat{b}(t) = (\hat{x}_t = \underbrace{\hat{x}_t} + \overbrace{\hat{x}_t}, \hat{y_{0_t}}, \hat{y_{1_t}}, \hat{y_{2_t}}, \ldots, \hat{y_{T_1-1_t}}, \hat{z_{0_t}}, \hat{z_{1_t}}, \hat{z_{2_t}}, \ldots, \hat{z_{t_2-1_t}}), \quad (5.2)$$

where $\hat{x}_t, \hat{y_{0_t}}, \hat{y_{1_t}}, \hat{y_{2_t}}, \ldots, \hat{y_{T_1-1_t}}, \hat{z_{0_t}}, \hat{z_{1_t}}, \hat{z_{2_t}}, \ldots, \hat{z_{t_2-1_t}} \in \mathbb{Z}_+$ are nonnegative observed constant values for each component of $B(t)$, at time $t = 0, 1, 2, 3, \ldots$.

The population $B(t)$ is observed over the time units, $t = 0, 1, 2, \ldots, T$, where the initial state $B(0) = \hat{b}(0)$ is assumed to be known. That is, $B(0)$ is deterministic, and the observed data consists of the measurements

$$\hat{b}(0), \hat{b}(1), \hat{b}(2), \ldots, \hat{b}(T). \quad (5.3)$$

We define the collection of random variables $B(0), B(1), B(2), \ldots, B(T)$ representing the population over times $t = 0, 1, 2, \ldots, T$ as follows:

$$D_T = \{B(0), B(1), B(2), \ldots, B(T)\} \quad (5.4)$$

and from (5.2), the observed values of D_T are given as

$$\hat{D}_T = \{\hat{b}(0), \hat{b}(1), \hat{b}(2), \ldots, \hat{b}(T)\}. \quad (5.5)$$

We use the observed sample path $\hat{D}_T$ of the process $\{B(t) : t = 0, 1, 2, \ldots\}$ to find maximum likelihood estimates for the parameters $\Theta = (p, \phi)$. The generation of the sample path $\hat{D}_T$ in (5.5) from the population $B(t)$ over times $t = 0, 1, 2, \ldots, T$ is illustrated in Fig. 2.

Remark 5.1 It must be noted that inferences for the parameters $\Theta = (p, \phi)$ such as confidence intervals and tests of significance, and consistency of estimators for the parameters are beyond the scope of this work, and will appear elsewhere.

We assume that we have data for influenza over time units $t = 0, 1, 2, \ldots, T$ denoted $\hat{D}_T$, where $\hat{D}_T$ is defined in (5.5), and $\hat{D}_T$ is one realization of the human population over time denoted D_T, defined in (5.4). From (5.2), (5.4), and (5.5), the likelihood function of $\Theta = (p, \phi)$ is defined as follows:

$$\begin{aligned} L(\Theta|\hat{D}_T) &= L(p, \phi|\hat{D}_T) = P(D_T = \hat{D}_T|p, \phi) \\ &= P(B(T) = \hat{b}(T), B(T-1) = \hat{b}(T-1), \ldots, B(0) = \hat{b}(0)|p, \phi). \end{aligned} \quad (5.6)$$

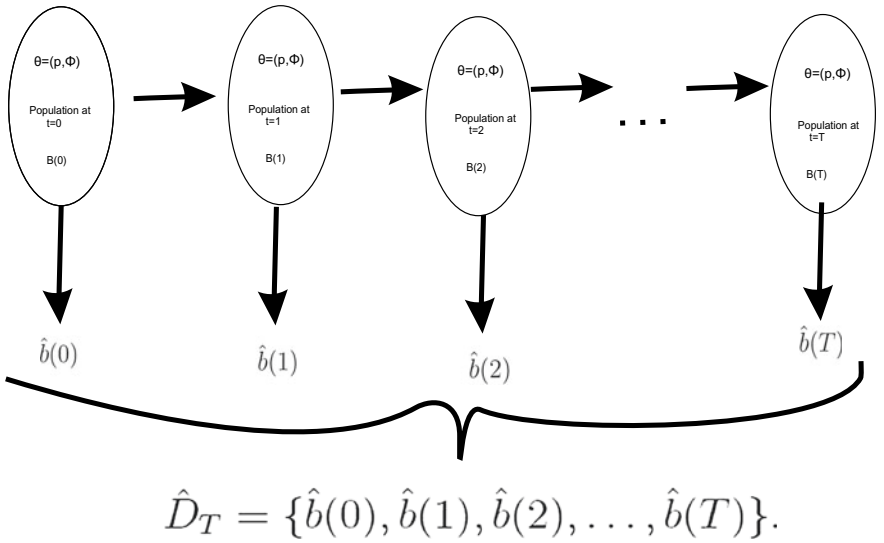

Fig. 2 Shows the transition of the process $\{B(t), t = 0, 1, 2, \ldots\}$ over time $t = 0, 1, 2, \ldots, T$, and observed data $\hat{D}_T = \{\hat{b}(0), \hat{b}(1), \hat{b}(2), \ldots, \hat{b}(T)\}$. The parameters $\Theta = (p, \phi)$ are constant in the population at all times $t = 0, 1, 2, \ldots, T$

From (5.6), applying the multiplication rule, it is easy to see that

$$\begin{aligned} L(p, \phi|D) = P(B(T) = \hat{b}(T)|B(T-1) = \hat{b}(T-1), \ldots, B(0) = \hat{b}(0); p, \phi)\times \\ \times P(B(T-1) = \hat{b}(T-1)|B(T-2) = \hat{b}(T-2), \ldots, B(0) = \hat{b}(0); p, \phi)\times \\ \vdots \\ \times P(B(1) = \hat{b}(1)|B(0) = \hat{b}(0); p, \phi) \times P(B(0) = \hat{b}(0); p, \phi). \end{aligned} \tag{5.7}$$

But, since $\{B(t), t = 0, 1, 2, 3, \ldots\}$ is a Markov Chain, and since it is assumed $B(0)$ is known, it is easy to see that (5.7) reduces to

$$L(p, \phi|\hat{D}_T) = \prod_{k=1}^{T} P(B(k) = \hat{b}(k)|B(k-1) = \hat{b}(k-1); p, \phi). \tag{5.8}$$

It follows from (5.8) and (3.9) that for $S(k) = x_k \in (0, x_{k-1}), \forall k = 1, 2, \ldots, T$,

$$L(p, \phi|\hat{D}_T) = \prod_{k=1}^{T} P(V_0(k) = \hat{y}_{0_k}, I_0(k) = \hat{z}_{0_k}|B(k-1) = \hat{b}(k-1); p, \phi). \tag{5.9}$$

Observe that substituting (4.8) into (5.9) leads to the likelihood function with respect to the parameters p, and ϕ. We should note that applying the maximization technique

to find the MLE $\hat{p}$, and $\hat{\phi}$, for p, and ϕ, respectively, using the likelihood function L defined in (5.9) leads to an intractable equation for the derivative of the log-likelihood of L with respect to p or ϕ, set to zero. Thus, we apply the expectation–maximization (EM) algorithm to find an appropriate MLE for p-the probability of passing the infection from one independent infectious contact, and for ϕ-the probability that a susceptible person gets vaccinated, given that the individual has escaped infection.

5.1 The EM Algorithm and Jensen's Inequality

In this section, we introduce the EM algorithm, where missing information is incorporated into the incomplete likelihood function, at random, and Jensen's inequality is used to find a lower-bound for the complete log-likelihood function.

Recall, the expectation–maximization (EM) algorithm is an iterative algorithm used to find the MLE of a parameter Θ of a given distribution [31, 32]. There are two cases where the algorithm is most useful: (1) when the data available for the maximum likelihood estimation technique has missing components and (2) when maximizing the likelihood function leads to an intractable equation, but adding missing data can simplify the process. It is for the second case in our problem that we utilize this EM algorithm.

Suppose we have observed data Y, and likelihood function $L(\Theta|Y) = P(Y|\Theta)$, and suppose the vector Z is missing data or a missing component, so that $X = (Y, Z)$ is the complete data. The complete log-likelihood function $\log L(\Theta|X) = \log P(Y, Z|\Theta)$ can be maximized to find the MLE of Θ in two basic EM algorithm steps, namely the expectation (E) step and the maximization (M)-step.

The E-step consists of finding the expected value of the complete log-likelihood function $\log P(Y, Z|\Theta)$ with respect to the conditional mass of Z given Y and Θ. That is, we find

$$\begin{aligned} E_{Z|Y;\Theta}[\log L(\Theta|X)] &= E_{Z|Y;\Theta}[\log P(Y, Z|\Theta)] \\ &= \sum_{Z} \log(P(Y, Z|\Theta)P(Z|Y; \Theta)). \end{aligned} \tag{5.10}$$

The M-step consists of maximizing $E_{Z|Y;\Theta}[\log L(\Theta|X)]$ to find an estimate $\hat{\Theta}$ for Θ. This process is summarized in the following steps:

i. Let $m = 0$ and $\hat{\Theta}^m$ be an initial guess for Θ.

ii. Given the observed data Y, and assuming that the guess $\hat{\Theta}^m$ is correct, calculate the conditional probability distribution $P(Z|Y, \hat{\Theta}^m)$ for the missing data Z.

iii. Find the conditional expected log-likelihood referred to as Q, that is,

$$\begin{aligned} Q(\Theta|\hat{\Theta}^m) &= \sum_Z \log(P(Y,Z|\Theta)P(Z|Y,\hat{\Theta}^m)) \\ &= E_{Z|Y,\hat{\Theta}^m}[\log(P(X|\Theta))], \end{aligned} \tag{5.11}$$

where $X = (Y, Z)$.

iv. Find the Θ that maximizes $Q(\Theta|\hat{\Theta}^m)$. The result will be the new $\hat{\Theta}^{m+1}$. That is,

$$\hat{\Theta}^{m+1} = \text{argmax}_{\Theta} Q(\Theta|\hat{\Theta}^m). \tag{5.12}$$

v. Update $\hat{\Theta}^m$ and repeat step (iv) until Θ stops noticeably changing.

The E-step can be obtained by applying Jensen's inequality. We recall Jensen's inequality [33] in the following:

Lemma 5.1 *Suppose f is a convex function, and X is a random variable, then*

$$E[f(X)] \geq f(E[X]). \tag{5.13}$$

Conversely, if you have a concave function (e.g., a logarithmic function), then

$$E[f(x)] \leq f(E[X]). \tag{5.14}$$

From (5.10), let $Y = \hat{D}_T$ represent the observed data defined in (5.5). The following random missing information Z are incorporated to make the log-likelihood function $\log(L)$ more tractable, where L is given in (5.9).

(i) the collection $\mathbf{e}_T^i = \{e_0^i, e_1^i, e_2^i, \ldots, e_t^i, \ldots, e_T^i\}$, where for each $t \in \{0, 1, 2, \ldots, T\}$ and $i \in \{1, 2, 3, \ldots, x_{t-1} = S(t-1)\}$, e_t^i is a discrete random variable representing the number of infectious individuals that the ith susceptible person of the $(t-1)$th generation meets at time t (i.e. in the interval $(t-1, t]$). Since from (4.3), a susceptible person only meets the fixed number of people, N, at any time t, therefore

$$e_t^i = j, j = 1, 2, 3, \ldots, N. \tag{5.15}$$

(ii) the collection $\mathbf{d}_{T,j}^i = \{d_{0,j}^i, d_{1,j}^i, d_{2,j}^i, \ldots, d_{t,j}^i, \ldots, d_{T-1,j}^i, d_{T,j}^i\}$, where for each $t \in \{0, 1, 2, \ldots, T\}, i \in \{1, 2, 3, \ldots, x_{t-1} = S(t-1)\}$, and $j \in \{1, 2, 3, \ldots, N\}$, $d_{t,j}^i$ is a categorical random variable indicating the event that the lth infectious individual passes the infection with probability p, where $l = 1, 2, 3, \ldots, j$, given

that the ith susceptible person meets j infectious people among the fixed number of people N, at time t. Thus,

$$d^i_{t,j} = l, l = 1, 2, 3, \ldots, j. \tag{5.16}$$

We consider a step-by-step approach to add the missing data $\mathbf{e}^i_T$ and $\mathbf{d}^i_{T,j}$ into the incomplete likelihood function L.

Lemma 5.2 *Let the assumptions of Theorem 4.1 be satisfied. Given the missing at random information* $\mathbf{e}^i_T$ *and* $\mathbf{d}^i_{T,j}$ *defined in (5.15) and (5.16), then it follows from (4.8) and (5.9), that the log-likelihood function* $\log L(p, \phi|\hat{D}_T)$ *satisfies the following inequality:*

$$\begin{aligned}
\log L(p, \phi|\hat{D}_T) \geq & \sum_{k=1}^{T}\sum_{j=1}^{N}\sum_{l=1}^{j}\Big[P(e^i_k = j|B(k-1) = \hat{b}(k-1); p, \phi) \\
& \times P(d^i_{k,j} = l|e^i_k = j, B(k-1) = \hat{b}(k-1); p, \phi) \\
& \times \log(P(V_0(k) = \hat{y}_{0_k}, e^i_k = j, d^i_{k,j} = l|B(k-1) = \hat{b}(k-1); p, \phi))\Big] \\
& + \sum_{k=1}^{T}\sum_{j=1}^{N}\sum_{l=1}^{j}\Big[P(e^i_k = j|V_0(k) = \hat{y}_{0_k}, B(k-1) = \hat{b}(k-1); p, \phi) \\
& \times P(d^i_{k,j} = l|e^i_k = j, V_0(k) = \hat{y}_{0_k}, B(k-1) = \hat{b}(k-1); p, \phi) \\
& \times \log(P(I_0(k) = \hat{y}_{0_k}, e^i_k = j, d^i_{k,j} = l|V_0(k) = \hat{y}_{0_k}, B(k-1) = \hat{b}(k-1); p, \phi))\Big] \\
& + \sum_{k=1}^{T}\sum_{j=1}^{N}\sum_{l=1}^{j}\Big[P(e^i_k = j|I_0(k) = \hat{z}_{0_k}, V_0(k) = \hat{y}_{0_k}, B(k-1) = \hat{b}(k-1); p, \phi) \\
& \times P(d^i_{k,j} = l|e^i_k = j, I_0(k) = \hat{z}_{0_k}, V_0(k) = \hat{y}_{0_k}, B(k-1) = \hat{b}(k-1); p, \phi) \\
& \times \log(P(not(V_0(k) \vee I_0(k)) = \hat{u}_{0_k}, e^i_k = j, d^i_{k,j} = l|I_0(k) \\
& = \hat{z}_{0_k}, V_0(k) = \hat{y}_{0_k}, B(k-1) = \hat{b}(k-1); p, \phi))\Big] \quad - \lambda_1 - \lambda_2
\end{aligned} \tag{5.17}$$

where $\hat{u}_{0_k} = \hat{x}_{k-1} - \hat{y}_{0_k} - \hat{z}_{0_k}, \forall k = 1, 2, \ldots, T$, *and* λ_1, *and also* λ_2 *are probability terms that depends on* $\mathbf{e}^i_T$ *and* $\mathbf{d}^i_{T,j}$.

Proof From (5.9), denote the log-likelihood $l(p, \phi|\hat{D}_T) \equiv \log L(p, \phi|\hat{D}_T)$. It follows from (5.9) that adding the missing random data $\mathbf{e}_T^i$, we obtain

$$\begin{aligned} l(p, \phi|\hat{D}_T) &= \log \prod_{k=1}^{T} P(V_0(k) = y_{0_k}, I_0(k) = z_{0_k}|B(k-1) = \hat{b}(k-1); p, \phi) \\ &= \sum_{k=1}^{T} \log \left[\sum_{j=1}^{N} P(V_0(k) = y_{0_k}, e_k^i = j|B(k-1) = \hat{b}(k-1); p, \phi) \right] \\ &\quad + \sum_{k=1}^{T} \log \left[\sum_{j=1}^{N} P(I_0(k) = z_{0_k}, e_k^i = j|V_0(k) = y_{0_k}, \right. \\ &\quad \left. B(k-1) = \hat{b}(k-1); p, \phi) \right] \\ &\quad + \sum_{k=1}^{T} \log \left[\sum_{j=1}^{N} P(not(V_0(k) \vee I_0(k)) = u_{0_k}, e_k^i = j|I_0(k) = z_{0_k}, , \right. \\ &\quad \left. V_0(k) = y_{0_k}, B(k-1) = \hat{b}(k-1); p, \phi) \right]. \end{aligned} \tag{5.18}$$

Equation (5.18) can be expressed further as follows

$$\begin{aligned} l(p, \phi|\hat{D}_T) &= \sum_{k=1}^{T} \log \left[\sum_{j=1}^{N} \frac{P(V_0(k) = y_{0_k}, e_k^i = j|B(k-1) = \hat{b}(k-1))}{P(e_k^i = j|B(k-1) = \hat{b}(k-1); p, \phi)}; p, \phi) \right. \\ &\left. \times P(e_k^i = j|B(k-1) = \hat{b}(k-1); p, \phi) \right] \\ &+ \sum_{k=1}^{T} \log \left[\sum_{j=1}^{N} \frac{P(I_0(k) = y_{0_k}, e_k^i = j|V_0(k) = y_{0_k}, B(k-1) = \hat{b}(k-1); p, \phi)}{P(e_k^i = j|V_0(k) = y_{0_k}, B(k-1) = \hat{b}(k-1)p, \phi)} \right. \\ &\left. \times P(e_k^i = j|V_0(k) = y_{0_k}, B(k-1) = \hat{b}(k-1); p, \phi) \right]. + \sum_{k=1}^{T} \log \left[\sum_{j=1}^{N} \right. \\ &\frac{P(not(V_0(k) \vee I_0(k)) = u_{0_k}, e_k^i = j|I_0(k) = z_{0_k}, , V_0(k) = y_{0_k}, B(k-1) = \hat{b}(k-1); p, \phi)}{P(e_k^i = j|I_0(k) = \hat{z}_{0_k}, V_0(k) = y_{0_k}, B(k-1) = \hat{b}(k-1); p, \phi)} \\ &\left. \times P(e_k^i = j|I_0(k) = z_{0_k}, , V_0(k) = y_{0_k}, B(k-1) = \hat{b}(k-1); p, \phi) \right]. \end{aligned} \tag{5.19}$$

Applying Jensen's inequity to (5.19), leads to the following

$$
\begin{aligned}
l(p,\phi|\hat{D}_T) \geq & \sum_{k=1}^{T}\sum_{j=1}^{N} \log\Big\{P(V_0(k)=y_{0_k}, e_k^i=j|B(k-1)=\hat{b}(k-1);p,\phi)\Big\} \\
& P(e_k^i=j|B(k-1)=\hat{b}(k-1);p,\phi) \\
& + \sum_{k=1}^{T}\sum_{j=1}^{N} \log\Big\{P(I_0(k)=z_{0_k}, e_k^i=j|V_0(k)=y_{0_k}, \\
& B(k-1)=\hat{b}(k-1);p,\phi)\Big\} \\
& \times P(e_k^i=j|V_0(k)=y_{0_k}, B(k-1)=\hat{b}(k-1);p,\phi) \\
& + \sum_{k=1}^{T}\sum_{j=1}^{N} \log\Big\{P(not(V_0(k)\vee I_0(k))=u_{0_k}, e_k^i=j|I_0(k) \\
& =z_{0_k},, V_0(k)=y_{0_k}, B(k-1)=\hat{b}(k-1);p,\phi)\Big\} \\
& \times P(e_k^i=j|I_0(k)=z_{0_k}, V_0(k)=y_{0_k}, B(k-1)=\hat{b}(k-1);p,\phi)-\lambda_1,
\end{aligned}
\tag{5.20}
$$

where λ_1 in (5.20) is given as follows

$$
\begin{aligned}
\lambda_1 = & \sum_{k=1}^{T}\sum_{j=1}^{N} \log\Big\{P(e_k^i=j|B(k-1)=\hat{b}(k-1);p,\phi)\Big\} \\
& P(e_k^i=j|B(k-1)=\hat{b}(k-1);p,\phi) \\
& + \sum_{k=1}^{T}\sum_{j=1}^{N} \log\Big\{P(e_k^i=j|V_0(k)=y_{0_k}, B(k-1)=\hat{b}(k-1);p,\phi)\Big\} \\
& \times P(e_k^i=j|V_0(k)=y_{0_k}, B(k-1)=\hat{b}(k-1);p,\phi) \\
& + \sum_{k=1}^{T}\sum_{j=1}^{N} \log\Big\{P(e_k^i=j|I_0(k)=z_{0_k}, V_0(k)=y_{0_k}, B(k-1)=\hat{b}(k-1);p,\phi)\Big\} \\
& \times P(e_k^i=j|I_0(k)=z_{0_k}, V_0(k)=y_{0_k}, B(k-1)=\hat{b}(k-1);p,\phi)
\end{aligned}
\tag{5.21}
$$

We add the missing data $d_{T,j}^i$ in (5.16) into the partially complete log-likelihood function $\log P(V_0(k)=y_{0_k}, e_k^i=j|B(k-1)=\hat{b}(k-1);p,\phi)$, $\log P(I_0(k)=z_{0_k}, e_k^i=j|V_0(k)=y_{0_k}, B(k-1)=\hat{b}(k-1);p,\phi)$ and $\log\Big\{P(not(V_0(k)\vee I_0(k))=u_{0_k}, e_k^i=j|I_0(k)=z_{0_k},, V_0(k)=y_{0_k}, B(k-1)=\hat{b}(k-1);p,\phi)\Big\}$,

$\forall k \in \{1, 2, 3, \ldots, T\}; j \in \{1, 2, 3, \ldots, N\}$, and apply the same technique in (5.18)-(5.21), as follows.

From (5.20)

$$
\begin{aligned}
l(p, \phi|\hat{D}_T) \geq & \sum_{k=1}^{T}\sum_{j=1}^{N} \log \left\{ \sum_{l=1}^{j} P(V_0(k) = y_{0_k}, e_k^i = j, d_{k,j}^i = l|B(k-1) = \hat{b}(k-1)) \right\} \\
& \times P(e_k^i = j|B(k-1) = \hat{b}(k-1); p, \phi) \\
& + \sum_{k=1}^{T}\sum_{j=1}^{N} \log \left\{ \sum_{l=1}^{j} P(I_0(k) = y_{0_k}, e_k^i = j, d_{k,j}^i = l|V_0(k) = y_{0_k}, \right. \\
& \left. B(k-1) = \hat{b}(k-1); p, \phi) \right\} \\
& \times P(e_k^i = j|V_0(k) = y_{0_k}, B(k-1) = \hat{b}(k-1); p, \phi) \\
& + \sum_{k=1}^{T}\sum_{j=1}^{N} \log \left\{ \sum_{l=1}^{j} P(not(V_0(k) \vee I_0(k)) \right. \\
& \left. = u_{0_k}, e_k^i = j, d_{k,j}^i = l|I_0(k) = z_{0_k}, V_0(k) = y_{0_k}, B(k-1) = \hat{b}(k-1); p, \phi) \right\} \\
& \times P(e_k^i = j|I_0(k) = z_{0_k}, V_0(k) = y_{0_k}, B(k-1) = \hat{b}(k-1); p, \phi) - \lambda_1,
\end{aligned}
\tag{5.22}
$$

Applying Jensen's inequality on (5.22), we obtain the following

$$
\begin{aligned}
l(p, \phi|\hat{D}_T) \geq & \sum_{k=1}^{T}\sum_{j=1}^{N}\sum_{l=1}^{j} \log \left\{ P(V_0(k) = y_{0_k}, e_k^i = j, d_{k,j}^i = l|B(k-1) \right. \\
& \left. = \hat{b}(k-1); p, \phi) \right\} \\
& \times P(d_{k,j}^i = l|e_k^i = j, B(k-1) = \hat{b}(k-1); p, \phi) P(e_k^i = j|B(k-1) \\
& = \hat{b}(k-1); p, \phi) \\
& + \sum_{k=1}^{T}\sum_{j=1}^{N}\sum_{l=1}^{j} \log \left\{ P(I_0(k) = z_{0_k}, e_k^i = j, d_{k,j}^i = l|V_0(k) = y_{0_k},) \right. \\
& \left. B(k-1) = \hat{b}(k-1); p, \phi) \right\} \\
& \times P(d_{k,j}^i = l|e_k^i = j, V_0(k) = y_{0_k}, B(k-1) = \hat{b}(k-1); p, \phi) \\
& P(e_k^i = j|V_0(k) = y_{0_k}, B(k-1) = \hat{b}(k-1); p, \phi) \\
& + \sum_{k=1}^{T}\sum_{j=1}^{N}\sum_{l=1}^{j} \log \left\{ P(not(V_0(k) \vee I_0(k)) = u_{0_k}, e_k^i = j, d_{k,j}^i \right. \\
& \left. = l|I_0(k) = z_{0_k}, V_0(k) = y_{0_k}, B(k-1) = \hat{b}(k-1); p, \phi) \right\} \\
& \times P(d_{k,j}^i = l|e_k^i = j, I_0(k) = z_{0_k}, V_0(k) = y_{0_k}, B(k-1) = \hat{b}(k-1); p, \phi) \\
& P(e_k^i = j|I_0(k) = z_{0_k}, V_0(k) = y_{0_k}, B(k-1) = \hat{b}(k-1); p, \phi) - \lambda_1 - \lambda_2,
\end{aligned}
\tag{5.23}
$$

where

$$\begin{aligned}
\lambda_2 &= \sum_{k=1}^{T}\sum_{j=1}^{N}\log\left\{P(d_{k,j}^i = l|e_k^i = j, B(k-1) = \hat{b}(k-1); p, \phi)\right\} \\
&\times P(d_{k,j}^i = l|e_k^i = j, B(k-1) = \hat{b}(k-1); p, \phi)P(e_k^i = j|B(k-1) = \hat{b}(k-1); p, \phi) \\
&+ \sum_{k=1}^{T}\sum_{j=1}^{N}\log\left\{P(d_{k,j}^i = l|e_k^i = j, V_0(k) = y_{0_k}, B(k-1) = \hat{b}(k-1); p, \phi)\right\} \\
&\times P(d_{k,j}^i = l|e_k^i = j, V_0(k) = y_{0_k}, B(k-1) = \hat{b}(k-1); p, \phi) \\
&\times P(e_k^i = j|V_0(k) = y_{0_k}, B(k-1) = \hat{b}(k-1); p, \phi) \\
&+ \sum_{k=1}^{T}\sum_{j=1}^{N}\sum_{l=1}^{j}\log\left\{P(d_{k,j}^i = l|e_k^i = j, I_0(k) = z_{0_k}, V_0(k) = y_{0_k}, \right. \\
&\left. B(k-1) = \hat{b}(k-1); p, \phi)\right\} \\
&\times P(d_{k,j}^i = l|e_k^i = j, I_0(k) = z_{0_k}, V_0(k) = y_{0_k}, B(k-1) = \hat{b}(k-1); p, \phi) \\
&\times P(e_k^i = j|I_0(k) = z_{0_k}, V_0(k) = y_{0_k}, B(k-1) = \hat{b}(k-1); p, \phi)
\end{aligned} \tag{5.24}$$

Remark 5.2 We note from (5.17) that the E-step of the EM algorithm consists of finding the conditional expectation term

$$\begin{aligned}
Q(\Theta|\hat{\Theta}^m) &= \sum_{k=1}^{T}\sum_{j=1}^{N}\sum_{l=1}^{j}\Big[P(e_k^i = j|B(k-1) = \hat{b}(k-1); p^m, \phi^m) \\
&\times P(d_{k,j}^i = l|e_k^i = j, B(k-1) = \hat{b}(k-1); p^m, \phi^m) \\
&\times \log(P(V_0(k) = \hat{y}_{0_k}, e_k^i = j, d_{k,j}^i = l|B(k-1) = \hat{b}(k-1); p, \phi))\Big] \\
&+ \sum_{k=1}^{T}\sum_{j=1}^{N}\sum_{l=1}^{j}\Big[P(e_k^i = j|V_0(k) = \hat{y}_{0_k}, B(k-1) = \hat{b}(k-1); p^m, \phi^m) \\
&\times P(d_{k,j}^i = l|e_k^i = j, V_0(k) = \hat{y}_{0_k}, B(k-1) = \hat{b}(k-1); p^m, \phi^m) \\
&\times \log(P(I_0(k) = \hat{y}_{0_k}, e_k^i = j, d_{k,j}^i = l|V_0(k) = \hat{y}_{0_k}, B(k-1) = \hat{b}(k-1); p, \phi))\Big] \\
&+ \sum_{k=1}^{T}\sum_{j=1}^{N}\sum_{l=1}^{j}\Big[P(e_k^i = j|I_0(k) = \hat{z}_{0_k}, V_0(k) = \hat{y}_{0_k}, B(k-1) = \hat{b}(k-1); p^m, \phi^m) \\
&\times P(d_{k,j}^i = l|e_k^i = j, I_0(k) = \hat{z}_{0_k}, V_0(k) = \hat{y}_{0_k}, B(k-1) = \hat{b}(k-1); p^m, \phi^m) \\
&\times \log(P(not(V_0(k) \vee I_0(k)) = \hat{u}_{0_k}, e_k^i = j, d_{k,j}^i = l|I_0(k) \\
&= z_{0_k}, V_0(k) = y_{0_k}, B(k-1) = \hat{b}(k-1); p, \phi))\Big]
\end{aligned} \tag{5.25}$$

where $\Theta = (p, \phi)$, and $(\hat{p}^m, \hat{\phi}^m)$ is the estimate of (p, ϕ) in the mth step of the EM algorithm.

We specify an explicit expression for components of the E-step (5.25) in the following result.

Lemma 5.3 *For each $k \in \{1, 2, 3, \ldots, T\}$, $j \in \{1, 2, 3, \ldots, N\}$, and $l \in \{1, 2, 3, \ldots, j\}$, the following holds:*

$$P(e_k^i = j | B(k-1) = \hat{b}(k-1); \hat{p}^{(m)}, \hat{\phi}^{(m)}) = \binom{N}{j} \left(\frac{\hat{I}(k-1)}{n-1}\right)^j \left(1 - \frac{\hat{I}(k-1)}{n-1}\right)^{N-j}, \tag{5.26}$$

$$P(e_k^i = j | V_0(k) = y_{0_k}, B(k-1) = \hat{b}(k-1); \hat{p}^{(m)}, \hat{\phi}^{(m)}) = \binom{N}{j} \left(\frac{\hat{I}(k-1)}{n-1}\right)^j \left(1 - \frac{\hat{I}(k-1)}{n-1}\right)^{N-j}, \tag{5.27}$$

and

$$P(e_k^i = j | I_0(k) = \hat{z}_{0_k}, V_0(k) = \hat{y}_{0_k}, B(k-1) = \hat{b}(k-1); \hat{p}^{(m)}, \hat{\phi}^{(m)}) \binom{N}{j} \left(\frac{\hat{I}(k-1)}{n-1}\right)^j \left(1 - \frac{\hat{I}(k-1)}{n-1}\right)^{N-j}. \tag{5.28}$$

Also,

$$P(d_{k,j}^i = l | e_k^i = j, B(k-1) = \hat{b}(k-1); \hat{p}^{(m)}, \hat{\phi}^{(m)}) = \hat{p}^{(m)}, \tag{5.29}$$

$$P(d_{k,j}^i = l | e_k^i = j, V_0(k) = y_{0_k}, B(k-1) = \hat{b}(k-1); \hat{p}^{(m)}, \hat{\phi}^{(m)}) = \hat{p}^{(m)}, \tag{5.30}$$

and

$$P(d_{k,j}^i = l | e_k^i = j, I_0(k) = z_{0_k}, V_0(k) = y_{0_k}, B(k-1) = \hat{b}(k-1); \hat{p}^{(m)}, \hat{\phi}^{(m)}) = \hat{p}^{(m)}. \tag{5.31}$$

Furthermore,

$$P(V_0(k) = \hat{y}_{0_k}, e_k^i = j, d_{k,j}^i = l | B(k-1) = \hat{b}(k-1); p, \phi) = \binom{\underbrace{\hat{x}_{k-1}}}{\hat{y}_{0_k}} \binom{N}{j} \left(\frac{\hat{I}(k-1)}{n-1}\right)^j \left(1 - \frac{\hat{I}(k-1)}{n-1}\right)^{N-j} (\phi(1-p))^{y_{0_k}} (1 - \phi(1-p))^{\underbrace{\hat{x}_{k-1}} - \hat{y}_{0_k}} p, \tag{5.32}$$

$$P(I_0(k)=\hat{z}_{0_k}, e_k^i=j, d_{k,j}^i=l|V_0(k)=\hat{y}_{0_k}, B(k-1)=\hat{b}(k-1);p,\phi)=$$
$$\binom{\hat{x}_{k-1}-\hat{y}_{0_k}}{\hat{z}_{0_k}}\binom{N}{j}\left(\frac{\hat{I}(k-1)}{n-1}\right)^j\left(1-\frac{\hat{I}(k-1)}{n-1}\right)^{N-j}p^{(\hat{z}_{0_k}+1)}(1-p)^{\hat{x}_{k-1}-\hat{y}_{0_k}-\hat{z}_{0_k}}, \tag{5.33}$$

and

$$P(not(V_0(k)\vee I_0(k))=\hat{u}_{0_k}, e_k^i=j, d_{k,j}^i=l|V_0(k)=\hat{y}_{0_k}, B(k-1)=\hat{b}(k-1);p,\phi)=$$
$$(1)\binom{N}{j}\left(\frac{\hat{I}(k-1)}{n-1}\right)^j\left(1-\frac{\hat{I}(k-1)}{n-1}\right)^{N-j}((1-p)(1-\phi))^{\hat{u}_{0_k}}p, \tag{5.34}$$

where $\hat{u}_{0_k}=\hat{x}_{k-1}-\hat{y}_{0_k}-\hat{z}_{0_k}, \forall k.$

Proof Equations (5.26)–(5.31) follow immediately from assumptions (a)–(d) in Sect. 4.1. For (5.32) and (5.34), we apply the multiplication rule and also apply assumptions (a)–(d) in Sect. 4.1. That is,

$$\begin{aligned}&P(V_0(k)=\hat{y}_{0_k}, e_k^i=j, d_{k,j}^i=l|B(k-1)=\hat{b}(k-1);p,\phi)=\\&P(V_0(k)=\hat{y}_{0_k}, |e_k^i=j, d_{k,j}^i=lB(k-1)=\hat{b}(k-1);p,\phi)\\&\times P(d_{k,j}^i=l|e_k^i=j, B(k-1)=\hat{b}(k-1);p,\phi)\\&\times P(e_k^i=j|B(k-1)=\hat{b}(k-1);p,\phi).\end{aligned} \tag{5.35}$$

Observe from assumptions (a)–(d) in Sect. 4.1 that, given infection is passed across only by the lth infectious person among the j infectious persons encountered for that given instant, and also given that ϕ is the probability that a susceptible person changes the mind, and becomes vaccinated within that time instant after escaping infection from the lth infectious person, it follows that $\phi(1-p)$ is the probability that a susceptible person gets vaccinated at any instant, and the conditional distribution of the random variable $V_0(k)$ is binomial with parameters $\phi(1-p)$ and $\underbrace{\hat{x}_{k-1}}$. Thus,

$$\begin{aligned}&P(V_0(k)=\hat{y}_{0_k}|e_k^i=j, d_{k,j}^i=l, B(k-1)\\&\quad=\hat{b}(k-1);p,\phi)=\binom{\underbrace{\hat{x}_{k-1}}}{\hat{y}_{0_k}}(\phi(1-p))^{y_{0_k}}(1-\phi(1-p))^{\underbrace{\hat{x}_{k-1}}-\hat{y}_{0_k}},\end{aligned} \tag{5.36}$$

Also, the probability that the lth infectious person passes infection at any instant given j infectious individuals present at the instant is given by

$$P(d_{k,j}^i=l|e_k^i=j, B(k-1)=\hat{b}(k-1);p,\phi)=p, \tag{5.37}$$

and the probability that the ith susceptible person meets j infectious people at time k is given by

$$P(e_k^i = j|B(k-1) = \hat{b}(k-1); p, \phi) = \binom{N}{j} \left(\frac{\hat{I}(k-1)}{n-1}\right)^j \left(1 - \frac{\hat{I}(k-1)}{n-1}\right)^{N-j}. \tag{5.38}$$

Substituting (5.36)–(5.38) into (5.35) gives (5.32).

Similarly,

$$\begin{aligned}
&P(I_0(k) = \hat{z}_{0_k}, e_k^i = j, d_{k,j}^i = l|V_0(k) = \hat{y}_{0_k}, B(k-1) = \hat{b}(k-1); p, \phi) = \\
&P(I_0(k) = \hat{z}_{0_k}, |e_k^i = j, d_{k,j}^i = l, V_0(k) = \hat{y}_{0_k}, B(k-1) = \hat{b}(k-1); p, \phi) \\
&\times P(d_{k,j}^i = l|e_k^i = j, V_0(k) = \hat{y}_{0_k}, B(k-1) = \hat{b}(k-1); p, \phi) \\
&\times P(e_k^i = j|V_0(k) = \hat{y}_{0_k}, B(k-1) = \hat{b}(k-1); p, \phi).
\end{aligned} \tag{5.39}$$

From assumptions (a)–(d) in Sect. 4.1, it is easy to see that

$$\begin{aligned}
&P(I_0(k) = \hat{z}_{0_k}|e_k^i = j, d_{k,j}^i = l, V_0(k) = \hat{y}_{0_k}, \\
&B(k-1) = \hat{b}(k-1); p) = \binom{\hat{x}_{k-1} - \hat{y}_{0_k}}{\hat{z}_{0_k}} (1-p)^{\hat{x}_{k-1} - \hat{y}_{0_k} - \hat{z}_{0_k}} (p)^{\hat{z}_{0_k}}.
\end{aligned} \tag{5.40}$$

Furthermore, all the other components of (5.39) are obtained similarly as in (5.37)–(5.38).

Finally,

$$\begin{aligned}
&P(not(V_0(k) \vee I_0(k)) = \hat{u}_{0_k}, e_k^i = j, d_{k,j}^i = l|V_0(k) = \hat{y}_{0_k}, \\
&\quad B(k-1) = \hat{b}(k-1); p, \phi) = \\
&P(not(V_0(k) \vee I_0(k)) = \hat{u}_{0_k}, |e_k^i = j, d_{k,j}^i = l, I_0(k) = \hat{z}_{0_k}, V_0(k) = \hat{y}_{0_k}, \\
&\quad B(k-1) = \hat{b}(k-1); p, \phi) \\
&\times P(d_{k,j}^i = l|e_k^i = j, I_0(k) = \hat{z}_{0_k}, V_0(k) = \hat{y}_{0_k}, B(k-1) = \hat{b}(k-1); p, \phi) \\
&\times P(e_k^i = j|I_0(k) = \hat{z}_{0_k}, V_0(k) = \hat{y}_{0_k}, B(k-1) = \hat{b}(k-1); p, \phi).
\end{aligned} \tag{5.41}$$

From assumptions (a)–(d) in Sect. 4.1, it is easy to see that for $\hat{u}_{0_k} = \hat{x}_{k-1} - \hat{y}_{0_k} - \hat{z}_{0_k}$,

$$\begin{aligned}
&P(not(V_0(k) \vee I_0(k)) = \hat{u}_{0_k}|e_k^i = j, d_{k,j}^i = l, I_0(k) \\
&\quad = \hat{z}_{0_k}, V_0(k) = \hat{y}_{0_k}, B(k-1) = \hat{b}(k-1); p) \\
&= \binom{\hat{x}_{k-1} - \hat{y}_{0_k} - \hat{z}_{0_k}}{\hat{u}_{0_k}} (p + \phi(1-p))^{\hat{x}_{k-1} - \hat{y}_{0_k} - \hat{z}_{0_k} - \hat{u}_{0_k}} (1 - p - \phi(1-p))^{\hat{u}_{0_k}} \\
&= (1 - p - \phi(1-p))^{\hat{u}_{0_k}}.
\end{aligned} \tag{5.42}$$

Furthermore, all the other components of (5.41) are obtained similarly as in (5.37)–(5.38). Thus, from (5.39) to (5.42), the result in (5.34) follows immediately.

The following result presents an expression for the E-step of the EM algorithm.

Theorem 5.1 *Assume that the results in Lemma 5.3 hold. For* $m = 0, 1, 2, \ldots$, *the E-step of the EM algorithm in (5.25) in Remark 5.2 is expressed as follows for* $\Theta = (p, \phi)$

$$\begin{aligned} Q(\Theta|\hat{\Theta}^{(m)}) \equiv \mathfrak{K} + \sum_{k=1}^{T} N \left(\frac{\hat{I}(k-1)}{n-1} \right) \hat{p}^{(m)} \times \\ \times \Big([1 + (\hat{z}_{0_k} + 1) + 1] \log(p) + (\hat{x}_{k-1} - \hat{z}_{0_k} + \hat{u}_{0_k}) \log(1-p) \\ (\underbrace{\hat{x}_{k-1}} - \hat{y}_{0_k}) \log(1 - \phi(1-p)) + \hat{y}_{0_k} \log(\phi) + \hat{u}_{0_k} \log(1-\phi) \Big), \end{aligned} \tag{5.43}$$

where $\hat{u}_{0_k} = \hat{x}_{k-1} - \hat{y}_{0_k} - \hat{z}_{0_k}$, $\forall k$, $\mathfrak{K}$ *denotes a constant term, and* $\hat{p}^{(m)}$ *is an estimate of p at the mth step. Also*

$$\hat{I}(k-1) = \hat{z}_{0_0} + \hat{z}_{0_1} + \cdots + \hat{z}_{0_{k-1}}. \tag{5.44}$$

Proof From Lemma 5.2 and (5.25), it is easy to see that

$$\begin{aligned} Q(\Theta|\hat{\Theta}^{(m)}) &\equiv Q(p, \phi|\hat{p}^{(m)}, \hat{\phi}^{m}) \\ &\equiv \sum_{k=1}^{T} \sum_{j=1}^{N} \sum_{l=1}^{j} \binom{N}{j} \left(\frac{\hat{I}(k-1)}{n-1} \right)^{j} \left(1 - \frac{\hat{I}(k-1)}{n-1} \right)^{N-j} \hat{p}^{(m)} \times \\ &\quad \left\{ \log \left[\binom{\underbrace{\hat{x}_{k-1}}}{\hat{y}_{0_k}} \binom{N}{j} \left(\frac{\hat{I}(k-1)}{n-1} \right)^{j} \left(1 - \frac{\hat{I}(k-1)}{n-1} \right)^{N-j} \right] \right. \\ &\quad \left. + (\underbrace{\hat{x}_{k-1}} - \hat{y}_{0_k}) \log(1 - \phi(1-p)) + (\hat{y}_{0_k}) \log(1-p) + (\hat{y}_{0_k}) \log(\phi) + \log(p) \right\} \\ &\quad + \sum_{k=1}^{T} \sum_{j=1}^{N} \sum_{l=1}^{j} \binom{N}{j} \left(\frac{\hat{I}(k-1)}{n-1} \right)^{j} \left(1 - \frac{\hat{I}(k-1)}{n-1} \right)^{N-j} \hat{p}^{(m)} \times \\ &\quad \left\{ \log \left[\binom{\hat{x}_{k-1} - \hat{y}_{0_k}}{\hat{z}_{0_{k-1}}} \binom{N}{j} \left(\frac{\hat{I}(k-1)}{n-1} \right)^{j} \left(1 - \frac{\hat{I}(k-1)}{n-1} \right)^{N-j} \right] \right. \\ &\quad \left. + (\hat{z}_{0_k} + 1) \log(p) + (\hat{x}_{k-1} - \hat{y}_{0_k} - \hat{z}_{0_k}) \log(1-p) \right\} \\ &\quad + \sum_{k=1}^{T} \sum_{j=1}^{N} \sum_{l=1}^{j} \binom{N}{j} \left(\frac{\hat{I}(k-1)}{n-1} \right)^{j} \left(1 - \frac{\hat{I}(k-1)}{n-1} \right)^{N-j} \hat{p}^{(m)} \times \\ &\quad \left\{ \log \left[\binom{N}{j} \left(\frac{\hat{I}(k-1)}{n-1} \right)^{j} \left(1 - \frac{\hat{I}(k-1)}{n-1} \right)^{N-j} \right] \right. \\ &\quad \left. + (\hat{u}_{0_k}) \log(1-p) + (\hat{u}_{0_k}) \log(1-\phi) + \log(p) \right\}, \end{aligned} \tag{5.45}$$

where $\hat{u}_{0_k} = \hat{x}_{k-1} - \hat{y}_{0_k} - \hat{z}_{0_k}, \forall k$. Observe that

$$\sum_{j=1}^{N}\sum_{l=1}^{j}\binom{N}{j}\left(\frac{\hat{I}(k-1)}{n-1}\right)^{j}\left(1-\frac{\hat{I}(k-1)}{n-1}\right)^{N-j} = N\left(\frac{\hat{I}(k-1)}{n-1}\right). \tag{5.46}$$

Thus, (5.43) follows immediately from (5.45), where

$$\begin{aligned}
\Re \equiv & \sum_{k=1}^{T}\sum_{j=1}^{N}\sum_{l=1}^{j}\binom{N}{j}\left(\frac{\hat{I}(k-1)}{n-1}\right)^{j}\left(1-\frac{\hat{I}(k-1)}{n-1}\right)^{N-j}\hat{p}^{(m)} \times \\
& \left[\log\left[\binom{\underbrace{\hat{x}_{k-1}}}{\hat{y}_{0_k-1}}\binom{N}{j}\left(\frac{\hat{I}(k-1)}{n-1}\right)^{j}\left(1-\frac{\hat{I}(k-1)}{n-1}\right)^{N-j}\right]\right] \\
& + \sum_{k=1}^{T}\sum_{j=1}^{N}\sum_{l=1}^{j}\binom{N}{j}\left(\frac{\hat{I}(k-1)}{n-1}\right)^{j}\left(1-\frac{\hat{I}(k-1)}{n-1}\right)^{N-j}\hat{p}^{(m)} \times \\
& \left[\log\left[\binom{\hat{x}_{k-1}-\hat{y}_{0_k}}{\hat{z}_{0_k-1}}\binom{N}{j}\left(\frac{\hat{I}(k-1)}{n-1}\right)^{j}\left(1-\frac{\hat{I}(k-1)}{n-1}\right)^{N-j}\right]\right] \\
& + \sum_{k=1}^{T}\sum_{j=1}^{N}\sum_{l=1}^{j}\binom{N}{j}\left(\frac{\hat{I}(k-1)}{n-1}\right)^{j}\left(1-\frac{\hat{I}(k-1)}{n-1}\right)^{N-j}\hat{p}^{(m)} \times \\
& \left[\log\left[\binom{N}{j}\left(\frac{\hat{I}(k-1)}{n-1}\right)^{j}\left(1-\frac{\hat{I}(k-1)}{n-1}\right)^{N-j}\right]\right].
\end{aligned} \tag{5.47}$$

Also, (5.44) follows from Definition 2.4.

Remark 5.3 It follows from Theorem 5.1 that the M-step of the EM algorithm consists of maximizing $Q(p, \phi|\hat{p}^{(m)}, \hat{\phi}^{(m)})$ with respect to p, ϕ. This is equivalent to maximizing the non-constant term of (5.43).

In the next result, we present the M-step of the EM algorithm, and an implicit MLE for p, ϕ.

Theorem 5.2 *Let the E-step of the EM algorithm be as defined in Theorem 5.1. The M-step of the EM algorithm consists of solving the following nonlinear system of equations for p and ϕ.*

$$\frac{\phi}{1-\phi(1-p)}\sum_{k=1}^{T} N\left(\frac{\hat{I}(k-1)}{n-1}\right)(\underbrace{\hat{x}_{k-1}}-\hat{y}_{0_k})$$
$$-\left(\frac{1}{1-p}\right)\sum_{k=1}^{T} N\left(\frac{\hat{I}(k-1)}{n-1}\right)(\underbrace{\hat{x}_{k-1}}-\hat{z}_{0_k}+\hat{u}_{0k})$$
$$+\left(\frac{1}{p}\right)\sum_{k=1}^{T} N\left(\frac{\hat{I}(k-1)}{n-1}\right)(1+(\hat{z}_{0_k}+1)+1)=0, \tag{5.48}$$
$$-\frac{(1-p)}{1-\phi(1-p)}\sum_{k=1}^{T} N\left(\frac{\hat{I}(k-1)}{n-1}\right)(\underbrace{\hat{x}_{k-1}}-\hat{y}_{0_k})+\left(\frac{1}{\phi}\right)\sum_{k=1}^{T} N\left(\frac{\hat{I}(k-1)}{n-1}\right)(\hat{y}_{0k})$$
$$-\left(\frac{1}{1-\phi}\right)\sum_{k=1}^{T} N\left(\frac{\hat{I}(k-1)}{n-1}\right)(\hat{u}_{0_k})=0. \tag{5.49}$$

Moreover, the MLE of p and ϕ are given implicitly as the solutions of the system (5.48)–(5.49).

Proof From (5.43), observe that at the mth step, $m = 0, 1, 2, \ldots$, maximizing the Q-function defined in the E-step $Q(\Theta|\hat{\Theta}^{(m)})$ with respect to p and ϕ, consists of taking the derivatives of $Q(\Theta|\hat{\Theta}^{(m)})$ with respect to p and ϕ, that is,

$$\frac{\partial Q}{\partial p}=\frac{\phi}{1-\phi(1-p)}\sum_{k=1}^{T} N\left(\frac{\hat{I}(k-1)}{n-1}\right)(\underbrace{\hat{x}_{k-1}}-\hat{y}_{0_k})\hat{p}^{(m)}$$
$$-\left(\frac{1}{1-p}\right)\sum_{k=1}^{T} N\left(\frac{\hat{I}(k-1)}{n-1}\right)(\underbrace{\hat{x}_{k-1}}-\hat{z}_{0_k}+\hat{u}_{0k})\hat{p}^{(m)}$$
$$+\left(\frac{1}{p}\right)\sum_{k=1}^{T} N\left(\frac{\hat{I}(k-1)}{n-1}\right)(1+(\hat{z}_{0_k}+1)+1)\hat{p}^{(m)}, \tag{5.50}$$
$$\frac{\partial Q}{\partial \phi}=-\frac{(1-p)}{1-\phi(1-p)}\sum_{k=1}^{T} N\left(\frac{\hat{I}(k-1)}{n-1}\right)(\underbrace{\hat{x}_{k-1}}-\hat{y}_{0_k})\hat{p}^{(m)}$$
$$+\left(\frac{1}{\phi}\right)\sum_{k=1}^{T} N\left(\frac{\hat{I}(k-1)}{n-1}\right)(\hat{y}_{0k})\hat{p}^{(m)}$$
$$-\left(\frac{1}{1-\phi}\right)\sum_{k=1}^{T} N\left(\frac{\hat{I}(k-1)}{n-1}\right)(\hat{u}_{0_k})\hat{p}^{(m)}, \tag{5.51}$$

and solving the simultaneous system of equations $\frac{\partial Q}{\partial p}=0$, and $\frac{\partial Q}{\partial \phi}=0$ for p and ϕ. Observe that beyond the initial step, and the initial estimates $\hat{p}^{(0)}, \hat{\phi}^{(0)} \in (0, 1)$ for the parameters p and ϕ, the solutions for the system $\frac{\partial Q}{\partial p}=0$, and $\frac{\partial Q}{\partial \phi}=0$ have no

dependence on $\hat{p}^{(m)} \in (0, 1), \forall m = 0, 1, 2, \ldots$. This implies that the MLE for the parameters p and ϕ are obtained by solving the system $\frac{\partial Q}{\partial p} = 0$, and $\frac{\partial Q}{\partial \phi} = 0$, which reduces to (5.48)-(5.49).

6 Some Epidemiological Parameters for Evaluating the Occurrence of Epidemics

In this section, we calculate some epidemiological parameters to evaluate the prevalence of influenza. We consider disease control parameters, such as the basic reproduction number, and the probability of no spread. These parameters are used in [33–37]. Furthermore, these epidemiological parameters are calculated for the random process $\{B(t), t = 0, 1, 2, \ldots\}$, whenever the transition probabilities are defined in Theorem 4.1.

An important first step to evaluate the prevalence of a new disease, or to determine whether a new disease is strongly established in the population beyond the outbreak, is to compute the expected number of infectious cases present in the population at any time. If at any time, more people are infected than they are susceptible or immune to the disease, then the prevalence of the disease spread is aggressive and immediate control measures are required. For a random process such as $\{B(t), t \geq 0\}$, the expected number of infectious people at any time, for example, $E[I_0(t)|B(0)]$ is ensemble means, whereas available data for the disease epidemics from sources such as CDC and WHO [38–40] are time-series data. It is necessary to find estimators for the ensemble means using time-series data. Indeed, in an extension of this project, it is shown that the SVIR Markov chain model $\{B(t), t \geq 0\}$ is *ergodic and has a unique limiting distribution*. Moreover, the consistency of the estimators is exhibited.

In the following, we characterize the prevalence of influenza from the initial infected population. That is, we calculate the expected number of infected individuals that occur over time, given an initial infected population. This information is useful to determine whether an epidemic will occur from the initial infected population.

6.1 Expected Number of Infected Individuals

Recall Definition 2.4, for $t < \min\{T_1, T_2\}$, and $T_1 \leq t < T_2$,

$$I(t) = I_0(t) + I_1(t) + I_2(t) + \cdots + I_t(t). \tag{6.1}$$

Furthermore, for $T_2 \leq t < T_1$ and $t \geq \max\{T_1, T_2\}$,

$$I(t) = I_0(t) + I_1(t) + \cdots + I_{T_2-2} + I_{T_2-1}. \tag{6.2}$$

In the following result, we show that the expected infectious population over time, given the initial outbreak of influenza depends only the state of the process at one-time lag.

Lemma 6.1 *For any* $t = 0, 1, 2, \ldots,$

$$E[I_0(t)|B(t-1), B(t-2), \ldots, B(1), B(0)] = E[I_0(t)|B(t-1)], \tag{6.3}$$

and

$$E[I_0(t)|B(0)] = E[E[I_0(t)|B(t-1)]|B(0)]. \tag{6.4}$$

Proof It is easy to see from Theorem 3.1 and Theorem 4.1 that

$$\begin{aligned}
&E[I_0(t)|B(t-1), B(t-2), \ldots, B(1), B(0)] \\
&= \sum_z \sum_y zP(V_0(t) = y, I_0(t) = z|B(t-1), B(t-2), \ldots, B(1), B(0)) \\
&= \sum_z \sum_y zP(V_0(t) = y, I_0(t) = z|B(t-1)) \\
&= E[I_0(t)|B(t-1)].
\end{aligned} \tag{6.5}$$

Also, by applying the properties of conditional expectations, for any $t = 0, 1, 2, \ldots,$

$$E[I_0(t)|B(0)] = E[E[I_0(t)|B(t-1), B(t-2), \ldots, B(1), B(0)]|B(0)]. \tag{6.6}$$

From (6.5), it follows that (6.6) reduces to,

$$E[I_0(t)|B(0)] = E[E[I_0(t)|B(t-1)]|B(0)] \tag{6.7}$$

definitely.

Using Lemma 6.1, we present in general form the expected number of infectious people present at any time t, given the population at the initial outbreak.

Theorem 6.1 *Let the assumptions of Theorem 3.1 and Theorem 4.1 hold. For* $t < min\{T_1, T_2\}$ *and* $t \in [T_1, T_2)$*, it follows that*

$$E[I(t)|B(0)] = I_0(0) + \sum_{k=1}^{t-1} E\left[S(t-k-1)\left(1 - \left(1 - \frac{pI(t-k-1)}{n-1}\right)^N\right)|B(0)\right]. \tag{6.8}$$

For $t \in [T_2, T_1)$ *and* $t \geq \max\{T_1, T_2\}$,

$$E[I(t)|B(0)] = \sum_{k=1}^{T_2-1} E\left[S(t-k-1)\left(1 - \left(1 - \frac{pI(t-k-1)}{n-1}\right)^N\right)|B(0)\right]. \tag{6.9}$$

Proof For $t < min\{T_1, T_2\}$,

$$\begin{aligned} I(t) &= I_0(t) + I_1(t) + I_2(t) + \cdots + I_t(t) \\ &= I_0(t) + I_0(t-1) + I_0(t-2) + \cdots + I_0(1) + I_0(0). \end{aligned} \tag{6.10}$$

$$\begin{aligned} E[I(t)|B(0)] &= E[I_0(t)|B(0)] + E[I_0(t-1)|B(0)] + \ldots \\ &\quad + E[I_0(1)|B(0)] + E[I_0(0)|B(0)] \\ &= I_0(0) + \sum_{k=1}^{t-1} E[I_0(t-k)|B(0)]. \end{aligned} \tag{6.11}$$

For each $k = 1, 2, 3, \ldots, t-1$, applying Lemma 6.1

$$\begin{aligned} E[I_0(t-k)|B(0)] &= E[E[I_0(t-k)|B(t-k-1)]|B(0)] \\ &= E[S(t-k-1)P_I(t-k)|B(0)] \\ &= E\left[S(t-k-1)\left(1 - \left(1 - \frac{pI(t-k-1)}{n-1}\right)^N\right)|B(0)\right], \end{aligned} \tag{6.12}$$

where $P_I(t-k)$ is defined in (4.4). Substituting (6.12) into (6.11), we obtain the result in (6.8). Observe that the result for $t \in [T_1, T_2)$ is obtained similarly as above.

For $t \in [T_2, T_1)$ and $t > \max\{T_1, T_2\}$

$$\begin{aligned} I(t) &= I_0(t) + I_1(t) + I_2(t) + \cdots + I_{T_2-1}(t) \\ &= I_0(t) + I_0(t-1) + I_0(t-2) + \cdots + I_0(t-(T_2-1)). \end{aligned} \tag{6.13}$$

$$\begin{aligned} E[I(t)|B(0)] &= E[I_0(t)|B(0)] + E[I_0(t-1)|B(0)] + \ldots \\ &\quad + E[I_0(t-(T_2-1)|B(0)] \\ &= \sum_{k=0}^{T_2-1} E[I_0(t-k)|B(0)]. \end{aligned} \tag{6.14}$$

For each $k = 0, 1, 2, 3, \ldots, (T_2-1)$ applying Lemma 6.1

$$
\begin{aligned}
E[I_0(t-k)|B(0)] &= E[E[I_0(t-k)|B(t-k-1)]|B(0)] \\
&= E[S(t-k-1)P_I(t-k-1)|B(0)] \\
&= E\left[S(t-k-1)\left(1-\left(1-\frac{pI(t-k-1)}{n-1}\right)^N\right)|B(0)\right],
\end{aligned}
\tag{6.15}
$$

where P_I is defined in (4.4). Substituting (6.15) into (6.14), we obtain (6.9).

Remark 6.1 It should be observed from Theorem 6.1 that an explicit form for the conditional expectation (6.8) and (6.9) can only be obtained provided the joint distribution of $(S(t), I(t)), \forall t \geq 0$ is known. However, since (6.8) and (6.9) represent population parameters at time t (conditional population means), which are a sum of random variables that represent observations over time until the time t, these parameters can be estimated point-wise using sample paths of the process $\{B(t), t = 0, 1, 2, \dots\}$, and the MLE of p obtained in Theorem 5.2.

For example, for $t > \max\{T_1, T_2\}$, (6.9) can be estimated using the sample path of

$$
\begin{aligned}
&(S(t-k-1), I_0(t-k-1), I_1(t-k-1), \dots, I_{t-k-1}(t-k-1)) = \\
&(\hat{x}_{t-k-1}, \hat{z}_{0_{t-k-1}}, \hat{z}_{1_{t-k-1}}, \dots, \hat{z}_{t-k-1_{t-k-1}}), \\
&k = 0, 1, 2, \dots, T_2 - 1.
\end{aligned}
\tag{6.16}
$$

The next result presents the estimates for the conditional population means at any time t,

Theorem 6.2 *Assume that the conditions of Theorem 6.1 are satisfied. For* $t > \max\{T_1, T_2\}$, *the conditional expected value in (6.9) denoted* $\mu_{I(t)|B(0)} = E[I(t)|B(0)]$ *can be estimated using the sample path of the process* $\{B(t), t = 0, 1, 2, \dots\}$ *namely:-*

$$
\begin{aligned}
&(S(t-k-1), I_0(t-k-1), I_1(t-k-1), \dots, I_{t-k-1}(t-k-1)) = \\
&(\hat{x}_{t-k-1}, \hat{z}_{0_{t-k-1}}, \hat{z}_{1_{t-k-1}}, \dots, \hat{z}_{t-k-1_{t-k-1}}), \\
&k = 0, 1, 2, \dots, T_2 - 1.
\end{aligned}
\tag{6.17}
$$

In fact, for $t > \max\{T_1, T_2\}$ *and* $t \in [T_2, T_1)$

$$
\hat{\mu}_{I(t)|B(0)} = \sum_{k=0}^{T_2-1}\left[\hat{x}_{t-k-1}\left(1-\left(1-\frac{\hat{p}\sum_{j=0}^{t-k-1}\hat{z}_{j_{t-k-1}}}{n-1}\right)^N\right)\right] \tag{6.18}
$$

estimates $\mu_{I(t)|B(0)} = E[I(t)|B(0)]$ *defined in (6.9).*

Also, for $t < min\{T_1, T_2\}$ *and* $t \in [T_1, T_2)$

$$\hat{\mu}_{I(t)|B(0)} = \hat{z}_{0_0} + \sum_{k=1}^{t-1} \left[\hat{x}_{t-k-1} \left(1 - \left(1 - \frac{\hat{p} \sum_{j=0}^{t-k-1} \hat{z}_{j_{t-k-1}}}{n-1} \right)^N \right) \right] \tag{6.19}$$

estimates $\mu_{I(t)|B(0)} = E[I(t)|B(0)]$ *defined in (6.8), where* $\hat{p}$ *is the MLE of p defined in (5.48).*

Proof The results follow simply from (5.44) and the definition of $\mu_{I(t)|B(0)} = E[I(t)|B(0)]$ defined in (6.9) and (6.8).

6.2 The Basic Reproduction Number for the SVIR Influenza Epidemic

The basic reproduction number, generally denoted R_0, is the expected number of secondary cases of infection from one infectious person or from an initial number of infectious people, $I(0) = z_{0_0}$, placed in a completely susceptible population, and it is the most widely used predictor of an epidemic outbreak. If $R_0 < 1$, the disease is expected to die out. If $R_0 > 1$, the disease is expected to spread out of control.

The basic reproduction number is highly dependent on the initial infectiousness of the disease and the duration of the disease in the initial infectious population. The basic reproduction number is important to determine disease control factors for an epidemic [33–36]. In the absence of an explicit formula for the basic reproduction number R_0, it can be estimated empirically using the methods in this section.

Observe from (6.8) that while $I_0(0)$ is the initial infectious population, the second term $\sum_{k=1}^{t-1} E\left[S(t-k-1) \left(1 - \left(1 - \frac{pI(t-k-1)}{n-1} \right)^N \right) |B(0) \right]$ represents the expected number of secondary infectious cases present at time t, given that the initial disease outbreak had only $I_0(0)$ number of infectious cases. Therefore, $\sum_{k=1}^{T_2-1} E\left[S(T_2-k-1) \left(1 - \left(1 - \frac{pI(T_2-k-1)}{n-1} \right)^N \right) |B(0) \right]$ must be the basic reproduction number given that $I_0(0) = 1$, where T_2 is the constant infectious period of every infectious person in the population. Using the results of Theorem 6.2, the basic reproduction number R_0 can be estimated in the following.

Corollary 1 *Let the assumptions of Theorem 6.1 and Theorem 6.2 be satisfied. The basic reproduction number is given implicitly as follows:*

$$R_0 = E[I(T_2)|B(0)] = \sum_{k=1}^{T_2-1} E\left[S\,(T_2-k-1) \left(1 - \left(1 - \frac{pI(T_2-k-1)}{n-1} \right)^N \right) |B(0) \right], \tag{6.20}$$

For $t \leq T_2$, (6.20) can be estimated using the following sample path of the process $\{B(t), t = 0, 1, 2, \dots\}$

$$\begin{aligned}&\big(S(T_2-k-1), I_0(T_2-k-1), I_1(T_2-k-1), \dots, I_{T_2-k-1}(T_2-k-1)\big) = \\ &(\hat{x}_{T_2-k-1}, \hat{z}_{0_{T_2-k-1}}, \hat{z}_{1_{T_2-k-1}}, \dots, \hat{z}_{T_2-k-1_{T_2-k-1}}), \\ &k = 1, 2, \dots, T_2 - 1. \end{aligned} \tag{6.21}$$

Furthermore, the estimate for R_0 is given as follows

$$\hat{R}_0 = \sum_{k=1}^{T_2-1} \hat{x}_{T_2-k-1} \left(1 - \left(1 - \frac{\hat{p} \sum_{j=0}^{T_2-k-1} \hat{z}_{j_{T_2-k-1}}}{n-1}\right)^N\right). \tag{6.22}$$

Proof The result follows very easily from the definition of the basic reproduction number, (6.19), and setting $t = T_2$, since T_2 is the infectious period of individuals in the population.

Remark 6.2 It should be observed from Corollary 1 that an explicit form for the basic reproduction number in (6.20) can only be obtained provided the joint distribution of $(S(t), I(t))\forall t \geq 0$ is known. However, since (6.20) represents a population parameter at time t, which is a sum of random variables that represent observations over time until the time t, this parameter is easily estimated point-wise using the sample path of the process $\{B(t), t = 0, 1, 2, \dots\}$ given in (6.21), and the MLE of p obtained in (5.51).

The advantage of $\hat{R}_0$ in (6.22) as an initial point estimate for the actual value R_0 is its dependence primarily on empirical data for influenza obtained over time, and also the dependence on the feasible estimated value of the probability of passing infection from one infectious contact p. Furthermore, with limited real data over several possible sample realizations for the stochastic process $\{B(t), t = 0, 1, 2, \dots\}$ over a given time interval, the statistic $\hat{R}_0$ can be studied numerically and the approximate sampling distribution generated and studied.

More interval estimates for the parameter R_0 in (6.20), require explicit sampling distribution for the point estimate $\hat{R}_0$, which are beyond the scope of this work.

Observe from (4.4) and (6.22) that for each $k \in \{1, 2, \dots, T_2 - 1\}$, the term $\left(1 - \left(1 - \frac{\hat{p} \sum_{j=0}^{T_2-k-1} \hat{z}_{j_{T_2-k-1}}}{n-1}\right)^N\right)$ is the estimated probability of getting infection at every time step over the remaining infectious period $T_2 - 1$ of the initial infectious population $I_0(0) = 1$. It is easy to see that the estimated basic reproduction number $\hat{R}_0$ in (6.22) is a weighted sum of the susceptible population $\hat{x}_{T_2-k-1}$ at each time step $k \in \{1, 2, \dots, T_2 - 1\}$ in the sample path (6.21), where the weights are $\left(1 - \left(1 - \frac{\hat{p} \sum_{j=0}^{T_2-k-1} \hat{z}_{j_{T_2-k-1}}}{n-1}\right)^N\right)$. One way the estimated basic reproduction

number $\hat{R}_0 < 1$ is when the weights $\left(1 - \left(1 - \frac{\hat{p}\sum_{j=0}^{T_2-k-1}\hat{z}_{jT_2-k-1}}{n-1}\right)^N\right) \ll 1$. Moreover, the weights are infinitesimally small, whenever $\hat{p} \ll 1$. This observation suggests that one way to eradicate the disease from the population is to ensure the chance of getting infected at any time step $k \in \{1, 2, \ldots, T_2 - 1\}$ is infinitesimally small. Thus, in addition to enforcing vaccination as a disease control measure against influenza, other measures that prevent contact with infected people must also be enforced, to fully eradicate the disease.

7 Example for the EM Algorithm

To illustrate the EM algorithm presented in Sect. 5.1, the influenza data [38–40] for the state of Georgia, USA, collected over 52 weeks in the years 2017–2018 by the collaborating WHO and National Respiratory And Enteric Virus Surveillance System (NREVSS) laboratories that are reporting to the CDC, is used to formulate the characteristics of a hypothetical population suffering from an influenza epidemic, and further used to calculate the MLEs for the parameters p and ϕ of the influenza model. The following assumptions are made about the hypothetical population.

(1) It is assumed that the population has a fixed size $n = 10{,}519{,}475$ which is equivalent to the population size of the state of Georgia in 2018 [40], and over the period of 52 weeks considered in this problem, the population is closed. In addition,
(2) The influenza epidemic is caused by the influenza type A virus, and the total number of new infections reported each week are assumed to follow the data in Fig. 3 exhibited in [38].
(3) It is also assumed that vaccination occurs each week and follows the weekly estimates also exhibited in Fig. 3, which are constructed by randomly selecting numbers in the local monthly cumulative influenza-vaccination coverage interval estimates in [39], for adults 18 years of age, and older. Observe from Fig. 3 that vaccination rises with the rise in infection. This observation is very typical for most influenza epidemics which are seasonal, and more people seek vaccination, whenever there is a rise in infection.
(4) The period of effective artificial immunity is assumed to be more than 52 weeks, that is, $T_1 > 52$, such that the class $\widetilde{S(t)} = 0$ for the entire duration over which observations are made. It is also assumed that the infectious period T_2 is only one week, beyond which all infectious persons are fully recovered and removed with permanent immunity against the disease. The condition (4) implies that the initial susceptible population continuously decreases over the 52 weeks of observing the epidemic, owing to continuous infection, and vaccination. Furthermore, the infectious population present at the end of any week will be only those who are just infected on that week.

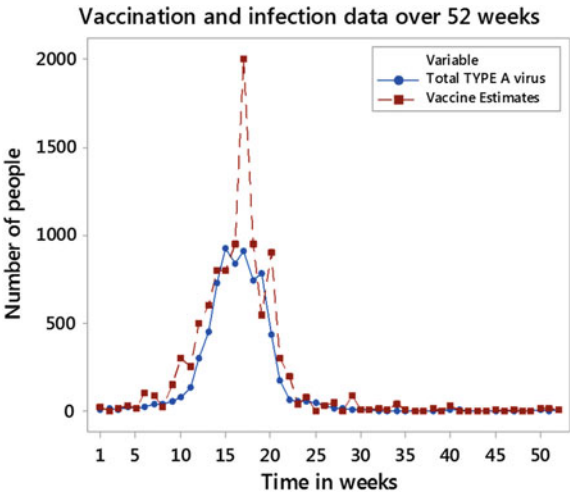

Fig. 3 Shows a time-series graph for the number of people vaccinated and infected with influenza type A virus every week, and over a period of 52 weeks

(5) It is also assumed for simplicity that every susceptible person meets a fixed number $N = 5$ other people per unit time. The initial infectious population is assumed to be 8 people, and nobody is assumed to be vaccinated or removed in the population initially.

From the above assumptions (1)–(5), and the data in [38–40] exhibited in Fig. 3, it follows from Theorem 5.2 that the M-step of the EM algorithm consists of solving the nonlinear system of equations[1]

$$1339359\frac{\phi}{1-\phi(1-p)} - 2678625\left(\frac{1}{1-p}\right) + 81.82526\left(\frac{1}{p}\right) = 0, \quad (7.1)$$

$$-1339359\frac{(1-p)}{1-\phi(1-p)} + 105.9085\left(\frac{1}{\phi}\right) - 1339080\left(\frac{1}{1-\phi}\right) = 0. \quad (7.2)$$

It follows that using the convenient choice of initial estimates $\hat{p}^{(0)} = 0.001$, $\hat{\phi}^{(0)} = 0.001$ for the parameters p and ϕ, the MLEs using MATLAB are $\hat{\phi} = 0.3954 * 1.0e - 04$, and $\hat{p} = 0.3055 * 1.0e - 04$.

These numbers- $\hat{\phi} = 0.3954 * 1.0e - 04$, and $\hat{p} = 0.3055 * 1.0e - 04$ seem to be plausible estimates for p and ϕ, since clearly from Fig. 3, the vaccination rate is greater than the infection rate.

When the fixed infectious period T_2 in (4) is increased to two weeks for every infectious person, and the other parameters remain the same as above, it follows that using the convenient choice of initial estimates $\hat{p}^{(0)} = 0.001$, $\hat{\phi}^{(0)} = 0.001$ for the parameters p and ϕ, the MLEs using MATLAB are $\hat{\phi} = 0.2836 * 1.0e - 03$, and $\hat{p} = 0.2165 * 1.0e - 03$. The basic reproduction number in (6.20) reduces to

[1]The cumulative sums in (5.48)–(5.49) were calculated using "for-loops" in *R*.

$$R_0 = E[I(2)|B(0)] = E\left[S(0)\left(1-\left(1-\frac{pI(0)}{n-1}\right)^N\right)|B(0)\right]$$
$$= S(0)\left(1-\left(1-\frac{pI(0)}{n-1}\right)^5\right), \tag{7.3}$$

where $S(0)$ and $I(0)$ are positive constants. Moreover, using the assumptions (1)–(5), the estimate for R_0 defined in (6.22) is given as follows

$$\hat{R}_0 = \hat{x}_0\left(1-\left(1-\frac{\hat{p}\hat{z}_{00}}{n-1}\right)^N\right)$$
$$= (1{,}051{,}475-8)\left(1-\left(1-\frac{(0.2165*1.0e-03)(8)}{10{,}519{,}475-1}\right)^5\right)$$
$$= 0.0175287. \tag{7.4}$$

Based on the value of $\hat{R}_0 = 0.0175287 < 1$, this suggests the disease is under control through the vaccination process.

8 Conclusion

In this study, we have sufficiently defined an SVIR Markov chain model for influenza which effectively shows the progression of the disease and effectiveness of the vaccine to control the disease over time for an individual in the population. Moreover, we defined the transition probabilities for the model. We presented two special cases of our model-(1) based on the assumption that the event of getting vaccinated at any instant depends on encounter with infectious people, and (2) the vaccination occurring over time with as a Poisson process. We present detailed derivations of the probabilities of the ith susceptible individual getting vaccinated or infected at any instant and further define the transition probabilities for each special case of the model.

We further used the maximum likelihood estimation technique and the expectation–maximization (EM) algorithm to approximate the fixed parameters of the model. To evaluate the occurrence and prevalence of the epidemic, we derived estimators for the basic reproduction number R_0 and the expected number of infected individuals at any time t.

Finally, we presented numerical simulation examples for the influenza epidemic and approximate the distribution of the total number of people in the population who ever get infected. Given these scenarios, we see how vaccination can curb the spread of influenza, and that the most limiting factor when trying to control the spread of influenza is the number of infectious people one interacts with per unit time.

Acknowledgements This work was completed during the graduate studies of Cameron Newman, Omotomilola Jegede and Mymuna Monem in the department of Mathematical Sciences of Georgia Southern University (GSU) in 2018–2019 academic year, supervised by Dr. Wanduku. Mymuna Monem was part of the general group discussions.

References

1. CDC Estimating Seasonal Influenza-Associated Deaths. https://www.cdc.gov/flu/about/disease/us_flu-related_deaths.htm
2. D. Iuliano, K.Roguski, H. Chang, D. Muscatello, R. Palekar, S. Tempia et al., Estimates of global seasonal influenza-associated respiratory mortality: a modelling study. Lancet **391**(10127), 1285–1300, 31 Mar 2018
3. WHO Influenza, burden of disease. http://www.who.int/influenza/surveillance_monitoring/bod/en/
4. CDC Flu symptoms and complications. https://www.cdc.gov/flu/consumer/symptoms.htm/
5. CDC Types of Influenza Viruses. https://www.cdc.gov/flu/about/viruses/types.htm
6. CDC How Flu Spreads. https://www.cdc.gov/flu/about/disease/spread.htm
7. CDC Different types of flu vaccines. https://www.cdc.gov/flu/vaccines/index.htm
8. H.C. Tuckwell, R,J. Williams, Some properties of a simple stochastic epidemic model of SIR type. Math. Biosci. **208**, 76–97 (2007)
9. D. Wanduku, Threshold conditions for a family of epidemic dynamic models for malaria with distributed delays in a non-random environment, Int. J. Biomath. **11**(6) 1850085 (46 pages) (2018). https://doi.org/10.1142/S1793524518500857
10. P. Witbooi, G.E. Muller, G.J. Van Schalkwyk, Vaccination control in a stochastic SVIR epidemic model. Comput. Math. Methods Med. **2015**, Article ID 271654, 9 pages (2015). https://doi.org/10.1155/2015/271654
11. D. Wanduku, Complete global analysis of a two-scale network SIRS epidemic dynamic model with distributed delay and random perturbation. Appl. Math. Comput. **294**, 49–76 (2017)
12. D. Wanduku, G.S. Ladde, Global properties of a two-scale network stochastic delayed human epidemic dynamic model. Nonlinear Anal. Real World Appl. **13**, 794–816 (2012)
13. F. Etbaigha, A. Willms, Z. Poljak, An SEIR model of influenza A virus infection and reinfection within a farrow-to-finish swine farm. PLOS ONE **13**(9), e0202493. https://doi.org/10.1371/journal.pone.0202493
14. M.E. Alexander, C. Bowman, S.M. Moghadas et al., Vaccination model for transmission dynamics of influenza. SIAM J. Appl. Dyn. Syst. **3**, 503–524 (2004)
15. D. Wanduku, The stochastic extinction and stability conditions for nonlinear malaria epidemics. Math. Biosci. Eng. **16**, 3771–3806 (2019)
16. A. Scherer, A.R. McLean, Mathematical models of vaccination. Brit. Med. Bull. **62**, 187–199 (2002)
17. H.S. Rodrigues, M.T.T. Monteiro, D.F.M. Torres, Vaccination models and optimal control strategies to dengue. Math. Biosci. **247**, 1–12 (2014)
18. A. Lloyd, *Introduction to Epidemiological Modeling: Basic Models and Their Properties* 23 Jan. 2017
19. M. Li, J.R. Graef, L. Wang, J. Karsai, Global dynamics of a SEIR model with varying total population size. Math. Biosci. **160**, 191–213 (1999)
20. C.M. Kribs-Zaleta, J.X. Velasco-Hernández, A simple vaccination model with multiple endemic states. J. Math. Biosci. **164**, 183–201 (2000)
21. D. Wanduku, G.S. Ladde, Fundamental properties of a two-scale network stochastic human epidemic dynamic model. Neural Parallel Sci. Comput. **19**, 229–270 (2011)
22. M. Ferrante, E. Ferraris, C. Rovira, On a stochastic epidemic SEIHR model and its diffusion approximation. TEST **25**, 482 (2016). https://doi.org/10.1007/s11749-015-0465-z

23. R. Yaesoubi, T. Cohen, Generalized Markov models of infectious disease spread: a novel framework for developing dynamic health policies. Eur. J. Oper. Res. **215**(3) (2011)
24. M. Greenwood, On the statistical measure of infectiousness. J. Hyg. Camb. **31**, 336 (1931)
25. H. Abbey, An examination of the Reed-Frost theory of epidemics. Hum. Biol. **24**, 201 (1952)
26. J. Jacquez, A note on chain binomial models of epidemic spread: what is wrong with the Reed-Frost Model. Mathem. Biosci. **87**(1), 73–82 (1987)
27. J. Gani, D. Jerwood, Markov chain methods in chain binomial epidemic models. Biometrics **27** (1971)
28. J. Lin, V. Andreasen, S.A. Levin, Dynamics of influenza A; the linear three strain model. Math. Biosci. **162**, 33–51 (1999)
29. M. Ajelli, P. Poletti, A. Melegaro S. Merler, The role of different social contexts in shaping influenza transmission during the 2009 pandemic. Sci. Rep. **4**, Article number: 7218 (2014)
30. L. Allen, An introduction to stochastic epidemic models, in *Mathematical Epidemiology* ed. by Brauer F., van den Driessche P., Wu J. Lecture Notes in Mathematics, vol. 1945 (Springer, Berlin, Heidelberg), pp. 81–130
31. M. Gupta, Y. Chen, Theory and use of the EM Algorithm. Found. Trends Sig. Process. **4**(3) (2010)
32. J. Bilmes, A gentle tutorial of the EM algorithm and it's Application to parameter estimation for Gausian mixture and hidden Markov models. Int. Comput. Sci. Inst. (1998)
33. G. Casella, R. Berger, *Statistical Inference*, 2 edn. (Duxbury, 2002)
34. K. Dietz, The estimation of the basic reproduction number for infectious diseases. Stat Methods Med Res. **2**(1), 23–41 (1993)
35. J. Jones, *Notes on* R_0 (Stanford University, Department of Anthropological Sciences, 2007)
36. P. Holme, N. Masuda, The basic reproduction number as a predictor for epidemic outbreaks in temporal networks. PLoS ONE **10**(3) (2015)
37. E. Vergu, H. Busson, P. Ezanno, Impact of the infection period distribution on the epidemic spread in a metapopulation model. PLoS ONE **5**(2) (2010)
38. CDC-FLUVIEW(1-17-2019). https://gis.cdc.gov/grasp/fluview/fluportaldashboard.html; https://www.cdc.gov/flu/weekly/weeklyarchives2017-2018/Week39.htm
39. FluVaxView 2017-18 Season. https://www.cdc.gov/flu/fluvaxview/coverage-1718estimates.htm
40. US census Bureau, 2018 National and State Population Estimates. https://www.census.gov/newsroom/press-kits/2018/pop-estimates-national-state.html

A Two-Dimensional Dynamical System for Local Transmission of Dengue with Time Invariant Mosquito Density

W. P. T. M. Wickramaarachchi and S. S. N. Perera

1 Introduction

Dengue fever (DF) and its severe form, the dengue hemorrhagic fever (DHF), is one of the most common widespread vector-borne diseases in the world. According to the World Health Organization (WHO), dengue disease is ranked as one of the most critical infectious diseases with severe impact on public health and well-being in the society [1, 2]. The disease has spread to almost all tropical and sub-tropical parts in the world, and it has been estimated that nearly 2.5 billion people in more than 100 countries are at risk [3]. Globally, every year, approximately 50 million dengue infections occur; half a million DHF cases require hospitalization with over 20,000 deaths [1, 3, 4]. The economic impact of DF/DHF is massive, placing significant burdens on affected nations and their communities. This impact varies and can include deaths, medical expenditures for hospitalization of patients and their careful clinical management, loss in productivity of the affected workforce, strain on healthcare services due to sudden, high demand during an epidemic, considerable expenditures for large-scale emergency control actions taken by the government in an outbreak, etc [5].

Dengue fever (DF) and dengue hemorrhagic fever (DHF) are endemic in Sri Lanka now since the first reported outbreak of dengue fever in 1965 [6]. There has been recurring outbreaks for the last five decades created some severe damages to public health and well-being of Sri Lankan people. During the first four decades of dengue in Sri Lanka, the burden had not been very severe. However, due to population growth, urbanization, unsystematic development, and climate change, dengue became a serious public health concern since 2008. The trend in dengue cases in Sri Lanka since year 2002 till 2018 is illustrated in Fig. 1.

W. P. T. M. Wickramaarachchi (✉)
Department of Mathematics, The Open University of Sri Lanka, Nawala, Nugegoda, Sri Lanka
e-mail: wpwic@ou.ac.lk

S. S. N. Perera
Research and Development Center for Mathematical Modeling, Department of Mathematics, University of Colombo, Colombo 03, Sri Lanka
e-mail: ssnp@maths.cmb.ac.lk

H. Dutta (ed.), *Mathematical Modelling in Health, Social and Applied Sciences*, Forum for Interdisciplinary Mathematics, https://doi.org/10.1007/978-981-15-2286-4_3

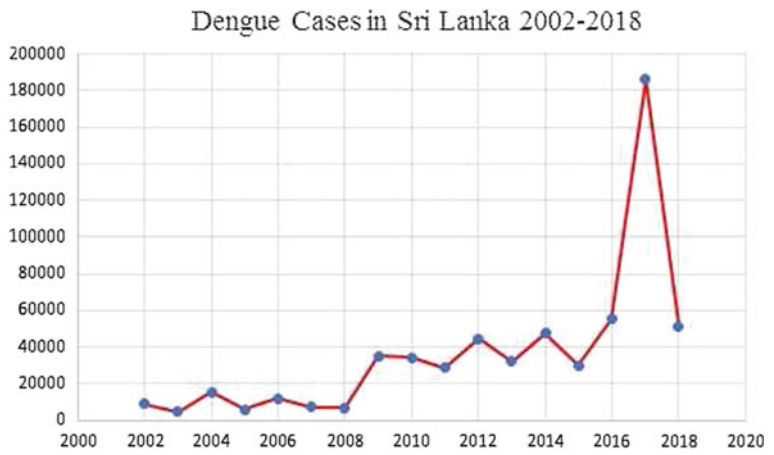

Fig. 1 Dengue trend in Sri Lanka from year 2002 to 2018. *Source* http://www.epid.gov.lk/web

In the year 2012, a total of 44,461 cases of dengue have been reported around the country. However, in the year 2013, number of cases has dropped to 32,063 but increased to 47,502 cases in the year 2014. Over the history of dengue in Sri Lanka, country went through its extremely high outbreak in year 2017 where cases amounted up to 180,000. Of them, the largest proportion was reported from the Colombo District which is the most urbanized and densely populated of the country [7]. Colombo is the capital and the largest city in Sri Lanka; its rapid urbanization and increased human movements have created Colombo a highly vulnerable geographic area for dengue disease. Out of them, the majority of the cases were reported in Colombo city area where the urban population is at high risk to be infected. Figure 2 shows the trend of dengue cases in Colombo Municipal Council (CMC) Area from the year 2006 to 2017.

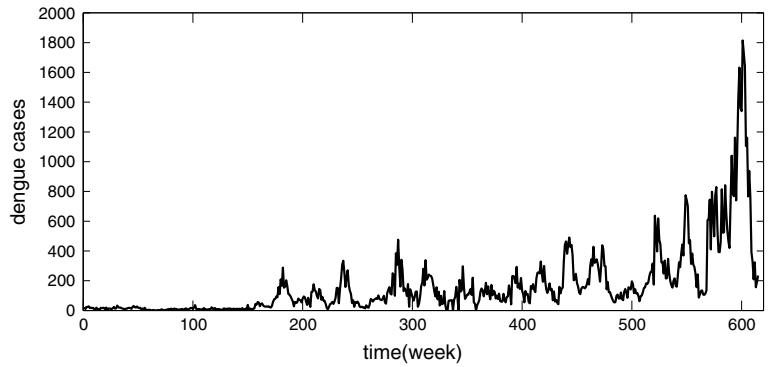

Fig. 2 Weekly reported dengue cases in Colombo Municipal Council area from 2006 to 2017

During the outbreak period, mainly after the monsoon season in Sri Lanka, a country usually goes through emergency states to control the negative impact to the national economy and the social stability and well-being of people. Government allocates a reasonable portion of funds for dengue control programs, awareness session for public and school children and dengue patient management in hospitals. Though the mortality rate due to dengue in Sri Lanka is fairly low compared to the number of cases reported, households face serious socio-economic problems as the patients may be advised to rest for months.

There is no vaccine or any specific treatment found for dengue disease yet and several researches for a vaccine are currently in progress [3, 8]. For the time being, the only mechanism for preventing and controlling DF/DHF is to ensure prompt diagnosis of cases of fever and appropriate clinical management during the hospitalization, to reduce human–vector contact, and to control larval habitats [8]. Therefore, it is very critical to investigate the dynamic of the dengue transmission by identifying the driving factors for disease propagation in the population. Having a thorough understanding of the dynamic may help the decision makers and public health professional to minimize the burden of the disease.

Dengue is a multi-factorial vector-borne disease as the transmission depends on numerous factors such as climate, demography in the area, geo-spatial characteristics, and the biological factors in the dengue mosquito. Due to this nature of the transmission, dengue has been identified as a disease with a very complex and uncertain transmission process. Among the factors of dengue disease transmission, climate variations play a major role. It is known that water bodies are essential for mosquitoes for breeding. Most of these sites are made by the rainfall [10, 11]. This has been justified that in Sri Lanka, we experience dengue outbreaks a few weeks after the monsoon periods. In addition to rainfall, temperature variation is also a sensitive factor in the dengue transmission dynamic. Researchers have found that a reasonably high-temperature level has increased the vectorial capacity and these favorable levels of temperature have an impact on the incubation period of mosquitoes in a way which supports the transmission positively [14, 15, 22]. Due to these facts, it is very critical to identify the relationship of these climate variation to the transmission of disease [10].

Dengue cases time series data are highly noisy due to the complexity and multifactor nature of the transmission so are climate data such as rainfall and temperature. As a result of this, classical time series models are not appropriate to identify the relationships. Thus, in this study, we use wavelet analysis and it enables us to investigate the spectral properties of the time series along with the correlations of the oscillations. These properties are essential to estimate out parameters in the transmission models.

Identification of these relationships may not only be sufficient to estimate the critical parameters in the model. It is known that most of these climate factors are uncertain. For example, high level of rainfall is not suitable for mosquito reproduction as the breeding sites may be washed out. Further, mosquitoes are unable to survive in extremely high-temperature levels [10]. It is also found that one factor may be in a favorable level while another is highly unfavorable for mosquitoes. This

unpredictable nature in the transmission process has to be addressed. The traditional approach to model parameters randomly has been the probabilistic by identifying a suitable probability density. However, this is very challenging with epidemic data since they are not reliable or they are not sufficient enough to figure out the probability distributions precisely. Thus, it is proposed a fuzzy set theory approach to model the parameters considering uncertainty, which is now being highly used in modeling data. Membership functions are defined for two factors, namely rainfall and temperature, considering their level of influence to make a favorable environment for mosquitoes not only to reproduce but also to propagate the virus.

It is also known that the mosquito density is critical when we consider the transmission locally; however, the human mobility is responsible to transmit the disease globally among multiple geographic locations. Many studies suggest that the mosquito density is an extremely sensitive factor and it is very responsive to climate variation induced mainly by temperature and rainfall. A favorable level of rainfall and temperature increases the reproduction of dengue mosquitoes; hence, it supports to rise the mosquito density in the environment.

Mathematical models are used to describe various real-world processes. Over the last century, a large number of these models have been developed to investigate the dynamic of numerous epidemic diseases [21]. They describe how the disease propagates over the population with interactions between the human and vector populations. However, most of them describe the dynamical behavior with considering fixed parameter values [9, 21, 23]. In order to study the dynamical behavior with varying parameters is still a challenging task. The estimation of these with respect to external factors should be done under uncertainty and the fully stochastic models are not appropriate since we do not know the underlying probability distributions and lack of reliable epidemiological data. This study aims to develop a mathematical model for dengue disease transmission in which the critical parameters are time invariant and they vary with respect to external forces. The techniques of estimating these dynamic parameters under uncertainty are also developed.

This chapter is organized into two sections. First, it is discussed how the critical parameters are estimated using available data. Noisy data are analyzed using wavelet transformation, and significant relationships between dengue incidents and external factors such as climate are identified. These results may then be used to model the critical parameters considering the uncertainty nature of the process. Since sufficiently reliable data are unavailable, probabilistic techniques may not be applicable to model the uncertainty. Thus, fuzzy set theory is used to overcome this challenge. Membership functions are developed considering the impact from rainfall and temperature to create a suitable environment for dengue mosquitoes to grow and transmit the virus. Next, a discrete time dynamic model for mosquito density is developed in which the fuzzy-based climate force for dengue disease is an input.

Secondly, a two-dimensional mathematical model for dengue transmission is also derived using only susceptible and infected human population proportions and considering quasi-equilibrium status for mosquitoes. We assume there are sufficiently

enough number of infected mosquitoes in the environment and this population is stable. Possible analytical and numerical results are obtained and discussed. Next, the two-dimensional system is solved together with the discrete time mosquito density model and the results are critically compared with the deterministic case. For this model, an aggregate control measure is also introduced and it is investigated how the infected human proportion is reduced as a result of increasing efficacy of the control actions. For model validation and comparison, reported dengue incidence cases in Colombo are used. Hence, model development and methods comparison are done using Colombo data.

2 Analysis of Factors of Dengue Transmission in Colombo

In this study, we analyze dengue incidents time series using wavelet approach which is a more sophisticated tool to analyze dengue data compared to statistical techniques. The influence of climate variation to dengue transmission is analyzed using cross-wavelet approach and wavelet coherence analysis.

Climate variations play an important role in occurring dengue outbreaks in Colombo. After the rainy season, it is reported large dengue outbreaks in Colombo each year. Therefore, it is important to identify the patterns of dengue outbreaks and the relationship between climate variation and dengue incidents in Colombo so that this relationship can be used to model the parameters in mathematical model of dengue transmission dynamically.

2.1 Wavelet Transform

Wavelets are finite energy functions which are capable of representing time–frequency localization of a transient signal with only a small finite number of coefficients [12, 24].

Definition 1 If $\psi \in L^2(\mathbb{R})$ satisfies the *admissibility* condition given by

$$C_\psi = \int_{-\infty}^{\infty} \frac{|\hat{\psi}(\omega)|^2}{|\omega|} d\omega < \infty, \tag{1}$$

then, ψ is called a *basic wavelet* and, with respect to any basic wavelet ψ, the integral/continuous wavelet transform (IWT/CWT) of function $f \in L^2(\mathbb{R})$ is defined as

$$(W_\psi f)(ba) = |a|^{-\frac{1}{2}} \int_{-\infty}^{\infty} f(t) \overline{\psi(\tfrac{t-b}{a})} dt,$$

where $a, b \in \mathbb{R}$ with $a \neq 0$.

Wavelet implies a *small wave*, thus the area under the graph of the wavelet $\psi(t)$ is zero. That is, $\int_{-\infty}^{\infty} \psi(t)dt = 0$. By setting

$$\psi_{ba}(t) = |a|^{-\frac{1}{2}} \psi(\frac{t-b}{a}), \tag{2}$$

the IWT can be represented as

$$(W_\psi f)(ba) = \langle f, \psi_{ba} \rangle. \tag{3}$$

Definition 2 Any original signal $f \in L^2(\mathbb{R})$ can be uniquely recovered by the inverse transform defined as

$$f(t) = \frac{1}{C_\psi} \int_{-\infty}^{\infty} \int_{-\infty}^{\infty} [(W_\psi f)(ba)] \psi_{ba} \frac{da}{a^2} db \tag{4}$$

where ψ_{ba} is as in (2).

For this analysis, the Morlet wavelet is used as the basic (mother) wavelet function. The Morlet wavelet is defined as

$$\psi(t) = K \exp(-i2\omega_0 t). \exp(-t^2/2), \tag{5}$$

where ω_0 represents the central angular frequency of the wavelet. In order ψ to have unit energy, the normalization constant K [12] is selected such that $K = \pi^{-1/4}$. The relationship between the frequencies f and wavelet scales can be derived as

$$\frac{1}{f} = \frac{4\pi a}{\omega_0 + \sqrt{2+\omega_0^2}}.$$

It is obviously seen that if $\omega_0 \approx 2\pi$ then $f \approx 1/a$. An example of the Morlet wavelet is given in Fig. 3.

2.2 Wavelet Power Spectrum

The wavelet transform can be considered as a generalization of the classical Fourier transform so that the spectral properties of any time series $x(t), t \in \mathbb{R}$ can be visualized. The wavelet power spectrum of the wavelet transform $(W_\psi x)(ba)$ of the time series $x(t)$ with the basic wavelet ψ is defined as

$$(S_\psi x)(ba) = \|(W_\psi x)(ba)\|^2. \tag{6}$$

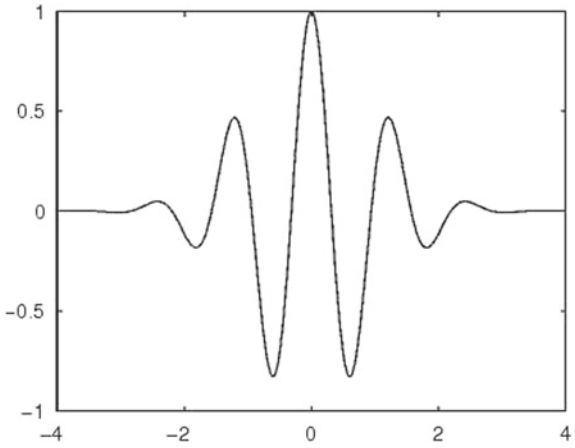

Fig. 3 The Morlet wavelet function

The global wavelet power spectrum $(\overline{S}_\psi x)(a)$ which is comparable with the Fourier spectrum of a signal can be defined as the averaged energy of all wavelet coefficients of the same scale a and given by

$$(\overline{S}_\psi x)(a) = \frac{\sigma_x^2}{T} \int_0^T \|(W_\psi x)(ba)\|^2 db, \tag{7}$$

where σ_x is the standard deviation of the time series $x(t)$ and T is the duration of the time series. Averaging the scale components gives the mean variance of each time location defined as

$$(\overline{S}_\psi x)(b) = \frac{\sigma_x^2 \pi^{1/4} b^{1/2}}{C_\psi} \int_0^\infty a^{1/2} \|(W_\psi x)(ba)\|^2 da, \tag{8}$$

where C_ψ as in 1.

2.3 Wavelet Coherency and Phase Difference

It is useful to quantify the statistical relationship between two signals if we have two non-stationary time series. The wavelet coherence function measures the correlation between two time series $x(t)$ and $y(t)$ [12]. The wavelet cross-spectrum of the two time series $x(t)$ and $y(t)$ can be defined as

$$(W_\psi xy)(ba) = (W_\psi x)(ba)(W_\psi y)(ba)^*. \tag{9}$$

Here $'*'$ denotes the complex conjugate. The cross-spectrum normalized by the spectrum of each signal gives the wavelet coherence which is defined as

$$(R_\psi xy)(ba) = \frac{\|\langle (W_\psi xy)(ba)\rangle\|}{\|\langle (W_\psi xx)(ba)\rangle\|^{1/2}\|\langle (W_\psi yy)(ba)\rangle\|^{1/2}}. \tag{10}$$

The notation $'\langle\rangle'$ stands for the smoothing operator in both time and scale parameters [12]. The wavelet coherency is similar to simple statistical correlation but $0 \leq (R_\psi xy)(ba) \leq 1$. This measure equals to 1 implies a perfect relationship between the two signals in both time and scale, however this goes to 0 if the two time series are independent.
As with the complex wavelets (for an example, Morlet wavelet), the local phase ζ is proportional to the ratio between imaginary part ($\Im$) and the real part ($\Re$) of the wavelet transform defined as [12, 13]

$$(\zeta_\psi x)(ba) = \tan^{-1}\frac{\Im[(W_\psi x)(ba)]}{\Re[(W_\psi x)(ba)]}. \tag{11}$$

The phase difference of two time series $x(t)$ and $y(t)$ is useful in identifying anti-phase relationships and it is defined as

$$(\zeta_\psi xy)(ba) = \tan^{-1}\frac{\Im[\langle (W_\psi xy)(ba)\rangle]}{\Re[\langle (W_\psi xy)(ba)\rangle]}. \tag{12}$$

2.4 Statistical Significance and Cone of Influence

Similarly, in time series methods, we need to assess the statistical significance of the patterns identified by the wavelet approach. The bootstrapping methods simply re-sampling procedures are employed to evaluate the statistical significance. The observed time series data are used to construct the time series defined under the null hypothesis, which share some properties with the original series. A procedure based on a re-sampling of the observed data with a Markov process scheme is used that preserves only the short temporal correlations. We focus to test whether the wavelet power spectra or wavelet coherence observed at a particular position on the time-scale plane are not resulted from a random process with the same Markov transitions (time order) as the original time series. The procedure of computing the bootstrapped series is discussed in [12, 18]. the significant regions are covered in a black line inside the power spectrum. Wavelet transformations are used for the time series which are short and noisy. The values of the wavelet transform are generally corrupted as the wavelet approaches the edges of the noisy time series, producing a boundary effect. This affected area increases as the size of the scale parameter a increases. This region is said to be cone of influence and it is generally represented as a cone in the wavelet power spectra.

2.5 Data Analysis

The weekly dengue data are analyzed from year 2006 to 2017 using wavelet transformation. Figure 4 shows the power spectrum of dengue incidents time series in Colombo city. According to this figure, dengue incident data show some seasonal oscillations and these fluctuations are in 16–32 weekly band period and this region is shown in orange and red in color.

The climate data were obtained from the Department of Meteorology, Sri Lanka, and weekly dengue cases data were obtained from Colombo Municipal Council. There time series data are analyzed using wavelet theory to identify any phase relationships among climate, mainly temperature and rainfall and dengue cases. The cross-wavelet power spectra obtained from a MATLAB program is given in Fig. 5.

The cross-wavelet power spectrum obtained for maximum temperature versus dengue incidents shows an anti-phase relationship (arrows pointing left). However, Fig. 5 suggests this relationship is not significant. In contrast, there exists a significant anti-phase relationship between dengue cases and rainfall with a $\sim$ 16-period band. This suggests a possible lead time of rainfall for an outbreak of dengue in Colombo during the period.

3 Modeling the Uncertainty

We aim to construct an index which explains the climate risk and the degree of favorability to dengue disease transmission in Colombo. We analyze incident data in Colombo with climate factors such as temperature and rainfall which are found to be

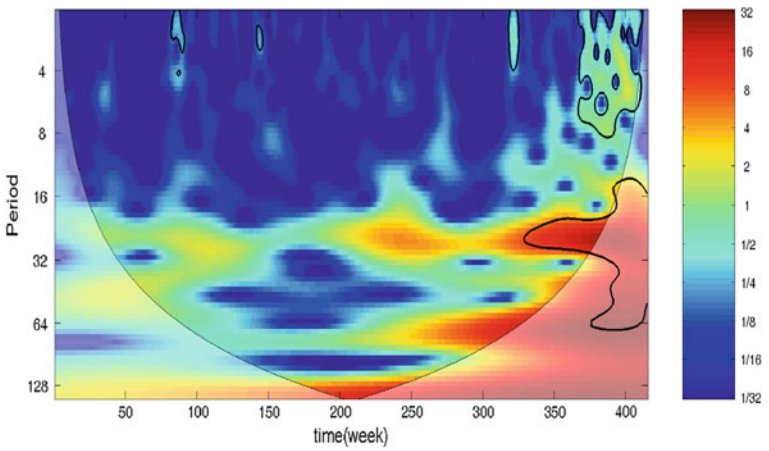

Fig. 4 Wavelet power spectrum of dengue data in Colombo Municipal Council from year 2006 to 2017

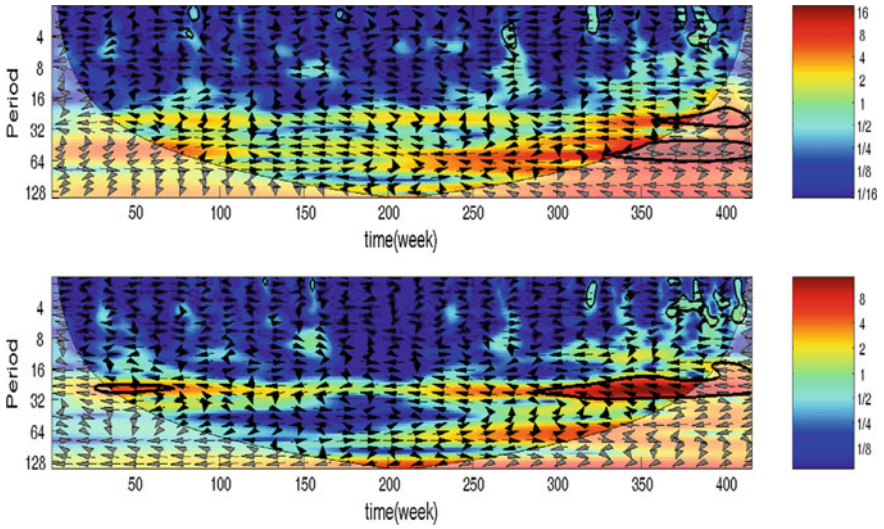

Fig. 5 Top: Cross-wavelet power spectrum of weekly dengue cases versus average maximum temperature and Bottom: Cross-wavelet power spectrum of weekly dengue cases versus average rainfall in Colombo from year 2006 to 2017

the most significant climate drivers to dengue. We use fuzzy set theory to investigate the influence from rainfall (RF) and the weekly averaged maximum temperature (TEMP) for dengue transmission. Based on the results obtained using cross-wavelet approach, the membership functions for weekly average rainfall with lead time and immediate maximum temperature are defined with the degree of membership value in [0,1] as the response variable which is the effect from each, respectively, to establish unfavorable environmental conditions for dengue transmission.

3.1 Fuzzy Set: Preliminaries

Definition 3 Let U be a non-empty set and A, a subset of U. The characteristic function of A is given by

$$A(x) = \begin{cases} 1, & \text{if } x \in A; \\ 0, & \text{if } x \notin A; \end{cases} \tag{13}$$

Definition 4 A fuzzy subset F of U is described by the function $F : U \to [0, 1]$ called the membership function of fuzzy set F where U is a classical non-empty set. The value $F(x) \in [0, 1]$ indicates the membership degree of the element x of U in

fuzzy set F, with $F(x) = 1$ and $F(x) = 0$ representing, respectively, the belongingness and non-belongingness of x in F [20, 28].

Definition 5 A fuzzy set is concentrated by reducing the grade of membership of all elements that are only partly in the set, in such a way that the less an element is in the set, the more its grade of membership is reduced. The concentration of a fuzzy set A can be defined by [19]

$$U_{CONC(A)}(x) = U_A^a(x) \text{ with } a > 1. \tag{14}$$

The opposite of the concentration is the dilation. A fuzzy set is dilated or stretched by increasing the grade of membership of all elements that are partly in the set. The dilation of a fuzzy set A can be defined by [19]

$$U_{DIL(A)}(x) = U_A^a(x) \text{ with } a < 1. \tag{15}$$

Definition 6 The trapezoidal curve is a function of a vector, x, and depends on four scalar parameters a, b, c, and d, as given by

$$f(x; a, b, c, d) = \begin{cases} 0, & \text{if } x \le a; \\ \dfrac{x-a}{b-a}, & \text{if } a \le x \le b; \\ 1, & \text{if } b \le x \le c; \\ \dfrac{d-x}{d-c}, & \text{if } c \le x \le d; \\ 0, & \text{if } d \le x. \end{cases} \tag{16}$$

The parameters a and d locate the "feet" of the trapezoid and the parameters b and c locate the "shoulders."

3.2 Fuzzy Membership Functions for Climate Factors

It is identified that at least 5 mm averaged weekly rainfall is required to make breeding sites available for mosquitoes and the breeding sites are washed out due to the heavy rainfall which is over 55 mm [14, 15, 25]. Further, it is identified that a weekly average temperature less than 16° C is unfavorable for mosquitoes to transmit the virus and a temperature between 30 and 34° C is ideal for mosquitoes to rapidly transmit of the virus due to the increased vector capacity and reduced incubation period. Further, it is noted that extreme heating conditions do not support dengue virus transmission so that we assume that the threshold temperature to be 37° C

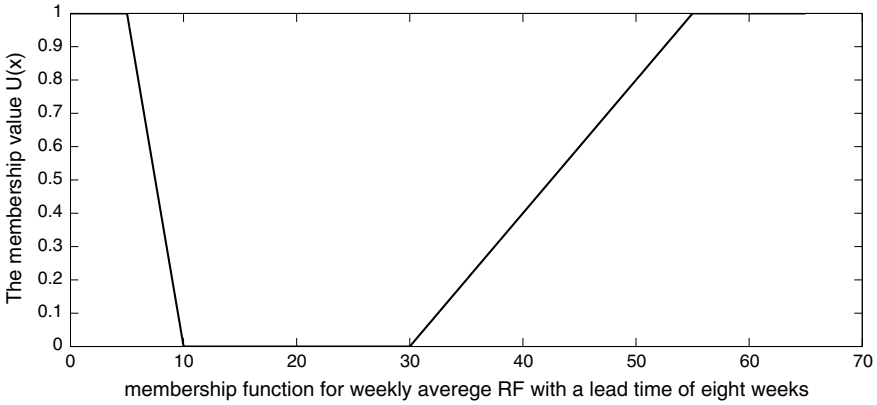

Fig. 6 Membership function for average weekly rainfall with eight weeks lag (RF)

[14, 15, 25]. Based on these conditions, the trapezoidal-shaped membership functions $U_{RF}(x) : A \subseteq \mathbb{R} \to [0, 1]$ and $U_{RF}(x) : B \subseteq \mathbb{R} \to [0, 1]$ are defined, respectively, to represent the effect from leading RF and immediate TEMP to create an unfavorable environment for dengue as

$$U_{RF}(x) = \begin{cases} 1, & \text{if } x \leq 5; \\ \frac{-x+10}{5}, & \text{if } 5 \leq x \leq 10; \\ 0, & \text{if } 10 \leq x \leq 30; \\ \frac{x-30}{25}, & \text{if } 30 \leq x \leq 55; \\ 1, & \text{if } x \geq 55; \end{cases} \tag{17}$$

$$U_{TEMP}(x) = \begin{cases} 1, & \text{if } x \leq 16; \\ \frac{-x+30}{14}, & \text{if } 16 \leq x \leq 30; \\ 0, & \text{if } 30 \leq x \leq 34; \\ \frac{x-34}{3}, & \text{if } 34 \leq x \leq 37; \\ 1, & \text{if } x \geq 37. \end{cases} \tag{18}$$

The trapezoidal-shaped membership functions given in (17) and (18) are illustrated in Figs. 6 and 7, respectively.

3.2.1 Fuzzy Operator of Overall Risk for Dengue

In the previous section, the individual effect from RF and TEMP is investigated to create an unfavorable environmental condition for dengue. Now, we try to define a fuzzy operator which computes the measure of combined effect from RF and TEMP.

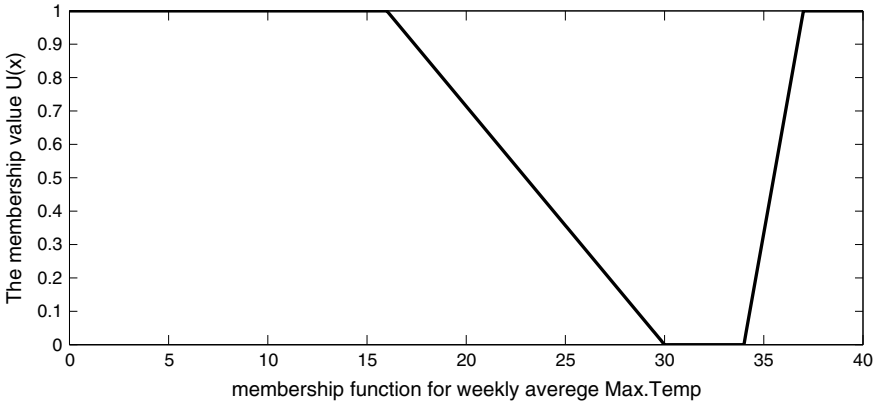

Fig. 7 Membership function for average weekly rainfall with eight weeks lag (RF)

A modified version of the Einstein Sum fuzzy operator in is used to measure the combined effect from above factors. This operator overcomes the disadvantages of the Hamacher operator where the it computes the combined effect to be zero if one individual membership value is zero no matter how much the other membership value is. For an example, if the RF is totally favorable (membership = 0) while TEMP is slightly favorable (membership > 0), then the Hamacher operator produces a membership value of zero which implies a totally favorable climate condition for dengue transmission and is sometimes misleading.

Definition 7 We define the modified Einstein Sum operator which computes the overall effect as a function $U_{MES}(x) : ([0, 1] \times [0, 1]) \rightarrow [0, 1]$ given by

$$U_{MES}(x) = \frac{U_{RF}^2(x) + U_{TEMP}^2(x)}{1 + U_{RF}(x) \cdot U_{TEMP}(x)}. \tag{19}$$

It is obviously seen that,

- If $U_{RF}(x) = 0$ and $U_{TEMP}(x) = 0$ then $U_{MES}(x) = 0$.
- If $U_{RF}(x) = 0$ and $U_{TEMP}(x) \neq 0$ then $U_{MES}(x) = U_{TEMP}^2(x) \leq U_{TEMP}(x)$ or if $U_{TEMP}(x) = 0$ and $U_{RF}(x) \neq 0$ then $U_{MES}(x) = U_{RF}^2(x) \leq U_{RF}(x)$.

Further, it can be shown that if $U_{TEMP}(x) < U_{RF}(x)$ then $U_{MES}(x) < U_{RF}$. The behavior of the overall effect $U_{MES}(x)$ for different membership values of RF and TEMP is represented in Fig. 8. This plot is generated such that we input membership values obtained for rainfall and temperature through the trapezoidal membership functions and the combined effect is computed according to Eq. (19) representing the third axis.

Then, we define the potential risk index of dengue transmission again as a function $M : ([0, 1] \times [0, 1]) \rightarrow [0, 1]$ defined by

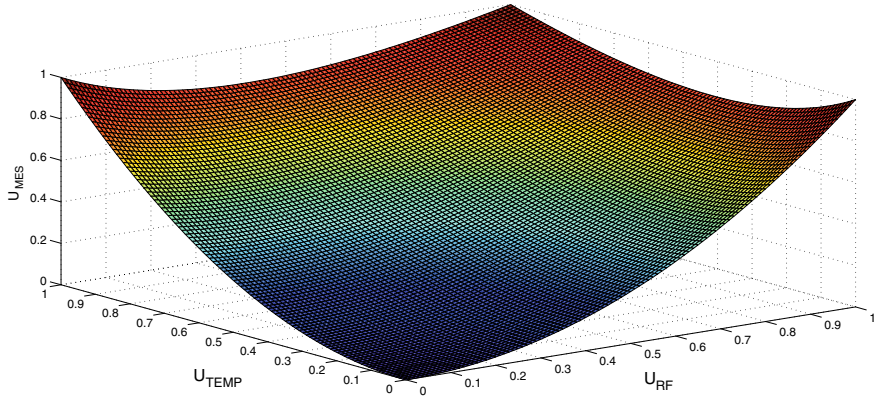

Fig. 8 Behavior of the overall effect for different membership values of RF and TEMP

$$M(x) = 1 - U_{MES}(x). \tag{20}$$

This risk index is constructed from time series data for rainfall and temperature. Thus the index described in equation (20) is a fuzzy valued time series where each observation is in [0,1].

4 Mathematical Model of Dengue Transmission

For the dengue transmission, both host (human) and vector (mosquito) populations are divided into several compartments. Host population is divided into three compartments, namely susceptible (S^h), infected (I^h), and recovered (R^h), and the vector population is divided into two compartments, namely susceptible (S^v) and infected (I^v). Since the life span of the vector population is too short, the recovery of the vectors is not considered [9]. The schematic diagram for the SIR model is represented in Fig. 9, where
$S^h(t)$ be the number of susceptible humans at time t,
$I^h(t)$ be the number of infected and infectious humans at time t,
$R^h(t)$ be the number of recovered humans at time t,
$S^v(t)$ be the number of susceptible mosquitoes at time t,
$I^v(t)$ be the number of infected and infectious mosquitoes at time t.

The model assumes all newborns are susceptible in both populations (no vertical transmission) and a uniform birth rate. The per capita birth rates for humans is λ, and the constant recruitment rate for mosquitoes is D. A susceptible, infectious, or recovered human can disappear from the respective compartment with a natural death, at a per capita rate of μ_h and the infectious human can recover from the infection

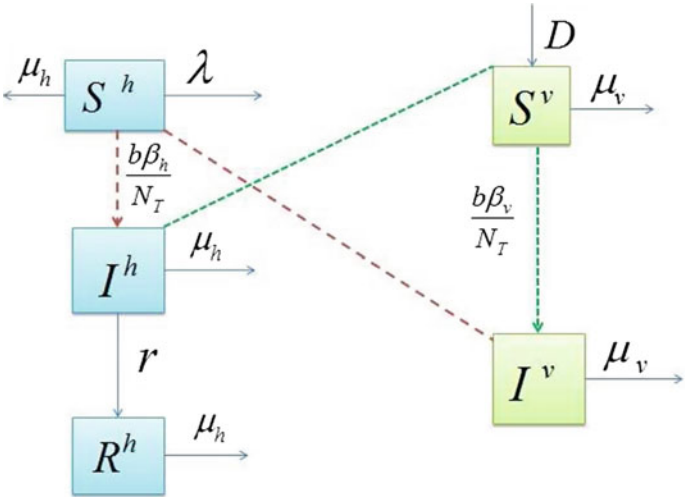

Fig. 9 Schematic diagram for SIR model of dengue disease transmission which describes the interactions between human and mosquito populations

and join the recovered population with a per capita rate of r. The natural death rate of mosquitoes is μ_v. The effective contact rates between the two populations, which may be defined as the average number of contacts per time that leads to the infection of one party if the other party is infectious, depends on a number of factors: the man biting rate of the mosquitoes b, the transmission probabilities between vectors and hosts namely the transmission probability of the virus from mosquitoes to humans, β_h and the transmission probability of the virus from humans to mosquitoes, β_v. Further, the effective contact rates between the populations depend on the number of individuals in both human and mosquito populations, N_T and N_v respectively. Since b is the average number of bites per mosquito per unit time, there are $b\frac{N_v}{N_T}$ number of bites per human per time. Since there are S^h susceptible humans and the proportion of the total number of bites that are potentially infectious to humans is $\frac{I^v}{N_v}$, the number of potentially infectious bites given to susceptible humans is $\frac{b}{N_T}S^hI^v$ bites per time. However, only a fraction of these bites, namely β_h, successfully infect humans. We thus have infected humans per unit time is given by $\frac{b\beta_hI^v}{N_T}S^h$. Similarly, we obtain the mosquitoes infected per unit time as $\frac{b\beta_vI^h}{N_T}S^v$. Based on this inflows and outflows of each compartment, we describe the dengue transmission between humans and mosquitoes by a system of nonlinear differential equations as in (21)

$$\begin{aligned}
\frac{dS^h}{dt} &= \lambda N_T - \frac{b\beta_h}{N_T} S^h I^v - \mu_h S^h \\
\frac{dI^h}{dt} &= \frac{b\beta_h}{N_T} S^h I^v - (\mu_h + r) I^h \\
\frac{dR^h}{dt} &= r I^h - \mu_h R^h \\
\frac{dS^v}{dt} &= D - \frac{b\beta_v}{N_T} S^v I^h - \mu_v S^v \\
\frac{dI^v}{dt} &= \frac{b\beta_v}{N_T} S^v I^h - \mu_v I^v
\end{aligned} \tag{21}$$

with the conditions

$$\begin{aligned}
N_T &= S^h + I^h + R^h \\
N_v &= S^v + I^v
\end{aligned}$$

and
$S_h(0) \geq 0, I_h(0) \geq 0, R_h(0) \geq 0, S_v(0) \geq 0$ and $I_v(0) \geq 0$. It is assumed that rate of change in the human and mosquito populations are zero ($\frac{dN_T}{dt} = 0$ and $\frac{dN_v}{dt} = 0$). Now it can be easily obtained that $\lambda = \mu_h$ and $N_v = \frac{D}{\mu_v}$. Now we introduce, $S = \frac{S^h}{N_T}$, $I = \frac{I^h}{N_T}$, $R = \frac{R^h}{N_T}$, $S_v = \frac{S^v}{N_v}$ and $I_v = \frac{I^v}{N_v}$. Now we obtain the dimensionless form of the system (21) as

$$\begin{aligned}
\frac{dS}{dt} &= \lambda - b\beta_h S I_v \frac{N_v}{N_T} - \mu_h S \\
\frac{dI}{dt} &= b\beta_h S I_v \frac{N_v}{N_T} - (\mu_h + r) I \\
\frac{dR}{dt} &= r I - \mu_h R \\
\frac{dS_v}{dt} &= \mu_v - b\beta_v S_v I - \mu_v S_v \\
\frac{dI_v}{dt} &= b\beta_v S_v I - \mu_v I_v.
\end{aligned} \tag{22}$$

Here,

$$S + I + R = 1$$

and

$$S_v + I_v = 1.$$

Since $R = 1 - I - S$ and $S_v = 1 - I_v$, the system (22) now reads as

$$\begin{aligned}\frac{dS}{dt} &= \lambda - \gamma_h S I_v - \mu_h S \\ \frac{dI}{dt} &= \gamma_h S I_v - (\mu_h + r) I \\ \frac{dI_v}{dt} &= \gamma_v (1 - I_v) I - \mu_v I_v\end{aligned} \tag{23}$$

where $\gamma_v = b\beta_v$, $\gamma_h = b\beta_h n$ and n is a measure of mosquito density which is defined as $n = \frac{N_v}{N_T}$ with $S(0) > 0, I(0) > 0$ and $I_v(0) > 0$.++

4.1 The Equilibrium States of the Model

We let the set of solutions denoted by Ω to the system of nonlinear differential equations in (23) as

$$\Omega = \{(S, I, I_v) \in R_+^3 : S + I \leq 1, S, I, I_v \geq 0\}.$$

The equilibrium points can be found by solving the system of equations given by

$$\begin{aligned}\lambda - \gamma_h S I_v - \mu_h S &= 0 \\ \gamma_h S I_v - (\mu_h + r) I &= 0 \\ \gamma_v (1 - I_v) I - \mu_v I_v &= 0.\end{aligned} \tag{24}$$

The disease-free equilibrium point E_0 can be easily obtained as

$$E_0 = (1, 0, 0).$$

The endemic equilibrium point is $E_1 = (S^*, I^*, I_v^*)$ where

$$\begin{aligned}S^* &= \frac{P + Q}{Q + PA}, \\ I^* &= \frac{A - 1}{Q + PA}, \\ I_v^* &= \frac{Q(A - 1)}{A(Q + P)},\end{aligned}$$

with $P = \frac{\mu_h + r}{\mu_h}$, $Q = \frac{\gamma_v}{\mu_v}$ and $A = \frac{\gamma_h \gamma_v}{\mu_v(\mu_h + r)}$.

Definition 8 The basic reproductive number R_0 for the system (23) is defined as $\sqrt{A}$ which is given by

$$R_0 = \sqrt{\frac{\gamma_h \gamma_v}{\mu_v(\mu_h + r)}}.$$

The Jacobian matrix of the right-hand side of the system (23) is computed as follows to analyze the stability of the equilibrium points E_0 and E_1.

$$J = \begin{pmatrix} -\gamma_h I_v - \mu_h & 0 & -\gamma_h S \\ \gamma_h I_v & -(\mu_h + r) & \gamma_h S \\ 0 & \gamma_v(1 - I_v) & -\mu_v - \gamma_v I \end{pmatrix} \tag{25}$$

The Jacobian matrix J_{E_0} for the system (23) at the disease-free equilibrium point E_0 is computed as

$$J_{E_0} = \begin{pmatrix} -\mu_h & 0 & -\gamma_h \\ 0 & -(\mu_h + r) & \gamma_h \\ 0 & \gamma_v & -\mu_v \end{pmatrix}. \tag{26}$$

We diagonalize the Jacobian matrix J_{E_0} for the disease-free equilibrium and the characteristic equation is given by

$$det(J_{E_0} - \eta I_d) = 0 \tag{27}$$

where η is the eigenvalue of J_{E_0} and I_d is the identity matrix. The eigenvalues can be obtained by solving Eq. (28)

$$\eta^3 + a_2\eta^2 + a_1\eta + a_0 = 0 \tag{28}$$

where

$$a_0 = \mu_h^2\mu_v + r\mu_h\mu_v - \mu_h\gamma_h\gamma_v,$$

$$a_1 = \mu_h^2 + 2\mu_h\mu_v + (\mu_h + \mu_v)r - \gamma_h\gamma_v,$$

$$a_2 = r + \mu_v + 2\mu_h.$$

Equation (28) is solved and the three eigenvalues can be obtained as

$$-\mu_h, \ \frac{-(\mu_v + \mu_h + r) + \sqrt{(\mu_v + \mu_h + r)^2 - 4\mu_v(\mu_h + r)(1 - R_0^2)}}{2},$$

$$\frac{-(\mu_v + \mu_h + r) - \sqrt{(\mu_v + \mu_h + r)^2 - 4\mu_v(\mu_h + r)(1 - R_0^2)}}{2}.$$

Theorem 1 *If all eigenvalues obtained by Jacobian matrix have negative real parts, then the equilibrium solution is locally stable.*

Clearly, all three eigenvalues in the Jacobian matrix J_{E_0} have negative real parts as long as R_0 is less than 1. Thus, the disease-free equilibrium E_0 is locally asymptotically stable if $R_0 < 1$.

Now, we discuss the local stability of the endemic equilibrium E_1. Then, the Jacobian matrix J_{E_1} for the system (23) at the endemic equilibrium point E_1 is computed as

$$J_{E_1} = \begin{pmatrix} -\gamma_h I_v^* - \mu_h & 0 & -\gamma_h S^* \\ \gamma_h I_v^* & -(\mu_h + r) & \gamma_h S^* \\ 0 & \gamma_v(1 - I_v^*) & -\mu_v - \gamma_v I^* \end{pmatrix}. \tag{29}$$

Again we diagonalize the Jacobian matrix J_{E_1} for the endemic equilibrium and the characteristic equation is given by

$$det(J_{E_1} - \eta I_d) = 0 \tag{30}$$

where η is the eigenvalue of J_{E_0} and I_d is the identity matrix. The eigenvalues can be obtained by solving Eq. (31)

$$\eta^3 + c_2\eta^2 + c_1\eta + c_0 = 0 \tag{31}$$

where

$$\begin{aligned} c_0 =& \mu_v \mu_h^2 P(R_0^2 - 1), \\ c_1 =& \mu_h^2 P \left(\frac{Q + PR_0^2}{P + Q} \right) + \mu_v \mu_h R_0^2 + (R_0^2 - 1) \left(\frac{\mu_v \mu_h QP}{Q + PR_0^2} \right), \\ c_2 =& \mu_h \left(\frac{Q + PR_0^2}{P + Q} \right) + \mu_h P + \mu_v R_0^2 \left(\frac{P + Q}{Q + PR_0^2} \right). \end{aligned} \tag{32}$$

Routh–Hurwitz stability criterion for third-order polynomials is used to determine the stability of the endemic equilibrium E_1.

Corollary 1 *If $P(x)$ is a third-order polynomial (i.e., $P(x) = x^3 + e_2x^2 + e_1x + e_0$), and its coefficients e_0, e_1 and e_2 satisfy the conditions given by*

$$e_2 > 0$$

$$e_1 > 0$$

$$e_2 e_1 > e_0,$$

then the equilibrium point is locally stable.

By using corollary 1, the local stability of endemic equilibrium point, E_1 of the system (23) is determined. It is clear that coefficients of (31) satisfy the conditions in corollary 1 as long as $R_0 > 1$. Thus the endemic equilibrium E_1 is locally stable whenever $R_0 > 1$.

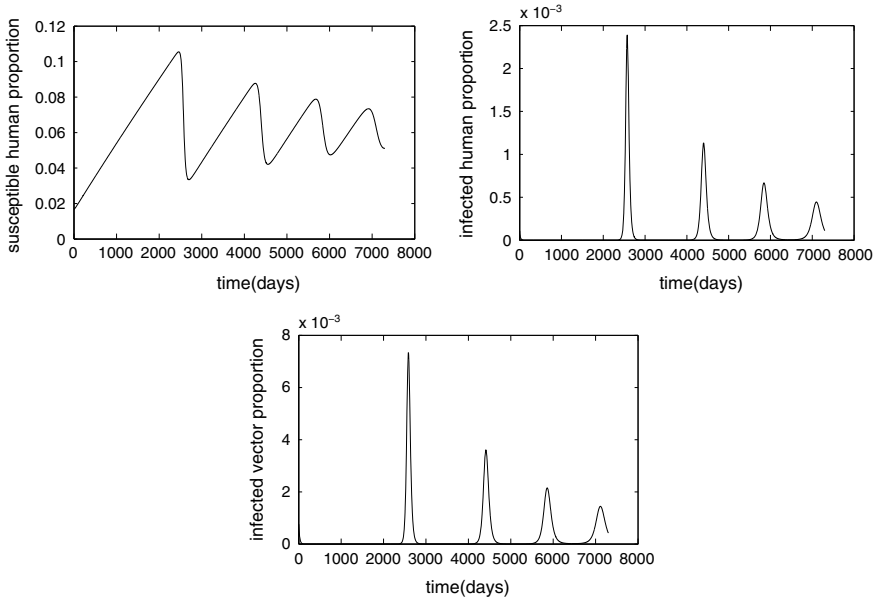

Fig. 10 Susceptible human, infected human, and infected mosquito proportion dynamics

4.2 Numerical Results

The system of equations of the mathematical model in 23 is solved numerically using MATLAB ODE solver. The solutions are illustrated in Fig. 10. The parameters are $\mu_h = 0.0000391$ per day, $\mu_v = 0.071$ per day, $b = 1/3$ per day, $\beta_h = 0.5$, $\beta_v = 0.7$, $n = 10$, and $r = 1/3$ per day. The initial conditions are $(S(0), I(0), I_v(0)) = (0.000001, 0.0000625, 0.006)$ [9].

According to Fig. 10, it can be seen that each population proportions show periodic oscillations and the proportional limit to their corresponding equilibrium point in the long run. However, this behavior is unrealistic compared to actual dynamic shown by the dengue cases data and Fig. 11 shows the solution trajectories.

5 Two-Dimensional Model for Dengue

We consider the system of Eqs. 23. This three-dimensional system includes susceptible humans (S), infected humans (I), and infected mosquitoes (I_v). However, it is very difficult to measure (I_v) in practice. Thus, we now attempt to reduce the three-dimensional system into a two-dimensional system by eliminating the infected mosquito proportion. We assume that there are sufficient infected mosquitoes in

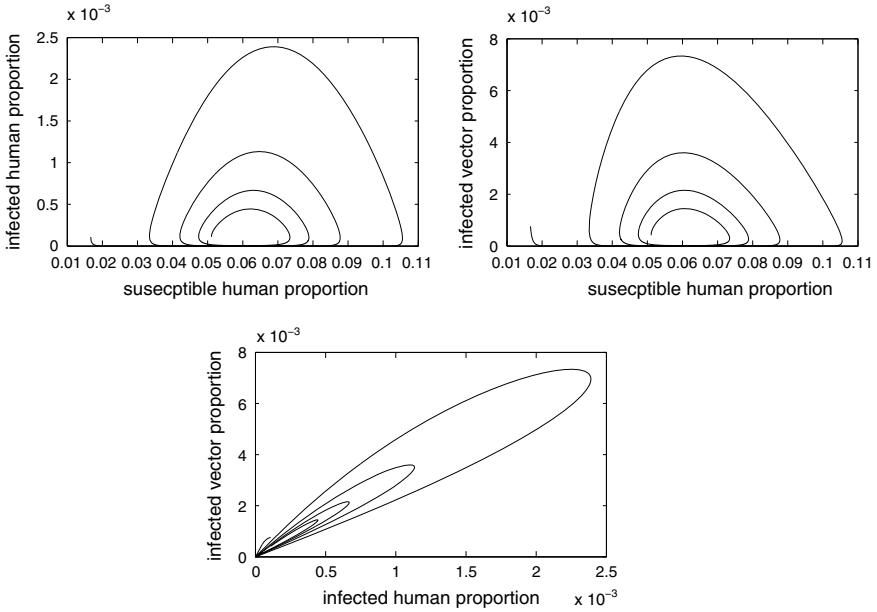

Fig. 11 Solution trajectories, projected onto (S, I), (S, I_v) and (I, I_v). The same parameter values are used as in Fig. 10

the environment who can transmit the virus to humans and this population is in an equilibrium. Thus,

$$\frac{dI_v}{dt} = 0.$$

This condition gives

$$\begin{aligned} \gamma_v(1 - I_v)I - \mu_v I_v &= 0 \\ I_v &= \frac{\gamma_v I}{\gamma_v I + \mu_v}. \end{aligned} \tag{33}$$

Substituting this I_v into the first two equations and using $\gamma_h = b\beta_h n$ and $\gamma_v = b\beta_v$ we get

$$\begin{aligned} \frac{dS}{dt} &= \lambda - \frac{b^2 n\beta_h\beta_v I}{b\beta_v I + \mu_v} - \mu_h S, \\ \frac{dI}{dt} &= \frac{b^2 n\beta_h\beta_v I}{b\beta_v I + \mu_v} - (\mu_h + r)I, \end{aligned} \tag{34}$$

with $S(0) > 0$ and $I(0) > 0$.

5.1 The Equilibrium States of the Model

In this section, we discuss the stability analysis of the two-dimensional model. We let the set of solutions denoted by Ω to the system of nonlinear differential equations in (34) as

$$\Omega^{'} = \{(S, I) \in R_{+}^{2} : S + I \leq 1, S, I \geq 0\}.$$

The Jacobian matrix of the system in (34) is obtained as

$$J^{'} = \begin{pmatrix} -\mu_h & \dfrac{b^2 n\beta_h\beta_v\mu_v}{(b\beta_v I + \mu_v)^2} \\ 0 & \dfrac{b^2 n\beta_h\beta_v\mu_v}{(b\beta_v I + \mu_v)^2} - (\mu_h + r) \end{pmatrix} \tag{35}$$

Clearly, the disease-free equilibrium state is $E_0^{'} = (1, 0)$. Thus, the Jacobian matrix at the disease-free equilibrium can be obtained as

$$J_{E_0}^{'} = \begin{pmatrix} -\mu_h & \dfrac{b^2 n\beta_h\beta_v}{\mu_v} \\ 0 & \dfrac{b^2 n\beta_h\beta_v}{\mu_v} - (\mu_h + r) \end{pmatrix} \tag{36}$$

We diagonalize the Jacobian matrix $J_{E_0}^{'}$ for the disease-free equilibrium and the characteristic equation is given by

$$det(J_{E_0}^{'} - \eta I_d) = 0 \tag{37}$$

where η is the eigenvalue of $J_{E_0}^{'}$ and I_d is the identity matrix. The eigenvalues can be obtained by solving Eq. (28)

$$\eta^2 + a_1\eta + a_0 = 0 \tag{38}$$

The two eigenvalues can be obtained as $\eta_1 = -\mu_h$ and $\eta_2 = \dfrac{b^2 n\beta_h\beta_v}{\mu_v} - (\mu_h + r)$. According to Theorem 1, if all eigenvalues obtained by Jacobian matrix have negative real parts, then the equilibrium solution is locally stable. Clearly, $\eta_1 < 0$. Thus, the disease-free equilibrium is locally stable if

$$\frac{b^2 n\beta_h\beta_v}{\mu_v} < \mu_h + r \tag{39}$$

Now, let the endemic equilibrium state of the model is denoted by $E^* = (S^*, I^*)$. This state can be obtained by solving $\frac{dS^*}{dt} = 0$ and $\frac{dI^*}{dt} = 0$. By solving these two equations, we obtain

$$I^* = \frac{M - L\mu_v}{NL} \tag{40}$$

and

$$S^* = \frac{1}{\mu_h}\left[\lambda - \frac{M - L\mu_v}{N}\right], \tag{41}$$

where $M = b^2 n\beta_h\beta_v$, $L = \mu_h + r$ and $N = b\beta_v$.
Substituting this state into the Jacobian matrix $J^{'}$, we now obtain the Jacobian matrix at the endemic equilibrium as

$$J^{'}_{E_1} = \begin{pmatrix} -\mu_h & \frac{L^2\mu_v}{M} \\ 0 & \frac{L^2\mu_v}{M} - L \end{pmatrix}. \tag{42}$$

Routh–Hurwitz stability criterion for second-order polynomials is used to determine the stability of the endemic equilibrium $E^{'}_1$. According to this criteria, the endemic equilibrium is stable if all the coefficients of the second-order polynomial is positive. We again diagonalize the matrix $J^{'}_{E_1}$ and obtain the characteristic polynomial in which the coefficients are

$$c_1 = 1,$$

$$c_2 = \frac{L(M - L) + \mu_v + M\mu_h}{M},$$

$$c_3 = \frac{\mu_h[L(M - L) + \mu_v]}{M}.$$

Obviously $c_1 > 0$. Now $c_2, c_3 > 0$ whenever $M > L$. Thus the system s n the endemic equilibrium whenever $b^2 n\beta_h\beta_v > \mu_h + r$.

5.2 Numerical Results

The two-dimensional deterministic system in 34 with is numerically solved using MATLAB. The parameter values are $n = 0.75$, $\mu_h = 3.42 \times 10^{-5}$, $\mu_v = 1/21$, $\beta_h = 0.07$, $\beta_v = 0.7$, $r = 1/14$, $\lambda = 0.0000456$, and $b = 1/3$. The dynamic of susceptible and infected population proportions are illustrated in Fig. 12.

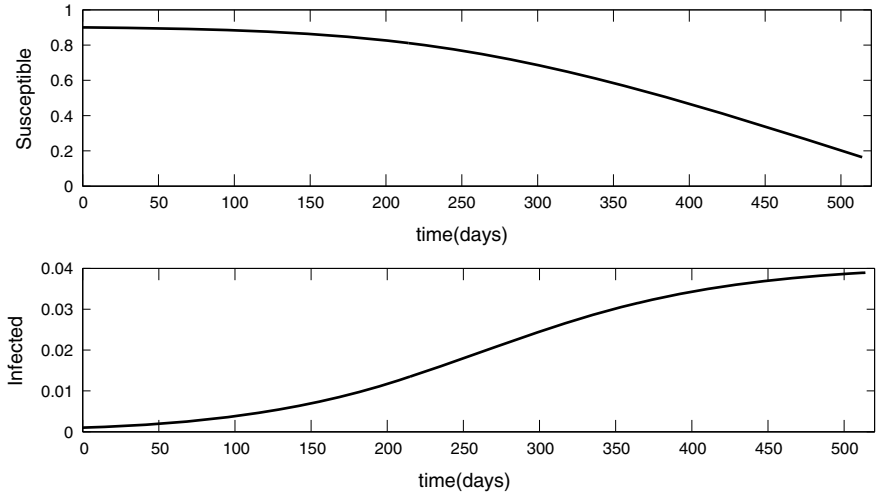

Fig. 12 Numerical solution of the two-dimensional system in 34

5.3 Sensitivity of the Parameters

It is clearly seen that the model expressed in system 34, there are number of parameters such as transmission probabilities from mosquitoes to humans and humans to mosquitoes, biting rate, mosquito density, and birth and death rates of humans and mosquitoes. Therefore, it is critical to investigate the sensitivity of these parameters to change the behavior of the transmission dynamic of the disease. However, the sensitivity analysis of the parameters are not carried out of which whose changes are negligible with respect to outside environment such as birth and death rates of humans. Figure 13 shows the variation in the dynamic as the mosquito density changes in small amount. Figures 14 and 15 show the sensitivity of the solution as the values of the transmission probabilities β_h and β_v change their value while Fig. 16 shows the sensitivity when the biting rate b varies in a considerably small interval.

As these Fig. 13, 14, 15 and 16 suggest, it can be clearly identified that the dynamic of the transmission of dengue diseases changes with respect to model parameter values. It is also clear that some parameters are more sensitive than others. However, we may have to pick the parameters which are influenced by the external forces significantly. Estimating each and every parameter value as a function of external variables is not practical and the system may become extremely complex to analyze.

6 Mosquito Density Model

We discussed previously that the mosquito density is a vital parameter in the model which is responsible to transmit the disease in a local environment. The impact of this parameter in the transmission dynamic of the disease is clearly shown in Fig. 13.

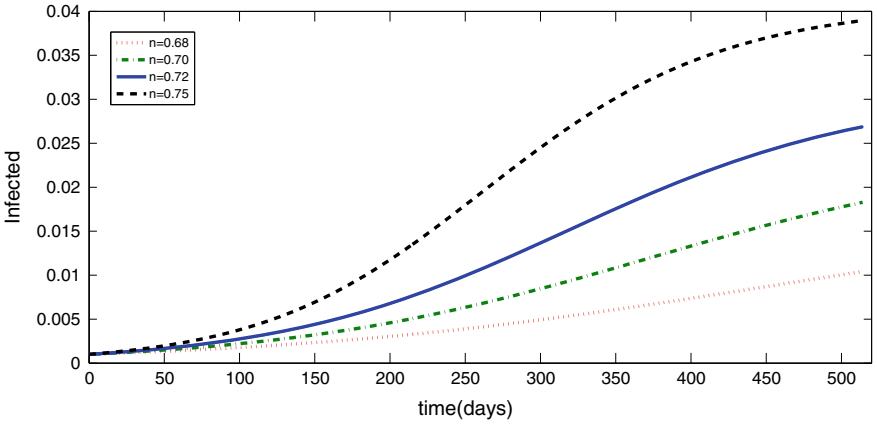

Fig. 13 Sensitivity of the infected human proportion when mosquito density n changes

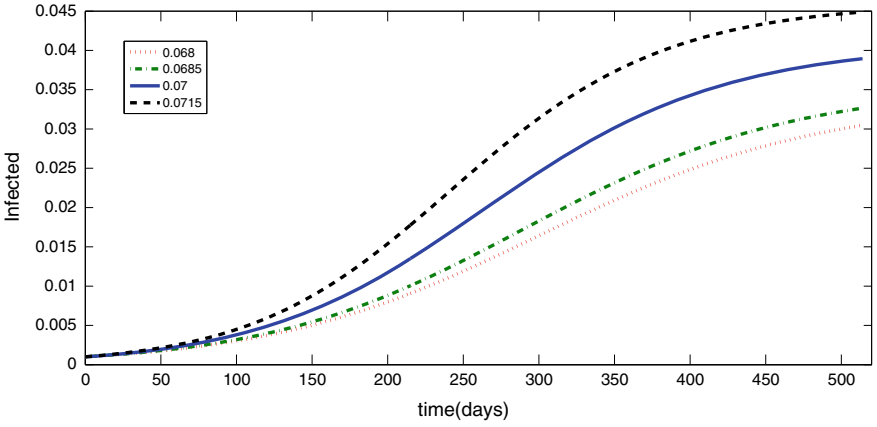

Fig. 14 Sensitivity of the infected human proportion when transmission probability humans to mosquitoes β_h changes

Further, it should be noted that the mosquito density is not constant over time and takes different values with respect to climate variations. Thus, it is time-dependent and its value changes with respect to climate factors, mainly due to rainfall and temperature. Though this is critical parameter in our model, finding reliable mosquito density data is extremely challenging. Therefore, we attempt to model the dynamic of this mosquito density in functional form. The development of this model is disused in detail here.

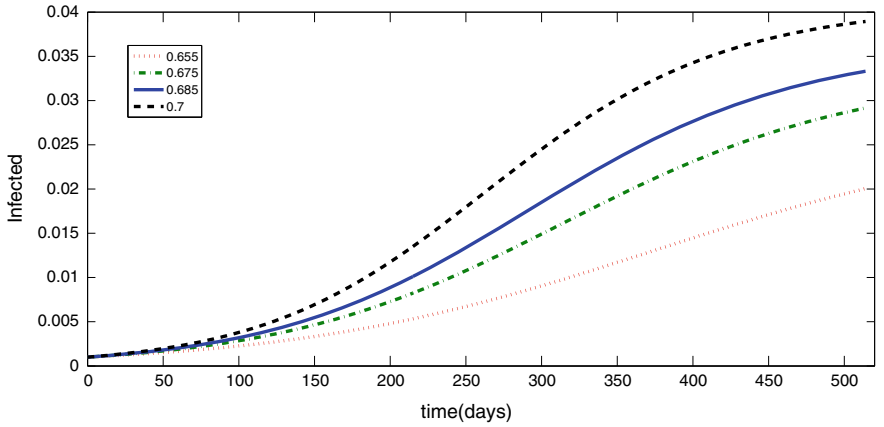

Fig. 15 Sensitivity of the infected human proportion when transmission probability from mosquitoes to humans β_v changes

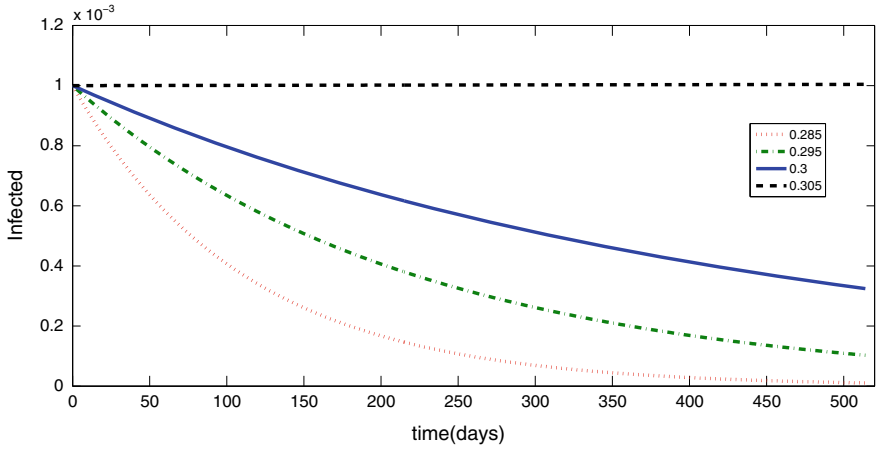

Fig. 16 Sensitivity of the infected human proportion when biting rate b changes

6.1 Gompertz Model

The Gompertz model is defined as [17, 26]

$$N(t+1) = \lambda_0 N(t)^{\theta} \tag{43}$$

where $\theta \in [0, 1]$ is an exponent, $\lambda_0 = \exp(r_0)$, $N(t)$ is the size of the population at time t and r_0 is the growth rate of the population.
Now, we start with a simple model in which we suppose that the number of vectors in time t, $(N_v(t))$ depends on the number of adult vectors in time $t-1$, $(N_v(t-1))$

and the number of growing juvenile vectors in time $t-1$, $J(t-1)$. This model can be expressed as [16, 17]

$$N_v(t) = sN_v(t-1) + pJ(t-1) \tag{44}$$

where $s \in [0, 1]$ is the per capita survival rate of the adult vectors and p is the per capita growing probability of juveniles [16].
The number of juveniles at time t, $(J(t))$ is regulated by the adult vector density in the previous time step. Thus we can write [16]

$$J(t) = F(N_v(t-1)). \tag{45}$$

Using Gompertz model in (43), the number of juveniles at time t, $J(t)$ in (44) can be expressed as

$$J(t) = \lambda_0 N_v^{\theta}(t-1). \tag{46}$$

Now Eq. (43) can be written as

$$N_v(t) = sN_v(t-1) + p(\lambda_0 N_v^{\theta}(t-2)). \tag{47}$$

6.2 Mathematical Analysis of the Density Model

Here, we discuss the stability analysis of the mosquito density model obtained as in Eq. (47). We view this as a system of first-order difference equation and it is given in (48),

$$\begin{aligned} N_v(t) &= sN_v(t-1) + pJ(t-1) \\ J(t) &= \lambda_0 N_v^{\theta}(t-1). \end{aligned} \tag{48}$$

It is easily found that the trivial equilibrium of the system (48) is

$$(N_v^*, J^*) = (0, 0).$$

The non-trivial equilibrium can be found as

$$(N_v^*, J^*) = \left(\left(\frac{p\lambda_0}{1-s} \right)^{1/1-\theta}, \lambda_0 \left(\frac{p\lambda_0}{1-s} \right)^{\theta/1-\theta} \right), \tag{49}$$

with $s \neq 1$. The Jacobian matrix (ϕ^*) for the system (48) is obtained at the equilibrium as

$$\phi^* = \begin{pmatrix} s & p \\ \theta\lambda_0 N_v^{*(\theta-1)} & 0 \end{pmatrix}. \tag{50}$$

Let the eigenvalues of the Jacobian matrix ϕ^* be η. We let $det(\phi^* - \eta I_d) = 0$ where I_d is the identity matrix and the characteristic polynomial can be obtained as

$$P(\eta) = \eta^2 - s\eta - p\lambda_0\theta N_v^{*(\theta-1)}. \tag{51}$$

We solve $P(\eta) = 0$ and the expression for the eigenvalue is obtained as

$$\eta = \frac{s}{2} \pm \sqrt{\left(\frac{s}{2}\right)^2 + \theta N^{*(\theta-1)}}. \tag{52}$$

The trivial equilibrium is always unstable since $\theta \in (0, 1)$ and $N^{*(\theta-1)}$ converges to a value outside the unit circle [16]. However for the non-trivial equilibrium, the largest eigenvalue of the Jacobian matrix is

$$\eta = \frac{s}{2} + \sqrt{\left(\frac{s}{2}\right)^2 + \theta(1-s)}. \tag{53}$$

Theorem 2 *The non-trivial equilibrium in (49) is asymptotic stability if* $|\eta| < 1$.

Theorem 2 gives us

$$\frac{s}{2} + \sqrt{\left(\frac{s}{2}\right)^2 + \theta(1-s)} < 1$$

if and only if

$$\left(\frac{s}{2}\right)^2 + \theta(1-s) < \left(1 - \frac{s}{2}\right)^2.$$

This leads to obtain the condition for asymptotic stability of the system (48) as

$$\theta < 1.$$

6.3 Model for Mosquito Density with Climate Force

In this section, we modify the model in Eq. (47) considering the external force induced by the rainfall and temperature. For this purpose, the climate risk index developed in Sect. 3 is used. There, the risk index is given in Eq. (20) and the new model can be expressed as

$$N_v(t) = se^{cM(t-1)}N_v(t-1) + p(\lambda_0 N_v^{\theta}(t-2)), \tag{54}$$

where c is the coefficient of climate force and $c \in [0, 1]$. If $c = 0$, then climatic variation does not influence the mosquito reproduction and then the model is simplified back to (47). If $c = 1$, then the climate force fully acts on mosquito propagation. Since density $n(t) = \frac{N_v(t)}{N_T(t)}$, then we obtain

$$n(t) = se^{cM(t-1)}n(t-1) + p(\lambda_0 n^{\theta}(t-2)) \tag{55}$$

(It is assumed that the mosquito life time is negligible compared to the life time of a human and $n^{\theta}(t) \approx \frac{N_v^{\theta}(t)}{N_T(t)}$).

7 Two-Dimensional Mathematical Model with Varying Mosquito Density

In this section, we transform the deterministic two-dimensional mathematical model of dengue transmission discussed in Sect. 5 into a non-deterministic system where the mosquito density parameter n is time invariant as in Eq. (55). Now, we let $n = n(t) = F(temp, rf)$. Thus, the system 34 can be rewritten as

$$\begin{aligned} \frac{dS}{dt} &= \lambda - \frac{b^2 n(t)\beta_h\beta_v I}{b\beta_v I + \mu_v} - \mu_h S, \\ \frac{dI}{dt} &= \frac{b^2 n(t)\beta_h\beta_v I}{b\beta_v I + \mu_v} - (\mu_h + r)I. \end{aligned} \tag{56}$$

We aim to investigate the dynamic of the dengue transmission with respect to climate variation only. Thus, other parameters are kept as constants. Since the system is now non-deterministic, the stability analysis of the equilibrium states may not be feasible to perform. Thus, the model is analyzed numerically.

7.1 Numerical Results

We solve system 56 and Eq. (55) together using a MATLAB program. The parameter values in the system 56 are , $\mu_h = 3.42 \times 10^{-5}$, $\mu_v = 1/21$, $\beta_h = 0.07$, $\beta_v = 0.7$, $r = 1/14$, $\lambda = 0.0000456$, $b = 1/3$ and the parameter values in Eq. (55) are $s = 0.105$, $\rho = 0.61$, $\theta = 0.115$ and $c = 0.65$. The dynamic of the susceptible and infected human proportions are shown in Fig. 17. It can be clearly seen that the dynamic is now different to results obtained from the deterministic model. Instead for a very smooth logistic growth of the infected population, this non-deterministic model produces some oscillation together with a trend in time mostly due to the

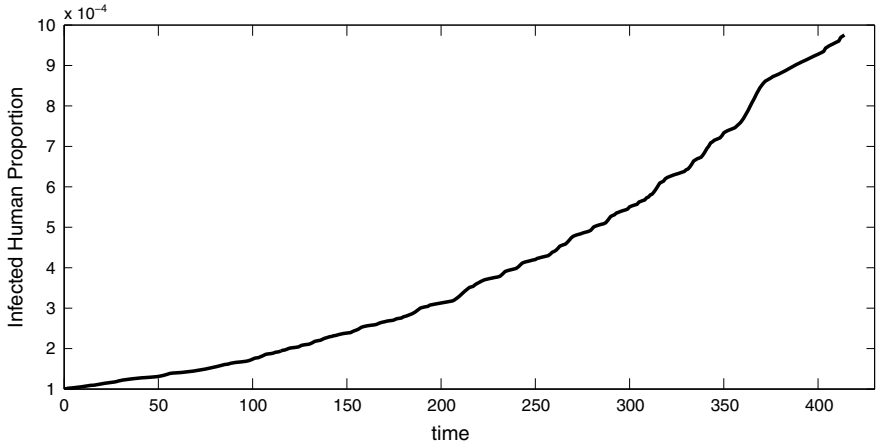

Fig. 17 Numerically simulated infected human proportion of the two-dimensional system in 56 and Eq. (55) simulated together

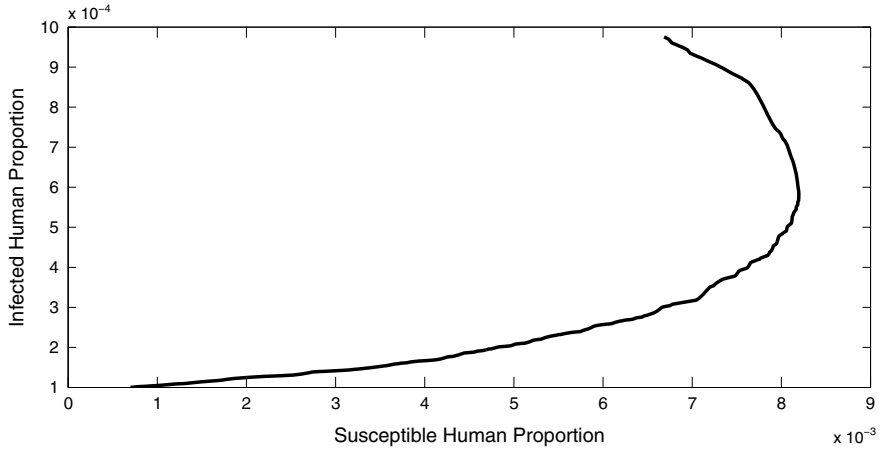

Fig. 18 Solution trajectory of the plotted infected proportion onto susceptible

climate variation considered. Figures 18 shows the solution trajectory plotted the infected proportion onto susceptible. Figures 18 shows the solution trajectory plotted the infected proportion onto susceptible.

The simulated dengue infections in humans is validated with the actual dengue incidents reported in Colombo Municipal Council area from year 2006 to 2017. The Comparison is illustrated in Fig. 19. It is clearly shown in this figure that the model captured the trend in dengue cases during the period and the fitted curve passes through most of the peak outbreaks. It should be noted that the outbreak occurred in mid 2017 is not predicted by the model since this peak is irregular compared to the pattern shown in the historical data.

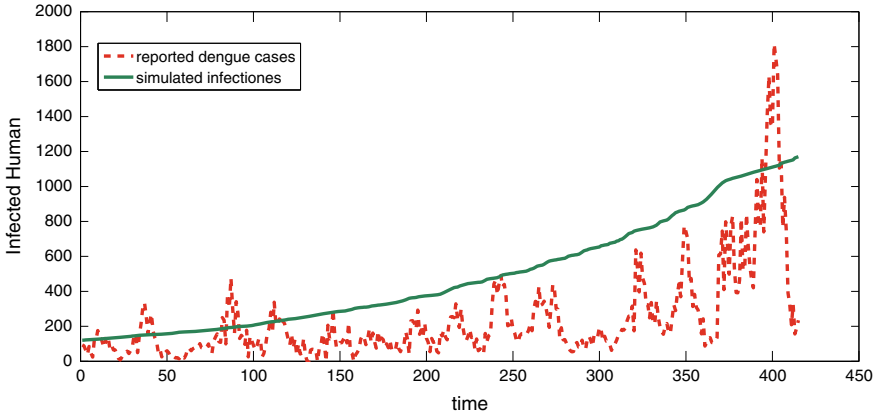

Fig. 19 Comparison of actual dengue cases reported from year 2006 to 2017 and the fitted dengue infections by the model

7.2 Introducing Control Measures

Now, we try to illustrate how the dynamics of mosquito density change as we introduce control measures to the model given in system 56. It should be understood that, we do not have any control over the climate since it is a natural phenomenon, but the impact of climate conditions to the mosquito propagation in the environment can be controlled [27]. Here, we introduce an aggregated control measure $u \in [0, 1]$. This measure is a composition of several control actions such as

- Controlling the adult mosquitoes which is referred to reducing the survival of adult mosquitoes. Practically this control measure includes chemical methods directed against adult mosquitoes, such as insecticide space sprays or residual applications [8, 27].
- Controlling the growing juveniles which is referred to reducing the growth of juveniles. This control measure includes the biological methods (e.g., fish, copepods small crustaceans that feed on mosquito larvae) to kill or reduce larval mosquito populations in water containers and the chemical methods against the mosquito's aquatic stages for use in water containers (e.g., temephos sand granules) [8, 27].

The mathematical model with control can then be established as

$$\begin{aligned} \frac{dS}{dt} &= \lambda - \frac{b^2 n(t)(1-u)\beta_h \beta_v I}{b\beta_v I + \mu_v} - \mu_h S, \\ \frac{dI}{dt} &= \frac{b^2 n(t)(1-u)\beta_h \beta_v I}{b\beta_v I + \mu_v} - (\mu_h + r)I. \end{aligned} \tag{57}$$

The change in the dynamic with respect to the varying effective levels of control actions is given in Fig. 20. Arbitrary levels of control measures considered for the

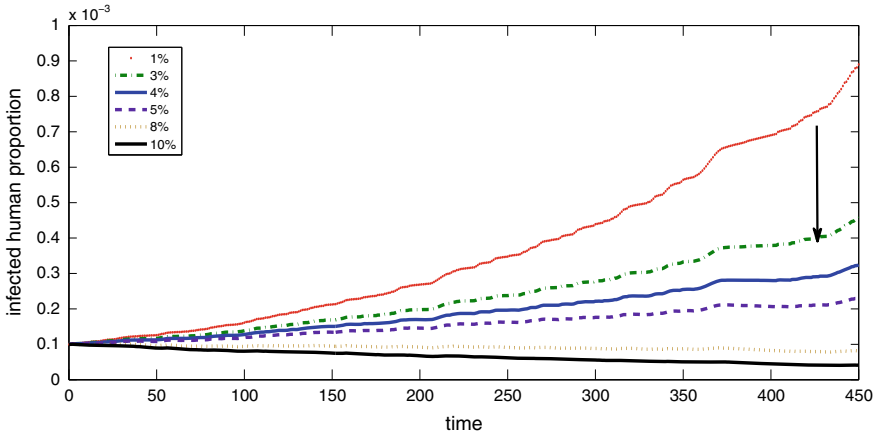

Fig. 20 Simulation of the model with different levels of control actions

simulation. According to Fig. 20, it is very clear that the proportion of humans who are infected with the dengue virus reduces as the efficacy of the control actions improved. It should also be noted that the effectiveness of this control measures depends on multiple factors such as amount of available resources such as human capital and funding, human motivation level, and attitude of public. Thus, 100% efficacy is not achieved in the real world.

8 Conclusion

Dengue is one of the very critical public health concerns in the tropical and sub-tropical regions around the world damaging the socio-economic stability and the well-being of people living in the countries exposed to the disease. The impact of this to Sri Lanka is extremely serious as a developing nation as every year a large number of cases of dengue reported island wide, among them some are life ending.

Biomedical researchers are progressing to find out a potential vaccine to treat dengue, however, none of them have been successful yet. Thus, health professionals and public health officials suggest that the best way to fight with the disease is to control the transmission over the population. Controlling may be only achieved by identifying the dynamic of the disease and hence effectively introducing control measures to reduce the mosquitoes.

Mathematical models are used to model and simulate the dynamics and they reveal very useful information supporting the control. The transmission process of dengue itself is complex and the virus gets changes with respect to time, so do the behavior and biting patterns of dengue mosquitoes vary. Thus, classical SIR models alone

with a deterministic parameter space may not be applicable. The results generated from these classical models have been far away explaining the real picture.

In this study, a two-dimensional differential system involving susceptible and infected human populations derives from a classical SIR model. Dengue data in Colombo is analyzed with respect to climate variation mainly by rainfall and temperature and the mosquito density parameter is modeled using a discrete time nonlinear model. The uncertainty in the process induced by the climate is modeled using fuzzy set theory. The two-dimensional system and the model equation for mosquito density are solved together using a MATLAB program. Possible mathematical analysis is carried out for the deterministic model and sensitivity of critical parameters is analyzed numerically.

The fitted dengue infections are validated with the actual cases reported and the model seems to have predicted the trend and fitted curve goes through most of the peak outbreaks. Therefore, the outcomes of this mathematical model can be used to establish early warning systems thus the disease burden can be minimized if the appropriate control measures are implemented in correct time.

References

1. D. Thai, *Dengue: a trilogy of people, mosquitoes and the virus. Current epidemiology and pathogenesis in (non-)endemic settings*, Thesis Dissertation, Faculty of Medicine, Oxford Clinical Research Unit (OUCRU), Ho Chi Minh City, Vietnam, 2012
2. V. Racloz, R. Ramsey, S. Tong, W. Hu, Surveillance of dengue fever virus: a review of epidemiological models and early warning systems. Plos Negl.Ed Trop. Dis. **6**(5), 1–9 (2012)
3. R. Bhatia, A.P. Dash, T. Sunyoto, Changing epidemiology of dengue in South-East Asia. WHO South-East Asia J. Public Health. 23–27 (2013)
4. E.A. Murray, M. Quam, A.W. Smith, Epidemiology of dengue: past, present and future prospects. Clin. Epidemiol. **5**, 299–309 (2013)
5. L.S. Lloyd, *Best Practices for Dengue Prevention and Control in the Americas, Environmental Health Project* (U.S, Agency for International Development Washington, DC, 2003), p. 20523
6. National Plan of Action for Prevention and Control of Dengue Fever 2005–2009, Epidemiology Unit, Ministry of Health, Sri Lanka
7. N. Thalagala, *Health system Cost for Dengue control and Management in Colombo District, Sri Lanka in 2012* (Dengue Tool Surveillance Project, Epidemiology Unit, Ministry of Health, Sri Lanka, 2012)
8. W. Parks, L. Lloyd, *Planning Social Mobilization and Communication for Dengue Fever Prevention and Control*, (WHO, Geneva, 2004)
9. P. Pongsumpun, Transmission model for dengue disease with and without the effect of extrinsic incubation period. KMITL Sci. Tech. J. **6**, 74–82 (2006)
10. C. Pratchaya, P. Puntani, T. Ming, Effect of rainfall for the dynamical transmission model of the dengue disease in Thailand. Hindawi Comput. Math. Methods Med. 1–17 (2017). https://doi.org/10.1155/2017/2541862
11. A. Ahmed, B. Abba, Mathematical assessment of the role of temperature and rainfall on mosquito population dynamics, in Mathematical Biology (Springer, New Yprk, 2016), pp. 1352-1395. https://doi.org/10.1007/s00285-016-1054-9
12. B. Cazelles, M. Chavez, G.C. Magny, S. Hales, Time-dependent spectral analysis of epidemiological time-series with wavelets. J. R. Soc. Interface **4**, 625–636 (2007)

13. B. Cazelles, M. Chavez, S. Hales, Nonstationary influence of El nino on the synchronous dengue epidemics in Thailand. Plos Med. **2**(4), 313–318 (2005)
14. X. Huang, C.A. Clements, G. Williams, G. Milinovich, W. Hu, A threshold analysis of dengue transmission in terms of weather variables and imported dengue cases in Australia. Emerg. Microbes Infect. **2**(1), 1–7 (2013)
15. S. Naish, P. Dale, J.S. Mackenzie, Climate change and dengue: a critical and systematic review of quantitative modeling approaches. BMC Infect. Dis. **14**(1), 1–14 (2014)
16. L. Chaves, A.C. Morrison, U.D. Kirtron, T.W. Scott, Nonlinear impacts of climatic variability on the density dependent regulation of an insect vector of disease. Glob. Chang. Biol. **18**, 457–468 (2011)
17. P. Turchin, Complex population dynamics, *Monographs in Population Biology* (Princeton University Press, New Jersey, 2003), pp. 19–98
18. B. Cazelles, M. Chavez, D. Berteaux, F. Menard, J.O. Vik, S. Jenouvrier, N.C. Stenseth, Wavelet analysis of ecological time series. Oecologia **156**, 287–304 (2008)
19. Lemaire J., Fuzzy Insurance, ASTIN Bull. **20**(1), 33–55 (1990)
20. H. Zimmermann, *Advanced Review*, Fuzzy set theory (Wiley, Hoboken, 2010), pp. 332–371
21. L. Esteva, C. Vargas, Analysis of a dengue disease transmission model. Math. Bio Sci. **150**, 131–151 (1998)
22. R.A. Erickson, K. Hayhoe, Potential impacts of climate change on the ecology of dengue and its mosquito vector the Asian tiger mosquito (Aedes albopictus). Environ. Res. Lett. **7**, 1–6 (2012)
23. Y. Wei, S. Chengjun, Global analysis for a general epidemiological model with vaccination and varying population. J. Math. Anal. Appl. **372**, 208–233 (2010)
24. W.P.T.M. Wickramaarachchi, S.S.N. Perera, Modeling and analysis of dengue disease transmission in urban Colombo: A wavelets and cross wavelets approach. J. Natl. Found. **43**(4), 337–345 (2014)
25. W.P.T.M. Wickramaarachchi, S.S.N. Perera, Developing a two-dimensional climate risk model for dengue disease transmission in urban Colombo. J. Basic Appl. Res. Int. **20**(3), 168–177 (2017)
26. W.P.T.M. Wickramaarachchi, S.S.N. Perera, The nonlinear dynamics of the dengue mosquito reproduction with respect to climate in urban Colombo: A discrete time density dependent fuzzy model. Int. J. Math. Model. Numer. Optim. **8**(2), 145–161 (2017)
27. W.P.T.M. Wickramaarachchi, S.S.N. Perera, A mathematical model with control to analyse the dynamics of dengue disease transmission in urban Colombo. J. Natl. Found. **46**(1), 41–49 (2018)
28. W.P.T.M. Wickramaarachchi, S.S.N. Perera, *Investigating the impact of climate on dengue disease transmission in urban Colombo: A fuzzy logic model*, in 4th Annual International Conference on Computational Mathematics, Computational Geometry and Statistics (CMCGS) (Singapore, 2015), pp. 20–24

A Mathematical Study of a Model for HPV with Two High-Risk Strains

A. Omame, D. Okuonghae and S. C. Inyama

1 Introduction

Cervical cancer is the most common cancer in women globally [1]. About 85% of the cervical cancer cases and roughly 90% of the 270,000 deaths due to the disease occur in lower- and middle-income countries [2]. Human papillomavirus (HPV) is the most important risk factor associated with cervical cancer, accounting for over 75% of cervical cancer cases [1, 3]. HPV has been classified, based on their oncogenic potentials, into high and low-risk HPV [3]. Low-risk types include types 6, 11, 42, 43 and 44 while types 16, 18, 31, 33, 35, 39, 45, 51, 52, 56, 58, 59, 68, 73, and 82 form the high-risk HPV types [3, 4]. HPV type 16 and type 18 are the most common high-risk types and are responsible for about 70% of global cervical cancer cases. Overall, HPV 16 is the most prevalent type, found in about 54% of cervical cancer cases, and HPV 18 is the second most prominent [5, 6]. Other oncogenic HPV types cause the remaining cancers. Particularly, HPV 45 and HPV 31, being the third and the fourth most prevalent types, are responsible for approximately 10% of cervical cancers. Generally, the four HPV types, HPV 16, 18, 45, and 31 all together account for 80% of global cervical cancer cases [6, 7]. Epidemiological data have shown interactions among HPV types [8]. Liaw et al. [9] pointed out that women could be susceptible to subsequent infections with HPV types 18, 39, 45, 59, and 68, if they have suffered an initial infection with HPV type 16. However, with subsequent infections with HPV, there may be a reduced risk of getting infected with the same strain [10]. Studies have recently shown that HPV vaccines offer cross-protection

A. Omame · S. C. Inyama
Department of Mathematics, Federal University of Technology, Owerri, Nigeria

D. Okuonghae (✉)
Department of Mathematics, University of Benin, Benin City, Nigeria
e-mail: daniel.okuonghae@uniben.edu; danny.okuonghae@corpus-christi.oxon.org

H. Dutta (ed.), *Mathematical Modelling in Health, Social and Applied Sciences*, Forum for Interdisciplinary Mathematics, https://doi.org/10.1007/978-981-15-2286-4_4

against related HPV strains [1, 5, 11, 12]. Vaccination against one strain of HPV can confer some cross-protection against other HPV infections [5, 11, 13].

Harari et al. [12] reported "partial cross-protection by the bivalent human papillomavirus (HPV) vaccine, which targets HPV 16 and HPV 18, against HPV 31, 33, and 45 infection." These claims were strongly supported by recent findings carried out in Scotland [14] and the Netherlands [15]. Ho et al. [10] observed that susceptibility to subsequent infection with HPV types 16, 31, 33, 35, 52, and 58 could be reduced by *IgG* antibodies against HPV type 16. There are currently three major anti-HPV vaccines: the bivalent *Cervarix* vaccine (which targets HPV 16 and 18), the quadrivalent *Gardasil* vaccine (which targets the oncogenic HPV types 16 and 18 and the warts causing HPV types 6 and 11) and the recently introduced nonavalent *Gardasil 9* vaccine (which targets the high-risk HPV types 16, 18, 31, 33, 45, 52, and 58 and the low-risk HPV types 6 and 11) [16]. The newly developed nonavalent *Gardasil 9* HPV vaccine, though very effective, may likely be too expensive for low-income and middle-income countries, where cervical cancer continues to remain a major cause of female mortality, and as such the poorest countries may not easily have access to it [2, 13]. Although the costs of the quadrivalent *Gardasil* vaccine and the bivalent *Cervarix* vaccine do not differ much, the higher cross-protection potential of the bivalent vaccine gives it preference over the quadrivalent vaccine [17].The cross-protection offered by the bivalent vaccine has been proven to be lasting and effective in women [13]. Kudo et al. [18] confirmed this thus: "The bivalent HPV vaccine is highly effective against HPV 16 and 18. Furthermore, significant cross-protection against HPV 31, 45, and 52 was demonstrated and sustained up to 6 years after vaccination. These findings should reassure politicians about the vaccine effectiveness (VE) of bivalent HPV vaccine in a Japanese population." Therefore, the bivalent vaccine's role in the global fight against cervical cancer cannot be underestimated [13].

Several mathematical models have been developed to analyze interactions among strains of different disease types (see, for instance, [19–23]). Garba et al. [24] discussed the dynamics of two strains of influenza, where they showed that cross-immunity due to infection could induce the phenomenon of backward bifurcation. Okuonghae et al. [23] studied the dynamics of a vaccination model of wild and vaccine-derived polio strains. Their model exhibited the phenomenon of competitive exclusion, where the strain with the higher reproduction number (greater than one) drives the other strain to extinction. In a another paper, Elbasha and Galvani [21] studied the interactions among HPV types and showed that mass vaccination may reduce the prevalence of HPV types not included in the vaccine. Their model was based on a simple Susceptible-Infected-Recovered (SIR) structure. Elbasha et al. [22] considered a multi-type HPV transmission model. Their model incorporated the epidemiology of HPV infection, disease and economics into its transmission dynamics. The analyses of the model were mainly based on numerical simulations.

In this work, we consider a two-sex, two-strain HPV mathematical model that rigorously assesses the impact of cross-immunity due to vaccination, in a population where two high-risk strains coexist and there is vaccination for one of the strains, which cross-protects against the strain not included in the vaccine. We are concerned with a vaccination strategy that makes use of the bivalent *Cervarix* vaccine targeted

at one group of high-risk HPV: type 16/18 but with cross-immunity property against other high-risk HPV: type 31/45. This has not been done for any two-sex, two-strain HPV model before. The paper is organized as follows. The model is formulated in Sect. 2 and analyzed qualitatively in Sect. 3. Existence and global stability of the boundary equilibria (for a special case) of the model are investigated in Sect. 4. Numerical simulations are carried out in Sect. 5 while Sect. 6 gives the concluding remarks.

2 Model Formulation

The model is based on the transmission dynamics of two-sex, two-strain HPV infection. In this study, strain 1 is HPV type 16/18 while HPV type 31/45 is considered as strain 2. The total population at time t, denoted by $N(t)$, is subdivided into $N_f(t)$ and $N_m(t)$. $N_f(t)$is further subdivided into susceptible females ($S_f(t)$), females vaccinated with the bivalent *Cervarix* vaccine ($V_f(t)$), females infected with strain 1 (I_{f1}), females with persistent HPV (strain i $(i = 1, 2)$ (P_{fi})), females with cancer (C_f), females who have recovered from strain i $(i = 1, 2)$ (R_{fi}), unvaccinated females infected with strain 2, (I_{f2}), vaccinated females infected with strain 2, (I^p_{f2}), females who have recovered from cancer (R^c_f) , females who have recovered from strain i and are infected with strain $j(I_{fij})$, and females who have recovered from both strains ($M_f(t)$). Similarly, $N_m(t)$ is subdivided into susceptible males ($S_m(t)$), males infectious with strain i $(i = 1, 2)$ (I_{mi}), males who have recovered from strain i $(i = 1, 2)$ (R_{mi}), males who have recovered from strain i and are infected with strain $j(I_{mij})$. Thus

$$N(t) = N_f(t) + N_m(t)$$

$$\begin{aligned} N_f &= S_f + V_f + I_{f1} + P_{f1} + C_f + R^c_f + R_{f1} + I_{f2} + I^p_{f2} \\ &\quad + P_{f2} + R_{f2} + I_{f12} + I_{f21} + M_f \\ N_m &= S_m + I_{m1} + R_{m1} + I_{m2} + R_{m2} + I_{m12} + I_{m21} + M_m \end{aligned}$$

It follows that the two-strain model for the transmission of HPV in a sexually active population is given by the following system of differential equations (Tables 1 and 2 describe the associated state variables and parameters in the model (1) while Figs. 1 and 2 give the flow diagrams of the model (1)):

$$\begin{aligned} \frac{dS_f}{dt} &= (1-f)\Lambda_f - \left(\lambda_{m1} + \lambda_{m2} + \mu_f\right) S_f \\ \frac{dV_f}{dt} &= f\Lambda_f - \left[(1-\xi)\lambda_{m1} + \eta_I(1-\xi)\lambda_{m2} + \mu_f\right] V_f \\ \frac{dI_{f1}}{dt} &= (1-\xi)\lambda_{m1} V_f + \lambda_{m1} S_f - \left(\tau_{f1} + \delta_{f1} + \mu_f\right) I_{f1} + \varepsilon_1 \lambda_{m1} R_{f1} + \alpha_1 \lambda_{m1} M_f \end{aligned}$$

$$
\begin{aligned}
\frac{dP_{f1}}{dt} &= (1-p_1)\tau_{f1}I_{f1} + (1-p_{21})\tau_{f21}I_{f21} - \left(\kappa_{f1}+\mu_f\right)P_{f1}\\
\frac{dC_f}{dt} &= (1-q_1)\kappa_{f1}P_{f1} + \eta_c(1-q_2)\kappa_{f2}P_{f2} - \left(\pi_f+\mu_f+\delta_{fc}\right)C_f\\
\frac{dR_f^c}{dt} &= \pi_f C_f - \mu_f R_f^c\\
\frac{dR_{f1}}{dt} &= p_1\tau_{f1}I_{f1} + q_1\kappa_{f1}P_{f1} - \left(\mu_f+\lambda_{m2}+\varepsilon_1\lambda_{m1}\right)R_{f1}\\
\frac{dI_{f2}}{dt} &= \lambda_{m2}S_f - \left(\tau_{f2}+\delta_{f2}+\mu_f\right)I_{f2} + \varepsilon_2\lambda_{m2}R_{f2} + \alpha_2\lambda_{m2}M_f\\
\frac{dI_{f2}^p}{dt} &= \eta_I(1-\xi)\lambda_{m2}V_f - \left(\eta_p\tau_{f2}+\delta_{f2}^p+\mu_f\right)I_{f2}^p\\
\frac{dP_{f2}}{dt} &= (1-p_2)\eta_p\tau_{f2}I_{f2}^p + (1-p_2)\tau_{f2}I_{f2} + (1-p_{12})\tau_{f12}I_{f12} - \left(\eta_c\kappa_{f2}+\mu_f\right)P_{f2}\\
\frac{dR_{f2}}{dt} &= p_2\eta_p\tau_{f2}I_{f2}^p + p_2\tau_{f2}I_{f2} + q_2\eta_c\kappa_{f2}P_{f2} - \left(\mu_f+\lambda_{m1}+\varepsilon_2\lambda_{m2}\right)R_{f2}\\
\frac{dS_m}{dt} &= \Lambda_m - \left(\lambda_{f1}+\lambda_{f2}+\mu_m\right)S_m\\
\frac{dI_{m1}}{dt} &= \lambda_{f1}S_m - (\tau_{m1}+\delta_{m1}+\mu_m)I_{m1} + \varepsilon_3\lambda_{f1}R_{m1} + \alpha_3\lambda_{f1}M_m\\
\frac{dR_{m1}}{dt} &= \tau_{m1}I_{m1} - \left(\mu_m+\lambda_{f2}+\varepsilon_3\lambda_{f1}\right)R_{m1}\\
\frac{dI_{m2}}{dt} &= \lambda_{f2}S_m + \varepsilon_4\lambda_{f2}R_{m2} + \alpha_4\lambda_{f2}M_m - (\tau_{m2}+\delta_{m2}+\mu_m)I_{m2}\\
\frac{dR_{m2}}{dt} &= \tau_{m2}I_{m2} - \left(\mu_m+\lambda_{f1}+\varepsilon_4\lambda_{f2}\right)R_{m2}\\
\frac{dI_{f12}}{dt} &= \lambda_{m2}R_{f1} - \left(\tau_{f12}+\delta_{f12}+\mu_f\right)I_{f12}\\
\frac{dI_{f21}}{dt} &= \lambda_{m1}R_{f2} - \left(\tau_{f21}+\delta_{f21}+\mu_f\right)I_{f21}\\
\frac{dM_f}{dt} &= p_{12}\tau_{f12}I_{f12} + p_{21}\tau_{f21}I_{f21} - \left(\mu_f+\alpha_1\lambda_{m1}+\alpha_2\lambda_{m2}\right)M_f\\
\frac{dI_{m12}}{dt} &= \lambda_{f2}R_{m1} - (\tau_{m12}+\delta_{m12}+\mu_m)I_{m12}\\
\frac{dI_{m21}}{dt} &= \lambda_{f1}R_{m2} - (\tau_{m21}+\delta_{m21}+\mu_m)I_{m21}\\
\frac{dM_m}{dt} &= \tau_{m12}I_{m12} + \tau_{m21}I_{m21} - \left(\mu_m+\alpha_3\lambda_{f1}+\alpha_4\lambda_{f2}\right)M_m
\end{aligned}
\tag{1}
$$

where,

$$
\lambda_{m1} = \frac{\beta_{m1}(I_{m1}+I_{m21})}{N_m} \tag{2}
$$

Table 1 Description of variables in the model (1)

Variable	Description
$S_f\,(S_m)$	Population of susceptible females (males)
V_f	Population of females vaccinated against strain 1
$I_{f\,1}(I_{m\,1}),\ \ i{=}1{,}2$	Population of females (males) infected with strain 1
$P_{f\,i},\ \ i{=}1{,}2$	Population of females with persistent strain i infection
C_f	Population of females with cervical cancer
$R_{f\,i}(R_{m\,i})\ \ i{=}1{,}2$	Population of females (males) who have recovered naturally from strain i
I_{m2}	Population of infected males with strain 2
I_{f2}	Population of unvaccinated infected females with strain 2
I_{f2}^{p}	Population of vaccinated infected females with strain 2
R_f^c	Population of females who have recovered from cervical cancer
$I_{f\,ij}(I_{m\,ij})$ $i,j{=}1{,}2;\ i{\neq}j$	Population of females (males) who have recovered from strain i and are infected with strain j
$M_f\,(M_m)$	Population of females (males) who have recovered from both strains
$N_f\,(N_m)$	Total female (male) population

and

$$\lambda_{m2} = \frac{\beta_{m2}(I_{m2} + I_{m12})}{N_m} \tag{3}$$

$$\lambda_{f1} = \frac{\beta_{f1}(I_{f1} + I_{f21} + \theta_{p1}P_{f1})}{N_f} \tag{4}$$

and

$$\lambda_{f2} = \frac{\beta_{f2}(I_{f2} + I_{f12} + \phi_p I_{f2}^{p} + \theta_{p2}P_{f2})}{N_f} \tag{5}$$

In (2) and (3), β_{m1} and β_{m2} are the effective contact rates for male-to-female transmission of strain 1 and strain 2 infections, respectively. β_{m1} is the product of c_1^f and β_1^m (i.e., $\beta_{m1} = c_1^f\beta_1^m$), while β_{m2} is the product of c_1^f and β_2^m (that is, $\beta_{m2} = c_1^f\beta_2^m$), where β_1^m and β_2^m denote the probabilities of transmitting strain 1 and strain 2 infections from male-to-female, respectively, and c_1^f denotes the rate at which females acquire new sexual partners. In (4) and (5), β_{f1} and β_{f2} are the effective contact rates for female-to-male transmission of strain 1 and strain 2 infections, respectively. β_{f1} is the product of c_1^f and β_1^f (i.e., $\beta_{f1} = c_1^m\beta_1^f$), while β_{f2} is the product of c_1^m and β_2^f (that is, $\beta_{f2} = c_1^m\beta_2^f$), where β_1^f and β_2^f denote the probabilities of transmitting strain 1 and strain 2 infections from female-to-male and c_1^m denotes the rate at which males acquire new sexual partners.

Table 2 Description of parameters in the model (1)

Parameter	Description
$\Lambda_f\,(\Lambda_m)$	Recruitment rate for females (males)
f	Proportion of susceptible females vaccinated against strain 1
$\mu_f\,(\mu_m)$	Natural death rate for females (males)
ξ	Bivalent vaccine efficacy for females
η_I	Modification parameter for cross-protection of vaccinated females against incident infection with strain 2
η_p	Modification parameter for cross-protection of vaccinated females against persistent infection with strain 2
η_c	Modification parameter for reduced rate of progression to cancer by females with persistent strain 2 infection relative to those with persistent strain 1 infection
$\tau_{f\,i}\,(\tau_{m\,i})_{,\ i=1,2}$	Recovery rate of females (males) infected with strain i
$\delta_{f\,i}\,(\delta_{m\,i})_{,\ i=1,2}$	Disease induced death rate for females (males) infected with strain i
$\delta_{f\,ij}\,(\delta_{m\,ij})$ $_{i,j=1,2;i\neq j}$	HPV induced death rate for females (males) who have recovered from strain i and infected with strain j
δ_{fc}	Cervical cancer induced death rate for females
δ_{f2}^{p}	Disease induced death rate for females in I_{f2}^{p} class
$\varepsilon_i\,,\ \alpha_i$	Modification parameters for reduced susceptibility of individuals who have recovered naturally from either one or both strains relative to those in the susceptible class
$\tau_{f\,ij}\,(\tau_{m\,ij})$	Recovery rate for females (males) who have recovered from strain i and are infected with strain j
$p_i,\ \ p_{ij}$	Proportion of females who recover naturally from HPV and do not progress to persistent HPV infection
q_i	Proportion of females who recover from persistent strain i infection and do not progress to cervical cancer
$\theta_{p\,i,\ i=1,2}$	Modification parameter for the infectiousness of females with persistent strain i infection relative to those in $I_{f1},\ \ I_{f2},\ \ I_{f21},\ \ I_{f12}$ classes
ϕ_p	Modification parameter for the infectiousness of females in I_{f2}^{p} class relative to those in I_{f2} class
π_f	Rate of recovery from cancer for females
κ_{f2}	Transition rate out of P_{f2} class for females

The model will be studied subject to the group contact constraint given by

$$c_m N_m = c_f N_f\,, \tag{6}$$

a consistency condition which states that in any small interval of time $[t, t+\Delta t]$, the total number of partnerships formed by females with males must equal total number of partnerships formed by males with females [25, 26].

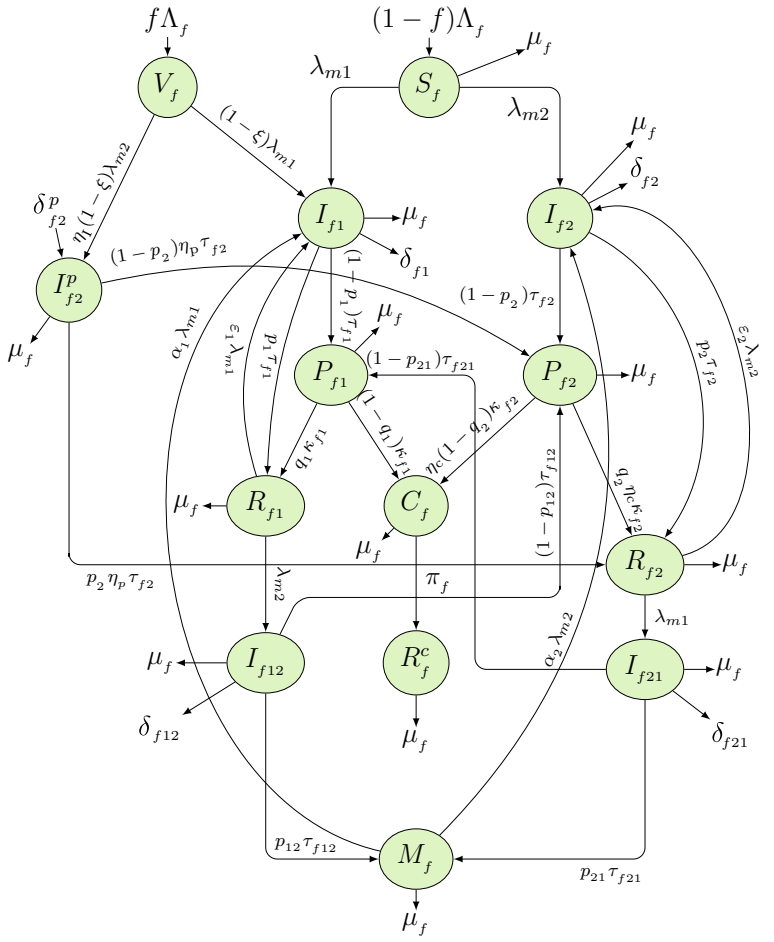

Fig. 1 Schematic diagram of the female components of the model (1)

Since the model monitors human population, it is easy to show that the state variables remain non-negative for all non-negative initial conditions (i.e., all the state variables and parameters of the model are non-negative for all $t > 0$).

Some of the new features of our work include incorporating the dynamics of cross-immunity due to vaccination ($\eta_I \neq 0, \eta_p \neq 0$) [5, 12, 18], allowing for heterogeneity in infectiousness of vaccinated and unvaccinated females with strain 2 (HPV type 31/45) [27], including compartments for females (males) who recover from one strain and are infected with the other strain, $I_{fij}(I_{mij})$, $i \neq j$, for females (males), and allowing for disease transmission by individuals who recover from one strain and are infected with the other strain (clinical studies have shown that subsequent infections with other strains are possible after an initial infection with HPV [10].

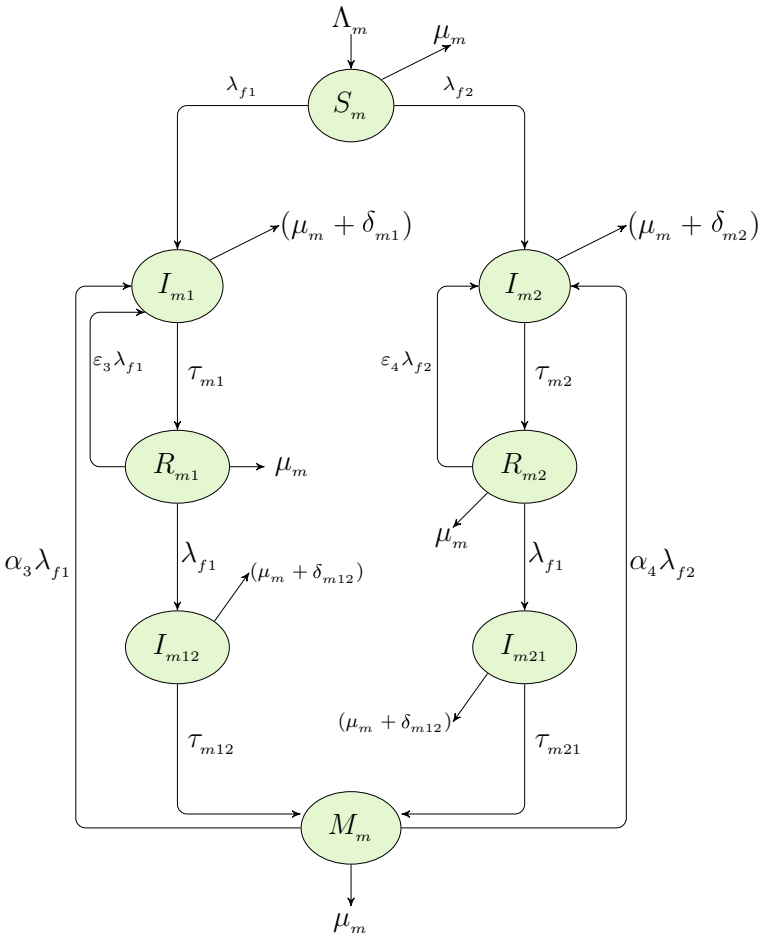

Fig. 2 Schematic diagram of the male components of the model (1)

3 Mathematical Analysis of the Model

We shall now rigorously analyze the model to gain insights into its dynamical features. We first show that the system (1) is dissipative (i.e., all feasible solutions are uniformly bounded in a proper subset $\mathcal{D} \subset \mathcal{R}_+^{22}$). The system (1) is split into two parts, namely the female population (N_f) (with $N_f = S_f + V_f + I_{f1} + P_{f1} + C_f + R_f^c + R_{f1} + I_{f2} + I_{f2}^p + P_{f2} + R_{f2} + I_{f12} + I_{f21} + M_f$) and the male population (N_m) (with $N_m = S_m + I_{m1} + R_{m1} + I_{m2} + R_{m2} + I_{m12} + I_{m21} + M_m$). Consider the feasible region

$$\mathcal{D} = \mathcal{D}_f \cup \mathcal{D}_m \subset \mathcal{R}_+^{14} \times \mathcal{R}_+^{8},$$

with

$$\mathcal{D}_f = \Bigg\{(S_f, V_f, I_{f1}, P_{f1}, C_f, R_f^c, R_{f1}, I_{f2}, I_{f2}^p, P_{f2}, R_{f2}, I_{f12}, I_{f21}, M_f) \in \mathcal{R}_+^{14} : S_f + V_f + I_{f1} + P_{f1} + C_f + R_f^c + R_{f1} + I_{f2} + I_{f2}^p + P_{f2} + R_{f2} + I_{f12} + I_{f21} + M_f \leq \frac{\Lambda_f}{\mu_f}\Bigg\}$$

and

$$\mathcal{D}_m = \Bigg\{(S_m, I_{m1}, R_{m1}, I_{m2}, R_{m2}, I_{m12}, I_{m21}, M_m) \in \mathcal{R}_+^{8} : S_m + I_{m1} + R_{m1} + I_{m2} + R_{m2} + I_{m12} + I_{m21} + M_m \leq \frac{\Lambda_m}{\mu_m}\Bigg\}$$

Adding the female compartments and the male compartments in the differential system (1), respectively, gives

$$\frac{dN_f}{dt} = \Lambda_f - \mu_f N_f(t) - [\delta_{f1} I_{f1} + \delta_{fc} C_f + \delta_{f2} I_{f2} + \delta_{f2}^p I_{f2}^p + \delta_{f12} I_{f12} + \delta_{f21} I_{f21}]$$
$$\frac{dN_m}{dt} = \Lambda_m - \mu_m N_m(t) - [\delta_{m1} I_{m1} + \delta_{m2} I_{m2} + \delta_{m12} I_{m12} + \delta_{m21} I_{m21}]$$

We have that,

$$\begin{aligned} \Lambda_f - (\mu_f + 6\delta_f) N_f \leq \frac{dN_f}{dt} < \Lambda_f - \mu_f N_f, \\ \Lambda_m - (\mu_m + 4\delta_m) N_m \leq \frac{dN_m}{dt} < \Lambda_m - \mu_m N_m \end{aligned} \tag{7}$$

where $\delta_f = \min\Big\{\delta_{f1}, \delta_{fc}, \delta_{f2}, \delta_{f2}^p, \delta_{f12}, \delta_{f21}\Big\}$,
$\delta_m = \min\{\delta_{m1}, \delta_{m2}, \delta_{m12}, \delta_{m21}\}$,
It follows from (7) that,

$$\frac{dN_f}{dt} \leq \Lambda_f - \mu_f N_f(t),$$
$$\frac{dN_m}{dt} \leq \Lambda_m - \mu_m N_m(t)$$

A standard comparison theorem [28] can be used to show that $N_f(t) \leq N_f(0)e^{-\mu_f t} + \frac{\Lambda_f}{\mu_f}(1 - e^{-\mu_f t})$ and $N_f(t) \leq N_f(0)e^{-\mu_f t} + \frac{\Lambda_f}{\mu_f}(1 - e^{-\mu_f t})$. In particular, $N_f(t) \leq \frac{\Lambda_f}{\mu_f}$ and $N_f(t) \leq \frac{\Lambda_f}{\mu_f}$ if $N_f(0) \leq \frac{\Lambda_f}{\mu_f}$ and $N_m(0) \leq \frac{\Lambda_m}{\mu_m}$, respectively. Thus, the region $\mathcal{D}$ is positively invariant. Hence, it is sufficient to consider the dynamics of the flow generated by (1) in $\mathcal{D}$. Thus, the result is summarized.

Lemma 3.1 *The region* $\mathcal{D}=\mathcal{D}_f\cup\mathcal{D}_m\subset \mathcal{R}_+^{14}\times\mathcal{R}_+^{8}$ *is positively invariant for the two-strain HPV model (1) with initial conditions in* $\mathcal{R}_+^{22}$

3.1 Local Stability of Disease-Free Equilibrium (DFE)

The model (1) has a DFE, obtained by setting the right-hand sides of the equations in the model (1) to zero, given by

$$\begin{aligned}\xi_0 &= \Big(S_f^*, V_f^*, I_{f1}^*, P_{f1}^*, C_f^*, R_f^{c*}, R_{f1}^*, I_{f2}^*,\\ &\quad I_{f2}^{p*}, P_{f2}^*, R_{f2}^*, S_m^*, I_{m1}^*, R_{m1}^*, I_{m2}^*, R_{m2}^*, I_{f12}^*, I_{f21}^*, M_f^*, I_{m12}^*, I_{m21}^*, M_m^*\Big)\\ &= \Big(S_f^*, V_f^*, 0,0,0,0,0,0,0,0,0, S_m^*, 0,0,0,0,0,0,0,0,0,0\Big)\end{aligned}$$

with,

$$S_f^* = \frac{(1-f)\Lambda_f}{\mu_f}, \quad V_f^* = \frac{f\Lambda_f}{\mu_f}, \quad S_m^* = \frac{\Lambda_m}{\mu_m}$$

The linear stability of the disease-free equilibrium, ξ_0 can be established using the next-generation operator principle [29] on the system (1).

The next-generation matrices are, respectively, given by

$$F = \begin{bmatrix}
0 & 0 & 0 & 0 & 0 & 0 & \frac{\beta_{m1}Q_1}{N_m^*} & 0 & 0 & 0 & 0 & \frac{\beta_{m1}Q_1}{N_m^*}\\
0 & 0 & 0 & 0 & 0 & 0 & 0 & 0 & 0 & 0 & 0 & 0\\
0 & 0 & 0 & 0 & 0 & 0 & 0 & 0 & 0 & 0 & 0 & 0\\
0 & 0 & 0 & 0 & 0 & 0 & 0 & \frac{\beta_{m2}S_f^*}{N_m^*} & 0 & 0 & \frac{\beta_{m2}S_f^*}{N_m^*} & 0\\
0 & 0 & 0 & 0 & 0 & 0 & 0 & \frac{\beta_{m2}S_f^*}{N_m^*} & 0 & 0 & \frac{\beta_{m2}Q_2}{N_m^*} & 0\\
0 & 0 & 0 & 0 & 0 & 0 & 0 & 0 & 0 & 0 & 0 & 0\\
\frac{\beta_{f1}S_m^*}{N_f^*} & \frac{\beta_{f1}\theta_{p1}S_m^*}{N_f^*} & 0 & 0 & 0 & 0 & 0 & 0 & 0 & \frac{\beta_{f1}S_m^*}{N_f^*} & 0 & 0\\
0 & 0 & 0 & \frac{\beta_{f2}S_m^*}{N_f^*} & \frac{\beta_{f2}\phi_pS_m^*}{N_f^*} & \frac{\beta_{f2}\theta_{p2}S_m^*}{N_f^*} & 0 & 0 & \frac{\beta_{f2}S_m^*}{N_f^*} & 0 & 0 & 0\\
0 & 0 & 0 & 0 & 0 & 0 & 0 & 0 & 0 & 0 & 0 & 0\\
0 & 0 & 0 & 0 & 0 & 0 & 0 & 0 & 0 & 0 & 0 & 0\\
0 & 0 & 0 & 0 & 0 & 0 & 0 & 0 & 0 & 0 & 0 & 0\\
0 & 0 & 0 & 0 & 0 & 0 & 0 & 0 & 0 & 0 & 0 & 0
\end{bmatrix}$$

$$V = \begin{bmatrix} K_1 & 0 & 0 & 0 & 0 & 0 & 0 & 0 & 0 & 0 & 0 & 0 \\ -G_1 & K_2 & 0 & 0 & 0 & 0 & 0 & 0 & 0 & -G_2 & 0 & 0 \\ 0 & 0 & K_3 & 0 & 0 & -G_4 & 0 & 0 & 0 & 0 & 0 & 0 \\ 0 & 0 & 0 & K_4 & 0 & 0 & 0 & 0 & 0 & 0 & 0 & 0 \\ 0 & 0 & 0 & 0 & K_5 & 0 & 0 & 0 & 0 & 0 & 0 & 0 \\ 0 & 0 & 0 & -G_6 & -G_5 & K_6 & 0 & 0 & -G_7 & 0 & 0 & 0 \\ 0 & 0 & 0 & 0 & 0 & 0 & K_7 & 0 & 0 & 0 & 0 & 0 \\ 0 & 0 & 0 & 0 & 0 & 0 & 0 & K_8 & 0 & 0 & 0 & 0 \\ 0 & 0 & 0 & 0 & 0 & 0 & 0 & 0 & K_9 & 0 & 0 & 0 \\ 0 & 0 & 0 & 0 & 0 & 0 & 0 & 0 & 0 & K_{10} & 0 & 0 \\ 0 & 0 & 0 & 0 & 0 & 0 & 0 & 0 & 0 & 0 & K_{11} & 0 \\ 0 & 0 & 0 & 0 & 0 & 0 & 0 & 0 & 0 & 0 & 0 & K_{12} \end{bmatrix}$$

where,

$$Q_1 = S_f^* + (1-\xi)V_f^* = \frac{(1-f\xi)\Lambda_f}{\mu_f}, \quad Q_2 = (1-\xi)\eta_I V_f^* = \frac{(1-\xi)f\eta_I\Lambda_f}{\mu_f}$$

$$K_1 = \tau_{f1} + \delta_{f1} + \mu_f,\ K_2 = \kappa_{f1} + \mu_f,\ K_3 = \pi_f + \mu_f + \delta_{fc},\ K_4 = \tau_{f2} + \delta_{f2} + \mu_f,$$

$$K_5 = \eta_p\tau_{f2} + \delta_{f2}^p + \mu_f, \quad K_6 = \eta_c\kappa_{f2} + \mu_f, \quad K_7 = \tau_{m1} + \delta_{m1} + \mu_m,$$

$$K_8 = \tau_{m2} + \delta_{m2} + \mu_m, \quad K_9 = \tau_{f12} + \delta_{f12} + \mu_m, \quad K_{10} = \tau_{f21} + \delta_{f21} + \mu_f,$$

$$K_{11} = \tau_{m12} + \delta_{m12} + \mu_m, \quad K_{12} = \tau_{m21} + \delta_{m21} + \mu_m, \quad G_1 = (1-p_1)\tau_{f1},$$

$$G_2 = (1-p_{21})\tau_{f21},\ G_3 = (1-q_1)\kappa_{f1},\ G_4 = \eta_c(1-q_2)\kappa_{f2},\ G_5 = (1-p_2)\eta_p\tau_{f2},$$

$$G_6 = (1-p_2)\tau_{f2},\ G_7 = (1-p_{12})\tau_{f12},\ G_8 = p_2\eta_p\tau_{f2},\ G_9 = q_2\eta_c\kappa_{f2},$$

$$G_{10} = p_{12}\tau_{f12}, G_{11} = p_{21}\tau_{f21}$$

Hence, it follows from [29] that the basic reproduction number of the model (1), denoted by $\mathcal{R}_0$, is given by (where ρ is the spectral radius)
$\mathcal{R}_0 = \rho(FV^{-1}) = \max\{\mathcal{R}_{01}, \mathcal{R}_{02}\}$ where $\mathcal{R}_{01}$ and $\mathcal{R}_{02}$ are the associated reproduction numbers for strain 1 and strain 2, respectively, given by

$$\mathcal{R}_{01} = \sqrt{\frac{\beta_{f1}\beta_{m1}(K_2 + G_1\theta_{p1})(1-f\xi)}{K_1K_2K_7}}, \quad \mathcal{R}_{02} = \sqrt{\frac{\beta_{f2}\beta_{m2}(K_6 + G_6\theta_{p2})}{K_4K_6K_8}}$$

The result below follows from Theorem 2 in [29].

Lemma 3.2 *The DFE* (ξ_0) *of the model* (1) *is locally asymptotically stable (LAS) if* $\mathcal{R}_0 < 1$, *and unstable if* $\mathcal{R}_0 > 1$.

3.2 Backward Bifurcation Analysis of the Model (1)

We shall investigate the type of bifurcation the model (1) may undergo, using the center manifold theory as discussed in [30]. The following result can be obtained using the approach in [30].

Theorem 3.1 *If $\mathcal{R}_0 < 1$ and a backward bifurcation coefficient $a > 0$, where*

$$
\begin{aligned}
a = &-\frac{2K_1\nu_3\omega_3}{N_m^*X_1^*}\Big\{\omega_{12}X_1^* - \varepsilon_1\omega_7N_m^* + (\omega_{13}+\omega_{14}+\omega_{15}+\omega_{16})X_1^* \\
&- \{\omega_1 + (1-\xi)\omega_2\}N_m^*\Big\} - \frac{2\beta_{m2}\beta_{f2}(K_6+\theta_{p2}G_6)\nu_{15}\omega_{15}}{K_4K_6N_m^*N_f^*} \\
&\Big\{\omega_{12}X_1^* - \varepsilon_2\omega_{11}N_m^* + (\omega_{13}+\omega_{14}+\omega_{15}+\omega_{16})x_1^* - \omega_1N_m^*\Big\} \\
&- \frac{2\beta_{m2}\beta_{f2}\eta_I(1-\xi)\nu_{15}\omega_{15}}{K_5K_6N_m^*N_f^*}\Big\{\omega_{12}x_{12}^* + (\omega_{13}+\omega_{14}+\omega_{15}+\omega_{16})x_2^* - \omega_2N_m^*\Big\} \\
&- \frac{2K_1\nu_3\omega_3}{N_m^*N_f^*}\Big\{\{\omega_1+\omega_2\}x_{12}^* - \varepsilon_3\omega_{14}N_f^* + n_1x_{12}^* - \omega_{12}N_f^*\Big\} \\
&- \frac{2\beta_{f2}\beta_{m2}\Big\{K_5(K_6+\theta_{p2}G_6)x_1^* + K_5(\phi_pK_6+\theta_{p2}G_5)\eta_I(1-\xi)x_2^*\Big\}\nu_{15}\omega_{15}}{K_4K_5K_6N_m^*N_f^{*2}} \\
&\times\Big\{\{\omega_1+\omega_2\}x_{12}^* - \varepsilon_4\omega_{16}N_f^* + n_1x_{12}^* - \omega_{12}N_f^*\Big\},
\end{aligned}
$$

then model (1) exhibits backward bifurcation at $\mathcal{R}_0 = 1$. If the inequality sign is reversed, then the system (1) exhibits a forward bifurcation at $\mathcal{R}_0 = 1$.

Proof Suppose

$$
\begin{aligned}
\xi_e = (&S_f^{**}, V_f^{**}, I_{f1}^{**}, P_{f1}^{**}, C_f^{**}, R_f^{c**}, R_{f1}^{**}, I_{f2}^{**}, I_{f2}^{p**}, P_{f2}^{**}, R_{f2}^{**}, S_m^{**}, I_{m1}^{**}, R_{m1}^{**}, I_{m2}^{**}, \\
&R_{m2}^{**}, I_{f12}^{**}, I_{f21}^{**}, M_f^{**}, I_{m12}^{**}, I_{m21}^{**}, M_m^{**})
\end{aligned}
$$

represents any arbitrary endemic equilibrium of the model (i.e., an endemic equilibrium in which at least one of the infected components is nonzero). The existence (or otherwise) of backward bifurcation will be explored using the center manifold theory [30]. To apply this theory, it is necessary to carry out the following change of variables.

Let

$$\begin{aligned}
&S_f = x_1,\ V_f = x_2,\ I_{f1} = x_3,\ P_{f1} = x_4,\ C_f = x_5,\ R_f^c = x_6,\\
&R_{f1} = x_7,\ I_{f2} = x_8,\ I_{f2}^p = x_9,\\
&P_{f2} = x_{10},\ R_{f2} = x_{11},\ S_m = x_{12},\ I_{m1} = x_{13},\ R_{m1} = x_{14},\\
&I_{m2} = x_{15},\ R_{m2} = x_{16},\ I_{f12} = x_{17},\\
&I_{f21} = x_{18},\ M_f = x_{19},\ I_{m12} = x_{20},\ I_{m21} = x_{21},\ M_m = x_{22}
\end{aligned}$$

so that

$$N = \sum_{i=1}^{22} x_i.$$

Further, using the vector notation

$$\begin{aligned}
X = (&x_1, x_2, x_3, x_4, x_5, x_6, x_7, x_8, x_9, x_{10}, x_{11}, x_{12}, x_{13}, x_{14},\\
&x_{15}, x_{16}, x_{17}, x_{18}, x_{19}, x_{20}, x_{21}, x_{22})^T
\end{aligned}$$

the model (1) can be rewritten in the form

$$\begin{aligned}
\frac{dX}{dt} = f = (&f_1, f_2, f_3, f_4, f_5, f_6, f_7, f_8, f_9, f_{10}, f_{11}, f_{12}, f_{13},\\
&f_{14}, f_{15}, f_{16}, f_{17}, f_{18}, f_{19}, f_{20}, f_{21}, f_{22})^T
\end{aligned}$$

as follows:

$$\begin{aligned}
\frac{dx_1}{dt} &\equiv f_1 = (1-f)\Lambda_f - \left(\lambda_{m1} + \lambda_{m2} + \mu_f\right)x_1\\
\frac{dx_2}{dt} &\equiv f_2 = f\Lambda_f - \left[(1-\xi)\lambda_{m1} + \eta_I(1-\xi)\lambda_{m2} + \mu_f\right]x_2\\
\frac{dx_3}{dt} &\equiv f_3 = (1-\xi)\lambda_{m1}x_2 + \lambda_{m1}x_1 + \varepsilon_1\lambda_{m1}x_7 + \alpha_1\lambda_{m1}x_{19} - (\tau_{f1} + \delta_{f1} + \mu_f)x_3\\
\frac{dx_4}{dt} &\equiv f_4 = (1-p_1)\tau_{f1}x_3 + (1-p_{21})\tau_{f21}x_{18} - (\kappa_{f1} + \mu_f)x_4\\
\frac{dx_5}{dt} &\equiv f_5 = (1-q_1)\kappa_{f1}x_4 + \eta_c(1-q_2)\kappa_{f2}x_{10} - (\pi_f + \mu_f + \delta_{fc})x_5\\
\frac{dx_6}{dt} &\equiv f_6 = \pi_f x_5 - \mu_f x_6\\
\frac{dx_7}{dt} &\equiv f_7 = p_1\tau_{f1}x_3 + q_1\kappa_{f1}x_4 - \left(\mu_f + \lambda_{m2} + \varepsilon_1\lambda_{m1}\right)x_7\\
\frac{dx_8}{dt} &\equiv f_8 = \lambda_{m2}x_1 + \varepsilon_2\lambda_{m2}x_{11} + \alpha_2\lambda_{m2}x_{19} - (\tau_{f2} + \delta_{f2} + \mu_f)x_8
\end{aligned}$$

$$
\begin{aligned}
\frac{dx_9}{dt} &\equiv f_9 = \eta_I(1-\xi)\lambda_{m2}x_2 - (\eta_p\tau_{f2} + \delta_{f2}^p + \mu_f)x_9\\
\frac{dx_{10}}{dt} &\equiv f_{10} = (1-p_2)\eta_p\tau_{f2}x_9 + (1-p_2)\tau_{f2}x_8 + (1-p_{12})\tau_{f12}x_{17} - (\eta_c\kappa_{f2} + \mu_f)x_{10}\\
\frac{dx_{11}}{dt} &\equiv f_{11} = p_2\eta_p\tau_{f2}x_9 + p_2\tau_{f2}x_8 + q_2\eta_c\kappa_{f2}x_{10} - \left(\lambda_{m1} + \varepsilon_2\lambda_{m2} + \mu_f\right)x_{11}\\
\frac{dx_{12}}{dt} &\equiv f_{12} = \Lambda_m - \left(\lambda_{f1} + \mu_m + \lambda_{f2}\right)x_{12}\\
\frac{dx_{13}}{dt} &\equiv f_{13} = \lambda_{f1}x_{12} + \varepsilon_3\lambda_{f1}x_{14} + \alpha_3\lambda_{f1}x_{22} - (\tau_{m1} + \delta_{m1} + \mu_m)x_{13}\\
\frac{dx_{14}}{dt} &\equiv f_{14} = \tau_{m1}x_{13} - \left(\lambda_{f2}x_{14} + \varepsilon_3\lambda_{f1}x_{14} + \mu_m\right)x_{14}\\
\frac{dx_{15}}{dt} &\equiv f_{15} = \lambda_{f2}x_{12} + \varepsilon_4\lambda_{f2}x_{16} + \alpha_4\lambda_{f2}x_{22} - (\tau_{m2} + \delta_{m2} + \mu_m)x_{15}\\
\frac{dx_{16}}{dt} &\equiv f_{16} = \tau_{m2}x_{15} - \left(\mu_m + \lambda_{f1} + \varepsilon_4\lambda_{f2}\right)x_{16}\\
\frac{dx_{17}}{dt} &\equiv f_{17} = \lambda_{m2}x_7 - \left(\tau_{f12} + \delta_{f12} + \mu_f\right)x_{17}\\
\frac{dx_{18}}{dt} &\equiv f_{18} = \lambda_{m1}x_{11} - \left(\tau_{f21} + \delta_{f21} + \mu_f\right)x_{18}\\
\frac{dx_{19}}{dt} &\equiv f_{19} = p_{12}\tau_{f12}x_{17} + p_{21}\tau_{f21}x_{18} - \left(\mu_f + \alpha_1\lambda_{m1} + \alpha_2\lambda_{m2}\right)x_{19}\\
\frac{dx_{20}}{dt} &\equiv f_{20} = \lambda_{f2}x_{14} - (\tau_{m12} + \delta_{m12} + \mu_m)\,x_{20}
\end{aligned}
\tag{8}
$$

$$
\begin{aligned}
\frac{dx_{21}}{dt} &\equiv f_{21} = \lambda_{f1}x_{16} - (\tau_{m21} + \delta_{m21} + \mu_m)\,x_{21}\\
\frac{dx_{22}}{dt} &\equiv f_{22} = \tau_{m12}x_{20} + \tau_{m21}x_{21} - \left(\mu_m + \alpha_3\lambda_{f1} + \alpha_4\lambda_{f2}\right)x_{22}
\end{aligned}
$$

where,

$$
\begin{aligned}
\lambda_{f1} &= \frac{\beta_{f1}(x_3 + x_{18} + \theta_{p1}x_4)}{\sum_{i=1}^{11}x_i + \sum_{i=17}^{19}x_i}\\
\lambda_{f2} &= \frac{\beta_{f2}(x_8 + x_{17} + \phi_p x_9 + \theta_{p2}x_{10})}{\sum_{i=1}^{11}x_i + \sum_{i=17}^{19}x_i}\\
\lambda_{m1} &= \frac{\beta_{m1}(x_{13} + x_{21})}{\sum_{i=12}^{16}x_i + \sum_{i=20}^{22}x_i}\\
\lambda_{m2} &= \frac{\beta_{m2}(x_{15} + x_{20})}{\sum_{i=12}^{16}x_i + \sum_{i=20}^{22}x_i}
\end{aligned}
$$

Without loss of generality, consider the case when $\mathcal{R}_{01} = 1$. Suppose, further, that β_{f1} is chosen as a bifurcation parameter. Solving for $\beta_{f1} = \beta_{f1}^*$ from $\mathcal{R}_{01} = 1$ gives

$$
\beta_{f1} = \beta_{f1}^* = \frac{K_1K_2K_7}{\beta_{m1}\left(K_2 + G_1\theta_{p1}\right)(1 - f\xi)}
$$

The Jacobian of the transformed system (8), evaluated at the DFE (ξ_0) with $\beta_{f1} = \beta_{f1}^*$, is given by

$$J(\xi_0)|_{\beta_{f1}=\beta_{f1}^*} = \begin{bmatrix} J_{11} & J_{12} \\ J_{21} & J_{22} \end{bmatrix}$$

where

$$J_{11} = \begin{bmatrix} -\mu_f & 0 & 0 & 0 & 0 & 0 & 0 & 0 & 0 & 0 & 0 \\ 0 & -\mu_f & 0 & 0 & 0 & 0 & 0 & 0 & 0 & 0 & 0 \\ 0 & 0 & -K_1 & 0 & 0 & 0 & 0 & 0 & 0 & 0 & 0 \\ 0 & 0 & G_1 & -K_2 & 0 & 0 & 0 & 0 & 0 & 0 & 0 \\ 0 & 0 & 0 & 0 & -K_3 & 0 & 0 & 0 & 0 & G_4 & 0 \\ 0 & 0 & 0 & 0 & 0 & -\mu_f & 0 & 0 & 0 & 0 & 0 \\ 0 & 0 & p_1\tau_{f1} & q_1\kappa_{f1} & 0 & 0 & -\mu_f & 0 & 0 & 0 & 0 \\ 0 & 0 & 0 & 0 & 0 & 0 & 0 & -K_4 & 0 & 0 & 0 \\ 0 & 0 & 0 & 0 & 0 & 0 & 0 & 0 & -K_5 & 0 & 0 \\ 0 & 0 & 0 & 0 & 0 & 0 & 0 & G_6 & G_5 & -K_6 & 0 \\ 0 & 0 & 0 & 0 & 0 & 0 & 0 & p_2\tau_{f2} & G_8 & G_9 & -\mu_f \end{bmatrix}$$

$$J_{12} = \begin{bmatrix} 0 & \frac{-\beta_{m1}x_1^*}{N_m^*} & 0 & \frac{-\beta_{m2}x_1^*}{N_m^*} & 0 & 0 & 0 & 0 & \frac{-\beta_{m2}x_1^*}{N_m^*} & \frac{-\beta_{m1}x_1^*}{N_m^*} & 0 \\ 0 & \frac{-\beta_{m1}(1-\xi)x_2^*}{N_m^*} & 0 & \frac{-\beta_{m2}\eta_I(1-\xi)x_2^*}{N_m^*} & 0 & 0 & 0 & 0 & \frac{-\beta_{m2}\eta_I(1-\xi)x_2^*}{N_m^*} & \frac{-\beta_{m2}(1-\xi)x_2^*}{N_m^*} & 0 \\ 0 & \frac{\beta_{m1}X_1^*}{N_m^*} & 0 & 0 & 0 & 0 & 0 & 0 & 0 & \frac{\beta_{m2}X_1^*}{N_m^*} & 0 \\ 0 & 0 & 0 & 0 & 0 & 0 & G_2 & 0 & 0 & 0 & 0 \\ 0 & 0 & 0 & 0 & 0 & 0 & 0 & 0 & 0 & 0 & 0 \\ 0 & 0 & 0 & 0 & 0 & 0 & 0 & 0 & 0 & 0 & 0 \\ 0 & 0 & 0 & 0 & 0 & 0 & 0 & 0 & 0 & 0 & 0 \\ 0 & 0 & 0 & \frac{\beta_{m2}x_1^*}{N_m^*} & 0 & 0 & 0 & 0 & \frac{\beta_{m2}x_1^*}{N_m^*} & 0 & 0 \\ 0 & 0 & 0 & \frac{\beta_{m2}\eta_I(1-\xi)x_2^*}{N_m^*} & 0 & 0 & 0 & 0 & \frac{\beta_{m2}\eta_I(1-\xi)x_2^*}{N_m^*} & 0 & 0 \\ 0 & 0 & 0 & 0 & 0 & G_7 & 0 & 0 & 0 & 0 & 0 \\ 0 & 0 & 0 & 0 & 0 & 0 & 0 & 0 & 0 & 0 & 0 \end{bmatrix}$$

$$J_{21} = \begin{bmatrix} 0 & 0 & \frac{-\beta_{f1}x_{12}^*}{N_f^*} & \frac{-\beta_{f1}\theta_{p1}x_{12}^*}{N_f^*} & 0 & 0 & 0 & \frac{-\beta_{f2}x_{12}^*}{N_f^*} & \frac{-\beta_{f2}\phi_p x_{12}^*}{N_f^*} & \frac{-\beta_{f2}\theta_{p2}x_{12}^*}{N_f^*} & 0 \\ 0 & 0 & \frac{\beta_{f1}x_{12}^*}{N_f^*} & \frac{\beta_{f1}\theta_{p1}x_{12}^*}{N_f^*} & 0 & 0 & 0 & 0 & 0 & 0 & 0 \\ 0 & 0 & 0 & 0 & 0 & 0 & 0 & 0 & 0 & 0 & 0 \\ 0 & 0 & 0 & 0 & 0 & 0 & 0 & \frac{\beta_{f2}x_{12}^*}{N_f^*} & \frac{\beta_{f2}\phi_p x_{12}^*}{N_f^*} & \frac{\beta_{f2}\theta_{p2}x_{12}^*}{N_f^*} & 0 \\ 0 & 0 & 0 & 0 & 0 & 0 & 0 & 0 & 0 & 0 & 0 \\ 0 & 0 & 0 & 0 & 0 & 0 & 0 & 0 & 0 & 0 & 0 \\ 0 & 0 & 0 & 0 & 0 & 0 & 0 & 0 & 0 & 0 & 0 \\ 0 & 0 & 0 & 0 & 0 & 0 & 0 & 0 & 0 & 0 & 0 \\ 0 & 0 & 0 & 0 & 0 & 0 & 0 & 0 & 0 & 0 & 0 \\ 0 & 0 & 0 & 0 & 0 & 0 & 0 & 0 & 0 & 0 & 0 \\ 0 & 0 & 0 & 0 & 0 & 0 & 0 & 0 & 0 & 0 & 0 \end{bmatrix}$$

$$J_{22} = \begin{bmatrix} -\mu_m & 0 & 0 & 0 & 0 & \frac{-\beta_{f2}x_{12}^*}{N_f^*} & \frac{-\beta_{f1}x_{12}^*}{N_f^*} & 0 & 0 & 0 & 0 \\ 0 & -K_7 & 0 & 0 & 0 & 0 & \frac{\beta_{f1}x_{12}^*}{N_f^*} & 0 & 0 & 0 & 0 \\ 0 & \tau_{m1} & -\mu_m & 0 & 0 & 0 & 0 & 0 & 0 & 0 & 0 \\ 0 & 0 & 0 & -K_8 & 0 & \frac{\beta_{f2}x_{12}^*}{N_f^*} & 0 & 0 & 0 & 0 & 0 \\ 0 & 0 & 0 & \tau_{m2} & -\mu_m & 0 & 0 & 0 & 0 & 0 & 0 \\ 0 & 0 & 0 & 0 & 0 & -K_9 & 0 & 0 & 0 & 0 & 0 \\ 0 & 0 & 0 & 0 & 0 & 0 & -K_{10} & 0 & 0 & 0 & 0 \\ 0 & 0 & 0 & 0 & 0 & G_{10} & G_{11} & -\mu_f & 0 & 0 & 0 \\ 0 & 0 & 0 & 0 & 0 & 0 & 0 & 0 & -K_{11} & 0 & 0 \\ 0 & 0 & 0 & 0 & 0 & 0 & 0 & 0 & 0 & -K_{12} & 0 \\ 0 & 0 & 0 & 0 & 0 & 0 & 0 & 0 & \tau_{m12} & \tau_{m21} & -\mu_m \end{bmatrix}$$

where $N_f^* = x_1^* + x_2^*$, $N_m^* = x_{12}^*$, $X_1^* = x_1^* + (1-\xi)x_2^*$.

It can be shown that the Jacobian of (1) has a right eigenvector (associated with the nonzero eigenvalue) given by

$$w = [\omega_1, \omega_2, \omega_3, \omega_4, \omega_5, \omega_6, \omega_7, \omega_8, \omega_9, \omega_{10}, \omega_{11}, \omega_{12}, \omega_{13}, \omega_{14}, \omega_{15}, \omega_{16}, \omega_{17}, \omega_{18}, \omega_{19}, \omega_{20}, \omega_{21}, \omega_{22}]^T$$

where,

$$\omega_1 = -\frac{1}{\mu_f}\left\{\frac{K_1 x_1^* \omega_3}{N_f^*(1-f\xi)} + \frac{\beta_{m2}x_1^*\omega_{15}}{N_m^*}\right\},$$

$$\omega_2 = -\frac{1}{\mu_f}\left\{\frac{K_1(1-\xi)x_2^*\omega_3}{N_f^*(1-f\xi)} + \frac{\beta_{m2}\eta_I(1-\xi)x_2^*\omega_{15}}{N_m^*}\right\},$$

$$\omega_3 = \omega_3 > 0, \quad \omega_4 = \frac{G_1\omega_3}{K_2},$$

$$\omega_5 = \frac{G_1G_3\omega_3}{K_2K_3} + \frac{G_4\beta_{m2}\{G_6K_5x_1^* + G_5K_4\eta_I(1-\xi)x_2^*\}\omega_{15}}{K_3K_4K_5K_6N_m^*},$$

$$\omega_6 = \frac{\pi_f G_1G_3\omega_3}{\mu_f K_2K_3} + \frac{\pi_f G_4\beta_{m2}\{G_6K_5x_1^* + G_5K_4\eta_I(1-\xi)x_2^*\}\omega_{15}}{\mu_f K_3K_4K_5K_6N_m^*},$$

$$\omega_7 = \frac{(p_1\tau_{f1}K_2 + q_1\kappa_{f1}G_1)\omega_3}{\mu_f K_2},$$

$$\omega_8 = \frac{\beta_{m2}x_1^*\omega_{15}}{K_4N_m^*}, \quad \omega_9 = \frac{\beta_{m2}\eta_I(1-\xi)x_2^*}{K_5N_m^*},$$

$$\omega_{10} = \frac{\beta_{m2}\{G_6K_5x_1^* + G_5K_4\eta_I(1-\xi)x_2^*\}\omega_{15}}{K_4K_5K_6N_m^*},$$

$$\omega_{11} = \frac{\beta_{m2}\{(p_2\tau_{f2}K_5K_6 + G_6G_9K_5)x_1^* + (G_8K_4K_6 + G_5G_9K_4)\eta_I(1-\xi)x_2^*\}\omega_{15}}{\mu_f K_4K_5K_6N_m^*},$$

$$\omega_{12} = -\frac{1}{\mu_m}\left\{\frac{K_1K_2K_7x_{12}^*\omega_3}{\beta_{m1}N_f^*(1-f\xi)} + \frac{\beta_{f2}\beta_{m2}\{K_5(K_6+\theta_{p2}G_6)x_1^* + K_4(K_6\phi_p + \theta_{p2}G_5)\eta_I(1-\xi)x_2^*\}\omega_{15}}{K_4K_5K_6N_f^*}\right\}$$

$$\omega_{13} = \frac{\beta_{f1}^*x_{12}^*(K_2+\theta_{p1}G_1)\omega_3}{K_2K_7N_f^*}, \quad \omega_{14} = \frac{\tau_{m1}K_1x_{12}^*\omega_3}{\beta_{m1}\mu_m(1-f\xi)N_f^*},$$

$$\omega_{15} = \omega_{15} > 0, \quad \omega_{16} = \frac{\tau_{m2}\omega_{15}}{\mu_m}$$

Furthermore, (1) has a corresponding left eigenvector (associated with the zero eigenvalue) given by

$$v = [\nu_1, \nu_2, \nu_3, \nu_4, \nu_5, \nu_6, \nu_7, \nu_8, \nu_9, \nu_{10}, \nu_{11}, \nu_{12}, \nu_{13}, \nu_{14}, \nu_{15}, \nu_{16}, \nu_{17}, \nu_{18}, \nu_{19}, \nu_{20}, \nu_{21}, \nu_{22}]$$

where,

$$\nu_3 = \nu_3 > 0, \quad \nu_4 = \frac{\theta_{p1}\nu_3}{(K_2+\theta_{p1}G_1)},$$

$$\nu_8 = \frac{\beta_{f2}x_{12}^*\nu 15(K_6+\theta_{p2}G_6)}{K_4K_6N_f^*}, \quad \nu_9 = \frac{\beta_{f2}x_{12}^*\nu 15(K_6+\theta_{p2}G_6)}{K_5K_6N_f^*},$$

$$\nu_{10} = \frac{\beta_{f2}\theta_{p2}x_{12}^*\nu_{15}}{K_6N_f^*}, \quad \nu_{13} = \frac{\beta_{m1}X_1^*\nu_3}{K_7N_m^*},$$

$$\nu_{17} = \frac{\beta_{f2}x_{12}^*\nu 15(K_6+\theta_{p2}G_6)}{K_6K_9N_f^*}, \quad \nu_{18} = \frac{(\theta_{p1}G_2 + K_1K_2)\nu_3}{K_{10}(K_2+\theta_{p1}G_1)},$$

$$\nu_{20} = \frac{\beta_{f2}\beta_{m2}\{(K_6+\theta_{p2}G_6)x_1^* + (\phi_pK_6+\theta_{p2}G_5)\eta_I(1-\xi)x_2^*\}\nu_{15}}{K_4K_5K_6K_{11}N_f^*},$$

$$\nu_{21} = \frac{\beta_{m1}X_1^*\nu_3}{K_{12}N_m^*}$$

It follows from Theorem 4.1 in [30], by computing the nonzero partial derivatives of $F(x)$(evaluated at the disease-free equilibrium, DFE (ξ_0)) that the associated bifurcation coefficients defined by a and b, given by

$$a = \sum_{k,i,j=1}^{n} \nu_k\omega_i\omega_j\frac{\partial^2 f_k}{\partial x_i\partial x_j}(0,0) \quad \text{and} \quad b = \sum_{k,i=1}^{n}\nu_k\omega_i\frac{\partial^2 f_k}{\partial x_i\partial\beta_S^*}(0,0),$$

are computed to be

$$
\begin{aligned}
a = &-\frac{2\beta_{m1}\nu_3\omega_{13}}{N_m^{*2}}\Big\{\omega_{12}X_1^* - \varepsilon_1\omega_7 N_m^* + (\omega_{13}+\omega_{14}+\omega_{15}+\omega_{16})X_1^* \\
&- \{\omega_1 + (1-\xi)\omega_2\}N_m^*\Big\} \\
&- \frac{2\beta_{m2}\nu_8\omega_{15}}{N_m^{*2}}\Big\{\omega_{12}x_1^* - \varepsilon_2\omega_{11}N_m^* + (\omega_{13}+\omega_{14}+\omega_{15}+\omega_{16})x_1^* - \omega_1 N_m^*\Big\} \\
&- \frac{2\beta_{m2}\eta_I(1-\xi)\nu_9\omega_{15}}{N_m^{*2}}\Big\{\omega_{12}x_2^* + (\omega_{13}+\omega_{14}+\omega_{15}+\omega_{16})x_2^* - \omega_2 N_m^*\Big\} \\
&- \frac{2\beta_{f1}^*(\omega_3+\theta_{p1}\omega_4)\nu_{13}}{N_f^{*2}}\Big\{\{\omega_1+\omega_2\}x_{12}^* - \varepsilon_3\omega_{14}N_f^* + n_1 x_{12}^* - \omega_{12}N_f^*\Big\} \\
&- \frac{2\beta_{f2}(\omega_8+\phi_p\omega_9+\theta_{p2}\omega_{10})\nu_{15}}{N_f^{*2}}\Big\{\{\omega_1+\omega_2\}x_{12}^* - \varepsilon_4\omega_{16}N_f^* + n_1 x_{12}^* - \omega_{12}N_f^*\Big\}
\end{aligned}
\tag{9}
$$

Which is further simplified to give

$$
\begin{aligned}
a = &-\frac{2K_1\nu_3\omega_3}{N_m^*X_1^*}\Big\{\omega_{12}X_1^* - \varepsilon_1\omega_7 N_m^* + (\omega_{13}+\omega_{14}+\omega_{15}+\omega_{16})X_1^* \\
&- \{\omega_1 + (1-\xi)\omega_2\}N_m^*\Big\} \\
&- \frac{2\beta_{m2}\beta_{f2}(K_6+\theta_{p2}G_6)\nu_{15}\omega_{15}}{K_4K_6N_m^*N_f^*}\Big\{\omega_{12}X_1^* - \varepsilon_2\omega_{11}N_m^* \\
&+ (\omega_{13}+\omega_{14}+\omega_{15}+\omega_{16})x_1^* - \omega_1 N_m^*\Big\} \\
&- \frac{2\beta_{m2}\beta_{f2}\eta_I(1-\xi)\nu_{15}\omega_{15}}{K_5K_6N_m^*N_f^*}\Big\{\omega_{12}x_{12}^* + (\omega_{13}+\omega_{14}+\omega_{15}+\omega_{16})x_2^* - \omega_2 N_m^*\Big\} \\
&- \frac{2K_1\nu_3\omega_3}{N_m^*N_f^*}\Big\{\{\omega_1+\omega_2\}x_{12}^* - \varepsilon_3\omega_{14}N_f^* + n_1 x_{12}^* - \omega_{12}N_f^*\Big\} \\
&- \frac{2\beta_{f2}\beta_{m2}\Big\{K_5(K_6+\theta_{p2}G_6)x_1^* + K_5(\phi_pK_6+\theta_{p2}G_5)\eta_I(1-\xi)x_2^*\Big\}\nu_{15}\omega_{15}}{K_4K_5K_6N_m^*N_f^{*2}} \\
&\times \Big\{\{\omega_1+\omega_2\}x_{12}^* - \varepsilon_4\omega_{16}N_f^* + n_1 x_{12}^* - \omega_{12}N_f^*\Big\}
\end{aligned}
$$

and

$$
b = \frac{x_{12}^*}{N_f^*}\nu_{13}\left(\omega_3 + \theta_{p1}\omega_4 + \omega_{18}\right) > 0
$$

Here,

$$n_1 = \omega_3 + \omega_4 + \omega_5 + \omega_6 + \omega_7 + \omega_8 + \omega_9 + \omega_{10} + \omega_{11}$$

Since the bifurcation coefficient b is positive, it follows from Theorem 4.1 in [30] that the model (1), or the transformed model (8), will undergo a backward bifurcation if the backward bifurcation coefficient, a, given by (9) is positive. □

Consider the model (1) with $\varepsilon_1 = \varepsilon_2 = \varepsilon_3 = \varepsilon_4 = 0$ and $\xi = 1$. The expression for the backward bifurcation coefficient, a, given as (9) (and noting that all parameters of the model (1) are positive), reduces to

$$\begin{aligned} a = -2K_7\omega_3\nu_3 \Bigg\{ & \frac{1}{N_m^*}(\omega_{13} + \omega_{14} + \omega_{15} + \omega_{16}) \\ & + \frac{1}{N_f^*}(\omega_3 + \omega_4 + \omega_5 + \omega_6 + \omega_7 + \omega_8 + \omega_9 + \omega_{10} + \omega_{11}) \\ & + \omega_1\Big(\frac{1}{N_f^*} - \frac{1}{x_1^*}\Big)\Bigg\} - \frac{2\beta_{m2}\beta_{f2}(K_2 + \theta_{p2}G_6)\omega_{15}\nu_{15}}{K_4K_6N_f^*} \\ & \Bigg\{\frac{x_1^*}{N_m^*}(\omega_{13} + \omega_{14} + \omega_{15} + \omega_{16}) + \omega_1\Big(\frac{x_1^*}{N_f^*} - 1\Big) \\ & + \frac{x_1^*}{N_f^*}(\omega_3 + \omega_4 + \omega_5 + \omega_6 + \omega_7 + \omega_8 + \omega_9 + \omega_{10} + \omega_{11})\Bigg\} < 0, \end{aligned}$$

since $N_f^* > x_1^*$, then $\left(\frac{1}{N_f^*} - \frac{1}{x_1^*}\right) < 0$, and $\left(\frac{x_1^*}{N_f^*} - 1\right) < 0$, and noting that $(\omega_{13} + \omega_{14} + \omega_{15} + \omega_{16}) > 0$ and $(\omega_3 + \omega_4 + \omega_5 + \omega_6 + \omega_7 + \omega_8 + \omega_9 + \omega_{10} + \omega_{11}) > 0$ while $\omega_1 < 0$. Hence, it follows from Theorem 4.1 in [30] that the model (1) does not undergo a backward bifurcation if $\varepsilon_1 = \varepsilon_2 = \varepsilon_3 = \varepsilon_4 = 0$ and $\xi = 1$. Imperfect HPV vaccine also induced backward bifurcation in the two-sex vaccination model in [31] while reinfection and imperfect vaccine caused backward bifurcation in the two-sex HPV vaccination model in [32].

Remark It is interesting to note that, in the absence of reinfection of recovered individuals with the same strain, if we set the cross-immunity parameter η_I to zero, backward bifurcation still persists due to the presence of an imperfect vaccine, ξ. However, setting $\xi = 1$, rules out the possibility of backward bifurcation in the model (1). This implies that, in the absence of reinfection of recovered individuals with the same strain, the overriding parameter inducing backward bifurcation is the imperfect vaccine.

4 Existence and Stability of Boundary Equilibria

The existence and stability of boundary equilibria of the model (1) is now investigated for a special case when the disease-induced death rates are assumed to be negligible (that is, $\delta_{f1} = \delta_{f2} = \delta_{f2}^{p} = \delta_{f12} = \delta_{f21} = \delta_{m1} = \delta_{m2} = \delta_{m12} = \delta_{m21} = \delta_{fc} = 0$). This is fitting in places like Northern America, Western Europe, Australia, and New Zealand where the average annual HPV and cancer mortality rates are less than four persons per 100,000 of the population [33, 34]. It should be noted that setting $\delta_{f1} = \delta_{f2} = \delta_{f2}^{p} = \delta_{f12} = \delta_{f21} = \delta_{m1} = \delta_{m2} = \delta_{m12} = \delta_{m21} = \delta_{fc} = 0$ in (1) gives $N_f \to \frac{\Lambda_f}{\mu_f}$ and $N_m \to \frac{\Lambda_m}{\mu_m}$ as $t \to \infty$.

The approach in [23] will be used to explore the existence and stability of the positive boundary equilibria. Let,

$$\lambda_{f1}^{**} = \frac{\beta_{f1}\mu_f\left(I_{f1}^{**} + I_{f21}^{**} + \theta_{p1}P_{f1}^{**}\right)}{\Lambda_f} \quad \text{and} \quad \lambda_{m1}^{**} = \frac{\beta_{m1}\mu_m(I_{m1}^{**} + I_{m21}^{**})}{\Lambda_m}$$
$$\lambda_{f2}^{**} = \frac{\beta_{f2}\mu_f\left(I_{f2}^{**} + I_{f12}^{**} + \phi_p I_{f2}^{p**} + \theta_{p2}P_{f2}^{**}\right)}{\Lambda_f} \quad \text{and} \quad \lambda_{m2}^{**} = \frac{\beta_{m2}\mu_m(I_{m2}^{**} + I_{m12}^{**})}{\Lambda_m} \tag{10}$$

be the forces of infection for strain 1 and strain 2, respectively, at the endemic steady state.

The equilibria of the model (1) can then be obtained by finding the fixed points of the equation

$$X = \Phi(X) = \begin{pmatrix} \theta_1(\lambda_1^{**}, \lambda_2^{**}) \\ \theta_2(\lambda_1^{**}, \lambda_2^{**}) \end{pmatrix}, \quad \text{where} \quad X = \begin{pmatrix} \lambda_1^{**} \\ \lambda_2^{**} \end{pmatrix} \tag{11}$$

with,
$\lambda_1^{**} = \lambda_{f1}^{**} + \lambda_{m1}^{**}, \quad \lambda_2^{**} = \lambda_{f2}^{**} + \lambda_{m2}^{**}$

4.1 Strain 1-Only Boundary Equilibrium (ξ_{e1})

In the absence of strain 2, [obtained by setting $I_{f2} = I_{f2}^{p} = P_{f2} = R_{f2} = I_{f12} = I_{f21} = M_f = I_{m2} = R_{m2} = I_{m12} = I_{m21} = M_m = 0$ in the model (1)], the strain 1-only submodel with $\delta_{f1} = \delta_{m1} = \delta_{fc} = 0$ is given by:

$$\begin{aligned}
\frac{dS_f}{dt} &= (1-f)\Lambda_f - \left(\lambda_{m1} + \mu_f\right) S_f \\
\frac{dV_f}{dt} &= f\Lambda_f - (1-\xi)\lambda_{m1} V_f - \mu_f V_f \\
\frac{dI_{f1}}{dt} &= (1-\xi)\lambda_{m1} V_f + \lambda_{m1} S_f - \bar{K}_1 I_{f1} + \varepsilon_1 \lambda_{m1} R_{f1} \\
\frac{dP_{f1}}{dt} &= G_1 I_{f1} - \bar{K}_2 P_{f1} \\
\frac{dC_f}{dt} &= G_3 P_{f1} - \bar{K}_3 C_f \\
\frac{dR_f^c}{dt} &= \pi_f C_f - \mu_f R_f^c \\
\frac{dR_{f1}}{dt} &= p_1 \tau_{f1} I_{f1} + q_1 \kappa_{f1} P_{f1} - \left(\mu_f + \varepsilon_1 \lambda_{m1}\right) R_{f1} \\
\frac{dS_m}{dt} &= \Lambda_m - \left(\lambda_{f1} + \mu_m\right) S_m \\
\frac{dI_{m1}}{dt} &= \lambda_{f1} S_m - \bar{K}_7 I_{m1} + \varepsilon_3 \lambda_{f1} R_{m1} \\
\frac{dR_{m1}}{dt} &= \tau_{m1} I_{m1} - \left(\mu_m + \varepsilon_3 \lambda_{f1}\right) R_{m1}
\end{aligned} \tag{12}$$

with,
$\bar{K}_1 = \bar{K}_1|_{\delta_{f1}=0}, \bar{K}_2 = K_2|_{\delta_{f1}=0}, \bar{K}_3 = K_3|_{\delta_{fc}=0}, \bar{K}_7 = K_7|_{\delta_{m1}=0}$.
The analysis of the sub-model (12) will be considered in the following positively invariant region

$$\mathcal{D}_1 = \mathcal{D}_1^f \cup \mathcal{D}_1^m$$

with

$$\begin{aligned}
\mathcal{D}_1^f &= \left\{ (S_f, V_f, I_{f1}, P_{f1}, C_f, R_f^c, R_{f1}) \in \mathfrak{R}_+^7 : N_f \leq \frac{\Lambda_f}{\mu_f} \right\}, \text{and} \\
\mathcal{D}_1^m &= \left\{ (S_m, I_{m1}, R_{m1}) \in \mathfrak{R}_+^3 : N_m \leq \frac{\Lambda_m}{\mu_m} \right\}
\end{aligned}$$

The DFE of the strain 1-only sub-model (12) is given by

$$\begin{aligned}
\xi_{01} &= (S_f^*, V_f^*, I_{f1}^*, P_{f1}^*, C_f^*, R_f^{c*}, R_{f1}^*, S_m^*, I_{m1}^*, R_{m1}^*) \\
&= (\frac{f\Lambda_f}{\mu_f}, \frac{(1-f)\Lambda_f}{\mu_f}, 0, 0, 0, 0, 0, \frac{\Lambda_m}{\mu_m}, 0, 0)
\end{aligned} \tag{13}$$

It follows from (11), that (by setting $\lambda_2^{**} = 0$) the strain 1-only boundary equilibrium (denoted by ξ_{e1}) is given by

$$\xi_{e1} = \left(S_f^{**}, V_f^{**}, I_{f1}^{**}, P_{f1}^{**}, C_f^{**}, R_f^{c**}, R_{f1}^{**}, 0, 0, 0, 0, S_m^{**}, I_{m1}^{**}, R_{m1}^{**}, 0, 0, 0, 0, 0, 0, 0, 0\right)$$

(It should be noted here that N_f^{**} and N_m^{**} are replaced with their limiting values $\frac{\Lambda_f}{\mu_f}$ and $\frac{\Lambda_m}{\mu_m}$, respectively, as all disease-induced death rates are assumed zero). It should be noted that setting $\delta_{f1} = \delta_{m1} = \delta_{fc} = 0$ in (12) gives $N_f \to \frac{\Lambda_f}{\mu_f}$ and $N_m \to \frac{\Lambda_m}{\mu_m}$ as $t \to \infty$. Let $\bar{\beta}_{f1} = \frac{\mu_f \beta_{f1}}{\Lambda_f}$ and $\bar{\beta}_{m1} = \frac{\mu_m \beta_{m1}}{\Lambda_m}$ so that

$$\lambda_{f1} = \bar{\beta}_{f1}(I_{f1} + \theta_{p1} P_{f1}) \quad \text{and} \quad \lambda_{m1} = \bar{\beta}_{m1} I_{m1} \tag{14}$$

Define

$$\lambda_{f2}^{**} = \frac{\beta_{f2}\mu_f \left(I_{f2}^{**} + \theta_{p2} P_{f2}^{**}\right)}{\Lambda_f}, \quad \text{and} \quad \lambda_{m2}^{**} = \frac{\beta_{m2} I_{m2}^{**} \mu_m}{\Lambda_m} \tag{15}$$

where,

$$\begin{aligned}
S_f^{**} &= \frac{(1-f)\,\Lambda_f}{\left(\lambda_{m1}^{**} + \mu_f\right)}, \quad V_f^{**} = \frac{f\,\Lambda_f}{\left[(1-\xi)\,\lambda_{m1}^{**} + \mu_f\right]}, \\
I_{f1}^{**} &= \frac{\left\{(1-\xi)\Lambda_f(\lambda_{m1}^{**})^2 + (1-\xi f)\Lambda_f \mu_f \lambda_{m1}^{**}\right\}\bar{K}_2(\mu_f + \varepsilon_1 \lambda_{m1}^{**})}{C_1(\lambda_{m1}^{**})^3 + C_2(\lambda_{m1}^{**})^2 + C_3\lambda_{m1}^{**} + C_4}, \\
P_{f1}^{**} &= \frac{\left\{(1-\xi)\Lambda_f(\lambda_{m1}^{**})^2 + (1-\xi f)\Lambda_f \mu_f \lambda_{m1}^{**}\right\}G_1(\mu_f + \varepsilon_1 \lambda_{m1}^{**})}{C_1(\lambda_{m1}^{**})^3 + C_2(\lambda_{m1}^{**})^2 + C_3\lambda_{m1}^{**} + C_4}, \\
R_{f1}^{**} &= \frac{\left\{(1-\xi)\Lambda_f(\lambda_{m1}^{**})^2 + (1-\xi f)\Lambda_f \mu_f \lambda_{m1}^{**}\right\}(G_1 + \bar{K}_2)}{C_1(\lambda_{m1}^{**})^3 + C_2(\lambda_{m1}^{**})^2 + C_3\lambda_{m1}^{**} + C_4}, \\
C_f^{**} &= \frac{\left\{(1-\xi)\Lambda_f(\lambda_{m1}^{**})^2 + (1-\xi f)\Lambda_f \mu_f \lambda_{m1}^{**}\right\}G_1 G_3(\mu_f + \varepsilon_1 \lambda_{m1}^{**})}{\bar{K}_3\left\{C_1(\lambda_{m1}^{**})^3 + C_2(\lambda_{m1}^{**})^2 + C_3\lambda_{m1}^{**} + C_4\right\}}, \\
R_f^{c**} &= \frac{\left\{(1-\xi)\Lambda_f(\lambda_{m1}^{**})^2 + (1-\xi f)\Lambda_f \mu_f \lambda_{m1}^{**}\right\}G_1 G_3 \pi_f(\mu_f + \varepsilon_1 \lambda_{m1}^{**})}{\mu_f K_3\left\{C_1(\lambda_{m1}^{**})^3 + C_2(\lambda_{m1}^{**})^2 + C_3\lambda_{m1}^{**} + C_4\right\}}, \\
S_m^{**} &= \frac{\Lambda_m}{(\mu_m + \lambda_{f1}^{**})}, \quad I_{m1}^{**} = \frac{\Lambda_m \lambda_{f1}^{**}(\mu_m + \varepsilon_3 \lambda_{f1}^{**})}{D_1(\lambda_{f1}^{**})^2 + D_2\lambda_{f1}^{**} + D_3} \\
R_{m1}^{**} &= \frac{\tau_{m1}\Lambda_m \lambda_{f1}^{**}}{D_1(\lambda_{f1}^{**})^2 + D_2\lambda_{f1}^{**} + D_3}
\end{aligned} \tag{16}$$

with,

$$
\begin{aligned}
C_1 &= (1-\xi)\varepsilon_1\big\{(1-p_1)(1-q_1)\tau_{f1}\kappa_{f1} + (1-p_1)\tau_{f1}\mu_f + \mu_f(\kappa_{f1+\mu_f})\big\} > 0\\
C_2 &= (1-\xi)\bar{K}_1\bar{K}_2\mu_f + (2-\xi)\mu_f\varepsilon_1\big\{(1-p_1)(1-q_1)\tau_{f1}\kappa_{f1}\\
&\quad + (1-p_1)\tau_{f1}\mu_f + \mu_f(\kappa_{f1}+\mu_f)\big\} > 0\\
C_3 &= (2-\xi)\mu_f^2(\tau_{f1}+\mu_f)(\kappa_{f1}+\mu_f) + \mu_f^2\varepsilon_1\big\{(1-p_1)(1-q_1)\tau_{f1}\kappa_{f1}\\
&\quad + (1-p_1)\tau_{f1}\mu_f + \mu_f(\kappa_{f1}+\mu_f)\big\} > 0\\
D_1 &= \varepsilon_3(\bar{K}_7+\tau_{m1}), \quad D_2 = \mu_m(\bar{K}_7+\varepsilon_3+\tau_{m1}\varepsilon_3), \quad D_3 = \mu_m^2\bar{K}_7
\end{aligned}
$$

The existence of the strain 1-only boundary equilibrium can be determined from fixed point problem $\theta_1(\lambda_1^{**}, 0) = \lambda_1^{**}$, which after some algebraic manipulations leads to the following polynomial (in terms of λ_{m1}^{**}):

$$
H_1(\lambda_{m1}^{**})^6 + H_2(\lambda_{m1}^{**})^5 + H_3(\lambda_{m1}^{**})^4 + H_4(\lambda_{m1}^{**})^3 + H_5(\lambda_{m1}^{**})^2 + H_6\lambda_{m1}^{**} + H_7 = 0, \tag{17}
$$

obtained from

$$
\begin{aligned}
\lambda_{f1}^{**} &= \frac{\lambda_{m1}^{**}\left[b_{02}(\lambda_{m1}^{**})^2 + b_{01}\lambda_{m1}^{**} + b_0\right]}{\left[b_{33}(\lambda_{m1}^{**})^3 + b_{22}(\lambda_{m1}^{**})^2 + b_{11}\lambda_{m1}^{**} + b_{00}\right]},\\
\lambda_{m1}^{**} &= \frac{\lambda_{f1}^{**}\left(c_{02}\lambda_{f1}^{**} + c_{01}\right)}{c_{22}(\lambda_{f1}^{**})^2 + c_{11}\lambda_{f1}^{**} + c_{00}}
\end{aligned} \tag{18}
$$

where,

$$
\begin{aligned}
b_0 &= \beta_{f1}\Lambda_f\mu_f^2(1-f\xi)(\bar{K}_2\mu_f + \theta_{p1}\mu_f G_1),\\
b_{01} &= \beta_{f1}\Lambda_f\mu_f(1-\xi)(\bar{K}_2\mu_f + \theta_{p1}\mu_f G_1) + \beta_{f1}\Lambda_f\mu_f^2(1-\xi)(\bar{K}_2\varepsilon_1 + \theta_{p1}G_1\varepsilon_1),\\
b_{02} &= \beta_{f1}\Lambda_f\mu_f(1-\xi)(\varepsilon_1\bar{K}_2 + \theta_{p1}G_1\varepsilon_1),\\
b_{00} &= \bar{K}_1\bar{K}_2\Lambda_f\mu_f^3,\\
b_{11} &= (2-\xi)\Lambda_f\mu_f^2(\tau_{f1}+\mu_f)(\kappa_{f1}+\mu_f)\\
&\quad + \Lambda_f\mu_f^2\varepsilon_1\big\{(1-p_1)(1-q_1)\tau_{f1}\kappa_{f1} + (1-p_1)\tau_{f1}\mu_f\\
&\quad + \mu_f(\kappa_{f1}+\mu_f)\big\} > 0\\
b_{22} &= (1-\xi)\Lambda_f\mu_f(\tau_{f1}+\mu_f)(\kappa_{f1}+\mu_f)\\
&\quad + (2-\xi)\Lambda_f\mu_f\varepsilon_1\big\{(1-p_1)(1-q_1)\tau_{f1}\kappa_{f1} + (1-p_1)\tau_{f1}\mu_f\\
&\quad + \mu_f(\kappa_{f1}+\mu_f)\big\} > 0\\
b_{33} &= (1-\xi)\Lambda_f\varepsilon_1\big\{(1-p_1)(1-q_1)\tau_{f1}\kappa_{f1} + (1-p_1)\tau_{f1}\mu_f^2(\kappa_{f1}+\mu_f)\big\} > 0\\
c_{00} &= \Lambda_m\mu_m^2\bar{K}_7, \quad c_{11} = \Lambda_m\mu_m\bar{K}_7 + \Lambda_m\mu_m\bar{K}_7\varepsilon_3 + \Lambda_m\mu_m\tau_{m1}\varepsilon_3,\\
c_{22} &= \varepsilon_3\Lambda_m(\bar{K}_7+\tau_{m1})\\
c_{01} &= \beta_{m1}\Lambda_m\mu_m^2, \quad c_{02} = \beta_{m1}\Lambda_m\mu_m\varepsilon_3
\end{aligned} \tag{19}
$$

with

$$
\begin{aligned}
H_1 &= b_{02}^2 c_{22} + c_{11} b_{02} b_{33} + c_{00} b_{33}^2 > 0 \\
H_2 &= 2b_{01} b_{02} c_{22} + c_{11} b_{02} b_{22} + c_{11} b_{01} b_{33} + 2c_{00} b_{22} b_{33} - b_{02}^2 c_{02} - b_{02} c_{01} b_{33}, \\
H_3 &= 2b_0 b_{02} c_{22} + b_{01}^2 c_{22} + c_{11} b_{02} b_{11} + c_{11} b_{01} b_{22} + c_{11} b_0 b_{33} + 2c_{00} b_{11} b_{33} \\
&\quad + c_{00} b_{22}^2 - 2b_{01} b_{02} c_{02} - b_{02} c_{01} b_{22} - b_{01} c_{01} b_{33}, \\
H_4 &= 2b_0 b_{01} c_{22} + b_{00} b_{02} c_{11} + b_{01} b_{11} c_{11} + b_0 b_{22} c_{11} - 2b_0 b_{02} c_{02} - b_{01}^2 c_{02} \\
&\quad - b_{02} b_{11} c_{01} - b_{01} b_{22} c_{01} + b_{00} b_{33} c_{00} (2 - \mathcal{R}_{01}^2) \\
H_5 &= (b_{01} c_{11} - b_{02} c_{01}) b_{00} + (b_{11} c_{11} - 2b_{01} c_{02}) b_0 + (b_{11} c_{00} - b_{01} c_{01}) b_{11} \\
&\quad + b_{00} c_{00} b_{22} (2 - \mathcal{R}_{01}^2) \\
H_6 &= b_0 b_{00} c_{11} - b_0^2 c_{02} - b_{00} b_{01} c_{01} + 2b_{00} b_{11} c_{00} (1 - \mathcal{R}_{01}^2) \\
H_7 &= b_{00}^2 c_{00} (1 - \mathcal{R}_{01}^2) > 0 \quad \text{if} \quad \mathcal{R}_{01} < 1
\end{aligned}
\tag{20}
$$

The components of the EEP are then obtained by solving for λ_{m1}^{**} from the polynomial (17) and substituting the positive values of λ_{m1}^{**} into the expressions in (16) [noting (19)]. Furthermore, it follows from (20) that the coefficient H_1 is always positive and H_7 is positive (negative) if $\mathcal{R}_{01}$ is less (greater) than unity. The following results can be deduced.

Theorem 4.1 *The strain 1-only sub-model* (12) *with* $\delta_{f1} = \delta_{m1} = \delta_{fc} = 0$ *has:*

(i) six or four endemic equilibria if $H_2 < 0, H_3 > 0, H_4 < 0, H_5 > 0, H_6 < 0$ *and* $\mathcal{R}_{01} < 1$,
(ii) four or two endemic equilibria if $H_2 > 0, H_3 < 0, H_4 > 0, H_5 < 0, H_6 > 0$ *and* $\mathcal{R}_{01} < 1$,
(iii) two endemic equilibria if $H_2 > 0, H_3 > 0, H_4 < 0, H_5 < 0, H_6 > 0$ *and* $\mathcal{R}_{01} < 1$
(iv) no endemic equilibrium otherwise, if $\mathcal{R}_{01} < 1$,

The first three items of Theorem 4.1 (i)–(iii) suggest the possibility of backward bifurcation in the strain 1-only sub-model (12) with negligible disease-induced deaths (i.e., $\delta_{f1} = \delta_{m1} = \delta_{fc} = 0$) when $\mathcal{R}_{01} < 1$.

4.1.1 Backward Bifurcation Analysis of Strain-1 only Sub-model

Following the application of the center manifold theory [30] (as used in Sect. 3.2), we observe that ε_1, ε_3, and ξ can cause backward bifurcation in the strain 1-only sub-model (the associated backward bifurcation diagram is depicted in Fig. 3). The following results can be established.

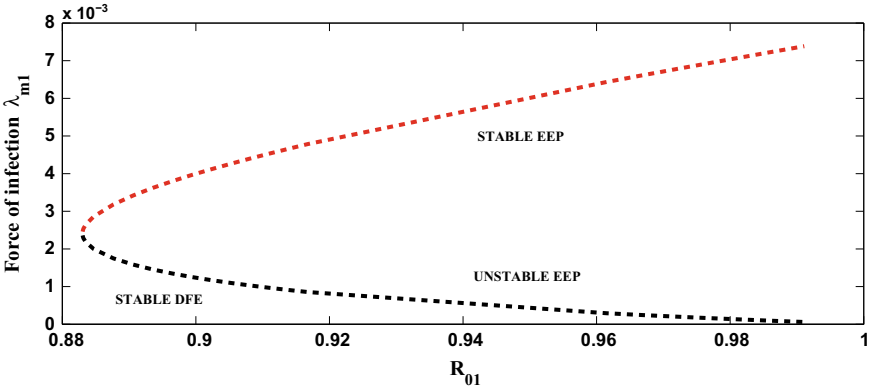

Fig. 3 Bifurcation diagram for the model (12). Parameter values used are: $\beta_{f1} = 0.7422$, $\beta_{m1} = 0.88$, $\varepsilon_1 = \varepsilon_3 = 10$, $\pi_f = 0.0000009$. All other parameters as in Table 4

Theorem 4.2 *In the absence of reinfection of recovered individuals with strain 1 ($\varepsilon_1 = \varepsilon_3 = 0$), the sub-model (12) with perfect vaccine ($\xi = 1$) does not undergo backward bifurcation.*

4.1.2 GAS of DFE of Strain-1 only Sub-model (12) for special case

Theorem 4.3 *In the absence of reinfection of recovered individuals with the same strain and imperfect vaccine (i.e., $\varepsilon_1 = \varepsilon_3 = 0, \xi = 1$), the DFE of the strain 1-only sub-model (12), given by ξ_{01}, is GAS in $\mathcal{D}$ whenever $\mathcal{R}_{01}|_{\xi=1} = \bar{\mathcal{R}}_{01} \leq 1$.*

Proof Consider the model (1) with strain 1-only (i.e., let $\mathcal{R}_{02} < 1$, so that strain 2 dies out) given by (12). Also, let $\varepsilon_1 = \varepsilon_3 = 0, \xi = 1$. Further, let us consider the Lyapunov function:

$$\mathcal{L}_1 = \frac{(K_2 + \theta_{p1} G_1)\beta_{f1}^f c_f S_f^*}{K_1 K_2 K_7 N_f^*} I_{f1} + \frac{\theta_{p1}\beta_{f1}^f c_f S_f^*}{K_2 K_7 N_f^*} P_{f1} + \frac{\bar{\mathcal{R}}_{01}}{K_7} I_{m1}$$

with Lyapunov derivative

$$\dot{\mathcal{L}}_1 = \frac{(K_2 + \theta_{p1} G_1)\beta_{f1}^f c_f S_f^*}{K_1 K_2 K_7 N_f^*} \dot{I}_{f1} + \frac{\theta_{p1}\beta_{f1}^f c_f S_f^*}{K_2 K_7 N_f^*} \dot{P}_{f1} + \frac{\bar{\mathcal{R}}_{01}}{K_7} \dot{I}_{m1}$$

Substituting the expressions for $\dot{I}_{f1}$, $\dot{P}_{f1}$ and $\dot{I}_{m1}$ from (12), we have that

$$\begin{aligned}\dot{\mathcal{L}}_1 &= \frac{(K_2+\theta_{p1}G_1)\beta^f_{f1}c_f S^*_f}{K_1K_2K_7N^*_f}[\lambda_{m1}S_f - K_1I_{f1}] + \frac{\theta_{p1}\beta^f_{f1}c_f S^*_f}{K_2K_7N^*_f}[G_1I_{f1} - K_2P_{f1}] \\ &\quad + \frac{\bar{\mathcal{R}}_{01}}{K_7}[\lambda_{f1}S_m - K_7I_{m1}] \\ &= \frac{(K_2+\theta_{p1}G_1)\beta^f_{f1}c_f S^*_f\lambda_{m1}S_f}{K_1K_2K_7N^*_f} + \frac{\bar{\mathcal{R}}_{01}\lambda_{f1}S_m}{K_7} \\ &\quad - I_{f1}\left[\frac{(K_2+\theta_{p1}G_1)\beta^f_{f1}c_f S^*_f}{K_2K_7N^*_f} - \frac{\theta_{p1}G_1\beta^f_{f1}c_f S^*_f}{K_2K_7N^*_f}\right] - P_{f1}\left[\frac{\theta_{p1}\beta^f_{f1}c_f S^*_f}{K_7N^*_f}\right] - \mathcal{R}_{01}I_{m1}\end{aligned}$$

which can be further simplified into

$$\begin{aligned}\dot{\mathcal{L}}_1 &= \frac{(K_2+\theta_{p1}G_1)\beta^f_{f1}c_f S^*_f\lambda_{m1}S_f}{K_1K_2K_7N^*_f} + \frac{\bar{\mathcal{R}}_{01}\lambda_{f1}S_m}{K_7} - \frac{\beta^f_{f1}c_f S^*_f(I_{f1}+\theta_{p1}P_{f1})}{K_7N^*_f} \\ &\quad - \bar{\mathcal{R}}_{01}I_{m1}\end{aligned}$$

Applying the group constraint in (6) and the definition of the forces of infection in (2)–(5), we have that

$$\begin{aligned}\dot{\mathcal{L}}_1 &= \frac{(K_2+\theta_{p1}G_1)\beta^f_{f1}c_f S^*_f\lambda_{m1}S_f}{K_1K_2K_7N^*_f} - \frac{\bar{\mathcal{R}}_{01}\lambda_{m1}N_f}{c_m\beta^m_{m1}} + \frac{\bar{\mathcal{R}}_{01}\lambda_{f1}S_m}{K_7} - \frac{S^*_f\lambda_{f1}N_m}{K_7N^*_f} \\ \dot{\mathcal{L}}_1 &\le \frac{\bar{\mathcal{R}}_{01}\lambda_{m1}N_f}{c_m\beta^m_{m1}}\left(\frac{\bar{\mathcal{R}}_{01}S_f}{N_f} - 1\right) + \frac{\lambda_{f1}N_m}{K_7}\left(\frac{\mathcal{R}_{01}S_m}{N_m} - 1\right) \quad \left(\text{since} \quad \frac{S^*_f}{N^*_f} < 1\right) \\ &\le \frac{\bar{\mathcal{R}}_{01}\lambda_{m1}N_f}{c_m\beta^m_{m1}}\left(\bar{\mathcal{R}}_{01} - 1\right) + \frac{\lambda_{f1}N_m}{K_7}\left(\bar{\mathcal{R}}_{01} - 1\right) \quad \left(\text{since} \quad \frac{S_f}{N_f} < 1, \text{and} \frac{S_m}{N_m} < 1\right)\end{aligned}$$

Since all the model parameters and variables are non-negative, it follows that $\dot{\mathcal{L}}_1 \le 0$ for $\mathcal{R}_{01} \le 1$ with $\dot{\mathcal{L}}_1 = 0$ if and only if $I_{f1} = P_{f1} = I_{m1} = 0$. Hence, $\mathcal{L}_1$ is a Lyapunov function on $\mathcal{D}$. Thus, using the LaSalle's invariance principle [35], $I_{f1} \to 0, P_{f1} \to 0$ and $I_{m1} \to 0$ as $t \to \infty$. Substituting $I_{f1} = P_{f1} = I_{m1} = 0$ in (12) shows that $C_f \to 0, R^c_f \to 0, R_{f1} \to 0, S_f \to S^*_f, V_f \to V^*_f, R_{m1} \to 0, S_m \to S^*_m$ as $t \to \infty$. Thus, every solution to the equations of the strain 1-only sub-model (12) with $\varepsilon_1 = \varepsilon_3 = 0, \xi = 1$, with initial conditions in $\mathcal{D}$, approaches the DFE (ξ_{01}) as $t \to \infty$ whenever $\bar{\mathcal{R}}_{01} \le 1$. □

Also, we prove the following result.

Theorem 4.4 *In the absence of reinfection of recovered individuals with strain 2 (i.e. $\varepsilon_2 = \varepsilon_4 = 0$), the DFE of the strain 2-only sub-model (27), given by ξ_{02}, is GAS in $\mathcal{D}$ whenever $\mathcal{R}_{02} \le 1$.*

Proof Consider the Lyapunov function

$$\mathcal{L}_2 = \frac{(K_6 + \theta_{p2} G_6)\beta^f_{f2} c_f}{K_4 K_6 K_8} I_{f2} + \frac{\theta_{p2}\beta^f_{f2} c_f}{K_6 K_8} P_{f2} + \frac{\mathcal{R}_{02}}{K_8} I_{m2}$$

with Lyapunov derivative

$$\dot{\mathcal{L}}_2 = \frac{(K_6 + \theta_{p2} G_6)\beta^f_{f2} c_f}{K_4 K_6 K_8} \dot{I}_{f2} + \frac{\theta_{p2}\beta^f_{f2} c_f}{K_6 K_8} \dot{P}_{f2} + \frac{\mathcal{R}_{02}}{K_8} \dot{I}_{m2}$$

Substituting the expressions for $\dot{I}_{f2}$, $\dot{P}_{f2}$ and $\dot{I}_{m2}$ from (12), we have that

$$\begin{aligned}
\dot{\mathcal{L}}_2 &= \frac{(K_6 + \theta_{p2} G_6)\beta^f_{f2} c_f}{K_4 K_6 K_8} [\lambda_{m2} S_f - K_4 I_{f2}] + \frac{\theta_{p2}\beta^f_{f2} c_f}{K_6 K_8} [G_6 I_{f2} - K_6 P_{f2}] \\
&\quad + \frac{\mathcal{R}_{02}}{K_8} [\lambda_{f2} S_m - K_8 I_{m2}] \\
&= \frac{(K_6 + \theta_{p2} G_6)\beta^f_{f2} c_f \lambda_{m2} S_f}{K_4 K_6 K_8} + \frac{\mathcal{R}_{02}\lambda_{f2} S_m}{K_8} \\
&\quad - I_{f2}\left[\frac{(K_6 + \theta_{p2} G_6)\beta^f_{f2} c_f}{K_6 K_8} - \frac{\theta_{p2} G_6 \beta^f_{f2} c_f}{K_6 K_8}\right] - P_{f2}\left[\frac{\theta_{p2}\beta^f_{f2} c_f}{K_8}\right] - \mathcal{R}_{02} I_{m2}
\end{aligned}$$

which can be further simplified into

$$\dot{\mathcal{L}}_2 = \frac{(K_6 + \theta_{p2} G_6)\beta^f_{f2} c_f \lambda_{m2} S_f}{K_4 K_6 K_8} + \frac{\mathcal{R}_{02}\lambda_{f2} S_m}{K_8} - \frac{\beta^f_{f2} c_f (I_{f2} + \theta_{p2} P_{f2})}{K_8} - \mathcal{R}_{02} I_{m2}$$

Applying the group constraint in (6) and the definition of the forces of infection in (2)–(5), we have that

$$\begin{aligned}
\dot{\mathcal{L}}_2 &= \frac{(K_6 + \theta_{p2} G_6)\beta^f_{f2} c_f \lambda_{m2} S_f}{K_4 K_6 K_8} - \frac{\mathcal{R}_{02}\lambda_{m2} N_f}{c_m \beta^m_{m2}} + \frac{\mathcal{R}_{02}\lambda_{f2} S_m}{K_8} - \frac{\lambda_{f2} N_m}{K_8} \\
\dot{\mathcal{L}}_2 &\le \frac{\mathcal{R}_{02}\lambda_{m2} N_f}{c_m \beta^m_{m2}} \left(\frac{\mathcal{R}_{02} S_f}{N_f} - 1\right) + \frac{\lambda_{f2} N_m}{K_8} \left(\frac{\mathcal{R}_{02} S_m}{N_m} - 1\right) \\
&\le \frac{\mathcal{R}_{02}\lambda_{m2} N_f}{c_m \beta^m_{m2}} (\mathcal{R}_{02} - 1) + \frac{\lambda_{f2} N_m}{K_8} (\mathcal{R}_{02} - 1) \quad \left(\text{since} \quad \frac{S_f}{N_f} < 1, \text{and} \frac{S_m}{N_m} < 1\right)
\end{aligned}$$

The proof is concluded as in the proof of Theorem 4.3 □

Theorem 4.5 *In the absence of reinfection of recovered individuals with the same strain (i.e., $\varepsilon_1 = \varepsilon_3 = 0$), the model (1) with $\delta_{f1} = \delta_{m1} = \delta_{fc} = 0, \xi = 1$, has a unique strain 1-only boundary equilibrium, ξ_{e1}, whenever $\mathcal{R}_{02} < 1 < \mathcal{R}_{01}|_{\xi=1} = \bar{\mathcal{R}}_{01} \le 1$*

Proof In the absence of reinfection of recovered individuals with the same strain and imperfect vaccine (i. e., $\varepsilon_1 = \varepsilon_3 = 0, \xi = 1$), the polynomial (17) reduces to

$$\bar{H}_5(\lambda_{m1}^{**})^2 + \bar{H}_6\lambda_{m1}^{**} + \bar{H}_7 = 0 \tag{21}$$

with,

$$\begin{aligned}
\bar{H}_5 &= \Lambda_f\mu_f^2(\tau_{f1}+\mu_f)(\kappa_{f1}+\mu_f)[\beta_{f1}\Lambda_m\Lambda_f\mu_f^2\bar{K}_7(1-f)(\bar{K}_2\mu_f+\theta_{p1}\mu_f G_1)\\
&\quad + \Lambda_m\Lambda_f\mu_m^2\mu_f^2\ldots\times(\tau_{f1}+\mu_f)(\kappa_{f1}+\mu_f)\bar{K}_7] > 0,\\
\bar{H}_6 &= \beta_{f1}\Lambda_f^2\Lambda_m\mu_f^5\mu_m\bar{K}_1\bar{K}_2\bar{K}_7(1-f)(\bar{K}_2\mu_f+\theta_{p1}\mu_f G_1)\\
&\quad + 2\Lambda_f^2\Lambda_m\mu_f^5\mu_m^2\bar{K}_1\bar{K}_2\bar{K}_7\ldots\times(\tau_{f1}+\mu_f)(\kappa_{f1}+\mu_f)(1-\bar{\mathcal{R}}_{01}^2),\\
\bar{H}_7 &= \Lambda_m\Lambda_f^2\mu_f^6\mu_m^2\bar{K}_2\bar{K}_2\bar{K}_7(1-\bar{\mathcal{R}}_{01}^2) < 0, \quad \text{if} \quad \bar{\mathcal{R}}_{01} > 1
\end{aligned} \tag{22}$$

It follows from (21) and (22) that, irrespective of the sign of $\bar{H}_6$, the quadratic (21) has a unique positive solution whenever $\bar{\mathcal{R}}_{01} > 1$. In addition, it should be pointed out that for the equilibrium ξ_{e1} to exist, it is necessary that strain 2 dies out asymptotically (i.e. $\mathcal{R}_{02} < 1$, in line with Theorem 4.4). Hence, the model (1) has a unique strain 1-only boundary equilibrium, ξ_{e1}, whenever $\mathcal{R}_{02} < 1 < \bar{\mathcal{R}}_{01}$.

□

4.1.3 GAS of the Strain-1 Only Boundary Equilibrium for Special Case

Theorem 4.6 *In the absence of reinfection of recovered individuals with the same strain and imperfect vaccine (i.e., $\varepsilon_1 = \varepsilon_3 =, \xi = 1$), the unique strain 1-only boundary equilibrium, ξ_{e1}, of the model (1), with $\delta_{f1} = \delta_{m1} = \delta_{fc} = 0$ is globally asymptotically stable (GAS) in $\mathcal{D}\setminus\mathcal{D}_{01}$ whenever $\mathcal{R}_{02} < 1 < \bar{\mathcal{R}}_{01} = \mathcal{R}_{01}|_{\xi=1}$, where*

$$\mathcal{D}_{01} = \Big\{(S_f, V_f, I_{f1}, P_{f1}, C_f, R_f^c, R_{f1}, S_m, I_{m1}, R_{m1}) \in \mathcal{D}_1 : I_{f1} = P_{f1} = C_f = R_f^c = R_{f1} = I_{m1} = 0\Big\}$$

Proof Consider the model (12) with (14), $\varepsilon_1 = \varepsilon_3 = 0$ and $\bar{\mathcal{R}}_{01} > 1$, so that the associated unique endemic equilibrium exists. Also, consider the nonlinear Lyapunov function of the Goh–Volterra type:

$$\mathcal{V}_1 = (K_2 + \theta_{p1} G_1)\bar{\beta}_{f1} S_m^{**}\left[S_f - S_f^{**} - S_f^{**} \ln\left(\frac{S_f}{S_f^{**}}\right) + V_f - V_f^{**} - V_f^{**} \ln\left(\frac{V_f}{V_f^{**}}\right)\right.$$
$$\left. + I_{f1} - I_{f1}^{**} - I_{f1}^{**} \ln\left(\frac{I_{f1}}{I_{f1}^{**}}\right)\right] + K_1 \theta_{p1} \bar{\beta}_{f1} S_m^{**}\left[P_{f1} - P_{f1}^{**} - P_{f1}^{**} \ln\left(\frac{P_{f1}}{P_{f1}^{**}}\right)\right]$$
$$K_1 K_2\left[S_m - S_m^{**} - S_m^{**} \ln\left(\frac{S_m}{S_m^{**}}\right) + I_{m1} - I_{m1}^{**} - I_{m1}^{**} \ln\left(\frac{I_{m1}}{I_{m1}^{**}}\right)\right]$$

with Lyapunov derivative,

$$\dot{\mathcal{V}}_1 = (K_2 + \theta_{p1} G_1)\bar{\beta}_{f1} S_m^{**}\left[\left(1 - \frac{S_f^{**}}{S_f}\right)\dot{S}_f + \left(1 - \frac{V_f^{**}}{V_f}\right)\dot{V}_f + \left(1 - \frac{I_{f1}^{**}}{I_{f1}}\right)\dot{I}_{f1}\right]$$
$$+ K_1 \theta_{p1} \bar{\beta}_{f1} S_m^{**}\left[\left(1 - \frac{P_{f1}^{**}}{P_{f1}}\right)\dot{P}_{f1}\right] + K_1 K_2\left[\left(1 - \frac{S_m^{**}}{S_m}\right)\dot{S}_m + \left(1 - \frac{I_{m1}^{**}}{I_{m1}}\right)\dot{I}_{m1}\right] \tag{23}$$

Substituting the derivatives in (12) into $\dot{\mathcal{V}}_1$, we have

$$\begin{aligned}
\dot{\mathcal{V}}_1 = (K_2 + \theta_{p1} G_1)\bar{\beta}_{f1} S_m^{**}\Bigg[& \left(1 - \frac{S_f^{**}}{S_f}\right)((1-f)\Lambda_f - (\bar{\beta}_{m1} I_{m1} + \mu_f) S_f) \\
& + \left(1 - \frac{V_f^{**}}{V_f}\right)(f\Lambda_f - \mu_f V_f) \\
& + \left(1 - \frac{I_{f1}^{**}}{I_{f1}}\right)(\bar{\beta}_{m1} I_{m1} S_f - K_1 I_{f1})\Bigg] \\
& + K_1 \theta_{p1} \bar{\beta}_{f1} S_m^{**}\left[\left(1 - \frac{P_{f1}^{**}}{P_{f1}}\right)(G_1 I_{f1} - K_2 P_{f1})\right] \\
& + K_1 K_2\Bigg[\left(1 - \frac{S_m^{**}}{S_m}\right)(\Lambda_m - \left(\bar{\beta}_{f1}(I_{f1} + \theta_{p1} P_{f1}) + \mu_m\right) S_m) \\
& + \left(1 - \frac{I_{m1}^{**}}{I_{m1}}\right)(\bar{\beta}_{f1}(I_{f1} + \theta_{p1} P_{f1}) S_m - K_7 I_{m1})\Bigg]
\end{aligned} \tag{24}$$

Observe from model (12) that, at steady state,

$$\begin{aligned}
(1-f)\Lambda_f = \left(\bar{\beta}_{m1} I_{m1}^{**} + \mu_f\right) S_f^{**}, \quad f\Lambda_f = \mu_f V_f^{**}, \quad \bar{\beta}_{m1} I_{m1} S_f^{**} = K_1 I_{f1}^{**}, \\
G_1 I_{f1}^{**} = K_2 P_{f1}^{**}, \ \Lambda_m = \left(\bar{\beta}_{f1}(I_{f1}^{**} + \theta_{p1} P_{f1}^{**}) + \mu_m\right) S_m^{**}, \ \bar{\beta}_{f1}(I_{f1}^{**} + \theta_{p1} P_{f1}^{**}) S_m^{**} \\
= K_7 I_{m1}^{**}
\end{aligned} \tag{25}$$

Substituting the expressions in (25) into (24) gives

$$\begin{aligned}\dot{\mathcal{V}}_1 = {} & (K_2+\theta_{p1}G_1)\bar{\beta}_{f1}S_m^{**}\left[\left(1-\frac{S_f^{**}}{S_f}\right)(\bar{\beta}_{m1}I_{m1}^{**}S_f^{**}+\mu_f S_f^{**}-\bar{\beta}_{m1}I_{m1}S_f-\mu_f S_f)\right.\\ & \left.+\left(1-\frac{V_f^{**}}{V_f}\right)(\mu_f V_f^{**}-\mu_f V_f)+\left(1-\frac{I_{f1}^{**}}{I_{f1}}\right)(\bar{\beta}_{m1}I_{m1}S_f-K_1I_{f1})\right]\\ & +K_1\theta_{p1}\bar{\beta}_{f1}S_m^{**}\left[\left(1-\frac{P_{f1}^{**}}{P_{f1}}\right)(G_1I_{f1}-K_2P_{f1})\right]\\ & +K_1K_2\left[\left(1-\frac{S_m^{**}}{S_m}\right)(\bar{\beta}_{f1}I_{f1}^{**}S_m^{**}+\bar{\beta}_{f1}\theta_{p1}P_{f1}^{**}S_m^{**}\right.\\ & +\mu_m S_m^{**}-\bar{\beta}_{f1}I_{f1}S_m-\bar{\beta}_{f1}\theta_{p1}P_{f1}S_m-\mu_m S_m)\\ & \left.+\left(1-\frac{I_{m1}^{**}}{I_{m1}}\right)(\bar{\beta}_{f1}I_{f1}S_m+\bar{\beta}_{f1}\theta_{p1}P_{f1}S_m-K_7I_{m1})\right]\end{aligned}$$

which can be simplified to

$$\begin{aligned}\dot{\mathcal{V}}_1 = {} & (K_2+\theta_{p1}G_2)\bar{\beta}_{f1}\mu_f S_m^{**}S_f^{**}\left(2-\frac{S_f^{**}}{S_f}-\frac{S_f}{S_f^{**}}\right)\\ & +K_1K_2\mu_m S_m^{**}\left(2-\frac{S_m^{**}}{S_m}-\frac{S_m}{S_m^{**}}\right)\\ & +K_1K_2\bar{\beta}_{f1}I_{f1}^{**}S_m^{**}\left(4-\frac{S_f^{**}}{S_f}-\frac{S_m^{**}}{S_m}-\frac{I_{m1}I_{f1}^{**}S_f}{I_{m1}^{**}I_{f1}S_f^{**}}-\frac{I_{f1}I_{m1}^{**}S_m}{I_{f1}^{**}I_{m1}S_m^{**}}\right)\\ & +K_1K_2\bar{\beta}_{f1}\theta_{p1}P_{f1}^{**}S_m^{**}\left(5-\frac{S_f^{**}}{S_f}-\frac{S_m^{**}}{S_m}-\frac{I_{m1}I_{f1}^{**}S_f}{I_{m1}^{**}I_{f1}S_f^{**}}-\frac{I_{m1}^{**}P_{f1}S_m}{I_{m1}P_{f1}^{**}S_m^{**}}-\frac{I_{f1}P_{f1}^{**}}{I_{f1}^{**}P_{f1}}\right)\end{aligned} \tag{26}$$

Finally, since arithmetic mean is greater that geometric mean, the following inequalities from (26) hold:

$$\left(2-\frac{S_f^{**}}{S_f}-\frac{S_f}{S_f^{**}}\right)\le 0,\quad \left(2-\frac{S_m^{**}}{S_m}-\frac{S_m}{S_m^{**}}\right)\le 0$$

$$\left(4-\frac{S_f^{**}}{S_f}-\frac{S_m^{**}}{S_m}-\frac{I_{m1}I_{f1}^{**}S_f}{I_{m1}^{**}I_{f1}S_f^{**}}-\frac{I_{f1}I_{m1}^{**}S_m}{I_{f1}^{**}I_{m1}S_m^{**}}\right)\le 0$$

$$\left(5-\frac{S_f^{**}}{S_f}-\frac{S_m^{**}}{S_m}-\frac{I_{m1}I_{f1}^{**}S_f}{I_{m1}^{**}I_{f1}S_f^{**}}-\frac{I_{m1}^{**}P_{f1}S_m}{I_{m1}P_{f1}^{**}S_m^{**}}-\frac{I_{f1}P_{f1}^{**}}{I_{f1}^{**}P_{f1}}\right)\le 0$$

Thus, $\dot{\mathcal{V}}_1 \le 0$ for $\bar{\mathcal{R}}_{01} > 1$. Hence, $\mathcal{V}_1$ is a Lyapunov function in $\mathcal{D}\setminus\mathcal{D}_{01}$ and it follows from the LaSalle's invariance principle [35], that every solution to the

equations of the model (12) with (14), and initial conditions in $\mathcal{D} \setminus \mathcal{D}_{01}$ approach the associated unique endemic equilibrium ξ_{e1}, of the model as $t \to \infty$ for $\bar{\mathcal{R}}_{01} > 1$.

4.2 Strain 2-Only Boundary Equilibrium

The strain 2-only sub-model (is obtained by setting $V_f = I_{f1} = P_{f1} = R_{f1} = I^p_{f2} = I_{f12} = I_{f21} = M_f = I_{m1} = R_{m1} = I_{m12} = I_{m21} = M_m = 0$ in the model (1)) is given by:

$$\begin{aligned}
\frac{dS_f}{dt} &= \Lambda_f - \left(\lambda_{m2} + \mu_f\right) S_f \\
\frac{dI_{f2}}{dt} &= \lambda_{m2} S_f - K_4 I_{f2} + \varepsilon_2 \lambda_{m2} R_{f2} \\
\frac{dP_{f2}}{dt} &= G_6 I_{f2} - K_6 P_{f2} \\
\frac{dC_f}{dt} &= G_4 P_{f2} - K_3 C_f \\
\frac{dR^c_f}{dt} &= \pi_f C_f - \mu_f R^c_f \\
\frac{dR_{f2}}{dt} &= p_2 \tau_{f2} I_{f2} + q_2 \eta_c \kappa_{f2} P_{f2} - \left(\mu_f + \varepsilon_2 \lambda_{m2}\right) R_{f2} \\
\frac{dS_m}{dt} &= \Lambda_m - \left(\lambda_{f2} + \mu_m\right) S_m \\
\frac{dI_{m2}}{dt} &= \lambda_{f2} S_m + \varepsilon_4 \lambda_{f2} R_{m2} - K_8 I_{m2} \\
\frac{dR_{m2}}{dt} &= \tau_{m2} I_{m2} - \left(\mu_m + \varepsilon_4 \lambda_{f2}\right) R_{m2}
\end{aligned} \tag{27}$$

where now

$$\lambda_{f2} = \frac{\beta_{f2}(I_{f2} + \theta_{p2} P_{f2})}{N_f}, \quad \lambda_{m2} = \frac{\beta_{m2} I_{m2}}{N_m}$$

with

$$\begin{aligned}
N_f &= S_f + I_{f2} + P_{f2} + C_f + R^c_f + R_{f2}, \quad \text{and} \\
N_m &= S_m + I_{m2} + R_{m2}
\end{aligned}$$

The sub-model (27) will be considered in the positively invariant region:

$$\mathcal{D}_2 = \mathcal{D}_2^f \cup \mathcal{D}_2^m$$

with

$$\mathcal{D}_2^f = \left\{ (S_f, I_{f2}, P_{f2}, C_f, R_f^c, R_{f2}) \in \mathfrak{R}_+^6 : N_f \leq \frac{\Lambda_f}{\mu_f} \right\}, \text{ and}$$
$$\mathcal{D}_2^m = \left\{ (S_m, I_{m2}, R_{m2}) \in \mathfrak{R}_+^3 : N_m \leq \frac{\Lambda_m}{\mu_m} \right\}$$

The strain 2-only sub-model (27) has a DFE, obtained by setting the right-hand sides of the equations in the model (27) to zero, given by

$$\begin{aligned} \xi_{02} =& (S_f^*, I_{f2}^*, P_{f2}^*, C_f^*, R_f^{c*}, R_{f2}^*, S_m^*, I_{m2}^*, R_{m2}^*) \\ =& (\frac{\Lambda_f}{\mu_f}, 0, 0, 0, 0, 0, \frac{\Lambda_m}{\mu_m}, 0, 0) \end{aligned} \tag{28}$$

Setting $\lambda_{f1} = \lambda_{m1} = 0$ in (1) gives the following general form of the strain 2-only boundary equilibrium (denoted by ξ_{e2})

$$\varepsilon_2 = \left(S_f^{**}, 0, 0, 0, C_f^{**}, R_f^{c**}, 0, I_{f2}^{**}, 0, P_{f2}^{**}, R_{f2}^{**}, S_m^{**}, 0, 0, I_{m2}^{**}, R_{m2}^{**}, 0, 0, 0, 0, 0, 0 \right)$$

(It should be noted here that N_f^{**} and N_m^{**} are replaced with their limiting values $\frac{\Lambda_f}{\mu_f}$ and $\frac{\Lambda_m}{\mu_m}$, respectively, as all disease-induced death rates are assumed zero). It should be noted that setting $\delta_{f2} = \delta_{m2} = \delta_{fc} = 0$ in (27) gives $N_f \to \frac{\Lambda_f}{\mu_f}$ and $N_m \to \frac{\Lambda_m}{\mu_m}$ as $t \to \infty$. Let $\bar{\beta}_{f2} = \frac{\mu_f \beta_{f2}}{\Lambda_f}$ and $\bar{\beta}_{m2} = \frac{\mu_m \beta_{m2}}{\Lambda_m}$ so that

$$\lambda_{f2} = \bar{\beta}_{f2}(I_{f2} + \theta_{p2} P_{f2}) \quad \text{and} \quad \lambda_{m2} = \bar{\beta}_{m2} I_{m2} \tag{29}$$

Define

$$\lambda_{f2}^{**} = \frac{\beta_{f2}\mu_f \left(I_{f2}^{**} + \theta_{p2} P_{f2}^{**} \right)}{\Lambda_f}, \quad \text{and} \quad \lambda_{m2}^{**} = \frac{\beta_{m2} I_{m2}^{**} \mu_m}{\Lambda_m} \tag{30}$$

Setting the right-hand sides of model (27) to zero gives the steady-state solutions

$$
\begin{aligned}
S_f^{**} &= \frac{\Lambda_f}{\left(\lambda_{m2}^{**}+\mu_f\right)},\\
I_{f2}^{**} &= \frac{K_6\Lambda_f\left(\varepsilon_2\lambda_{m2}^{**2}+\mu_f\lambda_{m2}^{**}\right)}{\left(\mu_f+\lambda_{m2}^{**}\right)\left[\lambda_{m2}^{**}\left(K_4K_6\varepsilon_2-K_6p_2\tau_{f2}\varepsilon_2+G_6G_9\varepsilon_2\right)+K_4K_6\mu_f\right]},\\
R_{f2}^{**} &= \frac{\Lambda_f\left(\varepsilon_2\lambda_{m2}^{**2}+\mu_f\lambda_{m2}^{**}\right)\left(K_6p_2\tau_{f2}+G_6G_9\right)}{\left(\mu_f+\lambda_{m2}^{**}\right)\left(\mu_f+\varepsilon_2\lambda_{m2}^{**}\right)\left[\lambda_{m2}^{**}\left(K_4K_6\varepsilon_2-K_6p_2\tau_{f2}\varepsilon_2+G_6G_9\varepsilon_2\right)+K_4K_6\mu_f\right]},\\
P_{f2}^{**} &= \frac{G_6\Lambda_f\left(\varepsilon_2\lambda_{m2}^{**2}+\mu_f\lambda_{m2}^{**}\right)}{\left(\mu_f+\lambda_{m2}^{**}\right)\left[\lambda_{m2}^{**}\left(K_4K_6\varepsilon_2-K_6p_2\tau_{f2}\varepsilon_2+G_6G_9\varepsilon_2\right)+K_4K_6\mu_f\right]},\\
C_f^{**} &= \frac{G_4G_6\Lambda_f\left(\varepsilon_2\lambda_{m2}^{**2}+\mu_f\lambda_{m2}^{**}\right)}{\left(\mu_f+\lambda_{m2}^{**}\right)K_3\left[\lambda_{m2}^{**}\left(K_4K_6\varepsilon_2-K_6p_2\tau_{f2}\varepsilon_2+G_6G_9\varepsilon_2\right)+K_4K_6\mu_f\right]},\\
R_f^{c**} &= \frac{G_4G_6\Lambda_f\pi_f\left(\varepsilon_2\lambda_{m2}^{**2}+\mu_f\lambda_{m2}^{**}\right)}{\mu_fK_3\left(\mu_f+\lambda_{m2}^{**}\right)\left[\lambda_{m2}^{**}\left(K_4K_6\varepsilon_2-K_6p_2\tau_{f2}\varepsilon_2+G_6G_9\varepsilon_2\right)+K_4K_6\mu_f\right]},\\
S_m^{**} &= \frac{\Lambda_m}{\left(\lambda_{f2}^{**}+\mu_m\right)},\\
I_{m2}^{**} &= \frac{\Lambda_m\lambda_{f2}^{**}\left(\varepsilon_4\lambda_{f2}^{**}+\mu_m\right)}{\left[\left(K_8\varepsilon_4-\tau_{m2}\varepsilon_4\right)\lambda_{f2}^{**2}+\left(K_8\mu_m+K_8\mu_m\varepsilon_4-\tau_{m2}\mu_m\varepsilon_4\right)\lambda_{f2}^{**}+K_8\mu_m^2\right]},\\
R_{m2}^{**} &= \frac{\tau_{m2}\lambda_{f2}^{**}\Lambda_m}{\left[\left(K_8\varepsilon_4-\tau_{m2}\varepsilon_4\right)\lambda_{f2}^{**2}+\left(K_8\mu_m+K_8\mu_m\varepsilon_4-\tau_{m2}\mu_m\varepsilon_4\right)\lambda_{f2}^{**}+K_8\mu_m^2\right]}
\end{aligned}
\tag{31}
$$

Substituting the above expressions into (30), gives

$$
\begin{aligned}
\lambda_{f2}^{**} &= \frac{h_{02}\lambda_{m2}^{**2}+h_{01}\lambda_{m2}^{**}}{h_{22}\lambda_{m2}^{**2}+h_{11}\lambda_{m2}^{**}+h_{00}},\\
\lambda_{m2}^{**} &= \frac{j_{02}\lambda_{f2}^{**2}+j_{01}\lambda_{f2}^{**}}{j_{22}\lambda_{f2}^{**2}+j_{11}\lambda_{f2}^{**}+j_{00}}
\end{aligned}
\tag{32}
$$

where,

$$
\begin{aligned}
&h_{02}=\beta_{f2}\mu_f\varepsilon_2(K_6+\theta_{p2}G_6),\quad h_{01}=\beta_{f2}\mu_f^2(K_6+\theta_{p2}G_6),\\
&h_{22}=K_4K_6\varepsilon_2-\varepsilon_2(K_6p_2\tau_{f2}+G_6G_9),\\
&h_{11}=K_4K_6\mu_f+K_4K_6\mu_f\varepsilon_2-\mu_f\varepsilon_2(K_2p_2\tau_{f2}+G_6G_9),\\
&h_{00}=K_4K_6\mu_f^2,\\
&j_{02}=\beta_{m2}\mu_m\varepsilon_4,\quad j_{01}=\beta_{m2}\mu_m^2,\quad j_{22}=K_8\varepsilon_4-\tau_{m2}\varepsilon_4,\\
&j_{11}=K_8\mu_m+K_8\mu_m\varepsilon_4-\tau_{m2}\mu_m\varepsilon_4,\quad j_{00}=K_8\mu_m^2
\end{aligned}
\tag{33}
$$

The existence of the strain 2-only boundary equilibrium can be determined from fixed point problem $\theta_2(0, \lambda_2^{**}) = \lambda_2^{**}$, which after some algebraic manipulations leads to the following polynomial (in terms of λ_{m2}^{**}):

$$Y_1(\lambda_{m2}^{**})^4 + Y_2(\lambda_{m2}^{**})^3 + Y_3(\lambda_{m2}^{**})^2 + Y_4\lambda_{m2}^{**} + Y_5 = 0 \tag{34}$$

with

$$\begin{aligned}
Y_1 &= h_{02}^2 j_{22} + h_{02}h_{22}j_{11} + h_{22}^2 j_{00} > 0\\
Y_2 &= 2h_{01}h_{02}j_{22} + h_{02}h_{11}j_{11} + h_{01}h_{22}j_{11} + 2h_{11}h_{22}j_{00} - h_{02}^2 j_{02} - h_{02}h_{22}j_{01},\\
Y_3 &= h_{01}^2 j_{22} + h_{02}h_{00}j_{11} + h_{01}h_{11}j_{11} + h_{11}^2 j_{00} - 2h_{01}h_{02}j_{02}\\
&\quad - h_{02}h_{11}j_{01} + h_{00}h_{22}j_{00}(2 - \mathcal{R}_{02}^2)\\
Y_4 &= h_{00}h_{01}j_{11} - h_{01}^2 j_{02} - h_{02}h_{00}j_{01} + h_{00}h_{11}j_{00}(1 - \mathcal{R}_{02}^2),\\
Y_5 &= h_{00}^2 j_{00}(1 - \mathcal{R}_{02}^2) > 0 \quad \text{if} \quad \mathcal{R}_{02} < 1
\end{aligned} \tag{35}$$

Using the approaches in Sect. 4.1 and the center manifold theory [30] (as applied in Sect. 3.2), the following results can be established.

Theorem 4.7 *In the absence of reinfection of recovered individuals with strain 2 ($\varepsilon_2 = \varepsilon_4 = 0$), the sub-model (27) does not undergo backward bifurcation.*

Theorem 4.8 *In the absence of reinfection of recovered individuals with strain 2 (i.e. $\varepsilon_2 = \varepsilon_4 = 0$), the model (1) with $\delta_{f2} = \delta_{m2} = \delta_{fc} = 0$ has a unique strain 2-only boundary equilibrium, ξ_{e2}, whenever $\mathcal{R}_{01} < 1 < \mathcal{R}_{02}$*

Theorem 4.9 *In the absence of re,infection of recovered individuals with strain 2 (i.e., $\varepsilon_2 = \varepsilon_4 =$), the unique strain 2-only boundary equilibrium, ξ_{e2}, of the model (1), with $\delta_{f2} = \delta_{m2} = \delta_{fc} = 0$, is globally asymptotically stable (GAS) in $\mathcal{D} \setminus \mathcal{D}_{02}$ whenever $\mathcal{R}_{01} < 1 < \mathcal{R}_{02}$, where*

$$\mathcal{D}_{02} = \Big\{ (S_f, I_{f2}, P_{f2}, C_f, R_f^c, R_{f2}, S_m, I_{m2}, R_{m2}) \in \mathcal{D}_2 : I_{f2} = P_{f2} = C_f = R_f^c = R_{f2} = I_{m2} = 0 \Big\}$$

5 Simulations of the Two-Strain HPV Model (1)

5.1 Uncertainty and Sensitivity Analysis

Uncertainties are expected to arise in estimates of the values of the parameters used in the numerical simulations. Applying the approach in Blower and Dowlatabadi [36], we carry out a Latin hypercube sampling (LHS) on the parameters of the model,

to ascertain the effect of these uncertainties and to determine the parameter(s) that have the greatest impact on the transmission dynamics of HPV. For the sensitivity analysis, a partial rank correlation coefficient (PRCC) was calculated between values of the parameters in the response function and the values of the response function derived from the sensitivity analysis. Using the reproduction numbers $\mathcal{R}_{01}$ and $\mathcal{R}_{02}$ as response functions, it follows from Table 3, that the top PRCC-ranked parameters are: the effective contact rates, β_{f1} (β_{m1}) and β_{f2} (β_{m2}) for strain 1 and strain 2, respectively, the fraction of vaccinated females f, the *Cervarix* vaccine efficacy, ξ, the treatment rates, τ_{f1} (τ_{m1}) and τ_{f2} (τ_{m2}) for strain 1 and strain 2, respectively, as well as the demographic parameters, μ_f and μ_m.

5.2 Numerical Simulations

We now simulate the model (1) numerically using the parameter estimates in Table 4 (unless otherwise stated), to assess the potential impact of various targeted control strategies on the transmission dynamics of HPV in the population. Demographic parameters relevant to South Africa were chosen. Specifically, since the total population of sexually active susceptible females and males (15–64 years) in South Africa are estimated to be 17,125,878, and 16,100,016, respectively, at disease-free equilibrium, $\frac{\Lambda_f}{\mu_f}$ = 16,751,173 and $\frac{\Lambda_m}{\mu_m}$ = 17,174,710 [37, 38]. In South Africa, the life expectancy for females and males is estimated at 64.6 years and 61.6 years, respectively [37]. Hence, we have that $\mu_f = 0.0162$ and $\mu_m = 0.0155$, so that Λ_f =271,369 and Λ_m = 266,208 per year, and the total HPV prevalence in South Africa was estimated around 5% in 2009 [39, 40].

The effect of the fraction of vaccinated females, f, on the cumulative new cases of strain 1 and strain 2 infections, depicted in Figs. 4 and 5, respectively, shows a decrease in the cumulative new cases of strain 1 infection with increasing fraction of vaccinated females, as expected. Also, increasing the fraction of vaccinated females leads to a corresponding decrease in the cumulative new cases of strain 2 infection. Numerical simulations for the cases $\mathcal{R}_{01} < 1$ and $\mathcal{R}_{01} > 1$, depicted in Fig. 6, show that strain 1 dies out when $\mathcal{R}_{01} < 1$ and persists at steady state when $\mathcal{R}_{01} > 1$. Similar conclusions are reached for the cases $\mathcal{R}_{02} < 1$ and $\mathcal{R}_{02} > 1$ (Figs. 6 and 7). The results of this study conform with the findings in [5, 11], that the bivalent *Cervarix* vaccine offers high protection not only against the most prevalent HPV types 16 and 18, but also against other oncogenic types like HPV 31 and 45. Moreover, the results of our findings will be very useful especially in poor and middle-income countries (where cervical cancer continues to be a major cause of deaths among women [2]) who may not be able to afford the high cost of the nonavalent *Gardasil 9* HPV vaccine.

Table 3 Partial rank correlation coefficients (PRCC) for $\mathcal{R}_{01}$ and $\mathcal{R}_{02}$ and each input parameter variable

Parameters	$\mathcal{R}_{01}$	$\mathcal{R}_{02}$
μ_f	$\mathbf{-0.5377}$	$\mathbf{-0.7109}$
μ_m	$\mathbf{-0.5396}$	$\mathbf{-0.6937}$
ε_1	0.0076	–
ε_2	–	−0.0014
ε_3	−0.0187	–
ε_4	–	0.0313
p_1	−0.0014	–
p_2	–	−0.0597
ξ	$\mathbf{-0.5644}$	–
q_1	0.0905	–
q_2	–	−0.0325
π_f	−0.0105	−0.0319
τ_{f1}	$\mathbf{-0.8511}$	–
τ_{m1}	$\mathbf{-0.8542}$	–
δ_{f1}	−0.0137	–
κ_{f1}	−0.0042	–
κ_{f2}	–	0.0315
δ_{m1}	−0.0210	–
δ_{fc}	0.0385	0.0551
f	$\mathbf{-0.9600}$	–
β_{f2}	–	$\mathbf{0.6088}$
β_{m2}	–	$\mathbf{0.9470}$
η_c	–	−0.0128
δ_{f2}	−0.0137	−0.0298
δ_{m2}	–	−0.0346
τ_{f2}	–	$\mathbf{-0.9285}$
τ_{m2}	–	$\mathbf{-0.9324}$
θ_{p1}	0.0142	–
θ_{p2}	–	0.0187
β_{f1}	$\mathbf{0.5001}$	–
β_{m1}	$\mathbf{0.8835}$	–

Table 4 Baseline values and ranges of the parameters of the model (1)

Parameter	Baseline value (*per* year)	Range (*per* year)	References
μ_f	0.0162	[0.0100, 0.2000]	[37]
μ_m	0.0155	[0.0100, 0.2000]	[37]
Λ_f	271,369	[250,000, 280,000]	[37]
Λ_m	26,6208	[25,0000, 280,000]	[37]
$\beta_1^f(\beta_2^f)$	0.5	[0.4,0.6]	[41, 42]
$\beta_1^m(\beta_2^m)$	0.4	[0.3,0.5]	[41, 42]
c_f	2	[1, 5]	[42]
$\eta_I(\eta_p)$	0.5	[0.5, 1.0]	Inferred from [5]
η_c	0.5	[0.5, 1.0]	Inferred from [5]
ϕ_p	0.7	[0.5, 1.0]	Assumed
$\varepsilon_1(\varepsilon_2)$	0.2	[0.1, 1.0]	Inferred from [10]
$\varepsilon_3(\varepsilon_4)$	0.3	[0.1, 1.0]	Inferred from [10]
$\theta_{p1}(\theta_{p2})$	0.9	[0.7, 0.9]	[32, 41, 42]
f	0.87	[0.5, 0.9]	[38]
ξ	0.9	[0.9, 1]	[42]
$\delta_{f1}(\delta_{m1})$	0.001	[0.0005, 0.002]	[41, 42]
$\delta_{f12}(\delta_{m12})$	0.001	[0.0005, 0.002]	[41, 42]
$\delta_{f2}(\delta_{m2})$	0.001	[0.0005, 0.002]	[41, 42]
$\delta_{f21}(\delta_{m21})$	0.001	[0.0005, 0.002]	[41, 42]
δ_{f2}^p	0.01	[0.005, 0.002]	Assumed
$\gamma_f(\gamma_m)$	0.5	[0.3, 0.7]	[41]
$\phi_f(\phi_m)$	0.9	[0.7, 0.9]	[42]
$\kappa_{f1}(\kappa_{f2})$	114	[110, 120]	[20]
$\tau_{f1}(\tau_{f2})$	0.9	[0.5, 2.5]	[42]
$\tau_{f21}(\tau_{f12})$	0.9	[0.5, 2.5]	[42]
$\tau_{m1}(\tau_{m2})$	0.9	[0.5, 2.5]	[42]
$\tau_{m21}(\tau_{m12})$	0.9	[0.5, 2.5]	[42]
$\kappa_{f1}(\kappa_{f2})$	0.3	[0.1, 0.5]	[41]
δ_f^c	0.01	[0.005, 0.002]	[42]
ω_f	0.01	[0.005, 0.02]	[32]
π_f	0.76	[0.56, 0.96]	[42, 43]
α_1	0.4	[0.1, 1.0]	Inferred from [10]
α_2	0.5	[0.1, 1.0]	Inferred from [10]
α_3	0.3	[0.1, 1.0]	Inferred from [10]
α_4	0.2	[0.1, 1.0]	Inferred from [10]
$p_1(p_2)$	0.5	[0.1, 1.0]	Assumed
$q_1(q_2)$	0.3	[0.1, 1.0]	Assumed
$p_{12}(p_{21})$	0.5	[0.1, 1.0]	Assumed

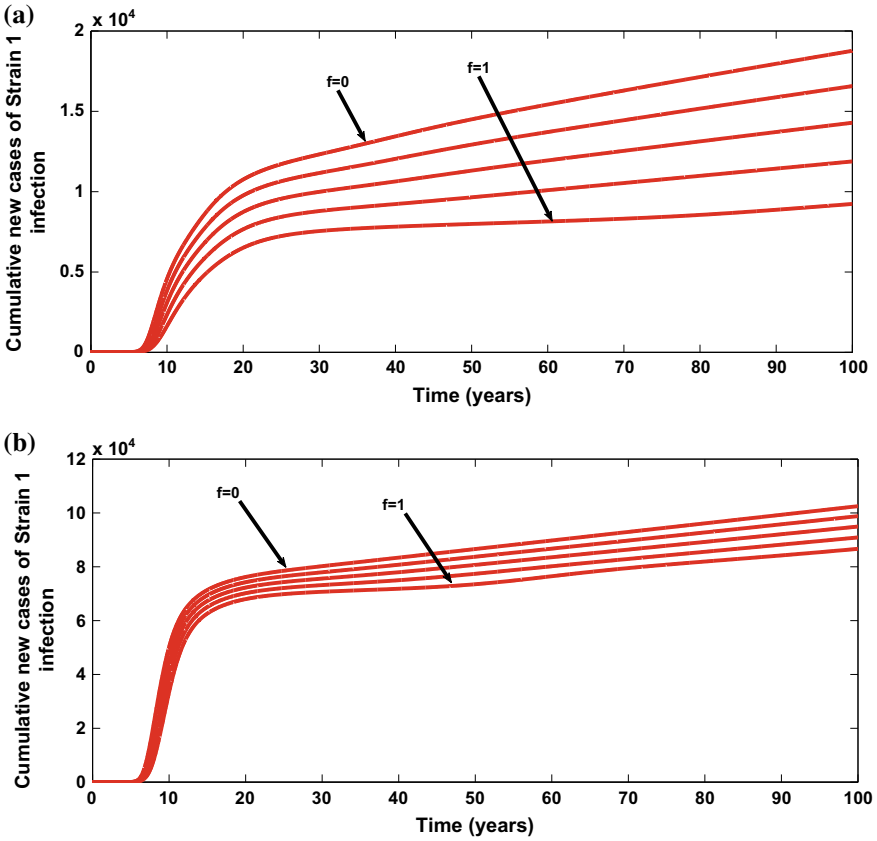

Fig. 4 Effect of the fraction of vaccinated susceptible females, f, on the cumulative new cases of strain 1 infection. **a** Here, $\beta_{f1} = 3.5$, $\beta_{m1} = 3.5$, **b** here, $\beta_{f1} = 4.7$, $\beta_{m1} = 4.7$. All other parameters as in Table 4

6 Conclusions

A new two-sex, two-strain HPV mathematical model that rigorously assesses the impact of cross-immunity due to vaccination, in a population where two strains coexist and there is vaccination for one of the strains, which cross-protects against the strain not included in the vaccine was considered. We discussed a vaccination strategy that makes use of the bivalent *Cervarix* vaccine targeted at one group of high-risk HPV: type 16/18 but with cross-immunity property against other high-risk HPV: type 31/45. The model (1) has a locally asymptotically stable disease-free equilibrium whenever the basic reproduction number ($\mathcal{R}_0$) is less than unity. The model was also shown to undergo the phenomenon of backward bifurcation, where the stable disease-free equilibrium coexists with one stable endemic equilibrium when the associated reproduction number is less than unity. The analysis showed that the phenomenon of

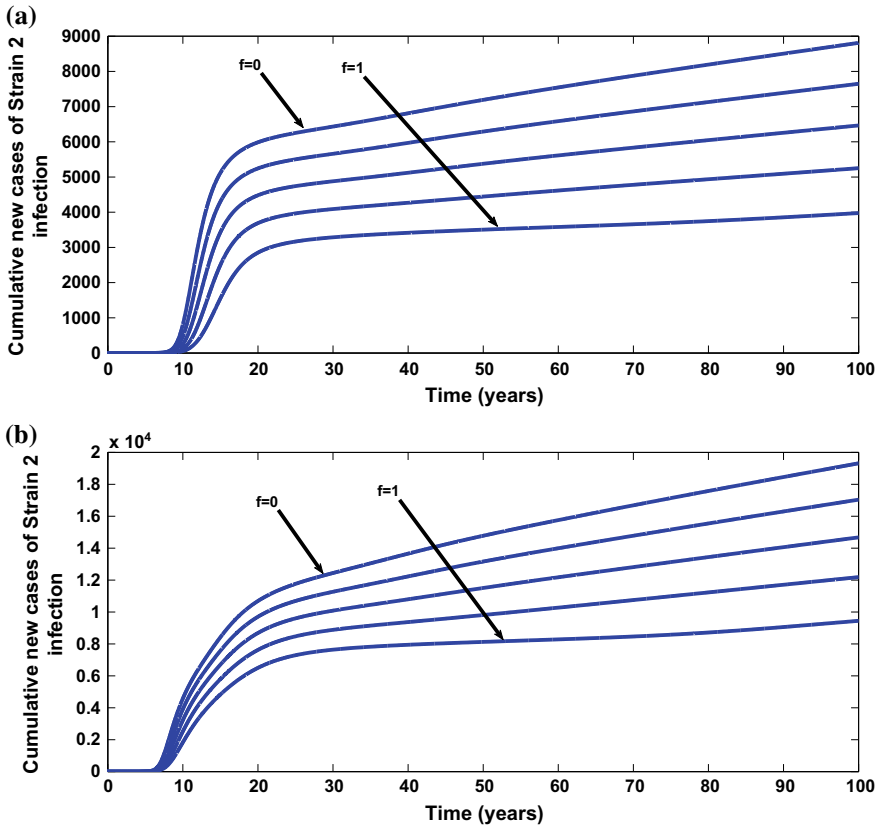

Fig. 5 Effect of the fraction of vaccinated susceptible females, f, on the cumulative new cases of strain 2 infection. **a** Here, $\beta_{f2} = 3.5$, $\beta_{m2} = 3.5$, **b** here, $\beta_{f2} = 4.7$, $\beta_{m2} = 4.7$. All other parameters as in Table 4

backward bifurcation is caused by the imperfect vaccine (that partially cross-protects the strain not included in the vaccine) as well as the reinfection of individuals who recover from a previous infection with the same strain.

Furthermore, the existence and stability of the boundary equilibrium of the strain 1-only sub-model was investigated. It is shown rigorously that the strain 1-only sub-model undergoes backward bifurcation due to the reinfection of recovered individuals and the presence of an imperfect vaccine. In the absence of reinfection of recovered individuals and imperfect vaccine for females, the DFE of the strain 1-only submodel is shown to be globally asymptotically stable when the associated reproduction number is less than one. Also, we observe that the strain 2-only sub-model does not undergo the phenomenon of backward bifurcation in the absence of reinfection of recovered individuals.

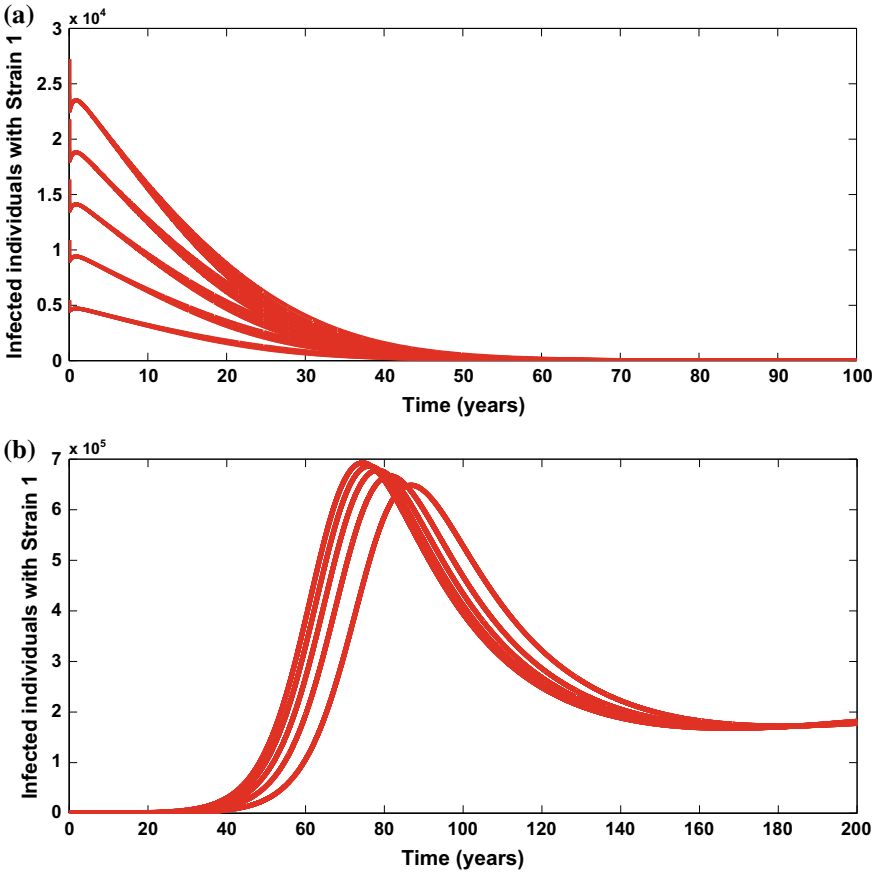

Fig. 6 Infected individuals with strain 1 at different initial conditions. **a** Here, $\beta_{f1} = \beta_{m1} = 1.7$, so that $\mathcal{R}_{01} = 0.865268 < 1$, **b** here, $\beta_{f1} = \beta_{m1} = 2.1$, so that $\mathcal{R}_{01} = 1.06886 > 1$. All other parameters as in Table 4

Moreover, numerical simulations of the model show that increasing the fraction of females vaccinated against a particular strain could significantly bring down the burden of the strain not included in the vaccine. Therefore, for effective control and prevention of oncogenic HPV types and cervical cancer, this study recommends wide vaccination of susceptible females with the bivalent *Cervarix* vaccine, especially in a population where HPV type 16/18 and type 31/45 are co-circulating. The findings in this study are consistent with the reports in Kudo et al. [18] that significant cross-protection against HPV 31, 45, and 52 was shown by the bivalent *Cervarix* vaccine which targets HPV types 16 and 18. One of the recommendations in [18] was a call on the government authorities of Japan to consider the effectiveness of this vaccine and ensure a continuous national vaccination program with the vaccine. Also, the results of our findings will be very useful especially in poor and developing countries

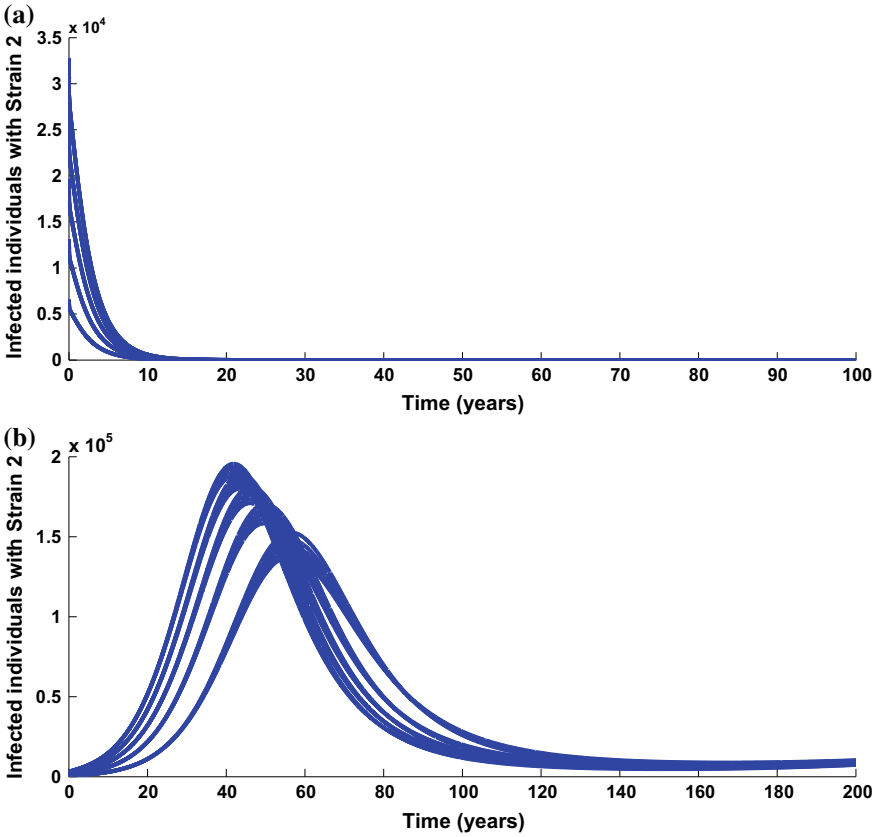

Fig. 7 Infected individuals with strain 2 at different initial conditions. **a** Here, $\beta_{f2} = \beta_{m2} = 0.8$, so that $\mathcal{R}_{02} = 0.875646 < 1$, **b** here, $\beta_{f2} = \beta_{m2} = 2.2$, so that $\mathcal{R}_{02} = 2.40803 > 1$. All other parameters as in Table 4

(where cervical cancer continues to be a major cause of deaths among women [2]) who may not be able to afford the high cost of the nonavalent *Gardasil 9* HPV vaccine. Sensitivity analysis of the model (1), using the reproduction numbers $\mathcal{R}_{01}$ and $\mathcal{R}_{02}$ as response functions, revealed that the top PRCC-ranked parameters are: the effective contact rates, β_{f1} (β_{m1}) and β_{f2} (β_{m2}) for strain 1 and strain 2, respectively, the fraction of vaccinated females f, the *Cervarix* vaccine efficacy, ξ, the treatment rates, τ_{f1} (τ_{m1}) and τ_{f2} (τ_{m2}) for strain 1 and strain 2, respectively, as well as the demographic parameters, μ_f and μ_m.

References

1. A. Jemal, F. Bray, M.M. Center, J. Ferlay, E. Ward, D. Forman, GLobal cancer statistics. Cancer J. Clin. **61**(2), 69–90 (2011)
2. C. Clendinen, Y. Zhang, R.W. Warburton, D.W. Light, Manufacturing costs of HPV vaccines for developing countries. Vaccine **34**, 5984–5989 (2016)
3. H.G. Ahmed, S.H. Bensumaidea, I.M. Ashankyty, Frequency of human papillomavirus (HPV) subtypes 31, 33, 35, 39 and 45 among Yemeni women with cervical cancer. Infect. Agents Cancer **10**(29), 1–6 (2015)
4. V. Kumar, A.K. Abbas, N. Fausto, R. Mitchell, Chapter 19 The female genital system and breast, in *Robbins Basic Pathology*, 8th edn. (Saunders, Philadelphia, 2007). ISBN 1-4160-2973-7
5. K.A. Ault, Human Papilloma Virus vaccines and the potential for cross-protection between related HPV types. Gynecol. Oncol. **107**, S31–S33 (2007)
6. J.S. Smith, L. Lindsay, B. Hoots, J. Keys, S. Franceschi, R. Winer, Human Papilloma Virus type distribution in invasive cervical cancer and high-grade cervical lesions: a meta-analysis update. Int. J. Cancer **121**(3), 621–632 (2007)
7. N. Munoz, F.X. Bosch, X. Castellsague, M. Diaz, S. de Sanjosé, D. Hammouda, Against which human papillomavirus types shall we vaccinate and screen? The international perspective. Int. J. Cancer **111**(2), 278–285 (2004)
8. K. Thomas, J. Hughes, J. Kuypers, N. Kiviat, S.-K. Lee, Concurrent and sequential acquisition of different genital human papillomavirus types. J. Infect. Dis. **182**, 1097 (2000)
9. K.-L. Liaw, A. Hildesheim, R. Burk, P. Gravitt, S. Wacholder, A prospective study of human papillomavirus (HPV) type 16 DNA detection by polymerase chain reaction and its association with acquisition and persistence of other HPV types. J. Infect. Dis. **183**, 8 (2001)
10. G.Y.F. Ho, Y. Studentsov, C.B. Hall, R. Bierman, L. Beardsley, Risk factors for subsequent cervicovaginal human papillomavirus (HPV) infection and the protective role of antibodies to HPV-16 virus-like particles. J. Infect. Dis. **186**, 737 (2002)
11. E.-M. de Villers, C. Fauquet, C. Broker, H.-U. Bernard, H. zur Harsen, Classification of human papillomavirus. Virology **324**, 17–27 (2004)
12. A. Harari, Z. Chen, A. Rodriguez, A.C. Hildesheim, C. Porras, R. Herrero, S. Wacholder, O.A. Panagiotou, B. Befano, R.D. Burk, M. Schiffman, Cross-protection of the bivalent Human papillomavirus (HPV) vaccine against variants of genetically related high-risk HPV infections. J. Infect. Dis. **213**, 939–947 (2016)
13. J.M.L. Brotherton, Confirming cross-protection of bivalent HPV vaccine. Lancet Inf. Dis. **17**(12), 1227–1228 (2017)
14. K. Kavanagh, K.G. Pollock, K. Cuschieri, Changes in the prevalence of Human Papillomavirus vaccination programme in Scotland: a 7-year cross-sectional study. Lancet Infect. Dis. **17**, 1293–1302 (2017)
15. P.J. Woestenberg, A.J. King, B.H.B. van Benthem, Bivalent vaccine effectiveness against type-specific oncogenic types among Dutch STI clinic visitors. J. Infect. Dis. **217**, 213–222 (2018)
16. P. van Damme, P. Bonanni, X. Bosch, E. Joura, S.K. Kjaer, C.J.L.M. Meijer, K.-U. Petry, B. Soubeyrand, T. Verstraeten, M. Stanley, Use of the nonavalent HPV vaccine in individuals previously fully or partially vaccinated with bivalent or quadrivalent HPV vaccines. Vaccine **34**, 757–761 (2016)
17. J. Bornstein, The HPV vaccine market: Cervarix competes with Gardasil. Therapy **7**(1), 71–75 (2010)
18. R. Kudo, M. Yamaguchi, M. Sekine, S. Adachi, Y. Ueda, E. Miyagi, M. Hara, S.J.B. Hanley, T. Enomoto, Bivalent Human papillomavirus vaccine effectiveness in a Japanese population: high vaccine type-specific effectiveness and evidence of cross-protection. J. Infect. Dis. (2018)
19. F.B. Agusto, A.B. Gumel, Qualitative dynamics of lowly- and highly-pathogenic Avian influenza strains. Math. Biosci. **243**, 147–162 (2013)
20. A.A. Alsaleh, A.B. Gumel, Analysis of a risk-structured vaccination model for the dynamics of oncogenic and warts-causing HPV types. Bull. Math. Biol. **76**, 1670–1726 (2014)

21. E.H. Elbasha, A.P. Galvani, Vaccination against multiple HPV types. Math. Biosci. **197**, 88–117 (2005)
22. E.H. Elbasha, E.J. Dasbach, R.P. Insinga, A multi-type HPV transmission model. Bull. Math. Biol. **70**(8), 2126–2176 (2008)
23. D. Okuonghae, A.B. Gumel, M.A. Safi, Dynamics of a two-strain vaccination model for polio. Nonlinear Anal. Real World Appl. **25**, 167–189 (2015)
24. S.M. Garba, M.A. Safi, A.B. Gumel, Cross-immunity induced backward bifurcation for a model of transmission dynamics of two strains of influenza. Nonlinear Anal. Real World Appl. **14**, 1384–1403 (2013)
25. C. Castillo-Chavez, W. Huang, Li, The effects of females' susceptibility on the coexistence of multiple pathogen strains of sexually transmitted diseases. J. Math. Biol. **35**, 503–522 (1997)
26. J. Dushoff, H. Wenzhang, C. Castillo-Chavez, Backward bifurcations and catastrophe in simple models of fatal diseases. J. Math. Biol. **36**, 227–248 (1998)
27. P. Bonanni, S. Boccalini, A. Bechini, Efficacy, duration of immunity and cross protection after HPV vaccination: a review of evidence. Vaccine **27**, A46–A53 (2009)
28. S. Lakshmikantham, S. Leela, A.A. Martynyuk, *Stability Analysis of Nonlinear Systems* (Marcel Dekker Inc., New York, 1989)
29. P. van den Driessche, J. Watmough, Reproduction numbers and sub-threshold endemic equilibria for compartmental models of disease transmission. Math. Biosci. **180**, 29–48 (2002)
30. C. Castillo-Chavez, B. Song, Dynamical models of tuberculosis and their applications. Math. Biosci. Eng. **2**, 361–404 (2004)
31. O. Sharomi, T. Malik, A model to assess the effect of vaccine compliance on Human Papilloma Virus infection and Cervical Cancer. Appl. Math. Model. **47**, 528–550 (2017)
32. A. Omame, R.A. Umana, D. Okuonghae, S.C. Inyama, Mathematical analysis of a two-sex Human Papillomavirus (HPV) model. Int. J. Biomath. **11**, 7 (2018)
33. D. Foreman, C. de Martel, C.J. Lacey, I. Soerjomataram, J. Lortet-Tieulent, L. Bruni, J. Vignat, Ferlay j, Bray F, Plummer M, Franceschi S, Global burden of human pappilomavirus and related diseases. Vaccine **30S**, F12–F23 (2012)
34. Human Papillomavirus and Related Diseases Report, ICO/IARC Information Centre on HPV and Cancer (2017). *www.hpvcentre.net*. Accessed: 21 Aug. 2018
35. J. La Salle, S. Lefschetz, *The Stability of Dynamical Systems* (SIAM, Philadelphia, 1976)
36. S.M. Blower, H. Dowlatabadi, Sensitivity and uncertainty analysis of complex models of disease transmission: an HIV model, as an example. Int. Stat. Rev. **2**, 229–243 (1994)
37. CIA World Factbook, South Africa Demographics Profile (2016). www.indexmundi.com/southafrica/demographics-profile_html. Accessed 24 Dec. 2016
38. Human Papillomavirus, Related Cancers, Fact Sheet, *South Africa summary report* (2016). www.hpvcentre.netAccessed: 26 Dec. 2016
39. Z.Z. Mbulawa, L.F. Johnson, D.J. Marais, I. Gustavsson, J.R. Moodley, D. Coetzee, U. Gyllensten, A.L. Williamson, Increased alpha-9 human papillomavirus species viral load in human immunodeficiency virus positive women. BioMed. Central (BMC) Infect. Dis. **14**(51) (2014)
40. T.B. Olesen, C. Munk, J. Christensen, K.K. Andersen, S.K. Kjaer, Human Papilloma Virus prevalence among men in sub-saharan Africa: a systematic review and meta-analysis. Sex. Transm. Infect. **90**, 455–462 (2014)
41. A.A. Alsaleh, A.B. Gumel, Dynamics of a vaccination model for HPV transmission. J. Biol. Syst. **22**(4), 555–599 (2014)
42. M.T. Malik, J. Reimer, A.B. Gumel, E.H. Elbasha, S.M. Mahmud, The impact of an imperfect vaccine and pap cytology screening on the transmission of Human Papillomavirus and occurrence of associated cervical dysplasia and cancer. Math. Biosci. Eng. **10**(4) (2013)
43. E.H. Elbasha, E.J. Dasbach, R.P. Insinga, Model for assessing Human Papillomavirus vaccination strategies. Emerg. Infect. Dis. **31**(1), 28–41 (2007)

The Impact of Fractional Differentiation in Terms of Fitting for a Prostate Cancer Model Under Intermittent Androgen Suppression Therapy

Ozlem Ozturk Mizrak, Cihan Mizrak, Ardak Kashkynbayev and Yang Kuang

1 Introduction

In the 1930s and 40s, Charles Huggins and his colleagues demonstrated that surgical castration often leads to significant regression of prostate cancer, and in 1966 he was awarded the Nobel Prize in Medicine and Physiology [1]. Today, androgen deprivation therapy (ADT) performs the same goal without surgery; however, the treatment is expensive and has many negative side effects such as sexual dysfunction and dementia [2].

Continuous androgen deprivation (CAD) treatment is a standard treatment method applied after the first radiation therapy that failed for localized advanced prostate cancer patients [2–5]. On the other hand, most patients eventually develop resistance to treatment, and then the disease becomes more aggressive and the prognosis is poor at this stage [6, 7]. Therefore, it is very important to estimate when resistance will occur in a patient, to improve the quality of life and to prevent treatment in

O. O. Mizrak (✉)
Department of Mathematics, Karabuk University, Baliklar Kayasi Mevkii, Demir Celik Kampusu, 78050 Karabuk, Turkey
e-mail: ozlemozturk@karabuk.edu.tr

C. Mizrak
Department of Mechatronics Engineering, Karabuk University, Baliklar Kayasi Mevkii, Demir Celik Kampusu, 78050 Karabuk, Turkey
e-mail: cihanmizrak@karabuk.edu.tr

A. Kashkynbayev
School of Science and Technology, Nazarbayev University, Astana 010000, Republic of Kazakhstan
e-mail: ardak.kashkynbayev@nu.edu.kz

Y. Kuang
School of Mathematical and Statistical Sciences, Arizona State University, Tempe, AZ 85287, USA
e-mail: kuang@asu.edu

H. Dutta (ed.), *Mathematical Modelling in Health, Social and Applied Sciences*, Forum for Interdisciplinary Mathematics, https://doi.org/10.1007/978-981-15-2286-4_5

vain. Intermittent androgen deprivation (IAD) aims to reduce side effects and delay development of resistance; however, the delay in resistance with this treatment is still controversial, and CAD remains the standard treatment method [4].

A solid understanding of the treatment of prostate cancer and the lack of standards trigger the need for mathematical models. Especially in the last 15 years, many mathematical models have been proposed to help explain the functioning dynamics of prostate cancer in the hope of answering the abovementioned questions.

Jackson [8] developed the first prostate cancer model in 2004, based on experimental data, under CAD treatment, which would lead to modeling efforts to be shown later. In 2008, Ideta et al. [9] demonstrated a mathematical model under IAD therapy, including the mutation of androgen-independent (AI) cells from androgen-dependent (AD) cells. Shimada and Aihara [10] investigated the competition between different prostate cell populations. Another approach to competition modeling is based on Ideta's model. [9]. Eikenberry et al. [11] developed Ideta's model to investigate the evolutionary role of androgens on prostate cancer, taking into account intracellular signals. This model was later described by Portz et al. [12] (PKN) to ensure compliance with clinical prostate-specific antigen (PSA) data, and the PKN model was then simplified by Baez and Kuang (BK) [13] to ensure compliance with both PSA and androgen data. As another expansion of the models of Ideta [9] and Eikenberry [11], Jain et al. [14] provided that the model they generate captures the biochemical dynamic of prostate cancer in detail. On the other hand, Hirata et al. [15] developed a fragmented linear model taking into account three populations of cells to ensure compliance with clinical PSA data. Many researchers have studied the parameter estimation [16, 17], optimum change times for IAD and control [16], Hirata et al. [18] and the prediction of progression of resistant prostate cancer [19] using the model of Hirata et al. [15].

Here, we especially focus on the BK model as it is one of the latest versions of PKN model and has good data fitting and forecasting ability. On the other hand, although cell quota phenomenon used in both PKN and BK models is an original approach to reflect the limiting effect of nutrient content in cancer cell populations, the minimum androgen amounts (cell quotas) required for survival of cell populations of castration sensitive (CS) and resistant (CR) are not easily measurable, while serum androgen data are easily available in the clinic. Therefore, this situation poses a problem in moving the model to clinical practice. In addition, in the BK model, the authors made data fitting and prediction under the hypothesis that the amount of androgen in the serum is equal to the amount of androgen in the cancer cells. However, this assumption is contrary to the biological fact that a portion of the serum androgen reaches the cell by diffusion, so it has misleading results, such as at the time of the discontinuation of IAD treatment, the intracellular androgen reaches its maximum level instantly.

At this point, the question is "Can we create a new model by demonstrating the growth of cancerous cells with the classic logistic growth model instead of the cell quota model?". The model and model dynamics created in response to this question are discussed in the following section.

2 Basic Logistic Growth Versus Cell Quota Model

Let us first recall the Model 1 (Single population model) and Model 2 (Two population model) of Baez and Kuang (BK):

2.1 Model 1: One Population Model

$$\frac{\mathrm{d}x}{\mathrm{d}t} = \mu\left(1 - \frac{q}{Q}\right)x - \left(\left(v\frac{R}{Q+R}\right) + \delta x\right)x,$$

$$\frac{\mathrm{d}v}{\mathrm{d}t} = -\mathrm{d}v,$$

$$\frac{\mathrm{d}Q}{\mathrm{d}t} = \gamma(Q_m - Q) - \mu(Q - q),$$

$$\frac{\mathrm{d}P}{\mathrm{d}t} = bQ + \sigma Qx - \varepsilon P$$

where

$$\gamma = \gamma_1 u(t) + \gamma_2, \quad u(t) = \begin{cases} 1, \text{ on treatment} \\ 0, \text{ off treatment} \end{cases}.$$

2.2 Model 2: Two Population Model

$$Dx_1 = \mu\left(1 - \frac{q_1}{Q}\right)x_1 - \left(D_1(Q) + \delta_{1X_1}\right)x_1 - \lambda(Q)x_1$$

$$Dx_2 = \mu\left(1 - \frac{q_2}{Q}\right)x_2 - \left(D_2(Q) + \delta_{2X_2}\right)x_2 - \lambda(Q)x_2$$

$$DQ = \gamma(Q_m - Q) - \frac{\mu(Q - q_1)x_1 + \mu(Q - q_2)x_2}{x_1 + x_2}$$

$$DP = bQ + \sigma(Qx_1 + Qx_2) - \varepsilon P$$

where

$$D_i(Q) = d_i \frac{R_i}{Q + R_i}, \quad i = 1, 2,$$

$$\lambda(Q) = c \frac{K}{Q + K}$$

In both of the BK models, the cell growth rate is determined by the androgen cell quota. Specifically, as in the PKN model [20], they model the growth rate by a two parameter function of androgen cell quota

$$G(Q) = \mu\left(1 - \frac{1}{Q}\right),$$

where Q is the androgen cell quota. Above equation is known as the Droop equation or a Droop growth rate model [21]. It assumes that Q is the concentration of the most limiting resource or nutrient, and q is the minimum level of Q required to prevent cell death [22]. BK models also assume androgen-dependent death rates for cancer cells (d_1, d_2). Besides this, for Model 1, they assume a time-dependent maximum baseline death rate v, which decreases exponentially at rate d to reflect the cell castration-resistance development due to the decreasing death rate and also include a density-independent death rate δ that constrains the total volume of cancer cells to be within realistic ranges. For a more detailed explanation of these models, the reader is referred to [19].

As stated before, our main problem is on investigating the androgen relevance of the CR cell proliferation. Even if CR cell proliferation has already been accepted to be effected positively with androgen concentration in the above cell quota models, we prefer to use logistic growth terms rather than cell quota to provide saturation effect of the population to be able to rebuild the BK models:

2.3 *Model 1*: One Population Logistic Model*

$$Dx(t) = r(A, x)x \tag{1}$$

$$Dv(t) = -\mathrm{d}v \tag{2}$$

$$\frac{\mathrm{d}A}{\mathrm{d}t} = \gamma(a_0 - A) - \mu \frac{A^\omega}{A^\omega + \rho^\omega} x, \tag{3}$$

$$\frac{\mathrm{d}P}{\mathrm{d}t} = bA + \sigma Ax - \varepsilon P \tag{4}$$

where

$$r(A,x) = \mu \frac{A^s}{A^s + k^s}\left(1 - \frac{x}{\theta}\right) - \left(v\frac{R}{A+R}\right) + \delta x), \tag{5}$$

$$\gamma = \gamma_1 u(t) + \gamma_2, \quad u(t) = \begin{cases} 1, \text{ on treatment} \\ 0, \text{ off treatment} \end{cases}. \tag{6}$$

2.4 Model 2*: Two Population Logistic Model

$$Dx_1(t) = r_1(A, x_1, x_2)x_1 - m(A)x_1 \tag{7}$$

$$Dx_2(t) = r_2(A, x_1, x_2)x_2 + m(A)x_1 \tag{8}$$

$$\frac{\mathrm{d}A}{\mathrm{d}t} = \gamma(a_0 - A) - \mu\frac{A^\omega}{A^\omega + \rho^\omega}(x_1 + x_2), \tag{9}$$

$$\frac{\mathrm{d}P}{\mathrm{d}t} = bA + \sigma A(x_1 + x_2) - \varepsilon P \tag{10}$$

where

$$r_1(A, x_1, x_2) = \mu\frac{A^m}{A^m + k^m}\left(1 - \frac{x_1 + x_2}{\theta}\right) - \left(d_1\frac{R_1}{A + R_1} + \delta_{_1X_1}\right)x_1, \tag{11}$$

$$r_2(A, x_1, x_2) = \mu\frac{A^n}{A^n + k^n}\left(1 - \frac{x_1 + x_2}{\theta}\right) - \left(d_2\frac{R_2}{A + R_2} + \delta_{_2X_2}\right)x_2 \tag{12}$$

$$m(A) = c\frac{K}{A + K}. \tag{13}$$

Since the terms other than growth and uptake are similar to those in the BK models, we avoid explaining them repeatedly. Here, we hypothesize that proliferative advantage of cells over each other changes as to androgen levels that are represented by A in the model formulizations. In other words, while below a threshold level of androgen, CR cells have greater capacity for proliferation compared to CS cells, above this threshold value CS cells gain a proliferative advantage over CR reversely. To be able to capture this assumption, we prefer to use Hill functions with constraint $n < m$. Thus, while we vary n between 0.01 and 2.99, m is assumed as $\|n\| + 1$. Due to the fact that we desire to have no significant change in Hill functions for androgen-rich environments, we vary k between 0.1 and 1. We also avoid to choose far less quantities for lower bounds of n and k not to encounter with any mathematical uncertainty in case of low androgen levels approaching zero. Likewise, as androgen within the cells is used for growth, we formulate the uptake term using

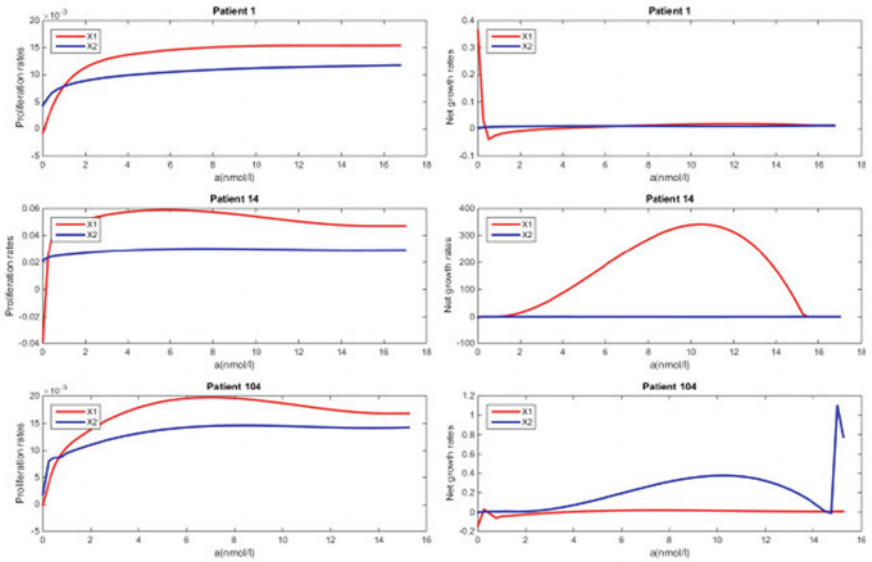

Fig. 1 Proliferation (left column) and net growth (right column) rates of CS and CR cells with respect to androgen for patients 1, 14, and 104, respectively, for 1.5 cycles of treatment

a Hill function that allows the uptake rate which approaches its maximum, μ, when the serum androgen concentration increases. In this term, we expect $\omega \in [1, 3]$ and $\rho \in [(a/2) - 2, (a/2)]$ where a is the maximum androgen level in the patient's serum. Other parameter values are nearly same as parameter values in BK models. Differently, the carrying capacity of cancer cells is taken as estimated by Rutter and Kuang [23] (Fig. 1).

2.5 Model Dynamics

2.5.1 Analysis of the Asymptotic Behavior of Model 1*

Let us rewrite Model 1^* in an explicit form:

$$\frac{\mathrm{d}x}{\mathrm{d}t} = \mu \frac{A^s}{A^s + k^s}\left(1 - \frac{x}{\theta}\right)x - \left(v\frac{R}{A+R} + \delta x\right)x, \tag{14}$$

$$\frac{\mathrm{d}v}{\mathrm{d}t} = -\mathrm{d}v, \tag{15}$$

$$\frac{\mathrm{d}A}{\mathrm{d}t} = \gamma(a_0 - A) - \mu\frac{A^\omega}{A^\omega + \rho^\omega}x, \tag{16}$$

$$\frac{\mathrm{d}P}{\mathrm{d}t} = bA + \sigma Ax - \varepsilon P. \tag{17}$$

Observe from the last equation that P is decoupled from the system. Therefore, we will restrict our attention only to the dynamics of Eqs. (14)–(17). For the convenience of the reader, let us introduce the function $q_i(A) = \mu \frac{A^i}{A^i + k^i}$. One can easily show that q_i is an increasing function for $A \geq 0$ and $i > 0$.

Proposition 1 The region $\left\{(x, v, A) : 0 \leq x \leq \frac{q_s(a_0)}{\delta}, v \geq 0, 0 \leq A \leq a_0\right\}$ is positive invariant.

Proof We want to prove that solutions of the system (14)–(17) which start positive remain positive. Since Eq. (15) is explicatively solvable, we obtain $v(t) = v_0 \mathrm{e}^{-\mathrm{d}t}$ which ensures its positivity for $v(0) \geq 0$ and boundedness for $t \geq 0$. The positivity of x easily follows since x appears in every term of Eq. (14). Further, note that from (16) we have $A'(0)$ and $A'(a_0) < 0$. *Thus, it easily follows that* $0 \leq A(t) \leq a_0$ for $t \geq 0$. It remains to show that x is bounded. From Eq. (14), we see that

$$\frac{\mathrm{d}x}{\mathrm{d}t} \leq q_s(a_0)x - \delta x^2,$$

which in tern implies that $\lim_{t\to\infty} \sup(x(t)) \leq \frac{q_s(a_0)}{\delta}$.

Proposition 2 The system of Eqs. (14)–(17) has an unstable cancer-free (disease-free) equilibrium $E_0 = (0, 0, a_0)$ and a locally asymptotically stable endemic equilibrium $E_1 = \frac{\theta q_s(\overline{A})}{\theta\delta + q_s(\overline{A})}, 0, \overline{A}, 0 < \overline{A} < a_0$.

Proof From Eq. (14), we see that there are two cases for the steady states: $x = 0$ or $x = \bar{x} > 0$. The case $x = 0$ gives us the cancer-free equilibrium E_0 which generates the following Jacobian matrix.

$$J(E_0) = \begin{bmatrix} q_s(a_0) & 0 & 0 \\ 0 & -d & 0 \\ q_\omega(a_0) & 0 & -\gamma \end{bmatrix}.$$

The set of eigenvalues are given by the diagonal elements: $\{q_s(a_0), -d, -\gamma\}$. Since $q_s(a_0) > 0$, we conclude that the cancer-free equilibrium is unstable.

Let us define a function $h(A) = \frac{q_s(A)}{\delta + \frac{q_s(A)}{\theta}} - \frac{\gamma(a_0 - A)}{q_\omega(A)}$. One can check that $\lim_{A\to 0^-} h(A) = -\infty$ and $h(a_0) > 0$. Thus, by the Intermediate Value Theorem (IVT) there exists $\overline{A} \in (0, a_0)$ such that $h(\overline{A}) = 0$. From Eqs. (14) and (16), we can find E_1 which satisfies the following equations $\bar{x} = \frac{q_s(\overline{A})}{\delta + \frac{q_s(\overline{A})}{\theta}} = \frac{\gamma(a_0 - \overline{A})}{q_\omega(\overline{A})}$. The Jacobian matrix evaluated at E_1 gives us the following matrix.

$$J(E_1) = \begin{bmatrix} -q_{s_0}(\overline{A}) & -\frac{R}{R+A}\bar{x} & q_s'(\overline{A})\left(1-\frac{\bar{x}}{\theta}\right)\bar{x} \\ 0 & -d & 0 \\ -q_\omega(\overline{A}) & 0 & -\gamma - q_\omega'(\overline{A})\bar{x} \end{bmatrix}.$$

Observe that $\lambda_2 = -d < 0$. The remaining two eigenvalues can be evaluated as

$$\lambda_{1,3} = \frac{\operatorname{Tr} J^1 \pm \sqrt{\left(\operatorname{Tr} J^1\right)^2 - 4 \det J^1}}{2},$$

where

$$J^1 = \begin{bmatrix} -q_{s_0}(\overline{A}) & q_s'(\overline{A})\left(1-\frac{\bar{x}}{\theta}\right)\bar{x} \\ -q_\omega(\overline{A}) & -\gamma - q_\omega'(\overline{A})\bar{x} \end{bmatrix}.$$

One can show that $\operatorname{Re}(\lambda_{1,3}) < 0$ since $TrJ^1 < 0$ and $\det J^1 > 0$. Thus, the endemic equilibrium E_1 is locally asymptotically stable. This completes the proof. □

In Proposition 1, for E_0 point, $v = 0$, $A = a_0$ is a sign that cancerous cells can be completely destroyed with androgen in abundance at a time when resistance to cancer in therapy has developed. However, the fact that this point is not stable means that cancer cells alone cannot be completely eliminated by IAD therapy. Since ADT is non-curative, this property is biologically reasonable. On the other hand, in the same proposition, for locally stable E_1 point, $v = 0$ indicates that at the time of the castration resistance, we can hold the tumor volume at a locally stable level for a certain amount of androgen levels.

2.5.2 Analysis of the Asymptotic Behavior of Model 2*

Let us rewrite Model 2* in an explicit form:

$$\frac{\mathrm{d}x_1}{\mathrm{d}t} = q_m(A)\left(1 - \frac{x_1 + x_2}{\theta}\right)x_1 - (D_1(A) + \delta_1 x_1)x_1 - m(A)x_1, \tag{18}$$

$$\frac{\mathrm{d}x_2}{\mathrm{d}t} = q_n(A)\left(1 - \frac{x_1 + x_2}{\theta}\right)x_2 - (D_2(A) + \delta_2 x_2)x_2 + m(A)x_1, \tag{19}$$

$$\frac{\mathrm{d}A}{\mathrm{d}t} = \gamma(a_0 - A) - \mu\frac{A^\omega}{A^\omega + \rho^\omega}(x_1 + x_2) \tag{20}$$

$$\frac{\mathrm{d}P}{\mathrm{d}t} = bA + \sigma A(x_1 + x_2) - \varepsilon P, \tag{21}$$

where $D_i(A) = d_i\frac{R_i}{A+R_i}$ and $m(A) = c\frac{K}{A+K}$.

As it was in Model 1*, we do not analyze Eq. (21) since P is decoupled from Eqs. (18)–(20).

Proposition 3 If $n < m$ and $\delta_2 \leq \delta_1$, then the region $\{(x_1, x_2, A) : x_1 \geq 0, x_2 \geq 0, x_1 + x_2 \leq \frac{q_m(a_0) - D_m}{\delta_2}, 0 \leq A \leq a_0\}$ is positive invariant, where $D_m = \min\{D_1(a_0), D_2(a_0)\}$.

Proof From Proposition 1, we know $0 \leq A(t) \leq a_0$ if $0 \leq A(O) \leq a_0$. Now assume on the contrary that the solutions $x(t)$ and x_2 do not remain positive. Then, there is $t_1 > 0$ *such that* $x_1(t_1) = 0$ or $x_2(t_1) = 0$. *Let us consider* $x_1(t_1) = 0$ *Then,* $x_1'(t) \geq -m(A)x_1$ for $t \in (0, t_1)$ which implies that $x_1(t_1) \geq x_1(0)\mathrm{e}^{-m(A)t_1} > 0$. *Contradiction*: *The latter case can be handled similarly since* x_2 appears in the first two terms and x_1 also appears in two terms. Set $X = x_1 + x_2$. Then, we have

$$\begin{aligned}\frac{\mathrm{d}X}{\mathrm{d}t} &\leq (q_m(A) - D_m)X - \delta_2 X^2 \\ &\leq (q_m(a_0) - D_m)X - \delta_2 X^2,\end{aligned}$$

which implies that $\lim_{t\to\infty} \sup X(t) \leq \frac{q_m(a_0) - D_m}{\delta_2}$.

Now, we study the steady states of Model 2*. We seek to understand the conditions under which one population will overtake the other, and the circumstances under which they may coexist.

Proposition 4 The system of Eqs. (18)–(20) has a cancer-free (disease-free) equilibrium $E_0 = (0, 0, a_0)$, a CR cell only equilibrium $E_2 = \left(0, \theta\frac{q_n(A_1) - D_2(A_1)}{q_n(A_1) + \theta\delta_2}, A_1\right)$, and a coexistence equilibrium $E_3 = \left(x_1^*, x_2^*, A^*\right)$, where $x_1^* > 0$, $x_2^* > 0$, $0 < A_1 < a_0$, and $0 < A^* < a_0$.

Proof From Eq. (18), we see that either $x_1 = 0$ or $x_1 > 0$.

If $x_1 = 0$, then there are two mutually exclusive cases: $x_2 = 0$ and $x_2 \neq 0$. In the first case, the steady state is $E_0 = (0, 0, a_0)$. In the latter case, the steady state is $E_2 = (0, \bar{x}, A_1)$, where $A_1 \in (0, a_0)$ and $\bar{x} = \theta\frac{q_n(A_1) - D_2(A_1)}{q_n(A_1) + \theta\delta_2} = \frac{\gamma(a_0 - A_1)}{\mu\frac{A^\omega}{A^\omega + \rho^\omega}} > 0$.

If $x_1 > 0$, it follows from Eq. (19) that $x_2 > 0$. Thus, there emerges the coexistence equilibrium $E_3 = \left(x_1^*, x_2^*, A^*\right)$.

Denote the functions $f(A) = q_m(A) - D_1(A) - m(A)$ and $g(A) = q_n(A) - D_2(A)$.

Proposition 4 demonstrates that if the CS cell population survives, then the CR must also survive. Biologically, this makes sense, as the CR will always receive new mutated CR cells as IAD continues.

Next, we study the extinction of cancer cell populations and stability conditions for each of these steady states when feasible.

Proposition 5 The cancer-free equilibrium $E_0 = (0, 0, a_0)$ is locally asymptotically stable if $f(a_0) < 0$ and $g(a_0) < 0$ and unstable if $f(a_0) > 0$ or $g(a_0) > 0$.

Proof Let us compute the Jacobian matrix at E_0.

$$J(E_0) = \begin{bmatrix} f(a_0) & 0 & 0 \\ m(a_0) & g(a_0) & 0 \\ -\mu \frac{(a_0^\omega)}{a_0^\omega + \rho^\omega} & a_0^\omega & -\gamma \end{bmatrix}$$

Since $J(E)$ is a lower triangular matrix, the set eigenvalues of $J(E)$ are given by the diagonal entries. Thus, the stability of E_0 is completely determined by the sign of $f(a)$ and $g(a_0)$. This finalizes the proof. □

Proposition 6 If $f(a_0) < 0$, then the CS population will die out. If, further, $g(a_0) < 0$, then both cancer populations will die out.

Proof One can easily check that f and g are increasing functions for $A > 0$. From Eq. (18), we have

$$\begin{aligned} \frac{x_1'}{x_1} &= q_m(A)\left(1 - \frac{x_1 + x_2}{\theta}\right) - D_1(A) - \delta_1 x_1 - m(A) \\ &\leq f(A) - \delta_1 x_1 \\ &\leq f(a_0). \end{aligned}$$

Thus, $x_1(t) \leq c_1 e^{f(a_0)t}$ which implies that $\lim_{t\to\infty} x_1(t) = 0$. Applying a similar argument to Eq. (19) along with $\lim_{t\to\infty} x_1(t) = 0$ and $g(a_0) < 0$ yields $\lim_{t\to\infty} x_2(t) = 0$.

Both for Propositions 5 and 6, $f(a_0) < 0$ and $g(a_0) < 0$, which means that CS and CR cells have too low growth rates, and if this condition is provided then both cancer cells will be eliminated producing a locally asymptotically stable E_0 point.

The following proposition provides a simple set of conditions that yields the biologically realistic final outcome when sensitive cells are overtaken by resistant cells.

Proposition 7 The CR only equilibrium E_2 is locally asymptotically stable if $f(A_1) < \frac{2q_m(A_1)g(A_1)}{q_n(A_1)+\theta\delta_2}$ and $g(A_1)(q_n(A_1) - \theta\delta_2 - 2) < 0$.

Proof The Jacobian matrix evaluated at E_2 is given by

$$J(E_2) = \begin{bmatrix} f(A_1) - \frac{2q_m(A_1)g(A_1)}{q_n(A_1)+\theta\delta_2} & 0 & 0 \\ m(A_1) - \frac{q_n(A_1)}{\theta}\overline{x_2} & \frac{g(A_1)(q_n(A_1)-\theta\delta_2-2)}{q_n(A_1)+\theta\delta_2} & q_n'(A_1)\left(1 - \frac{\overline{x_2}}{\theta}\right)\overline{x_2} - D_2'(A)\overline{x_2} \\ -\mu \frac{(A_1^\omega)}{A_1^\omega + \rho^\omega} & 0 & -\gamma - \mu \frac{\omega\rho^\omega A_1^{\omega-1}}{(A_1^\omega + \rho^\omega)}\overline{x_2} \end{bmatrix}.$$

It is seen that the set of eigenvalues are given by the diagonal entries of $J(E_2)$. If $f(A_1) < \frac{2q_m(A_1)g(A_1)}{q_n(A_1)+\theta\delta_2}$ and $g(A_1)(q_n(A_1) - \theta\delta_2 - 2) < 0$, then all diagonal entries are negative which yields the CR only equilibrium E_2 is locally asymptotically stable. This finalizes the proof. □

2.6 Clinical Trial Data

During the chapter, data from Bruchovsky et al. [24] are used for our analysis and model calibration. This clinical trial admitted patients who demonstrated a rising serum PSA level after they received radiotherapy and had no evidence of metastasis [24]. The treatment in each cycle consisted of administering cyproterone acetate for four weeks, followed by a combination of leuprolide acetate and cyproterone acetate, for an average of 36 weeks. If serum PSA is less than 4 μg/L by the end of this period, the androgen suppression therapy is stopped. If a patient's serum PSA stays above the threshold, the patient will be taken off of the study. After the treatment is interrupted, PSA and androgen are monitored every four weeks. The therapy is restarted when the patient's serum PSA increases to $\geq$10 μg/L [24]. The data set is available at [25].

2.7 Comparison of Models

In this section, we compare our logistic models with BK models giving an error table for 1.5 cycles data fitting. Unlike the BK model, we classify patients' cases as without relapse, with metastasis (without relapse) and with relapse to be able to conduct more detailed research.

To compare models, we conduct simulations with MATLAB's (MATLAB 9.4, R2018a) built-in function fmincon, which uses the Interior Point Algorithm, to find the optimum parameters for each patient. The algorithm searches for a minimum value in a range of pre-specified parameter ranges, which were estimated from various literature sources. We use this algorithm to minimize the MSE for PSA and androgen data. The MSE is calculated with the following equations:

$$P_{\text{error}} = \frac{\sum_{i=1}^{N}\left(P_i - \widehat{P_i}\right)^2}{N}$$

$$A_{\text{error}} = \frac{\sum_{i=1}^{N}\left(A_i - \widehat{A_i}\right)^2}{N}$$

where N represents the total number of data points, P_i represents the PSA data value, and $\hat{P}_i$ the value from the model. Likewise, A_i represents the androgen data value and $\hat{A}_i$ the value from the model. We then use an equally weighted combination of both errors

$$\text{error} = P_{\text{error}} + A_{\text{error}}$$

as our objective function, which is then minimized with fmincon.

Table 1 Comparison of mean squared error (MSE) for androgen and prostate-specific antigen (PSA) for the first 1.5 cycles

Model	PSA			Androgen		
	Min	Mean	Max	Min	Mean	Max
One pop logistic	0,173931	2,445644	36,51354	0,968212	10,34476	49,41232
One pop BK	0,058844	2,46837	25,04435	0,773269	8,656484	51,09163
Two pop logistic	0,088222	2,438892	44,1696	0,801594	10,16664	45,70097
Two pop BK	0,353765	3,766446	69,38941	0,998116	12,53949	55,10578

Table 2 Comparison of mean squared error (MSE) for androgen and prostate-specific antigen (PSA) for the first 1.5 cycles for one population BK (OPBK) and logistic (OPL) models with respect to fractional counterparts (OPFBK) and (OPFL)

Model	PSA			Androgen		
	Min	Mean	Max	Min	Mean	Max
OPL	0,173931	2,445644	36,51354	0,968212	10,34476	49,41232
OPFL	0,091858	2,164708	35,277998	0,864893	9,633965	42,721133
OPBK	0,058844	2,46837	25,04435	0,773269	8,656484	51,09163
OPFBK	0,057346	1,667311	25,201899	0,470016	8,138561	49,036617

OPL one population logistic, *OPBK* one population BK, *OPFL* one population fractional logistic, *OPFBK* one population fractional BK

Table 1 and simulations below show that one pop and two pop logistic and BK models fit data about the same accuracy. However, logistic models reduce the fitting error for PSA while one pop BK model serves better data fitting for androgen with respect to one pop logistic. Two pop logistic model again performs better data fitting for androgen when compared to two pop BK (Table 2).

2.7.1 Case 1: Without Relapse (Patients 1, 15, 17, 63)

See Figs. 2, 3, 4, and 5.

2.7.2 Case 2: With Metastasis (Without Relapse) (Patients 32, 64, 83)

See Figs. 6, 7, 8, and 9.

2.7.3 Case 3: With Relapse (Patients 12, 19, 36, 101)

See Figs. 10, 11, 12, and 13.

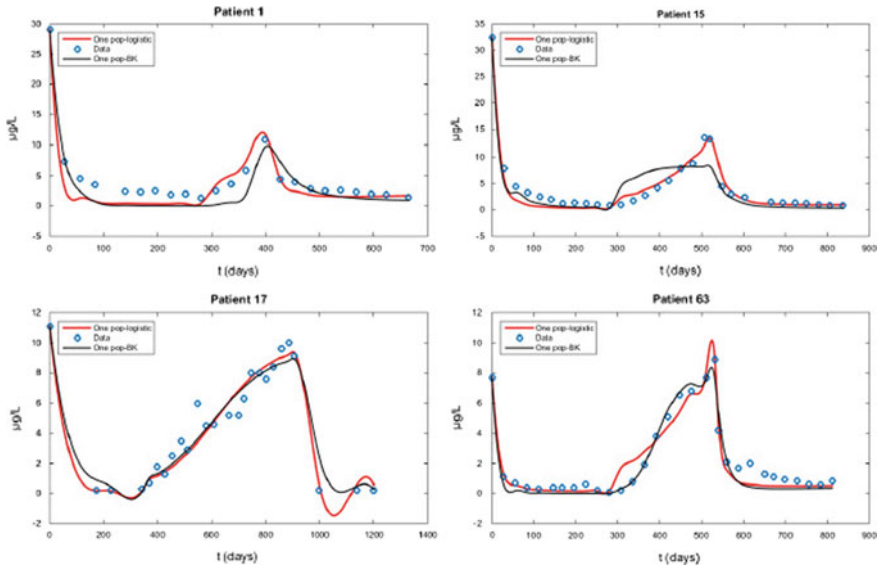

Fig. 2 Simulations of PSA fittings for every one population model for 1.5 cycles of treatment

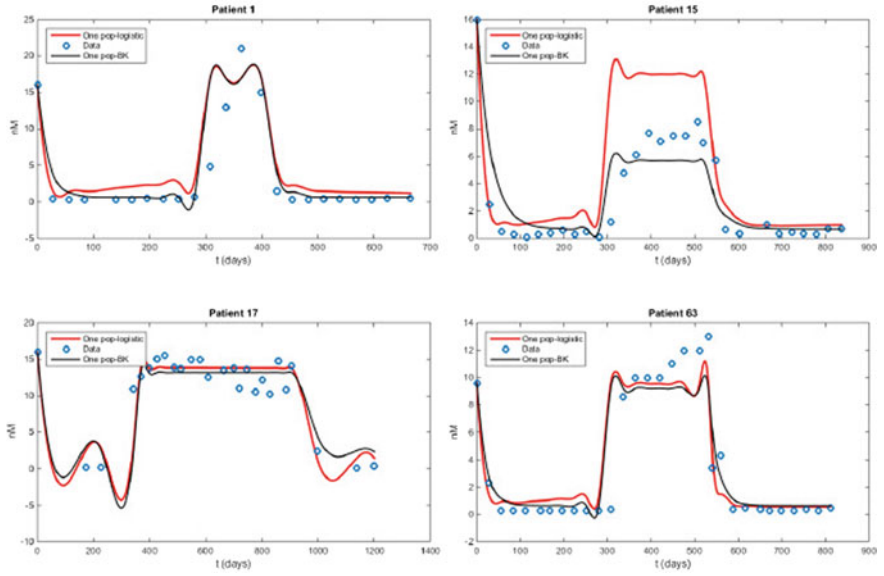

Fig. 3 Simulations of androgen fittings for every one population model for 1.5 cycles of treatment

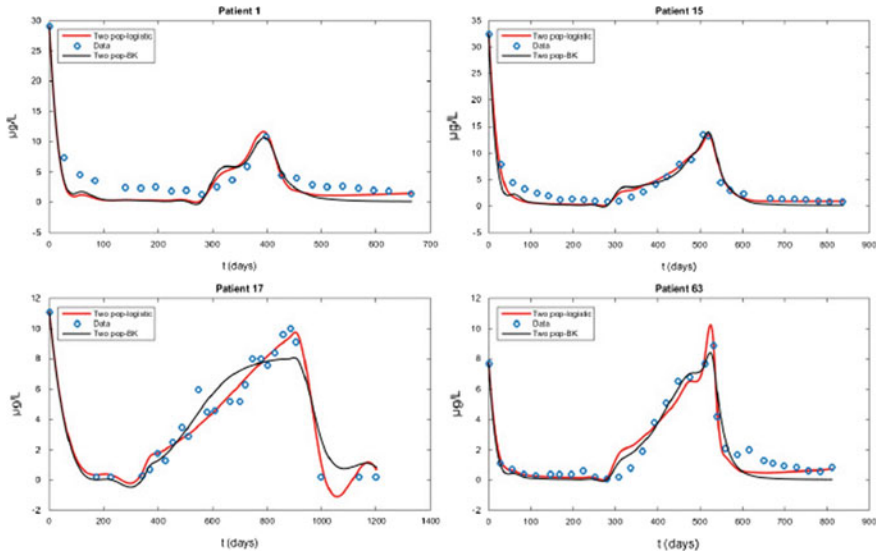

Fig. 4 Simulations of PSA fittings for every two population model for 1.5 cycles of treatment

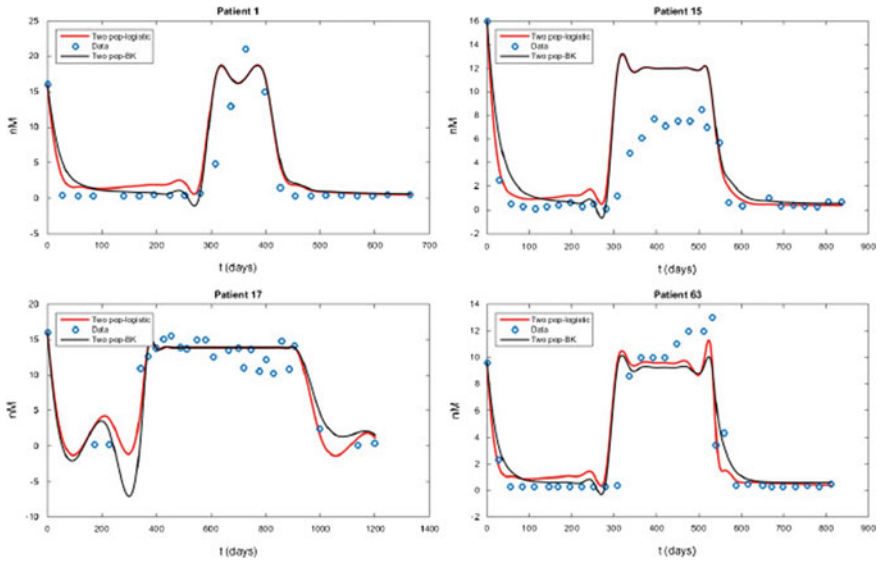

Fig. 5 Simulations of androgen fittings for every two population model for 1.5 cycles of treatment

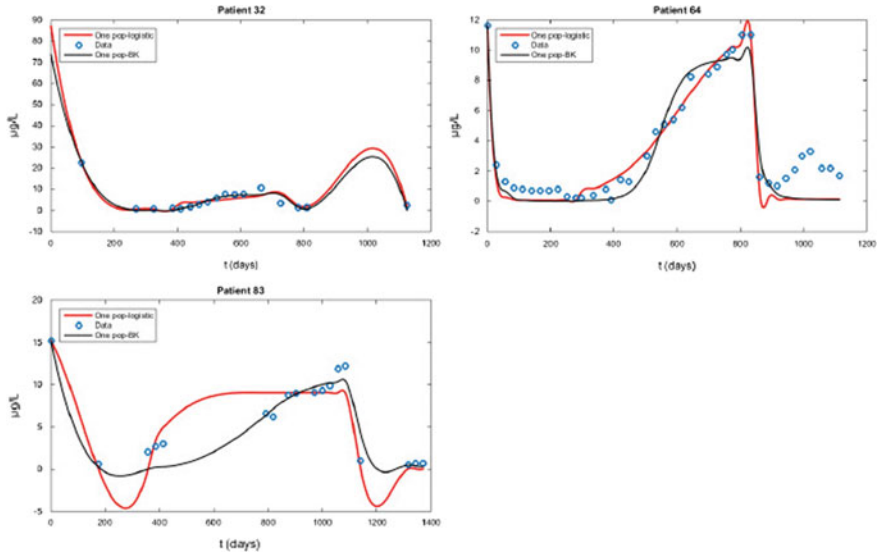

Fig. 6 Simulations of PSA fittings for every one population model for 1.5 cycles of treatment

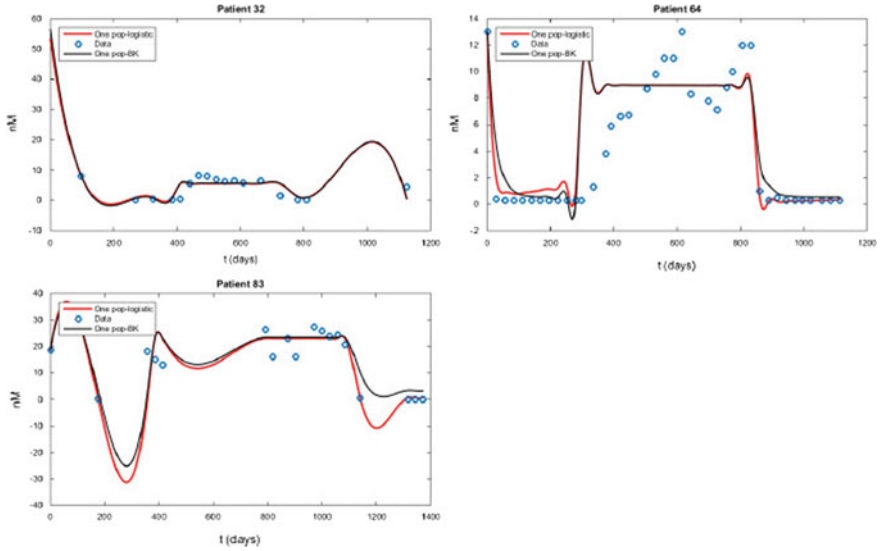

Fig. 7 Simulations of androgen fittings for every one population model for 1.5 cycles of treatment

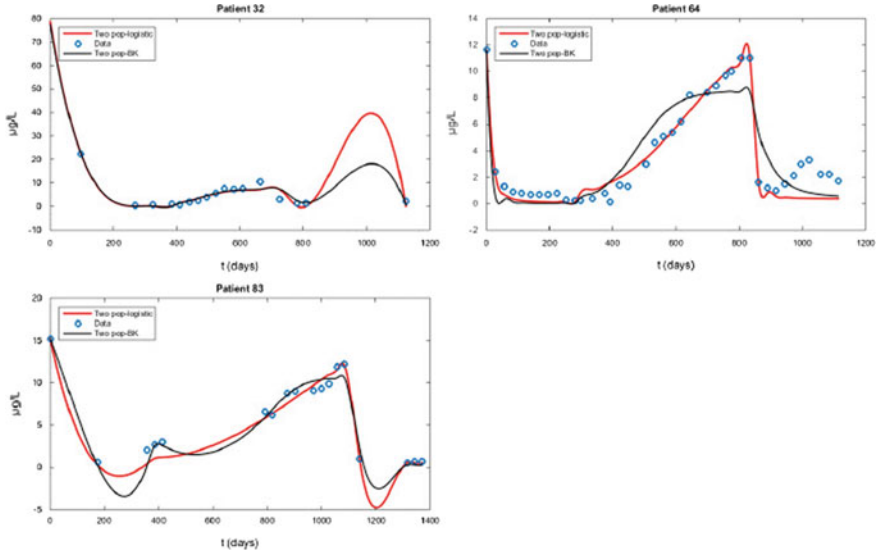

Fig. 8 Simulations of PSA fittings for every two population model for 1.5 cycles of treatment

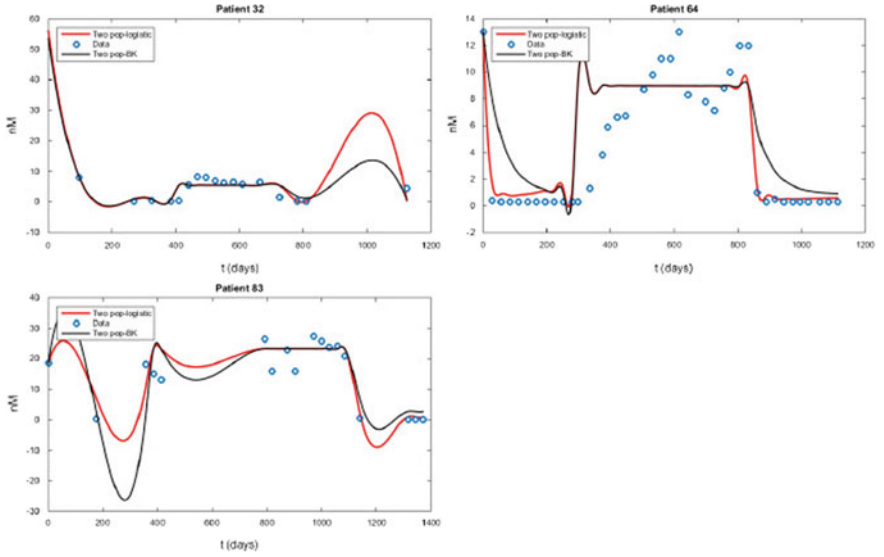

Fig. 9 Simulations of androgen fittings for every two population model for 1.5 cycles of treatment

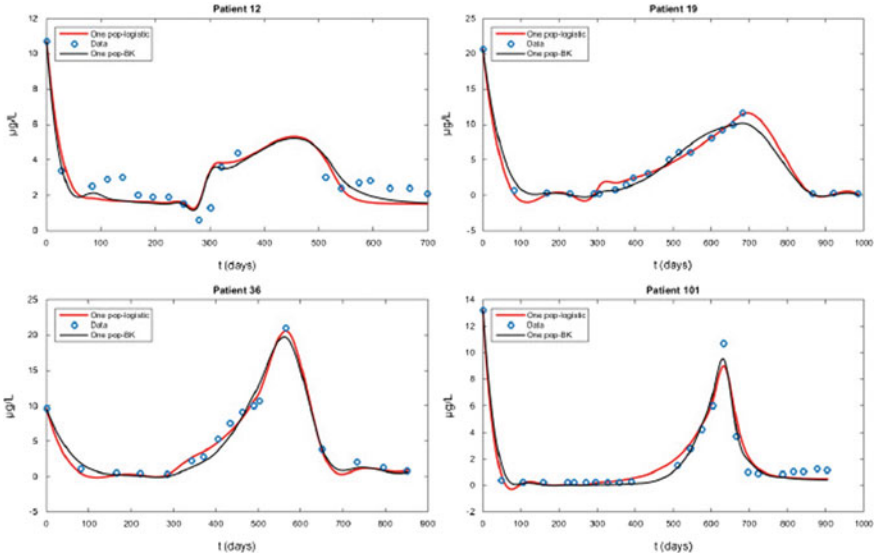

Fig. 10 Simulations of PSA fittings for every one population model for 1.5 cycles of treatment

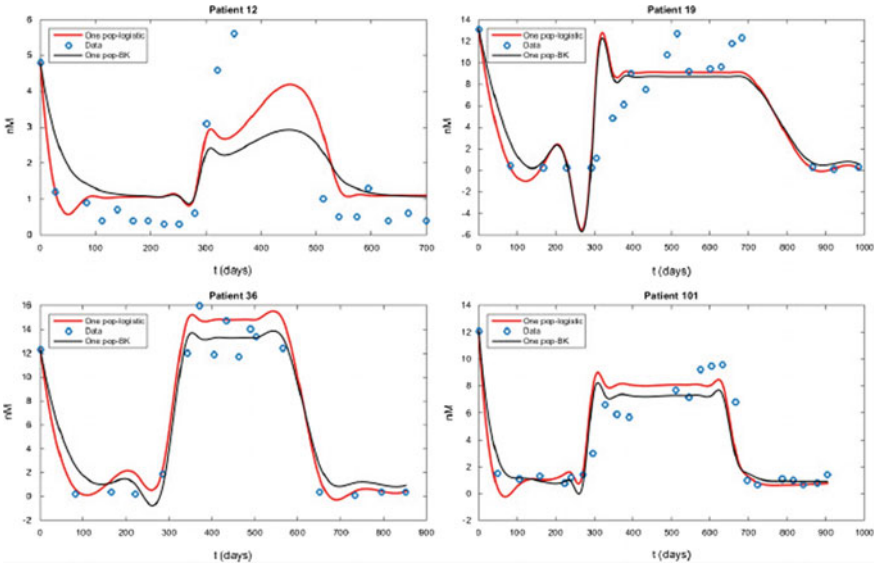

Fig. 11 Simulations of androgen fittings for every one population model for 1.5 cycles of treatment

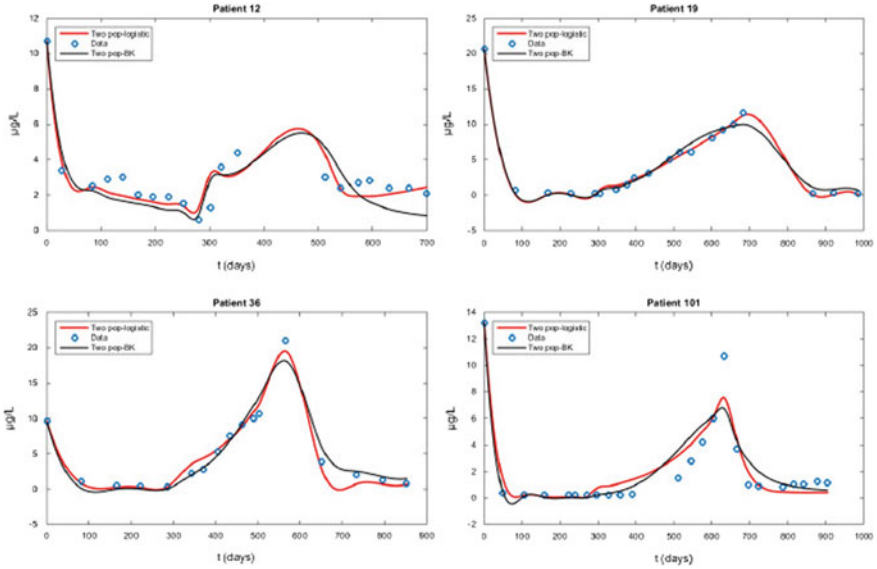

Fig. 12 Simulations of PSA fittings for every two population model for 1.5 cycles of treatment

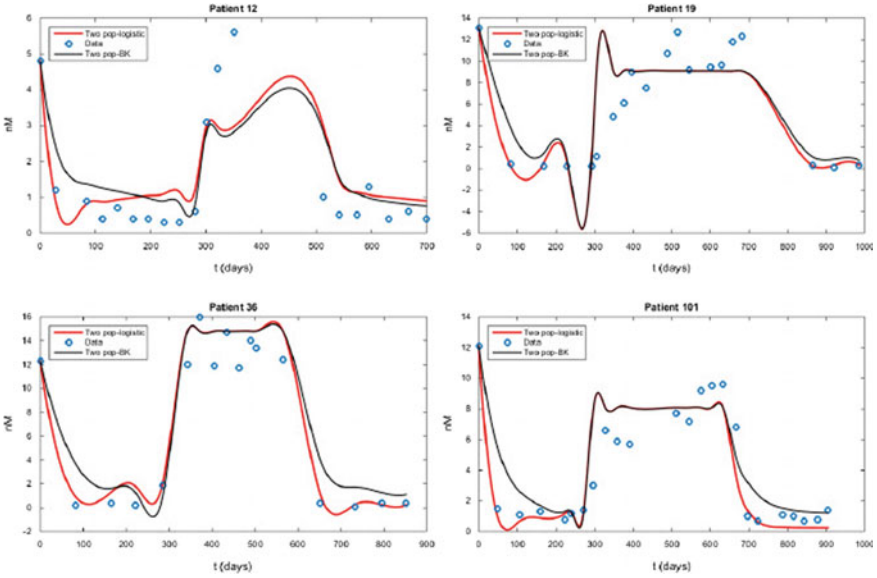

Fig. 13 Simulations of androgen fittings for every one population model for 1.5 cycles of treatment

2.8 Conclusion

With this chapter, we generate new models based on logistic growth terms alternatively to cell quota models. These models succeed to emphasize the role of androgens on the development of CR cells with accurate data fittings. Of course, simulations can be conducted for larger time intervals and also forecasting abilities of these proposed models should be investigated separately. What is more, all simulations in are for patients who do not encounter any relapse during the clinical trial. Forecasting situations should be investigated for other patients in Case 2 and Case 3 to monitor differences like the existence of any relapse.

3 Does Fractional Differentiation Provide Better Data Fitting for Clinical Data-Based Prostate Cancer Models Under Androgen Suppression Therapy?

In this section, we introduce the fractional versions of one and two population BK and logistic models shown in Sect. 2. Then, the stability analysis of them is examined, and outcomes are discussed with numerical simulations.

3.1 Fractional Model 1: One Population Fractional BK Model

$$\frac{\mathrm{d}^{\alpha_1} x}{\mathrm{d}t^{\alpha_1}} = \mu\left(1 - \frac{q}{Q}\right)x - \left(v\frac{R}{Q+R} + \delta x\right)x, \tag{22}$$

$$\frac{\mathrm{d}^{\alpha_2} v}{\mathrm{d}t^{\alpha_2}} = -\mathrm{d}v, \tag{23}$$

$$\frac{\mathrm{d}^{\alpha_3} Q}{\mathrm{d}t^{\alpha_3}} = \gamma(Q_m - Q) - \mu(Q - q), \tag{24}$$

$$\frac{\mathrm{d}^{\alpha_4} P}{\mathrm{d}t^{\alpha_4}} = bQ + \sigma Qx - \varepsilon P \tag{25}$$

where $\alpha_i \in (0, 1]$ for $i = 1, 2, 3, 4$ and represents Caputo-type fractional order and

$$\gamma = \gamma_1 u(t) + \gamma_2, u(t) = \begin{cases} 1; \text{ on treatment,} \\ 0, \text{ off treatment.} \end{cases} \tag{26}$$

3.2 Fractional Model 1*: One Population Fractional Logistic Model 1

$$\frac{\mathrm{d}^{\beta_1} x}{\mathrm{d}t^{\beta_1}} = \mu \frac{A^s}{A^s + k^s}\left(1 - \frac{x}{\theta}\right)x - \left(v\frac{R}{A+R} + \delta x\right)x, \tag{27}$$

$$\frac{\mathrm{d}^{\beta_2} v}{\mathrm{d}t^{\beta_2}} = -\mathrm{d}v, \tag{28}$$

$$\frac{\mathrm{d}^{\beta_3} A}{\mathrm{d}t^{\beta_3}} = \gamma(a_0 - A) - \mu \frac{A^\omega}{A^\omega + \rho^\omega}x, \tag{29}$$

$$\frac{\mathrm{d}^{\beta_4} P}{\mathrm{d}t^{\beta_4}} = bA + \sigma A(x_1 + x_2) - \varepsilon P \tag{30}$$

where $\beta_i \in (0, 1]$ for $i = 1, 2, 3, 4$ and represents Caputo-type fractional order.

3.3 Model Dynamics of One Population Fractional BK and Logistic Models

3.3.1 Stability Analysis of Fractional Model 1

Observe from the last equation that P is decoupled from the system. Therefore, we will restrict our attention only to the dynamics of Eqs. (22)–(24). The next auxiliary Lemma will be useful. We omit the proof because it easily follows from the Generalized Mean Value Theorem for fractional differential equations [4].

Lemma 1 [2] Assume that $F(t)$ and $\frac{\mathrm{d}^\alpha F(t)}{\mathrm{d}t^\alpha}$ are continuous in $[a, b]$ for $\alpha \in (0, 1]$. If $\frac{\mathrm{d}^\alpha F(t)}{\mathrm{d}t^\alpha} \geq 0$ for all $t \in (a, b)$, then $F(t)$ is non-decreasing in the interval $[a, b]$, and if $\frac{\mathrm{d}^\alpha F(t)}{\mathrm{d}t^\alpha} \leq 0$ for all $t \in (a, b)$, then $F(t)$ is non-increasing in the interval $[a, b]$.

Proposition 2 The region $\{(x, v, Q) : 0 \leq x \leq \frac{\mu}{\delta}\left(1 - \frac{q}{Q_m}\right), v \geq 0, q \leq Q \leq Q_m\}$ is positive invariant.

Proof One can easily show the existence and uniqueness of the solutions to the system (22)–(24) with the initial values $x(O), v(O)$ and $Q(O)$ on (0,1) by using Theorem 3.1 and Remark 3.2 in [3]. Next, we want to prove that solutions of (22)–(24) which start positive remain positive. It is easy to see that $\frac{\mathrm{d}^{\alpha_1} x}{\mathrm{d}t^{\alpha_1}}|_{x=0} = 0$, and $\frac{\mathrm{d}^{\alpha_2} v}{\mathrm{d}t^{\alpha_2}}|_{v=0} = 0$.

Thus, by Lemma 1, it follows that solutions which start positive remain positive. Further, observe that

$$\frac{\mathrm{d}^{\alpha_3} Q}{\mathrm{d}t^{\alpha_3}}|_{Q=q} = \gamma(Q_m - q) > 0 \quad and \quad \frac{\mathrm{d}^{\alpha_3} Q}{\mathrm{d}t^{\alpha_3}}|_{Q=Q_m} = -\mu(Q_m - q) < 0$$

Thus, the last inequality and Lemma 1 yield $q \leq Q \leq Q_m$. Further, note that from 1 we have

$$\frac{\mathrm{d}^{\alpha_1} x}{\mathrm{d}t^{\alpha_1}} \leq \mu\left(1 - \frac{q}{Q_m}\right)x - \delta x^2,$$

which in tern implies that $\frac{\mathrm{d}^{\alpha_1} x}{\mathrm{d}t^{\alpha_1}} \leq 0$. Thus, by Lemma 1, $x(t)$ is

$$x = \frac{\mu}{\delta}\left(1 - \frac{q}{Q_m}\right)$$

bounded above by $\frac{\mu}{\delta}\left(1 - \frac{q}{Q_m}\right)$. This finishes the proof. □

Next, we want to analyze the asymptotic behavior of the system (22)–(24). From the application point of view, it is convenient to assume that $\alpha_i, i = 1, 2, 3$ are rational numbers.

Proposition 3 The system of Eqs. (22)–(24) has an unstable cancer-free (disease-free) equilibrium $E_0 = \left(0, 0, \frac{\gamma Q_m + \mu q}{\mu + \gamma}\right)$ and a locally asymptotically stable endemic equilibrium $E_1 = \left(\frac{\mu\gamma}{\delta}\frac{Q_m - q}{\gamma Q_m + \mu q}, 0, \frac{\gamma Q_m + \mu q}{\mu + \gamma}\right)$.

Proof Let $E = (x^*, v^*, Q^*)$ be steady state of the system of Eqs. (22)–(24). From Eq. (22), we see that there are two cases for the steady states: $x^* = 0$ or $x^* > 0$. The case $x^* = 0$ gives us the cancer-free equilibrium E_0. If $x^* > 0$, then $x^* = \frac{\mu\gamma}{\delta}\frac{Q_m - q}{\gamma Q_m + \mu q}$ gives us the endemic equilibrium E_1.

Our model consists of multi-order fractional differential equations (FDEs), i.e., α_i do not have to be equal. Thus, we cannot evaluate the Jacobian matrix at the fixed points to analyze the stability. Instead, we convert the system (22)–(24) into its equivalent single-order system. Since all α_i are rational numbers, there exist relatively prime positive integer pairs (k_i, l_i) such that $\alpha_i = \frac{k_i}{l_i}$. Let L be the least common multiple of the denominators, i.e., $L = LCM(l_1, l_2, l_3)$. Set $\alpha = 1/L$ and $N = L(\alpha_1 + \alpha_2 + \alpha_3)$. Then, three-dimensional system (22)–(24) is equivalent to the following augmented N-dimensional system.

$$\begin{aligned}
\frac{\mathrm{d}^{\alpha} x_1}{\mathrm{d}t^{\alpha}} &= x_2, \\
\frac{\mathrm{d}^{\alpha} x_2}{\mathrm{d}t^{\alpha}} &= x_3, \\
\frac{\mathrm{d}^{\alpha} x_{L\alpha_1}}{\mathrm{d}t^{\alpha}} &= \mu\left(1 - \frac{q}{Q}\right)x - \left(v\frac{R}{Q+R} + \delta x\right)x, \\
\frac{\mathrm{d}^{\alpha} v}{\mathrm{d}t^{\alpha}} &= v_2,
\end{aligned}$$

$$\begin{aligned}
\frac{\mathrm{d}^{\alpha} v_2}{\mathrm{d}t^{\alpha}} &= v_3, \\
\frac{\mathrm{d}^{\alpha} v_{L\alpha_2}}{\mathrm{d}t^{\alpha}} &= -\mathrm{d}v, \\
\frac{\mathrm{d}^{\alpha} Q}{\mathrm{d}t^{\alpha}} &= Q_2, \\
\frac{\mathrm{d}^{\alpha} Q_2}{\mathrm{d}t^{\alpha}} &= Q_3, \\
\frac{\mathrm{d}^{\alpha} Q_{L\alpha_3}}{\mathrm{d}t^{\alpha}} &= \gamma(Q_m - Q) - \mu(Q - q),
\end{aligned} \tag{31}$$

where $x \in R$; for $2 \leq i \leq L\alpha_1$; $v_i \in R$; for $2 \leq i \leq L$; and $Q \in R$; for $2 \leq i \leq L$: The cancer-free equilibrium $E_0 = \left(0, 0, \frac{\gamma Q_m + \mu q}{\mu + \gamma}\right)$ and the endemic equilibrium $E_1 = \left(0, 0\frac{\gamma Q_m + \mu q}{\mu + \gamma}\right)$ of the system (22)–(24) correspond to the cancer-free equilibrium $\widetilde{E_0} = \left(\underbrace{0, \ldots, 0, 0}_{N-1}, \frac{\gamma Q_m + \mu q}{\mu + \gamma}\right)$ *and the endemic equilibrium* $\widetilde{E_1} = (\underbrace{0, \ldots, 0, 0}_{L\alpha_1 - 1}, \frac{\mu\gamma}{\delta}\frac{Q_m - q}{\gamma Q_m + \mu q}, \underbrace{0, \ldots, 0}_{L\alpha_2 + L\alpha_3 - 1}, \frac{\gamma Q_m + \mu q}{\mu + \gamma})$ of the system (31), respectively. Thus, *we* analyze the asymptotic behavior of the system (31). For more details how to convert a multi-order FDE to a *single*-order FDE, we refer the reader to the paper [1]. The cancer-free equilibrium $\widetilde{E_0}$ generates the following Jacobian matrix.

$$\mathrm{J}\left(\widetilde{E_0}\right) = \begin{bmatrix} 0 & 1 & \cdots & \cdots 0 \\ \vdots & & & \\ \mu\left(1 - \frac{q}{Q^*}\right) & 0 & \cdots & \cdots 0 \\ \vdots & & & \\ 0 & \cdots & -d & \cdots 0 \\ \vdots & & & \\ 0 & \cdots & -\gamma - \mu & \cdots 0 \end{bmatrix},$$

where $Q^* = \frac{\gamma Q_m + \mu q}{\mu + \gamma}$. By Theorem 4.1 in [1], the cancer-free equilibrium is stable if and only if the eigenvalues of the matrix $J\left(\overline{E}\right)$ satisfy either $|\arg(\lambda)| > \alpha\pi/2$ or solutions of the equation $|\arg(\lambda)| = \alpha\pi/2$ have geometric multiplicity one. Further, the eigenvalues of the matrix $\mathrm{J}\left(\widetilde{E_0}\right)$ are the roots of the polynomial $\det\left(\mathrm{diag}\left(\lambda^{L\alpha_1}, \lambda^{L\alpha_2}, \lambda^{L\alpha_3}\right) - J_6\right)$, where

$$J_6 = \begin{bmatrix} \mu\left(1 - \frac{q}{Q^*}\right) & 0 & 0 \\ 0 & -d & 0 \\ 0 & 0 & -\gamma - \mu \end{bmatrix}.$$

Since $\mu\left(1-\frac{q}{Q^*}\right) = \frac{\mu\gamma(Q_m-q)}{\gamma Q_m+\mu q} > 0$, the equation $\lambda^{L\alpha_1} = \mu\left(1-\frac{q}{Q^*}\right)$ has at least one positive root yielding $|\arg(\lambda)| = 0$. Thus, we conclude that the cancer-free equilibrium is unstable.

The Jacobian matrix evaluated at $\widetilde{E_1}$ gives us the following matrix.

$$\mathrm{J}\left(\widetilde{E_1}\right) = \begin{bmatrix} 0 & 1 & \cdots & \cdots & 0 \\ \vdots & & & & \\ -\frac{\mu\gamma(Q_m-q)}{\gamma Q_{m0}+\mu q0} & \cdots & \cdots & \frac{\mu q x^*}{(Q^*)^2} & 0 \\ \vdots & & & & \\ 0 & \cdots & -d & \cdots & 0 \\ \vdots & & & & \\ 0 & 0 & -\gamma-\mu & \cdots & 0 \end{bmatrix}$$

Again by Theorem 4.1 in [1], the eigenvalues of the matrix $\mathrm{J}\left(\widetilde{E_1}\right)$ are determined by finding the roots of the polynomial $\det\left(\mathrm{diag}\left(\lambda^{L\alpha_1}, \lambda^{L\alpha_2}, \lambda^{L\alpha_3}\right) - J_2\right)$, where

$$J_7 = \begin{bmatrix} -\frac{\mu\gamma(Q_m-q)}{\gamma Q_{m0}+\mu q0} & -\frac{R}{R+Q^*}x^* & \frac{\mu q x^*}{(Q^*)^2} \\ 0 & -d & 0 \\ 0 & 0 & -\gamma-\mu \end{bmatrix}$$

Thus, the eigenvalues satisfy the following algebraic equations $\lambda^{L\alpha_1} = -\frac{\mu\gamma(Q_m-q)}{\gamma Q_m+\mu q} < 0$, $\lambda^{L\alpha_2} = -d < 0$, and $\lambda^{L\alpha_3} = -\gamma-\mu < 0$.

Thus, one can show that all eigenvalues satisfy the inequality $|\arg(\lambda)| > \alpha\pi/2$. Theorem 4.1 in [1] implies that the endemics equilibrium E_1 is locally asymptotically stable. This completes the proof. □

3.3.2 Stability Analysis of Fractional Model 1*

Observe from the last equation that P is decoupled from the system. Therefore, we will restrict our attention only to the dynamics of Eqs. (27)–(29). For convenience, let us introduce the function $q_i(A) = \mu\frac{A^i}{A^i+k^i}$. One can easily show that q_i is an increasing function for $A \geq 0$ and $i > 0$.

Proposition 4 The region $\left\{(x, v, A) : 0 \leq x \leq \frac{q_s(a_0)}{\delta}, v \geq 0, 0 \leq A \leq a_0\right\}$ is positive invariant.

Proof One can easily show the existence and uniqueness of the solutions to the system (27)–(29) with the initial values $x(O)$, $v(O)$, and $A(O)$ on (0,1) by using

Theorem 3.1 and Remark 3.2 in [3]. Next, we want to prove that solutions of (27)–(29) which start positive remain positive. It is easy to see that $\frac{d^{\beta_1}x}{dt^{\beta_1}}x = 0 = 0$, $\left.\frac{d^{\beta_2}v}{dt^{\beta_2}}\right|_{v=0} = 0$, and $\left.\frac{d^{\beta_3}A}{dt^{\beta_3}}\right|_{A=0} = \gamma a_0 > 0$.

Thus, by Lemma 1, it follows that solutions which start positive remain positive. Further, note that from 6 we have

$$\frac{d^{\beta_1}x}{dt} \leq q_s(a_0)x - \delta x^2,$$

which in tern implies that $\left.\frac{d^{\beta_1}x}{dt^{\beta_1}}\right| \leq 0$.

$$x = \frac{q_s(a_0)}{\delta, to}$$

Thus, by Lemma 1, $x(t)$ is bounded above by $q_s(a_0)$. It remains to show that A is bounded. Observe from Eq. (29) that we have $\left.\frac{d^{\beta_3}A}{dt^{\beta_3}}\right| < 0$.

$$A = a_0$$

Therefore, again by Lemma 1, we obtain $A(t)$ bounded by a_0. This *finishes* the proof. □

Next, we want to analyze the asymptotic behavior of the system (27)–(29). From the application point of view, it is convenient to assume that $\beta, i = 1, 2, 3$ are rational numbers.

Proposition 5 The system of Eqs. (27)–(29) has an unstable cancer-free (disease-free) equilibrium $E_0 = (0, 0, a_0)$ and a locally asymptotically stable endemic equilibrium $E_1 = \left(\frac{\theta q_s(\overline{A})}{\theta\delta + q_s(\overline{A})}, 0, \overline{A}\right)$, $0 < \overline{A} < a_0$.

Proof From Eq. (27), we see that there are two cases for the steady states: $x = 0$ or $x = \bar{x} > 0$. The case $x = 0$ gives us the cancer-free equilibrium E_0. If $x = \bar{x} > 0$, consider a function $h(A) = \frac{q_s(A)}{\delta + \frac{q_s(A)}{\theta}} - \frac{\gamma(a_0 - A)}{q_\omega(A)}$. One can check that $\lim_{A\to 0^-} h(A) = -1$ and $h(a_0) > 0$. Thus, by the Intermediate Value Theorem (IVT), there exists $\overline{A} \in (0, a_0)$ such that $h(\overline{A}) = 0$. From Eqs. (27) and (29), we can find E_1 which satisfies the following equations $\bar{x} = \frac{q_s(\overline{A})}{\delta + \frac{q_s(\overline{A})}{\theta}} = \frac{\gamma(a_0 - \overline{A})}{q_\omega(\overline{A})}$.

Our model consists of multi-order fractional differential equations (FDEs), i.e., α_i do not have to be equal. Thus, we cannot evaluate the Jacobian matrix at the fixed points to analyze the stability. Instead, we convert the system (27)–(29) into its equivalent single-order system. Since all β_i are rational numbers, there exist relatively prime positive integer pairs (k_i, l_i) such that $\beta_i = \frac{k_i}{l_i}$. Let L be the least common multiple of the denominators, i.e., $L = LCM(l_1, l_2, l_3)$. Set $\alpha = 1/L$ and

$N = L(\beta_1 + \beta_2 + \beta_3)$. Then, three-dimensional system (27)–(29) is equivalent to the following augmented N-dimensional system.

$$\begin{aligned}
\frac{\mathrm{d}^{\beta}x}{\mathrm{d}f^{\beta}} &= x_2,\\
\frac{\mathrm{d}x_2}{\mathrm{d}t^{\beta}} &= x_3,\\
&\vdots\\
\frac{\mathrm{d}^{\beta}x_{L\beta_1}}{\mathrm{d}t^{\beta}} &= \mu\frac{A^s}{A^s+k^s}\Big(1-\frac{x}{\theta}\Big)x-\Big(v\frac{R}{A+R}+\delta x\Big)x,\\
\frac{\mathrm{d}^{\beta}v}{\mathrm{d}t^{\beta}} &= v_2,\\
\frac{\mathrm{d}^{\beta}v_2}{\mathrm{d}t^{\beta}} &= v_3,\\
&\vdots\\
\frac{\mathrm{d}^{\beta}v_{\beta_2}}{\mathrm{d}t^{\beta}} &= -\mathrm{d}v,\\
\frac{\mathrm{d}^{\beta}\mathrm{A}}{\mathrm{d}t^{\beta}} &= A_2,\\
\frac{\mathrm{d}^{\beta}A_2}{\mathrm{d}t^{\beta}} &= A_3,\\
&\vdots\\
\frac{\mathrm{d}^{\beta}A_{L\beta_3}}{\mathrm{d}t^{\beta}} &= \gamma(a_0-A)-\mu\frac{A^{\omega}}{A^{\omega}+\rho^{\omega}}x,
\end{aligned} \tag{32}$$

where $x_i \in R$; for $2 \le i \le L\beta_1$; $v_i \in R$; for $2 \le i \le L\beta_2$; and $A_i \in R$; for $2 \le i \le L$: The cancer-free equilibrium $E_0 = (0, 0, a_0)$ and the endemic equilibrium $E_1 = \left(\frac{\theta q_s(\overline{A})}{\theta\delta+q_s(\overline{A})}, 0, \overline{A}\right)$ of the system (27)–(29) correspond to the cancer-free equilibrium $\overline{E_0} = \left(\underbrace{0, \ldots, 0, 0}_{N-1}, a_0\right)$ *and the endemic equilibrium* $\overline{E_1} = (\underbrace{0, \ldots, 0, 0}_{L\beta_1-1}, \frac{\theta q_s(\overline{A})}{\theta\delta+q_s(\overline{A})}, \underbrace{0, \ldots, 0}_{L\beta_2+L\beta_3-1}, \overline{A})$ of the system (32), respectively. Thus, *we* analyze the asymptotic behavior of the system (32). For more details how to convert a multi-order FDE to a *single*-order FDE, we refer the reader to the paper [1]. The cancer-free equilibrium $\overline{E_0}$ generates the following Jacobian matrix

$$\mathrm{J}\left(\overline{E_0}\right) = \begin{bmatrix} 0 & 1 & \cdots & \cdots & 0 \\ \vdots & & & & \\ q_s(a_0) & 0 & \cdots & \cdots & 0 \\ \vdots & & & & \\ 0 & \cdots & -d & \cdots & 0 \\ \vdots & & & & \\ q_\omega(a_0) & \cdots & \cdots & -\gamma & 0 \end{bmatrix}.$$

By Theorem 4.1 in [1], the cancer-free equilibrium is stable if and only if the eigenvalues of the matrix $J\left(\overline{E_0}\right)$ satisfy either $|\arg(\lambda)| > \alpha\pi/2$ or solutions of the equation $|\arg(\lambda)| = \alpha\pi/2$ have geometric multiplicity one. Further, the eigenvalues of the matrix $J\left(\overline{E_0}\right)$ are the roots of the polynomial $\det\left(\mathrm{diag}\left(\lambda^{L\beta_1}, \lambda^{L\beta_2}, \lambda^{L\beta_3}\right) - J_7\right)$, where

$$J_1 = \begin{bmatrix} q_s(a_0) & 0 & 0 \\ 0 & -d & 0 \\ q_\omega(a_0) & 0 & -\gamma \end{bmatrix}.$$

Since $q_s(a_0) > 0$, the equation $\lambda^{L\beta_1} = q_s(a_0)$ has at least one positive root. Thus, we conclude that the cancer-free equilibrium is unstable.

The Jacobian matrix evaluated at $\overline{E_1}$ gives us the following matrix.

$$\mathrm{J}\left(\overline{E_1}\right) \begin{bmatrix} 0 & 1 & \cdots & & & \cdots & 0 \\ \vdots & & & & & & \\ -q_s\left(\overline{A}\right) & \cdots & -\frac{R}{R+\overline{A}}\bar{x} & \cdots & & q_s'\left(\overline{A}\right)\left(1-\frac{\bar{x}}{\theta}\right)\bar{x} & 0 \\ \vdots & & & & & & \\ 0 & \cdots & & -d & & \cdots & 0 \\ \vdots & & & & & & \\ q_\omega\left(\overline{A}\right) & 0 & \cdots & -\gamma - q_\omega'\left(\overline{A}\right)\bar{x} & & \cdots & 0 \end{bmatrix}$$

Again by Theorem 4.1 in [1], the eigenvalues of the matrix $J\left(\overline{E_1}\right)$ are determined by finding the roots of the polynomial $\det\left(\mathrm{diag}\left(\lambda^{L\beta_1}, \lambda^{L\beta_2}, \lambda^{L\beta_3}\right) - J_2\right)$, where

$$J_2 = \begin{bmatrix} -q_s\left(\overline{A}\right) & -\frac{R}{R+\overline{A}}\bar{x} & q_s'\left(\overline{A}\right)\left(1-\frac{\bar{x}}{\theta}\right)\bar{x} \\ 0 & -d & 0 \\ q_\omega\left(\overline{A}\right) & 0 & -\gamma - q_\omega'\left(\overline{A}\right)\bar{x} \end{bmatrix}.$$

Thus, the eigenvalues satisfy the following equation

$$\left(\lambda^{L\beta_2}+d\right)\left(q_\omega\left(\overline{A}\right)q_s'\left(\overline{A}\right)\left(1-\frac{\bar{x}}{\theta}\right)\bar{x}+q_s\left(\overline{A}\right)\left(\gamma+q_\omega'\left(\overline{A}\right)\bar{x}\right)\lambda^{L\beta_1+L\beta_3}\right.$$
$$\left.+\,q_s\left(\overline{A}\right)\lambda^{L\beta_3}+\left(\gamma+q_\omega'\left(\overline{A}\right)\bar{x}\right)\lambda^{L\beta_1}\right)=0.$$

Observe that λ is a solution for $\lambda^{L\beta_2}=-d<0$, and the remaining eigenvalues can be evaluated from

$$\lambda^{L\beta_1+L\beta_3}+q_s\left(\overline{A}\right)\lambda^{L\beta_3}+\left(\gamma+q_\omega'\left(\overline{A}\right)\bar{x}\right)\lambda^{L\beta_1}$$
$$+\,q_\omega\left(\overline{A}\right)q_s'\left(\overline{A}\right)\left(1-\frac{\bar{x}}{\theta}\right)\bar{x}+q_s\left(\overline{A}\right)\left(\gamma+q_\omega'\left(\overline{A}\right)\bar{x}\right)=0.$$

Since $q_s\left(\overline{A}\right)>0$, $\gamma+q_\omega'\left(\overline{A}\right)\bar{x}>0$, $q_s\left(\overline{A}\right)\left(\gamma+q_\omega'\left(\overline{A}\right)\bar{x}\right)>0$, and $q_\omega\left(\overline{A}\right)q_s'\left(\overline{A}\right)\left(1-\frac{\bar{x}}{\theta}\right)\bar{x}>0$, Descartes' rule of signs guarantees that there is no positive real root. This completes the proof. □

As we stated in the paper [1], every process in nature has its own specific speed so it needs to be represented by their own specific fractional derivative orders, too. For example here, we cannot say that serum androgen and PSA have to diffuse at the same rate or CS and CR cells have to proliferate at the same rate in a patient. Hence, we prefer to model each equation above using different differential orders. Due to the microscopic environment of the above processes, we consider derivative orders between 0 and 1 and investigate which order would fit our data set best. Doing this, we provide a justification on that fractional-order modeling could improve the fit to a particular set of experimental data when compared with the ordinary form.

In the literature, there are several papers including numerical methods, parameter estimate, and stability analysis for the fractional models in biology and medicine. To be able to obtain numerical solutions of the above fractional systems, we impose the explicit product integration (PI) rectangular rule [2] to the process of finding optimum parameters fitting data for each patient. To compare models, we conduct simulations with MATLAB's (MATLAB 9.4, R2018a) built-in function fmincon, which uses the Interior Point Algorithm, to find the optimum parameters for each patient. The algorithm searches for a minimum value in a range of pre-specified parameter ranges, which were estimated from various literature sources. We use this algorithm to minimize the MSE for PSA and androgen data. The MSE is calculated with the following equations:

$$P_{\text{error}}=\frac{\sum_{i=1}^{N}(P_i-\widehat{P})^2}{N} \tag{33}$$

$$A_{\text{error}}=\frac{\sum_{i=1}^{N}(A_i-\widehat{A_i})^2}{N} \tag{34}$$

where N represents the total number of data points, P_i represents the PSA data value, and $\widehat{P}$ the value from the model. Likewise, A_i represents the androgen data value

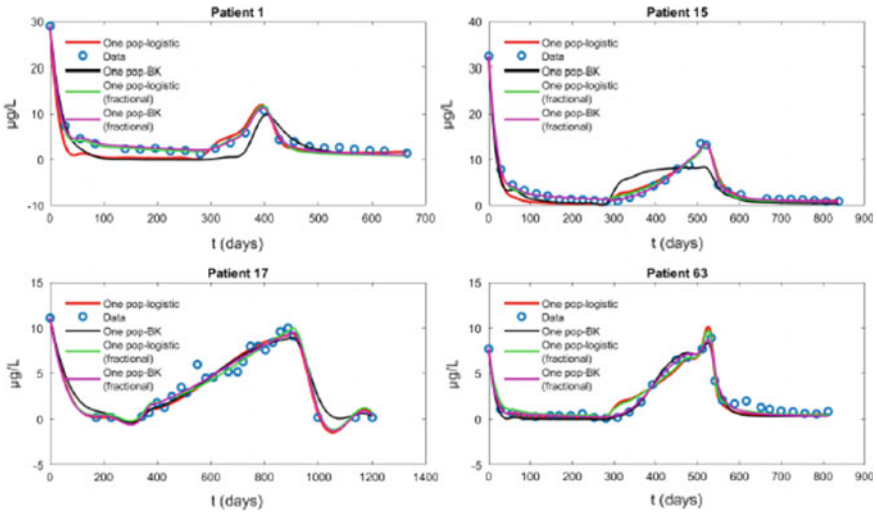

Fig. 14 Simulations of PSA fittings for every one population model for 1.5 cycles of treatment

and $\widehat{A_i}$ the value from the model. We then use an equally weighted combination of both errors

$$\text{error} = P_{\text{error}} + A_{\text{error}} \tag{35}$$

as our objective function, which is then minimized with fmincon.

When the MSE values of the PSA values of the OPBK and OPL models are examined, it is clear that the fractional conjugates of these models reduce the error. When the same study is done for androgen values, it is seen that the MSE values are still less for the fractional conjugates.

3.4 Case 1: Without Relapse (Patients 1, 15, 17, 63)

See Figs. 14 and 15.

3.5 Case 2: With Metastasis (Without Relapse) (Patients 32, 64, 83)

See Figs 16 and 17.

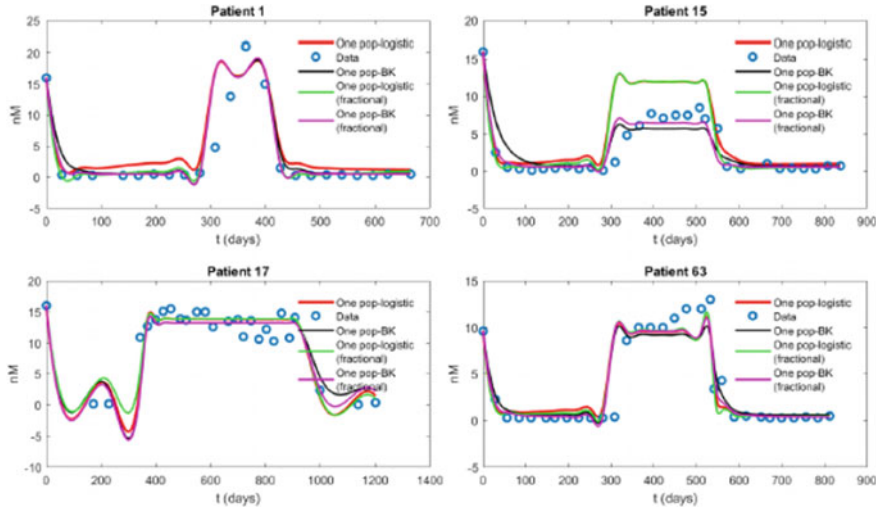

Fig. 15 Simulations of androgen fittings for every one population model for 1.5 cycles of treatment

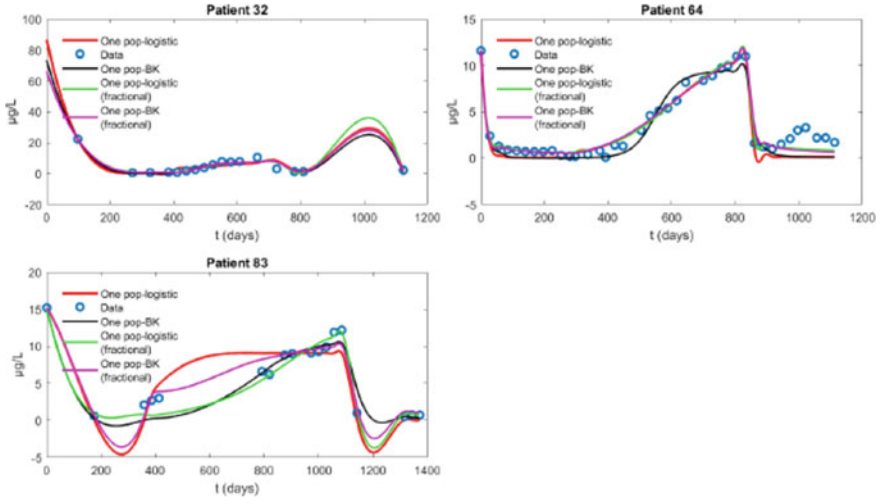

Fig. 16 Simulations of PSA fittings for every one population model for 1.5 cycles of treatment

3.6 Case 3: With Relapse (Patients 12, 19, 36, 101)

See Figs. 18 and 19.

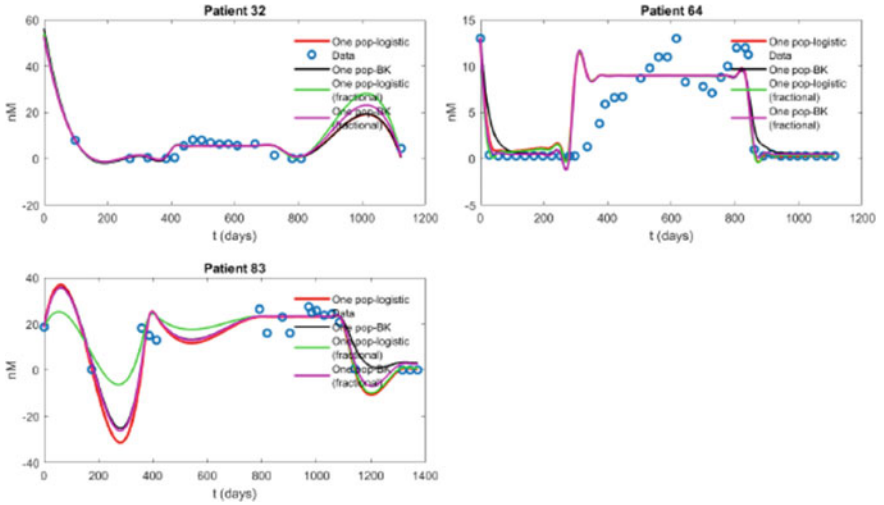

Fig. 17 Simulations of androgen fittings for every one population model for 1.5 cycles of treatment

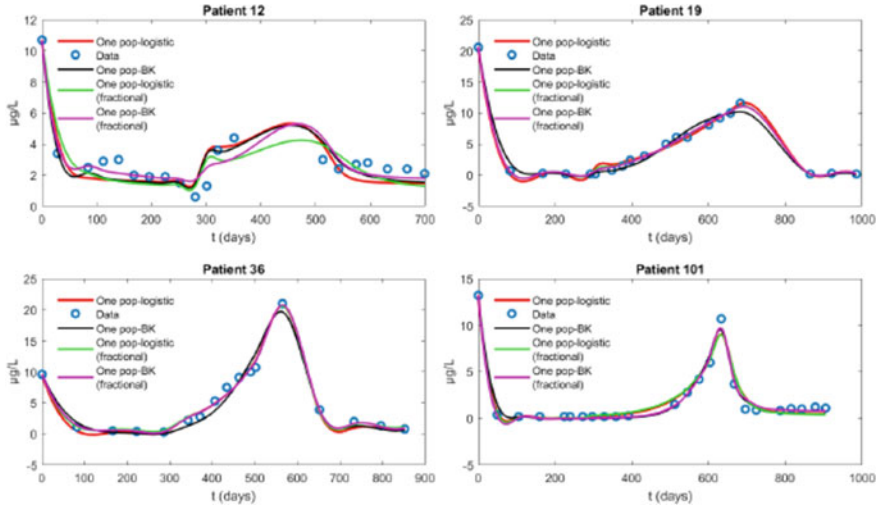

Fig. 18 Simulations of PSA fittings for every one population model for 1.5 cycles of treatment

3.7 Fractional Model 2: Two Population Fractional BK Model

$$\frac{\mathrm{d}^{\chi_1} x_1}{\mathrm{d}t} = \mu\left(1 - \frac{q_1}{Q}\right)x_1 - \left(D_1(Q) + \delta_{1X_1}\right)x_1 - \lambda(Q)x_1 \tag{36}$$

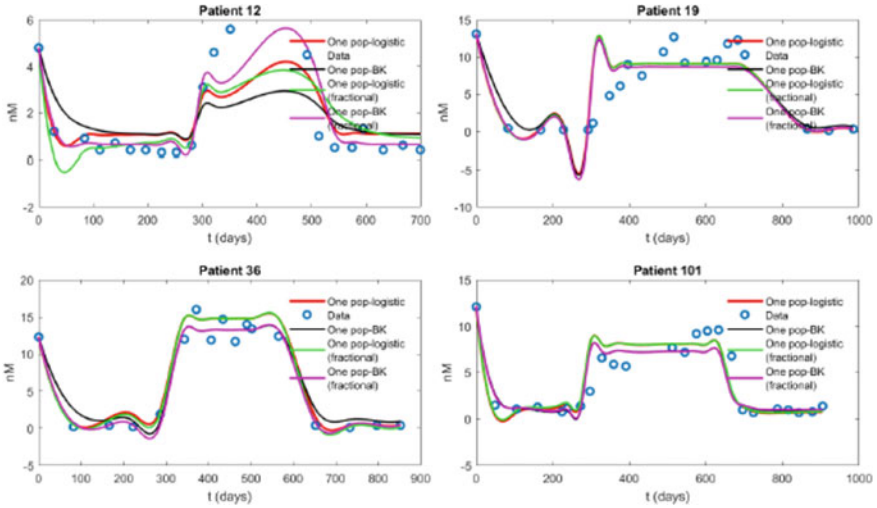

Fig. 19 Simulations of PSA fittings for every one population model for 1.5 cycles of treatment

$$\frac{\mathrm{d}^{\chi_2} x_2}{\mathrm{d}t} = \mu\left(1 - \frac{q_2}{Q}\right)x_2 - \left(D_2(Q) + \delta_{_2 X_2}\right)x_2 - \lambda(Q)x_2 \tag{37}$$

$$\frac{\mathrm{d}^{\chi_3} Q}{\mathrm{d}t} = \gamma(Q_m - Q) - \frac{\mu(Q - q_1)x_1 + \mu(Q - q_2)x_2}{x_1 + x_2} \tag{38}$$

$$\frac{\mathrm{d}^{\chi_4} P}{\mathrm{d}t} = bQ + \sigma(Qx_1 + Qx_2) - \varepsilon P \tag{39}$$

where $\chi_i \in (0, 1]$ for $i = 1, 2, 3, 4$ and represents Caputo-type fractional order and

$$D_i(Q) = d_i \frac{R_i}{Q + R_i}, i = 1, 2 \tag{40}$$

$$\lambda(Q) = c\frac{K}{Q + K} \tag{41}$$

3.8 *Fractional Model 2*: Two Population Fractional Logistic Model*

$$\frac{\mathrm{d}^{\psi_1} x_1}{\mathrm{d}t} = r_1(A, x_1, x_2)x_1 - m(A)x_1 \tag{42}$$

$$\frac{\mathrm{d}^{\psi_2} x_2}{\mathrm{d}t} = r_2(A, x_1, x_2)x_2 + m(A)x_1 \tag{43}$$

$$\frac{\mathrm{d}^{\psi_3} A}{\mathrm{d}t} = \gamma(a_0 - A) - \mu\frac{A^{\omega}}{A^{\omega} + \rho^{\omega}}(x_1 + x_2), \tag{44}$$

$$\frac{\mathrm{d}^{\beta_4} P}{\mathrm{d}t^{\beta_4}} = bA + \sigma A(x_1 + x_2) - \varepsilon P \tag{45}$$

where $\psi_i \in (0, 1]$ for $i = 1, 2, 3, 4$ and represents Caputo-type fractional order and

$$r_1(A, x_1, x_2) = \mu\frac{A^m}{A^m + k^m}\left(1 - \frac{x_1 + x_2}{\theta}\right) - \left(d_1\frac{R_1}{A + R_1} + \delta_{_1 X_1}\right)x_1, \tag{46}$$

$$r_2(A, x_1, x_2) = \mu\frac{A^n}{A^n + k^n}\left(1 - \frac{x_1 + x_2}{\theta}\right) - \left(d_2\frac{R_2}{A + R_2} + \delta_{_2 X_2}\right)x_2 \tag{47}$$

$$m(A) = c\frac{K}{A + K}. \tag{48}$$

3.9 Model Dynamics of Two Population Fractional BK and Logistic Models

3.9.1 Stability Analysis of Fractional Model 2

Proposition 6 Suppose that $q_2 \leq q_1 \leq Q_m$. Then, the region $\{(x_1, x_2, Q) : x_1 \geq 0, x_2 \geq 0, q_2 \leq Q \leq Q_m\}$ is positive invariant.

Proof It follows from Eqs. (36)–(38) that

$$\frac{\mathrm{d}^{\chi_1} x_1}{\mathrm{d}t^{\chi_1}}|_{x_1=0} = 0 \text{ and } \frac{\mathrm{d}^{\chi_2} x_2}{\mathrm{d}t^{\chi_1}}|_{x_2=0} = \rho(Q)x_1 \geq 0.$$

The above inequalities guarantee by Lemma 1 the positiveness of x_1 and x_2. Next, one can see that

$$\frac{\mathrm{d}^{\chi_3} Q}{\mathrm{d}t^{\chi_3}}|_{Q=q_2} = \gamma(Q_m - q_2) + \mu\frac{(q_1 - q_2)x_2}{x_1 + x_2} > 0$$

and

$$\frac{\mathrm{d}^{\chi_3} Q}{\mathrm{d}t^{\chi_3}}|_{Q=Q_m} = -\mu\frac{(Q_m - q_1)x_1 + (Q_m - q_2)x_2}{x_1 + x_2} < 0$$

Thus, by Lemma 1, it follows that $q_2 \leq Q \leq Q_m$. □

Remark 7 If in addition, we assume that $\chi_1 = \chi_2$ and $\delta_2 \leq \delta_1$, then $x_1 + x_2 \leq \frac{G_2(Q_m)-D_m}{\delta_2}$, where $D_m = \min\{D_1(q_2), D_2(q_2)\}$.

Proof Since $q_2 \leq q_1$, we have $G_1(Q) \leq G_2(Q)$. Further, one can easily show that the growth rate $G_i(Q)$, $i = 1, 2$ is increasing function of Q. Now, set $X = x_1 + x_2$. Then, we have

$$\begin{aligned}\frac{\mathrm{d}^{\chi_1} X}{\mathrm{d}t^{\chi_1}} &= \frac{\mathrm{d}^{\chi_1} x_1}{\mathrm{d}t} + \frac{\mathrm{d}^{\chi_2} x_2}{\mathrm{d}t} \\ &\leq (G_2(Q) - D_m)X - \delta_2 X^2 \\ &\leq (G_2(Q_m) - D_m)X - \delta_2 X^2.\end{aligned}$$

Thus, $\frac{\mathrm{d}^{\chi_1} X}{\mathrm{d}t^{\chi_1}}|_{x=\frac{G_2(Q_m)-D_m}{\delta_2}} \leq 0$.

By virtue of Lemma 1, we have $\lim_{t\to\infty} \sup X(t) \leq \frac{G_2(Q_m)-D_m}{\delta_2}$.

Proposition 8 The system of Eqs. (36)–(38) has a cancer-free (disease-free) equilibrium $F_0 = (0, 0, Q_m)$, a CR cell only equilibrium $F_1 = \left(0, \frac{G_1(Q_1)-D_2(Q_1)}{\delta_2}, Q_1\right)$, and a coexistence equilibrium $F_2 = \left(\frac{G_1(Q_2)-D_2(Q_2)-\rho(Q_2)}{\delta_1}, x_2^*, Q_2\right)$, where $x_2^* > 0$, $Q_1 < Q_2$ and $Q_1 = \frac{\gamma Q_m + \mu q_2}{\gamma+\mu}$.

Proof From Eq. (36), we see that either $x_1 = 0$ or $x_1 > 0$.

If $x_1 = 0$, then there are two mutually exclusive cases: $x_2 = 0$ and $x_2 \neq 0$. In the first case, the steady state is $F_0 = (0, 0, Q_m)$. In the latter case, the steady state is $F_1 = \left(0, \frac{G_1(Q_1)-D_2(Q_1)}{\delta_2}, Q_1\right)$, where Q_1 can be found to be $Q_1 = \frac{\gamma Q_m + \mu q_2}{\gamma+\mu}$.

If $x_1 > 0$, it follows from Eq. (37) that $x_2 > 0$. Thus, there emerges the coexistence equilibrium $F_2 = \left(\frac{G_1(Q_2')-D_2(Q_2')-\rho(Q_2')}{\delta_1}, x_2^*, Q_2\right)$,. Further, from 17 we have

$$\begin{aligned}0 &= \frac{(Q_2 - q_1)x_1^* + (Q_2 - q_2)x_2^*}{x_1 + x_2} \\ &\geq (Q_m - Q_2) - \mu(Q_2 - q_2).\end{aligned}$$

The last inequality implies that $Q_2 \geq \frac{\gamma Q_m + \mu q_2}{\gamma+\mu} = Q_1$. □

From the application point of view, we assume that χ_i, $i = 1, 2, 3$, are rational numbers. For convenience, denote the functions $u(Q) = G_1(Q) - D_1(Q) - \rho(Q)$ and $v(Q) = G_2(Q) - D_2(Q)$.

Proposition 9 The cancer-free equilibrium $F_0 = (0, 0, Q_m)$ is unstable *if* $u(Q_m) > 0$ or $v(Q_m) > 0$ and locally asymptotically stable if $u(Q_m) < 0$ and $v(Q_m) < 0$.

Proof We convert the system (36)–(38) into its equivalent single-order system. Since all χ_i are rational numbers, there exist relatively prime positive integer pairs (k_i, l_i) such that $\alpha_i = \frac{k_i}{l_i}$. Let M be the least common multiple of the denominators, i.e., $M = LCM(l_1, l_2, l_3)$. Set $\chi = 1/M$ and $N = M(\chi_1 + \chi_2 + \chi_3)$. Then, three-dimensional system (36)–(38) is equivalent to the following augmented N-dimensional system.

$$
\begin{aligned}
\frac{\mathrm{d}^{\chi} x_1}{\mathrm{d}t^{\chi}} &= y_2,\\
\frac{\mathrm{d}^{\chi} y_2}{\mathrm{d}t^{\chi}} &= y_3,\\
&\vdots\\
\frac{\mathrm{d}^{\chi} y_{M\alpha_1}}{\mathrm{d}t^{\chi}} &= \mu\left(1-\frac{q_1}{Q}\right)x_1 - (D_1(Q)+\delta_1 x_1)x_1 - \rho(Q)x_1,\\
\frac{\mathrm{d}^{\chi} x_2}{\mathrm{d}^{\chi}\mathrm{t}} &= z_2,\\
\frac{\mathrm{d}^{\chi} z_2}{\mathrm{d}^{\chi}\mathrm{t}} &= z_3,\\
&\vdots\\
\frac{\mathrm{d}^{\chi} z_{M\alpha_2}}{\mathrm{d}t^{\chi}} &= \mu\left(1-\frac{q_2}{Q}\right)x_2 - (D_2(Q)+\delta_2 x_2)x_2 + \rho(Q)x_1,\\
\frac{\mathrm{d}^{\chi} Q}{\mathrm{d}t^{\chi}} &= Q_2,\\
\frac{\mathrm{d}^{\chi} Q_2}{\mathrm{d}t^{\chi}} &= Q_3,\\
&\vdots\\
\frac{\mathrm{d}^{\chi} Q_{M\alpha_3}}{\mathrm{d}t^{\chi}} &= \gamma(Q_m - Q) - \mu\frac{(Q-q_1)x_1 + (Q-q_2)x_2}{x_1+x_2}.
\end{aligned}
\tag{49}
$$

Thus, we analyze the asymptotic behavior of the system (49). Let us compute the Jacobian matrix at F_0.

$$
J\left(\widetilde{F}_0\right) = \begin{Bmatrix}
0 & 1 & 0 & \cdots & 0\\
\vdots & & & & \\
u(Q_m) & 0 & \cdots & \cdots & 0\\
\vdots & & & & \\
\rho(Q_m) & \cdots & v(Q_m) & 0 & 0\\
\vdots & & & & \\
0 & \cdots & \cdots & -\gamma Q_m - \mu & 0
\end{Bmatrix}.
$$

By Theorem 4.1 in [1], the cancer-free equilibrium is stable if and only if the eigenvalues of the matrix $J\left(\widetilde{F}_0\right)$ satisfy either $|\arg(\lambda)| > \chi\pi/2$ or solutions of the equation $|\arg(\lambda)| = \chi\pi/2$ have geometric multiplicity one. Further, the eigenvalues of the matrix $J(F)$ are determined by the roots of the polynomial

$$\det\left(\operatorname{diag}\left(\lambda^{M\chi_1}, \lambda^{M\chi_2}, \lambda^{M\chi_3}\right) - J_4\right),$$

where

$$J_4 = \begin{Bmatrix} u(Q_m) & 0 & 0 \\ \rho(Q_m) & v(Q_m) & 0 \\ 0 & 0 & -\gamma Q_m - \mu \end{Bmatrix}$$

Since J_4 is a lower triangular matrix, the set eigenvalues of $J\left(\widetilde{F}_0\right)$ are given by the following algebraic equations.

$$\lambda^{M\chi_1} = u(Q_m), \lambda^{M\chi_2} = v(Q_m), \quad \text{and} \quad \lambda^{M\chi_3} = -\gamma Q_m - \mu < 0. \tag{50}$$

If $u(Q_m) > 0$ or $v(Q_m) > 0$, then at least one eigenvalue is positive which in tern implies that $\arg(\lambda) = 0$. Thus, the cancer-free equilibrium is unstable.

If $u(Q_m) < 0$ and $v(Q_m) < 0$, then one can show that all solutions of the (50) satisfy $|\arg(\lambda)| > \chi\pi/2$. Thus, by Theorem 4.1 in [1], we conclude that the cancer-free equilibrium is locally asymptotically stable. This finalizes the proof. □

Proposition 10 The CR only equilibrium F_1 is locally asymptotically stable if $u(Q_1) < 0$ and $v(Q_1) > 0$.

Proof In order to analyze the asymptotic behavior of *F,* we again consider the system (49). The CR only equilibrium $\widetilde{F}_1$ of the system (36)–(37) corresponds $\widetilde{F}_1 = (\underbrace{0, \ldots, 0, 0}_{M\chi_1+M\chi_2-1}, \frac{\mu\gamma}{\delta}\frac{Q_m-q}{\gamma Q_m+\mu q}, \underbrace{0, \ldots, 0}_{M\chi_3-1}, \frac{\gamma Q_m+\mu q}{\mu+\gamma})$ of the system (49). The Jacobian matrix evaluated at $\widetilde{F}_1$ is given by

$$\mathrm{J}\left(\widetilde{F}_1\right) = \begin{bmatrix} 0 & 1 & \cdots & \cdots & \cdots & 0 \\ \vdots & & & & & \\ u(Q_1) & 0 & \cdots & \cdots & \cdots & 0 \\ \vdots & & -v(Q_1) & & \left(\frac{\mu q_2}{Q_1^2} + \frac{d_2 R_2}{(R_2'+Q_1)^2}\right)\frac{G_2(Q_1)-D_2(Q_1)}{\delta_2'} & \\ \rho(Q_1) & \cdots & & \cdots & & 0 \\ \vdots & & & & & \\ \frac{\mu\delta_2(q_1-q_2)}{G_2(Q_1)-D_2'(Q_1)} & 0 & \cdots & -\gamma-\mu & \cdots & 0 \end{bmatrix}.$$

By Theorem 4.1 in [1], the CR only equilibrium is asymptotically stable if the eigenvalues of the matrix $J\left(\widetilde{F}_1\right)$ satisfy $|\arg(\lambda)| > \chi\pi/2$. Further, the

eigenvalues of the matrix $J\left(\widetilde{F}_1\right)$ are determined by the roots of the polynomial $\det\left(\text{diag}\left(\lambda^{M\chi_1}, \lambda^{M\chi_2}, \lambda^{M\chi_3}\right) - J_5\right)$, where

$$J_5 = \begin{Bmatrix} u(Q_1) & 0 & 0 \\ \rho(Q_1) & -v(Q_1)\left(\frac{\mu q_2}{Q_1^2} + \frac{d_2 R_2}{(R_2+Q_1)^2}\right) & \frac{G_2(Q_1)-D_2'(Q_1)}{\delta_2} \\ \frac{\mu\delta_2(q_1-q_2)}{G_2(Q_1)-D_2'(Q_1)} & 0 & -\gamma-\mu \end{Bmatrix}.$$

It is seen that the set of eigenvalues satisfy the following algebraic equations

$$\begin{aligned} \lambda^{M\chi_1} &= u(Q_1), \\ \lambda^{M\chi_2} &= -v(Q_1), \\ \lambda^{M\chi_3} &= -\gamma-\mu < 0. \end{aligned}$$

If $u(Q_1) < 0$ and $v(Q_1) > 0$, then it is easy to show that all eigenvalues satisfy the inequality $|\arg(\lambda)| > \chi\pi/2 = \pi/2M$. Thus, the CR only equilibrium F_1 is locally asymptotically stable. This finalizes the proof. □

3.9.2 Stability Analysis of Fractional Model 2*

As it was in Model 2, we do not analyze Eq. (45) since P is decoupled from Eqs. (42)–(44).

Proposition 11 The region $\{(x_1, x_2, A) : x_1 \geq 0, x_2 \geq 0, 0 \leq A \leq a_0\}$ is positive invariant.

Proof From Proposition 3, we know that $0 \leq A(t) \leq a_0$ if $0 \leq A(O) \leq a_0$. Next, observe that

$$\left.\frac{\mathrm{d}^{\psi_1} x_1}{\mathrm{d}t}\right|_{x_1=0} = 0 \quad \text{and} \quad \left.\frac{\mathrm{d}^{\psi_2} x_2}{\mathrm{d}t}\right|_{x_2=0} = m(A)x_1 \geq 0.$$

Thus, by Lemma 1, it follows that solutions which start positive remain positive.

Remark 12 If in addition, we assume that $\psi_1 = \psi_2$, $n < m$, and $\delta_2 \leq \delta_1$, then $x_1 + x_2 \leq \frac{q_m(a_0)-D_m}{\delta_2}$.

Proof Set $X = x_1 + x_2$. Then, we have

$$\begin{aligned} \frac{\mathrm{d}^{\psi_1} X}{\mathrm{d}t} &= \frac{\mathrm{d}^{\psi_1} x_1}{\mathrm{d}t} + \frac{\mathrm{d}^{\psi_2} x_2}{\mathrm{d}t} \\ &\leq (q_m(A) - D_m)X - \delta_2 X^2 \end{aligned}$$

$$\leq (q_m(a_0) - D_m)X - \delta_2 X^2.$$

Thus, $\frac{\mathrm{d}^{\psi_1} X}{\mathrm{d}t}|_{X=\frac{q_m(a_0)-D_m}{\delta_2}} \leq 0$. By virtue of Lemma 1, we have $\lim_{t\to\infty} \sup X(t) \leq \frac{q_m(a_0)-D_m}{\delta_2}$.

Proposition 13 The system of Eqs. (42)–(44) has a cancer-free (disease-free) equilibrium $E_0 = (0, 0, a_0)$, a CR cell only equilibrium $E_2 = \left(0, \theta\frac{q_n(A_1)-D_2(A_1)}{q_n(A_1)+\theta\delta_2}, A_1\right)$, and a coexistence equilibrium $E_3 = \left(x_1^*, x_2^*, A^*\right)$, where $x_1^* > 0, x_2^* > 0, 0 < A_1 < a_0$, and $0 < A^* < a_0$.

Proof From Eq. (42), we see that either $x_1 = 0$ or $x_1 > 0$.

If $x_1 = 0$, then there are two mutually exclusive cases: $x_2 = 0$ and $x_2 \neq 0$. In the first case the steady state is $E_0 = (0, 0, a_0)$. In the latter case, the steady state is $E_2 = (0, \bar{x}, A_1)$, where $A_1 \in (0, a_0)$ and $\bar{x} = \theta\frac{q_n(A_1)-D_2(A_1)}{q_n(A_1)+\theta\delta_2} = \frac{\gamma(a_0-A_1)}{\mu\frac{A_1^{\omega}}{A_1^{\omega}+\rho^{\omega}}} > 0$.

If $x_1 > 0$, it follows from Eq. (43) that $x_2 > 0$. Thus, there emerges the coexistence equilibrium $E_3 = \left(x_1^*, x_2^*, A^*\right)$.

As in Model 2, in order to carry out the asymptotic behavior we assume that $\psi_i, i = 1, 2, 3$, are rational numbers. Denote the functions $f(A) = q_m(A) - D_1(A) - m(A)$ and $g(A) = q_n(A) - D_2(A)$.

Proposition 14 The cancer-free equilibrium $E_0 = (0, 0, a_0)$ is unstable if $f(a_0) > 0$ or $g(a_0) > 0$ and locally asymptotically stable if $f(a_0) < 0$ and $g(a_0) < 0$.

Proof We convert the system (42)–(44) into its equivalent single-order system. Since all ψ_i are rational numbers, there exist relatively prime positive integer pairs (k_i, l_i) such that $\psi_i = \frac{k_i}{l_i}$. Let M be the least common multiple of the denominators, i.e., $M = LCM(l_1, l_2, l_3)$. Set $\psi = 1/M$ and $N = M(\psi_1 + \psi_2 + \psi_3)$. Then, three-dimensional system (42)–(44) is equivalent to the following augmented N-dimensional system

$$\begin{aligned}
&\frac{\mathrm{d}^{\psi} x_1}{\mathrm{d}t^{\psi}} = y_2,\\
&\frac{\mathrm{d}^{\psi} y_2}{\mathrm{d}t^{\psi}} = y_3,\\
&\vdots\\
&\frac{\mathrm{d}^{\psi} y_{M\psi_1}}{\mathrm{d}t^{\psi}} = q_m(A)\left(1 - \frac{x_1 + x_2}{\theta}\right)x_1 - (D_1(A) + \delta_1 x_1)x_1 - m(A)x_1,\\
&\frac{\mathrm{d}^{\psi} x_2}{\mathrm{d}t^{\psi}} = z_2,\\
&\frac{\mathrm{d}^{\psi} z_2}{\mathrm{d}t^{\psi}} = z_3\\
&\vdots
\end{aligned}$$

$$\begin{aligned}
&\frac{\mathrm{d}^{\psi} z_{M\psi_2}}{\mathrm{d}t^{\psi}} = q_n(A)\left(1 - \frac{x_1 + x_2}{\theta}\right)x_2 - (D_2(A) + \delta_2 x_2)x_2 + m(A)x_1,\\
&\frac{\mathrm{d}^{\psi} A}{\mathrm{d}t^{\psi}} = A_2,\\
&\frac{\mathrm{d}^{\psi} A_2}{\mathrm{d}t^{\psi}} = A_3,\\
&\vdots\\
&\frac{\mathrm{d}^{\psi} A_{M\psi_3}}{\mathrm{d}t^{\psi}} = \gamma(a_0 - A) - \mu\frac{A^{\omega}}{A^{\omega} + \rho^{\omega}}(x_1 + x_2)
\end{aligned} \tag{51}$$

Thus, we analyze the asymptotic behavior of the system (51). Let us compute the Jacobian matrix at cancer-free equilibrium $\widetilde{E_0} = \left(\underbrace{0, \ldots, 0, 0}_{N-1}, a_0\right)$.

$$\mathrm{J}\left(\widetilde{E_0}\right) = \begin{Bmatrix} 0 & 1 & 0 & \cdots & 0 \\ \vdots & & & & \\ f(a_0) & 0 & \cdots & \cdots & 0 \\ \vdots & & & & \\ m(a_0) & 0 & & g(a_0) & 0 \\ \vdots & & & & \\ -\mu\frac{a_0^{\omega}}{a_0^{\omega}+\rho^{\omega}} & \cdots & -\mu\frac{a_0^{\omega}}{a_0^{\omega}+\rho^{\omega}} & \cdots & \cdots \end{Bmatrix}.$$

By Theorem 4.1 in [1], the cancer-free equilibrium is stable if and only if the eigenvalues of the matrix $J\left(\widetilde{E_0}\right)$ satisfy either $|\arg(\lambda)| > \psi\pi/2$ or solutions of the equation $|\arg(\lambda)| = \psi\pi/2$ have geometric multiplicity one. Further, the eigenvalues of the matrix $J\left(\widetilde{E_0}\right)$ are determined by the roots of the polynomial $\det\left(\mathrm{diag}\left(\lambda^{M\psi_1}, \lambda^{M\psi_2}, \lambda^{M\psi_3}\right) - J_2\right)$, where

$$J_2 = \begin{Bmatrix} f(a_0) & 0 & 0 \\ m(a_0) & g(a_0) & 0 \\ -\mu\frac{a_0^{\omega}}{a_0^{\omega}+\rho^{\omega}} & -\mu\frac{a_0^{\omega}}{a_0^{\omega}+\rho^{\omega}} & -\gamma \end{Bmatrix}.$$

Since J_2 is a lower triangular matrix, the set eigenvalues of $J\left(\widetilde{E_0}\right)$ are given by the following algebraic equations.

$$\lambda^{M\psi_1} = f(a_0), \lambda^{M\psi_2} = g(a_0), \quad \text{and} \quad \lambda^{M\psi_3} = -\gamma < 0. \tag{52}$$

If $f(a_0) > 0$ or $g(a_0) > 0$, then at least one eigenvalue is positive which in tern implies that $\arg(\lambda) = 0$. Thus, the cancer-free equilibrium is unstable.

If $f(a_0) < 0$ and $g(a_0) < 0$, then one can show that all solutions of the (52) satisfy $|\arg(\lambda)| > \psi\pi/2$. Thus, by Theorem 4.1 in [1], we conclude that the cancer-free equilibrium is locally asymptotically stable. This finalizes the proof. □

Proposition 15 The CR only equilibrium E_2 is locally asymptotically stable if $f(A_1) < \frac{2q_m(A_1)g(A_1)}{q_n(A_1)+\theta\delta_2}$ and $g(A_1)(q_n(A_1) - \theta\delta_2 - 2) < 0$.

Proof In order to analyze the asymptotic behavior of E_2, we again consider the system (51). The CR only equilibrium E_2 of the system (42)–(44) corresponds to the CR only equilibrium $\widetilde{E_2} = (\underbrace{0, \ldots, 0, 0}_{M\chi_1+M\chi_2-1}, \theta\frac{(q_n(A_1)-D_2A_1)}{q_n(A_1)+\theta\delta_2}, \underbrace{0, \ldots, 0}_{M\chi_3-1}, A_1)$ of the system (51). The Jacobian matrix evaluated at $\widetilde{E_2}$ is given by

$$\mathrm{J}(\widetilde{E_2}) = \begin{bmatrix} 0 & 1 & 0 & \cdots & \cdots & 0 \\ \vdots & & & & & \\ f(A_1) - \frac{2q_m(A_1)g(A_1)}{q_n(A_1)+\theta\delta_2} & 0 & \cdots & \cdots & \cdots & 0 \\ \vdots & & & & & \\ m(A_1) - \frac{q_n(A_1)}{\theta}\overline{x_2} & 0 & \cdots & \cdots & \frac{g(A_1)(q_n(A_1)-\theta\delta_2-2)}{q_n(A_1)+\theta\delta_2} & 0 \\ \vdots & & & & & \\ q_n'(A_1)\big(1 - \frac{\overline{x_2}}{\theta}\big)\overline{x_2} - D_2'(A_1)\overline{x_2} & 0 & \cdots & \cdots & -\gamma - \mu\frac{\omega\rho^\omega A_1^{\omega-1}}{(A_1^\omega+\rho^\omega)^2}\overline{x_2} & 0 \end{bmatrix}$$

By Theorem 4.1 in [1], the CR only equilibrium is asymptotically stable if the eigenvalues of the matrix $J\big(\overline{E}\big)$ satisfy $|\arg(\lambda)| > \psi\pi/2$. Further, the eigenvalues of the matrix $J\big(\overline{E}\big)$ are determined by the roots of the polynomial $\det\big(\mathrm{diag}\big(\lambda^{M\psi_1}, \lambda^{M\psi_2}, \lambda^{M\psi_3}\big) - J_3\big)$, where

$$J_3 = \begin{Bmatrix} f(A_1) - \frac{2q_m(A_1)g(A_1)}{q_n(A_1)+\theta\delta_2} & 0 & 0 \\ m(A_1) - \frac{q_n(A_1)}{\theta}\overline{x_2} & \frac{g(A_1)(q_n(A_1)-\theta\delta_2-2)}{q_n(A_1)+\theta\delta_2} & q_n'(A_1)\big(1 - \frac{\overline{x_2}}{\theta}\big)\overline{x_2} - D_2'(A_1)\overline{x_2} \\ -\mu\frac{A_1^\omega}{A_1^\omega+\rho^\omega} & 0 & -\gamma - \mu\frac{\omega\rho^\omega A_1^{\omega-1}}{(A_1^\omega+\rho^\omega)^2}\overline{x_2} \end{Bmatrix}$$

It is seen that the set of eigenvalues satisfy the following algebraic equations

$$\begin{aligned} \lambda^{M\psi_1} &= f(A_1) - \frac{2q_m(A_1)g(A_1)}{q_n(A_1)+\theta\delta_2}, \\ \lambda^{M\psi_2} &= g(A_1)(q_n(A_1) - \theta\delta_2 - 2), \\ \lambda^{M\psi_3} &= -\gamma - \mu\frac{\omega\rho^\omega A_1^{\omega-1}}{(A_1^\omega+\rho^\omega)^2}\bar{x} < 0. \end{aligned}$$

If $f(A_1) < \frac{2q_m(A_1)g(A_1)}{q_n(A_1)+\theta\delta_2}$ and $g(A_1)(q_n(A_1) - \theta\delta_2 - 2) < 0$, then it is easy to show that all eigenvalues satisfy the inequality $|\arg(\lambda)| > \beta\pi/2 = \pi/2M$. Thus, the CR only equilibrium E_2 is locally asymptotically stable. This finalizes the proof. □

Table 3 Comparison of mean squared error (MSE) for androgen and prostate-specific antigen (PSA) for the first 1.5 cycles for two population BK (TPBK) and logistic (TPL) models with respect to fractional counterparts (TPFBK) and (TPFL)

Model	PSA			Androgen		
	Min	Mean	Max	Min	Mean	Max
TPL	0,088222	2,438892	44,1696	0,801594	10,16664	45,70097
TPFL	0,076367	1,994876	33,404229	0,699228	10,893238	42,223214
TPBK	0,353765	3,766446	69,38941	0,998116	12,53949	55,10578
TPFBK	1,225462	2,079395	34,058538	0,741277	11,467617	52,934657

TPL two population logistic, *TPFL* two population fractional logistic, *TPBK* two population BK, *TPFBK* two population fractional BK

Following the same methodology expressed for one population models above, we find the MSE values of the PSA and androgen values of the TPBK and TPL models. When a MSE comparison is made for PSA values, it is clear that the fractional conjugates of these models reduce the error. When the same study is done for androgen values, it is seen that the MSE values either remain almost the same for fractional conjugates or fall (Table 3).

3.10 Case 1: Without Relapse (Patients 1, 15, 17, 63)

See Figs. 20 and 21.

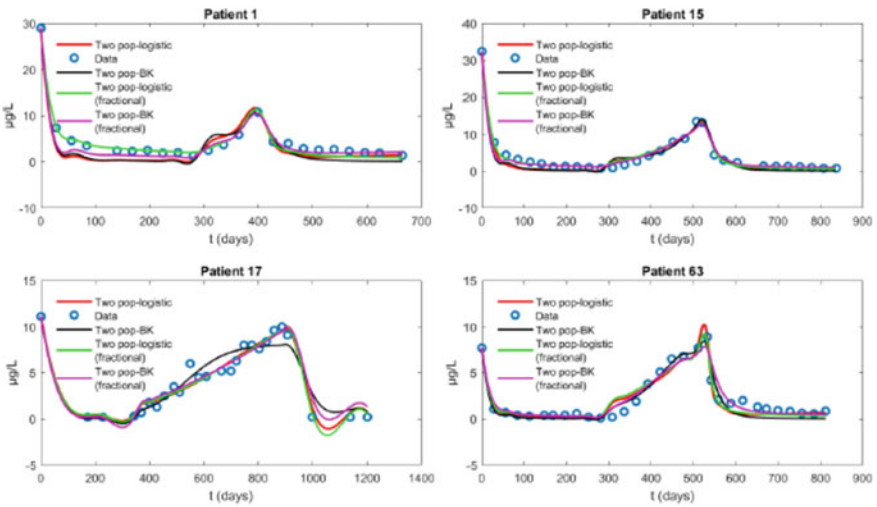

Fig. 20 Simulations of PSA fittings for every one population model for 1.5 cycles of treatment

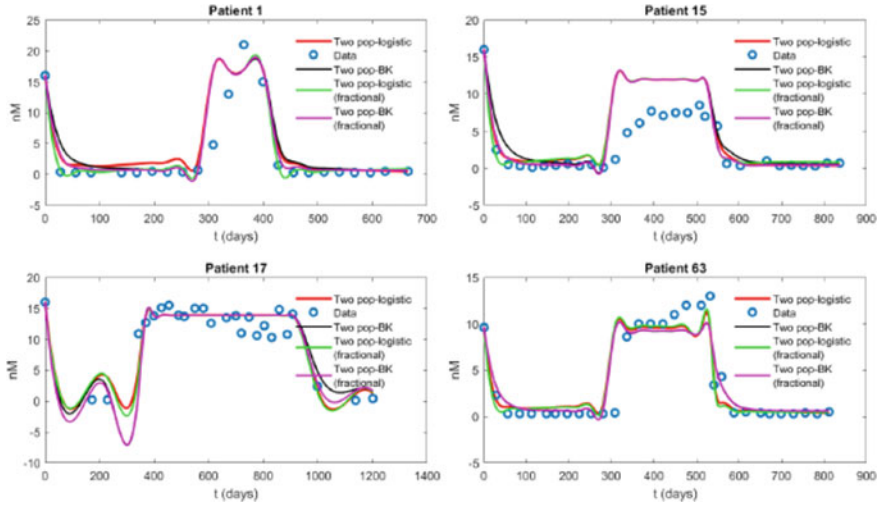

Fig. 21 Simulations of androgen fittings for every one population model for 1.5 cycles of treatment

3.11 Case 2: With Metastasis (Without Relapse) (Patients 32, 64, 83)

See Figs. 22 and 23.

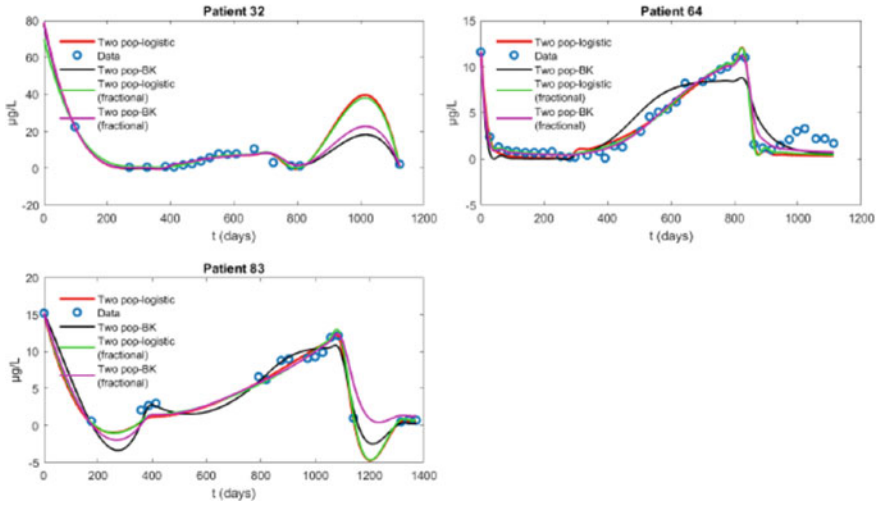

Fig. 22 Simulations of PSA fittings for every one population model for 1.5 cycles of treatment

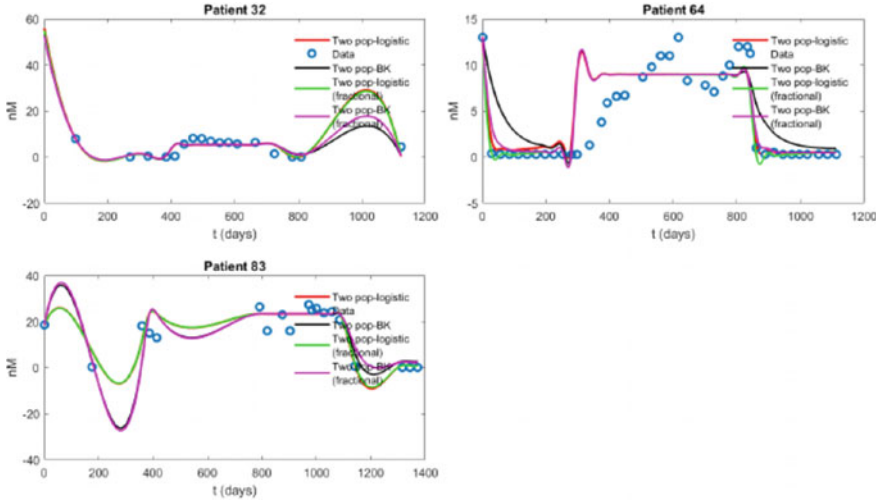

Fig. 23 Simulations of androgen fittings for every one population model for 1.5 cycles of treatment

3.12 Case 3: With Relapse (Patients 12, 19, 36, 101)

Here, α_i $(i = 1, 2, 3, 4)$ values represent the net growth rate of CS and CR cells and the diffusion rate of serum androgen and PSA, respectively. For example, for Patient 1 (in OPFBK model), while CS cells show a bit faster growth than CR cells, and androgen is diffusing faster than PSA. The values of other patients can be similarly interpreted (Figs. 24 and 25; Tables 4, 5, 6, and 7).

3.13 Conclusion

With this section, we generate the fractional versions of one and two population BK and logistic models and reach this result that the fractional conjugates of these models either reduce the MSE values or leave them almost the same. Therefore, fractional derivation generally occurs as a good alternative to modeling with better data fitting. On the other hand, multi-order fractional systems created in this section are not very desirable to include more parameters than ordinary equivalents. To this end, the focus should be on creating fractional models with fewer parameters without compromising on the basis of biological facts in future studies. Also, these fractional models should be solved especially with the implicit PI trapezoidal rule about which is emphasized that it is more reliable than the other methods stated in the paper [2] with fewer errors and then should be analyzed with respect to the change of MSE values. In addition to this, fractional and delay versions of TPBK and TPL models can be compared, and the advantages and disadvantages against each other

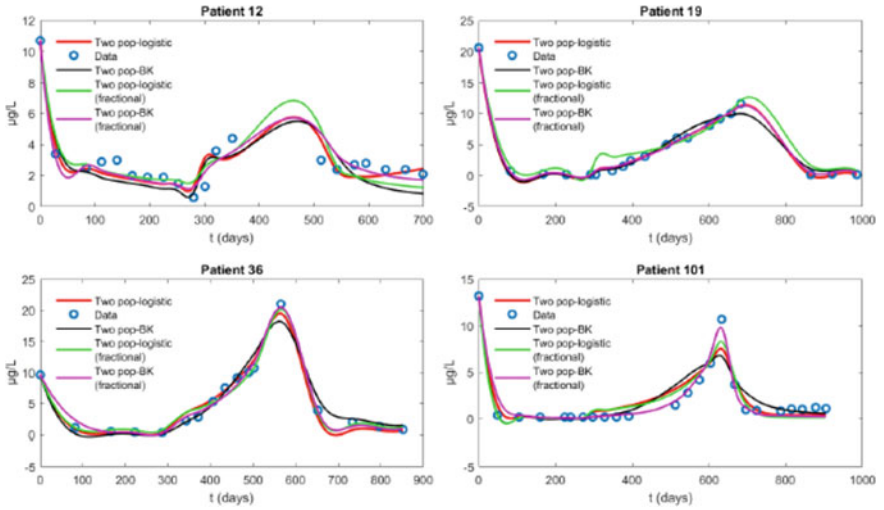

Fig. 24 Simulations of PSA fittings for every one population model for 1.5 cycles of treatment

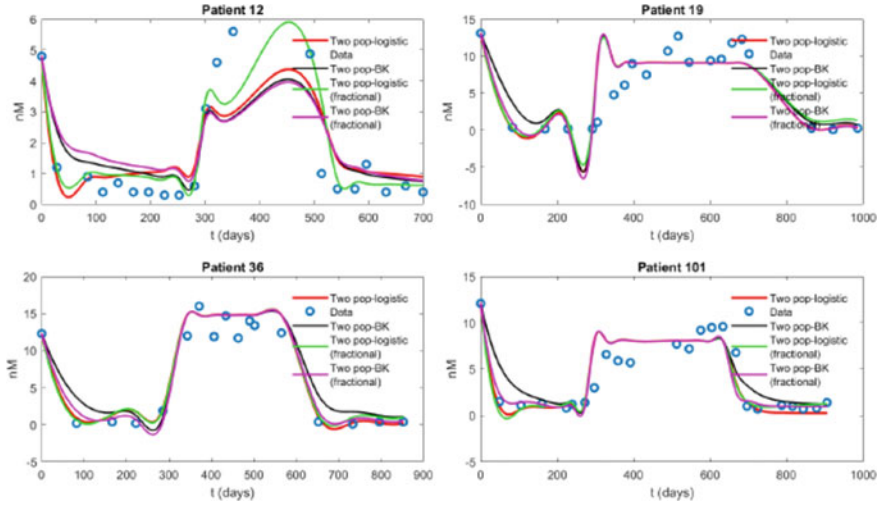

Fig. 25 Simulations of androgen fittings for every one population model for 1.5 cycles of treatment

can be investigated. Finally, to make predictions on resistance, imposing an ensemble Kalman filter into these fractional models may be another direction for future work.

Table 4 Optimal alpha values for patients in numerical simulations (for OPFBK model)

Patient	α_1	α_2	α_3	α_4
1	0,624761	0,500000	0,990000	0,500000
15	0,832262	0,743663	0,988468	0,516263
17	0,766818	0,513626	0,989989	0,989332
63	0,795169	0,964573	0,911281	0,500004
32	0,989981	0,588649	0,989991	0,538456
64	0,594303	0,724906	0,989996	0,500006
83	0,500006	0,500150	0,989998	0,575342
12	0,500000	0,743973	0,989999	0,500000
19	0,714895	0,500859	0,989668	0,644767
36	0,733337	0,500071	0,989991	0,716358
101	0,989984	0,775649	0,989987	0,989843

Table 5 Optimal beta values for patients in numerical simulations (for OPFL model)

Patient	β_1	β_2	β_3	β_4
1	0,989966	0,501054	0,969879	0,500121
15	0,989404	0,515919	0,953509	0,502991
17	0,989557	0,561484	0,989507	0,971678
63	0,989626	0,506515	0,856649	0,501253
32	0,989494	0,552440	0,805364	0,515453
64	0,987768	0,630501	0,989197	0,500776
83	0,990000	0,747626	0,989999	0,504897
12	0,935231	0,726912	0,920229	0,595430
19	0,964345	0,833712	0,972717	0,654057
36	0,988691	0,524407	0,989012	0,510935
101	0,989789	0,724291	0,989215	0,981611

4 Research Results

The results of the research presented so far can be summarized as follows:

- First of all, the mathematical model we have formed by accepting that androgens have a positive effect on CR cell proliferation has created proliferation terms using logistic growth terms. Moreover, this model, which provides generally better data fittings than the BK model, does not compete only with the BK model but also compete with other models in the literature.
- The stability analysis of the logistic models reveals whether the cancer cells can be completely eliminated, what restrictions should be made if they cannot be, what conditions should be provided to keep them at a local stable level, what the CS and

Table 6 Optimal chi values for patients in numerical simulations (for TPFBK model)

Patient	χ_1	χ_2	χ_3	χ_4
1	0,500519	0,715126	0,989899	0,500083
15	0,628557	0,707221	0,989803	0,500245
17	0,989421	0,705671	0,989774	0,972518
63	0,747118	0,826512	0,989854	0,528226
32	0,725712	0,819878	0,966505	0,709687
64	0,622157	0,705622	0,989871	0,500917
83	0,989976	0,731043	0,989981	0,986780
12	0,947467	0,537256	0,656281	0,516388
19	0,939402	0,718373	0,989187	0,684748
36	0,969878	0,680010	0,989877	0,635165
101	0,989781	0,603203	0,989088	0,712237

Table 7 Optimal psi values for patients in numerical simulations (for TPFL model)

Patient	ψ_1	ψ_2	ψ_3	ψ_4
1	0,977256	0,602088	0,941998	0,524273
15	0,955527	0,779392	0,934645	0,547061
17	0,928922	0,765377	0,884623	0,832938
63	0,852426	0,862360	0,911937	0,617110
32	0,982154	0,536804	0,913867	0,533610
64	0,949548	0,533055	0,943829	0,500418
83	0,989897	0,783728	0,989889	0,957508
12	0,876736	0,917007	0,717897	0,572673
19	0,989981	0,588552	0,989951	0,617169
36	0,989994	0,582408	0,989987	0,500968
101	0,989936	0,501915	0,967355	0,967479

CR cells are meant to live together, or the conditions in which CR cells override CS cells.

- Afterward, the fractional versions of both the proposed logistic models and the BK model have been built to show that they provide better data fittings with respect to ordinary forms by reducing the MSE value, as we have claimed before. For fractional models, stability analysis was performed, too, and conditions affecting cancer dynamics were determined.
- This research process, above all, has provided the opportunity to get in touch with other researchers, especially Professor Yang Kuang, in the courses and seminars that have been attended from time to time in an internationally educated university and benefit from their knowledge and experience, and has opened a horizon that is difficult to win without coming here. In addition, this research period has provided

the opportunity to follow new trends and the latest studies in the field of mathematical biology closely. With these studies, which we initiated as an introduction to mathematical oncology, we will try to create domestic research groups that will lead to similar studies in our country and will try to make the studies most suitable for clinical use. We will also continue to expand our international connections while continuing to move across this field with new competitive project ideas.

Acknowledgements: O.O.M. is supported by the Scientific and Research Council of Turkey within the context of 2214-A-Ph.D. Research Fellowship Abroad and by the Scientific Research Unit of Ankara University with the grant number 17L0430006. We are also grateful to Nicholas Bruchovsky for the clinical data set.

References

1. W. Deng, C. Li, Analysis of fractional differential equations with multi- orders. Fractals **15**(2), 173–182 (2007)
2. Y. Ding, H. Ye, A fractional-order differential equation model of HIV infection of CD4 + T-Cells. Math. Comput. Model. **50**, 386–392 (2009)
3. W. Lin, Global existence theory and chaos control of fractional differential equations. J. Math. Anal. Appl. **332**, 709–726 (2007)
4. Z.M. Odibat, N.T. Shawagfeh, Generalized Taylors formula. Appl. Math. Comput. **186**, 286–293 (2007)
5. O.O. Mizrak, N. Ozalp, Fractional analog of a chemical system inspired by Braess' paradox. Comp. Appl. Math. **37**, 2503–2518 (2018). https://doi.org/10.1007/s40314017-0462-9
6. R. Garrappa, Numerical solution of fractional differential equations: A survey and a software tutorial. Mathematics **6**, 16 (2018). https://doi.org/10.3390/math6020016
7. S.R. Denmeade, J.T. Isaacs, A history of prostate cancer treatment. Nat. Rev. Cancer **2**(5), 389–396 (2002)
8. N. Bruchovsky, L. Klotz, J. Crook, S. Malone, C. Ludgate, W.J. Morris, M.E. Gleave, S.L. Goldenberg, Final results of the Canadian prospective phase II trial of intermittent androgen suppression for men in biochemical recurrence after radiotherapy for locally advanced prostate cancer: Clinical parameters. Cancer **107**(2), 389–395 (2006)
9. T. Nishiyama, Serum testosterone levels after medical or surgical androgen deprivation: A comprehensive review of the literature. Urol. Oncol. **32**(1), 38–e17–28 (2013)
10. J.M. Crook, C.J. O'Callaghan, G. Duncan, D.P. Dearnaley, C.S. Higano, E.M. Horwitz, E. Frymire, S. Malone, J. Chin, A. Nabid, P. Warde, T. Corbett, S. Angyal, S.L. Goldenberg, M.K. Gospodarowicz, F. Saad, J.P. Logue, E. Hall, P.F. Schellhammer, K. Ding, L. Klotz, Intermittent androgen suppression for rising PSA level after radiotherapy. N. Engl. J. Med. **367**(10), 895–903 (2012)
11. A.H. Bryce, E.S. Antonarakis, Androgen receptor splice variant 7 in castration resistant prostate cancer: Clinical considerations. Int. J. Urol. **23**(8), 646–653 (2016)
12. B. Feldman, D. Feldman, The development of androgen-independent prostate cancer. Nat. Rev. Cancer **1**(1), 34–45 (2001)
13. P.C. Deaths, Cancer Statistics, 2011 The impact of eliminating socioeconomic and racial disparities on premature cancer deaths (2011)
14. T.L. Jackson, A mathematical model of prostate tumor growth and androgen-independent relapse. Discret. Contin. Dyn. Syst.-Ser. B **4**, 187–202 (2004)
15. A.M. Ideta, G. Tanaka, T. Takeuchi, K. Aihara, A mathematical model of intermittent androgen suppression for prostate cancer. J. Nonlinear Sci. **18**, 593–614 (2008)

16. T. Shimada, K. Aihara, A nonlinear model with competition between prostate tumor cells and its application to intermittent androgen suppression therapy of prostate cancer. Math. Biosci. **214**, 134–139 (2008)
17. S.E. Eikenberry, J.D. Nagy, Y. Kuang, The evolutionary impact of androgen levels on prostate cancer in a multi-scale mathematical model. Biol. Direct **5**, 24 (2010)
18. T. Portz, Y. Kuang, J.D. Nagy, A clinical data validated mathematical model of prostate cancer growth under intermittent androgen suppression therapy. AIP Adv. **2**, 011002 (2012)
19. J. Baez, Y. Kuang, Mathematical models of androgen resistance in prostate cancer patients under intermittent androgen suppression therapy. Appl. Sci. 6, 352 (2016). doi: 10.3390/app6110352
20. T. Portz, Y. Kuang, J. Nagy, A clinical data validated mathematical model of prostate cancer growth under intermittent androgen suppression therapy. AIP Adv. **2**, 1–14 (2012)
21. Y. Kuang, J.D. Nagy, S.E. Eikenberry, in *Introduction to Mathematical Oncology* (Chapman and Hall/CRC Mathematical and Computational Biology, 2016)
22. M. Droop, Some thoughts on nutrient limitation in algae1. J. Phycol. **9**(264), 272 (1973)
23. E.M. Rutter, Y. Kuang, Global dynamics of a model of joint hormone treatment with dendritic cell vaccine for prostate cancer. DCDS-B **22**, 1001–1021 (2017)
24. N. Bruchovsky, L. Klotz, J. Crook, S. Malone, C. Ludgate, W.J. Morris, M.E. Gleave, S.L. Goldenberg, Final results of the Canadian prospective phase II trial of intermittent androgen suppression for men in biochemical recurrence after radiotherapy for locally advanced prostate cancer. Cancer **107**, 389–395 (2006)
25. N. Bruchovsky, Clinical Research. 2006. Available online: http://www.nicholasbruchovsky.com/clinicalResearch.html. Accessed on 18 July 2018
26. H. Vardhan Jain, A. Friedman, Modeling prostate cancer response to continuous versus intermittent androgen ablation therapy. Discret. Contin. Dyn. Syst.-Ser. B. **18**
27. Y. Hirata, N. Bruchovsky, K. Aihara, Development of a mathematical model that predicts the outcome of hormone therapy for prostate cancer. J. Theor. Biol. **264**, 517–527 (2010)
28. Q. Guo, Z. Lu, Y. Hirata, K. Aihara, Parameter estimation and optimal scheduling algorithm for a mathematical model of intermittent androgen suppression therapy for prostate cancer. Chaos **23**(4), 43125 (2013)
29. Y. Tao, Q. Guo, K. Aihara, A partial deferential equation model and its reduction to an ordinary differential equation model for prostate tumor growth under intermittent hormone therapy. J. Math. Biol. 1–22 (2013)
30. Y. Hirata, K. Akakura, C.S. Higano, N. Bruchovsky, K. Aihara, Quantitative mathematical modeling of PSA dynamics of prostate cancer patients treated with intermittent androgen suppression. J. Mol. Cell Biol. **4**(3), 127–132 (2012)
31. Y. Hirata, S.-I. Azuma, K. Aihara, Model predictive control for optimally scheduling intermittent androgen suppression of prostate cancer. Methods **67**(3), 278–281 (2014)

Toward the Realization of the "Europe 2020" Agenda for Economic Growth in the European Union: An Empirical Analysis Based on Goal Programming

Cinzia Colapinto, Davide La Torre, Danilo Liuzzi and Aymeric Vié

1 Introduction

As awareness on environmental issue has spiked, with dissemination of social movements in favor of stronger environmental respect and profusion of international treaties, optimal resource allocation and economic growth cannot be distinguished from sustainability and ecological considerations. Nowadays, countries are subject to numerous binding frameworks for policy making (i.e., the 1992 United Nations Framework Convention on Climate Change and the more recent Cop 21 conference organized in Paris in 2016), introducing greenhouse gas emission targets. As scientific reports (such as the Intergovernmental Panel on Climate Change) encounter large media coverage, the importance of these targets can be expected to increase, further adding constraints on economic policies design and implementation.

These added international and social incentives to more environment-friendly measures yet encounter complex national and international economic situations.

C. Colapinto
Department of Management, Ca' Foscari University of Venice, Venice, Italy

D. La Torre (✉)
SKEMA Business School, Sophia Antipolis Campus, Sophia Antipolis, France
e-mail: davide.latorre@skema.edu

D. Liuzzi
Department of Economic, Business, Mathematical and Statistical Sciences, University of Trieste, Trieste, Italy

A. Vié
Department of Economics and Management, and Quantitative Methods, University of Milan, Milan, Italy

Paris School of Economics, Paris, France

New England Complex Systems Institute, Cambridge, MA, USA

Sciences Po Saint Germain en Laye, Saint Germain en Laye, France

H. Dutta (ed.), *Mathematical Modelling in Health, Social and Applied Sciences*, Forum for Interdisciplinary Mathematics, https://doi.org/10.1007/978-981-15-2286-4_6

Indeed, after the last global financial crisis most developed countries show low growth and budget recovery, and improving, but still stagnant, labor markets, thus balancing these fundamental policy topics with the more recent environmental stakes is evidently a struggle. An illustrative example did arise in France, when important social unrest from the "yellow jackets" originally emerged from an increase in the taxation of most polluting fuels. These elements further demonstrate the importance of careful consideration of each of the goals in the design of public policy. While such arbitrages are difficult to make by decision makers, several tools can bring a substantial help and support in policy design. The problem of simultaneously conciliating economic, environmental, social, and energy policy targets is well captured by the mathematical models of multiple criteria decision analysis (MCDA), which indeed allow to identify the optimal policy design accounting for all different objectives.

The European Union is a typical and interesting case study. After the 2008 economic crisis, in 2010 European institutions and notably the European Council, and European Commission, proposed the introduction of numerical multi-criteria policy targets, the so-called Europe 2020 strategy [1]. This highly varied set of national targets covers a large subset of national issues, such as economic growth, employment, education and research, reduction of greenhouse gas emissions, progress toward higher energy efficiency, and struggle against poverty and social exclusion. While these sets of actions and associated objectives (such as a decrease by 20% of GHG emissions or an increase in energy efficiency by 20%) are formulated at the European Union scale, the objectives are nationally transposed, leaving European Union members a relative margin of freedom in their implementation. This feature creates a context in which MCDA techniques can be applied to evaluate the satisfaction of Europe 2020 objectives by European Union states.

The application of MCDA techniques, and specifically goal programming (GP) and its variants and extensions, to macroeconomic policies is not novel. They have been widely used to tackle similar issues of decision making with competing objectives, as they allow to identify a Pareto optimal solution with respect to the goals involved. Nevertheless, the use of GP models has before emerged in engineering, where they have been implemented to analyze supply chain optimization problems facing imprecise assessment of both demand and information [2, 3], vendor problems [4, 5], production planning [6], or also decision making in manufacturing [7, 8]. The increasing popularity of GP models, already noticed by Ignizio [9], gave birth for instance to financial portfolio selection applications [10, 11], with consideration of manager preferences [12], highlighting the flexibility of GP approaches to integrate these constraints as well, and also in the context of optimal allocation of renewable energies with quota constraints [13]. In marketing, decision-making problems seeing an application of GP methods are sales operation [14] and media planning [15, 16]. In agricultural and environmental management, as the GP methodology constitutes an adequate tool to model environmental interactions [17], uses of MCDA approaches have dealt with agricultural land planning [18, 19], outsourcing management [20], and crop selection [21].

The extant MCDA literature covers a large variety of models and applications reviewed by Colapinto et al. [22], and the GP formulation has been applied to macroeconomic policy design and evaluation. Some researchers [23–25] have used weighted goal programming (WGP) to study the global sustainability and development of the GCC countries. Other authors employ this methodology to study macroeconomic policies in Spain [26, 27] through the joint analysis of optimal economic and environmental policies. More recently, Omrani et al. [28] have applied a WGP model to more efficiently plan regional sustainable development and workforce allocation in Iran. Zografidou et al. [29] have suggested an optimal design of renewable energy production in Greece by weighting social, financial, and production goals. Nomani et al. [30] implemented a fuzzy goal programming approach to evaluate the satisfaction of sustainability policy targets in India. Finally, Bravo et al. [31] have studied the robustness of WGP models applied to offshore wind-farm site location determination. Indeed, GP and its variants offer the ability to balance different objectives and are relevant tools to study the satisfaction of several mutually conflicting objectives. Recent economic works provide multi-criteria models emphasizing the comparison of welfare criteria [32] and studying the economy/environment trade-off through externality modeling, notably establishing that "independently of the relative importance of economic and environmental factors, it is paradoxically optimal for the economy to asymptotically reach the maximum pollution level that the environment is able to bear" in the multi-criteria decision making [33].

Our chapter proposes a GP model to describe and measure the progress of each European country toward the satisfaction of the main Europe 2020 goals, and expands the following authors' previous work with the use of a fuzzy GP model [34]. With respect to Vié et al. [34], this chapter presents a more detailed analysis with updated and more complete data. The Europe 2020 strategy is used as a reference framework for activities in the EU at national and regional levels. Our model is linear and includes seven economic sectors and four different criteria. The data have been collected using information provided by the European Commission and the EU statistics office, Eurostat. Eurostat regularly publishes comprehensive progress reports for the targets. We referred to the targets for different sectors indicated in the Europe 2020 agenda, including employment, research and development (R&D), climate change and energy, education, and poverty and social exclusion. In particular, the climate change and energy targets are:

(a) greenhouse gas emissions 20% lower than 1990 levels
(b) 20% of energy coming from renewables
(c) 20% increase in energy efficiency.

Our model mainly focuses on the analysis of a sustainable economic growth and combines the economic objective (GDP) together with GHG emissions and energy efficiency. Our model does not distinguish skilled from unskilled labor force and supposes that population level is equal to the labor force.

The chapter is organized as follows. Section 2 reviews some basic notions in MCDA and GP. Section 3 presents the model formulation, including a detailed description of the economic sectors and the criteria. Section 4 describes how the data

have been collected, while Sect. 5 illustrates the results. As usual, Sect. 6 concludes. In the appendices (1–10), we report data calculation and model results.

2 A Review of Multiple Criteria Decision Analysis and Goal Programming

Multiple criteria decision analysis or multiple criteria decision making (MCDM) is a discipline that considers decision-making situations involving multiple and conflicting criteria. Some examples of conflicting criteria that have been considered in the literature are quality, cost, price, satisfaction, risk, and others. Considering multiple criteria with respect to a single criterion leads to more informed and better decisions. However, typically there does not exist a unique optimal solution and it is necessary to use a decision maker's preferences to differentiate between solutions. Many important advances have been developed in this field in the last sixty years including new approaches, innovative methods, and sophisticated computational algorithms. A classical MCDA model involves several criteria, objectives, or attributes, to be considered simultaneously. These dimensions are usually conflicting, and the decision maker will look for the solution of the best compromise.

MCDA models are based on the notion of partial or Pareto order which can be summarized as follows: Given two vectors $a, b \in R^P$, we say that $a \leq b$ if and only if $a_i \leq b_i$ for all $i = 1 \ldots p$. The general formulation of a MCDA model can be stated as follows [35]: Given a set of p criteria $f_1, f_2, \ldots, f_p$, determine the optimal solution of the vector function $f(x) := \left[f_1(x),\ f_2(x), \ldots, f_p(x)\right]$ under the condition that $x \in D \subseteq \Re^n$ where D designates the set of feasible solutions. The optimal solution has to be understood in Pareto sense: We say that a point $\hat{x} \in D$ is a global Pareto optimal solution or global Pareto efficient solution if $f(x) \in f(\hat{x}) + (-R_+^p \backslash \{0\})^c$ for all $x \in D$. Practically speaking, a Pareto optimal solution describes a state in which goods and resources are distributed in such a way that it is not possible to improve a single criterion without also causing at least one other criterion to become worse off than before the change. In other words, a state is not Pareto efficient if there exists a certain change in the allocation of goods and resources that may result in some criteria being in a better position with no criterion being in a worse position than before the change. If a point $x \in D$ is not Pareto efficient, there is potential for a Pareto improvement and an increase in Pareto efficiency.

GP is a well-known technique to solve MCDA models. The GP model is based on a notion of distance, and it seeks to minimize positive or negative deviations of the achievement levels with respect to the aspiration ones. It is an aggregating methodology that allows obtaining a solution representing the best compromise that can be achieved by the decision maker, as noted by Jayaraman et al. [24].

The WGP model is one of the possible variants of the GP model that have been proposed in the literature. In this context, the decision maker can show different appreciation of the positive and negative deviations based on the relative importance

of the objective and this is expressed by introducing different weights w_i^+ and w_i^-. The mathematical formulation of the WGP model reads as follows:

$$\text{Minimize} \sum_{i=1}^{p} w_i^+ \delta_i^+ + w_i^- \delta_i^-$$

subject to:

$$f_i(x) + \delta_i^- - \delta_i^+ = g_i \quad i = 1 \ldots p$$
$$x \in F$$
$$\delta_i^-,\ \delta_i^+ \geq 0 \quad i = 1 \ldots p$$

3 Model Formulation

As previously mentioned, MCDA usually deals with decision making with multiple and conflicting criteria, objectives, or attributes and considers decision makers' preferences to determine the best compromise among optimal solutions. GP was first introduced by Charnes and Cooper [36]. Given a set of n linear criteria $F_i(X_1, X_2, \ldots, X_n) = \sum_{j=1}^{n} A_{ij} X_{ij}$ and a set of goals G_i the WGP model reads as

$$\sum_{i=1}^{p} \alpha_i^+ D_i^+ + \alpha_i^- D_i^-$$

Subject to:

$$\begin{gathered} \sum_{j=1}^{n} A_{ij} X_j + D_i^- + D_i^+ = G_i,\ i = 1 \ldots p \\ X \in \Omega \\ D_i^-,\ D_i^+ \geq 0,\ i = 1 \ldots p \end{gathered} \tag{1}$$

where Ω is a feasible set, α_i^+ and α_i^- are weights, X_j are the input variables representing the number of employees in each economic sector, the coefficient A_{ij} states the contribution of the jth variable to the achievement of the ith criterion, and D_i^- and D_i^+ are the positive and negative deviations with respect to the aspirational goal levels $G_i, i = 1, \ldots, n$, respectively.

Previous researchers—see, i.e., Andre' et al. [26] and San Cristóbal [27] in Spain, Jayaraman et al. [23, 25] in the GCC countries—have shown how the government can determine its optimal policy according to different criteria using the GP approach. Considering the Europe 2020 objectives established by the European Commission, our macroeconomic model simultaneously considers the following four criteria with their respective units:

(a) F_1 is the economic output (in million US$)

(b) F_2 is the GHG emissions (in Gg of CO_2 equivalent kilo tonnes)
(c) F_3 is the electric consumption (in thousand tonnes of oil equivalent)
(d) F_4 is the number of employees (in thousands).

The decision variables in our GP model are all relevant economic sectors for the analysis. They are equivalent to the main activities identified by NACE Rev. 2 classification:

- X_1: agriculture, forestry, and fishing
- X_2: energy industry
- X_3: manufacturing industry
- X_4: construction and residential
- X_5: trade, transports, distribution, and repairing
- X_6: commercial services (information, communication, financial, and insurance activities)
- X_7: general services (administrative, state, technical, scientific, education, health, and social services).

Each criterion F_i is linear with respect to each decision variable X_j and takes the form:

$$\begin{aligned}
F_1(X_1, X_2, \ldots, X_7) &= A_{11}X_1 + A_{12}X_2 + \cdots + A_{17}X_7 \\
F_2(X_1, X_2, \ldots, X_7) &= A_{21}X_1 + A_{22}X_2 + \cdots + A_{27}X_7 \\
F_3(X_1, X_2, \ldots, X_7) &= A_{31}X_1 + A_{32}X_2 + \cdots + A_{37}X_7 \\
F_4(X_1, X_2, \ldots, X_7) &= A_{41}X_1 + A_{42}X_2 + \cdots + A_{47}X_7
\end{aligned}$$

The seven economic categories aim to represent—for each country—its economic, social, environmental, and energy characteristics. We also replicate the choice made in previous publications [23, 27] that fit well the NACE (second revision) classification of economic activities created within the European Union. Such a classification is complete, aiming to describe efficiently whole economic patterns. Our choice of categories is restricted either to specific global categories, such as agriculture combined with fishing and forestry, either to an aggregate category as commercial services, which includes both financial and insurance activities and information and communication economics.

The GP problem we intend to solve can then be written in the following form:

$$\begin{aligned}
\text{Minimize } & (\alpha_1^+ D_1^+ + \alpha_1^- D_1^-) + \left(\alpha_2^+ D_2^+ + \alpha_2^- D_2^-\right) + \left(\alpha_3^+ D_3^+ + \alpha_3^- D_3^-\right) \\
& + \left(\alpha_4^+ D_4^+ + \alpha_4^- D_4^-\right) \\
\text{Subject to :}
\end{aligned}$$

$$
\begin{gathered}
A_{11}X_1 + A_{12}X_2 + \cdots + A_{17}X_7 - D_1^+ + D_1^- = G_1 \\
A_{21}X_1 + A_{22}X_2 + \cdots + A_{27}X_7 - D_2^+ + D_2^- = G_2 \\
A_{31}X_1 + A_{32}X_2 + \cdots + A_{37}X_7 - D_3^+ + D_3^- = G_3 \\
X_1 + X_2 + \cdots + X_7 - D_4^+ + D_4^- = G_4 \\
X_1 \geq \Omega_1, X_2 \geq \Omega_2, X_3 \geq \Omega_3, X_4 \geq \Omega_4, X_5 \geq \Omega_5, X_6 \geq \Omega_6, X_7 \geq \Omega_7 \\
X_j,\ j = 1, 2, \ldots, 7 \text{ are positive and integer} \\
D_i^+, D_i^- \geq 0, \quad i = 1, 2, 3, 4
\end{gathered}
\tag{2}
$$

The variables D_i^+, D_i^- describe the positive and the negative deviations. The input variables X_j take integer values and must be at least equal to the positive number Ω_j which is the number of employees in each sector of our analysis (see Appendix 1). A_{1j} is the economic output per capita (worker) for the jth economic sector (see Appendix 2). A_{2j} describes the GHG emission per capita (worker) for the jth economic sector (see Appendix 3). A_{3j} models the energy consumption per capita (worker) for the jth economic sector (see Appendix 4).

For each country, we solve the above model (2) which takes then the form of a mixed-integer linear programming (MILP) model. We have implemented it using LINGO. So far, we have assumed equal weights for each objective. In other words, all the weights α_n^+ and α_n^-, $n = 1, \ldots, 4$, are equal. Our choice is motivated by the fact that the Europe 2020 agenda does not provide any priority or ranking among the objectives and all of them must be jointly met. However, these weights might be modified at the regional level when the national preferences and the economic situation of each country have to be taken into account.

4 Data Collection and Computation

In this section, we briefly discuss how we have estimated all parameters involved in the model. For each constraint, we describe how the data have been collected and how the estimations have been computed. We also provide their interpretation.

4.1 The Gross Domestic Product Constraint

The GDP per capita denoted A_{1i} (see Appendix 2) is expressed in US$ thousands per capita. It is computed for a given sector i in each country by taking the ratio of the economic output (GDP) for the selected sector i in US$ millions in 2015 [37–40, 35] and the number of employees (expressed in thousands) in the same year for the same economic sector i [41, 42]. Following the Europe 2020 recommendation that the economic output must be at least conserved with respect to the year of analysis, and following GDP growth rate projections of the International Monetary Fund (IMF)

and the OECD up to 2020, we defined the economic GDP objective G_1 as the sum of the forecast GDP of all sectors. For instance, a country with a GDP of 100 in 1990 forecasted to grow by 10% to 2020 will have an economic output target of 110. The resulting GDP constraint can be expressed as follows: The economic output of the country needs to be at least as good as current projections.

4.2 The Greenhouse Gas Constraint

The average sectorial greenhouse gas (GHG) emissions per capita A_{2i} (see Appendix 3 for the data) is expressed in tonnes of CO_2 equivalent per capita, for a given sector i in each country. It is computed by dividing sectorial GHG emissions (in thousands of tonnes) in the selected country in 2015 and the number of employees (expressed in thousands) in the same year for the same economic sector and country [37–42]. This delivers the benchmark from which the environmental policy target G_2 is computed, according to the Europe 2020 objective consisting in a decrease by 20% of GHG emissions at the scale of the national economy, an objective that we apply to all sectors separately. For instance, a country with a GHG emission level of 100 in 1990 will have a GHG emission target of 80 at the horizon 2020.

4.3 The Energy Constraint

The average sectorial energy consumption per capita A_{i3} (see Appendix 4 for the data) is expressed in tonnes of oil equivalent per capita, for a given economic sector i in each country. In order to obtain its numerical values, we took the ratio of the energy consumption for the selected sector i in the selected country in thousands of tonnes of oil equivalent in 2015 [43],[1] and of the number of employees (expressed in thousands) in the same year for the same sector i and country [37–42]. The determination of the energy consumption targets G_3 proceeded by transforming the resulting consumption with the 20%[2] increases in energy efficiency imposed by the Europe 2020 strategy, with respect to the 1990 level constituting the benchmark of the policy set.

[1] Eurostat data in thousands of tonnes of oil equivalent (ktoe) on a net calorific value basis.

[2] Europe 2020 objectives in energy sector deal with an increasing of energy efficiency by 20%, which mathematically implies a reduction of energy consumption by 16.66% from the 1990 consumption to the horizon 2020.

4.4 The Employment Constraint

This constraint is simple, as the model aims at maintaining employment at the benchmark level set in the year of analysis. This constraint is declined in each economic sector, based on the number of jobs recorded in the year of data collecting [41, 42]. Natural population growth (and estimated forecasts for later years) was considered to formulate the aggregate employment goal G_4. Note that this constraint operates in the aggregate level, offering countries flexibility in the allocation of incoming workforce across economic sectors.

5 Model Implementation and Discussion

As said above, we implement our model using the software LINGO and the results are presented in Appendix 9. We have ticked with "x" any time there is a significant deviation value (detailed results table can be found in Appendix 10). In all simulations, we have normalized the weights to 1. We would like to point out that confidential and missing data for Cyprus, Croatia, and Malta restrict us to make less precise conclusions than those done for other countries.

From what we observed, the current trend will allow all European countries to have $D_4^+ = 0$, which means that the entire available labor force will be used for creating a sustainable development. This result outlines the need for a better integration of unemployed workforce, possibly through intensified training policies and inclusive measures in the labor market. In the context of automation, improving the effectiveness of changes in qualification seems relevant to ensure optimal economic performance, employment, and social inclusion.

In several countries, we observe a significant nonzero value for the deviation D_4^-, meaning that the satisfaction of the objectives of the model requires additional workforce to be integrated within the economy in specific sectors. In a context of increasing immigration toward European countries, this study outlines the necessity and the benefits coming from a more efficient integration of newcomers within the labor market in Eastern and Northern countries (for instance, Germany).

Some countries present a significant deviation in the values taken by D_1^-, standing for a negative deviation from the economic goal. For these countries, the satisfaction of the simultaneous objectives leads to a slower economic output than targeted. This can be interpreted as a lack of productivity that can be verified empirically comparing the average economic product of these countries, with economically well-performing countries. Improving competitiveness and production efficiency may result from organizational changes or evolutions in the length of work time permitted.

A significant deviation in the parameter D_1^+, a positive deviation from the economic goal, shows a great economic performance of the country, for which the

optimal allocation of workers to reach Europe 2020 goals leads to higher economic growth than expected (for instance, Eastern countries, Belgium, Luxemburg, Germany show this result).

Only two countries show a significant negative deviation from the environmental goal D_2^-. The optimal allocation of workers provides the achievement of the environmental goals in Czech and Slovak Republics. These results can be explained by the transformations of national economic patterns following the collapse of USSR during the early nineties and the dissolution of Czechoslovakia in 1993. It illustrates the significant progress made in switching to a cleaner energy production system after the Soviet period. A large number of European countries include in their optimal allocation a positive deviation D_2^+, stressing that GHG emissions at the optimal allocation are significantly higher than the objective (especially in the UK, France, and Spain). The importance and the wide diffusion of these positive deviations outlines the need for an increased transformation of European production systems leading to lower environmental impact sectors, especially in industry and agriculture, for which these countries show higher GHG emissions than average.

Five countries (Cyprus, Czech and Slovak Republics, Romania, and Sweden) show significant values in the deviation D_3^-. This result stands for a negative deviation from the energy consumption reduction goal which means that their optimal allocation goes beyond the required reduction of energy consumption. This result for the Czech and Slovak Republics and in Romania might be justified again by their national economic pattern transformation from former Soviet-linked countries into Eastern European countries.

Most countries in our sample show important and significant positive deviation D_3^+ from the energy production goal, outlining emergency and significant needs for a better energy efficiency, and development of renewable sources of energy, able to satisfy the Europe 2020 energy objective while keeping the other parameters—economic output, number of jobs, environmental impact—at least as good with respect to the sustainability objectives. Different measures may be implemented to reach these goals: for instance, development of renewable energies, intensified use of nuclear energy, or waste reduction.

6 Conclusion and Policy Implications

The GP model allows policy makers to identify the best combination of investments and choices that optimizes the multiple and competing objectives that usually coexist within a national strategy plan. To ensure that each member state tailors the Europe 2020 strategy in the most effective way, the European Commission has proposed that goals are translated into national targets and trajectories. The purpose of the European plan relies on the interactions among interrelated targets: indeed, investing in cleaner, low carbon technologies could help the environment, contribute to fighting climate change, and create new business and employment opportunities in Europe. However, some stakeholders will enjoy benefits only in the long term, and that is why these

changes meet resistance and conflicting objectives occur. Our implementation of a GP model for European countries, with respect to the Europe 2020 goals in reduction of GHG emissions and increase in energy efficiency, combined with economic output and employment constraints, outlines the need for a better integration and training of the incoming workforce in a context of increasing immigration flows, jointly with deep and sustained transformations of economic national systems toward a more energy-efficient production system, combined with the development of renewable energies in many EU countries.

Improving our model to represent more efficiently the reality and support public policies implies to identify the utility payoffs attached to each deviation that goes beyond the object of this chapter. For future research, it would be interesting considering that the utility, or preferences of the policy maker, can be taken into account by switching to a more sophisticated GP variant, where the appropriate coefficients for each sector of deviation are identified.

Acknowledgements The authors would like to thank the two anonymous referees for useful suggestions and thorough reviewing, and all the participants of the 12th Multi-objective Programming and Goal Programming (MOPGP) International Conference of Metz, France (2017), for their useful suggestions and remarks.

Appendix 1—Employment by Main Sector in EU (in Thousands)

Countries	Agriculture, forestry and fishing	Energy industry	Manufacturing industry	Construction and residential	Trade, transports, distribution, repairing	Commercial services (information, communication, financial, and insurance activities)	Public, administrative services, technical, scientific, education, health, and social services
Austria	176.4	57.8	631.5	297.2	1,171.6	241.4	1,510.8
Belgium	59.6	53.1	502	266.2	974,5	236.7	2,311
Bulgaria[a]	56.72	32.57	536.22	147.16	793,70	79.41	237.15
Croatia[b]	36.23	14.74	254.85	102.3	415,009	38.41	133.697
Cyprus[b]	0[c]	0[c]	27.68	18.51	116,087	9.13	33.22
Czech Rep.	158.9	128	1367.9	411.2	1246.4	226	1,458.1
Denmark	68	25	284	173	722	179	1,225
Estonia	24.3	13.6	117.9	51.9	151.9	35.7	197.1
Finland	108.1	31.6	339.3	189.8	525.8	144.4	1,022.8
France	766	318	2,678	1,789	6,238	1,618	12,572
Germany	620	571	7,516	2,450	9,961	2,301	17,011
Greece	471.7	50.3	337.9	181.4	1,300.8	163.2	1,227.6
Hungary	273.8	82.1	775.6	269.2	1,020.2	211.6	1,488.6
Ireland	110.2	22.6	202.9	139	564	152.2	716.9
Italy	910.4	312.4	3,833.2	1,552.1	6,164.6	1,260.8	7,756.6
Latvia	71.6	21.5	118.5	69.6	245.5	43.1	277.5

(continued)

(continued)

Countries	Agriculture, forestry and fishing	Energy industry	Manufacturing industry	Construction and residential	Trade, transports, distribution, repairing	Commercial services (information, communication, financial, and insurance activities)	Public, administrative services, technical, scientific, education, health, and social services
Lithuania	120.9	26.9	202.7	104.8	358.4	45.8	419.8
Luxembourg	4.6	4.4	32.3	41.5	93.5	62.4	149.3
Malta[b]	0[c]	0[c]	0[c]	9.99	57.72	6.91	26.28
Netherlands	192	67	767	457	2,19	503	4,249
Poland[b]	130.54	300.11	2,425.35	831.23	3,154.54	309.27	1,230.23
Portugal[d]	451.8	59.3	714.2	274	1,143.6	165.5	1,492.9
Romania[e]	85.466	123.239	1,180.1	365.32	1,384.74	157.36	44.20
Slovak Rep.	73.4	47.2	490.7	163.2	609	107.6	527.37
Slovenia	75.4	21.1	190.9	62.6	200.1	50.4	304.7
Spain	732	244.7	2057.7	1005.7	5,632.7	821.6	6,394.9
Sweden	112.3	66	580	340.4	981.5	270.7	2,233.3
UK	359.3	384.9	2,563	2,056.9	8,270.4	2,391.6	13,599.1

[a]Eurostat, Persons employed by NACE Rev. 2, 2014, data
[b]Eurostat source, cf. supra
[c]Data mentioned as confidential—Eurostat source
[d]Same source, OECD estimations
[e]Eurostat source, cf. supra. 2014
Source Eurostat [42] (if not otherwise specified)

Appendix 2—Economic Output (GDP) Per Economic Sector in EU Countries (US$ Millions)

Country	Agriculture, forestry, and fishing	Energy industry	Manufacturing industry	Construction and residential	Trade, transports, distribution, repairing	Commercial services (information, communication, financial and insurance activities)	Public, administrative services, technical, scientific, education, health, and social services
Austria	3,905.4	1,182.7	57,220.9	19,411.5	53,535.7	33,770	81,120.9
Belgium	2,745	233.5	52,417.2	19,956.6	65,047.5	38,275.1	133,183.7
Bulgaria	1,873.4	963.8	6,168.8	1,698.7	7,693.7	4,810.7	8,105.2
Croatia[a]	353	10	738.2	555.8	2,880.5	2,669.4	4,680.4
Cyprus	1,504.3	819.2	5,320.6	1,905.3	5,829.3	3,983.6	8,478.5
Czech Rep.	3,785.4	1,364.2	40,392.3	8,571.2	24,746.5	14,110.5	32,263
Denmark	2,900.8	3,477.8	34,516.9	11,031.9	43,738.1	25,541.2	74,420.8
Estonia	592.3	250.9	2,770.9	1,092.3	3,447.6	1,744	4,373.8
Finland	4,443	551	30,652	11,481	25,800	15,614	54,647
France	33,854	2,148	218,987	106,155	290,404	184,239	698,443
Germany	17,351	4,158	622,608	124,755	387,625	242,562	800,412
Greece	6,385.6	812.2	14,708.1	3,696.8	28,141.9	12,763	39,879.3
Hungary	3,800.8	152.9	22,618.7	3,816.2	15,443.7	7,980.1	24,123.4
Ireland	2,398	898.8	87,448.2	6,024.7	26,020.7	34,131.9	51,905.5
Italy	33,158.7	5,470	232,882	70.099	248,975.1	137,076.5	390,895.1
Latvia	723.9	105	2,652.4	1,381.7	5,057.1	1,919.5	4,924.3

(continued)

(continued)

Country	Agriculture, forestry, and fishing	Energy industry	Manufacturing industry	Construction and residential	Trade, transports, distribution, repairing	Commercial services (information, communication, financial and insurance activities)	Public, administrative services, technical, scientific, education, health, and social services
Lithuania	1,220.5	103.7	6,493.9	2,440.4	10,027.6	1,859.4	6,957.9
Luxembourg	112.9	31.3	2,461.8	2,340.4	7,538.8	15,240.8	12,295.6
Malta	103.6	0	728.2	345.6	1,361.7	1,081.8	2,426.3
Netherlands	10,965	12,573	71,120	28,048	116,686	74,264	221,426
Poland	9,921.8	6,170.6	75,087.1	29,881	91,052.8	30,637.6	86,313.4
Portugal	3,654.2	497.9	21,555.2	6,363.9	30,258.1	13,827.4	41,977.9
Romania	6,651.3	1,421	30,948.1	9,272.9	24,074.5	14,289.6	26,834.4
Slovak Rep.	794.3	127	7,737.8	1,826.3	6,032.5	2,782.6	8,815.3
Slovenia	2,600.5	362	15,940.8	5,577.4	9,519.4	5,927.7	14,916.6
Spain	25,004	2,110	138,914	54,554	163,329	78,783	265,940
Sweden	5,211.8	1.637	67,240	23,272.6	64,369.1	41,214.6	124,932.1
UK	14,981.3	23,174.5	224,465.4	141,518.8	357,250.9	315,841.9	708,262.2

[a]Due to missing data, Croatia data is extracted from Eurostat 2014 panel data

Source Eurostat data, NACE Rev. 2 classification, 2014, 2015

Appendix 3—Emissions of GHG[3] in Economic Sectors in EU Countries[4]

[3] CO_2, CH_4, N_2O, HFCs, PFCs, SF_6, NO_4, NO_X, NMVOC, PFC, PM (2, 5, and 10); summed and transformed in CO_2 equivalent and thousands of tonnes.

[4] United Nation—Framework Convention on Climate Change—Submitted National Communications, sixth edition, due January 1, 2014, data from 2011 in principle, in equivalent CO_2 emissions (Gg), data based on national accounts//Data confirmed in European Environment Agency Data//Eurostat—Air emissions national accounts by NACE Rev. 2 activity, 2014 data, in thousands of tonnes of CO_2 equivalent.

Countries	Agriculture, forestry, and fishing	Energy industry	Manufacturing industry	Construction and residential	Trade, transports, distribution, repairing	Commercial services (information, communication, financial and insurance activities)	Public, administrative services, technical, scientific, education, health, and social services
Austria	7,577.10	13,988.43	26,499.85	380.91	7,669.89	223.77	1,640.62
Belgium	9,365.88	21,862.84	33,771.89	439.74	9,999.41	1,183.62	6,221.01
Bulgaria	7,510.28	28,950.92	5,877.21	56. 7	4,830.7	50.59	393.02
Croatia	3,442.21	6,275.44	4,173.59	37.08	1,358.21	116.72	521.48
Cyprus	633	3,722	1,732.52	33.76	493.40	35.97	110.95
Czech Rep.	8,065	58,424	18,556.53	187.47	9,215.65	180.71	2,859.96
Denmark	9,671.85	19,747.81	5,580.18	103.51	39,777.66	117.05	1,180.64
Estonia	1,270.52	14,875.63	2,514.08	27.22	1,694.24	14.86	396.05
Finland	5,881.11	24,628.42	13,845.4	8,914	10,471.12	254.99	1,863.34
France	90,340	53,015.88	95,234.84	3,228.13	52,662.67	2,244.39	20,766.18
Germany	63,936	353,793	160,692.01	2,995.36	97,468.43	4,665.26	26,064.59
Greece	8,965.84	53,840.83	13,348.27	57.2	6,718.45	39.01	847.56
Hungary	5,925	17,459	9,699.31	100.21	5,387.57	561.29	2,264.7
Ireland	17,730	11,935	6,325.86	144.57	4,249.55	255.5	866.24
Italy	31,486	132,413	89,590.47	1,739.74	49,530.1	517.48	4,842.16
Latvia	2,456	2,084	1,342.62	18.84	2,509.77	14.25	290.3

(continued)

(continued)

Countries	Agriculture, forestry, and fishing	Energy industry	Manufacturing industry	Construction and residential	Trade, transports, distribution, repairing	Commercial services (information, communication, financial and insurance activities)	Public, administrative services, technical, scientific, education, health, and social services
Lithuania	3,756	4,467	4,823.88	14.3	7,480.83	18.38	218.76
Luxembourg	663	1,003	1,458.00	17.2	3,879.1	111.98	219.8
Malta	89	1,914	43.96	6.30[a]	3,443.38	12.95	61.88
Netherlands	18,097	63,000	42,131.76	941.46	32,802.36	635.74	8,057.37
Poland	29,930	174,672	62,271.56	548.26	33,550.04	1,430.56	9,534.95
Portugal	6,958	16,506	15,795.2	664.9	7,167.8	133.8	1,417.9
Romania	17,093	35,558	23,034.06	153.4	8,817.3	464.34	2,215.37
Slovak Rep.	2,935	9,280	17,598.00	16.65	4,884.97	5.02	888.43
Slovenia	1,691	6,359	2,289.37	50.13	4,011.70	8.68	220.23
Spain	36,262	87,124	75,513.46	957.57	37,214.06	617.25	4,408.9
Sweden	7,338	10,974	14,001.58	63.07	13,820.01	180.91	1,545.78
UK	43,735	178,850	83,588.16	3,020.55	94,951.03	1,523.58	19,002.70

[a]Eurostat estimate

Appendix 4—Energy Consumption[5] in Economic Sectors in EU Countries

[5] In thousands of tonnes of oil equivalent (ktoe) on a net calorific value basis.

Country	Agriculture, forestry, and fishing	Energy industry[a]	Manufacturing industry	Construction and residential	Trade, transports, distribution, repairing	Commercial services (information, communication, financial and insurance activities)	Public, administrative services, technical, scientific, education, health, and social services
Austria	539	1,935	7,517	5,627	8,197	565.2	2,260.8
Belgium	645	8,393	10,638	7,390	8,699	851.6	3,406.4
Bulgaria	191	518	2,622	2,165	2,946	185.2	740.8
Croatia	233	563	1,101	2,183	1,882	142.2	568.8
Cyprus	39	24	220	288	596	39.6	158.4
Czech Rep.	593	2,908	6,829	5,673	5,881	559.6	2,238.4
Denmark	727	251	2,090	3,956	4,014	364.8	1,459.2
Estonia	132	113	566	888	741	91.8	367.2
Finland	718	1,150	10,325	5,064	4,136	574.6	2,298.4
France	4,516	14,003	25,883	37,318	43,544	4,206.6	16,814.4
Germany	9,386[b]	22,120	54,882	51,287	54,998	6,581.4	26,325.6
Greece	281	705	3,088	3,786	5,640	342.4	1,369.6
Hungary	599	1,676	3,923	4,431	3,910	448.8	1,795.2
Ireland	221	216	2,233	2,561	3,677	246.4	985.6
Italy	2,776	7,187	25,280	29,541	37,009	2,933.2	11,732.8
Latvia	153	89	791	1,239	987	121.8	487.2

(continued)

(continued)

Country	Agriculture, forestry, and fishing	Energy industry[a]	Manufacturing industry	Construction and residential	Trade, transports, distribution, repairing	Commercial services (information, communication, financial and insurance activities)	Public, administrative services, technical, scientific, education, health, and social services
Lithuania	105	1,070	971	1,400	1,644	118	472
Luxembourg	25	36	613	478	2,096	78.8	315.2
Malta	5	4	47	72	185	21.5	102.5
Netherlands	3,546	14,186	13,181	9,120	10,280	1,265.2	5,060.8
Poland	3,401	5,323	14,166	18,945	15,639	1,559	6,236
Portugal	424	1,435	4,393	2,569	5,439	380.8	1,523.2
Romania	422	1,564	6,204	7,390	5,290	353.6	1,414.4
Slovak Rep.	138	919	3,296	1,952	2,199	261.4	1,045.6
Slovenia	74	147	1,230	1,040	1,797	85.4	341.6
Spain	2,766	4,106	19,229	14,698	28,098	1,767.6	7,070.4
Sweden	377	1,969	10,757	6,633	7,732	883.4	3,533.6
UK	973	6,892	23,124	35,140	39,784	3,177.8	12,711.2

[a]Non-energy use (consumption of raw materials)

[b]State of the Art on Energy Efficiency in Agriculture, Country data on energy consumption in different agro-production sectors in the European countries, agree, FP7 Program of the EU, 2012

Source International Energy Agency [43] data, Eurostat

Appendix 5—Europe 2020 GP Goals

Goals	Economy	Environment		Energy		Labor (in thousands)	
Country	GDP 2020 output, G_1^a	GHG 1990 adjusted emissions[b]	GHG 2020 adjusted emissions objective G_2^c	1990 adjusted level of consumption[d]	Europe 2020 objective adjusted consumption, G_3^e	Total number of jobs in 2015	Total number of jobs in 2020 (G_4)
Austria	25,3207.24	44,783.98751	37,318.4968	19,257.3521	16,047.1515	4086.7	4,127.7308
Belgium	219,980.146	104,774.2633	87,308.3936	36,863.2895	30,718.1791	4403.1	4,627.70235
Bulgaria	20,124.1921	86,528.42057	72,104.1329	17,070.5778	14,224.9125	1882.951	1,367.26662
Croatia	24,608.6206	13,146.9679	10,955.3684	6,995.8871	5,829.67272	995.229	811.482554
Cyprus	99,634.8986	4,698.694239	3,915.42191	938.4375	781.999969	204.633	247.772675
Czech Rep.	119,073.993	153,336.5209	127,775.323	34,344.7404	28,619.4722	4,996.5	4,996.5
Denmark	153,603.942	88,577.76917	73,811.855	12,862	10,717.9046	2,676	2,812.50289
Estonia	83,171.9581	11,192.33462	9,326.57244	5,901.53571	4,917.74971	592.4	563.366506
Finland	820,160.365	48,751.5178	40,624.6398	21,492.7429	17,909.9026	2,361.8	2,421.43841
France	2,190,576.46	371,294.9451	309,400.078	141,807.95	118,168.565	25,979	30,116.7812
Germany	1,239,551.34	965,454.0876	804,512.891	236,892.325	197,402.374	40,430	35,989.5619
Greece	103,397.869	86,248.26403	71,870.6784	14,426.8645	12,021.9062	3,732.9	3,255.44646
Hungary	173,794.38	67,836.52567	56,528.1768	21,972.4803	18,309.6678	4,121.1	3,360.23242
Ireland	692,546.877	39,259.86781	32,715.2478	6,853.88889	5,711.34561	1,907.8	2,764.46669
Italy	602,875.178	381,169.0226	317,628.147	110,702.862	92,248.6952	21,790.1	19,003.055
Latvia	32,592.0349	19,742.82409	16,451.6953	6,347.48718	5,289.36107	847.3	716.423094
Lithuania	23,923.4809	51,061.97919	42,549.9473	11,442.0408	9,534.65261	1,279.3	1,070.55496
Luxembourg	37,281.0115	8,118.19132	6,794.88883	3,004.65	2,503.77485	388	465.291916

(continued)

(continued)

Goals	Economy	Environment		Energy		Labor (in thousands)	
Country	GDP 2020 output, G_1^a	GHG 1990 adjusted emissions[b]	GHG 2020 adjusted emissions objective G_2^c	1990 adjusted level of consumption[d]	Europe 2020 objective adjusted consumption, G_3^e	Total number of jobs in 2015	Total number of jobs in 2020 (G_4)
Malta	269,440.916	3,692.682825	3,077.1126	262.2	218.49126	100.9	111.401753
Netherlands	544,074.804	189,398.4085	157,825.694	51,490	42,906.617	10148	10,878.5305
Poland	209,057.592	387,013.087	322,498.005	63,467.7451	52,887.672	8,381.264	8,091.99793
Portugal	137,296.491	44,726.91459	37,270.9379	12,174.1519	10,144.7208	4,301.3	3,848.52231
Romania	70,362.1455	199,171.7597	165,969.827	42,563.6129	35,468.2586	3,340.422	2,752.17912
Slovak Rep.	51,076.038	65,111.064	54,257.0496	14,912.72	12,426.7696	2,018.469	2,048.92824
Slovenia	482,344.805	16,395.04576	13,661.9916	3,792.5	3,160.29025	905.2	923.449412
Spain	530,605.115	205,972.288	171,636.708	30,622.8788	25,518.0449	16,889.3	16,805.0222
Sweden	1,069,709.51	61,950.71469	51,623.5306	58,353.6378	48,626.0864	4,584.2	5,161.35035
UK	1,107,326.7	619,593.5555	516,307.31	129,764.154	108,132.47	29,625.2	33,846.48

[a]Based on Eurostat data previously mentioned, combined with growth rate forecasts from IMF, European Commission, OECD for each year, in millions of US$

[b]In thousands of tonnes of CO_2 equivalent, adjusted to remain consistent and consider the representability of the global economic national patterns in respect to the GHG emissions criteria, Eurostat data

[c]In thousands of tonnes of CO_2 equivalent, adjusted in the same way, Eurostat data

[d]Eurostat data for Europe 2020 Statistics, 1990, in million tonnes of oil equivalent; adjusted data to remain consistent and consider the representability of the global economic national patterns

[e]Europe 2020 objectives in energy sector deal with an increasing of energy efficiency by 20%, which mathematically implies a reduction of energy consumption by 16.66% from the 1990 consumption to the horizon 2020: Assume that $X = a * Y$ where X is the energy consumption, a the efficiency and Y the total product, the possible uses of energy; if we increase a by 20%, we obtain $X' = 1,2 * a * Y$, so $a * Y = X'/1,2$ which implies $(5/6) * X = a \times Y$, so $X' = (1 - 5/6) * X$

Appendix 6—A_{ij} Coefficients for the Economic Constraint (in Thousands of US$ Per Capita)

Country	Agriculture, forestry, and fishing	Energy industry	Manufacturing industry	Construction and residential	Trade, transports, distribution, repairing	Commercial services (information, communication, financial and insurance activities)	Public, administrative services, technical, scientific, education, health, and social services
Austria	22.1394558	20.4619377	90.6110847	65.314603	45.6945203	139.892295	53.6940032
Belgium	46.057047	4.39736347	104.416733	74.9684448	66.7496152	161.703	57.6303332
Bulgaria	33.0277494	29.5889233	11.5043192	11.542983	9.69341215	60.57748	34.1762278
Croatia	9.74357559	0.67847208	2.89660585	5.43325252	6.94081333	69.4993361	35.007517
Cyprus[a]	–	–	192,218208	102,91131	50,214925	436,224266	255,222757
Czech Rep.	23.8225299	10.6578125	29.5286936	20.844358	19.8543806	62.4358407	22.1267403
Denmark	42.6588235	139.112	121.53838	63.7682081	60.5790859	142.688268	60.7516735
Estonia	24.3744856	18.4485294	23.5021204	21.0462428	22.6965109	48.8515406	22.1907661
Finland	41.1008326	17.4367089	90.3389331	60.4899895	49.0680867	108.130194	53.4288228
France	44.1958225	6.75471698	81.7725915	59.3376188	46.5540237	113.868356	55.5554407
Germany	27.9854839	7.28196147	82.8376796	50.9204082	38.9142656	105.415906	47.052613
Greece	13.5374179	16.1471173	43.5279669	20.3792723	21.634302	78.2046569	32.4855816
Hungary	13.8816654	1.86236297	29.1628417	14.1760773	15.1379141	37.713138	16.2054279
Ireland	21.7604356	39.7699115	430.991621	43.3431655	46.1359929	224.256899	72.4027061
Italy	36.4221221	17.5096031	60.7539393	0.04516397	40.3878759	108.721843	50.3951603
Latvia	10.1103352	4.88372093	22.3831224	19.8520115	20.5991853	44.5359629	17.7452252

(continued)

(continued)

Country	Agriculture, forestry, and fishing	Energy industry	Manufacturing industry	Construction and residential	Trade, transports, distribution, repairing	Commercial services (information, communication, financial and insurance activities)	Public, administrative services, technical, scientific, education, health, and social services
Lithuania	10.0951199	3.85501859	32.0370005	23.2862595	27.9787946	40.5982533	16.5743211
Lux.	24.5434783	7.11363636	76.2167183	56.3951807	80.628877	244.24359	82.35499
Malta[a]	–	–	–	34.5876701	23.5898413	156.623715	92.3355025
Neth.	5.7109375	187.656716	92.7249022	61.3741794	53.4032037	147.642147	52.1124971
Poland	76.0040753	20.5614702	30.9592842	35.9481056	28.8640225	99.0645684	70.1604906
Portugal	8.08809208	8.39629005	30.1809017	23.2259124	26.4586394	83.5492447	28.1183602
Romania	77.82393	11.5304409	26.2250254	25.3829519	17.3855993	90.8071834	607.126858
Slovak Rep.	10.8215259	2.69067797	15.7689016	11.1905637	9.90558292	25.8605948	16.7156204
Slovenia	34.4893899	17.1563981	83.5034049	89.0958466	47.5732134	117.613095	48.9550377
Spain	34.1584699	8.62280343	67.5093551	54.2448046	28.9965736	95.8897274	41.5862641
Sweden	46.4096171	24.8030303	115.931034	68.3683901	65.5823739	152.251939	55.9405812
UK	41.6957974	60.2091452	87.579165	68.8019836	43.1963267	132.063012	52.0815495

[a]Due to missing or confidential data, some coefficients for these countries were undetermined

Appendix 7—A_{ij} Coefficients for the Environmental Constraint (in Tonnes of CO_2 Equivalent Per Capita)

Countries	Agriculture, forestry, and fishing	Energy industry	Manufacturing industry	Construction and residential	Trade, transports, distribution, repairing	Commercial services (information, communication, financial and insurance activities)	Public, administrative services, technical, scientific, education, health, and social services
Austria	42.9540816	242.01436	41.9633001	1.28165882	6.54650905	0.92695112	1.08592799
Belgium	157.145638	411.729567	67.2746833	1.65191961	10.2610713	5.0005112	2.69191129
Bulgaria	132.405063	888.801154	10.9605196	0.38526668	6.08626768	0.63702874	1.65720044
Croatia	95.012559	425.771084	16.3766647	0.36249707	3.2727218	3.03874092	3.90046897
Cyprus[a]	–	–	62.5911127	1.82332289	4.25026919	3.93933421	3.33982541
Czech Rep.	50.7551919	456.4375	13.5657073	0.45590467	7.39381659	0.79959735	1.96142651
Denmark	142.233088	789.9124	19.6485282	0.59830636	55.0937161	0.6539162	0.96378857
Estonia	52.2847737	1093.79632	21.3237998	0.52454721	11.1536471	0.41627451	2.00936073
Finland	54.4043478	779.38038	40.8057619	46.9652266	19.9146482	1.76585873	1.8218068
France	117.937337	166.716604	35.5619279	1.80443432	8.44223549	1.38713597	1.65178086
Germany	103.122581	619.602452	21.3799912	1.22259592	9.78500452	2.02749544	1.53221974
Greece	19.0075048	1070.39423	39.5035987	0.31532525	5.16486009	0.23903186	0.69042033
Hungary	21.6398831	212.655298	12.505557	0.37224368	5.28089492	2.65258507	1.52136101
Ireland	160.889292	528.097345	31.1772351	1.04006475	7.53465957	1.67869251	1.20831915
Italy	34.5847979	423.857234	23.3722407	1.12089621	8.03460079	0.41043702	0.62426334
Latvia	34.301676	96.9302326	11.3301181	0.27066092	10.2231039	0.33055684	1.04611532

(continued)

(continued)

Countries	Agriculture, forestry, and fishing	Energy industry	Manufacturing industry	Construction and residential	Trade, transports, distribution, repairing	Commercial services (information, communication, financial and insurance activities)	Public, administrative services, technical, scientific, education, health, and social services
Lithuania	31.0669975	166.05948	23.798145	0.13640267	20.8728432	0.40135371	0.52110291
Lux	144.130435	227.954545	45.1394118	0.41445783	41.4877005	1.79450321	1.47220362
Malta[a]	–	–	–	–	59.6524149	1.87548863	2.35491114
Netherl.	9.42552083	940.298507	54.9305841	2.06008096	15.0125195	1.26389066	1.89629889
Poland	229.273113	582.036287	25.6752885	0.65958235	10.6354683	4.62561718	7.75055518
Portugal	15.4006197	278.347386	22.1159339	2.42664234	6.26775096	0.80845921	0.94976221
Romania	199.99766	288.528794	19.5187671	0.4199031	6.36748251	2.95076956	50.1226046
Slovak Rep.	39.986376	196.610169	35.8630589	0.10201593	8.02129228	0.04663569	1.68465344
Slovenia	22.4270557	301.374408	11.9924987	0.80079872	20.0484908	0.1722619	0.72278635
Spain	49.5382514	356.044136	36.6979929	0.95213781	6.60678946	0.75128286	0.6894394
Sweden	65.3428317	166.272727	24.1406586	0.18527615	14.0804982	0.6683044	0.69214973
UK	121.722794	464.666147	32.6134042	1.46849774	11.4808266	0.63705344	1.39734997

[a]Due to missing or confidential data, some coefficients for these countries were undetermined

Appendix 8—A_{ij} Coefficients for the Energy Constraint[6]

[6]In tonnes of oil equivalent.

Countries	Agriculture, forestry, and fishing	Energy industry	Manufacturing industry	Construction and residential	Trade, transports, distribution, repairing	Commercial services (information, communication, financial and insurance activities)	Public, administrative services, technical, scientific, education, health, and social services
Austria	3.05555556	33.4775087	11.9034046	18.9333782	6.99641516	2.34134217	1.49642573
Belgium	10.8221477	158.060264	21.1912351	27.7610819	8.92662904	3.59780313	1.47399394
Bulgaria	3.36730017	15.9027415	4.88982052	14.7115783	3.71171117	2.3320825	3.12364279
Croatia	6.43131193	38.1979782	4.32018835	21.3400328	4.53484141	3.70225728	4.25439613
Cyprus[a]	–	–	7.94797688	15.5557956	5.13408047	4.33639947	4.76821192
Czech Rep.	3.73190686	22.71875	4.992324	13.7962062	4.71838896	2.47610619	1.53514848
Denmark	10.6911765	10.04	7.35915493	22.867052	5.55955679	2.03798883	1.19118367
Estonia	5.43209877	8.30882353	4.80067854	17.1098266	4.87820935	2.57142857	1.8630137
Finland	6.64199815	36.3924051	30.4302977	26.6807165	7.86610879	3.97922438	2.24716465
France	5.89556136	44.0345912	9.66504854	20.8596982	6.98044245	2.59987639	1.3374483
Germany	15.1387097	38.7390543	7.30202235	20.9334694	5.5213332	2.86023468	1.54756334
Greece	0.59571762	14.0159046	9.13879846	20.8710033	4.33579336	2.09803922	1.11567286
Hungary	2.18772827	20.4141291	5.0580196	16.4598811	3.83258185	2.12098299	1.20596534
Ireland	2.00544465	9.55752212	11.0054214	18.4244604	6.51950355	1.61892247	1.3748082
Italy	3.04920914	23.0057618	6.595012	19.0329231	6.00347143	2.32645939	1.51262151
Latvia	2.13687151	4.13953488	6.67510549	17.8017241	4.0203666	2.82598608	1.75567568

(continued)

(continued)

Countries	Agriculture, forestry, and fishing	Energy industry	Manufacturing industry	Construction and residential	Trade, transports, distribution, repairing	Commercial services (information, communication, financial and insurance activities)	Public, administrative services, technical, scientific, education, health, and social services
Lithuania	0.86848635	39.7769517	4.79033054	13.3587786	4.58705357	2.57641921	1.12434493
Lux	5.43478261	8.18181818	18.9783282	11.5180723	22.4171123	1.26282051	2.11118553
Malta[a]	–	–	–	7.20576461	3.2049061	3.11278413	3.90074971
Netherl.	1.846875	211.731343	17.1851369	19.9562363	4.70480549	2.51530815	1.19105672
Poland	26.0527183	17.7371253	5.84080648	22.7916355	4.95761193	5.04091907	5.06897908
Portugal	0.93846835	24.1989882	6.15093811	9.37591241	4.75603358	2.30090634	1.02029607
Romania	4.93763602	12.6907878	5.2571905	20.2288405	3.82021725	2.24704821	32.000724
Slovak Rep.	1.88010899	19.470339	6.71693499	11.9607843	3.61083744	2.42936803	1.98267247
Slovenia	0.98143236	6.96682464	6.44316396	16.6134185	8.98050975	1.69444444	1.12110272
Spain	3.77868852	16.7797303	9.34489965	14.6146962	4.98837147	2.15141188	1.10563105
Sweden	3.35707925	29.8333333	18.5465517	19.4858989	7.87773816	3.26339121	1.58223257
UK	2.70804342	17.9059496	9.02223956	17.0839613	4.8104082	1.3287339	0.93470891

[a]Due to missing or confidential data, some coefficients for these countries were undetermined

Appendix 9—Model Results: Significant Deviations in the Results of the GP Model

	D_1^-	D_1^+	D_2^-	D_2^+	D_3^-	D_3^+	D_4^-	D_4^+
Austria	x			x		x		
Belgium		x				x		
Bulgaria		x						x
Croatia				x		x		x
Cyprus	x				x			
Czech Rep.	x		X		x			
Denmark		x		x		x		
Estonia				x		x		x
Finland	x			x		x		
France	x			x		x		
Germany		x				x		x
Greece		x		x		x		x
Hungary						x		x
Ireland	x			x		x		
Italy		x				x		x
Latvia								x
Lithuania		x				x		x
Luxembourg		x		x		x		
Malta	x			x		x		
Netherlands						x		
Poland		x				x		x
Portugal				x		x		x
Romania		x			x			x
Slovak Rep.	x		X		x			
Slovenia	x			x		x		
Spain		x		x		x		
Sweden	x				x			
UK		x		x		x		

Appendix 10—Model Results: Detailed Results of the GP Model

	D_1^-	D_1^+	D_2^-	D_2^+	D_3^-	D_3^+	D_4^-	D_4^+
Austria	44,601,580	0	0	20,677,980	0	10,695,990	0	0
Belgium	0	104,524,100	0	0	0	9,862,652	0	0
Bulgaria	0	15,466,390	0	0	0	0	0	843,812.3
Croatia	0	0	0	5,525,223	0	1,517,922	0	366,813
Cyprus	78,924,460	0	0	0	779,739,100	0	0	0
Czech Rep.	128,010,800	0	30,208,690	0	3,858,174	0	0	0
Denmark	0	50,315,840	0	2,490,308	0	2,306,434	0	0
Estonia	0	0	0	12,036,040	0	160,5637	0	1,439,487
Finland	614,629,900	0	0	25,281,090	0	477,1897	0	0
France	185,143,400	0	0	13,856,240	0	38,919,930	0	0
Germany	0	960,975,200	0	0	0	34,115,800	0	4,593,585
Greece	0	2,990,281	0	11,953,400	0	3,203,648	0	477,454
Hungary	0	0	0	0	0	4,439,730	0	3,559,426
Ireland	114,504,200	0	0	35,501,810	0	13,858,420	0	0
Italy	0	446,004,600	0	0	0	24,601,410	0	2,804,939
Latvia	0		0	0	0	0	0	560,002.7
Lithuania	0	5,675,707	0	0	0	1,462,300	0	339,897.1
Luxembourg	0	7,099,267	0	573,367.9	0	2,027,462	0	0
Malta	262,580,900		0	460,428.6	0	194,785.3	0	0
Netherlands	0	0	0	0	0	10,347,080	0	0
Poland	0	120,342,200	0	0	0	12,580,790	0	307,363

(continued)

(continued)

	D_1^-	D_1^+	D_2^-	D_2^+	D_3^-	D_3^+	D_4^-	D_4^+
Portugal	0	0	0	11,565,290	0	6,551,841	0	682,089.1
Romania	0	46,271,050	0	0	9,368,044	0	0	860,759.8
Slovak Rep.	22,878,340	0	500,978,300	0	2,023,232	0	0	0
Slovenia	425,353,700	0	0	970,167.7	0	1,611,453	0	0
Spain	0	198,577,300	0	706,137,600	0	52,337,540	0	0
Sweden	656,521,500	0	0	0	14,326,920	0	0	0
UK	0	898,065,800	0	396,765,400	0	1,751,931	0	0

References

1. European Commission, A Strategy for Smart, Sustainable and Inclusive Growth, COM 2020 (2010). Available at: http://ec.europa.eu/eu2020/pdf/COMPLET%20EN%20BARROSO%20%20%20007%20-%20Europe%202020%20-%20EN%20version.pdf
2. H. Selim, I. Ozkarahan, A supply chain distribution network design model: an interactive fuzzy goal programming-based solution approach. Int. J. Adv. Manuf. Technol. **36**(3–4), 401–418 (2008)
3. S.J.H. Tsai, A fuzzy goal programming approach for green supply chain optimization under activity-based costing and performance evaluation with a value-chain structure. Int. J. Prod. Res. **47**(18), 4991–5017 (2009)
4. M. Kumar, P. Vrat, R. Shankar, A fuzzy goal programming approach for vendor selection problem in a supply chain. Comput. Ind. Eng. **46**(1), 69–85 (2004)
5. C. Zhou, R. Zhao, W. Tang, Two-echelon supply chain games in a fuzzy environment. Comput. Ind. Eng. **55**(2), 390–405 (2008)
6. H. Selim, Ceyhun Araz, Irem Ozkarahan, Collaborative production–distribution planning in supply chain: a fuzzy goal programming approach. Transp. Res. Part E: Logistics Transp. Rev. **44**(3), 396–419 (2008)
7. M. Sheikhalishahi, S.A. Torabi, Maintenance supplier selection considering life cycle costs and risks: a fuzzy goal programming approach. Int. J. Prod. Res. **52**(23), 7084–7099 (2014)
8. K. Taghizadeh, M. Bagherpour, I. Mahdavi, An interactive fuzzy goal programming approach for multi-period multi-product production planning problem. Fuzzy Inf. Eng. **3**(4), 393–410 (2011)
9. J.P. Ignizio, Notes and communications of the (Re) discovery of fuzzy goal programming. Decis. Sci. **13**(2), 331–336 (1982)
10. M. Inuiguchi, J. Ramik, Possibilistic linear programming: a brief review of fuzzy mathematical programming and a comparison with stochastic programming in portfolio selection problem. Fuzzy Sets Syst. **111**(1), 3–28 (2000)
11. J. Watada, Fuzzy portfolio selection & its application to decision making. Tatra Mt. Math. Publ. **13**(4), 219–248 (1997)
12. N. Mansour, A. Rebaï, B. Aouni, Portfolio selection through the imprecise goal programming model: integration of Manager's preferences. J. Ind. Eng. Int. **3**(5), 1–8 (2007)
13. T.U. Daim, G. Kayakutlu, K. Cowan, Developing Oregon's renewable energy portfolio using fuzzy goal programming model. Comput. Ind. Eng. **59**(4), 786–793 (2010)
14. S.K. Tyagi, K. Yang, A. Tyagi, S.N. Dwivedi, Development of a fuzzy goal programming model for optimization of lead time and cost in an overlapped product development project using a Gaussian adaptive particle swarm optimization-based approach. Eng. Appl. Artif. Intell. **24**(5), 866–879 (2011)
15. A. Charnes, W.W. Cooper, J.K. Devoe, D.B. Learner, W. Reinecke W, A goal programming model for media planning. Manag. Sci. **14**(8), B-415–B-544 (1968)
16. P.C. Jha, R. Aggarwal, A. Gupta, Optimal media planning for multi-products in segmented market. Appl. Math. Comput. **217**(16), 6802–6818 (2011)
17. P. Linares, C. Romero, A multiple criteria decision-making approach for electricity planning in Spain: economic versus environmental objectives. J Oper. Res. Soc. **51**(6), 736–743 (2000)
18. A. Biswas, B.B. Pal, Application of fuzzy goal programming technique to land use planning in agricultural system. Omega **33**(5), 391–398 (2005)
19. D.K. Sharmar, R.K. Jana, A. Gaur, Fuzzy goal programming for agricultural land allocation problems. Yugoslav J. Oper. Res. **17**(1), 31–42 (2007)
20. C. Araz, P.M. Ozfirat, I. Ozkarahan, An integrated multicriteria decision-making methodology for outsourcing management. Comput. Oper. Res. **34**(12), 3738–3756 (2007)
21. S.H. Mirkarimi, R. Joolaie, F. Eshraghi, S.B. Abadi, Application of fuzzy goal programming in cropping pattern management of selected crops in Mazandaran province (case study Amol township). Int. J. Agric. Crop Sci. **6**(15), 1062–1067 (2013)

22. C. Colapinto, R. Jayaraman, S. Marsiglio, Multi-criteria decision analysis with goal programming in engineering, management and social sciences: a state-of-the art review. Ann. Oper. Res. **251**(1–2), 7–40 (2017)
23. R. Jayaraman, C. Colapinto, D. La Torre, T. Malik, A weighted goal programming model for planning sustainable development applied to gulf cooperation council countries. Appl. Energy, **185**(Part 2, 1), 1931–1939 (2017)
24. R. Jayaraman, C. Colapinto, D. La Torre, T. Malik, Multi-criteria model for sustainable development using goal programming applied to the United Arab Emirates. Energy Policy **87**, 447–454 (2015)
25. R. Jayaraman, D. Liuzzi, C. Colapinto, T. Malik, A fuzzy goal programming model to analyse energy, environmental and sustainability goals of the United Arab Emirates. Ann. Oper. Res. **251**(1–2), 255–270 (2017)
26. F.J. André, M.A. Cardenete, C. Romero, A goal programming approach for a joint design of macroeconomic and environmental policies: a methodological proposal and an application to the Spanish economy. Environ. Manage. **43**(5), 888–898 (2009)
27. J.R. San Cristóbal, A goal programming model for environmental policy analysis: application to Spain. Energy Policy **43**, 303–307 (2012)
28. H. Omrani, M. Valipour, A. Emrouznejad, Using weighted goal programming model for planning regional sustainable development to optimal workforce allocation: an application for provinces of Iran. Soc. Indic. Res. 1–29
29. E. Zografidou, K. Petridis, N.E. Petridis, G. Arabatzis, A financial approach to renewable energy production in Greece using goal programming. Renew. Energy **108**, 37–51 (2017)
30. M.A. Nomani, I. Ali, A. Fgenschuh, A. Ahmed, A fuzzy goal programming approach to analyze sustainable development goals of India. Appl. Econ. Lett. **24**(7), 443–447 (2017)
31. M. Bravo, D. Jones, D. Pla-Santamaria, G. Wall, Robustness of weighted goal programming models: an analytical measure and its application to offshore wind-farm site selection in United Kingdom. Ann. Oper. Res. **267**(1–2), 65–79 (2018)
32. C. Colapinto, D. Liuzzi, S. Marsiglio, Sustainability and intertemporal equity: a multicriteria approach. Ann. Oper. Res. **251**, 271–284 (2017)
33. S. Marsiglio, F. Privileggi, On the economic growth and environmental trade–off: a multi-objective analysis. Ann. Oper. Res. (2019). https://doi.org/10.1007/s10479-019-03217-y
34. A. Vié, D. Liuzzi, C. Colapinto, D. La Torre, The long-run sustainability of the European Union countries: assessing the Europe 2020 strategy through a fuzzy goal programming model. Manag. Decis. **57**(2), 523–542 (2019)
35. Y. Sawaragi, H. Nakayama, T. Tanino, Theory of multiobjective optimization, Academic Press, New York (1985)
36. A. Charnes, W.W. Cooper, *Management Models and Industrial Applications of Linear Programming* (Wiley, New York, 1961)
37. Eurostat/Economy and finance/National accounts/Annual national accounts/GDP and main components (2014)
38. Eurostat/Environment and energy/Energy/Energy Statistics/Quantities/Final energy consumption by product (2014), Final energy consumption by sector (2014)
39. Eurostat/General and regional statistics/European and national indicators for short-term analysis/Regional statistics by NUTS classification/Regional labour market statistics (2014)
40. Eurostat/General and regional statistics/European and national indicators for short term analysis/Regional statistics by NUTS classification/Regional labour market statistics/Regional employment—LFS annual series (2014)
41. OECD Statistics, National Accounts Data/Annual Aggregates/Main Aggregates/Population and Employment by main activity (2015). https://stats.oecd.org/Index.aspx?DataSetCode=SNA_TABLE3
42. Eurostat (2015) data available at https://ec.europa.eu/eurostat
43. International Energy Agency (2014)
44. A. Charnes, W.W. Cooper, R. Ferguson, Optimal estimation of executive compensation by linear programming. Manag. Sci. **1**, 138–151 (1955)

45. Eurostat/Environment and energy/Environment/Emissions of greenhouse gases and air pollutants (EEA)/Greenhouse gas emissions, Greenhouse gas emissions, base year 1990, Greenhouse gas emissions by sector (EEA) (2014)
46. Eurostat/General and regional statistics/European and national indicators for short-term analysis/National accounts—ESA (2010)
47. United Nation Framework Convention on Climate Change—Submitted National Communications

On the Poincaré-Andronov-Melnikov Method for Modelling of Grazing Periodic Solutions in Discontinuous Systems

Flaviano Battelli and Michal Fečkan

1 Introduction

Grazing is a typical phenomenon that may appear in discontinuous dynamical systems. This usually happens when a solution either has a zero velocity when touching an impact surface or when a solution just tangentially touching a switching surface. Grazing of a solution is well studied, so we refer the reader [1–5] and the references cited there in for motivation to discontinuous systems.

In this chapter, we investigate a persistence of a grazing solution under autonomous perturbation for the case of tangential grazing when a nearby dynamics is sliding. We derive a Melnikov like condition for the persistence of such grazing which is a generalization of periodic Melnikov method [6]. We also present an example for illustration. Both periodic and grazing solutions are itself interesting phenomenon in discontinuous systems, so the appearance of both simultaneously is much more interesting. This is the first reason why we study the persistence of such kind of solutions under perturbation. The second reason is that such kind of solutions determine borders in parametric discontinuous systems between the grazing, nongrazing and

Flaviano Battelli: This chapter has been performed within the activity of GNAMPA-INdAM-CNR.

Michal Fečkan: Partially supported by the Slovak Research and Development Agency under the contract No. APVV-18-0308 and by the Slovak Grant Agency VEGA No. 1/0358/20 and No. 2/0127/20.

F. Battelli
Department of Industrial Engineering and Mathematics,
Marche Polytechnic University, Ancona, Italy
e-mail: battelli@dipmat.univpm.it

M. Fečkan (✉)
Department of Mathematical Analysis and Numerical Mathematics,
Comenius University in Bratislava, Mlynská Dolina, 842 48 Bratislava, Slovakia
e-mail: Michal.Feckan@fmph.uniba.sk

Mathematical Institute of Slovak Academy of Sciences,
Štefánikova 49, 814 73 Bratislava, Slovakia

H. Dutta (ed.), *Mathematical Modelling in Health, Social and Applied Sciences*, Forum for Interdisciplinary Mathematics, https://doi.org/10.1007/978-981-15-2286-4_7

sliding, and periodicity and nonperiodicity phenomena as well. Consequently, this chapter fulfils a gap in the existing theory of modelling of discontinuous systems.

The chapter is organized as follows. In Sect. 2, we introduce the investigated problem and study the set of initial values near the periodic and grazing solution which determine grazing solutions under perturbation. The grazing Poincaré map is derived in Sect. 3. Section 4 is devoted for solving fixed points of the grazing Poincaré map via Lyapunov-Schmidt method in terms of the corresponding Melnikov conditions. Section 5 presents a class of examples to illustrate our theory.

2 Notations

Let $\Omega \subset \mathbb{R}^n$ be an open subset of $\mathbb{R}^n$ and $G, f_+, f_- : \Omega \to \mathbb{R}$ be C^r functions, $r \geq 2$. We set $\Omega_\pm := \{x \in \Omega \mid \pm G(x) > 0\}$ and assume the discontinuous equation

$$\dot{x} = f(x) := \begin{cases} f_+(x) \text{ if } x \in \Omega_+ \\ f_-(x) \text{ if } x \in \Omega_- \end{cases} \tag{2.1}$$

has a C^1 periodic solution touching tangentially the hypersurface $S := \{x \in \Omega \mid G(x) = 0\}$. With this, we mean that a C^1 periodic function $x_0(t)$ of period, say $T > 0$, exists such that $x_0(t) \in \Omega_+$ for all $t \in [0, T]$, $t \neq t_0 \in]0, T[$, $G(x_0(t_0)) = 0$ and the equation

$$\dot{x}_0(t) = f_+(x_0(t))$$

is satisfied for all $t \in [0, T]$. Let

$$g(x, \varepsilon, \mu) := \begin{cases} g_+(x, \varepsilon, \mu) \text{ if } x \in \Omega_+ \\ g_-(x, \varepsilon, \mu) \text{ if } x \in \Omega_- \end{cases}$$

where $g_+, g_- : \Omega \times B \to \mathbb{R}^n$ are C^r functions. Here $B \subseteq \mathbb{R}^2$ is an ball in $\mathbb{R}^2$ centred at $(0, 0)$. In this chapter, we study the problem of existence of a periodic solution of the perturbed discontinuous equation

$$\dot{x} = f_\pm(x) + \varepsilon g_\pm(x, \varepsilon, \mu), \quad x \in \Omega_\pm. \tag{2.2}$$

We suppose that 0 is a regular value of G. Since $d(t) := G(x_0(t))$ has a minimum at $t = t_0$ we have

$$d(t_0) = d'(t_0) = 0, \quad d''(t_0) \geq 0$$

we assume the minimum is strong that is $d''(t_0) > 0$. Let $x_0 := x_0(t_0)$ and $\bar{x} = x_0(0)$. Conditions $d'(t_0) = 0$, $d''(t_0) > 0$ are equivalent to

$$G'(x_0) f_+(x_0) = 0, \quad G''(x_0) f_+(x_0)^2 + G'(x_0) f'_+(x_0) f_+(x_0) > 0. \tag{2.3}$$

Let $B(\bar{x}, \rho)$ be the ball of radius ρ centred at $\bar{x}$ with $\rho < \rho_0$ and $B := B(\bar{x}, \rho_0) \subset \Omega_+$. For any $\tilde{x} \in B(\bar{x}, \rho)$ let $\phi(t, \tilde{x}, \varepsilon, \mu)$ be the solution of equation

$$\dot{x} = f_+(x) + \varepsilon g_+(x, \varepsilon, \mu) \tag{2.4}$$

such that $\phi(0, \tilde{x}, \varepsilon, \mu) = \tilde{x}$ [in other words $\phi(t, \tilde{x}, \varepsilon, \mu)$ is the flow of Eq. (2.4)]. When $\varepsilon = 0$ we get $\phi(t, x, 0, \mu) = \phi_0(t, x)$, the flow of equation $\dot{x} = f_+(x)$, which is independent of μ.

Lemma 2.1 *Let $x_0(t)$ be a periodic solution of Eq. (2.1) touching tangentially $S = \{x \in \Omega \mid G(x) = 0\}$ at $x_0 = x_0(t_0)$. Suppose $G'(x_0) \neq 0$ and that condition (2.3) holds. Then there exist $\rho > 0$, $\bar{\varepsilon} > 0$ such that for any $|\varepsilon| < \bar{\varepsilon}$ there exists a hypersurface $\mathcal{S}_{\varepsilon,\mu} \subset B(\bar{x}, \rho)$ such that for any $x \in \mathcal{S}_{\varepsilon,\mu}$, $\phi(t, x, \varepsilon, \mu)$ touches tangentially the manifold S at a point $\phi(t(x, \varepsilon, \mu), x, \varepsilon, \mu)$. Moreover $t(x, \varepsilon, \mu)$ is C^r, $t(\bar{x}, 0, \mu) = t_0$, and, for any $x \in \mathcal{S}_{\varepsilon,\mu}$, $G(\phi(t, x, \varepsilon, \mu))$ has a minimum at $t(x, \varepsilon, \mu)$.*

Proof. We consider the function $\delta(t, x, \varepsilon, \mu) := G(\phi(t, x, \varepsilon, \mu))$, $|\varepsilon| \leq \bar{\varepsilon}$. Let

$$h(t, x, \varepsilon, \mu) := \begin{pmatrix} \delta(t, x, \varepsilon, \mu) \\ \delta_t(t, x, \varepsilon, \mu) \end{pmatrix} : \mathbb{R} \times B(\bar{x}, \rho) \times [-\bar{\varepsilon}, \bar{\varepsilon}] \times \mathbb{R} \to \mathbb{R}^2.$$

Note that $\delta(t, x, 0, \mu) := d(t, x) = G(\phi_0(t, x))$ is independent of μ. Hence $h(t, x, 0, \mu) = h_0(t, x) := \begin{pmatrix} G(\phi_0(t, x)) \\ G'(\phi_0(t, x)) f_+(\phi_0(t, x)) \end{pmatrix}$ does not depend on μ and $h(t, \bar{x}, 0, \mu) = h_0(t, \bar{x}) = \begin{pmatrix} d(t) \\ d'(t) \end{pmatrix}$. We prove that the system

$$h(t, x, \varepsilon, \mu) = 0$$

has a C^r solution $t(x, \varepsilon, \mu)$ for any x belonging to a hypersurface $\mathcal{S}_{\varepsilon,\mu}$ of the ball $B(\bar{x}, \rho)$. We have

$$h_0(t_0, \bar{x}) = 0$$

and

$$\frac{\partial h_0}{\partial(x, t)}(t_0, \bar{x}, 0, \mu) = \begin{pmatrix} d_x(t_0, \bar{x}) & d_t(t_0, \bar{x}) \\ d_{xt}(t_0, \bar{x}) & d_{tt}(t_0, \bar{x}) \end{pmatrix} = \begin{pmatrix} d_x(t_0, \bar{x}) & 0 \\ d_{xt}(t_0, \bar{x}) & d''(t_0) \end{pmatrix}$$

Hence if rank $d_x(t_0, \bar{x}) = 1$, the implicit function theorem implies the existence of a submanifold $\mathcal{S}_{\varepsilon,\mu}$ of $B(\bar{x}, \rho)$, which is described by an equation like $x_j = X_j(x_{\hat{j}}, \varepsilon, \mu)$, for some $j = 1, \ldots, n$ (here $x_{\hat{j}}$ means that the coordinate x_j in x is missed) and of a function $t = t(x_{\hat{j}}, \varepsilon, \mu)$ such that $h(t, x, \varepsilon) = 0$ when $t = t(x_{\hat{j}}, \varepsilon, \mu)$ and $x_j = X_j(x_{\hat{j}}, \varepsilon, \mu)$. To be more precise, we can proceed in two steps. First to solve equation $\delta_t(t, x, \varepsilon, \mu) = 0$ in a neighbourhood of $(t_0, \bar{x}, 0, \mu)$, with μ in a compact set, for $t = t(x, \varepsilon, \mu)$, with $t(\bar{x}, 0, \mu) = t_0$. Then plug $t = t(x, \varepsilon, \mu)$ into $\delta(t, x, \varepsilon, \mu)$ to obtain:

$$\mathcal{S}_{\varepsilon,\mu} = \{x \in B(\bar{x}, \rho) \mid \delta(t(x, \varepsilon, \mu), x, \varepsilon, \mu) = 0\}.$$

Note that $t(x,0,\mu)=t_0(x)$ is independent of μ and is defined by the fact that $d_t(t_0(x),x)=0$.

We have:

$$d_x(t_0,\bar{x})=G'(\phi_0(t_0,\bar{x}))\phi_{0x}(t_0,\bar{x})=G'(x_0)\phi_{0x}(t_0,\bar{x})$$

and $\phi_{0x}(t_0,\bar{x})=\phi_x(t_0,\bar{x},0)$ is invertible being the fundamental matrix of the linear equation $\dot{x}=f'_+(x_0(t))x$. So $d_x(t_0,\bar{x})\neq 0$ if and only if $G'(x_0)\neq 0$ and this holds by the assumptions. Since $d''(t_0)>0$, rank $\left[\frac{\partial h_0}{\partial(x,t)}\right]=2$. Possibly reordering variables we can assume that $h(t,x,\varepsilon,\mu)=0$ if and only if

$$t=t(x_{\hat{1}},\varepsilon,\mu)\quad\text{and}\quad x_1=X_1(x_{\hat{1}},\varepsilon,\mu).$$

Next, from the implicit function theorem we get:

$$\bar{x}_1=X_1(\bar{x}_{\hat{1}},0,\mu),\quad t_0=t(\bar{x}_{\hat{1}},0,\mu).$$

In particular, $\bar{x}\in\mathcal{S}_0=\mathcal{S}_{0,\mu}$. Now we prove that $\delta(t,(X_1(x_{\hat{1}},\varepsilon,\mu),x_{\hat{1}}),\varepsilon,\mu)$ has a minimum at $t=t(x_{\hat{1}},\varepsilon,\mu)$. We already know that

$$\begin{aligned}&\delta(t(x_{\hat{1}},\varepsilon,\mu),(X_1(x_{\hat{1}},\varepsilon,\mu),x_{\hat{1}}),\varepsilon,\mu)\\ =&\delta_t(t(x_{\hat{1}},\varepsilon,\mu),(X_1(x_{\hat{1}},\varepsilon,\mu),x_{\hat{1}}),\varepsilon,\mu)=0.\end{aligned}$$

Next

$$\lim_{\substack{x_{\hat{1}}\to\bar{x}_{\hat{1}}\\ \varepsilon\to 0}}\delta_{tt}(t(x_{\hat{1}},\varepsilon,\mu),(X_1(\bar{x}_{\hat{1}},\varepsilon,\mu),x_{\hat{1}}),\varepsilon,\mu)=\delta_{tt}(t_0,\bar{x},0)=d''(t_0)>0.$$

Thus, $t(x_{\hat{1}},\varepsilon,\mu)$ is a local minimum point for $\delta(t,(X_1(\bar{x}_{\hat{1}},\varepsilon,\mu),x_{\hat{1}}),\varepsilon,\mu)$. This point is a global minimum in an interval like $\left[-\frac{T}{3},\frac{4}{3}T\right]$ because $\delta(t,x,\varepsilon,\mu)\to d(t)$ as $(\varepsilon,x)\to(0,\bar{x})$.

Remark 2.2 From the proof of Lemma 2.1, we see that $x\in\mathcal{S}_{\varepsilon,\mu}\cap B(\bar{x},\rho)$ if and only if

$$\min\{\delta(t,x,\varepsilon,\mu)\mid 0\le t\le T\}=0$$

which is equivalent to:

$$\begin{aligned}&G(\phi(t(x,\varepsilon,\mu),x,\varepsilon,\mu))=0,\\ &G'(\phi(t(x,\varepsilon,\mu),x,\varepsilon,\mu))\phi_t(t(x,\varepsilon,\mu),x,\varepsilon,\mu)=0\end{aligned}\tag{2.5}$$

Differentiating the first equality in (2.5) with respect to $x\in\mathcal{S}_{\varepsilon,\mu}$, we get

$$\begin{aligned}&G'(\phi(t(x,\varepsilon,\mu),x,\varepsilon,\mu))\\ &[\phi_t(t(x,\varepsilon,\mu),x,\varepsilon,\mu))t_x(x,\varepsilon,\mu)+\phi_x(t(x,\varepsilon,\mu),x,\varepsilon,\mu)]_{|T_x\mathcal{S}_{\varepsilon,\mu}}=0\end{aligned}\tag{2.6}$$

and then, using the second equality in (2.5):

$$[G'(\phi(t(x,\varepsilon,\mu),x,\varepsilon,\mu))\phi_x(t(x,\varepsilon,\mu),x,\varepsilon,\mu)]_{|T_x\mathcal{S}_{\varepsilon,\mu}}=0.$$

Since $\phi_x(t(x,\varepsilon,\mu),x,\varepsilon,\mu)$ is invertible, the kernel of

$$G'(\phi(t(x,\varepsilon,\mu),x,\varepsilon,\mu))\phi_x(t(x,\varepsilon,\mu),x,\varepsilon,\mu)$$

is $(n-1)$-dimensional. As a consequence,

$$\mathcal{N}[G'(\phi(t(x,\varepsilon,\mu),x,\varepsilon,\mu))\phi_x(t(x,\varepsilon,\mu),x,\varepsilon,\mu)]=T_x\mathcal{S}_{\varepsilon,\mu}.$$

When $\varepsilon=0$ and $x=\bar{x}$, this gives, due to $t(\bar{x},0,\mu)=t_0$, $\phi(t_0,\bar{x},0,\mu)=x_0$:

$$\mathcal{N}[G'(x_0)\phi_{0x}(t_0,\bar{x})]=T_{\bar{x}}\mathcal{S}_0.$$

Now, we remark that the equality $\delta_t(t(x,\varepsilon,\mu),x,\varepsilon,\mu)=0$ holds for any $x\in B(\bar{x},\rho)$ (since $t(x,\varepsilon,\mu)$ has been found solving first $\delta_t(t,x,\varepsilon,\mu)=0$). Hence

$$\frac{\partial}{\partial x}\delta(t(x,\varepsilon,\mu),x,\varepsilon,\mu)=\delta_x(t(x,\varepsilon,\mu),x,\varepsilon,\mu)\neq 0$$

for any $x\in B(\bar{x},\rho)$ (with ρ sufficiently small) since

$$\lim_{\substack{x\to\bar{x}\\ \varepsilon\to 0}}\delta_x(t(x,\varepsilon,\mu),x,\varepsilon,\mu)=d_x(t_0,\bar{x})=G'(x_0)\phi_{0,x}(t_0,\bar{x})\neq 0.$$

Moreover $\delta_{tt}(t(x,\varepsilon,\mu),x,\varepsilon,\mu)>0$ for $|x-\bar{x}|+|\varepsilon|$ sufficiently small since

$$\lim_{\substack{x\to\bar{x}\\ \varepsilon\to 0}}\delta_{tt}(t(x,\varepsilon,\mu),x,\varepsilon,\mu)=d''(t_0)>0.$$

Hence $t(x,\varepsilon,\mu)$ is a local strong minimum of $\delta(t,x,\varepsilon,\mu)$.

Now, the conditions $\delta(t(x,\varepsilon,\mu),x,\varepsilon,\mu)=0$ and $\delta_x(t(x,\varepsilon,\mu),x,\varepsilon,\mu)\neq 0$ for $x\in\mathcal{S}_{\varepsilon,\mu}$ imply that the hypersurface $\mathcal{S}_{\varepsilon,\mu}$ splits $B(\bar{x},\rho)$ in two connected open sets, say $B_-^{\varepsilon,\mu}(\bar{x},\rho)$ and $B_+^{\varepsilon,\mu}(\bar{x},\rho)$ characterized by the following.

$x\in B_+^{\varepsilon,\mu}(\bar{x},\rho)$ if and only if $\min\{G(\phi(t,x,\varepsilon,\mu))\mid 0\le t\le T\}>0$,
$x\in B_-^{\varepsilon,\mu}(\bar{x},\rho)$ if and only if $\min\{G(\phi(t,x,\varepsilon,\mu))\mid 0\le t\le T\}<0$.

Let $\varphi(t,x,\varepsilon,\mu)$ be the flow of the discontinuous system (2.2). The sign of $G(\varphi(t,x,\varepsilon,\mu))$ when $x\in B_-^{\varepsilon,\mu}(\bar{x},\rho)$ depends on the properties of the function $f_-(x)$. We distinguish between the following two cases:

(i) $G'(x_0)f_-(x_0)>0$;
(ii) $G'(x_0)f_-(x_0)<0$.

Suppose $x\in B_-^{\varepsilon,\mu}(\bar{x},\rho)$. In this case, we have $\min\delta(t,x,\varepsilon,\mu)<0$.

Then there exists a unique $\tilde{t} = \tilde{t}(x, \varepsilon, \mu)$, with $\tilde{t}(\bar{x}, 0, \mu) = t_0$, such that $G(\phi(\tilde{t}, x, \varepsilon, \mu)) = 0$ and $G(\phi(t, x, \varepsilon, \mu)) > 0$, for $t < \tilde{t}$. We derive that

$$\delta_t(\tilde{t}, x, \varepsilon, \mu)) = G'(\phi(\tilde{t}, x, \varepsilon, \mu))[f_+(\phi(\tilde{t}, x, \varepsilon, \mu)) + \varepsilon g_+(\phi(\tilde{t}, x, \varepsilon, \mu), \varepsilon, \mu)] \leq 0.$$

Since $\delta(\tilde{t}, x, \varepsilon, \mu) = G(\phi(\tilde{t}, x, \varepsilon, \mu)) = 0$, we see that the equality holds if and only if $x \in \mathcal{S}_{\varepsilon,\mu}$ and $\tilde{t} = t(x, \varepsilon, \mu)$. So we conclude that

$$G'(\phi(\tilde{t}, x, \varepsilon, \mu))[f_+(\phi(\tilde{t}, x, \varepsilon, \mu)) + \varepsilon g_+(\phi(\tilde{t}, x, \varepsilon, \mu), \varepsilon, \mu)] < 0 \tag{2.7}$$

for any $x \in B_-^{\varepsilon,\mu}(\bar{x}, \rho)$. Because of the uniqueness, we see that $\phi(\tilde{t}, x, \varepsilon, \mu) \to x_0$ as $\varepsilon \to 0$ and $x \to \bar{x}$. Hence, if ρ and ε are small enough we get, in case (i),

$$G'(\phi(\tilde{t}, x, \varepsilon, \mu))[f_-(\phi(\tilde{t}, x, \varepsilon, \mu)) + \varepsilon g_-(\phi(\tilde{t}, x, \varepsilon, \mu), \varepsilon, \mu)] > 0.$$

This means that the vector field on Ω_- pushes the solution into Ω_+ while the vector field on Ω_+ pushes the solution into Ω_-. As a consequence, we have sliding. On the other hand, if (ii) holds then the solution enters into Ω_- at the point $\phi(\tilde{t}, x, \varepsilon, \mu) \in S$ that is $\phi(t, x, \varepsilon, \mu)$ crosses S transversally at $\phi(\tilde{t}, x, \varepsilon, \mu)$.

In this chapter, we study the problem of existence of grazing periodic solutions that is periodic solutions starting from a point in $\mathcal{S}_{\varepsilon,\mu}$. In Sect. 3, we construct the Poincaré map of Eq. (2.4). Then in Sect. 4, we study the problem of existence of fixed points in $\mathcal{S}_{\varepsilon,\mu}$ of the Poincaré map.

We conclude this section with the construction of another submanifold of S that will be useful in the next sections. Let

$$h_\pm(x, \varepsilon, \mu) = f_\pm(x) + \varepsilon g_\pm(x, \varepsilon, \mu)$$

and set

$$\mathcal{M}_{\varepsilon,\mu} = \{x \in S \mid G'(x)h_+(x, \varepsilon, \mu) = 0\}.$$

When $\varepsilon = 0$ we get

$$\begin{aligned} \mathcal{M}_{0,\mu} = \mathcal{M}_0 &= \{x \in S \mid G'(x)f_+(x) = 0\} \\ &= \{x \in \Omega \mid G(x) = 0,\ G'(x)f_+(x) = 0\}. \end{aligned}$$

The Jacobian matrix (with respect to x) at x_0 of the map $\begin{pmatrix} G(x) \\ G'(x)f_+(x) \end{pmatrix}$ is

$$\begin{pmatrix} G'(x_0) \\ G''(x_0)f_+(x_0) + G'(x_0)f'_+(x_0) \end{pmatrix}$$

whose rank equals 2 because of assumption (2.3). Indeed from (2.3) it follows that $G'(x_0)$ and $G''(x_0)f_+(x_0) + G'(x_0)f'_+(x_0)$ do not have the same kernel hence they

cannot be proportional. Hence for any μ in a given fixed compact subset of $\mathbb{R}$ there exists $\varepsilon_0 > 0$ and a (connected) neighbourhood U of x_0 such that for $|\varepsilon| < \varepsilon_0$, $\mathcal{M}_{\varepsilon,\mu}$ is a codimension 1 submanifold of $S \cap U$. Using $\phi_t(t(x,\varepsilon,\mu),x,\varepsilon,\mu) = h_+(\phi(t(x,\varepsilon,\mu),x,\varepsilon,\mu),\varepsilon,\mu)$ and (2.5) we see that

$$\phi(t(x,\varepsilon,\mu),x,\varepsilon,\mu) \in \mathcal{M}_{\varepsilon,\mu}.$$

Since the flow is invertible, we obtain (at least locally in a neigbborhood of x_0)

$$\mathcal{M}_{\varepsilon,\mu} = \{\phi(t(x,\varepsilon,\mu),x,\varepsilon,\mu) \mid x \in \mathcal{S}_{\varepsilon,\mu} \cap B(\bar{x},\rho)\}. \tag{2.8}$$

Since $\mathcal{M}_{\varepsilon,\mu}$ is a codimension one submanifold of S, for ε sufficiently small (and μ in a given compact subset of $\mathbb{R}$) it splits a given (small) neighbourhood of x_0, say $B(x_0,r)$, into two connected components characterized by the inequalities $G'(x)h_+(x,t,\varepsilon,\mu) > 0$ and $G'(x)h_+(x,t,\varepsilon,\mu) < 0$.

From Eq. (2.8), it follows that $\mathcal{M}_{\varepsilon,\mu}$ is the image under the flow $\phi(t(x,\varepsilon,\mu),x,\varepsilon,\mu)$ of $\mathcal{S}_{\varepsilon,\mu} \cap B(\bar{x},\rho)$. As a consequence, we deduce that $B_-^{\varepsilon,\mu}(\bar{x},\rho)$ is sent by the flow $\phi(\tilde{t}(x,\varepsilon,\mu),x,\varepsilon,\mu)$ into one of the two components of $B(x_0,r) \cap S] \setminus \mathcal{M}_{\varepsilon,\mu}$. From Eq. (2.7), it follows that the image under the flow of $B_-^{\varepsilon}(\bar{x},\rho)$ belongs to the connected component of $[B(x_0,r) \cap S] \setminus \mathcal{M}_{\varepsilon,\mu}$ where $G'(x)h_+(x,t,\varepsilon,\mu) < 0$. We collect all the above remarks in the following.

Proposition 2.3 *Suppose $x_0(t)$ is a periodic solution of Eq. (2.1) touching tangentially $S = \{x \in \mathbb{R}^n \mid G(x) = 0\}$ at $x_0 = x_0(t_0)$ and that condition (2.3) as well as $G'(x_0) \neq 0$ hold. Then there exist $B(x_0,r)$ and $\varepsilon_0 > 0$ such that for any $|\varepsilon| < \varepsilon_0$ and μ in a given compact subset of $\mathbb{R}$ the manifold $\mathcal{M}_{\varepsilon,\mu}$ splits $B(x_0,r) \cap S$ into two open (in the induced topology on S) subsets of $B(x_0,r) \cap S$ characterized by the inequalities*

$$G'(x)h_+(x,t,\varepsilon,\mu) > 0 \quad G'(x)h_+(x,t,\varepsilon,\mu) < 0$$

respectively. Moreover, the following holds:

(a) $\mathcal{M}_{\varepsilon,\mu} = \{\phi(t(x,\varepsilon,\mu),x,\varepsilon,\mu) \mid x \in \mathcal{S}_{\varepsilon,\mu} \cap B(\bar{x},\rho)\}$,
(b) if $x \in B_-^{\varepsilon,\mu}(\bar{x},\rho)$ *then*

$$G'(\phi(t(x,\varepsilon,\mu),x,\varepsilon,\mu))h_+(\phi(t(x,\varepsilon,\mu),x,\varepsilon,\mu),t,\varepsilon,\mu) < 0.$$

3 The Poincaré Map

In this section, we construct the Poincaré map of Eq. (2.4) in the sliding case (that is when (i) holds). This map is defined for $x \in B(\bar{x},\rho) \cap L$, L being any fixed hyperplane through $\bar{x}$ transverse to $f_+(\bar{x})$, for example $L = \{\bar{x}\} + \{f_+(\bar{x})\}^{\perp}$, and takes values on L. When $x \in B_+^{\varepsilon,\mu}(\bar{x},\rho) \cap L$, it is simply the Poincaré map of equation $\dot{x} = f_+(x) + \varepsilon g_+(x,\varepsilon,\mu)$.

Before giving the definition of the Poincaré map on $\overline{B_-^{\varepsilon,\mu}(\bar{x},\rho)} \cap L$, we need to make few remarks.

For $x \in \overline{B_-^{\varepsilon,\mu}(\bar{x},\rho)} \cap L$, consider the solution starting from $\phi(\tilde{t},x,\varepsilon) \in S$, with $\tilde{t} = \tilde{t}(x,\varepsilon,\mu)$. To this end, we define the vector field on S. For simplicity, assume that

$$S = \{x \in \mathbb{R}^n \mid x_n = 0\}.$$

Since the argument is local in a neighbourhood of x_0, we can always reduce to this situation by a (usually nonlinear) change of variables. Thus, we take $G(x) = x_n$ and Eqs. (2.3), (2.5) read, respectively:

$$f_{+,n}(x_0) = 0, \qquad f'_{+,n}(x_0) \cdot f_+(x_0) > 0$$

and

$$\phi_n(t(x,\varepsilon,\mu),x,\varepsilon,\mu) = 0, \quad [e_n^* \phi_x(t(x,\varepsilon,\mu),x,\varepsilon,\mu)]_{|T_x\mathcal{S}_\varepsilon} = 0$$

for any $x \in \mathcal{S}_\varepsilon$. Moreover $e_n^*\phi_t(t(x,\varepsilon,\mu),x,\varepsilon,\mu) = 0$, that is

$$f_{+,n}(\phi(t(x,\varepsilon,\mu),x,\varepsilon,\mu)) = 0.$$

The vector field on S is then given by the equation

$$\dot{x}_{\hat{n}} = h(x_{\hat{n}},\varepsilon,\mu) = h_0(x_{\hat{n}}) + \varepsilon h_1(x_{\hat{n}},\varepsilon,\mu) \tag{3.1}$$

where

$$h(x_{\hat{n}},\varepsilon,\mu) = \frac{h_{-,n}(x_{\hat{n}},\varepsilon,\mu)h_{+,\hat{n}}(x_{\hat{n}},\varepsilon,\mu) - h_{+,n}(x_{\hat{n}},\varepsilon,\mu)h_{-,\hat{n}}(x_{\hat{n}},\varepsilon,\mu)}{h_{-,n}(x_{\hat{n}},\varepsilon,\mu) - h_{+,n}(x_{\hat{n}},\varepsilon,\mu)}.$$

Note that

$$\lim_{\varepsilon\to 0} h_{-,n}(x_{\hat{n}},\varepsilon,\mu) - h_{+,n}(x_{\hat{n}},\varepsilon,\mu) = f_{-,n}(x_{\hat{n}}) - f_{+,n}(x_{\hat{n}}) \neq 0$$

for $|x - x_0|$ sufficiently small. Thus for ε sufficiently small, Eq. (3.1) is well defined in a neighbourhood of $x_{0,\hat{n}}$. To avoid misunderstanding, we emphasize that with $h_{\pm,n}(x_{\hat{n}},\varepsilon)$ we mean the function $h_{\pm,n}((x_{\hat{n}},0),\varepsilon)$ and similarly for $h_{\pm,\hat{n}}(x_{\hat{n}},\varepsilon)$. In the following, we write $x_{\hat{n}}$ to denote both $x_{\hat{n}}$ and $(x_{\hat{n}},0)$, the meaning being clear from the context. Solutions of (3.1) will remain in S until $h_{+,n}(x_{\hat{n}},\varepsilon) < 0 < h_{-,n}(x_{\hat{n}},\varepsilon)$. When $g(x,t,\varepsilon,\mu) = g(x,\varepsilon,\mu)$ the manifold $\mathcal{M}_{\varepsilon,\mu,t}$ are t-independent and, actually, being $G(x) = x_n$, we have:

$$\mathcal{M}_{\varepsilon,\mu} = \{x \in S \mid h_{+,n}(x,\varepsilon,\mu) = 0\}$$

and

$$\mathcal{M}_0 = \{x \in S \mid f_{+,n}(x) = 0\}.$$

Sliding will occur until the solution $x_{\hat{n}}(t, \tilde{t}, \phi_{\hat{n}}(\tilde{t}, x, \varepsilon, \mu), \varepsilon, \mu)$ of Eq. (3.1) starting, at $t = \tilde{t} = \tilde{t}(x, \varepsilon, \mu)$, from $\phi_{\hat{n}}(\tilde{t}, x, \varepsilon, \mu)$, $x \in B_-(\bar{x}, \rho)$, reaches the manifold $\mathcal{M}_{\varepsilon,\mu}$ that is until

$$h_{+,n}(x_{\hat{n}}(t, \tilde{t}, \phi_{\hat{n}}(\tilde{t}, x, \varepsilon, \mu), \varepsilon, \mu), \varepsilon, \mu) = 0.$$

Here $x_{\hat{n}}(t, \tilde{t}, \tilde{x}, \varepsilon, \mu)$ is the solution of (3.1) satisfying $x_{\hat{n}}(\tilde{t}, \tilde{t}, \tilde{x}, \varepsilon, \mu) = \tilde{x}$. Since $\mathcal{M}_{\varepsilon,\mu}$ is a codimension 1 submanifold of S and $x_0 \in \mathcal{M}_0$, there exists a neighbourhood $B(x_0, r)$ of x_0 such that $[B(x_0, r) \cap S] \setminus \mathcal{M}_{\varepsilon,\mu}$ has two connected components. These two connected components are characterized by the inequalities $h_{+,n}(x, \varepsilon) > 0$, $h_{+,n}(x, \varepsilon) < 0$.

In the previous section, we observed that the image under the flow of $V \cap B^{\varepsilon}_-(\bar{x}, \rho)$ belongs to the connected component of $[B(x_0, r) \cap S] \setminus \mathcal{M}_{\varepsilon,\mu}$ where $h_{+,n}(x, \varepsilon, \mu) < 0$.

In order to have sliding, we need that the solutions of Eq. (3.1) on S cross the manifold $\mathcal{M}_{\varepsilon,\mu}$. We prove that the solutions of (3.1) cross $\mathcal{M}_{\varepsilon,\mu}$ transversally. Indeed on $\mathcal{M}_{\varepsilon,\mu}$ we have:

$$x \in \mathcal{M}_{\varepsilon,\mu} \Rightarrow h(x_{\hat{n}}, \varepsilon, \mu) = h_{+,\hat{n}}(x_{\hat{n}}, \varepsilon, \mu).$$

Hence a solution of Eq. (3.1) crosses $\mathcal{M}_{\varepsilon,\mu}$ and going from $\{x \in S \mid h(x_{\hat{n}}, \varepsilon, \mu) < 0\}$ into $\{x \in S \mid h(x_{\hat{n}}, \varepsilon, \mu) > 0\}$ if

$$h'_{+,n}(x_{\hat{n}}, \varepsilon, \mu) h_{+,\hat{n}}(x_{\hat{n}}, \varepsilon, \mu) > 0$$

for any $x_{\hat{n}} \in B(x_0, r) \cap S$. Of course, this holds if it holds for $\varepsilon = 0$, that is

$$f'_{+,n}(x_{\hat{n}}) f_{+,\hat{n}}(x_{\hat{n}}) > 0 \tag{3.2}$$

for any $x_{\hat{n}} \in B(x_0, r) \cap S$. Note that $f'_{+,n}(x_{\hat{n}})$ and $h'_{+,n}(x_{\hat{n}}, \varepsilon)$ denote the derivative of $f_{+,n}(x_{\hat{n}})$, $h_{+,n}(x_{\hat{n}}, \varepsilon)$ with respect to $(x_1, \ldots, x_{n-1})$ at $(x_1, \ldots, x_{n-1}, 0)$.

Condition (3.2) implies that we have a sliding behaviour also for the solutions of Eq. (2.1) when x belongs to $B^0_-(\bar{x}, \rho)$.

Let $\bar{t}(x, \varepsilon, \mu)$ be the first time after $\tilde{t}(x, \varepsilon, \mu)$ such that

$$x_{\hat{n}}(t, \tilde{t}(x, \varepsilon, \mu), \phi_{\hat{n}}(\tilde{t}(x, \varepsilon, \mu), x, \varepsilon, \mu), \varepsilon, \mu) \in \mathcal{M}_{\varepsilon,\mu}.$$

Clearly, if $x \in \mathcal{S}_{\varepsilon,\mu}$ then $\bar{t}(x, \varepsilon, \mu) = \tilde{t}(x, \varepsilon, \mu) = t(x, \varepsilon, \mu)$. Finally we consider the solution

$$x_r(t, x, \varepsilon, \mu) = \phi(t, \bar{t}(x, \varepsilon, \mu), x_{\hat{n}}(\bar{t}(x, \varepsilon, \mu), \tilde{t}(x, \varepsilon, \mu), \phi_{\hat{n}}(\tilde{t}(x, \varepsilon, \mu), x, \varepsilon, \mu), \varepsilon, \mu))$$

of $\dot{x} = h_+(x, \varepsilon, \mu)$ such that

$$x_r(\bar{t}(x,\varepsilon,\mu),x,\varepsilon,\mu) = x_{\hat{n}}(\bar{t}(x,\varepsilon,\mu),\tilde{t}(x,\varepsilon,\mu),\phi_{\hat{n}}(\tilde{t}(x,\varepsilon,\mu),x,\varepsilon,\mu),\varepsilon,\mu).$$

Because of continuous dependence on the data, we see that

$$\sup_{t\in\left[\bar{t}(x,\varepsilon),\frac{3}{2}T\right]} |x_r(t,x,\varepsilon,\mu) - x_0(t)| \to 0$$

as $(x,\varepsilon)\to(\bar{x},0)$, uniformly for μ in compact sets. Hence there exists a smooth function $T(x,\varepsilon,\mu)$ such that

$$\begin{aligned}
&T(\bar{x},0,\mu) = T,\\
&x_r(t,x,\varepsilon,\mu)\notin L \quad \text{for}\, \bar{t}(x,\varepsilon,\mu)\le t < T(x,\varepsilon,\mu),\\
&x_r(T(x,\varepsilon,\mu),x,\varepsilon,\mu)\in L,\\
&\sup_{\bar{t}(x,\varepsilon,\mu)\le t\le T(x,\varepsilon,\mu)} |x_r(t,x,\varepsilon,\mu) - x_0(t)| \to 0, \quad \text{as}\,(x,\varepsilon)\to(\bar{x},0).
\end{aligned}$$

The map $\pi(\cdot,\varepsilon,\mu) : \overline{B^{\varepsilon}_{-}(\bar{x},\rho)}\cap L \to L$, $\pi(x,\varepsilon,\mu) = x_r(T(x,\varepsilon,\mu),x,\varepsilon,\mu)$ is the Poincaré map.

In the following section, we study the restriction of $\pi(x,\varepsilon,\mu)$ to $\mathcal{S}_{\varepsilon,\mu}$. In this case, we have grazing instead of sliding and the Poincaré map is still defined as $\pi(x,\varepsilon,\mu) = x_r(T(x,\varepsilon,\mu),x,\varepsilon,\mu)$, but

$$x_r(t,x,\varepsilon,\mu) = \phi(t,x,\varepsilon,\mu)$$

for any $x\in\mathcal{S}_{\varepsilon,\mu}$, $\phi(t,x,\varepsilon,\mu)$ being the flow of equation $\dot{x} = f_+(x) + \varepsilon g_+(x,\varepsilon,\mu)$. Hence

$$\pi(x,\varepsilon,\mu) = \phi(T(x,\varepsilon,\mu),x,\varepsilon,\mu), \quad \text{for any}\, x\in\mathcal{S}_{\varepsilon,\mu}. \tag{3.3}$$

4 Grazing Periodic Solutions

In this section, we prove that if a certain condition is satisfied there exists a grazing periodic solution of Eq. (2.4). Actually, we prove the following.

Theorem 4.1 *Suppose the equation $\dot{x} = f_+(x)$ has the T-periodic solution $x_0(t)\in\Omega_+$, for $t\neq t_0$ touching tangentially the manifold $G(x)=0$ at the point $x_0 = x(t_0)$. Suppose further that $G'(x_0)\neq 0$, and that (2.3) holds. Suppose that the generic condition*

$$\mathcal{N}(\mathbb{I} - P'(\bar{x}))/T_{\bar{x}}(\mathcal{S}_0\cap L) = \{0\} \tag{4.1}$$

holds, where $P : L\to L$ is the Poincaré map of $\dot{x} = f_+(x)$. Then the adjoint equation $\dot{x} = -f'_+(x_0(t))^* x$ has a unique, up to a multiplicative constant, solution $\psi(t)$ such that $\psi(T)\in T_{\bar{x}}L\cap\left[\mathcal{R}(\mathbb{I}-P'(\bar{x}))_{|T_{\bar{x}}(\mathcal{S}_0\cap L)}\right]^{\perp}$. Next let $\psi_1(t)$ be the solution of $\dot{x} = -f'_+(x_0(t))^* x$ such that $\psi_1(0) = \psi(T) - \psi(0)$. Then, if the function

$$\Delta(\mu) = \int_0^{t_0} \psi_1(s)^* g_+(x_0(s), 0, \mu) ds + \int_0^T \psi(s)^* g_+(x_0(s), 0, \mu) ds$$

has a simple zero at some point $\mu = \mu_0$, there exists $\mu(\varepsilon)$ such that for $\mu = \mu(\varepsilon)$ equation $\dot{x} = f_+(x) + \varepsilon g_+(x, \varepsilon, \mu)$ has a periodic and grazing solution $x_0(t, \varepsilon)$ whose period is a C^1-function of ε and tends to T as $\varepsilon \to 0$. Moreover, for any compact interval $I \subset \mathbb{R}$ we have

$$\lim_{\varepsilon \to 0} \sup_{t \in I} |x_0(t, \varepsilon) - x_0(t)| = 0.$$

Proof. We want to solve

$$\pi(x, \varepsilon, \mu) - x = 0, \quad x \in \mathcal{S}_{\varepsilon,\mu} \cap L. \tag{4.2}$$

Note, first, that $L = \bar{x} + T_{\bar{x}}L = \{\bar{x} + \xi \mid \xi \in T_{\bar{x}}L\}$. Hence, for any $x \in \mathcal{S}_{\varepsilon,\mu} \cap L$ we have $\pi(x, \varepsilon, \mu) - x \in T_{\bar{x}}L$. In the following, we take $T_{\bar{x}}L = \{f_+(\bar{x})\}^\perp$

Recalling that $P : L \to L$ is the Poincaré map of $\dot{x} = f_+(x)$, we get $\pi(\cdot, 0, \mu)/(\mathcal{S}_0 \cap L) = P/(\mathcal{S}_0 \cap L)$. Hence $\pi_x(\bar{x}, 0, \mu)\xi = P'(\bar{x})\xi$ for $\xi \in T_{\bar{x}}(\mathcal{S}_0 \cap L)$. To solve (4.2), we use the Lyapunov-Schmidt method. By (4.1), it holds $\operatorname{codim} \mathcal{R}(\mathbb{I} - P'(\bar{x}))/T_{\bar{x}}(\mathcal{S}_0 \cap L) = 1$ in $T_{\bar{x}}L$. So we take a projection $P_1 : T_{\bar{x}}L \to \mathcal{R}(\mathbb{I} - P'(\bar{x}))/T_{\bar{x}}(\mathcal{S}_0 \cap L)$, and split (4.2) into

$$P_1(\pi(x, \varepsilon, \mu) - x) = 0, \quad x \in \mathcal{S}_{\varepsilon,\mu} \cap L \tag{4.3}$$

and

$$(\mathbb{I} - P_1)(\pi(x, \varepsilon, \mu) - x) = 0, \quad x \in \mathcal{S}_{\varepsilon,\mu} \cap L. \tag{4.4}$$

We write Eq. (4.4) in a more explicit form. First of all Eq. (4.4) is equivalent to

$$\psi^*[\pi(x, \varepsilon, \mu) - x] = 0 \tag{4.5}$$

for some non-zero vector $\psi \in T_{\bar{x}}L$ orthogonal to $\mathcal{R}(\mathbb{I} - P'(\bar{x}))/T_{\bar{x}}(\mathcal{S}_0 \cap L)$, that is,

$$\psi \in T_{\bar{x}}L, \quad \text{and} \quad \psi^* v = 0 \tag{4.6}$$

for any $v \in V := \mathcal{R}(\mathbb{I} - P'(\bar{x}))/T_{\bar{x}}(\mathcal{S}_0 \cap L)$ or equivalently:

$$\psi \in T_{\bar{x}}L, \quad \text{and} \quad \psi^* \mathcal{A} w = 0$$

for any $w \in W := T_{\bar{x}}(\mathcal{S}_0 \cap L)$ with

$$\mathcal{A} = \mathbb{I} - P'(\bar{x}) : T_{\bar{x}}L \to T_{\bar{x}}L. \tag{4.7}$$

Note that V and W are codimension 1 subspaces of $T_{\bar{x}}L$. If ψ_1 is another non-zero vector satisfying (4.6) then $\psi_1 = \mu\psi$ for some scalar $\mu \neq 0$ and hence Eq. (4.5) and

$$\psi_1^*[\pi(x,\varepsilon,\mu)-x]=0$$

are equivalent.

The second equation reads also $[\mathcal{A}^*\psi]^*w=0$ for any $w\in W:=T_{\bar{x}}(\mathcal{S}_0\cap L)$, that is,

$$\mathcal{A}^*\psi=\tilde{b}$$

for some vector $\tilde{b}\in T_{\bar{x}}L\cap T_{\bar{x}}(\mathcal{S}_0\cap L)^{\perp}$. Indeed, from (4.7) it follows

$$\mathcal{A}^*: T_{\bar{x}}L\to T_{\bar{x}}L.$$

Let

$$b=\phi_{0,x}(t_0,\bar{x})^*G'(x_0)^*.$$

It is clear that $b\in T_{\bar{x}}L$. In fact:

$$b^*f_+(\bar{x})=G'(x_0)\phi_{0,x}(t_0,\bar{x})\dot{x}_0(0)=G'(x_0)\dot{x}_0(t_0)=0.$$

Next, we know that

$$T_{\bar{x}}(\mathcal{S}_0\cap L)=\{\xi\in T_{\bar{x}}L\mid G'(x_0)\phi_{0,x}(t_0,\bar{x})\xi=0\}.$$

So, for any $\xi\in T_{\bar{x}}(\mathcal{S}_0\cap L)$, we have (using $\bar{P}=\bar{P}^*$):

$$b^*\xi=G'(x_0)\phi_{0,x}(T,\bar{x})\xi=0.$$

Note also that $\psi\in T_{\bar{x}}L$ implies

$$\bar{P}\psi=\psi,$$

where $\bar{P}:\mathbb{R}^n\to T_{\bar{x}}L$ is the orthogonal projection onto $T_{\bar{x}}L$ along $f_+(\bar{x})$.

Thus, we can write

$$\mathcal{A}^*\psi=\lambda b=\lambda\phi_{0,x}(t_0,\bar{x})^*G'(x_0)^*.$$

for some $\lambda\in\mathbb{R}$.

Now we consider Eq. (4.3). When $\varepsilon=0$ it reads: $P_1(P(x)-x)=0$, $x\in\mathcal{S}_0\cap L$ and has the solution $x=\bar{x}\in\mathcal{S}_0\cap L$. Differentiating the lefthand side with respect to x at $\bar{x}$, we get: $P_1(P'(\bar{x})-\mathbb{I})_{|T_{\bar{x}}\mathcal{S}_0\cap L}=(P'(\bar{x})-\mathbb{I})_{|T_{\bar{x}}\mathcal{S}_0\cap L}$ whose kernel reduces to $\{0\}$ because of (4.1). So $P_1(P'(\bar{x})-\mathbb{I})_{|T_{\bar{x}}\mathcal{S}_0\cap L}$ is an isomorphism from $T_{\bar{x}}\mathcal{S}_0\cap L$ onto $\mathcal{R}(\mathbb{I}-P'(\bar{x}))/T_{\bar{x}}\mathcal{S}_0\cap L$. Then, for ε sufficiently small and any μ from a compact subset of $\mathbb{R}$, (4.3) has a unique solution $x(\varepsilon,\mu)\in\mathcal{S}_{\varepsilon,\mu}\cap L$ such that $x(0,\mu)=\bar{x}$. Now we insert $x(\varepsilon,\mu)$ into (4.5) to get the equation

$$\tilde{\mathcal{G}}(\mu,\varepsilon)=0,$$

where $\tilde{\mathcal{G}}(\mu,\varepsilon) := \psi^*[\pi(x(\varepsilon,\mu),\varepsilon,\mu) - x(\varepsilon,\mu)]$. We have

$$\tilde{\mathcal{G}}(\mu,0) = \psi^*[\pi(x(0,\mu),0,\mu) - x(0,\mu) = \psi^*[P(\bar{x}) - \bar{x}] = 0$$

since $P(\bar{x}) = \bar{x}$. As a consequence, we set

$$\mathcal{G}(\mu,\varepsilon) := \begin{cases} \varepsilon^{-1}\tilde{\mathcal{G}}(\mu,\varepsilon) & \text{if } \varepsilon \neq 0 \\ \tilde{\mathcal{G}}_\varepsilon(\mu,0) & \text{if } \varepsilon = 0. \end{cases}$$

We want to apply the implicit function theorem to the function $\mathcal{G}(\mu,\varepsilon)$. To this end, we need that $\mu_0 \in \mathbb{R}$ exists such that

$$\mathcal{G}(\mu_0,0) = 0 \quad \text{and} \quad \mathcal{G}_\mu(\mu_0,0) \neq 0.$$

It is easy to check that

$$\mathcal{G}(\mu,0) = \psi^*[(P'(\bar{x}) - \mathbb{I})x_\varepsilon(0,\mu) + \pi_\varepsilon(\bar{x},0,\mu)].$$

From Eq. (3.3) we get

$$\begin{aligned} \pi_\varepsilon(\bar{x},0,\mu) &= \phi_{0t}(T,\bar{x})T_\varepsilon(\bar{x},0) + \phi_\varepsilon(T,\bar{x},0,\mu) \\ &= f_+(\bar{x})T_\varepsilon(\bar{x},0) + \phi_\varepsilon(T,\bar{x},0,\mu). \end{aligned} \tag{4.8}$$

So, from $\bar{P}\psi = \psi$, $\bar{P}f_+(\bar{x}) = 0$ and $\bar{P} = \bar{P}^*$ we get:

$$\psi^*\pi_\varepsilon(\bar{x},0,\mu) = \psi^*\bar{P}\pi_\varepsilon(\bar{x},0,\mu) = \psi^*\bar{P}\phi_\varepsilon(T,\bar{x},0,\mu) = \psi^*\phi_\varepsilon(T,\bar{x},0,\mu).$$

Next from $\mathcal{A}^*\psi = \lambda\bar{P}\phi_{0,x}(t_0,\bar{x})^*G'(x_0)^*$, $\mathcal{A} = \mathbb{I} - P'(\bar{x})$, we derive

$$\begin{aligned} \psi^*(P'(\bar{x}) - \mathbb{I})x_\varepsilon(0,\mu) &= -(\mathcal{A}^*\psi)^*x_\varepsilon(0,\mu) \\ &= -\lambda G'(x_0)\phi_{0,x}(t_0,\bar{x})\bar{P}x_\varepsilon(0,\mu) \\ &= -\lambda G'(x_0)\phi_x(t_0,\bar{x},0,\mu)x_\varepsilon(0,\mu) \end{aligned}$$

because $x(\varepsilon,\mu) \in \mathcal{S}_{\varepsilon,\mu} \cap L$ and then $\bar{P}x(\varepsilon,\mu) = x(\varepsilon,\mu)$. Now, from the proof of Lemma 2.1 we know that $\mathcal{S}_{\varepsilon,\mu} = \{x \in L \mid \delta(\bar{t}(x,\varepsilon,\mu),x,\varepsilon,\mu) = 0\}$, where $\bar{t}(x,\varepsilon,\mu)$ is such that

$$\delta_t(\bar{t}(x,\varepsilon,\mu),x,\varepsilon,\mu) = 0 \quad \text{for any } x \in \mathcal{S}_{\varepsilon,\mu}.$$

As a consequence,

$$\delta(\bar{t}(x(\varepsilon,\mu),\varepsilon,\mu),x(\varepsilon,\mu),\varepsilon,\mu) = 0.$$

Differentiating with respect to $\varepsilon = 0$ and using

$$\delta_t(\bar{t}(x,\varepsilon,\mu),x,\varepsilon,\mu) = 0 \quad \text{for any } x \in \mathcal{S}_{\varepsilon,\mu}$$

we get:

$$\delta_x(\bar{t}(x(\varepsilon,\mu),\varepsilon,\mu),x(\varepsilon,\mu),\varepsilon,\mu)x_\varepsilon(\varepsilon,\mu)+\delta_\varepsilon(\bar{t}(x(\varepsilon,\mu),\varepsilon,\mu),x(\varepsilon,\mu),\varepsilon,\mu)=0.$$

Setting $\varepsilon=0$ and recalling that $x(0,\mu)=\bar{x}$, $\bar{t}(\bar{x},0,\mu)=t_0$, $\phi_0(t_0,\bar{x})=x_0$, the previous equation gives:

$$G'(x_0)[\phi_{0x}(t_0,\bar{x})x_\varepsilon(0,\mu)+\phi_\varepsilon(t_0,\bar{x},0,\mu)]=0.$$

Thus:

$$\begin{aligned}\psi^*(P'(\bar{x})-\mathbb{I})x_\varepsilon(0,\mu)&=-\lambda G'(x_0)\phi_x(t_0,\bar{x},0,\mu)x_\varepsilon(0,\mu)\\&=\lambda G'(x_0)\phi_\varepsilon(t_0,\bar{x},0,\mu).\end{aligned}$$

As a consequence:

$$\mathcal{G}(\mu,0)=\lambda G'(x_0)\phi_\varepsilon(t_0,\bar{x},0,\mu)+\psi^*\phi_\varepsilon(T,\bar{x},0,\mu).$$

Now we observe that $(\mathbb{I}-\bar{P})[\pi(x,\varepsilon,\mu)-x]=0$, for any $x\in\overline{B^\varepsilon_-(\bar{x},\rho)}\cap L$ since $\pi(x,\varepsilon,\mu)-x\in T_{\bar{x}}L$. Let $x(\varepsilon)\in\overline{B^\varepsilon_-(\bar{x},\rho)}\cap L$ be such that $x(0)=\bar{x}$. Write $x(\varepsilon)=\bar{x}+\varepsilon\tilde{x}(\varepsilon)$, where $\tilde{x}(\varepsilon)$ is a C^1 function taking values in $\in T_{\bar{x}}L$. Then differentiating $(\mathbb{I}-\bar{P})[\pi(\bar{x}+\varepsilon\tilde{x}(\varepsilon),\varepsilon,\mu)-\bar{x}-\varepsilon\tilde{x}(\varepsilon)]=0$ at $\varepsilon=0$ we get:

$$(\mathbb{I}-\bar{P})[P'(\bar{x})\tilde{x}(0)-\tilde{x}(0)+\pi_\varepsilon(\bar{x},0,\mu)]=0$$

since $P'(\bar{x})=\pi_x(\bar{x},0,\mu)$. However $P'(\bar{x}):T_{\bar{x}}L\to T_{\bar{x}}L$ and hence $(\mathbb{I}-\bar{P})P'(\bar{x})=0$. Thus $(\mathbb{I}-\bar{P})\pi_\varepsilon(\bar{x},0,\mu)=0$ for any $\mu\in\mathbb{R}$. Then, using (4.8) we get:

$$f_+(\bar{x})T_\varepsilon(\bar{x},0)=-(\mathbb{I}-\bar{P})\phi_\varepsilon(T,\bar{x},0,\mu).$$

Now $\phi(t,\bar{x},\varepsilon,\mu)$ is the solution of the Cauchy problem:

$$\begin{cases}\dot{z}=f_+(z)+\varepsilon g_+(z,\varepsilon,\mu)\\ z(0)=\bar{x}\end{cases}$$

and hence differentiating with respect to ε and recalling that $\phi(t,\bar{x},0,\mu)=x_0(t)$, we see that $\phi_\varepsilon(t,\bar{x},0,\mu)$ satisfies:

$$\begin{cases}\dot{z}=f'_+(x_0(t))z+g_+(x_0(t),0,\mu)\\ z(0)=0.\end{cases}$$

Hence

$$\phi_\varepsilon(t,\bar{x},0,\mu)=\int_0^t X(t)X(s)^{-1}g_+(x_0(s),0,\mu)ds$$

with $X(t) = \phi_{0x}(t, \bar{x})$. Hence

$$\begin{aligned}
&\mathcal{G}(\mu, 0) = \lambda G'(x_0) \int_0^{t_0} X(t_0)X(s)^{-1} g_+(x_0(s), 0, \mu)ds \\
&+\psi^* \int_0^T X(T)X(s)^{-1} g_+(x_0(s), 0, \mu)ds \\
&= \int_0^{t_0} \psi_1(s)^* g_+(x_0(s), 0, \mu)ds + \int_0^T \psi(s)^* g_+(x_0(s), 0, \mu)ds
\end{aligned}$$

for

$$\psi_1(t) = X(t)^{-1*} X(t_0)^* [\lambda G'(x_0)]^*, \quad \psi(t) = X(t)^{-1*} X(T)^* \psi.$$

Note $\psi_1(t)$ and $\psi(t)$ solve the adjoint linear equation

$$\dot{x} = -f'_+(x_0(t))x$$

together with

$$\begin{aligned}
&\psi_1(0) = \lambda X(t_0)^* G'(x_0)^* = \lambda \phi_{0x}(t_0, \bar{x})^* G'(x_0)^* = \mathcal{A}^* \psi, \\
&\psi(T) - \psi(0) = \psi_1(0).
\end{aligned}$$

The first is obvious, as for the second we have indeed:

$$\psi(T) - \psi(0) = (\mathbb{I} - X(T))^* \psi = [\psi^* (\mathbb{I} - X(T))]^*.$$

Differentiating $P(x) = \phi_0(T(x), x)$ at $x = \bar{x}$ we get: $P'(\bar{x}) = f_+(\bar{x})T'(\bar{x}) + \phi_{0x}(T, \bar{x})$ i.e. $X(T) = P'(\bar{x}) - f_+(\bar{x})T'(\bar{x})$. So, recalling that $\psi^* f_+(\bar{x}) = 0$,

$$\psi^*(\mathbb{I} - X(T)) = \psi^*(\mathbb{I} - P'(\bar{x})) = \psi^* \mathcal{A} = \lambda b^* = \lambda G'(x_0) X(t_0)$$

and then

$$\psi(T) - \psi(0) = \lambda X(t_0)^* G'(x_0)^* = \psi_1(0).$$

Since $\psi_1(t)$ solves the adjoint equation, condition $\psi_1(0) = \psi(T) - \psi(0)$ defines $\psi_1(t)$ uniquely in terms of $\psi(t)$.

5 Example

Consider the unperturbed Hamiltonian system

$$\begin{cases}
\dot{x} = H_y(x, y) := \frac{\partial H}{\partial y}(x, y) \\
\dot{y} = -H_x(x, y) := -\frac{\partial H}{\partial x}(x, y) \\
\dot{z} = h(z)
\end{cases} \tag{5.1}$$

where $h(0) = 0$, $h'(0) \neq 0$ and $h \in C^2$, $H \in C^3$. Let the discontinuity manifold be defined by the equation $G(x, y, z) := x - c = 0$, $c \in \mathbb{R}$ and suppose the equation

$$\begin{cases} \dot{x} = H_y(x, y) \\ \dot{y} = -H_x(x, y) \end{cases}$$

has the T-periodic solution $(x_0(t), y_0(t))$ such that $x_0(t) > c$ for any $t \in [0, T] \setminus \{t_0\}$ and $x_0(t_0) = c$. We take $\gamma(t) := (x_0(t), y_0(t), 0)^*$ as the T-periodic solution of Eq. (5.1) to which we apply Theorem 4.1. Note that $\gamma(t)$ has been denoted by $x_0(t)$ in the previous sections. We use this different notation to avoid misunderstanding. We write $\bar{x}$ for $(x_0, y_0, 0) := (x_0(0), y_0(0), 0)$. With reference to the notation of the previous sections, we have:

$$T_{\bar{x}}L = \left\{ \begin{pmatrix} H_y(x, y) \\ -H_x(x, y) \\ 0 \end{pmatrix} \right\}^{\perp} = \left\{ \begin{pmatrix} u \\ v \\ w \end{pmatrix} \mid H_y(x_0, y_0)u = H_x(x_0, y_0)v \right\},$$

hence

$$T_{\bar{x}}L = \left\{ \begin{pmatrix} uH_x(x_0, y_0) \\ uH_y(x_0, y_0) \\ w \end{pmatrix} \mid u, w \in \mathbb{R} \right\} = \left\{ \begin{pmatrix} -u\dot{y}_0(0) \\ u\dot{x}_0(0) \\ w \end{pmatrix} \mid u, w \in \mathbb{R} \right\}$$

and

$$L = \bar{x} + T_{\bar{x}}L = \left\{ \begin{pmatrix} x_0 - u\dot{y}_0(0) \\ y_0 + u\dot{x}_0(0) \\ w \end{pmatrix} \mid u, w \in \mathbb{R} \right\}.$$

For $(x, y, z) \in L$, the Poincaré map is then given by

$$P(x, y, z) = P(x_0 + uH_x(x_0, y_0), y_0 + uH_y(x_0, y_0), w).$$

Next, the flow of Eq. (5.1) can be written as:

$$\phi_0(t, x, y, z) = (\phi_1(t, x, y), \phi_2(t, x, y), \phi_3(t, z))^*. \tag{5.2}$$

and then $\phi_0(t, x, y, z) \in L$ if and only if $\phi_1(t, x, y) = x_0 + uH_x(x_0, y_0)$ and $\phi_2(t, x, y) = y_0 + uH_y(x_0, y_0)$ for some u, that is, if and only if

$$H_y(x_0, y_0)[\phi_1(t, x, y) - x_0] = H_x(x_0, y_0)[\phi_2(t, x, y) - x_0].$$

Hence the time needed to a solution starting from L to reach again L is a function of (x, y) only. Thus

$$P(x, y, z) = \phi(T(x, y), x, y, z), \text{ for any } (x, y, z) \in L.$$

We derive, using also (5.2)

$$\frac{\partial P}{\partial x}(x_0, y_0, 0) = \phi_t(T, x_0, y_0, 0)T_x(x_0, y_0) + \phi_x(T, x_0, y_0, 0)$$
$$= \dot{\gamma}(T)T_x(x_0, y_0) + \phi_x(T, x_0, y_0, 0),$$

$$\frac{\partial P}{\partial y}(x_0, y_0, 0) = \phi_t(T, x_0, y_0, 0)T_y(x_0, y_0) + \phi_y(T, x_0, y_0, 0)$$
$$= \dot{\gamma}(T)T_x(x_0, y_0) + \phi_x(T, x_0, y_0, 0),$$

$$\frac{\partial P}{\partial z}(x_0, y_0, 0) = \phi_z(T, x_0, y_0, 0) = (0, 0, \phi_{3,z}(T, 0))^* = (0, 0, e^{h'(0)t})^*,$$

since $\phi_{3,z}(t, 0)$ is a solution of equation $\dot{z} = h'(0)z$, $z(0) = 1$.

Then:

$$P'(\bar{x}) = \begin{pmatrix} \pi_0 & 0 \\ 0 & e^{h'(0)T} \end{pmatrix},$$

where π_0 is the derivative of the Poincaré map of the Hamiltonian system (5.1) without the z-equation. We take the basis of $T_{\bar{x}}L$:

$$e = \begin{pmatrix} -\dot{y}_0(0) \\ \dot{x}_0(0) \\ 0 \end{pmatrix}, \quad e_3 = \begin{pmatrix} 0 \\ 0 \\ 1 \end{pmatrix}.$$

Now we look at $\mathcal{S}_0$. Since the (x, y)-equations and the z-equation are uncoupled, we see that $(x_0(t), y_0(t), z(\tau)) \in \mathcal{S}_0$, for all t and τ in a small neighbourhood of $t = 0$. Hence

$$T_{\bar{x}}\mathcal{S}_0 = \text{span}\left\{ \begin{pmatrix} \dot{x}_0(0) \\ \dot{y}_0(0) \\ 0 \end{pmatrix}, \begin{pmatrix} 0 \\ 0 \\ 1 \end{pmatrix} \right\}.$$

We conclude that, being $T_{\bar{x}}(\mathcal{S}_0 \cap L)$ one-dimensional:

$$T_{\bar{x}}(\mathcal{S}_0 \cap L) = \text{span}\,\{e_3\}.$$

We have

$$(\mathbb{I} - P'(\bar{x}))e_3 = \begin{pmatrix} 0 \\ 0 \\ 1 - e^{h'(0)T} \end{pmatrix} = (1 - e^{h'(0)T})e_3.$$

Thus, since $h'(0) \neq 0$, we see that $\mathcal{R}(\mathbb{I} - P'(\bar{x}))_{|T_{\bar{x}}(\mathcal{S}_0 \cap L)} = \text{span}\{e_3\}$ from which assumption (4.1) follows.

Next, the adjoint equation reads:

$$\begin{cases} \dot{x} = -H_{xy}(x_0(t), y_0(t))x + H_{xx}(x_0(t), y_0(t))y \\ \dot{y} = -H_{yy}(x_0(t), y_0(t))x + H_{xy}(x_0(t), y_0(t))y \\ \dot{z} = -h'(0)z \end{cases}$$

and it follows from the previous considerations that

$$T_{\bar{x}}L \cap \text{span}\{e_3\}^{\perp} = \text{span}\{e\}.$$

Thus, since $(x_0(t), y_0(t))$ is $T-$periodic, we see that, up to a multiplicative constant, $\psi(t)$ solves

$$\begin{cases} \dot{x} = -H_{xy}(x_0(t), y_0(t))x + H_{xx}(x_0(t), y_0(t))y \\ \dot{y} = -H_{yy}(x_0(t), y_0(t))x + H_{xy}(x_0(t), y_0(t))y \\ \dot{z} = -h'(0)z \\ x(T) = -\dot{y}_0(0) = -\dot{y}_0(T), \quad y(T) = \dot{x}_0(0) = \dot{x}_0(T), \quad z(T) = 0. \end{cases}$$

So $\psi(t) = (-\dot{y}_0(t), \dot{x}_0(t), 0)$ is T-periodic and then $\psi_1(0) = \psi(T) - \psi(0) = 0, \psi_1(t)$ being a solution of the adjoint equation. We conclude that

$$\Delta(\mu) = \int_0^T (-\dot{y}_0(t), \dot{x}_0(t), 0)^* g_+(x_0(t), y_0(t), 0, \mu)dt.$$

For concreteness, let us consider

$$\begin{cases} \dot{x} = y \\ \dot{y} = -x + \varepsilon(y(\mu - y^2) + z) \\ \dot{z} = \sin z + \varepsilon(x + y + z), \end{cases} \tag{5.3}$$

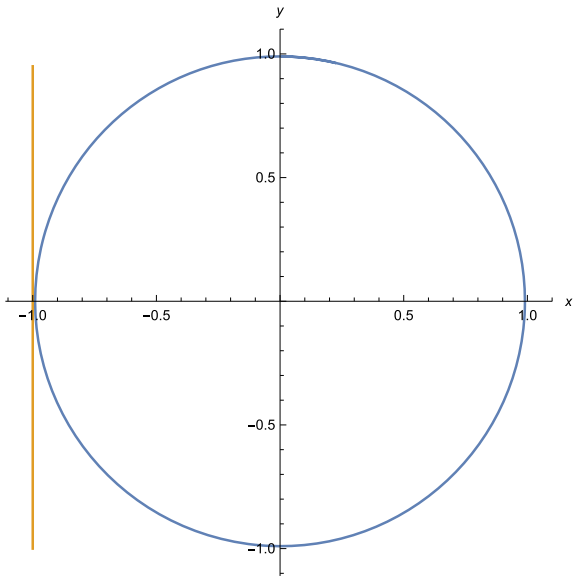

Fig. 1 The plot of solutions $(x(t), y(t))$ of (5.3) with $\mu = 0.751$, $\varepsilon = 0.01$ and $x(0) = 0.01$, $y(0) = 0.99$, $z(0) = -0.01$ on $[0, 6.5]$

so $H(x, y) = \frac{x^2+y^2}{2}$, $h(z) = \sin z$, $G(x, y, z) = x + 1$ and $g_+(x, y, \varepsilon, \mu) = (0, y(\mu - y^2) + z, x + y + z)^*$. Then $x_0(t) = \sin t$, $y_0(t) = \cos t$, $t_0 = \pi$, $T = 2\pi$ and

$$\Delta(\mu) = \int_0^{2\pi} \cos^2 t(\mu - \cos^2 t)dt = \pi\left(\mu - \frac{3}{4}\right).$$

Clearly $\mu = \frac{3}{4}$ is a simple zero of $\Delta(\mu)$, so applying Theorem 4.1, there is a smooth function $\mu(\varepsilon)$ defined for ε small such that $\mu(0) = \frac{3}{4}$ and (5.3) possesses a periodic and grazing solution for $\mu = \mu(\varepsilon)$ which is located near $(\sin t, \cos t, 0)$ (see Fig. 1).

Acknowledgements We thank the referees for careful reading and valuable comments that helped to improve the chapter.

References

1. M. Akhmet, A. Kivilcim, Stability in non-autonomous periodic systems with grazing stationary impacts. Carpathian J. Math. **33**, 1–8 (2017)
2. J. Awrejcewicz, M.M. Holicke, *Smooth and Nonsmooth High Dimensional Chaos and the Melnikov-Type Methods* (World Scientific Publishing Co., Singapore, 2007)
3. P. Olejnik, J. Awrejcewicz, M. Fečkan, *Modeling, Analysis and Control of Dynamical Systems: With Friction and Impacts* (World Scientific Publishing Co. Pte. Ltd., New Jersey, 2018)
4. M. di Bernardo, C.J. Budd, A.R. Champneys, P. Kowalczyk, *Piecewise-Smooth Dynamical Systems: Theory and Application* (Springer, London, 2008)
5. O. Makarenkov, J.S.W. Lamb, Dynamics and bifurcations of nonsmooth systems: a survey. Phys. D Nonlinear Phenom. **241**, 1826–1844 (2012)
6. J. Guckenheimer, P. Holmes, *Nonlinear Oscillations, Dynamical Systems and Bifurcations of Vector Fields* (Springer, New York, 1983)

Modelling and Analysis of Predation System with Nonlocal and Nonsingular Operator

Kolade M. Owolabi and Hemen Dutta

1 Introduction

A general time-dependent partial differential equation (PDE) of reaction-diffusion type is an equation of the form

$$u_t = \delta Lg(x,t) + Fg(x,t), \tag{1.1}$$

where L is the stiff part that stands for the linear operator, and F is non-stiff or mildly stiff part that represents the nonlinear operator [1, 2], which accounts for the local reaction, and δ is the diffusion coefficient, $g(x,t)$ denotes density or concentration of species at time t and position x. Reaction-diffusion system is a set of mathematical equations that illustrate the manner in which the density of species or concentration of substances is being distributed in space under the influence of reaction and diffusion. Many physical problems encountered in various fields of applied sciences and engineering, such as the Gray-Scott, Fisher-KPP, Allen-Cahn, and many other biological systems are modelled in the form (1.1).

Fractional reaction-diffusion system that governs the nonlinear interaction between the predator and prey species are considered in this work for spatial pattern formations. Population dynamics has become an important area of research, which is aimed to analyse how various dynamical behaviours may influence the ecosystem distribution. The spatial pattern formation is regarded as one of the key areas of study in mathematical biology [3]. The most widely studied dynamic for spatial pattern formation process is the reaction-diffusion system that was suggested by Alan Turing

K. M. Owolabi (✉)
Faculty of Mathematics and Statistics, Ton Duc Thang University,
Ho Chi Minh City, Vietnam
e-mail: kolademattheowolabi@tdtu.edu.vn

H. Dutta
Department of Mathematics, Gauhati University, Guwahati 781014, India

H. Dutta (ed.), *Mathematical Modelling in Health, Social and Applied Sciences*, Forum for Interdisciplinary Mathematics, https://doi.org/10.1007/978-981-15-2286-4_8

in 1952 [4]. It was demonstrated that a system of reacting and diffusing chemical species could give arise from initial near-homogeneity into a spatial structure of chemical concentration. The scenario called Turing instability or diffusion-driven instability has now been proved to arise in chemistry. Numerical experiments have shown and lead to the formation of spots, stripes, mitotic spots and stripes and other complex patterns, see [3, 5–10] for theoretical and experimental literature on spatial pattern formation processes.

In recent years, research has shown that models with fractional-order case are most reliable and accurate when compared to classical order problems [11, 12]. Fractional calculus is considered as the generalization of standard derivatives and integrals to fractional derivatives and integrals, and it has been the focus of many studies over the years due to their wide range of applicability such as fluid mechanics, physics, biology, viscoelasticity, fractals, groundwater analysis and other engineering applications, see [12–15] for more details. Various numerical methods have been proposed for solving fractional reaction-diffusion equations, see [11, 16–24].

There are several existing definitions and properties of fractional calculus. In what follows, we briefly report some definitions based on fractional derivatives and integrals that are connected to this study.

Let g to be a not necessarily differentiable function, let γ be real such that $\gamma > 0$, then the Caputo derivative of fractional power γ is defined as [15]

$$ {}_0^C\mathcal{D}_t^{\gamma} g(t) = \frac{1}{\Gamma(\gamma)} \int_0^t (t-\xi)^{\gamma-1} g(\xi) d\xi. \tag{1.2} $$

We adapt the Sobolev space given by

$$ \mathcal{H}^1[a,b] := \left\{ g \in L^2[a,b] : \frac{dg}{dt} \in L^2[a,b] \right\} $$

to define the Caputo-Fabrizio and Atangana-Baleanu fractional derivatives for the Caputo and Riemann-Liouville cases.

Let $g \in \mathcal{H}^1(a,b)$, for $b > a$ and $\gamma \in [0,1]$ then the Caputo-Fabrizio fractional derivative of order γ with exponential law is defined by [25]

$$ {}^{CF}\mathcal{D}_t^{\gamma} g(t) = \frac{M(\gamma)}{(1-\gamma)} \int_a^t g'(\xi) \exp\left[-\gamma \frac{t-\xi}{1-\gamma} \right] d\xi, \tag{1.3} $$

where $M(\alpha)$ denotes a normalized function such that $M(0) = 1$ and $M(1) = 1$.

For $g \in \mathcal{H}^1[a,b]$ and $0 < \gamma < 1$, the left and right Atangana-Baleanu operators in the sense of Caputo are given by

$$ {}^{ABC}_{a}\mathcal{D}^{\gamma}_{t} g(t) = \frac{M(\gamma)}{1-\gamma} \int_a^t g'(\xi) E_\gamma \left(-\frac{\gamma}{1-\gamma}(t-\xi)^\gamma \right) d\xi, \tag{1.4} $$

and

$$ {}^{ABC}_{b}\mathcal{D}^{\gamma}_{t} g(t) = \frac{-M(\gamma)}{1-\gamma} \int_t^b g'(\xi) E_\gamma \left(-\frac{\gamma}{1-\gamma}(\xi-t)^\gamma \right) d\xi, \tag{1.5} $$

respectively. Similarly, with $g \in \mathcal{H}^1[a,b]$ and $0 < \gamma < 1$, the left and right Atangana-Baleanu operators in Riemann-Liouville sense are defined as

$$ {}^{ABC}_{a}\mathcal{D}^{\gamma}_{t} g(t) = \frac{M(\gamma)}{1-\gamma} \frac{d}{dt} \int_a^t g(\xi) E_\gamma \left(-\frac{\gamma}{1-\gamma}(t-\xi)^\gamma \right) d\xi, \tag{1.6} $$

and

$$ {}^{ABC}_{b}\mathcal{D}^{\gamma}_{t} g(t) = \frac{-M(\gamma)}{1-\gamma} \frac{d}{dt} \int_t^b g(\xi) E_\gamma \left(-\frac{\gamma}{1-\gamma}(\xi-t)^\gamma \right) d\xi, \tag{1.7} $$

where $M(\gamma) > 0$ denotes the normalization function as in the case of Caputo-Fabrizio derivative.

The left and right fractional integrals for the Atangana-Baleanu derivative are given by

$$ {}^{AB}_{a}I^{\gamma} g(t) = \frac{1-\gamma}{M(\gamma)} g(t) + \frac{\gamma}{M(\gamma)} {}_{a}I^{\gamma} g(t) $$

and

$$ {}^{AB}_{b}I^{\gamma} g(t) = \frac{1-\gamma}{M(\gamma)} g(t) + \frac{\gamma}{M(\gamma)} {}_{b}I^{\gamma} g(t)\xi. $$

The Laplace transform of the left Atangana-Baleanu derivatives in both sense of Caputo and Riemann-Liouville operators is respectively given as

$$ \mathscr{L}\left\{ {}^{ABC}_{a}\mathcal{D}^{\gamma}_{t} g(t) \right\} = \frac{M(\gamma)}{1-\gamma} \frac{s^\gamma \mathfrak{L}\{g(t)\}(s) - s^{\gamma-1} g(a)}{s^\gamma + \frac{\gamma}{1+\gamma}} $$

and

$$ \mathscr{L}\left\{ {}^{ABR}_{a}\mathcal{D}^{\gamma}_{t} g(t) \right\} = \frac{M(\gamma)}{1-\gamma} \frac{s^\gamma \mathfrak{L}\{g(t)\}(s)}{s^\gamma + \frac{\gamma}{1+\gamma}}. $$

Mittag-Leffler function is an important operator which has been described by many authors in several books and excellent papers [26–29]. Some authors through the Laplace transform have reported the associated integral to ABC nonlocal and

nonsingular fractional derivative in [30, 31]. We define the one parameter Mittag-Leffler kernel in (1.4) by

$$E_\gamma(z) = \sum_{k=0}^{\infty} \frac{z^k}{\Gamma(\gamma k + 1)}, \quad Re(\gamma) > 0. \tag{1.8}$$

The two-parameter Mittag-Leffler kernel is given by the series expansion

$$E_{\gamma,\eta}(z) = \sum_{k=0}^{\infty} \frac{z^k}{\Gamma(\gamma k + \eta)}, \ (\gamma, \eta \in C, Re(\gamma) > 0). \tag{1.9}$$

Lemma 1.1 *[32] Let $s, s_1, s_2, s_3 \in C$, $(Re(s), Re(s_1), Re(s_2) > 0)$. Then*

$$\int_0^y (y-t)^{s_1-1} E_{s,s_1}(s_3(y-t)^s) t^{s_2-1} dt = \Gamma(s_2) y^{s_1+s_2-1} E_{s,s_1+s_2}(s_3 y^s). \tag{1.10}$$

The choice of using the ABC derivative in this paper is due to a number of the merits the operator has over some of the existing derivatives that have been applied over the years. This new derivative has brought new weapons into applied mathematics to model complex real-world scenarios more accurately because the operator has both Markovian and non-Markovian properties, while the Riemann-Liouville and Caputo derivatives have just Markovian and non-Markovian, respectively. The ABC waiting time combined the power law, stretched exponential and Brownian motion, while Riemann-Liouville and Caputo derivatives have only power law and exponential decay, respectively. Atangana-Baleanu derivative in the sense of Caputo has probability distribution which is both Gaussian and non-Gaussian and can switch over from Gaussian to non-Gaussian without steady state.

The aim of this chapter is to extend the concept of fractional calculus to study pattern formation process in a range of multicomponent predator-prey dynamics of fractional reaction-diffusion systems. The remainder part of this work is broken into sections as follows. General reaction-diffusion system modelled with the novel Atangana-Baleanu operator of fractional order is presented in Sect. 2, with suggested numerical method of solution. Predator-prey system of two-, three-species and their linear stability analysis are given in Sect. 3. Numerical experiments are given in Sect. 4. Finally, conclusion is made in Sect. 5.

2 Approximation Techniques

In this section, a numerical technique for solving the general partial differential equation with non-integer order is derived in the sense of Atangana-Baleanu fractional operator. To achieve this, we replace the classical time derivative in (1.1) with the ABC derivative to obtain

$$^{ABC}{}_0\mathcal{D}_t^{\gamma} g(x,t) = \delta L g(x,t) + F g(x,t), \tag{2.11}$$

where $^{ABC}{}_0\mathcal{D}_t^{\gamma}$ is defined as the left ABC derivative given in (1.4), L and F remain as the linear and nonlinear operators, respectively. For simplicity, we relax the diffusion constant by setting it to unity. Next, we apply Laplace transform to both sides of the above equation to obtain

$$\begin{aligned} \mathscr{L}\left\{^{ABC}{}_0\mathcal{D}_t^{\gamma} g(x,t)\right\} &= \mathscr{L}\left\{L g(x,t) + F g(x,t)\right\}, \\ ^{ABC}{}_0\mathcal{D}_t^{\gamma} g(s,t) &= \mathscr{L}\left\{L g(x,t) + F g(x,t)\right\}. \end{aligned} \tag{2.12}$$

By substituting $g(s,t) = g(t)$ and $\mathscr{L}\{Lg(x,t) + Fg(x,t)\} = G(g,t)$ we get

$$^{ABC}{}_0\mathcal{D}_t^{\gamma} g(t) = G(g,t). \tag{2.13}$$

With the use of Atangana-Baleanu fractional integral, we have

$$g(x,t) = g(x,0) + \frac{1-\gamma}{M(\gamma)} G(g,t) + \frac{\gamma}{M(\gamma)\Gamma(\gamma)} \int_0^t G(g,\xi)(t-\xi)^{\gamma-1} d\xi. \tag{2.14}$$

At $g(x,t_n) = g_n$, we have

$$g_{n+1} = g_0 + \frac{1-\gamma}{M(\gamma)} G(g,t_{n+1}) + \frac{\gamma}{M(\gamma)\Gamma(\gamma)} \int_0^{t_{n+1}} G(g,\xi)(t_{n+1}-\xi)^{\gamma-1} d\xi \tag{2.15}$$

and

$$g_n = g_0 + \frac{1-\gamma}{M(\gamma)} G(g,t_n) + \frac{\gamma}{M(\gamma)\Gamma(\gamma)} \int_0^{t_n} G(g,\xi)(t_n-\xi)^{\gamma-1} d\xi. \tag{2.16}$$

By subtracting (2.16) from (2.15), one obtains

$$\begin{aligned} g_{n+1} = g_n &+ \frac{1-\gamma}{M(\gamma)}[G_{n+1} - G_n] \\ &+ \frac{\gamma}{M(\gamma)\Gamma(\gamma)} \left[\int_0^{t_{n+1}} G(g,\xi)(t_{n+1}-\xi)^{\gamma-1} - \int_0^{t_n} G(g,\xi)(t_n-\xi)^{\gamma-1}\right] d\xi \end{aligned} \tag{2.17}$$

Next, we approximate the function $G(g,t)$ in terms of the Lagrangian polynomial as

$$G(g,t) \approx P(t) = \frac{t-t_{n-1}}{t_n - t_{n-1}} G_n + \frac{t-t_n}{t_{n-1}-t_n} G_{n-1} \tag{2.18}$$

By following the procedure in [33], we finally have

$$g_{n+1} = g_n + \frac{1-\gamma}{M(\gamma)}[G_{n+1} - G_n] + \frac{\gamma}{M(\gamma)\Gamma(\gamma)} \begin{bmatrix} h^\gamma \left(\frac{2(n+1)^\gamma}{\gamma} - \frac{(n+1)^{\gamma+1}}{\gamma+1} \right) G_n \\ -h^\gamma \left(\frac{(n+1)^\gamma}{\gamma} - \frac{(n+1)^{\gamma+1}}{\gamma+1} \right) G_{n-1} \\ -h^\gamma \left(\frac{n^\gamma}{\gamma} - \frac{n^{\gamma+1}}{\gamma+1} \right) G_n + \frac{n^{\gamma+1}}{\gamma+1} G_{n-1} \end{bmatrix} \tag{2.19}$$

which after further factorization becomes

$$\begin{aligned} g_{n+1} = g_n &+ \frac{1-\gamma}{M(\gamma)}[G_{n+1} - G_n] \\ &+ \frac{\gamma h^\gamma}{M(\gamma)\Gamma(\gamma)} \left\{ \left(\frac{2(n+1)^\gamma - n^\gamma}{\gamma} + \frac{n^{\gamma+1} - (n+1)^{\gamma+1}}{\gamma+1} \right) G_n \right. \\ &\left. - \left(\frac{2(n+1)^\gamma - n^\gamma}{\gamma} + \frac{n^{\gamma+1} - (n+1)^{\gamma+1}}{\gamma+1} \right) G_{n-1} \right\} \end{aligned} \tag{2.20}$$

It should be mentioned that we recover the classical Adams-Bashforth method as $\gamma \to 1$. For stability and convergence properties of this scheme, see [33].

To define the scheme in real space, we then apply the inverse Laplace transform technique as

$$g(x, t_{n+1}) = \mathscr{L}^{-1} \left\{ \begin{array}{r} g(x, t_n) + \frac{1-\gamma}{M(\gamma)}[G_{n+1} - G_n] \\ + \frac{\gamma h^\gamma}{M(\gamma)\Gamma(\gamma)} \left(\frac{2(n+1)^\gamma - n^\gamma}{\gamma} + \frac{n^{\gamma+1} - (n+1)^{\gamma+1}}{\gamma+1} \right) G_n \\ - \frac{\gamma h^\gamma}{M(\gamma)\Gamma(\gamma)} \left(\frac{2(n+1)^\gamma - n^\gamma}{\gamma} + \frac{n^{\gamma+1} - (n+1)^{\gamma+1}}{\gamma+1} \right) G_{n-1} \end{array} \right\}. \tag{2.21}$$

At this junction, any standard method can be used to discretize in space variable x in the form

$$g(x_j, t_{n+1}) = \mathscr{L}^{-1} \left\{ \begin{array}{r} g(x_j, t_n) + \frac{1-\gamma}{M(\gamma)}[G_j^{n+1} - G_j^n] \\ + \frac{\gamma h^\gamma}{M(\gamma)\Gamma(\gamma)} \left(\frac{2(n+1)^\gamma - n^\gamma}{\gamma} + \frac{n^{\gamma+1} - (n+1)^{\gamma+1}}{\gamma+1} \right) G_j^n \\ - \frac{\gamma h^\gamma}{M(\gamma)\Gamma(\gamma)} \left(\frac{2(n+1)^\gamma - n^\gamma}{\gamma} + \frac{n^{\gamma+1} - (n+1)^{\gamma+1}}{\gamma+1} \right) G_j^{n-1} \end{array} \right\}. \tag{2.22}$$

The linear and nonlinear operators on the right-hand side of Eq. (2.11) are discretized using the finite difference scheme, see [2] for details.

3 Main Models and Mathematical Analysis

In this section, we introduce two- and three-species models and carry out their linear stability analysis. The objective here is to seek for conditions under which the nontrivial steady-state solution is linearly stable in the absence of diffusion but unstable in the presence of diffusion. This phenomenon is popularly called the Turing instability or diffusion-driven instability. Spatial pattern formation will be examined by the numerical method.

3.1 Two-Species Predator-Prey System

A classical predator-prey model with logistic growth is given by [34]

$$\begin{aligned}\frac{\partial U}{\partial t} &= \delta_1 \Delta U + rU\left(1 - \frac{U}{K}\right) - (\lambda + aV)UV \\ \frac{\partial V}{\partial t} &= \delta_2 \Delta V - mV + e(\lambda + aV)UV,\end{aligned} \tag{3.23}$$

where $U(x, t)$, $V(x, t)$ are the population densities of prey and predator, respectively; $(x, t) \in \Omega \times \mathbb{R}^+$ with bounded boundary Ω, r and K are the prey intrinsic growth rate and carrying capacity, respectively. The food conversion rate is denoted by e, m denotes death rate of predator, the attack and cooperation in hunting rates are respectively, given as λ and a, diffusion coefficients for prey and predator are represented by δ_1 and δ_2. We assumed all parameters are positive. To ensure that nothing is going in and out of the domain, we impose homogeneous or zero-flux boundary conditions

$$\partial U \cdot \mathbf{n} = 0, \quad \partial V \cdot \mathbf{n} = 0, \quad \text{on } \partial\Omega \times \mathbb{R}^+,$$

where $\mathbf{n}$ is the outward normal to $\partial\Omega$, and subject to initial function

$$U(x, 0) = U_0(x), \quad V(x, 0) = V_0(x), \quad x \in \Omega.$$

To reduce the number of parameters, we adopt non-dimensional idea in [3, 9], by setting $x = x/d$, (with d, the diameter of Ω), $\tau = r/m$, $\kappa = e\lambda/m$, $\alpha = am/\lambda^2$, $\beta_i = \delta_i/d^2$, $i = 1, 2$. So that (3.23) becomes

$$\begin{aligned}\frac{\partial u}{\partial t} &= \delta_1 \Delta u + \tau u\left(1 - \frac{u}{\kappa}\right) - (1 + \alpha v)uv \\ \frac{\partial v}{\partial t} &= \delta_2 \Delta v - v + (1 + \alpha v)uv,\end{aligned} \tag{3.24}$$

By replacing the classical time derivative in (3.24) with the Atangana-Baleanu fractional-order operator, we have nonlinear system

$$\begin{aligned} {}^{ABC}{}_0\mathcal{D}_t^{\gamma} u &= \delta_1 \Delta u + \tau u\left(1 - \frac{u}{\kappa}\right) - (1 + \alpha v)uv \\ {}^{ABC}{}_0\mathcal{D}_t^{\gamma} v &= \delta_2 \Delta v - v + (1 + \alpha v)uv, \end{aligned} \tag{3.25}$$

Following the procedures in [3, 35], we denote the biologically meaningful equilibrium point which guarantees the coexistence of species u and v by $E^* = (u^*, v^*)$, where v^* is the solution of

$$g(x) := \kappa\rho^2 x^3 + 2\rho\kappa x^2 + \kappa(1 - \tau\rho)x + \tau(1 - \kappa) = 0$$

and

$$u^* = \frac{1}{1 + \rho v^*}.$$

For linear stability of (3.25), we let ${}^{ABC}{}_0\mathcal{D}_t^{\gamma} u = 0$ and ${}^{ABC}{}_0\mathcal{D}_t^{\gamma} v = 0$. Also, we assume

$$0 = \lambda_0 < \lambda_1 < \lambda_2 < \cdots < \lambda_n < \cdots \tag{3.26}$$

be the eigenvalues of the Jacobian or community matrix arising from

$${}^{ABC}{}_0\mathcal{D}_t^{\gamma}\begin{pmatrix} P \\ Q \end{pmatrix} = \begin{pmatrix} a_{11} & a_{12} \\ a_{21} & a_{22} \end{pmatrix}\begin{pmatrix} P \\ Q \end{pmatrix} + \begin{pmatrix} \delta_1 \Delta P \\ \delta_2 \Delta Q \end{pmatrix} + \begin{pmatrix} G_1 \\ G_2 \end{pmatrix} \tag{3.27}$$

where $P = u - u^*$ and $Q = v - v^*$ are the perturbation parameters, and

$$\begin{aligned} a_{11} &= -\frac{\tau}{\kappa(1 + \rho v^*)}, \quad a_{12} = -\frac{1 + 2\rho v^*}{1 + \rho v^*}, \\ a_{21} &= (1 + \rho v^*)v^*, \quad a_{22} = \frac{\rho v^*}{1 + \rho v^*} \\ G_1 &= -\frac{\tau P^2}{\kappa} - (1 + \rho v^*)PQ - \rho Q(PQ + u^* Q + v^* P), \\ G_2 &= (1 + \rho v^*)PQ + \rho Q(PQ + u^* Q + v^* P). \end{aligned} \tag{3.28}$$

For simplicity, we let

$${}^{ABC}{}_0\mathcal{D}_t^{\gamma}\mathbf{U} = \mathcal{A}\mathbf{U}, \tag{3.29}$$

where

$$\mathbf{U} = \begin{pmatrix} P \\ Q \end{pmatrix}, \quad \mathcal{A} = \begin{pmatrix} -\frac{\tau}{\kappa(1+\rho v^*)} + \delta_1 \Delta & -\frac{1+2\rho v^*}{1+\rho v^*} \\ (1 + \rho v^*)v^* & \frac{\rho v^*}{1+\rho v^*} + \delta_2 \Delta \end{pmatrix}. \tag{3.30}$$

For $i = 0, 1, 2, \ldots, \Lambda_i$ is an eigenvalue of $\mathcal{A}$ provided Λ_i is an eigenvalue of the following matrix

$$\mathcal{B} = \begin{pmatrix} -\left(\frac{\tau}{\kappa(1+\rho v^*)} + \lambda_i \delta_1\right) & -\frac{1+2\rho v^*}{1+\rho v^*} \\ (1+\rho v^*)v^* & \frac{\rho v^*}{1+\rho v^*} - \lambda_i \delta_2 \end{pmatrix}. \tag{3.31}$$

The characteristic polynomial equation of matrix $\mathcal{B}$ becomes

$$\Lambda_i^2 - \phi_i \Lambda_i + \varphi_i = 0, \tag{3.32}$$

where

$$\begin{aligned} \phi_i &= \phi_0 - \lambda_i(\delta_1 + \delta_2) \Longrightarrow \mathrm{tr}(\mathcal{B}_i), \\ \varphi_i &= \varphi_0 + \delta_1\delta_2\lambda_i^2 + \frac{\tau\delta_2 - \kappa\rho v^*\delta_1}{\kappa(1+\rho v^*)}\lambda_i \Longrightarrow \det(\mathcal{B}_i) \end{aligned} \tag{3.33}$$

and

$$\begin{aligned} \phi_0 &= -\frac{\tau}{\kappa(1+\rho v^*)} + \frac{\rho v^*}{1+\rho v^*} = \frac{\kappa\rho v^* - \tau}{\kappa(1+\rho v^*)}, \\ \varphi_0 &= \left(-\frac{\tau}{\kappa(1+\rho v^*)}\right)\left(\frac{\rho v^*}{1+\rho v^*}\right) - \left(-\frac{1+2\rho v^*}{1+\rho v^*}\right)\left((1+\rho v^*)v^*\right) \\ &= v^*\left(2\rho v^* - \frac{\tau\rho}{\kappa(1+\rho v^*)^2} + 1\right) \end{aligned} \tag{3.34}$$

being the main invariants without diffusion [35]. It should be noted that the necessary and sufficient condition for linear stability of equilibrium point E^* in the absence of diffusion is that $\phi_0 < 0$ and $\varphi_0 > 0$, see [3, 9] for details. it is obvious that in the absence of diffusion, the equilibrium point E^* is stable, provided the condition

$$\kappa\rho v^* < \tau < \frac{(1+2\rho v^*)(\kappa(1+\rho v^*))}{\rho} \tag{3.35}$$

is satisfied, and unstable if otherwise. Hence, the above inequality can be taken as necessary condition for stability in the presence of diffusion. The phase portraits and time series results for system (3.25) in the absence of diffusion for some γ are reported in Fig. 1.

Theorem 3.1 *For any of the conditions*

$$\kappa\rho v^* < \tau < \frac{(1+2\rho v^*)(\kappa(1+\rho v^*))}{\rho}, \quad \frac{\delta_2}{\delta_1} \geq \frac{\kappa\rho v^*}{\tau}, \tag{3.36}$$

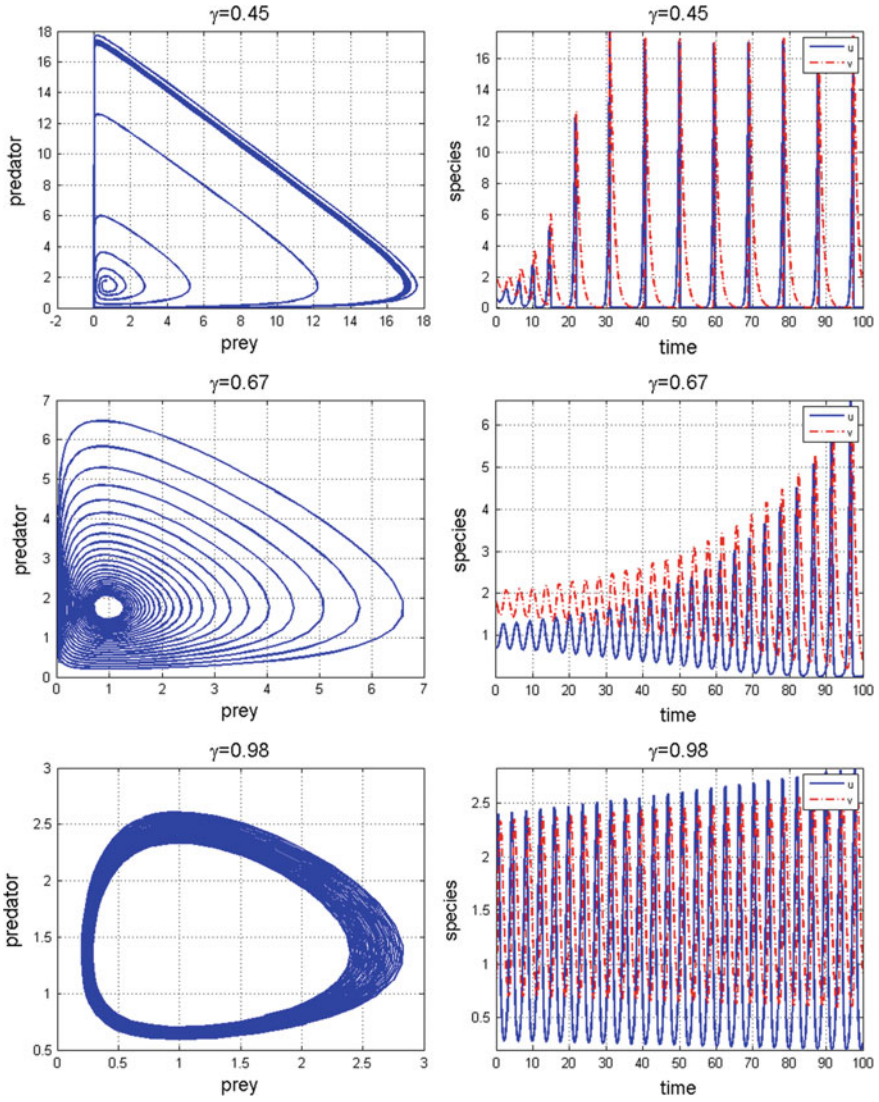

Fig. 1 Phase portraits and time series result for system (3.25) in the absence of diffusion for some instances of fractional order γ. Parameters are; $(u_0, v_0) = (1.7, 0.8)$, $\tau = 3$, $\alpha = 0.3$, $\kappa = 4.5$ for $t = 100$

and

$$\kappa\rho v^* < \tau < \frac{(1+2\rho v^*)(\kappa(1+\rho v^*))}{\rho}, \quad \frac{\delta_2}{\delta_1} < \frac{\kappa\rho v^*}{\tau},$$
$$\frac{(\kappa\delta_1\rho v^* - \tau\delta_2)^2}{\delta_1\delta_2} < 4\kappa v^*[(1+2\rho v^*)(1+\rho v^*)^2\kappa - \tau\rho] \tag{3.37}$$

to be satisfied,it implies the coexistence equilibrium state is linearly stable.

The proof follows directly, when inequality in (3.35) is satisfied, then $\phi_0 < 0\ \forall i$ such that $\phi_i < 0$. By virtue of the second condition in (3.33), it is obvious that any of conditions (3.36) or (3.37) indicate that for every i, $\varphi_i > 0$.

It is known that the equilibrium point E^* is stable and unstable in the absence and presence diffusion, respectively. This phenomenon is popularly referred to as diffusion-driven instability or Turing instability. For $\phi_0 < 0$ implies that $\phi_i < 0$, for all i. Then, diffusion-driven instability may arise if $\varphi_0 > 0$ and $\varphi_i < 0$. In addition, by virtue of necessary condition for the occurrence of Turing instability is that

$$\frac{\delta_2}{\delta_1} < \frac{\kappa\rho v^*}{\tau} \quad \delta_1 > \delta_2. \tag{3.38}$$

For further details on stability analysis of diffusive systems, readers are referred to the classical books by Murray [3, 9].

Theorem 3.2 *If conditions*

$$\kappa\rho v^* < \tau < \frac{(1+2\rho v^*)(\kappa(1+\rho v^*))}{\rho}$$

and

$$\frac{\delta_2}{\delta_1} < \frac{\kappa\rho v^*}{\tau} \quad \delta_1 > \delta_2$$

with either

$$\delta_1 > \frac{\kappa(1+\rho v^*)\varphi_0 + \tau\lambda_1\delta_2}{\kappa\lambda_1[\rho v^* - \lambda_1\delta_2(1+\rho v^*)]}$$
$$\delta_2 < \frac{\rho v^*}{\lambda_1(1+\rho v^*)} \tag{3.39}$$

or

$$\frac{(\kappa\delta_1\rho v^* - \tau\delta_2)^2}{\delta_1\delta_2} > 4\kappa v^*[\kappa(1+2\rho v^*)(1+\rho v^*)^2 - \tau\rho] \tag{3.40}$$

hold, then diffusion-driven instability is occurred.

3.2 Three-Species Predator-Prey-Mutualist System

The three component system here consists of the prey, predator and mutualist of species, interacting in nonlinear fashion to form the following partial differential equation

$$\begin{aligned}
&\frac{\partial u}{\partial t} - \delta_1 \Delta u = f_1(u, v, w) = u\left(1 - u - \frac{av}{1 + cw}\right), \quad x \in \Omega, t > 0,\\
&\frac{\partial v}{\partial t} - \delta_2 \Delta(v + \delta_4 uv) = f_2(u, v, w) = v(2 - v + bu), \ x \in \Omega, t > 0,\\
&\frac{\partial w}{\partial t} - \delta_3 \Delta w = f_3(u, v, w) = w\left(1 - \frac{w}{1 + du}\right), \qquad x \in \Omega, t > 0, \ (3.41)\\
&\partial_n u = 0, \ \partial_n v = 0, \ \partial_n w = 0, \qquad x \in \partial\Omega, t > 0,
\end{aligned}$$

where $u(x, t)$, $v(x, t)$ and $w(x, t)$ are respective prey, predator and mutualist population densities. In the model, $v-$prey serves as food to $u-$predator, the relationship between w and u is of symbiotic mutualist, c and d are mutualistic parameters, the maximum predator growth rate and predation coefficients are denoted by b and a, respectively. The constants $\delta_i (i = 1, 2, 3)$ are self-diffusion coefficients while $\delta_2\delta_4$ is the cross-diffusion pressure which represents the mutual interaction between the individual species. Here, Ω is the domain-habitat for the three species, which is bounded in $\mathbb{R}^N$ with smooth boundary $\partial\Omega$. The homogeneous Neumann boundary condition imposed here shows that there is zero-flux population across the boundary. For further biological background, see [3, 35–37].

Similarly, we replace the classical time derivative in system (3.41) with the ABC operator with fractional order $\gamma \in (0, 1]$ and set $\delta_4 = 0$ to obtain

$$\begin{aligned}
&{}^{ABC}{}_0\mathcal{D}_t^{\gamma} u - \delta_1 \Delta u = f_1(u, v, w) = u\left(1 - u - \frac{av}{1 + cw}\right), \quad x \in \Omega, t > 0,\\
&{}^{ABC}{}_0\mathcal{D}_t^{\gamma} v - \delta_2 \Delta v = f_2(u, v, w) = v(2 - v + bu), \qquad x \in \Omega, t > 0, \qquad (3.42)\\
&{}^{ABC}{}_0\mathcal{D}_t^{\gamma} w - \delta_3 \Delta w = f_3(u, v, w) = w\left(1 - \frac{w}{1 + du}\right), \qquad x \in \Omega, t > 0,
\end{aligned}$$

For spatial pattern formation analysis, we require to know the condition under which the nontrivial steady state is stable in the absence of diffusion and unstable in the presence of diffusion. By setting $f_i(u, v, w) = 0, i = 1, 2, 3$, and after some algebraic calculations we obtain the equilibrium state solution $E^* = (u^*, v^*, w^*)$, where

$$
\begin{aligned}
u^* &= \frac{c(d-1) - ab - 1 + \sqrt{[c(1-d) + ab + 1]^2 + 4cd(-2a + c + 1)}}{2cd} \\
v^* &= bu^* + 2 \\
w^* &= du^* + 1.
\end{aligned} \tag{3.43}
$$

To start with, we require to show that point E^* in the absence of diffusion ($\delta_i = 0, i = 1, 2, 3$) is locally stable, we have the fractional autonomous system

$$
\begin{aligned}
{}^{ABC}{}_0\mathcal{D}_t^{\gamma} u(t) &= u\left(1 - u - \frac{av}{1 + cw}\right), \quad t > 0, \\
{}^{ABC}{}_0\mathcal{D}_t^{\gamma} v(t) &= v(2 - v + bu), \ t > 0, \\
{}^{ABC}{}_0\mathcal{D}_t^{\gamma} w(t) &= w\left(1 - \frac{w}{1 + du}\right), t > 0.
\end{aligned} \tag{3.44}
$$

Numerical results for some values of γ are given in Fig. 2.

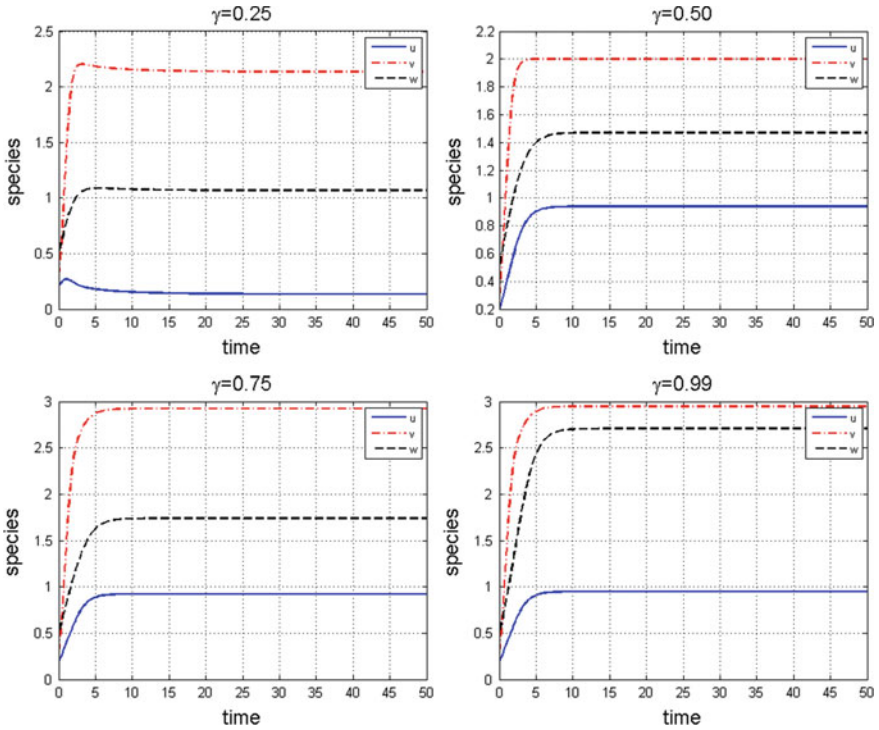

Fig. 2 Time series result of system (3.44) for different γ. Parameters are; $a = 3, b = 1, c = 6, d = 0.5$ for $t = 50$

Theorem 3.3 *The point E^* of system (3.44) which corresponds to the coexistence of the species is locally asymptotically stable if the following conditions hold:*

$$a \leq 4,\ b \leq 1,\ ad \leq 2,\ 1 = c > 2a. \tag{3.45}$$

Proof For notational convenience, we let

$$\mathbf{D}(z) = \begin{pmatrix} {}^{ABC}{}_0\mathcal{D}_t^{\gamma} u \\ {}^{ABC}{}_0\mathcal{D}_t^{\gamma} v \\ {}^{ABC}{}_0\mathcal{D}_t^{\gamma} w \end{pmatrix} = \begin{pmatrix} u\left(1 - u - \frac{av}{1+cw}\right) \\ v(2 - v + bu) \\ w\left(1 - \frac{w}{1+du}\right) \end{pmatrix} \tag{3.46}$$

Obviously, with $\mathbf{D}(z)|_{E^*} = 0$, we have

$$\mathbf{A}|_{E^*} = \begin{pmatrix} -u^* & -\frac{au^*}{1+cw^*} & \frac{acu^*v^*}{(1+cw^*)^2} \\ bv^* & -v^* & 0 \\ \frac{dw^{*3}}{(1+du^*)^2} & 0 & \frac{-w^*}{1+du^*} \end{pmatrix} \tag{3.47}$$

with corresponding characteristic equation

$$\zeta(\lambda) = \lambda^3 + q_1\lambda^2 + q_2\lambda + q_3, \tag{3.48}$$

where

$$\begin{aligned} q_1 &= u^* + v^* + \frac{w^*}{1+du^*}, \\ q_2 &= u^*v^* + \frac{w^*(u^*+v^*)}{1+du^*} + \frac{abu^*v^*}{1+cw^*} - \frac{acdu^*v^*w^{*2}}{(1+cw^*)^2(1+du^*)^2}, \\ q_3 &= \frac{abu^*v^*w^*}{(1+cw^*)(1+du^*)} - \frac{acdu^*v^{*2}w^{*2}}{(1+cw^*)^2(1+du^*)^2} + \frac{u^*v^*w^*}{1+du^*}. \end{aligned} \tag{3.49}$$

By following the Routh-Hurwitz criterion, we can deduce that point E^* is locally asymptotically stable since conditions in (3.45) hold, we say that $q_1q_2 - q_3 > 0$ for all $q_1 > 0$, $q_2 > 0$ and $q_3 > 0$.

In the presence of diffusion, we consider model (3.42) and discuss its locally stability. We assume $0 = \sigma_1 < \sigma_2 < \cdots \to \infty$ to be eigenvalues of the Laplacian operator $-\Delta$ on Ω subject to zero-flux boundary condition, we also let $\psi(\sigma_i)$ be the corresponding space eigenfunctions to σ_i. By following authors in [38, 39], we have (i) $\chi_{ij} := \{\nu \cdot \theta_{ij};\ \nu \in \mathbb{R}^3\}$, where $\{\theta_{ij}\}$ are orthonormal basis functions of $\psi(\sigma_i)$ for $j = 1, \ldots, \dim \psi(\sigma_i)$, and (ii) $\chi := \{z \in [C^1(\Omega)]^3 : \partial_n u = \partial_n v = \partial_n w = 0,\ \text{on } \partial\Omega\}$, and $\chi = \oplus_{i=1}^{\infty}\chi_i$ where $\chi = \oplus_{i=1}^{\dim \psi(\sigma_i)}\chi_{ij}$.

Theorem 3.4 *The equilibrium solution E^* of system (3.42) is locally asymptotically stable if conditions*

$$a \leq 4,\ b \leq 1,\ ad \leq 2,\ 1 = c > 2a$$

are satisfied.

Proof The linearized form of fractional system (3.42) at $\gamma = 1$ and point E^* can be written in the form

$$z_t = z(D\Delta + \mathbf{A}|_{E^*}),$$

where

$$D = \begin{pmatrix} \delta_1 & 0 & 0 \\ 0 & \delta_2 & 0 \\ 0 & 0 & \delta_3 \end{pmatrix}.$$

Clearly, it is not difficult to see that under the operator $D\Delta + \mathbf{A}|_{E^*}$, χ_i is considered as its invariant, and λ is the eigenvalue of χ_i provided it is an eigenvalue of matrix $-\sigma_i D + \mathbf{A}|_{E^*}$. By calculating its characteristic polynomial, we have

$$\vartheta(\lambda) = \lambda^3 + p_1\lambda^2 + p_2\lambda + p_3, \tag{3.50}$$

where

$$\begin{aligned}
p_1 &= u^* + v^* + \frac{w^*}{1+du^*} + \sigma_i(\delta_1 + \delta_2 + \delta_3), \\
p_2 &= u^*v^* + u^*\sigma_i\delta_2 + v^*\sigma_i\delta_1 + \sigma_i^2\delta_1\delta_2 + (u^* + v^* + \sigma_i(\delta_1 + \delta_2))\left(\frac{w^*}{1+du^*} + \delta_3\sigma_i\right) \\
&\quad + \frac{abu^*v^*}{1+cw^*} - \frac{acdu^*v^*w^{*2}}{(1+cw^*)^2(1+du^*)^2}, \\
p_3 &= \left(\frac{w^*}{1+du^*} + \delta_3\sigma_i\right)\left\{u^*v^* + u^*\sigma_i\delta_2 + v^*\sigma_i\delta_1 + \sigma_i^2\delta_1\delta_2 + \frac{abu^*v^*}{1+cw^*}\right\} \\
&\quad - \frac{acdu^*v^*w^{*2}}{(1+cw^*)^2(1+du^*)^2}(v^* + \delta_2\sigma_i).
\end{aligned} \tag{3.51}$$

Similarly, by applying the conditions $a \leq 4,\ b \leq 1,\ ad \leq 2,\ 1 = c > 2a$, we can see that p_1, p_2, p_3 are all positive, and $p_1p_2 - p_3 > 0$. It directly follows from Routh-Hurwitz criterion that for every $i > 0$, the roots $\lambda_{i,1}$, $\lambda_{i,2}$ and $\lambda_{i,3}$ of $\vartheta_i(\lambda) = 0$ have negative real parts. □

4 Experimental Results

In this section, we present numerical results for both systems (3.25) and (3.42) to justify the theoretical findings, for different instances of fractional order γ. As suggested in [2, 40], the domain size has to be chosen large enough to give enough room for the species to propagate in space. Throughout our analysis here, we choose the zero-flux boundary conditions clamped at the ends of domain size $x \in [0, D]$ in one-dimension with discretization step $h = 0.05$. In both systems, we initial conditions that are neighbourhood of equilibrium values subject to a small noise perturbation. Figures 3 and 4 show the behaviour of fractional predator-prey systems (3.25) and (3.42) for some values of γ.

We extend our experiment to two-dimensional results. Fractional model (3.25) is numerically solved on a square domain $[0, D] \times [0, D]$, for $D = 200$, with time-step $\Delta t = 0.25$ and a space-step $\Delta x = 0.05$. We employ the standard five-point approximation technique for the 2D Laplacian operator subject to the zero-flux boundary conditions [40] and initial conditions

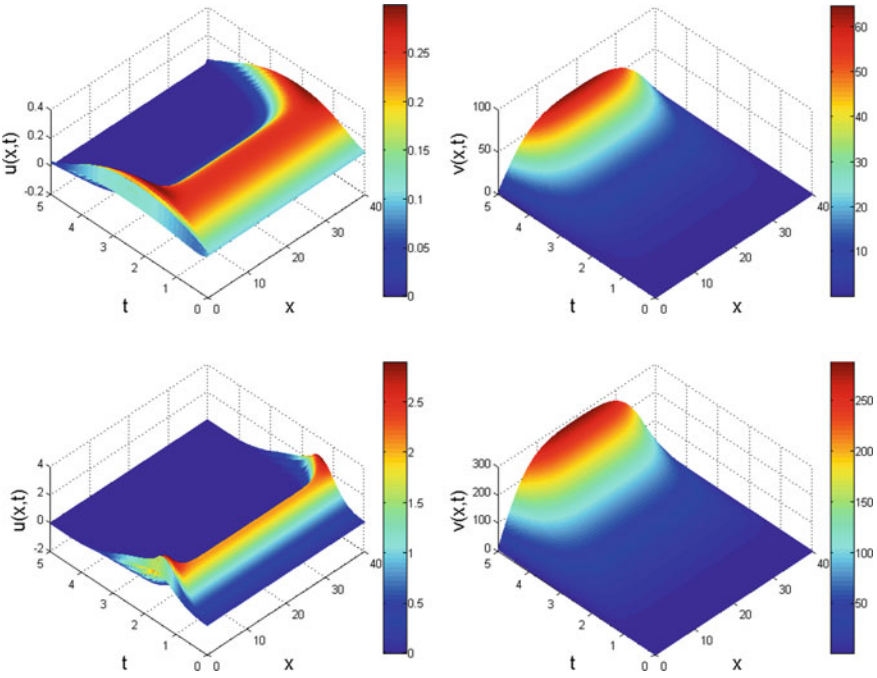

Fig. 3 One-dimensional distribution of system (3.25) at $\gamma = (0.50, 0.75)$ for upper and lower rows, respectively with $D = 40$, $\tau = 3$, $\alpha = 0.3$ and $\kappa = 5$

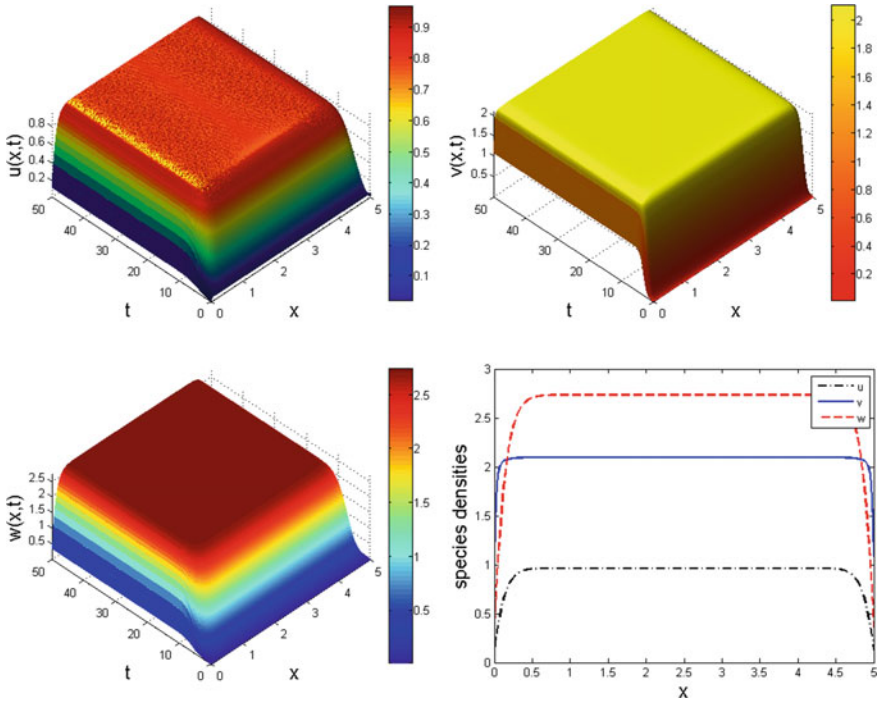

Fig. 4 One-dimensional distribution of system (3.42) at $\gamma = 0.63$ with $D = 5$, $\tau = 3$, $\alpha = 0.3$ and $\kappa = 5$

$$u(x, y, 0) = 1 - \exp(-10((x - \nu/2)^2 + (y - \nu/2)^2)),$$
$$v(x, y, 0) = \exp(-10((x - \nu/2)^2 + (y - \nu/2)^2)) \tag{4.52}$$

to obtain results in Figs. 5 and 6 for different instances of γ. When $\gamma < 0.5$, we observed a mixed population of stripes and spots patterns denoting spatial interaction between a zebra and cheetah species, this assertion is evident in Fig. 5. When $\gamma > 0.5$, only the predator class is becoming dominant, they occupied the whole domain-habitat. At $\gamma = 0.94$, it is obvious that the situation has turned to survival of the fittest, only the matured and strongest among the predator could survive due to shortage of prey which serves as food. A serious decline in densities is noticeable.

In the 2D simulations, we noticed that the distributions of prey- and predator-species are of the same type. Thus, we continue simulation analysis of pattern formations with that of the predator (v) species. In Fig. 7, we fixed $\gamma = 0.99$ and vary the simulation time as seen in the figure caption.

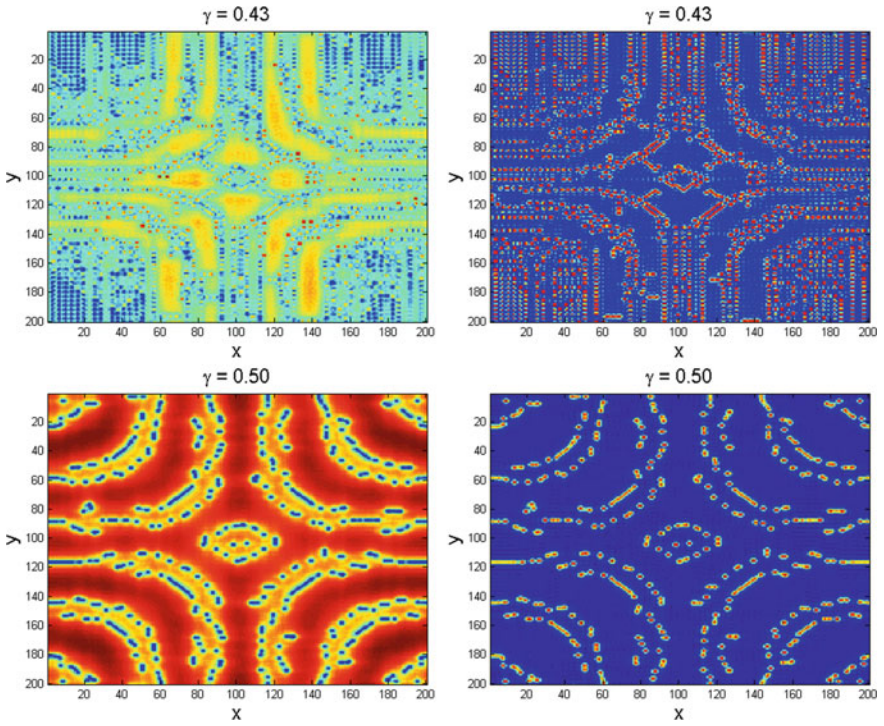

Fig. 5 Numerical results showing the dynamical evolution of fractional predator-prey system (3.25) obtained for $0 < \gamma \leq 0.5$ with $\tau = 3$, $\alpha = 0.3$ and $\kappa = 5$. simulation runs for $N = 200$ and $t = 1000$

5 Conclusion

Two notable dynamics of fractional reaction-diffusion models which describe spatial interaction between the predator and prey species are studied in this work for pattern formations. The classical derivatives in each of the models are replaced with the new Atangana-Baleanu fractional-order derivative in the sense of Caputo. The models are examined for stability and conditions for equilibrium state to be locally asymptotically stable are revealed. The condition for the occurrence of Turing instability is equally given. Some numerical results for different instances of fractional order are reported in one and two dimensions.

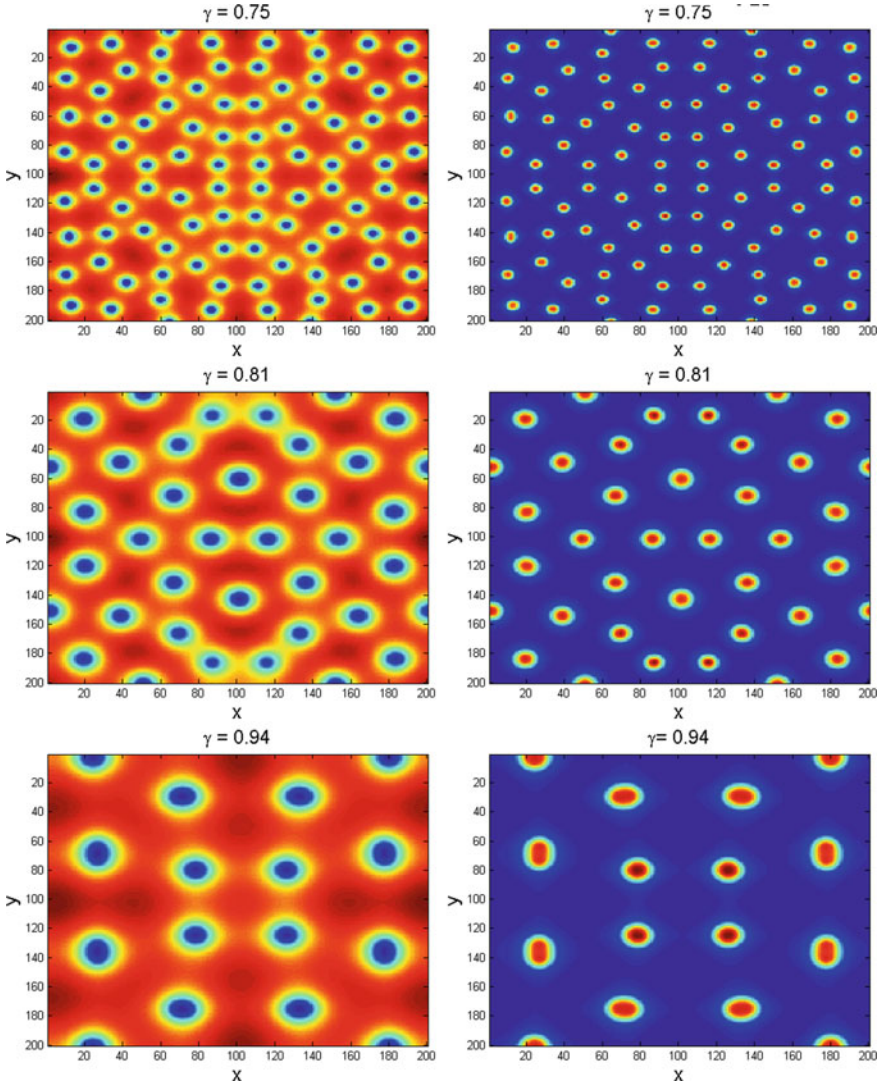

Fig. 6 Numerical results showing the dynamical evolution of fractional predator-prey system (3.25) obtained for $0.5 < \gamma \leq 1$ with $\tau = 3$, $\alpha = 0.3$ and $\kappa = 5$. simulation runs for $N = 200$ and $t = 1000$

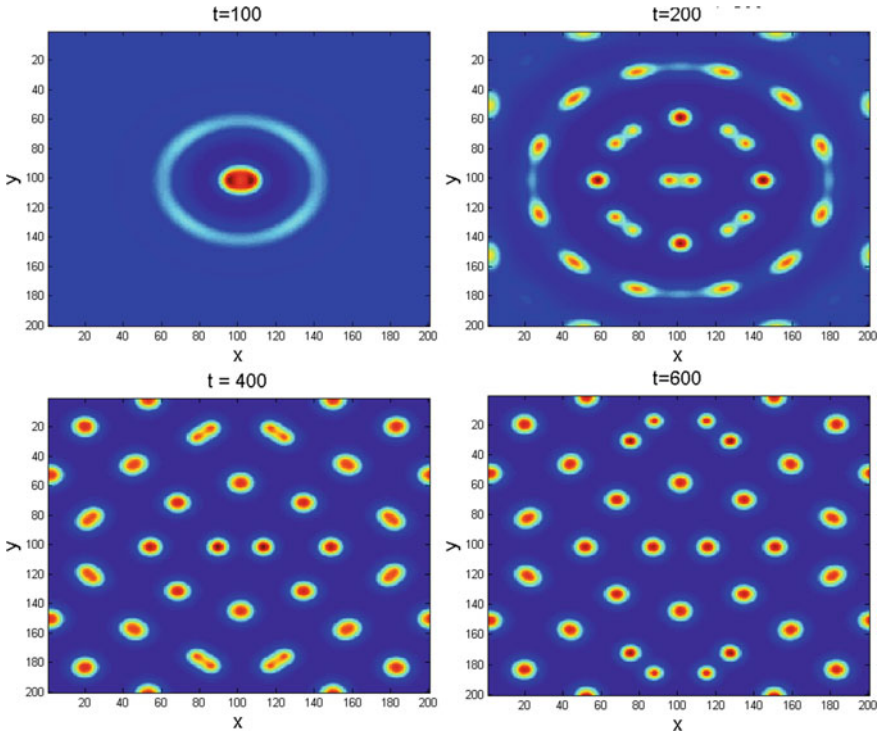

Fig. 7 Evolution of $v-$species in system (3.25) for different instances of time at $\gamma = 0.99$. Other parameters are given in Fig. 6

References

1. A.K. Kassam, L.N. Trefethen, Fourth-order time-stepping for stiff PDEs. SIAM J. Sci. Comput. **26**, 1214–1233 (2005)
2. K.M. Owolabi, K.C. Patidar, Higher-order time-stepping methods for time-dependent reaction-diffusion equations arising in biology. Appl. Math. Comput. **240**, 30–50 (2014)
3. J.D. Murray, *Mathematical Biology I: An Introduction* (Springer, New York, 2002)
4. A.M. Turing, The chemical basis for morphogenesis. Philos. Trans. R. Soc. B **237**, 37–72 (1952)
5. E.J. Crampin, E. Gaffney, P.K. Maini, Reaction and diffusion growing domains: scenarios for robust pattern formation. Bull. Math. Biol. **61**, 1093–1120 (1999)
6. E.J. Crampin, E. Gaffney, P.K. Maini, Mode-doubling and tripling in reaction-diffusion patterns on growing domains: a piecewise linear model. J. Math. Biol. **44**, 107–128 (2002)
7. P.K. Maini, D.L. Benson, J.A. Sherratt, Pattern formation in reaction diffusion models with spatially inhomogeneous diffusion coefficients. IMA J. Math. Appl. Med. Biol. **9**, 197–213 (1992)
8. T. Miura, P.K. Maini, Speed of pattern appearance in reaction-diffusion models: implications in the pattern formation of limb bud mesenchyme cells. Bull. Math. Biol. **66**, 627–649 (2004)
9. J.D. Murray, *Mathematical Biology II: Spatial Models and Biomedical Applications* (Springer, New York, 2003)

10. R.A. Satnoianu, M. Menzinger, P.K. Maini, Turing instabilities in general systems. J. Math. Biol. **41**, 493–512 (2000)
11. K.M. Owolabi, J.F. Gómez-Aguilar, B. Karaagac, Modelling, analysis and simulations of some chaotic systems using derivative with Mittag-Leffler kernel. Chaos Soliton. Fract. **125**, 54–63 (2019)
12. I. Podlubny, *Fractional Differential Equations* (Academic Press, San Diego, CA, 1999)
13. B.S.T. Alkahtani, Chua's circuit model with Atangana-Baleanu derivative with fractional order. Chaos Soliton. Fract. **89**, 547–551 (2016)
14. M.A. Dokuyucu, D. Baleanu, E. Çelik, Analysis of Keller-Segel model with Atangana-Baleanu fractional derivative. Filomat **32**, 5633–5643 (2018)
15. S.G. Samko, A.A. Kilbas, O.I. Marichev, *Fractional Integrals and Derivatives: Theory and Applications* (Gordon and Breach Science Publishers, Yverdon, 1993)
16. B.I. Henry, S.L. Wearne, Fractional reaction-diffusion. Phys. A **276**, 448–455 (2000)
17. K.M. Owolabi, Analysis and numerical simulation of multicomponent system with Atangana-Baleanu fractional derivative. Chaos Soliton. Fract. **115**, 127–134 (2018)
18. K.M. Owolabi, Numerical patterns in system of integer and non-integer order derivatives. Chaos Soliton. Fract. **115**, 143–153 (2018)
19. K.M. Owolabi, Numerical patterns in reaction-diffusion system with the Caputo and Atangana-Baleanu fractional derivatives. Chaos Soliton. Fract. **115**, 160–169 (2018)
20. K.M. Owolabi, Numerical solutions and pattern formation process in fractional diffusion-like equations, in *Fractional Derivatives with Mittag-Leffler Kernel: Trends and Applications in Science and Engineering*, ed. by J.F. Gómez, L. Torres, R.F. Escobar (Springer, Switzerland, 2019), pp. 195–216
21. K.M. Owolabi, Behavioural study of symbiosis dynamics via the Caputo and Atangana-Baleanu fractional derivatives. Chaos Soliton. Fract. **122**, 89–101 (2019)
22. K.M. Owolabi, E. Pindza, Numerical simulation of multidimensional nonlinear fractional Ginzburg-Landau equations. Discr. Contin. Dyn. Syst. Ser. S **12**, 835–851 (2019)
23. K.M. Owolabi, H. Dutta, Numerical solution of space-time-fractional reaction-diffusion equations via the Caputo and Riesz derivatives, in *Mathematics Applied to Engineering, Modelling, and Social Issues*, ed. by F.T. Smith, H. Dutta, J.N. Mordeson (Springer, Switzerland, 2019), pp. 161–188
24. K.M. Owolabi, Numerical analysis and pattern formation process for space-fractional superdiffusive systems. Discr. Contin. Dyn. Syst. Ser. S **12**, 543–566 (2019)
25. M. Caputo, M. Fabrizio, Applications of new time and spatial fractional derivatives with exponential kernels. Progr. Fract. Differ. Appl. **2**, 1–11 (2016)
26. A. Atangana, D. Baleanu, New fractional derivatives with nonlocal and non-singular kernel: theory and application to heat transfer model. Thermal Sci. **20**, 763–769 (2016)
27. D. Baleanu, B. Shiri, Collocation methods for fractional differential equations involving non-singular kernel. Chaos Soliton. Fract. **116**, 136–145 (2018)
28. R. Gorenflo, A.A. Kilbas, F. Mainardi, S.V. Rogosin et al., *Mittag-Leffler Functions Related Topics and Applications* (Springer, Berlin, Heidelberg, 2016)
29. H. Srivastava, Z. Tomovski, Fractional calculus with an integral operator containing a generalized Mittag-Leffler function in the kernel. Appl. Math. Comput. **211**, 198–210 (2009)
30. D. Baleanu, A. Fernandez, On some new properties of fractional derivatives with Mittag-Leffler kernel. Commun. Nonlinear Sci. Numer. Simul. **59**, 444–462 (2018)
31. I. Koca, Efficient numerical approach for solving fractional partial differential equations with non-singular kernel derivatives. Chaos Soliton. Fract. **116**, 278–286 (2018)
32. A.A. Kilbas, M. Saigo, R. Saxena, Generalized Mittag-Leffler function and generalized fractional calculus operators. Integr. Trans. Spec. Funct. **15**, 31–49 (2004)
33. A. Atangana, K.M. Owolabi, New numerical approach for fractional differential equations. Math. Model. Nat. Phenom. **13**, 3 (2018)
34. M. Alves, F. Hilker, Hunting cooperation and Allee effects in predators. J. Theoret. Biol. **419**, 13–22 (2017)

35. R. Cantrell, C. Cosner, *Spatial Ecology via Reaction-Diffusion Equations* (Wiley, Chichester, UK, 2003)
36. C. Tian, Z. Ling, Z. Lin, Turing pattern formation in a predator-prey-mutualist system. Nonlinear Anal. Real World Appl. **12**, 3224–3237 (2011)
37. P.H. Thrall, M.E. Hochberg, J.J. Burdon, J.D. Bever, Coevolution of symbiotic mutualists and parasites in a community context. Trends Ecol. Evol. **22**, 120–126 (2007)
38. P.Y.H. Pang, M.X. Wang, Strategy and stationary pattern in a three-species predator-prey model. J. Differ. Equ. **200**, 245–273 (2004)
39. M. Rietkerk, J. van de Koppel, Regular pattern formation in real ecosystems. Trends Ecol. Evol. **23**, 169–175 (2008)
40. K.M. Owolabi, K.C. Patidar, Numerical simulations of multicomponent ecological models with adaptive methods. Theoret. Biol. Med. Model. **13**, 1 (2016)

New Aspects of Fractional Epidemiological Model for Computer Viruses with Mittag–Leffler Law

Devendra Kumar and Jagdev Singh

1 Introduction

In recent years, computer virus is a major problem in hardware and software technology. The computer virus is a particular kind of computer program which propagates itself and spreads from one computer to another. The file system generally damaged by the viruses and worms employs system vulnerability to look and attack computers. Consequently, for improving the safety and reliability in the computer setups and networks, the test on excellent examination of the computer virus spreading dynamical process is an important instrument. There are mainly two methods to examine the considered problem similar to the biological viruses as microscopic and macroscopic mathematical models. To describe and control the spreading of computer virus, many engineers and scientists suggested several ways to formulate mathematical models [1–18]. In recent work, Singh et al. [19] have reported a new mathematical model for describing spreading of computer virus by making use of a new fractional derivative with the exponential kernel. Fractional order calculus (FOC) has been employed to formulate the mathematical models of real-life problems. Nowadays, the FOC is acting a pivotal role in the areas of physics, computer science, chemistry, earth science, economics, etc. In recent years, many mathematicians and scientists paid their attention in this very special branch of mathematical analysis [20–32]. In 2016, Atangana–Baleanu (AB) fractional derivative was studied by Atangana and Baleanu [33] connected with the Mittag–Leffler function in its kernel. The AB fractional derivative has been used in describing various physical problems such as mathematical model of exothermic reactions having fixed heat source in porous media [34], Biswas–Milovic model in optical communications [35], regularized long-wave equation in plasma waves [36], Fornberg–Whitham equation in wave breaking [37],

D. Kumar (✉)
Department of Mathematics, University of Rajasthan, Jaipur, Rajasthan 302004, India

J. Singh
Department of Mathematics, JECRC University, Jaipur, Rajasthan 303905, India

H. Dutta (ed.), *Mathematical Modelling in Health, Social and Applied Sciences*, Forum for Interdisciplinary Mathematics, https://doi.org/10.1007/978-981-15-2286-4_9

rumor spreading dynamical model [38], dynamical system for competition between commercial and rural banks in Indonesia [39], etc.

The principal aim of the present study is to suggest a novel epidemiological model for describing the spreading for computer viruses with Mittag–Leffler-type memory. A new numerical algorithm, namely q-HATM [40, 41] is used for solving the epidemiological model of arbitrary order for computer viruses associated with Mittag–Leffler-type kernel. The q-HATM is the combination of q-homotopy analysis method (q-HAM) [42, 43] and Laplace transform method [44–47].

Motivated and very useful consequences of fractional operators in mathematical modeling of real word problems, we present a fractional modified epidemiological model (FMEM) for computer viruses. The key aim of this investigation is to apply a novel fractional operator in describing the spreading of viruses in computers. The existence and uniqueness of the solution of the FMEM for computer viruses are investigated by using the concept of the well-known fixed-point theory. The article is organized as follows: Sect. 2 presents the key results related to AB fractional derivative. Section 3 is dedicated to the fractional modeling of computer viruses. In Sect. 4, we report the existence and uniqueness of the solution of the FMEM for computer viruses. In Sect. 5, the efficiency of q-HATM is used to obtain the analytical solution of the FMEM for computer viruses. Section 6 reports the numerical results and discussions. Section 7, which is the last portion of the article, points out the conclusions.

2 The AB Fractional Derivative and Its Properties

Definition 2.1 Assume that $S \in H^1(\alpha, \beta)$, $\beta > \alpha$, $\kappa \in (0, 1]$ and differentiable, then the AB fractional derivative in terms of Caputo is presented as [33]

$$ {}^{ABC}_{\alpha}D^{\kappa}_{\tau}(S(\tau)) = \frac{B(\kappa)}{1-\kappa}\int_{\alpha}^{\tau} S'(\eta)E_{\kappa}\left[-\frac{\kappa}{1-\kappa}(\tau-\eta)^{\kappa}\right]\mathrm{d}\eta. \tag{1} $$

In Eq. (1), $B(\kappa)$ is satisfying the property $B(0) = B(1) = 1$.

Definition 2.2 Let $S \in H^1(\alpha, \beta)$, $\beta > \alpha$, $\kappa \in (0, 1]$ and non-differentiable, then the AB fractional derivative in Riemann–Liouville sense is presented as [33]

$$ {}^{ABR}_{\alpha}D^{\kappa}_{\tau}(S(\tau)) = \frac{B(\kappa)}{1-\kappa}\frac{\mathrm{d}}{\mathrm{d}\tau}\int_{\alpha}^{\tau} S(\eta)E_{\kappa}\left[-\frac{\kappa}{1-\kappa}(\tau-\eta)^{\kappa}\right]\mathrm{d}\eta. \tag{2} $$

Definition 2.3 Consider $0 < \kappa < 1$, and S be a function of τ, then the fractional integral operator associated with AB fractional derivative of order κ is drafted as [33]

$$ {}^{AB}_{0}I^{\kappa}_{\tau}(S(\tau)) = \frac{(1-\kappa)}{B(\kappa)}S(\tau) + \frac{\kappa}{B(\kappa)\Gamma(\kappa)}\int_{0}^{\tau} S(\vartheta)(\tau-\vartheta)^{\kappa-1}\mathrm{d}\vartheta, \quad \tau \geq 0. \tag{3} $$

3 FMEM of Computer Viruses with Mittag–Leffler Memory

In this section, we extend the epidemiological model for computer viruses formulated by Piqueira and Araujo [5] by using the theory of AB fractional derivative to induce the strong memory in the model description. Here, we denote the total population by T. We divide the total population T into the following four categories:

Category I: The number of computers which are not infected is inclined to probable infection and is indicated by the symbol $S(\tau)$.
Category II: The number of computers which are not infected is associated with the anti-virus and represented by the symbol $A(\tau)$.
Category III: The number of computers which are infected by virus is denoted by the symbol $I(\tau)$.
Category IV: The number of removed computers because of infection or not is represented by the symbol $R(\tau)$.

In the mathematical formulation of the problem, the influx parameter mortality parameters are taken in the following manner:

ϖ indicates the influx rate, which is representing the involvement of novel computers to the interconnected system, and θ stands for the proportion coefficient connected to the mortality rate, not due to the virus.

In order to decorate the magnificent report with infected ones, the susceptible category $S(\tau)$ is converted into the infected category with a rate that is pertaining to the chance of susceptible computers. Consequently, ξ represents the equivalent factor and this rate is straightforwardly equivalent to the multiplication of $S(\tau)$ and $I(\tau)$. The conversion of susceptible into antidotal is straightforwardly equivalent to the product of $S(\tau)$ and $A(\tau)$ with the equivalent factor represented via μ_{SA}. On making use of the anti-virus programs, the computers affected by virus can be got back to normal ones and being converted in the antidotal one with a rate straightforwardly equivalent to the product of $A(\tau)$ and $I(\tau)$ with the equivalent factor indicated via μ_{IA}. Here, we indicate the rate of reducing the computer into the useless and computer is removed from the system by the symbol ε, while we represent the proportion factor of the computers that can be restored and converted into the susceptible category by the symbol ρ.

The dynamical process of the spreading of the infection of a recognized virus is investigated with the aid of the present approach and, so, the conversion of antidotal into infected is not studied. Consequently, a scheme of vaccination can be described,

and a cost-effective application of anti-virus programs can be clarified with the help of the understudy model.

Considering all these suppositions, the mathematical representations can be presented in the following manner

$$\begin{aligned}
\frac{\mathrm{d}S(\tau)}{\mathrm{d}\tau} &= \varpi - \mu_{SA}S(\tau)A(\tau) - \xi S(\tau)I(\tau) - \theta S(\tau) + \rho R(\tau),\\
\frac{\mathrm{d}I(\tau)}{d\tau} &= \xi S(\tau)I(\tau) - \mu_{IA}A(\tau)I(\tau) - \varepsilon I(\tau) - \theta I(\tau),\\
\frac{\mathrm{d}R(\tau)}{\mathrm{d}\tau} &= \varepsilon I(\tau) - \rho R(\tau) - \theta R(\tau),\\
\frac{\mathrm{d}A(\tau)}{\mathrm{d}\tau} &= \mu_{SA}S(\tau)A(\tau) + \mu_{IA}A(\tau)I(\tau) - \theta A(\tau).
\end{aligned} \tag{4}$$

In considered model, the influx rate is investigated to be $\varpi = 0$, as action of viruses is very fast than the extension of system, so it is assumed that no new computer is involved in the system all the while the spreading of the assessed virus. On the similar manner, the fraction coefficient is taken to be $\theta = 0$, supposing that the machine obsolescence time is very bigger than the time of the virus movement.

Consequently, mathematical model (4) becomes as follows:

$$\begin{aligned}
\frac{\mathrm{d}S(\tau)}{\mathrm{d}\tau} &= -\mu_{SA}S(\tau)A(\tau) - \xi S(\tau)I(\tau) + \rho R(\tau),\\
\frac{\mathrm{d}I(\tau)}{\mathrm{d}\tau} &= \xi S(\tau)I(\tau) - \mu_{IA}A(\tau)I(\tau) - \varepsilon I(\tau),\\
\frac{\mathrm{d}R(\tau)}{\mathrm{d}\tau} &= \varepsilon I(\tau) - \rho R(\tau),\\
\frac{\mathrm{d}A(\tau)}{\mathrm{d}\tau} &= \mu_{SA}S(\tau)A(\tau) + \mu_{IA}A(\tau)I(\tau).
\end{aligned} \tag{5}$$

It is well known that the mathematical models with classical derivatives do not carry the memory of the system, so we extend the mathematical model (5) with the aid of AB fractional derivative, then it reduces as follows:

$$\begin{aligned}
{}_0^{ABC}D_\tau^\kappa S(\tau) &= -\mu_{SA}S(\tau)A(\tau) - \xi S(\tau)I(\tau) + \rho R(\tau),\\
{}_0^{ABC}D_\tau^\kappa I(\tau) &= \xi S(\tau)I(\tau) - \mu_{IA}A(\tau)I(\tau) - \varepsilon I(\tau),\\
{}_0^{ABC}D_\tau^\kappa R(\tau) &= \varepsilon I(\tau) - \rho R(\tau),\\
{}_0^{ABC}D_\tau^\kappa A(\tau) &= \mu_{SA}S(\tau)A(\tau) + \mu_{IA}A(\tau)I(\tau).
\end{aligned} \tag{6}$$

The initial conditions associated with fractional model (6) are presented as

$$S = \alpha_1, \quad I = \alpha_2, \quad R = \alpha_3 \quad \text{and} \quad A = \alpha_4 \quad \text{at } \tau = 0. \tag{7}$$

In this investigation, we have taken $T(\tau) = S(\tau) + I(\tau) + R(\tau) + A(\tau)$ to be fixed at a time τ. We suppose that Ψ stands for the Banach space of continuous real-valued functions over the interval Δ having the norm

$$\|(S(\tau), I(\tau), R(\tau), A(\tau))\| = \|S(\tau)\| + \|I(\tau)\| + \|R(\tau)\| + \|A(\tau)\|. \quad (8)$$

In Eq. (8), $\|S(\tau)\| = \sup\{|S(\tau) : \tau \in \Delta|\}$, $\|I(\tau)\| = \sup\{|I((\tau) : \tau \in \Delta|\}$, $\|R(\tau)\| = \sup\{|R(\tau) : \tau \in \Delta|\}$ and $\|A(\tau)\| = \sup\{|A(\tau) : \tau \in \Delta|\}$. Specially $\Psi = C(\Delta) \times C(\Delta) \times C(\Delta) \times C(\Delta)$, here $C(\Delta)$ is the Banach space of continuous $\Re$ valued functions on the interval Δ possessing the sup norm.

4 Existence and Uniqueness of a Solution of FMEM for Computer Viruses with Mittag–Leffler Memory

In the present part, we investigate the existence of the solution with the help of the concept of the well-known fixed-point approach.

Firstly, we employ the fractional integral operator on the fractional order model (6), and it gives

$$\begin{aligned}
S(\tau) - S(0) &= {}^{AB}_{0}I^{\kappa}_{\tau}\{-\mu_{SA}S(\tau)A(\tau) - \xi S(\tau)I(\tau) + \rho R(\tau)\},\\
I(\tau) - I(0) &= {}^{AB}_{0}I^{\kappa}_{\tau}\{\xi S(\tau)I(\tau) - \mu_{IA}A(\tau)I(\tau) - \varepsilon I(\tau)\},\\
R(\tau) - R(0) &= {}^{AB}_{0}I^{\kappa}_{\tau}\{\varepsilon I(\tau) - \rho R(\tau)\},\\
A(\tau) - A(0) &= {}^{AB}_{0}I^{\kappa}_{\tau}\{\mu_{SA}S(\tau)A(\tau) + \mu_{IA}A(\tau)I(\tau)\}.
\end{aligned} \quad (9)$$

On using the representation given in Eq. (3), it reduces to the following system

$$\begin{aligned}
S(\tau) - S(0) &= \frac{(1-\kappa)}{B(\kappa)}\{-\mu_{SA}S(\tau)A(\tau) - \xi S(\tau)I(\tau) + \rho R(\tau)\}\\
&\quad + \frac{\kappa}{B(\kappa)\Gamma(\kappa)}\int_0^{\tau}\{-\mu_{SA}S(\vartheta)A(\vartheta) - \xi S(\vartheta)I(\vartheta) + \rho R(\vartheta)\}(\tau-\vartheta)^{\kappa-1}\mathrm{d}\vartheta,\\
I(\tau) - I(0) &= \frac{(1-\kappa)}{B(\kappa)}\{\xi S(\tau)I(\tau) - \mu_{IA}A(\tau)I(\tau) - \varepsilon I(\tau)\}\\
&\quad + \frac{\kappa}{B(\kappa)\Gamma(\kappa)}\int_0^{\tau}\{\xi S(\vartheta)I(\vartheta) - \mu_{IA}A(\vartheta)I(\vartheta) - \varepsilon I(\vartheta)\}(\tau-\vartheta)^{\kappa-1}\mathrm{d}\vartheta,\\
R(\tau) - R(0) &= \frac{(1-\kappa)}{B(\kappa)}\{\varepsilon I(\tau) - \rho R(\tau)\}\\
&\quad + \frac{\kappa}{B(\kappa)\Gamma(\kappa)}\int_0^{\tau}\{\varepsilon I(\vartheta) - \rho R(\vartheta)\}(\tau-\vartheta)^{\kappa-1}\mathrm{d}\vartheta,\\
A(\tau) - A(0) &= \frac{(1-\kappa)}{B(\kappa)}\{\mu_{SA}S(\tau)A(\tau) + \mu_{IA}A(\tau)I(\tau)\}\\
&\quad + \frac{\kappa}{B(\kappa)\Gamma(\kappa)}\int_0^{\tau}\{\mu_{SA}S(\vartheta)A(\vartheta) + \mu_{IA}A(\tau)I(\vartheta)\}(\tau-\vartheta)^{\kappa-1}\mathrm{d}\vartheta.
\end{aligned} \quad (10)$$

In order to clarify the system, we use the subsequent notations

$$\begin{aligned}
&\Omega_1(\tau, S) = -\mu_{SA} S(\tau) A(\tau) - \xi S(\tau) I(\tau) + \rho R(\tau),\\
&\Omega_2(\tau, I) = \xi S(\tau) I(\tau) - \mu_{IA} A(\tau) I(\tau) - \varepsilon I(\tau),\\
&\Omega_3(\tau, R) = \varepsilon I(\tau) - \rho R(\tau),\\
&\Omega_4(\tau, A) = \mu_{SA} S(\tau) A(\tau) + \mu_{IA} A(\tau) I(\tau).
\end{aligned} \tag{11}$$

Theorem 4.1 The kernels $\Omega_1(\tau, S), \Omega_2(\tau, I), \Omega_3(\tau, R)$ and $\Omega_4(\tau, A)$ fulfill the Lipschitz condition and contraction if the subsequent result is satisfied

$$0 \leq (\mu_{SA}\beta_4 + \xi\beta_2) < 1. \tag{12}$$

Proof We initiate with $\Omega_1(\tau, S)$. Let $S(\tau)$ and $S^*(\tau)$ are two functions, then we get

$$\left\|\Omega_1(\tau, S) - \Omega_1(\tau, S^*)\right\| = \left\|-\mu_{SA}\left\{S(\tau) - S^*(\tau)\right\}A(\tau) - \xi\left\{S(\tau) - S^*(\tau)\right\}I(\tau)\right\|. \tag{13}$$

On utilizing of the inequality of triangular on Eq. (13), it gives

$$\begin{aligned}
\left\|\Omega_1(\tau, S) - \Omega_1(\tau, S^*)\right\| &\leq \left\|\mu_{SA}\left\{S(\tau) - S^*(\tau)\right\}A(\tau)\right\| + \left\|\beta\left\{S(\tau) - S^*(\tau)\right\}I(\tau)\right\|\\
&\leq \{\mu_{SA}\beta_4 + \xi\beta_2\}\left\|S(\tau) - S^*(\tau)\right\|\\
&\leq \lambda_1\left\|\left(S(\tau) - S^*(\tau)\right)\right\|.
\end{aligned} \tag{14}$$

Letting $\lambda_1 = \mu_{SA}\beta_4 + \xi\beta_2$, where $\|S(\tau)\| \leq \beta_1$, $\|I(\tau)\| \leq \beta_2$, $\|R(\tau)\| \leq \beta_3$ and $\|A(\tau)\| \leq \beta_4$ are bounded functions, then Eq. (14) gives

$$\left\|\Omega_1(\tau, S) - \Omega_1(t, S^*)\right\| \leq \lambda_1\left\|S(\tau) - S^*(\tau)\right\|. \tag{15}$$

Thus, the $\Omega_1(\tau, S)$ satisfy the Lipschitz condition and if $0 \leq \mu_{SA}\beta_4 + \xi\beta_2 < 1$, then it is also a contraction.

In the similar way, we can easily prove the following results

$$\begin{aligned}
&\|\Omega_2(\tau, I) - \Omega_2(\tau, I^*)\| \leq \lambda_2\|I(\tau) - I^*(\tau)\|,\\
&\|\Omega_3(\tau, R) - \Omega_3(\tau, R^*)\| \leq \lambda_3\|R(\tau) - R^*(\tau)\|,\\
&\|\Omega_4(\tau, A) - \Omega_4(\tau, A^*)\| \leq \lambda_4\|A(\tau) - A^*(\tau)\|.
\end{aligned} \tag{16}$$

On making use of the abovementioned kernels, Eq. (10) reduces as follows:

$$
\begin{aligned}
S(\tau) &= S(0) + \tfrac{(1-\kappa)}{B(\kappa)}\Omega_1(\tau, S) + \tfrac{\kappa}{B(\kappa)\Gamma(\kappa)}\int_0^\tau \Omega_1(\vartheta, S)(\tau-\vartheta)^{\kappa-1}\mathrm{d}\vartheta,\\
I(\tau) &= I(0) + \tfrac{(1-\kappa)}{B(\kappa)}\Omega_2(\tau, I) + \tfrac{\kappa}{B(\kappa)\Gamma(\kappa)}\int_0^\tau \Omega_2(\vartheta, I)(\tau-\vartheta)^{\kappa-1}\mathrm{d}\vartheta,\\
R(\tau) &= R(0) + \frac{(1-\kappa)}{B(\kappa)}\Omega_3(\tau, R) + \frac{\kappa}{B(\kappa)\Gamma(\kappa)}\int_0^\tau \Omega_3(\vartheta, R)(\tau-\vartheta)^{\kappa-1}\mathrm{d}\vartheta,\\
A(\tau) &= A(0) + \frac{(1-\kappa)}{B(\kappa)}\Omega_4(\tau, A) + \frac{\kappa}{B(\kappa)\Gamma(\kappa)}\int_0^\tau \Omega_4(\vartheta, A)(\tau-\vartheta)^{\kappa-1}\mathrm{d}\vartheta.
\end{aligned}
\tag{17}
$$

Now, we present the following recursive formula

$$
\begin{aligned}
S_n(\tau) &= \tfrac{(1-\kappa)}{B(\kappa)}\Omega_1(\tau, S_{n-1}) + \tfrac{\kappa}{B(\kappa)\Gamma(\kappa)}\int_0^\tau \Omega_1(y, S_{n-1})(\tau-\vartheta)^{\kappa-1}\mathrm{d}y,\\
I_n(\tau) &= \tfrac{(1-\kappa)}{B(\kappa)}\Omega_2(\tau, I_{n-1}) + \tfrac{\kappa}{B(\kappa)\Gamma(\kappa)}\int_0^\tau \Omega_2(\vartheta, I_{n-1})(\tau-\vartheta)^{\kappa-1}\mathrm{d}\vartheta,\\
R_n(\tau) &= \tfrac{(1-\kappa)}{B(\kappa)}\Omega_3(\tau, R_{n-1}) + \tfrac{\kappa}{B(\kappa)\Gamma(\kappa)}\int_0^\tau \Omega_3(\vartheta, R_{n-1})(\tau-\vartheta)^{\kappa-1}\mathrm{d}\vartheta,\\
A_n(\tau) &= \tfrac{(1-\kappa)}{B(\kappa)}\Omega_4(\tau, A_{n-1}) + \tfrac{\kappa}{B(\kappa)\Gamma(\kappa)}\int_0^\tau \Omega_4(\vartheta, A_{n-1})(\tau-\vartheta)^{\kappa-1}\mathrm{d}\vartheta.
\end{aligned}
\tag{18}
$$

The associated initial conditions are presented as

$$
S_0(\tau) = S(0), \quad I_0(\tau) = I(0), \quad R_0(\tau) = R(0), \quad A_0(\tau) = A(0). \tag{19}
$$

The difference formulas are written in the following manner

$$
\begin{aligned}
\wp_{1,n}(\tau) &= S_n(\tau) - S_{n-1}(\tau) = \frac{(1-\kappa)}{B(\kappa)}(\Omega_1(\tau, S_{n-1}) - \Omega_1(\tau, S_{n-2}))\\
&\quad + \frac{\kappa}{B(\kappa)\Gamma(\kappa)}\int_0^\tau (\Omega_1(\vartheta, S_{n-1}) - \Omega_1(\vartheta, S_{n-2}))(\tau-\vartheta)^{\kappa-1}\mathrm{d}\vartheta\\
\wp_{2,n}(\tau) &= I_n(\tau) - I_{n-1}(\tau) = \frac{(1-\kappa)}{B(\kappa)}(\Omega_2(\tau, I_{n-1}) - \Omega_2(\tau, I_{n-2}))\\
&\quad + \frac{\kappa}{B(\kappa)\Gamma(\kappa)}\int_0^\tau (\Omega_2(\vartheta, I_{n-1}) - \Omega_2(\vartheta, I_{n-2}))\,(\tau-\vartheta)^{\kappa-1}\mathrm{d}\vartheta,\\
\wp_{3,n}(\tau) &= R_n(\tau) - R_{n-1}(\tau) = \frac{(1-\kappa)}{B(\kappa)}(\Omega_3(\tau, R_{n-1}) - \Omega_3(\tau, R_{n-2}))\\
&\quad + \frac{\kappa}{B(\kappa)\Gamma(\kappa)}\int_0^\tau (\Omega_3(\vartheta, R_{n-1}) - \Omega_3(\vartheta, R_{n-2}))(\tau-\vartheta)^{\kappa-1}\mathrm{d}\vartheta,
\end{aligned}
$$

$$\wp_{4,n}(\tau) = A_n(\tau) - A_{n-1}(\tau) = \frac{(1-\kappa)}{B(\kappa)}(\Omega_4(\tau, A_{n-1}) - \Omega_4(\tau, A_{n-2})) + \frac{\kappa}{B(\kappa)\Gamma(\kappa)}\int_0^t (\Omega_4(\vartheta, A_{n-1}) - \Omega_4(\vartheta, A_{n-2}))(\tau-\vartheta)^{\kappa-1}\mathrm{d}\vartheta. \quad (20)$$

It is worth to observe that

$$\begin{aligned} S_n(\tau) &= \sum_{i=0}^{n} \wp_{1,i}(\tau), \\ I_n(\tau) &= \sum_{i=0}^{n} \wp_{2,i}(\tau), \\ R_n(\tau) &= \sum_{i=0}^{n} \wp_{3,i}(\tau), \\ A_n(\tau) &= \sum_{i=0}^{n} \wp_{4,i}(\tau). \end{aligned} \quad (21)$$

We can easily obtain the subsequent result

$$\begin{aligned} \left\|\wp_{1,n}(\tau)\right\| &= \|S_n(\tau) - S_{n-1}(\tau)\| \\ &= \left\| \begin{array}{l} \frac{(1-\kappa)}{B(\kappa)}(\Omega_1(\tau, S_{n-1}) - \Omega_1(\tau, S_{n-2})) \\ +\frac{\kappa}{B(\kappa)\Gamma(\kappa)}\int_0^\tau (\Omega_1(\vartheta, S_{n-1}) - \Omega_1(\vartheta, S_{n-2}))(\tau-\vartheta)^{\kappa-1}\,\mathrm{d}\vartheta \end{array} \right\|. \end{aligned} \quad (22)$$

On utilization of the triangular inequality on Eq. (22) enables us to get the result

$$\left\|S_n(\tau) - S_{n-1}(\tau)\right\| \le \frac{(1-\kappa)}{B(\kappa)}\left\|\left(\Omega_1(\tau, S_{n-1}) - \Omega_1(\tau, S_{n-2})\right)\right\| + \frac{\kappa}{B(\kappa)\Gamma(\kappa)}\left\|\int_0^\tau \left(\Omega_1(\vartheta, S_{n-1}) - \Omega_1(\vartheta, S_{n-2})\right)(\tau-\vartheta)^{\kappa-1}\mathrm{d}\vartheta\right\|. \quad (23)$$

We have already proved that $\Omega_1(\tau, S)$ holds the Lipchitz condition, so we get

$$\|S_n(\tau) - S_{n-1}(\tau)\| \le \frac{(1-\kappa)}{B(\kappa)}\lambda_1\|S_{n-1}(\tau) - S_{n-2}(\tau)\| + \frac{\kappa}{B(\kappa)\Gamma(\kappa)}\lambda_1\int_0^\tau \|S_{n-1}(\vartheta) - S_{n-2}(\vartheta)\|(\tau-\vartheta)^{\kappa-1}\mathrm{d}\vartheta, \quad (24)$$

Then, we have

$$\left\|\wp_{1,n}(\tau)\right\| \leq \frac{(1-\kappa)}{B(\kappa)}\lambda_1\left\|\wp_{1,n-1}(\tau)\right\| + \frac{\kappa}{B(\kappa)\Gamma(\kappa)}\lambda_1\int_0^\tau \left\|\wp_{1,n-1}(\vartheta)\right\|(\tau-\vartheta)^{\kappa-1}\mathrm{d}\vartheta. \tag{25}$$

On employing the same way, we get

$$\begin{aligned}
\left\|\wp_{2,n}(\tau)\right\| &\leq \tfrac{(1-\kappa)}{B(\kappa)}\lambda_2\left\|\wp_{2,n-1}(\tau)\right\| + \tfrac{\kappa}{B(\kappa)\Gamma(\kappa)}\lambda_2\int_0^\tau \left\|\wp_{2,n-1}(\vartheta)\right\|(\tau-\vartheta)^{\kappa-1}\mathrm{d}\vartheta,\\
\left\|\wp_{3,n}(\tau)\right\| &\leq \tfrac{(1-\kappa)}{B(\kappa)}\lambda_3\left\|\wp_{3,n-1}(\tau)\right\| + \tfrac{\kappa}{B(\kappa)\Gamma(\kappa)}\lambda_3\int_0^\tau \left\|\wp_{3,n-1}(\vartheta)\right\|(\tau-\vartheta)^{\kappa-1}\mathrm{d}\vartheta,\\
\left\|\wp_{4,n}(\tau)\right\| &\leq \tfrac{(1-\kappa)}{B(\kappa)}\lambda_4\left\|\wp_{4,n-1}(\tau)\right\| + \tfrac{\kappa}{B(\kappa)\Gamma(\kappa)}\lambda_4\int_0^\tau \left\|\wp_{4,n-1}(\vartheta)\right\|(\tau-\vartheta)^{\kappa-1}\mathrm{d}\vartheta.
\end{aligned} \tag{26}$$

On making use of the abovementioned results, we establish the following theorems.

Theorem 4.2 The exact solution of the FMEM for computer viruses (6) exists if we can find τ_0 such that

$$\frac{(1-\kappa)}{B(\kappa)}\lambda_1 + \frac{\kappa}{B(\kappa)\Gamma(\kappa+1)}\lambda_1\tau_0^\kappa < 1. \tag{27}$$

Proof From the results (25) and (26), we have

$$\begin{aligned}
\left\|\wp_{1,n}(\tau)\right\| &\leq \|S_n(0)\|\left[\left(\tfrac{(1-\kappa)}{B(\kappa)}\lambda_1\right) + \left(\tfrac{\kappa}{B(\kappa)\Gamma(\kappa+1)}\lambda_1\tau^\kappa\right)\right]^n\\
\left\|\wp_{2,n}(\tau)\right\| &\leq \|I_n(0)\|\left[\left(\tfrac{(1-\kappa)}{B(\kappa)}\lambda_2\right) + \left(\tfrac{\kappa}{B(\kappa)\Gamma(\kappa+1)}\lambda_2\tau^\kappa\right)\right]^n,\\
\left\|\wp_{3,n}(\tau)\right\| &\leq \|R_n(0)\|\left[\left(\tfrac{(1-\kappa)}{B(\kappa)}\lambda_3\right) + \left(\tfrac{\kappa}{B(\kappa)\Gamma(\kappa+1)}\lambda_3\tau^\kappa\right)\right]^n,\\
\left\|\wp_{4,n}(\tau)\right\| &\leq \|A_n(0)\|\left[\left(\tfrac{(1-\kappa)}{B(\kappa)}\lambda_4\right) + \left(\tfrac{\kappa}{B(\kappa)\Gamma(\kappa+1)}\lambda_4\tau^\kappa\right)\right]^n.
\end{aligned} \tag{28}$$

Thus, the abovementioned solutions exist and are continuous. In order to demonstrate that Eq. (18) is a solution of FMEM for computer viruses (6), we suppose that

$$\begin{aligned}
S(\tau) - S(0) &= S_n(\tau) - W_{1,n}(\tau),\\
I(\tau) - I(0) &= I_n(\tau) - W_{2,n}(\tau),\\
R(\tau) - R(0) &= R_n(\tau) - W_{3,n}(\tau),\\
A(\tau) - A(0) &= A_n(\tau) - W_{4,n}(\tau).
\end{aligned} \tag{29}$$

Therefore, we have

$$\begin{aligned}\left\|W_{1,n}(\tau)\right\| &= \left\| \begin{array}{l} \frac{(1-\kappa)}{B(\kappa)}(\Omega_1(\tau, S) - \Omega_1(\tau, S_{n-1})) \\ +\frac{\kappa}{B(\kappa)\Gamma(\kappa)} \int_0^\tau (\Omega_1(\tau, S) - \Omega_1(\tau, S_{n-1}))(\tau-\tau)^{\kappa-1} d\tau \end{array} \right\|. \\ &\leq \frac{(1-\kappa)}{B(\kappa)} \|(\Omega_1(\tau, S) - \Omega_1(\tau, S_{n-1}))\| \\ &\quad + \frac{\kappa}{B(\kappa)\Gamma(\kappa)} \int_0^\tau \|(\Omega_1(\vartheta, S) - \Omega_1(\vartheta, S_{n-1}))\| (\tau-\vartheta)^{\kappa-1} \mathrm{d}\vartheta \\ &\leq \frac{(1-\kappa)}{B(\kappa)} \lambda_1 \|S(\tau) - S_{n-1}(\tau)\| + \frac{\kappa}{B(\kappa)\Gamma(\kappa+1)} \lambda_1 \|S(\tau) - S_{n-1}(\tau)\| \tau^\kappa. \end{aligned} \tag{30}$$

On making use of the abovementioned process recursively, it gives

$$\left\|W_{1,n}(\tau)\right\| \leq \left(\frac{(1-\kappa)}{B(\kappa)} + \frac{\kappa}{B(\kappa)\Gamma(\kappa+1)} \tau^\kappa \right)^{n+1} \lambda_1^{n+1} \beta_1. \tag{31}$$

Then at τ_0, we have

$$\left\|W_{4,n}(\tau)\right\| \leq \left(\frac{(1-\kappa)}{B(\kappa)} + \frac{\kappa}{B(\kappa)\Gamma(\kappa+1)} \tau_0^\kappa \right)^{n+1} \lambda_1^{n+1} \beta_1. \tag{32}$$

Next, on using the limit n tends to infinity, we have

$$\left\|W_{1,n}(\tau)\right\| \to 0.$$

In the same way, we get

$$\left\|W_{2,n}(\tau)\right\| \to 0, \left\|W_{3,n}(\tau)\right\| \to 0 \quad \text{and} \quad \left\|W_{4,n}(\tau)\right\| \to 0.$$

Hence, the exact solution of the FMEM for computer viruses (6) exists if condition (27) is satisfied.

Now, we show that the FMEM for computer viruses (6) has a unique solution.

In order to prove the uniqueness of the solutions, we assume that there exists another system of solutions of mathematical model (6) be $S^*(\tau)$, $I^*(\tau)$, $R^*(\tau)$ and $A^*(\tau)$ then

$$S(\tau) - S^*(\tau) = \frac{(1-\kappa)}{B(\kappa)} \big(\Omega_1(\tau, S) - \Omega_1(\tau, S^*)\big)$$

$$+\frac{\kappa}{B(\kappa)\Gamma(\kappa)}\int_0^{\tau}\big(\Omega_1(\vartheta,S)-\Omega_1(\vartheta,S^*)\big)(\tau-\vartheta)^{\kappa-1}\mathrm{d}\vartheta. \tag{33}$$

On operating the norm on Eq. (33), we get

$$\begin{aligned}\big\|S(\tau)-S^*(\tau)\big\| \le{}& \frac{(1-\kappa)}{B(\kappa)}\big\|\Omega_1(\tau,S)-\Omega_1(\tau,S^*)\big\| \\ &+\frac{\kappa}{B(\kappa)\Gamma(\kappa)}\int_0^{\tau}\big\|\big(\Omega_1(\vartheta,S)-\Omega_1(\vartheta,S^*)\big)\big\|(\tau-\vartheta)^{\kappa-1}\mathrm{d}\vartheta.\end{aligned} \tag{34}$$

The use of the Lipschitz condition of $\Omega_1(\tau, S)$ enables us to get

$$\big\|S(\tau)-S^*(\tau)\big\|\left(1-\frac{(1-\kappa)}{B(\kappa)}\lambda_1-\frac{\kappa}{B(\kappa)\Gamma(\kappa+1)}\lambda_1\tau^{\kappa}\right)\le 0. \tag{35}$$

Theorem 4.3 The FMEM for computer viruses (6) has a unique solution if

$$\left(1-\frac{(1-\kappa)}{B(\kappa)}\lambda_1-\frac{\kappa}{B(\kappa)\Gamma(\kappa+1)}\lambda_1\tau^{\kappa}\right)>0. \tag{36}$$

Proof From Eq. (35), we have

$$\big\|S(\tau)-S^*(\tau)\big\|\left(1-\frac{(1-\kappa)}{B(\kappa)}\lambda_1-\frac{\kappa}{B(\kappa)\Gamma(\kappa+1)}\lambda_1\tau^{\kappa}\right)\le 0. \tag{37}$$

If condition (36) holds, then Eq. (37) yields

$$\big\|S(\tau)-S^*(\tau)\big\|=0.$$

Thus, we have

$$S(\tau)=S^*(\tau). \tag{38}$$

On utilizing the similar methodology, we arrive at the following results

$$I(\tau)=I^*(\tau),\quad R(\tau)=R^*(\tau),\quad A(\tau)=A^*(\tau). \tag{39}$$

Thus, the proof of the uniqueness theorem is completed.

5 Application of q-HATM to Solve FMEM for Computer Viruses

First of all, we use the Laplace transform on FMEM for computer viruses (6), and it gives

$$\begin{aligned}
&L[S] - \tfrac{\alpha_1}{p} - \tfrac{p^\kappa+\kappa(1-p^\kappa)}{p^\kappa} L[-\mu_{SA} S(\tau)A(\tau) - \xi S(\tau)I(\tau) + \rho R(\tau)] = 0,\\
&L[I] - \tfrac{\alpha_2}{p} - \tfrac{p^\kappa+\kappa(1-p^\kappa)}{p^\kappa} L[\xi S(\tau)I(\tau) - \mu_{IA} A(\tau)I(\tau) - \varepsilon I(\tau)] = 0,\\
&L[R] - \tfrac{\alpha_3}{p} - \tfrac{p^\kappa+\kappa(1-p^\kappa)}{p^\kappa} L[\varepsilon I(\tau) - \rho R(\tau)] = 0,\\
&L[A] - \tfrac{\alpha_4}{p} - \tfrac{p^\kappa+\kappa(1-p^\kappa)}{p^\kappa} L[\mu_{SA} S(\tau)A(\tau) + \mu_{IA} A(\tau)I(\tau)] = 0.
\end{aligned} \tag{40}$$

The nonlinear operators are given as

$$\begin{aligned}
N_1[\Theta_1(\tau;z)] &= L[\Theta_1(\tau;z)] - \frac{\alpha_1}{p} - \frac{p^\kappa+\kappa(1-p^\kappa)}{p^\kappa} L[-\mu_{SA}\Theta_1(\tau;z)\,\Theta_4(\tau;z)\\
&\quad -\xi\Theta_1(\tau;z)\Theta_2(\tau;z) + \rho\Theta_3(\tau;z)] = 0,\\
N_2[\Theta_2(\tau;z)] &= L[\Theta_2(\tau;z)] - \frac{\alpha_2}{p} - \frac{p^\kappa+\kappa(1-p^\kappa)}{p^\kappa} L[\xi\Theta_1(\tau;z)\,\Theta_2(\tau;z)\\
&\quad -\mu_{IA}\Theta_4(\tau;z)\Theta_2(\tau;z) - \varepsilon\Theta_2(\tau;z)\,] = 0,\\
N_3[\Theta_3(\tau;z)] &= L[\Theta_3(\tau;z)] - \frac{\alpha_3}{p} - \frac{p^\kappa+\kappa(1-p^\kappa)}{p^\kappa} L[\varepsilon\Theta_2(\tau;z)\\
&\quad -\rho\Theta_3(\tau;z)] = 0,\\
N_4[\Theta_4(\tau;z)] &= L[\Theta_4(\tau;z)] - \frac{\alpha_4}{p} - \frac{p^\kappa+\kappa(1-p^\kappa)}{p^\kappa} L[\mu_{SA}\Theta_1(\tau;z)\,\Theta_4(\tau;z)\\
&\quad +\mu_{IA}\Theta_4(\tau;z)\Theta_2(\tau;z)] = 0,
\end{aligned} \tag{41}$$

and thus, we have

$$\begin{aligned}
\Re_{1,\ell}(\vec{S}_{(\ell-1)}) &= L\big[S_{(\ell-1)}\big] - \frac{\alpha_1}{p}\left(1-\frac{k_\ell}{n}\right)\\
&\quad - \frac{p^\kappa+\kappa(1-p^\kappa)}{p^\kappa} L\left[-\mu_{SA}\left(\sum_{r=0}^{\ell-1} S_r A_{(\ell-1-r)}\right)\right.\\
&\quad \left. -\xi\left(\sum_{r=0}^{\ell-1} S_r I_{(\ell-1-r)}\right) - \rho R_{(\ell-1)}\right],\\
\Re_{2,\ell}(\vec{I}_{(\ell-1)}) &= L\big[I_{(\ell-1)}\big] - \frac{\alpha_2}{p}\left(1-\frac{k_\ell}{n}\right)\\
&\quad - \frac{p^\kappa+\kappa(1-p^\kappa)}{p^\kappa} L\left[\xi\left(\sum_{r=0}^{\ell-1} S_r I_{(\ell-1-r)}\right)\right.
\end{aligned}$$

$$-\mu_{IA}\left(\sum_{r=0}^{\ell-1} A_r I_{(\ell-1-r)}\right) - \varepsilon I_{(\ell-1)}\Bigg],$$

$$\Re_{3,\ell}(\vec{R}_{(\ell-1)}) = L\big[R_{(\ell-1)}\big] - \frac{\alpha_3}{p}\left(1 - \frac{k_\ell}{n}\right) - \frac{p^\kappa + \kappa(1-p^\kappa)}{p^\kappa} L\big[\varepsilon I_{(\ell-1)} - \rho R_{(\ell-1)}\big],$$

$$\Re_{4,\ell}(\vec{A}_{(\ell-1)}) = L\big[A_{(\ell-1)}\big] - \frac{\alpha_4}{p}\left(1 - \frac{k_\ell}{n}\right) - \frac{p^\kappa + \kappa(1-p^\kappa)}{p^\kappa} L\Bigg[\mu_{SA}\left(\sum_{r=0}^{\ell-1} S_r A_{(\ell-1-r)}\right) + \mu_{IA}\left(\sum_{r=0}^{\ell-1} A_r I_{(\ell-1-r)}\right)\Bigg] \tag{42}$$

and k_ℓ is defined as

$$k_\ell = \begin{cases} 0, & \ell \le 1, \\ n, & \ell > 1. \end{cases} \tag{43}$$

Next, the deformation equations of ℓ^{th}-order are presented as

$$\begin{aligned} L\big[S_\ell(\tau) - k_\ell S_{(\ell-1)}(\tau)\big] &= \hbar \Re_{1,\ell}(\vec{S}_{(\ell-1)}), \\ L\big[I_\ell(\tau) - k_\ell I_{(\ell-1)}(\tau)\big] &= \hbar \Re_{2,\ell}(\vec{I}_{(\ell-1)}), \\ L\big[R_\ell(\tau) - k_\ell R_{(\ell-1)}(\tau)\big] &= \hbar \Re_{3,\ell}(\vec{R}_{(\ell-1)}), \\ L\big[A_\ell(\tau) - k_\ell A_{(\ell-1)}(\tau)\big] &= \hbar \Re_{4,\ell}(\vec{A}_{(\ell-1)}). \end{aligned} \tag{44}$$

The utilization the inversion of Laplace transform on Eq. (44) enables us to get

$$\begin{aligned} S_\ell(\tau) &= k_\ell S_{(\ell-1)}(\tau) + \hbar L^{-1}\Big[\Re_{1,\ell}(\vec{S}_{(\ell-1)})\Big], \\ I_\ell(\tau) &= k_\ell I_{(\ell-1)}(\tau) + \hbar L^{-1}\big[\Re_{1,\ell}(\vec{I}_{(\ell-1)})\big], \\ R_\ell(\tau) &= k_\ell R_{(\ell-1)}(\tau) + \hbar L^{-1}\Big[\Re_{1,\ell}(\vec{R}_{(\ell-1)})\Big], \\ A_\ell(\tau) &= k_\ell A_{(\ell-1)}(\tau) + \hbar L^{-1}\Big[\Re_{1,\ell}(\vec{A}_{(\ell-1)})\Big]. \end{aligned} \tag{45}$$

We take the initial guess $S_0(\tau) = \alpha_1$, $I_0(\tau) = \alpha_2$, $R_0(\tau) = \alpha_3$, $A_0(\tau) = \alpha_4$ and solving Eq. (45) for $\ell = 0, 1, 2, \ldots$, we determine the values of $S_\ell(\tau)$, $I_\ell(\tau)$, $R_\ell(\tau)$ and $A_\ell(\tau)$, $\forall \ell \ge 1$.

Finally, the solution of FMEM for computer viruses (6) is given as

$$\begin{aligned} S(\tau) &= S_0(\tau) + S_1(\tau)\left(\tfrac{1}{n}\right) + S_2(\tau)\left(\tfrac{1}{n}\right)^2 + \cdots, \\ I(\tau) &= I_0(\tau) + I_1(\tau)\left(\tfrac{1}{n}\right) + I_2(\tau)\left(\tfrac{1}{n}\right)^2 + \cdots, \\ R(\tau) &= R_0(\tau) + R_1(\tau)\left(\tfrac{1}{n}\right) + R_2(\tau)\left(\tfrac{1}{n}\right)^2 + \cdots, \\ A(\tau) &= A_0(\tau) + A_1(\tau)\left(\tfrac{1}{n}\right) + A_2(\tau)\left(\tfrac{1}{n}\right)^2 + \cdots. \end{aligned} \tag{46}$$

6 Numerical Simulations

In this part, we present the numerical computation for FMEM for computer viruses (6) as function of time at $\mu_{SA} = 0.025$, $\mu_{IA} = 0.25$, $\xi = 0.1$, $\varepsilon = 9$, $\rho = 0.8$, $\hbar = -1$ and $n = 3$ for defined values of order of AB fractional operator. The initial conditions are taken as $S(0) = 3$, $I(0) = 95$, $R(0) = 1$ and $A(0) = 1$. The numerical outcomes for different kind of computer populations are present through Figs. 1, 2, 3 and 4. Figure 1 presents the impact of order of AB fractional operator on the group of non-infected computers with the possibility of infection. Figure 2 demonstrates the impact

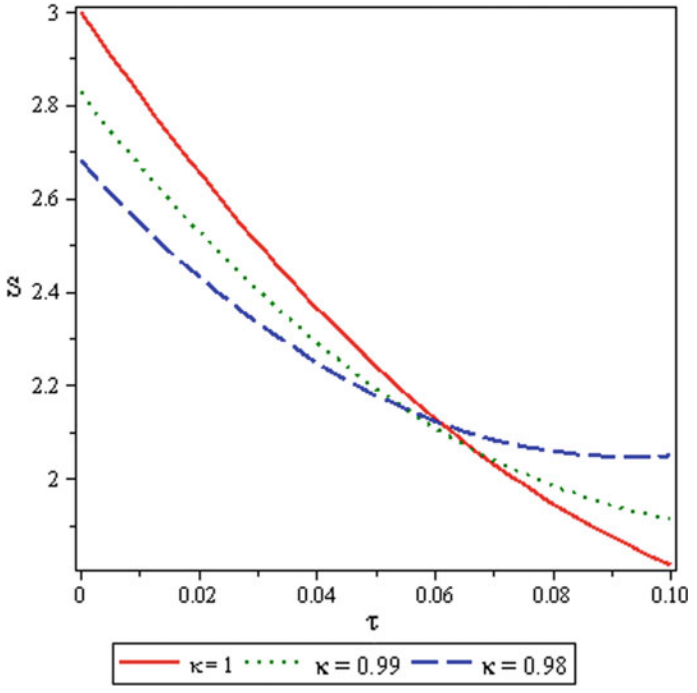

Fig. 1 Nature of $S(\tau)$ with respect to τ for distinct orders of AB fractional derivative

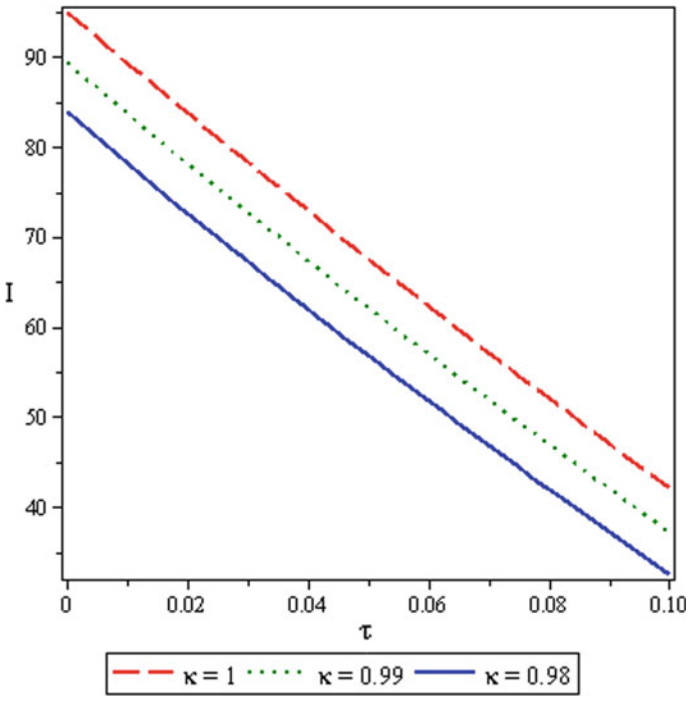

Fig. 2 Nature of $I(\tau)$ with respect to τ for distinct orders of AB fractional derivative

of order of AB fractional operator on the group of infected computers. Figure 3 presents the influence of order of AB fractional operator on the class of removed ones due to the infection or not. Figure 4 presents the effect of order of AB fractional derivative on non-infected computers associated with anti-virus. It can be noticed from Figs. 1, 2, 3 and 4 that there is a significant impact of order of AB fractional operator on different kind of populations of computers due to Mittag–Leffler memory.

7 Concluding Remarks, Observations and Suggestions

In this work, the FMEM for computer viruses is studied involving Mittag–Leffler memory effects. The existence and uniqueness of the solution of FMEM for computer viruses are examined. The solution of the FMEM for computer viruses is obtained with the aid of q-HATM. To demonstrate the effects of Mittag–Leffler memory on different groups of computer, some numerical simulations are conducted. The numerical outcomes give very clear indications that the use of AB fractional derivative in mathematical modeling of computer viruses is very fruitful, and the q-HATM is a very accurate and easy approach for solving such type of fractional models.

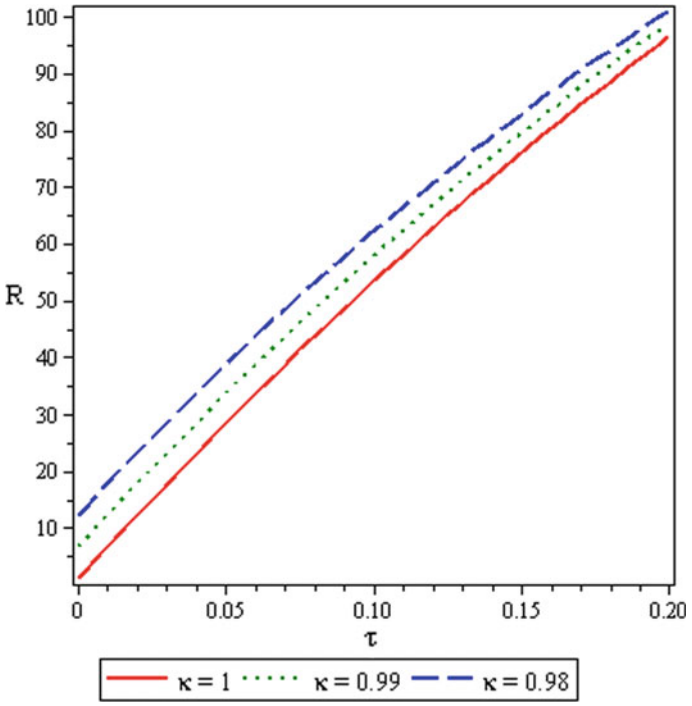

Fig. 3 Nature of $R(\tau)$ with respect to τ for distinct orders of AB fractional derivative

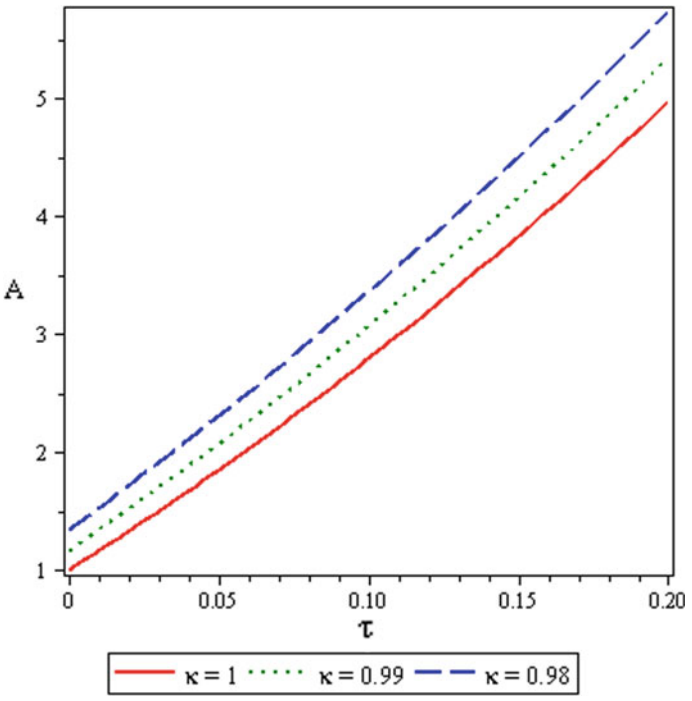

Fig. 4 Nature of $A(\tau)$ with respect to τ for distinct orders of AB fractional derivative

References

1. J.O. Kephart, S.R. White, Measuring and modelling computer virus prevalence, in *IEEE Computer Society Symposium on Research in Security and Privacy* (1993), pp. 2–15
2. J.O. Kephart, S.R. White, D.M. Chess, Computers and epidemiology. IEEE Spectr. **5**(30), 20–26 (1993)
3. L. Billings, W.M. Spears, I.B. Schwartz, A unified prediction of computer virus spread inconnected networks. Phys. Lett. A **297**, 261–266 (2002)
4. X. Han, Q. Tan, Dynamical behavior of computer virus on Internet. Appl. Math. Comput. **6**(217), 2520–2526 (2010)
5. J.R.C. Piqueira, V.O. Araujo, A modified epidemiological model for computer viruses. Appl. Math. Comput. **2**(213), 355–360 (2009)
6. J. Ren, X. Yang, Q. Zhu, L.X. Yang, C. Zhang, A novel computer virus model and its dynamics. Nonlinear Anal. **1**(13), 376–384 (2012)
7. J.C. Wierman, D.J. Marchette, Modeling computer virus prevalence with a susceptible-infected susceptible model with reintroduction. Comput. Stat. Data Anal. **1**(45), 3–23 (2004)
8. A.H. Handam, A.A. Freihat, A new analytic numeric method solution for fractional modified epidemiological model for computer viruses. Appl. Appl. Math. **10**(2), 919–936 (2015)
9. W. Murray, The application of epidemiology to computer viruses. Comput. Secur. **7**, 139–150 (1988)
10. W. Gleissner, A mathematical theory for the spread of computer viruses. Comput. Secur. **8**, 35–41 (1989)
11. J.O. Kephart, G.B. Sorkin, D.M. Chess, S.R. White, Fighting computer viruses, in *Scientific American* (1997), pp. 88–93

12. J.O. Kephart, S.R. White, Directed-graph epidemiological models of computer viruses, in *Proceedings of the IEEE Symposium on Security and Privacy* (1997), pp. 343–359
13. Z. Lu, X. Chi, L. Chen, The effect of constant and pulse vaccination of SIR epidemic model with horizontal and vertical transmission. Math. Comput. Model. **36**, 1039–1057 (2002)
14. A.G. Atta, M. Moatimid, Y.H. Youssri, Generalized fibonacci operational collocation approach for fractional initial value problems. Int. J. Appl. Comput. Math **5**, 9 (2019). https://doi.org/10.1007/s40819-018-0597-4
15. W.M. Abd-Elhameed, Y.H. Youssri, Sixth-kind Chebyshev spectral approach for solving fractional differential equations. Int. J. Nonlinear Sci. Numer. Simul. **20**(2), 191–203 (2019). https://doi.org/10.1515/ijnsns-2018-0118
16. R.M. Hafez, Y.H. Youssri, Jacobi collocation scheme for variable-order fractional reaction-subdiffusion equation. Comput. Appl. Math. **37**(4), 5315–5333 (2019)
17. S. Ullah, M.A. Khan, M. Farook, T. Gul, F. Hussain, A fractional order HBV model with hospitalization. Discr. Contin. Dyn. Syst. S (2019). https://doi.org/10.3934/dcdss.2020056
18. S. Ullah, M.A. Khan, M. Farooq, Z. Hammouch, D. Baleanu, A fractional model for the dynamics of tuberculosis infection using Caputo-Fabrizio derivative. Discr. Contin. Dyn. Syst. S (2019). https://doi.org/10.3934/dcdss.2020057
19. J. Singh, D. Kumar, Z. Hammouch, A. Atangana, A fractional epidemiological model for computer viruses pertaining to a new fractional derivative. Appl. Math. Comput. **316**, 504–515 (2018)
20. M. Caputo, Linear models of dissipation whose Q is almost frequency independent, part II. Geophys. J. Int. **13**(5), 529–539 (1967)
21. A.A. Kilbas, H.M. Srivastava, J.J. Trujillo, *Theory and applications of fractional differential equations* (Elsevier, Amsterdam, The Netherlands, 2006)
22. M. Caputo, M. Fabrizio, A new definition of fractional derivative without singular kernel. Progr. Fract. Differ. Appl. **1**, 73–85 (2015)
23. J. Losada, J.J. Nieto, Properties of the new fractional derivative without singular kernel. Progr. Fract. Differ. Appl. **1**, 87–92 (2015)
24. A. Atangana, B.T. Alkahtani, Analysis of the Keller-Segel model with a fractional derivative without singular kernel. Entropy **17**(6), 4439–4453 (2015)
25. A. Atangana, B.T. Alkahtani, Analysis of non- homogenous heat model with new trend of derivative with fractional order. Chaos Soliton. Fract. **89**, 566–571 (2016)
26. D. Kumar, J. Singh, D. Baleanu, Numerical computation of a fractional model of differential-difference equation. J. Comput. Nonlinear Dyn. **11**(6), 061004 (2016)
27. D. Kumar, J. Singh, D. Baleanu, M.A. Qurashi, Analysis of logistic equation pertaining to a new fractional derivative with non-singular kernel. Adv. Mech. Eng. **9**(1), 1–8 (2017)
28. J. Singh, D. Kumar, D. Baleanu, S. Rathore, *On the local fractional wave equation in fractal strings*. Math. Methods Appl. Sci. 42(5), 1588-1595 (2019).
29. X.J. Yang, A new integral transform operator for solving the heat-diffusion problem. Appl. Math. Lett. **64**, 193–197 (2017)
30. A. Debbouche, D.F.M. Torres, Sobolev type fractional dynamic equations and optimal multi-integral controls with fractional nonlocal conditions. Fract. Calc. Appl. Anal. **18**(1), 95–121 (2015)
31. D. Kumar, J. Singh, S.D. Purohit, R. Swroop, A hybrid analytical algorithm for nonlinear fractional wave-like equations. Math. Model. Nat. Phenom. **14**, 304 (2019)
32. A. Goswami, J. Singh, D. Kumar, Sushila, An efficient analytical approach for fractional equal width equations describing hydro-magnetic waves in cold plasma. Phys. A **524**, 563–575 (2019)
33. A. Atangana, D. Baleanu, New fractional derivative with nonlocal and non-singular kernel, theory and application to heat transfer model. Therm. Sci. **20**(2), 763–769 (2016)
34. D. Kumar, J. Singh, K. Tanwar, D. Baleanu, A new fractional exothermic reactions model having constant heat source in porous media with power, exponential and Mittag-Leffler Laws. Int. J. Heat Mass Transf. **138**, 1222–1227 (2019)
35. J. Singh, D. Kumar, D. Baleanu, New aspects of fractional Biswas-Milovic model with Mittag-Leffler law. Math. Model. Nat. Phenom. **14**, 303 (2019)

36. D. Kumar, J. Singh, D. Baleanu, Analysis of regularized long-wave equation associated with a new fractional operator with Mittag-Leffler type kernel. Phys. A **492**, 155–167 (2018)
37. D. Kumar, J. Singh, D. Baleanu, A new analysis of Fornberg-Whitham equation pertaining to a fractional derivative with Mittag-Leffler type kernel. Eur. J. Phys. Plus **133**(2), 70 (2018)
38. J. Singh, A new analysis for fractional rumor spreading dynamical model in a social network with Mittag-Leffler law. Chaos **29**, 013137 (2019)
39. Fatmawati, M.A. Khan, M. Khan, M. Azizah, Windarto, S. Ullah, Fractional model for the dynamics of competition between commercial and rural banks in Indonesia. Chaos Soliton. Fract. **122**, 32–46 (2019)
40. D. Kumar, J. Singh, D. Baleanu, A new analysis for fractional model of regularized long-wave equation arising in ion acoustic plasma waves. Math. Methods Appl. Sci. **40**(15), 5642–5653 (2017)
41. H.M. Srivastava, D. Kumar, J. Singh, An efficient analytical technique for fractional model of vibration equation. Appl. Math. Model. **45**, 192–204 (2017)
42. M.A. El-Tawil, S.N. Huseen, The q-homotopy analysis method (q-HAM). Int. J. Appl. Math. Mech. **8**, 51–75 (2012)
43. M.A. El-Tawil, S.N. Huseen, On convergence of the q-homotopy analysis method. Int. J. Contemp. Math. Sci. **8**, 481–497 (2013)
44. S.A. Khuri, A Laplace decomposition algorithm applied to a class of nonlinear differential equations. J. Appl. Math. **1**, 141–155 (2001)
45. D. Kumar, R.P. Agarwal, J. Singh, A modified numerical scheme and convergence analysis for fractional model of Lienard's equation. J. Comput. Appl. Math. 339, 405-413 (2018)
46. D. Kumar, J. Singh, D. Baleanu, A fractional model of convective radial fins with temperature-dependent thermal conductivity. Rom. Rep. Phys. **69**(1), 103 (2017)
47. D. Kumar, J. Singh, D. Baleanu, Analytic study of Allen-Cahn equation of fractional order. Bull. Math. Anal. Appl. **1**, 31–40 (2016)

Numerical Simulation of Nonlinear Ecological Models with Nonlocal and Nonsingular Fractional Derivative

Kolade M. Owolabi

1 Introduction

Over the years, the subject of ecology has been studied and becomes day-in and day-out activities. The meaning of ecology has gone beyond monitoring a flock of animals. In population dynamics, it has been used to address the interpersonal relationship between two or more species, where a functional response of the higher species (predator) to that of the lower species (prey) is known to be the change in the density of prey attached per unit time per predator as the prey density changes. Different types of functional response used to model various predation scenarios have been reported in [20, 21] to compliment the realistic standard Lotka–Voltera system. Zhang et al. [35] study the effect of periodic forcing and impulsive perturbations on predator–prey system with Holling type-IV functional response.

In contrast to the classical single or multicomponent species dynamics that were extensively reported in literature between the 1970s and 1980s and till date, respectively [19], predator–prey systems are known to give rise to period and spatiotemporal oscillations. Though most systems with steady-state equilibria often result to oscillatory transients with a stable frequency. Many (fluctuating) population scenarios appear to be modelled by such interactions. Nonetheless, fractional predator–prey models have been poorly reported with respect to the interaction of nonlinear dynamics. The total population of the mathematical model can be denoted by P, which is subdivided into two or three groups, that is, a group referred to as the prey on which the higher class depends for existence. The second group contains the species

K. M. Owolabi (✉)
Faculty of Natural and Agricultural Sciences, Institute for Groundwater Studies, University of the Free State, Bloemfontein 9300, South Africa
e-mail: kolademattheowolabi@tdtu.edu.vn

Faculty of Mathematics and Statistics, Ton Duc Thang University, Ho Chi Minh City, Vietnam

H. Dutta (ed.), *Mathematical Modelling in Health, Social and Applied Sciences*, Forum for Interdisciplinary Mathematics, https://doi.org/10.1007/978-981-15-2286-4_10

known as the predator, and this group of population depends on the lower or weak class to make living.

The dynamical system of predation consisting of the prey species $u(t)$, the lower or intermediate predator species $v(t)$ and the top predator species denoted by $w(t)$ are modelled by the following general food chain system

$$\frac{du}{dt} = f_1(u, v, w), \quad \frac{dv}{dt} = f_2(u, v, w), \quad \frac{dw}{dt} = f_3(u, v, w), \tag{1}$$

where the reaction functions f_i, $i = 1, 2, 3$ which account for the local kinetics are continuous and Lipschitzian on R^3_+; hence, the solution exists and is unique.

In the present case, we consider a fractional extension of the classical model (1) as

$$\frac{d^\alpha u}{dt^\alpha} = f_1(u, v, w), \quad \frac{d^\alpha v}{dt^\alpha} = f_2(u, v, w), \quad \frac{d^\alpha w}{dt^\alpha} = f_3(u, v, w), \tag{2}$$

where the functions f_i and parameters remain as earlier defined, and $\frac{d^\alpha u}{dt^\alpha}$ is given by the Atangana–Baleanu fractional derivative of order $\alpha \in (0, 1]$ in the sense of Caputo [5, 18, 26, 27]

$${}^{ABC}\mathcal{D}^\alpha_{a,t}[u(t)] = \frac{M(\alpha)}{1-\alpha}\int_a^t u'(\xi)E_\alpha\left[-\alpha\frac{(t-\xi)^\alpha}{1-\alpha}\right]d\xi \tag{3}$$

where $M(\alpha)$ is a normalized function as given by Caputo and Fabrizio [12, 13], and E_α is a one-parameter Mittag–Leffler function defined in terms of power series expansion

$$u(z) = E_\alpha(z) = \sum_{s=0}^{\infty}\frac{z^s}{\Gamma(\alpha s + 1)}, \quad \alpha > 0, \quad \alpha \in \mathbb{R}, \quad z \in \mathbb{C}. \tag{4}$$

The Laplace transform of (3) is defined as [5, 24, 25]

$$\begin{aligned}\mathscr{L}\left\{{}^{ABC}_{a}\mathcal{D}^{(\alpha)}_t u(t)\right\}(p) &= \frac{M(\alpha)}{1-\alpha}\mathscr{L}\left\{\int_a^t u'(\xi)E_\alpha\left[-\alpha\frac{(t-\xi)^\alpha}{1-\alpha}\right]d\xi\right\} \\ &= \frac{M(\alpha)}{1-\alpha}\,\frac{p^\alpha\mathscr{L}\{u(t)\}(p) - s^{\alpha-1}u(0)}{p^\alpha + \frac{\alpha}{1-\alpha}}.\end{aligned} \tag{5}$$

In a more compact form, modelling of system (2) with Atangana–Baleanu derivative becomes

$$ {}_{0}^{ABC}\mathcal{D}_{t}^{\alpha}[\cdot(t)] = \frac{1-\alpha}{AB(\alpha)} f_i(u, v, w, t) + \frac{\alpha}{AB(\alpha)\Gamma(\alpha)} \int_0^t f_i(u, v, w, \xi)(t-\xi)^{\alpha-1} d\xi \tag{6} $$

with similar expression for other components. The above derivative has both nonlocal and nonsingular kernel properties [5]. Recently, this new derivative as defined in (3) has been applied to model real-life phenomena, see for instance [5–10], and other applications can be found in [23, 24, 31, 32].

Due to some limitations of the Caputo, Riemann–Liouville and the Caputo–Fabrizio fractional operators, the Atangana–Baleanu derivative was able to bring new weapons into the field of applied mathematics to formulate accurately some of real-life problems in science and engineering. Some of the properties of this derivative over the existing ones include the ability to combine both Markovian and non-Markovian properties, while the Caputo operator is non-Markovian and Riemann–Liouville is Markovian. The ABC derivative waiting time is power law, Brownian motion and stretched exponential law, whereas the Riemann–Liouville formulation has only power law, and Caputo–Fabrizio is exponential decay.

Nonetheless, since Atangana–Baleanu fractional operator is still new, the level of work done based on its applicability is still poorly understood, most especially, the numerical approximation of the derivative. Some of the existing numerical methods which have been extended to handle noninteger order problems include the Laplace method, homotopy analysis method and predictor–corrector scheme, spectral algorithm [33], numerical spectral Legendre–Galerkin algorithm [14–17] and Tchebyshev–Galerkin operational matrix method [1, 11], to mention a few. Other applications of the Atangana–Baleanu operator can be found in [2–4]. In this chapter, we extend the use of Adams–Bashforth scheme to time-fractional reaction–diffusion systems of predation.

The aim of this chapter is to model two and three components predator–prey dynamics with Holling type-IV functional responses using the Atangana–Baleanu fractional derivative, and to compare the results to obtain for fractional order $\alpha \in (0, 1)$ with that of the classical case when $\alpha = 1$. Section 2 deals with the mathematical analysis of the main equations. Formulation of the numerical scheme for approximation of the Atangana–Baleanu fractional derivative is discussed in Sect. 3. We experiment for different values of fractional order in Sect. 4, and finally conclude with Sect. 5.

2 Mathematical Analysis of the Main Dynamics

In this section, stability analysis for two different predation systems with Holling type-IV functional response will be considered.

2.1 Fractional Predator–Prey Dynamics with Holling Response Function of Type-IV

We begin our analysis by considering a simplified form of predator–prey dynamics with Holling type-IV case

$$\begin{aligned}
{}_0^{ABC}\mathcal{D}_t^{\alpha} u &= f_1(u, v, w) = u(\phi - \varphi u) - \frac{\psi_1 uv}{\beta_1 + u^2}, \\
{}_0^{ABC}\mathcal{D}_t^{\alpha} v &= f_2(u, v, w) = \frac{\psi_2 uv}{\beta_1 + u^2} - \delta_1 v - \frac{\psi_3 vw}{\beta_2 + v}, \\
{}_0^{ABC}\mathcal{D}_t^{\alpha} w &= f_3(u, v, w) = \frac{\psi_4 vw}{\beta_2 + v} - \delta_2 w,
\end{aligned} \tag{7}$$

where ${}_0^{ABC}\mathcal{D}_t^{\alpha}(\cdot)$ is the Atangana–Baleanu fractional derivative of order $\alpha \in (0, 1]$, ϕ denotes the growth rate of species u, the intraspecific competition among species u is represented by φ, the half-saturation constant is given by $\beta_i (i = 1, 2)$, and the lower- and top-predators death rates are given by δ_1 and δ_2, respectively. The pair positive parameters (ψ_1, ψ_2) and (ψ_3, ψ_4) stand for the maximum per capital reduction values for which species u and v can attain, respectively. It is reasonable to assume that the initial populations $u(0) \geq 0$, $v(0) \geq 0$ and $w(0) \geq 0$, and continuous local kinetic functions f_i, $i = 1, 2, 3$.

To examine the equilibrium points of fractional system (7), we let

$${}_0^{ABC}\mathcal{D}_t^{\alpha}(\cdot) = 0, \quad \Longrightarrow f_i(u, v, w) = 0, \quad i = 1, 2, 3,$$

from which we can determine the equilibrium points u^*, v^* and w^*. A close look at model (7) shows there are four positive equilibrium. We will consider the stability analysis technique as discussed in [28] and consider only the nontrivial case which is expected to guarantee the existence of the three species. The point $S^* = (u^*, v^*, w^*)$ which represents the biologically meaningful equilibrium point exists, provided there is a positive solution that satisfies the system

$$\begin{aligned}
f_1(u, v, w) &= u(\phi - \varphi u) - \frac{\psi_1 uv}{\beta_1 + u^2} = 0, \\
f_2(u, v, w) &= \frac{\psi_2 uv}{\beta_1 + u^2} - \delta_1 v - \frac{\psi_3 vw}{\beta_2 + v} = 0, \\
f_3(u, v, w) &= \frac{\psi_4 vw}{\beta_2 + v} - \delta_2 w = 0,
\end{aligned} \tag{8}$$

Solving (8) directly results to $v^* = \delta_2 \beta 2/(\psi_4 - \delta_2)$, and u^* is determined from the root of equation

$$u^3 - \frac{\phi u^2}{\varphi} + \beta_1 u + \left(\frac{\psi_1 v^* - \phi \beta_2}{\varphi} \right) = 0, \tag{9}$$

bear in mind that $0 < u^* \leq /\varphi$ and $f(0) = \left(\frac{\psi_1 v^* - \phi\beta_2}{\varphi}\right) < 0$, if condition $v^* < \frac{\phi\beta_1}{\psi_1}$ holds. Again, $f(\phi/\varphi) = \psi_1 v^*/\varphi > 0$. This implies that $f(0)f(\phi/\varphi) < 0$, meaning that there exists a nonnegative root of (9). From the second dynamics in (8), we obtain

$$w^* = \left(\frac{\psi_2 u^*}{\beta_1 + u^{*2}} - \delta_1\right)\frac{\beta_2 + v^*}{\psi_3}.$$

So, we say that the point S^* exists subject to conditions

$$\psi_4 > \delta_2, \quad v^* < \frac{\phi\beta_1}{\psi_1}, \quad \frac{\psi_2 u^*}{\beta_1 + u^{*2}} - \delta_1.$$

Next, we examine the dynamical property of system (7) by computing the community matrix of the species as

$$\mathbf{A} = \begin{pmatrix} \phi - 2\varphi u^* - \frac{\psi_1 v^*(\beta_1 - u^{*2})^2}{(\beta_1 + u^{*2})^2} & -\frac{\psi_1 u^*}{\beta_1 + u^{*2}} & 0 \\ \frac{\psi_2 v^*(\beta_1 - u^{*2})^2}{(\beta_1 + u^{*2})^2} & \frac{\psi_2 u^*}{\beta_1 + u^{*2}} - \frac{\beta_2\psi_3 w^*}{\beta_2 + u^*} - \delta_1 & -\frac{\psi_3 v^*}{\beta_2 + u^*} \\ 0 & \frac{\beta_2\psi_4 w^*}{(\beta_2 + u^*)^2} & 0 \end{pmatrix}_{(u^*, v^*, w^*)} \tag{10}$$

which has the characteristic equation

$$\lambda^3 + \underbrace{[-(a_{11} + a_{22})]}_{X}\lambda^2 + \underbrace{a_{11}a_{22} - a_{12}a_{21} - a_{23}a_{32}}_{Y}\lambda + \underbrace{a_{11}a_{23}a_{32}}_{Z} = 0.$$

By following the Routh–Hurwitz condition, the equilibrium point S^* is locally asymptotically stable if and only if the conditions $X > 0$, $Y > 0$ and $XY - Z > 0$ are satisfied. Clearly, the conditions $X > 0$ and $Z > 0$ hold if

$$2\varphi u + \frac{\psi_1 v^*(\beta_1 - u^{*2}) - \psi_2 u^*(\beta_1 + u^{*2})}{(\beta_1 + u^{*2})^2} + \left(\frac{\beta_2\psi_2 w^*}{(\beta_2 + v^*)}\right) > \phi$$

and

$$u^{*2} < \beta_1, \quad \psi_2 < \frac{\psi_1 v^*(\beta_1 - u^{*2})}{u^*(\beta_1 + u^{*2})}.$$

Therefore, we can conclude that the necessary condition for $XY - Z > 0$ is when $(a_{12}a_{21} - a_{11}a_{22}) < 0$ holds, since $XY - Z = (a_{12}a_{21} - a_{11}a_{22})(a_{11} + a_{22}) + a_{22}a_{23}$ a_{32}, given that

$$\left[\frac{\psi_2^*}{\beta_1 + u^{*2}} - \left(\frac{\beta_2\psi_3 w^*}{(\beta_2 + v^*)^2} + \phi\right)\right](\phi - 2\varphi u^*) + \left(\frac{\beta_2\psi_3 w^*}{(\beta_2 + v^*)^2} + \delta_1\right)\frac{\varphi_1 v^*(\beta_1 - u^{*2})}{(\beta_1 + u^{*2})^2} > 0.$$

So, subject to the above conditions, the nontrivial point S^* is locally asymptotically stable. The essence of stability analysis reported here is to guide in the correct choice of parameter values when numerically simulating the full dynamical system.

2.2 Fractional Reaction–Diffusion Dynamics with Holling Type-IV Functional Response

In this section, we consider the dynamical system with Holling type-IV functional response

$$\begin{aligned} \mathcal{D}_t^\alpha u &= f_u(u,v) = \rho u\left(1-\frac{u}{\kappa}\right) - \frac{\mu u v}{1+\beta u+\gamma u^2}, \\ \mathcal{D}_t^\alpha v &= f_v(u,v) = \frac{\sigma\mu u v}{1+\beta u+\gamma u^2} - \delta v, \end{aligned} \tag{11}$$

where the u and v are the prey and predator populations, respectively, the term $\frac{\mu u}{1+\beta u+\gamma u^2}$ is also referred to as the Monod–Haldane-type functional response [30, 34], ρ is the growth rate of prey, the capture rate μ, κ denotes the carrying capacity, the prey–predator conversion rate is σ, and we denote the half-saturation parameter by γ. The parameter b is assumed to be greater than $-2\sqrt{\gamma}$ to ensure that the population of u-species is nonnegative. All parameters here are assumed to be positive.

An extension is given here by considering the time-fractional reaction–diffusion problem with Holling type-IV functional response formulated in the form

$$\begin{aligned} {}_0^{ABC}\mathcal{D}_t^\alpha u &= D_u\Delta u + f_u(u,v), \quad (x,t)\in L=[0,T]\times\Omega, \\ {}_0^{ABC}\mathcal{D}_t^\alpha v &= D_v\Delta v + f_v(u,v) \end{aligned} \tag{12}$$

subject to the Neumann (zero-flux) boundary conditions $\frac{\partial u}{\partial \nu} = \frac{\partial v}{\partial \nu} = 0, (x,t)\Sigma = (0,T)\times\partial\Omega$ and initial conditions $u(x,0) = u_0(x), \quad v(x,0) = v_0(x), \quad x\in\Omega$, where Ω is the domain assumed to be bounded in $\mathbb{R}^2$ with a smooth boundary $\partial\Omega$, Δ denotes the Laplacian operator on Ω, and the outward normal to $\partial\Omega$ is represented by ν. The parameters D_u, D_v are the diffusion coefficients, $u(x,t)$ and $v(x,t)$ are the population densities of the prey and predator species at time $t\in[0,T]$ and position $x\in\Omega, f_u, f_v$, and the associated parameters remain as defined in (11).

The nonspatial system (11) has at least two steady states that correspond to spatially homogeneous system (12). The interest of the this chapter is to report the nontrivial coexistence point $E=(u^*,v^*)$ where

$$u^* = \frac{\mu\sigma-\delta\beta}{2\delta\gamma}, \quad v^* = \frac{\rho\sigma(\beta\delta-\mu\sigma+\delta\gamma\kappa)u^*+\sigma\rho\delta}{\gamma\kappa\delta^2}$$

subject to conditions

$$(\rho, \kappa, \mu, \beta, \gamma, \delta, \sigma)|\mu\sigma > \delta\beta,$$
$$(\mu\sigma - \delta\beta)^2 > \gamma\delta^2,$$
$$\kappa + \frac{\beta}{\gamma} - \frac{\mu\sigma}{\delta\gamma} < 0,$$
$$\sqrt{(\mu\sigma - \delta\beta)^2 - 4\delta^2\gamma} > \frac{-(\delta^2\beta^2 + \mu^2\sigma^2 + \delta^2\gamma\beta\kappa) + 2(\delta^2\gamma + \delta\beta\mu\sigma) + \delta\gamma\mu\sigma\kappa}{(\delta\beta - \mu\sigma + \delta\gamma\kappa)} > 0.$$

So for linear stability analysis, dynamic system (11) is linearized at equilibrium point (u^*, v^*). Following stability technique applied in [22], we assume a solution

$$u(x, t) \equiv u^* e^{\lambda t + i\omega x}, \quad v(x, t) \equiv v^* e^{\lambda t + i\omega x} \tag{13}$$

where ω is the wave number, λ denotes the eigenvalue arising from the Jacobian or community matrix $\mathbf{A}$ of system (11). For Hopf bifurcation to occur, $Re(\lambda) = 0$ and $Im(\lambda) \neq 0$. The system undergoes Hopf bifurcation when

$$F_H = \{(\rho, \kappa, \mu, \beta, \gamma, \delta, \sigma)|\det(\mathbf{A}_0) > 0, \quad \mathrm{tr}(\mathbf{A}_0) = 0\}, \tag{14}$$

where

$$\det(\mathbf{A}_0) = \frac{\mu\delta v^* + \sigma\mu(\rho - 2(\rho u^*/\kappa))u^*}{1 + \beta u^* + \gamma u^{*2}} - \left(\rho - \frac{2\rho u^*}{\kappa}\right)\delta - \frac{(\beta + 2\gamma u^*)\mu\delta v^*}{(1 + \beta u^* + \gamma u^{*2})^2}$$

$$\mathrm{tr}(\mathbf{A}_0) = \frac{\mu(\sigma u^* - v^* + \gamma u^{*2} v^* + \beta\sigma u^{*2} + \sigma u^{*3}\gamma)}{(1 + \beta u^* + \gamma u^{*2})^2} + \frac{2\rho u^*}{\kappa} - \rho - \delta.$$

The bifurcation parameter is taken as κ here. The Turing bifurcation is defined as

$$F_T = \{(\rho, \kappa, \mu, \beta, \gamma, \delta, \sigma)|\det(\mathbf{A}_\omega) = 0, \quad \mathrm{tr}(\mathbf{A}_\omega) = 0\}, \tag{15}$$

where

$$\det(\mathbf{A}_\omega) = -(\delta + D_v\omega^2)\left[\rho - \frac{2\rho u^*}{\kappa} - D_u\omega^2\right] \times \frac{\left[\left(\rho - \frac{2\rho u^*}{\kappa} - D_u\kappa^2\right)\sigma\mu u^* + (\delta + D_v\omega^2)\mu v^*\right]}{(1 + \beta u^* + \gamma n^{*2})} - \frac{\mu(\beta + 2\gamma u^*)(\delta + D_v\omega^2)u^* v^*}{(1 + \beta u^* + \gamma u^{*2})^2},$$

$$\text{tr}(\mathbf{A}_\omega) = \frac{\mu(\sigma u^* - v^* + \gamma u^{*2} v^* + \beta\sigma u^{*2} + \sigma u^{*3}\gamma)}{(1+\beta u^* + \gamma u^{*2})^2} + \frac{2\rho u^*}{\kappa} + \rho - \delta - (D_u + D_v)\omega^2.$$

In Sect. 4, we give the numerical simulation experiments for both the nonspatially and spatially time-fractional dynamics (11) and (12).

3 Numerical Method for Atangana–Baleanu Fractional Derivative

In this section, we write the fractional differential system (6) in the form

$$^{ABC}_{0}\mathcal{D}^{\alpha}_{t} z(t) = f(z(t), t), \quad z(0) = z_0, \tag{16}$$

where $z = z(u, v, w)$, and $0 < \alpha \leq 1$. By applying the fundamental theorem of calculus, we transform the above differential equation into fractional integral type

$$z(t) - z(0) = \frac{(1-\alpha)}{ABC(\alpha)} f(z(t), t) + \frac{\alpha}{\Gamma(\alpha) ABC(\alpha)} \int_0^t f(z(\xi), \xi)(t-\xi)^{\alpha-1} d\xi. \tag{17}$$

At point $t = t_{n+1}$, for $n = 1, 2, \ldots$, we obtain

$$z(t_{n+1}) - z(0) = \frac{(1-\alpha)}{ABC(\alpha)} f(z(t_n), t_n) + \frac{\alpha}{\Gamma(\alpha) ABC(\alpha)} \int_0^{t_{n+1}} f(z(\xi), \xi)(t_{n+1}-\xi)^{\alpha-1} d\xi. \tag{18}$$

Similarly at point $t = t_n$ for $n = 1, 2, \ldots$, we get

$$z(t_n) - z(0) = \frac{(1-\alpha)}{ABC(\alpha)} f(z(t_{n-1}), t_{n-1}) + \frac{\alpha}{\Gamma(\alpha) ABC(\alpha)} \int_0^{t_n} f(z(\xi), \xi)(t_n-\xi)^{\alpha-1} d\xi. \tag{19}$$

On subtraction yields

$$\begin{aligned} z(t_{n+1}) - z(t_n) = {} & \frac{(1-\alpha)}{ABC(\alpha)} \{f(z(t_n)) - f(z(t_{n-1}), t_{n-1})\} \\ & + \frac{\alpha}{\Gamma(\alpha) ABC(\alpha)} \int_0^{t_{n+1}} f(z(\xi), \xi)(t_{n+1}-\xi)^{\alpha-1} d\xi \\ & - \frac{\alpha}{\Gamma(\alpha) ABC(\alpha)} \int_0^{t_n} f(z(\xi), \xi)(t_n-\xi)^{\alpha-1} d\xi. \end{aligned} \tag{20}$$

After some algebraic manipulations, we obtain

$$\begin{aligned}
&z(t_{n+1}) - z(t_n) \\
&= \frac{1-\alpha}{ABC(\alpha)}\{f(z_n, t_n) - f(z_{n-1}, t_{n-1})\} + \frac{\alpha f(z_n, t_n)}{ABC(\alpha)\Gamma(\alpha)h}\left\{\frac{2ht_{n+1}^{\alpha}}{\alpha} - \frac{t_{n+1}^{\alpha+1}}{\alpha+1}\right\} \\
&- \frac{\alpha f(z_{n-1}, t_{n-1})}{ABC(\alpha)\Gamma(\alpha)h}\left\{\frac{ht_{n+1}^{\alpha}}{\alpha} - \frac{t_{n+1}^{\alpha+1}}{\alpha+1}\right\} - \frac{\alpha f(z_n, t_n)}{ABC(\alpha)\Gamma(\alpha)h}\left\{\frac{ht_n^{\alpha}}{\alpha} - \frac{t_n^{\alpha+1}}{\alpha+1}\right\} \\
&+ \frac{f(z_{n-1}, t_{n-1})}{ABC(\alpha)\Gamma(\alpha)}t_n^{\alpha+1}.
\end{aligned} \tag{21}$$

Thus,

$$\begin{aligned}
z_{n+1} = z_n + f(z_n, t_n)&\left\{\frac{1-\alpha}{ABC(\alpha)} + \frac{\alpha}{ABC(\alpha)h}\left[\frac{2ht_{n+1}^{\alpha}}{\alpha} - \frac{t_{n+1}^{\alpha+1}}{\alpha+1}\right]\right. \\
&\left. - \frac{\alpha}{ABC(\alpha)\Gamma(\alpha)h}\left[\frac{ht_n^{\alpha}}{\alpha} - \frac{t_n^{\alpha+1}}{\alpha+1}\right]\right\} + f(z_{n-1}, t_{n-1}) \\
&\times\left\{\frac{\alpha-1}{ABC(\alpha)} - \frac{\alpha}{h\Gamma(\alpha)ABC(\alpha)}\left[\frac{ht_{n+1}^{\alpha}}{\alpha} - \frac{t_{n+1}^{\alpha+1}}{\alpha+1} + \frac{t^{\alpha+1}}{h\Gamma(\alpha)ABC(\alpha)}\right]\right\}.
\end{aligned} \tag{22}$$

This equation is referred to as the two-step Adams–Bashforth scheme for Atangana–Baleanu fractional derivative in Caputo sense. Details of convergence and stability results can be found in [9].

So when applied to fractional dynamic system (2) bear in mind that $z = z(u, v, w, t)$, we have

$$\begin{aligned}
&u_{n+1} - u_n \\
&= f_1(u_n, v_n, w_n, t_n)\left\{\frac{(1-\alpha)}{ABC(\alpha)} + \frac{\alpha}{ABC(\alpha)h} + \left(\frac{2ht_{n=1}^{\alpha}}{\alpha} - \frac{t_{n+1}^{\alpha+1}}{\alpha+1}\right)\right. \\
&\left. - \frac{\alpha}{h\Gamma(\alpha)ABC(\alpha)}\left(\frac{ht_n^{\alpha}}{\alpha} - \frac{t_n^{\alpha+1}}{\alpha+1}\right)\right\} + f_1(u_{n-1}, v_{n-1}, w_{n-1}, t_{n-1}) \\
&\times\left\{\frac{\alpha-1}{ABC(\alpha)} - \frac{\alpha}{h\Gamma(\alpha)ABC(\alpha)}\left(\frac{ht_{n+1}^{\alpha}}{\alpha} - \frac{t_{n+1}^{\alpha+1}}{\alpha+1} + \frac{t_{n+1}^{\alpha+1}}{h\Gamma(\alpha)ABC(\alpha)}\right)\right\},
\end{aligned}$$

$$
\begin{aligned}
&v_{n+1}-v_n\\
&=f_2(u_n,v_n,w_n,t_n)\left\{\frac{(1-\alpha)}{ABC(\alpha)}+\frac{\alpha}{ABC(\alpha)h}+\left(\frac{2ht_{n=1}^{\alpha}}{\alpha}-\frac{t_{n+1}^{\alpha+1}}{\alpha+1}\right)\right.\\
&\left.-\frac{\alpha}{h\Gamma(\alpha)ABC(\alpha)}\left(\frac{ht_n^{\alpha}}{\alpha}-\frac{t_n^{\alpha+1}}{\alpha+1}\right)\right\}+f_2(u_{n-1},v_{n-1},w_{n-1},t_{n-1})\\
&\times\left\{\frac{\alpha-1}{ABC(\alpha)}-\frac{\alpha}{h\Gamma(\alpha)ABC(\alpha)}\left(\frac{ht_{n+1}^{\alpha}}{\alpha}-\frac{t_{n+1}^{\alpha+1}}{\alpha+1}+\frac{t_{n+1}^{\alpha+1}}{h\Gamma(\alpha)ABC(\alpha)}\right)\right\},
\end{aligned}
$$

$$
\begin{aligned}
&w_{n+1}-w_n\\
&=f_3(u_n,v_n,w_n,t_n)\left\{\frac{(1-\alpha)}{ABC(\alpha)}+\frac{\alpha}{ABC(\alpha)h}+\left(\frac{2ht_{n=1}^{\alpha}}{\alpha}-\frac{t_{n+1}^{\alpha+1}}{\alpha+1}\right)\right.\\
&\left.-\frac{\alpha}{h\Gamma(\alpha)ABC(\alpha)}\left(\frac{ht_n^{\alpha}}{\alpha}-\frac{t_n^{\alpha+1}}{\alpha+1}\right)\right\}+f_3(u_{n-1},v_{n-1},w_{n-1},t_{n-1})\\
&\times\left\{\frac{\alpha-1}{ABC(\alpha)}-\frac{\alpha}{h\Gamma(\alpha)ABC(\alpha)}\left(\frac{ht_{n+1}^{\alpha}}{\alpha}-\frac{t_{n+1}^{\alpha+1}}{\alpha+1}+\frac{t_{n+1}^{\alpha+1}}{h\Gamma(\alpha)ABC(\alpha)}\right)\right\},
\end{aligned}
$$

By substituting the values of $f_i(u,v,w)$, $i=1,2,3$ as earlier given, we obtain

$$
\begin{aligned}
&u_{n+1}-u_n=u_n(t_n)(\phi-\varphi u_n(t_n))-\frac{\psi_1 u_n(t_n)v_n(t_n)}{\beta_1+u_n^2(t_n)}\\
&\times\left\{\frac{(1-\alpha)}{ABC(\alpha)}+\frac{\alpha}{ABC(\alpha)h}+\left(\frac{2ht_{n=1}^{\alpha}}{\alpha}-\frac{t_{n+1}^{\alpha+1}}{\alpha+1}\right)\right.\\
&\left.-\frac{\alpha}{h\Gamma(\alpha)ABC(\alpha)}\left(\frac{ht_n^{\alpha}}{\alpha}-\frac{t_n^{\alpha+1}}{\alpha+1}\right)\right\}\\
&+u_{n-1}(t_{n-1})(\phi-\varphi u_{n-1}(t_{n-1}))-\frac{\psi_1 u_{n-1}(t_{n-1})v_{n-1}(t_{n-1})}{\beta_1+u_{n-1}^2(t_{n-1})}\\
&\times\left\{\frac{\alpha-1}{ABC(\alpha)}-\frac{\alpha}{h\Gamma(\alpha)ABC(\alpha)}\left(\frac{ht_{n+1}^{\alpha}}{\alpha}-\frac{t_{n+1}^{\alpha+1}}{\alpha+1}+\frac{t_{n+1}^{\alpha+1}}{h\Gamma(\alpha)ABC(\alpha)}\right)\right\},
\end{aligned}
$$

$$
\begin{aligned}
v_{n+1} - v_n &= \frac{\psi_2 u_n(t_n) v_n(t_n)}{\beta_1 + u_n^2(t_n)} - \delta_1 v_n(t_n) - \frac{\psi_3 v_n(t_n) w_n(t_n)}{\beta_2 + v_n(t_n)} \\
&\times \left\{ \frac{(1-\alpha)}{ABC(\alpha)} + \frac{\alpha}{ABC(\alpha)h} + \left(\frac{2ht_{n=1}^{\alpha}}{\alpha} - \frac{t_{n+1}^{\alpha+1}}{\alpha+1} \right) \right. \\
&\left. - \frac{\alpha}{h\Gamma(\alpha)ABC(\alpha)} \left(\frac{ht_n^{\alpha}}{\alpha} - \frac{t_n^{\alpha+1}}{\alpha+1} \right) \right\} \\
&+ \frac{\psi_2 u_{n-1}(t_{n-1}) v_{n-1}(t_{n-1})}{\beta_1 + u_{n-1}^2(t_{n-1})} - \delta_1 v_{n-1}(t_{n-1}) - \frac{\psi_3 v_{n-1}(t_{n-1}) w_{n-1}(t_{n-1})}{\beta_2 + v_{n-1}(t_{n-1})} \\
&\times \left\{ \frac{\alpha - 1}{ABC(\alpha)} - \frac{\alpha}{h\Gamma(\alpha)ABC(\alpha)} \left(\frac{ht_{n+1}^{\alpha}}{\alpha} - \frac{t_{n+1}^{\alpha+1}}{\alpha+1} + \frac{t_{n+1}^{\alpha+1}}{h\Gamma(\alpha)ABC(\alpha)} \right) \right\},
\end{aligned}
$$

$$
\begin{aligned}
w_{n+1} - w_n &= \frac{\psi_4 v_n(t_n) w_n(t_n)}{\beta_2 + v_n(t_n)} - \delta_2 w_n(t_n) \\
&\times \left\{ \frac{(1-\alpha)}{ABC(\alpha)} + \frac{\alpha}{ABC(\alpha)h} + \left(\frac{2ht_{n=1}^{\alpha}}{\alpha} - \frac{t_{n+1}^{\alpha+1}}{\alpha+1} \right) - \frac{\alpha}{h\Gamma(\alpha)ABC(\alpha)} \right. \\
&\left. \times \left(\frac{ht_n^{\alpha}}{\alpha} - \frac{t_n^{\alpha+1}}{\alpha+1} \right) \right\} + \frac{\psi_4 v_{n-1}(t_{n-1}) w_{n-1}(t_{n-1})}{\beta_2 + v_{n-1}(t_{n-1})} - \delta_2 w_{n-1}(t_{n-1}) \\
&\times \left\{ \frac{\alpha - 1}{ABC(\alpha)} - \frac{\alpha}{h\Gamma(\alpha)ABC(\alpha)} \left(\frac{ht_{n+1}^{\alpha}}{\alpha} - \frac{t_{n+1}^{\alpha+1}}{\alpha+1} + \frac{t_{n+1}^{\alpha+1}}{h\Gamma(\alpha)ABC(\alpha)} \right) \right\},
\end{aligned}
$$

which is the numerical approximation of fractional dynamic system (2) using the Atangana–Baleanu fractional derivative in the sense of Caputo.

4 Numerical Experiment and Results

Our numerical experiments in this section are performed with a MATLAB package. We apply the fractional two-step Adams–Bashforth method formulated in Sect. 3 for the approximation of the Atangana–Baleanu fractional derivative. Two important predation models with Holling type-IV earlier studied theoretically are now considered for our numerical experiments.

We begin our simulation experiment of fractional system (7) with parameters: $\delta_1 = 0.037$, $\delta_2 = 0.053$, $\varphi = (0.30, 1.20)$, $\phi = (0.25, 0.5)$, $\psi_1 = 0.15$, $\psi_2 = 0.27$, $\psi_3 = 0.29$, $\psi_4 = 0.095$, $\beta_1 = 1$, $\beta 2 = 2$. Simulation time is fixed at $t = 1000$ to obtain 2D (columns 2, 3) and 3D (column 1) dynamics in Figs. 1, 2, 3, 4 and 5 which correspond to $\alpha = (0.25, 0.35, 0.67, 0.73, 1.0)$, respectively. We observed a drastic behaviour for classical case when $\alpha = 1$.

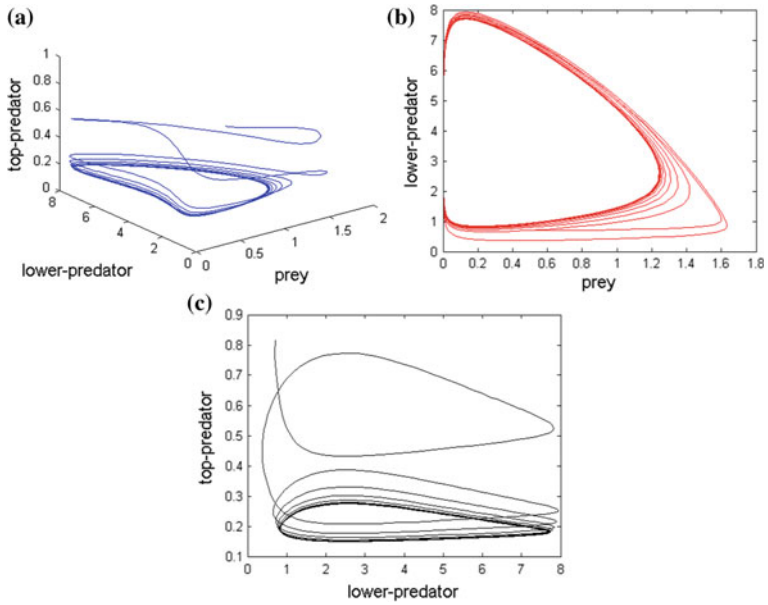

Fig. 1 Numerical results for system (7) with $\alpha = 0.25$

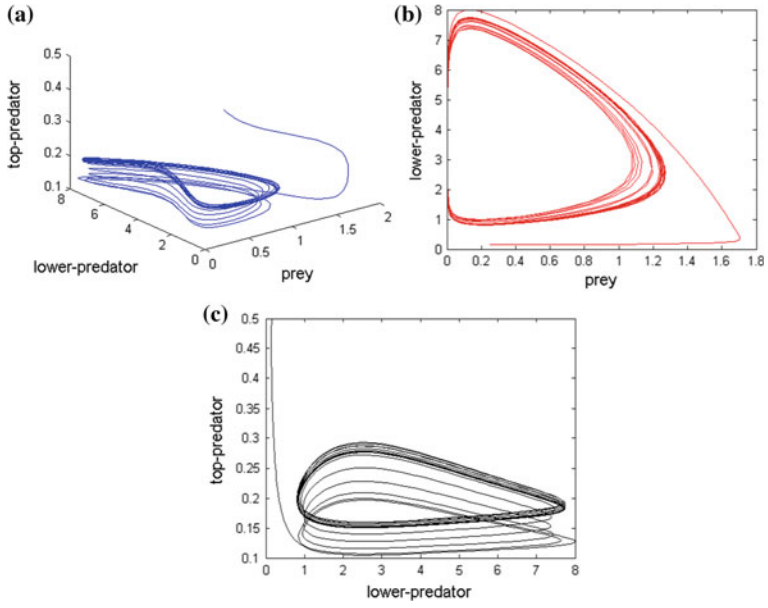

Fig. 2 Numerical results for system (7) with $\alpha = 0.35$

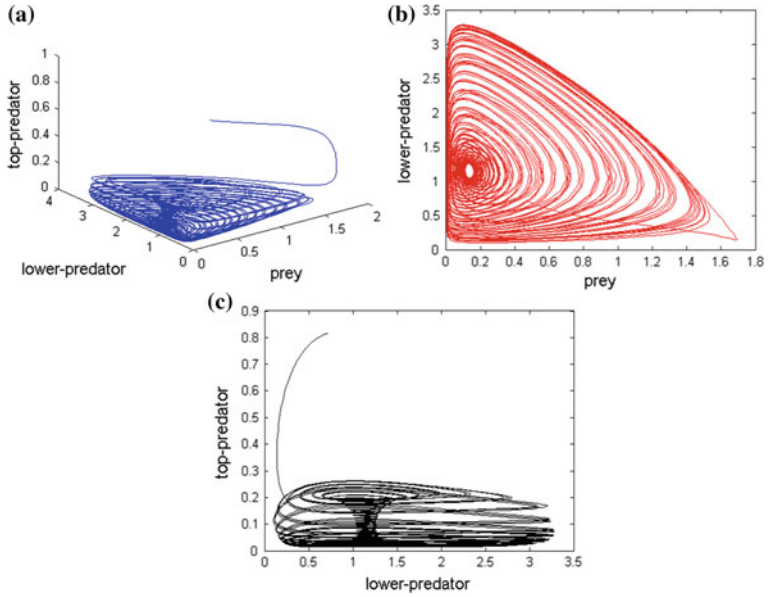

Fig. 3 Numerical results for system (7) with $\alpha = 0.67$

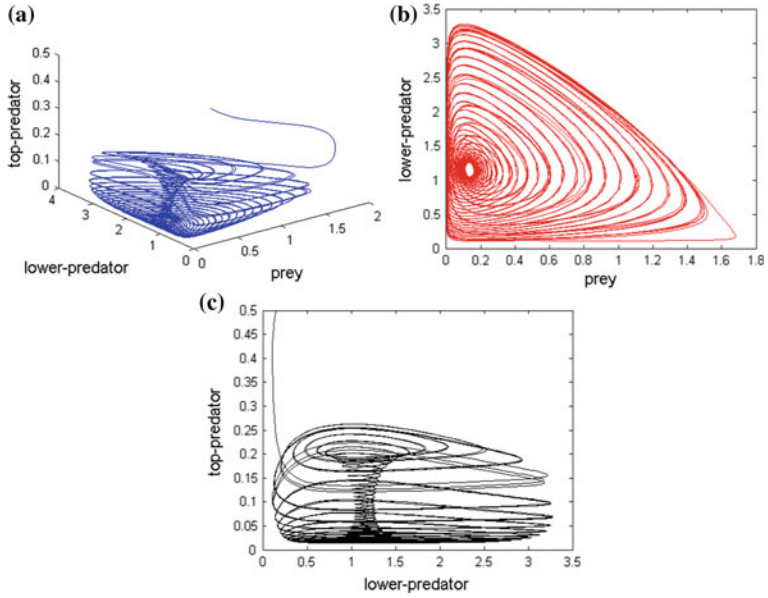

Fig. 4 Numerical results for system (7) with $\alpha = 0.73$

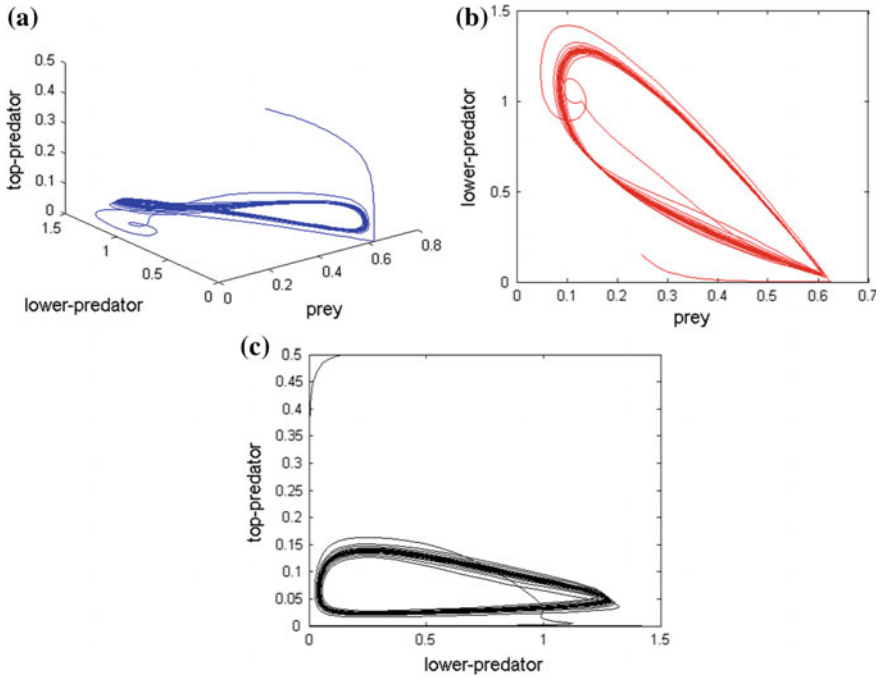

Fig. 5 Numerical results for system (7) with $\alpha = 1.00$

It should be mentioned that apart from the dynamical behaviours reported here, we observed several other scenarios that are not presented in this section. For instance, when ϕ which symbolizes the intrinsic growth rate of prey species u is decreasing, the dynamic undergoes periodic attractor. The chaotic attractor becomes stable, and the value of intraspecific competition φ is increasing. Increasing the parameters δ_1 and δ_2 which denote the death rates of the lower- and top-predators result to the dynamic to change from chaotic case to periodic, and from chaotic to stable distributions, respectively.

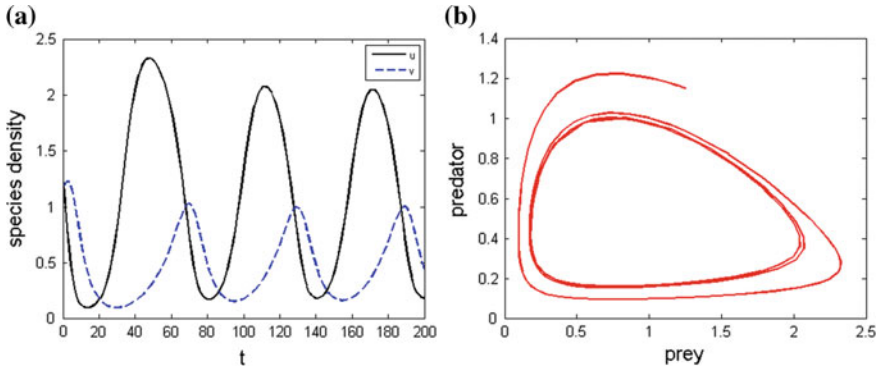

Fig. 6 Numerical results for fractional predator–prey system (11) with $\alpha = 0.25$

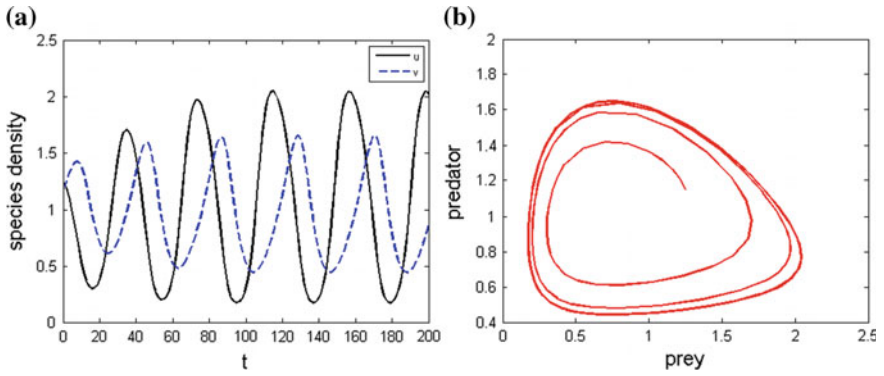

Fig. 7 Numerical results for fractional predator–prey system (11) with $\alpha = 0.50$

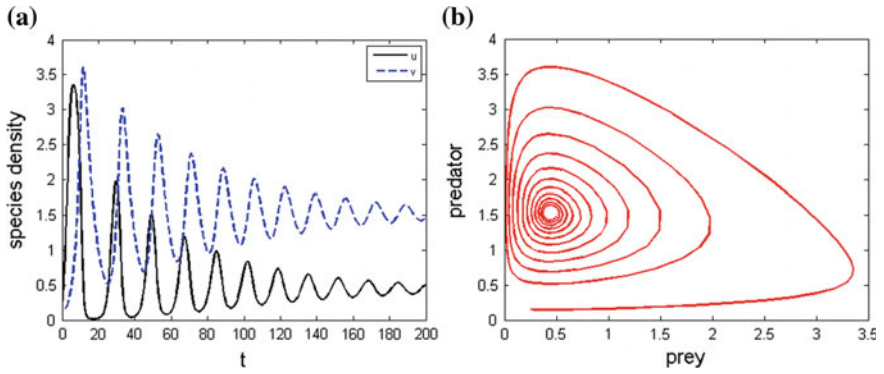

Fig. 8 Numerical results for fractional predator–prey system (11) with $\alpha = 0.98$

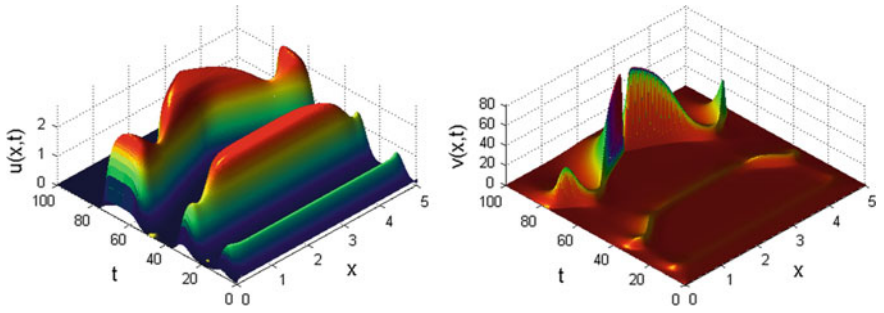

Fig. 9 Spatiotemporal dynamics of fractional reaction–diffusion system (12) with $\alpha = 0.38$

We simulate systems (11) and (12) by employing the zero-flux Neumann boundary conditions to examine some chaotic behaviour of the systems for different values of $\alpha \in (0, 1]$. The parameters used are $\kappa \in [2.8, 4.0]$, $\rho = 1$, $\mu = 0.625$, $\beta = 1$, $\gamma =$

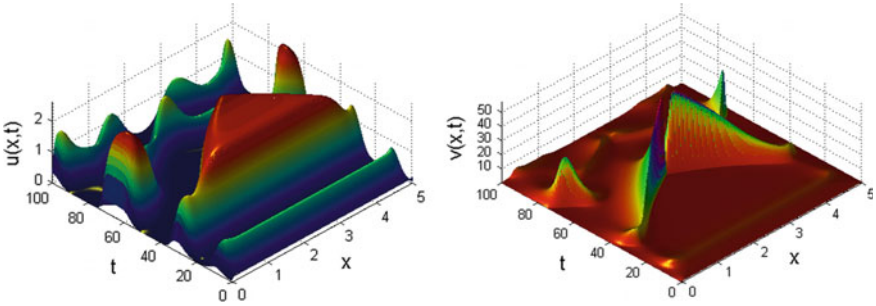

Fig. 10 Spatiotemporal dynamics of fractional reaction–diffusion system (12) with $\alpha = 0.52$

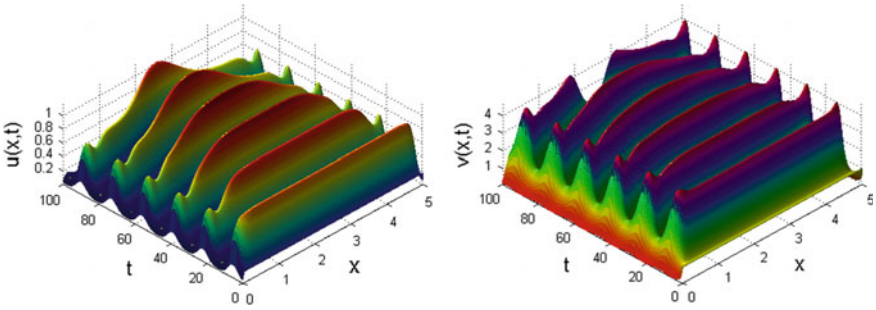

Fig. 11 Spatiotemporal dynamics of fractional reaction–diffusion system (12) with $\alpha = 0.71$

0.125, $\delta = 0.78$, $D_u = 0.05$, $D_v = 0.25$ and $\sigma = 0.69$, which satisfy (ρ, κ, μ, β, γ, δ, σ) in $E = (u^*, v^*)$. The initial condition is taken as a small amplitude random perturbation which is allowed to evolve naturally in the computation to induce a nontrivial result. We employ a finite difference approximation to discretize the Laplacian operator ($\Delta = \partial^2(\cdot)/\partial x^2$); see [9, 29] for details. The spatiotemporal behaviours reported in this work show the coexistence of the species. Figures 6, 7 and 8 correspond to time-evolution of non-diffusive system (11), while Figs. 9, 10 and 11 indicate chaotic behaviour of dynamic system (12) in the presence of diffusion. The behaviour of the dynamics obtained in the absence and presence of diffusion in this work has a lot of biological interpretation, and readers are referred to [20, 21] for further explanations.

5 Conclusion

In this work, different examples of predation systems whose dynamics are governed by the Holling type-IV functional responses are theoretically studied and numerically investigated. The classical time derivative in such systems is modelled in time with

the novel Atangana–Baleanu fractional order derivative in the sense of Caputo. To help in the correct choice of parameters, the local stability analysis for each of the models is examined. A fractional two-step Adams–Bashforth scheme is developed to approximate the fractional derivative of order $\alpha \in (0, 1]$. The biological importance of the comparative simulation results on the population densities of the prey and predators is presented. Numerical results for some instances of fractional order for both diffusive and nondiffusive revealing the behaviour of the species are presented. Extension of the mathematical techniques presented in this work to more complex models in engineering is left for future research.

References

1. W.M. Abd-Elhameed, E.H. Doha, Y.H. Youssri, M.A. Bassuony , New Tchebyshev-Galerkin operational matrix method for solving linear and nonlinear hyperbolic telegraph type equations, in *Numerical Methods for Partial Differential Equations* (2016). https://doi.org/10.1002/num.22074
2. O. Abu Arqub, M. Al-Smadi, Atangana-Baleanu fractional approach to the solutions of Bagley-Torvik and Painlevé equations in Hilbert space. Chaos, Solitons and Fractals **117**, 161–167 (2018)
3. O. Abu Arqub, B. Maayah, Numerical solutions of integrodifferential equations of Fredholm operator type in the sense of the Atangana-Baleanu fractional operator. Chaos Solitons Fractals **117**, 117–124 (2018)
4. O. Abu Arqub, B. Maayah, Modulation of reproducing kernel Hilbert space method for numerical solutions of Riccati and Bernoulli equations in the Atangana-Baleanu fractional sense. Chaos, Solitons Fractals **125**, 163–170 (2019)
5. A. Atangana, D. Baleanu, New fractional derivatives with nonlocal and non-singular Kernel: theory and application to heat transfer model. Thermal Sci. **20**, 763–769 (2016)
6. A. Atangana, *Derivative with a New Parameter: Theory Methods and Applications* (Academic Press, New York, 2016)
7. A. Atangana, J.F. Goméz-Aguilar, Fractional derivatives with no-index law property: application to chaos and statistics. Chaos, Solitons Fractals **114**, 516–535 (2018)
8. A. Atangana, Blind in a commutative world: simple illustrations with functions and chaotic attractors Chaos. Solitons Fractals **114**, 347–363 (2018)
9. A. Atangana, K.M. Owolabi, New numerical approach for fractional differential equations. Math. Modell. Nat. Phenom., **13**(3), 21 pages (2018). https://doi.org/10.1051/mmnp/2018010
10. A. Atangana, S. Jain, The role of power decay, exponential decay and Mittag-Leffler function's waiting time distribution: application of cancer spread. Phys. A **512**, 330–351 (2018)
11. M.A. Bassuony, W.M. Abd-Elhameed, E.H. Doha, Y.H. Youssri, A Legendre-Laguerre-Galerkin method for uniform Euler-Bernoulli beam equation. East Asian J. Appl. Math. **8**, 280–295 (2018)
12. M. Caputo, M. Fabrizio, A new definition of fractional derivative without singular kernel. Progr. Fractional Differ. Appl. **1**, 73–85 (2015)
13. M. Caputo, M. Fabrizio, Applications of new time and spatial fractional derivatives with exponential kernels. Progr. Fractional Differ. Appl. **2**, 1–11 (2016)
14. E.H. Doha, W.M. Abd-Elhameed, N.A. Elkot, Y.H. Youssri, Integral spectral Tchebyshev approach for solving space Riemann-Liouville and Riesz fractional advection-dispersion problems. Adv. Diff. Equ. (2017). https://doi.org/10.1186/s13662-017-1336-6
15. E.H. Doha, Y.H. Youssri, On the connection coefficients and recurrence relations arising from expansions in series of modified generalized Laguerre polynomials: applications on a semi-infinite domain. Nonlinear Eng. (2019). https://doi.org/10.1515/nleng-2018-0073

16. E.H. Doha, R.M. Hafez, Y.H. Youssri, Shifted Jacobi spectral-Galerkin method for solving hyperbolic partial differential equations. Comput. Math. Appl. (2019). https://doi.org/10.1016/j.camwa.2019.03.011
17. E.H. Doha, W.M. Abd-Elhameed, Y.H. Youssri, Fully Legendre spectral Galerkin algorithm for solving linear one-dimensional telegraph type equation. Int. J. Comput. Methods (2019). https://doi.org/10.1142/S0219876218501189
18. J.F. Gómez-Aguilar, Space-time fractional diffusion equation using a derivative with nonsingular and regular kernel. Phys. A: Stat. Mech. Appl. **465**(2017), 562–572 (2017)
19. B.E. Kendall, Cycles, chaos, and noise in predator-prey dynamics. Chaos Solitons Fractals **12**, 321–332 (2001)
20. J.D. Murray, *Mathematical Biology I: An Introduction* (Springer, New York, 2002)
21. J.D. Murray, *Mathematical Biology II: Spatial Models and Biomedical Applications* (Springer, Berlin, 2003)
22. K.M. Owolabi, Mathematical analysis and numerical simulation of patterns in fractional and classical reaction-diffusion systems. Chaos Solitons Fractals **93**, 89–98 (2016)
23. K.M. Owolabi, Numerical approach to fractional blow-up equations with Atangana-Baleanu derivative in Riemann-Liouville sense. Math. Modell. Nat. Phenom. **13**, 7 (2018). https://doi.org/10.1051/mmnp/2018006
24. K.M. Owolabi, Modelling and simulation of a dynamical system with the Atangana-Baleanu fractional derivative. Eur. Phys. J. Plus **133**, 15 (2018). https://doi.org/10.1140/epjp/i2018-11863-9
25. K.M. Owolabi, Numerical patterns in reaction-diffusion system with the Caputo and Atangana-Baleanu fractional derivatives. Chaos Solitons Fractals **115**, 160–169 (2018)
26. K.M. Owolabi, Chaotic behaviour in system of noninteger-order ordinary differential equations. Chaos Solitons Fractals **000**, 1–9 (2018)
27. K.M. Owolabi, Analysis and numerical simulation of multicomponent system with Atangana-Baleanu fractional derivative. Chaos Solitons Fractals **115**, 127–134 (2018)
28. K.M. Owolabi, Numerical patterns in system of integer and non-integer order derivatives. Chaos Solitons Fractals **115**, 143–153 (2018)
29. K.M. Owolabi, Numerical approach to fractional blow-up equations with Atangana-Baleanu derivative in Riemann-Liouville sense. Math. Modell. Nat. Phenom. **13**(7), [17 pages] (2018). https://doi.org/10.1051/mmnp/2018006
30. P.Y.H. Pang, M. Wang, Non-constant positive steady states of a predator-prey system with non-monotonic functional response and diffusion. Proc. Lond. Math. Soc. **88**, 135–157 (2004)
31. J.E. Solís-Pérez, J.F. Gómez-Aguilar, A. Atangana, Novel numerical method for solving variable-order fractional differential equations with power, exponential and Mittag-Leffler laws. Chaos Solitons Fractals **114**, 175–185 (2018)
32. J. Singh, D. Kumar, Z. Hammouch, A. Atangana, A fractional epidemiological model for computer viruses pertaining to a new fractional derivative. Appl. Math. Comput. **316**, 504–515 (2018)
33. Y.H. Youssri, W.M. Abd-Elhameed, Numerical spectral legendre-Galerkin algorithm for solving time fractional telegraph equation. Rom. J. Phys. **63**, 107 (2019)
34. L. Zhang, Z. Li, Spatial complexity of a predator-prey model with Holling-type response. Abstr. Appl. Anal., **2014**, Article ID 675378, 15 pages (2014). https://doi.org/10.1155/2014/675378
35. S. Zhang, D. Tan, L. Chen, Chaos in periodically forced Holling type IV predator-prey system with impulsive perturbations. Chaos Solitons Fractals **27**, 980–990 (2006)